frontiers | Research Topics

Advances in adult neurogenesis

Edited by
Seiji Hitoshi, Chitra Mandyam and Ashok K. Shetty

Published in
Frontiers in Neuroscience

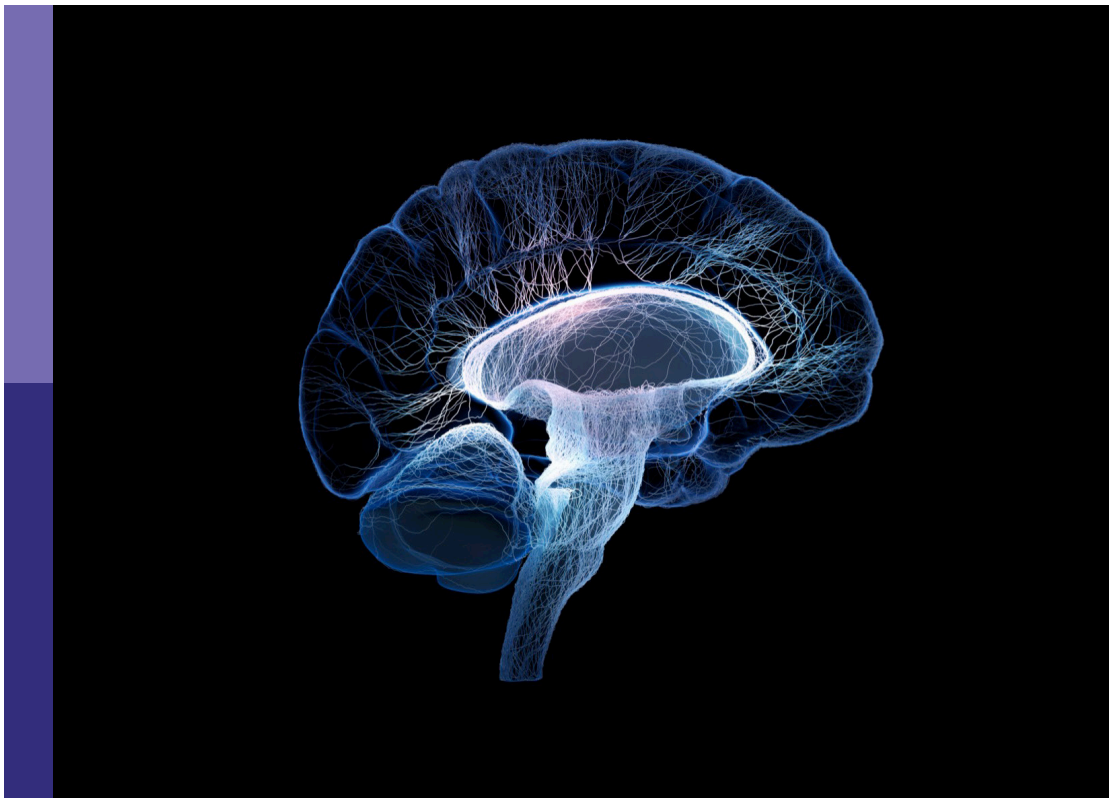

ISSN 1664-8714
ISBN 978-2-8325-4305-4
DOI 10.3389/978-2-8325-4305-4

About Frontiers

Frontiers is more than just an open access publisher of scholarly articles: it is a pioneering approach to the world of academia, radically improving the way scholarly research is managed. The grand vision of Frontiers is a world where all people have an equal opportunity to seek, share and generate knowledge. Frontiers provides immediate and permanent online open access to all its publications, but this alone is not enough to realize our grand goals.

Frontiers journal series

The Frontiers journal series is a multi-tier and interdisciplinary set of open-access, online journals, promising a paradigm shift from the current review, selection and dissemination processes in academic publishing. All Frontiers journals are driven by researchers for researchers; therefore, they constitute a service to the scholarly community. At the same time, the *Frontiers journal series* operates on a revolutionary invention, the tiered publishing system, initially addressing specific communities of scholars, and gradually climbing up to broader public understanding, thus serving the interests of the lay society, too.

Dedication to quality

Each Frontiers article is a landmark of the highest quality, thanks to genuinely collaborative interactions between authors and review editors, who include some of the world's best academicians. Research must be certified by peers before entering a stream of knowledge that may eventually reach the public - and shape society; therefore, Frontiers only applies the most rigorous and unbiased reviews. Frontiers revolutionizes research publishing by freely delivering the most outstanding research, evaluated with no bias from both the academic and social point of view. By applying the most advanced information technologies, Frontiers is catapulting scholarly publishing into a new generation.

What are Frontiers Research Topics?

Frontiers Research Topics are very popular trademarks of the *Frontiers journals series*: they are collections of at least ten articles, all centered on a particular subject. With their unique mix of varied contributions from Original Research to Review Articles, Frontiers Research Topics unify the most influential researchers, the latest key findings and historical advances in a hot research area.

Find out more on how to host your own Frontiers Research Topic or contribute to one as an author by contacting the Frontiers editorial office: frontiersin.org/about/contact

Advances in adult neurogenesis

Topic editors

Seiji Hitoshi — Shiga University of Medical Science, Japan

Chitra Mandyam — University of California, United States

Ashok K. Shetty — Texas A&M University School of Medicine, United States

Citation

Hitoshi, S., Mandyam, C., Shetty, A. K., eds. (2024). *Advances in adult neurogenesis*. Lausanne: Frontiers Media SA. doi: 10.3389/978-2-8325-4305-4

Table of contents

frontiers | Frontiers in Neuroscience

TYPE Editorial
PUBLISHED 05 January 2024
DOI 10.3389/fnins.2023.1307844

OPEN ACCESS

EDITED AND REVIEWED BY
Wendy Gold,
The University of Sydney, Australia

*CORRESPONDENCE
Seiji Hitoshi
shitoshi-tky@umin.ac.jp
Chitra D. Mandyam
cmandyam@scripps.edu
Ashok K. Shetty
ash.shetty@tamu.edu

RECEIVED 05 October 2023
ACCEPTED 12 December 2023
PUBLISHED 05 January 2024

CITATION
Hitoshi S, Mandyam CD and Shetty AK (2024) Editorial: Advances in adult neurogenesis. *Front. Neurosci.* 17:1307844. doi: 10.3389/fnins.2023.1307844

Editorial: Advances in adult neurogenesis

Seiji Hitoshi[1]*, Chitra D. Mandyam[2]* and Ashok K. Shetty[3]*

[1]Department of Integrative Physiology, Shiga University of Medical Science, Otsu, Japan, [2]VA San Diego Healthcare System, Veterans Health Administration, United States Department of Veterans Affairs, San Diego, CA, United States, [3]Department of Cell Biology and Genetics, Institute for Regenerative Medicine, Texas A&M University School of Medicine, College Station, TX, United States

KEYWORDS

adult neurogenesis, neural stem cells, dentate gyrus, olfactory bulb, V-SVZ

Editorial on the Research Topic
Advances in adult neurogenesis

Based on tremendous and elaborate work by Ramón y Cajal and other neuroanatomists around the beginning of 20th Century, it was generally believed that "once the development was ended, the fonts of growth and regeneration…dried up irrevocably (Cajal, 1991)." Pioneering studies by Joseph Altman in the 1960s, which unequivocally showed the generation of new neurons in the hippocampal dentate gyrus of adult mammals by [3H]-thymidine autoradiography (Altman, 1969), were, therefore, underappreciated, and adult neurogenesis remained a controversial field for more than a decade. It was not until the 1980s that the idea of adult neurogenesis was widely accepted following the development of several cell lineage markers and a culturing method of multipotent neural precursor cells from the adult brain (Lendahl et al., 1990; Reynolds and Weiss, 1992). Since then, this field has attracted significant attention, producing a multitude of papers spanning from basic mechanisms underlying the maintenance of the neurogenic niche to the functional significance of neurogenesis in the adult brain in healthy conditions or in a variety of diseases states.

We collected five review papers in this Research Topic of *Frontiers in Neuroscience*. Lampada and Taylor summarize our current knowledge regarding crucial roles of Notch signaling in maintaining neural precursor cell population in the ventricular-subventricular zone (V-SVZ) in the adult brain where quiescent, self-renewing neural stem cells reside. A comprehensive review by Singh et al., outlines transcription factors that play critical roles in preserving neural progenitor activity and promoting subsequent neurogenesis. A review by Inada et al., sheds light on a currently overlooked brain region, the subcommissural organ, and describes its potential in maintaining a neurogenic niche and stimulating neurogenesis in the adult brain. Since it was recognized that thousands of new neurons are born each day, although many of which die within several weeks, and a substantial number of them are incorporated into the granular cell layer of the adult hippocampus in rodents as well as in humans (Spalding et al., 2013), the possible function of the adult dentate neurogenesis in the memory formation and eradication has been extensively investigated. An excellent review by Fölsz et al., introduces preceding important studies and discusses the current situation of this research field. In contrast to the physiological function, a review by Kasahara et al., discusses aberrant neurogenesis in a pathological condition, such as epilepsy. As a whole, the review articles covered in this Research Topic update the state of the adult neurogenesis field, which we believe will help instigate future function questions and studies from scientist's novice to the field.

Seven original research papers also contribute to this Research Topic. Fang et al., provide novel data, demonstrating that one of the tissue inhibitors of metalloproteinases (TIMPs), TIMP3, promotes the maintenance of neural stem cells (NSCs). When newborn neurons are integrated into the existing neural network in the olfactory bulb, Sawada et al., demonstrate that PlexinD1 signaling plays a significant role. Olfactory bulb neurogenesis affects animal behavior when it is disturbed by chronic mild stress, which is shown by Athanassi et al.. Three groups scrutinized the dentate gyrus neurogenesis: Ohyama et al., propose phosphorylated Smad3-positive cells as a distinct subpopulation in the dentate gyrus; Kasakura et al., examined the effects of NT-3 overexpression on the differentiation of dentate gyrus neural precursor cells; and Amelchenko et al., provide evidence showing the correlation between age-related decline in cognitive flexibility and reduced hippocampal neurogenesis. Moreover, an article by Bazarek et al., demonstrates that overexpression of Neurogenin2 could modulate cortical oligodendrocyte progenitor cells to transdifferentiate into neurons, which could lead to a new strategy for functional recovery of the brain following injury or disease in the future.

In sum, this Research Topic aims to clarify what is vigorously explored in the Adult Neurogenesis field, and it would be our pleasure if it draws the attention of young neuroscientists and encourages them to explore this field and contribute studies supporting to the significance of neurogenesis in the adult brain.

Author contributions

SH: Writing – original draft. CM: Writing – review & editing. AS: Writing – review & editing.

Funding

The author(s) declare financial support was received for the research, authorship, and/or publication of this article. SH was supported by a Grant-in-Aid for Challenging Exploratory Research (22K19359) from the Ministry of Education, Culture, Sports, Science and Technology of Japan. AS was supported by grants from the National Institutes of Health (National Institute for Aging grants, RF1AG074256-01 and R01AG075440-01). CM was supported by a grant from the National Institute on Alcoholism and Alcohol Abuse (AA020098).

Acknowledgments

We thank all authors for their contributions to this Research Topic.

Conflict of interest

The authors declare that the research was conducted in the absence of any commercial or financial relationships that could be construed as a potential conflict of interest.

The author(s) declared that they were an editorial board member of Frontiers, at the time of submission. This had no impact on the peer review process and the final decision.

Publisher's note

References

Altman, J. (1969). "DNA metabolism and cell proliferation," in *Handbook of Neurochemistry, Vol. 2*, ed A. Lajtha (New York, NY: Plenum Press), 137–182.

Cajal, R. Y. (1991). "Cajal's degeneration and regeneration of the nervous system," in *Cajal's Degeneration and Regeneration of the Nervous System*, eds J. DeFelipe, E. G. Jones, and R. M. May (New York, NY: Oxford Academic).

Lendahl, U., Zimmerman, L. B., and McKay, R. D. (1990). CNS stem cells express a new class of intermediate filament protein. *Cell* 60, 585–595. doi: 10.1016/0092-8674(90)90662-X

Reynolds, B. A., and Weiss, S. (1992). Generation of neurons and astrocytes from isolated cells of the adult mammalian central nervous system. *Science* 255, 1707–1710. doi: 10.1126/science.1553558

Spalding, K. L., Bergmann, O., Alkass, K., Bernard, B., Salehpour, M., Huttner, H. B., et al. (2013). Dynamics of hippocampal neurogenesis in adult humans. *Cell* 153, 1219–1227. doi: 10.1016/j.cell.2013.05.002

frontiers | Frontiers in Neuroscience

TYPE Mini Review
PUBLISHED 15 February 2023
DOI 10.3389/fnins.2023.1128623

OPEN ACCESS

EDITED BY
Ashok K. Shetty,
Texas A&M University College of Medicine, United States

REVIEWED BY
Shawn Fletcher Sorrells,
University of Pittsburgh, United States

*CORRESPONDENCE
Vincent Croset
✉ vincent.croset@durham.ac.uk

SPECIALTY SECTION
This article was submitted to Neurodevelopment, a section of the journal Frontiers in Neuroscience

RECEIVED 20 December 2022
ACCEPTED 30 January 2023
PUBLISHED 15 February 2023

CITATION
Fölsz O, Trouche S and Croset V (2023) Adult-born neurons add flexibility to hippocampal memories.
Front. Neurosci. 17:1128623.
doi: 10.3389/fnins.2023.1128623

Adult-born neurons add flexibility to hippocampal memories

Orsolya Fölsz[1,2], Stéphanie Trouche[3] and Vincent Croset[1]*

[1]Department of Biosciences, Durham University, Durham, United Kingdom, [2]MSc in Neuroscience Programme, University of Oxford, Oxford, United Kingdom, [3]Institute of Functional Genomics, University of Montpellier, CNRS, INSERM, Montpellier, France

Although most neurons are generated embryonically, neurogenesis is maintained at low rates in specific brain areas throughout adulthood, including the dentate gyrus of the mammalian hippocampus. Episodic-like memories encoded in the hippocampus require the dentate gyrus to decorrelate similar experiences by generating distinct neuronal representations from overlapping inputs (pattern separation). Adult-born neurons integrating into the dentate gyrus circuit compete with resident mature cells for neuronal inputs and outputs, and recruit inhibitory circuits to limit hippocampal activity. They display transient hyperexcitability and hyperplasticity during maturation, making them more likely to be recruited by any given experience. Behavioral evidence suggests that adult-born neurons support pattern separation in the rodent dentate gyrus during encoding, and they have been proposed to provide a temporal stamp to memories encoded in close succession. The constant addition of neurons gradually degrades old connections, promoting generalization and ultimately forgetting of remote memories in the hippocampus. This makes space for new memories, preventing saturation and interference. Overall, a small population of adult-born neurons appears to make a unique contribution to hippocampal information encoding and removal. Although several inconsistencies regarding the functional relevance of neurogenesis remain, in this review we argue that immature neurons confer a unique form of transience on the dentate gyrus that complements synaptic plasticity to help animals flexibly adapt to changing environments.

KEYWORDS

neurogenesis, memory, hippocampus, forgetting, pattern separation, flexibility

Introduction

Brain plasticity enables animals to encode novel information and adapt to changing environments. A leading hypothesis suggests that memory representations are stored within connected neuronal ensembles called engrams in each brain region and throughout the brain (Semon, 1921). Neuronal ensembles activated together by a learning experience undergo persistent functional modifications upon learning and are reactivated together during memory recall. Learning triggers lasting changes in synaptic strength between co-activated neurons (Hebb, 2005), often underlain by long-term potentiation (LTP) of relevant synapses (Bliss and Lømo, 1973).

In the mammalian brain, episodic-like memories are stored in the hippocampus (**Figure 1A**). The dentate gyrus (DG) of the hippocampus integrates spatio-temporal and event-specific information from the medial and lateral entorhinal cortex (EC), respectively, and converts them into sparse neuronal representations (Engin et al., 2015). Pattern separation enables

highly analogous memories to be stored with little interference in distinct cell ensembles in the CA3 subfield (Leutgeb et al., 2007). The DG also attenuates the generalization of remote fear memories and may be involved in the remote memory retrieval (Bernier et al., 2017). CA3 performs the complementary process of pattern completion, enabling behavioral expression of a memory trace, even when the context or inputs of memory recall are different from encoding or incomplete (Leutgeb et al., 2007). Outputs from CA3 are compared with direct EC inputs in CA1 and sent back to the EC to be distributed across the neocortex for long-term storage. The EC also has direct connections with CA3, which are involved in discrimination of distinct stimuli (Fyhn et al., 2007).

In most mammals, hippocampal circuitry is constantly reformed by a unique form of structural and functional plasticity involving neurogenesis. Adult neurogenesis in rodents is present in at least two areas: the subventricular zone lining the lateral ventricles, and the subgranular zone of the DG (Lois and Alvarez-Buylla, 1993; Kempermann et al., 1997a). The former gives rise to cells that migrate to the olfactory bulb and differentiate into inhibitory olfactory neurons, while the latter generates excitatory glutamatergic granule cells (GCs). The vast majority of DG GCs are born perinatally, after which neurogenesis declines and is maintained at varying levels throughout adulthood (Ngwenya et al., 2015; Hochgerner et al., 2018). Of all DG GCs, ∼0.2% are generated daily in rats and ∼0.06% in mice (Kempermann et al., 1997a; Cameron and Mckay, 2001). Around half of adult-born GCs (abGCs) generated are eliminated through waves of programmed cell death during their maturation (Dayer et al., 2003; Ryu et al., 2016; Pilz et al., 2018). Surviving cells are stably maintained and ultimately become indistinguishable from developmental GCs (Dayer et al., 2003; Kempermann et al., 2003). Neurogenesis is balanced by the continuous removal of mostly perinatally-generated mature GCs (mGCs) (Ciric et al., 2019), resulting in a constant or slightly expanding DG cell number (Rapp and Gallagher, 1996; Kempermann et al., 1997b). In this review, we argue that integration of abGCs into the DG network confers plasticity to the classical cortico-hippocampal circuit.

Functional integration of adult-born neurons

Proliferation of neural progenitor cells (NPCs) in the subgranular zone of the DG produces neuronal fate-committed cells that undergo stereotypic stages of maturation (Hochgerner et al., 2018; Pilz et al., 2018). Maturing abGCs extend dendrites and an axon toward CA3 (or CA2; Llorens-Martín et al., 2015) of the hippocampus (Zhao et al., 2006), shifting excitation-inhibition balance. The ensuing critical period of hyperexcitability (Mongiat et al., 2009; Danielson et al., 2016; Li L. et al., 2017) is characterized by lower LTP induction threshold and higher LTP amplitude compared to mature mGCs (Schmidt-Hieber et al., 2004; Ge et al., 2007; Li et al., 2013). Maturing abGCs continuously reform their connections with the local circuitry, in an activity-dependent manner (Toni et al., 2007; Jungenitz et al., 2018).

During early maturation, abGCs receive inhibitory inputs from local interneurons and form transient direct connections with mGCs (Hendricks et al., 2017; Gozel and Gerstner, 2021). Electrophysiological recordings show that abGCs receiving lateral EC inputs inhibit mGCs, while abGCs receiving medial EC inputs excite mGCs (Luna et al., 2019). Later, abGCs switch from direct interactions to synaptic competition with mGCs for EC inputs and CA3 targets. Electron microscopy evidence shows that abGCs initially contact pre-existing axon terminals occupied by other neurons, but later outcompete mGC axons to become unique synaptic partners (Toni et al., 2007). Similar processes occur dendritically (Toni et al., 2008; McAvoy et al., 2016). Firing connections are stably maintained while inactive ones are pruned, therefore hyperexcitable abGCs tend to prevail, driving the elimination of existing mGC connections (Tashiro et al., 2007; Yasuda et al., 2011; Restivo et al., 2015; Murray et al., 2020). The selective survival of abGCs may also be regulated by synaptic activity, and in an information-specific manner (Tashiro et al., 2006). abGCs additionally form dynamic connections with hippocampal interneurons that inhibit neighboring mGCs (lateral inhibition), and exert inhibition even on CA3 and CA1 (feedforward inhibition) (Chawla et al., 2005; Guo et al., 2018; Berdugo-Vega et al., 2020). This results in the overall sparsification of population firing across the hippocampus (Lacefield et al., 2012; Temprana et al., 2015; McHugh et al., 2022).

Excitation or artificial LTP induction, as well as exposure to new experiences, such as spatial learning, voluntary exercise, or increased sensory stimulation (e.g., animal housing in groups, novel toys in home cages etc.) promote neurogenesis (Kempermann et al., 1997b; Gould et al., 1999; van Praag et al., 1999; Deisseroth et al., 2004; Bruel-Jungerman et al., 2006; Darcy et al., 2014). Stress, aging, and some neuropsychiatric conditions decrease proliferation rates and responsiveness of abGCs (Ben Abdallah et al., 2010; Snyder et al., 2011). This may contribute to intensified stress responses (Snyder et al., 2011), and decreased learning abilities in older animals (Montaron et al., 2020).

Contribution of adult-born neurons to memory encoding

The DG converts EC inputs into highly decorrelated representations in CA3 (Fyhn et al., 2007). This is achieved by changes in the correlated activity of the same sparse subset of GCs between similar contexts, such as when rats explore enclosures of slightly different shapes. Niibori et al. (2012) measured the overlap between CA3 cells activated during encoding and re-exposure using a cellular imaging approach, and found that suppressing neurogenesis disrupts the decorrelation of highly overlapping (but not dissimilar) contexts. Behavioral evidence suggests that critical period abGCs are important for tasks requiring separation of highly similar contexts, such as contextual fear discrimination or re-learning of a shock zone location (**Table 1**); however, these cells appear dispensable for learning a location in the water maze (Sahay et al., 2011, Burghardt et al., 2012). Intriguingly, blocking all outputs from GCs older than 3–4 weeks improves contextual fear conditioning (CFC) performance, suggesting that pattern separation not only relies on abGCs, but could be counteracted by mGCs (Nakashiba et al., 2012). abGCs might recruit inhibitory circuits to limit the activation of the same GCs in similar contexts *via* lateral and feedback inhibition, providing a potential mechanism for pattern separation (Kitamura et al., 2009; Engin et al., 2015; Temprana et al., 2015; **Figure 1B**).

Despite these advances, the extent of abGC contribution to pattern separation remains ambiguous, largely due to inconsistencies around defining and manipulating relevant neuronal populations,

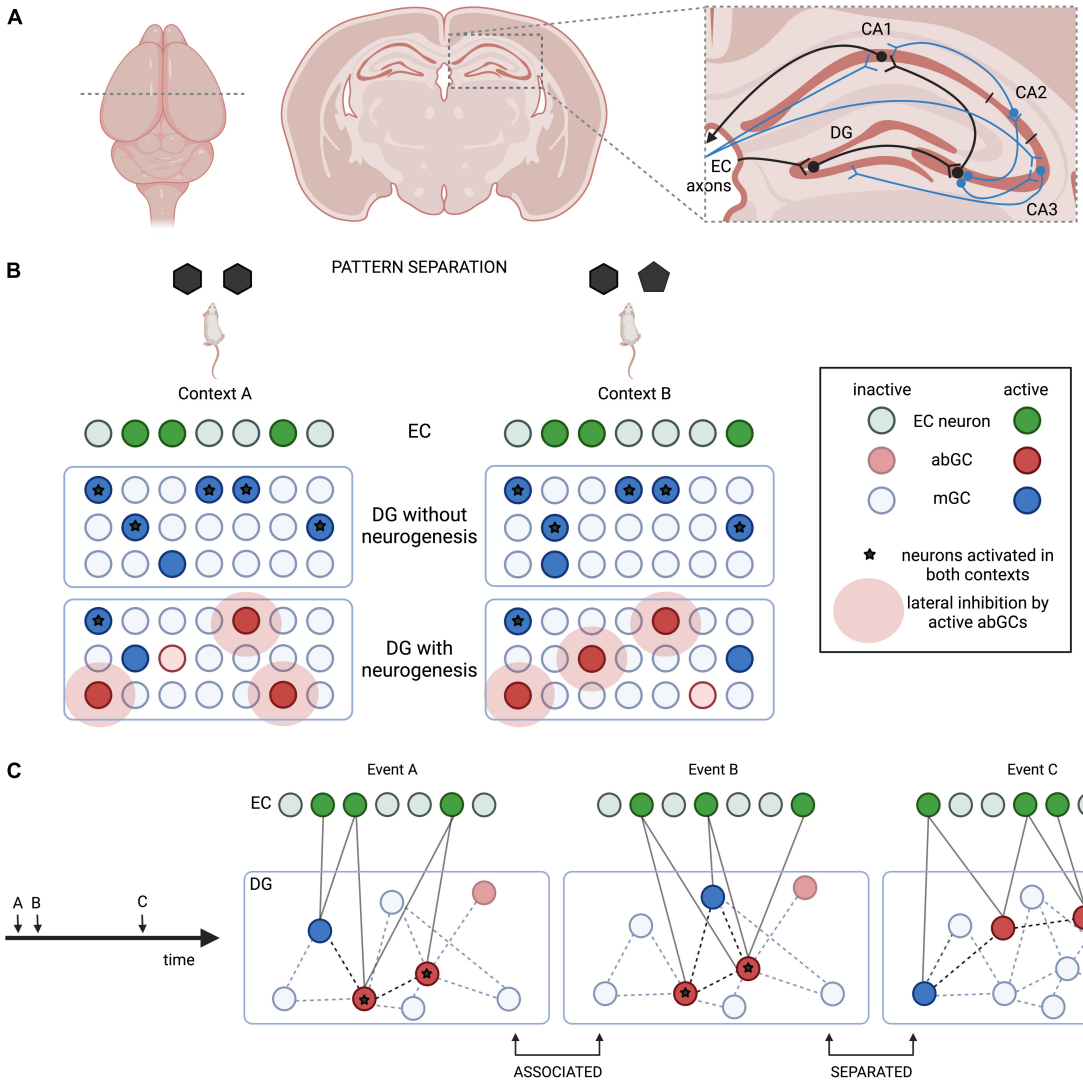

FIGURE 1
Simplified hippocampal circuitry and the role of adult neurogenesis in pattern separation in the dentate gyrus (DG). **(A)** Schematic hippocampal circuitry from a mouse brain coronal section. Beyond the basic trisynaptic loop (EC-DG-CA3-CA1, black), some entorhinal cortex (EC) inputs go directly to CA1/CA3, while some CA3 axons project to CA2, send collaterals to other CA3 neurons, and feed back to the DG (blue). **(B)** Adult-born GCs (abGCs) achieve pattern separation by limiting the activation of the same mature GCs (mGCs) in similar contexts. **(C)** "Time-stamping" could link contemporary events A and B, but separate remote event C by activating a changing population of abGCs.

and in the behavioral paradigms used (Table 1). More specific DG-based pattern separation paradigms, optogenetic manipulations, and simultaneous recordings of abGCs and mature hippocampal cell types may help elucidate the precise role of abGCs in memory formation. Disrupted pattern separation in some, but improved performance in other hippocampus-based tasks suggests that abGCs may serve additional functions beyond pattern separation, depending on the behavioral paradigm.

Aimone et al. (2006) proposed that abGCs link memories encoded in close succession, while separating remote memories (Figure 1C). Because hyperexcitable DG cells are preferentially included into engrams (Park et al., 2016), critical period abGCs may be more readily recruited into any memory trace. This generates overlapping representations in CA3 that can be activated by the context represented in any of the temporally associated engrams. Therefore, integration of young abGCs into hippocampal engrams may help connect contemporary memories (Cai et al., 2016), while more mature abGC populations support pattern separation (Aimone et al., 2010). The involvement of juvenile-born GCs (Kesner et al., 2014) in "time-stamping" has been described in a task where animals use spatial cues to generate preference for a temporally paired spatial location. Lesions in either cell population eliminated preference for the cued location, suggesting disrupted associations between events occurring close in time.

Recently, new findings have questioned the validity of the "time-stamping" hypothesis. Whereas abGCs are indeed more likely to be recruited during spatial memory encoding and activated during retrieval (Kee et al., 2007; Trouche et al., 2009; Stone et al., 2011; Gu et al., 2012; Martinez-Canabal et al., 2013), little overlap was found between abGCs activated during encoding or retrieval of contextual fear memories (Kumar et al., 2020). This suggests that either abGCs are activated by behavioral states rather than specific events or contexts (Erwin et al., 2020), or that limited overlap between the two populations could be a general property of DG

engrams (Denny et al., 2014). Another line of recent findings shows that maturing abGCs maintain their hyperexcitable properties for several months beyond the proposed critical period. These studies injected rats with various thymidine analogs to birthdate GC populations before quantifying their activity using immediate early gene expression. abGCs remained excitable especially in younger animals and animals that were offered environmental stimulation, and their activation supported learning even in older animals (Ohline et al., 2018; Montaron et al., 2020). This questions the idea of temporal integration and the long-standing view that abGCs exert their memory-related functions merely during their first weeks of existence (Alme et al., 2010).

Adult-born neurons and memory consolidation

abGCs stably integrated into the hippocampal circuitry may also influence later stages of memory processing. Classical views of systems consolidation have held that after encoding, memories progressively lose their hippocampal dependence before transferring completely to neocortex (Frankland and Bontempi, 2005). Prefrontal cortex engrams are strengthened by CA3 and CA1 ripples (Nakashiba et al., 2009), while hippocampal engrams are gradually silenced (Kitamura et al., 2017; Gao et al., 2018).

Some evidence suggests that abGCs promote memory consolidation during sleep, when hippocampal and neocortical engrams are reactivated, and synapses are selectively strengthened or renormalized by dendritic remodeling (Mirescu et al., 2006; de Vivo et al., 2017; Li W. et al., 2017). abGCs active during CFC learning are reactivated during rapid eye movement (REM) sleep, and both optogenetic stimulation and silencing of reactivated abGCs disrupt consolidation (Kumar et al., 2020). Blocking neurogenesis reduces non-REM sleep and disrupts consolidation-related oscillations and cortex-hippocampus interaction, leading to poor spatial memory performance (Sippel et al., 2020). Further, the rate of neurogenesis also seems to determine the hippocampus-dependent period of memories (Kitamura et al., 2009). Although none of these studies directly links abGC engrams to these changes, or specifically accounts for sleep-induced changes in neurogenesis levels, they do demonstrate that abGCs are involved in sleep-related consolidation.

Neurogenesis affects memory stability and causes forgetting

Hippocampal representations of consolidated remote memories are reactivated upon retrieval. This destabilizes engrams, allowing protein synthesis-dependent reconsolidation processes to update, strengthen, or silence them (Suzuki et al., 2004). Both immature and critical period abGCs are reactivated during retrieval, however, blocking protein synthesis in the immature population alone affects reconsolidation (Lods et al., 2021). Updating of memories is impaired in the novel object recognition task when an even younger abGC population is ablated, further supporting that highly immature abGCs mediate reconsolidation (Suárez-Pereira and Carrión, 2015). The emerging unique roles of abGCs in post-encoding memory strengthening was recently demonstrated; chemogenetic stimulation during retrieval of abGCs, but not mGCs, improved remote memory strength and accuracy in rats (Lods et al., 2022).

A growing body of evidence suggests that increased neurogenesis after memory encoding promotes forgetting (**Table 1**). For instance, pharmacologically enhancing neurogenesis increases the forgetting of remote CFC memories after long re-exposures to the original context make them return to the hippocampus (Ishikawa et al., 2016). This has been explained by gradual elimination of existing connections through synaptic competition with abGCs (Murray et al., 2020), and reduction in LTP persistence through feedback and feedforward inhibition (Alam et al., 2018). Neurogenesis also disrupts perineuronal nets in CA1, which otherwise protect memories from degradation by limiting interneuron activity (Evans et al., 2022).

Removal of a small number of connections may only reduce memory precision, allowing recall by cues slightly different from the original encoding context (generalization) (Ko and Frankland, 2021). This might involve pruning of synapses that mediate feedforward inhibition (Ruediger et al., 2011). Once more connections are weakened, memories become inaccessible. High postnatal neurogenesis may even explain why early childhood memories are forgotten in many species (infantile amnesia) (Akers et al., 2014). Memory representations are not fully erased, as optogenetic reactivation of DG engrams can partially recover these memories (Guskjolen et al., 2018).

Replacement of old memories with updated novel memories can occur in similar contexts without interference. Indeed, neurogenesis is involved specifically in tasks requiring high cognitive flexibility, such as re-learning of a changed spatial location. In this case, ablation of neurogenesis prevents, while expansion of the abGC population promotes better search strategies (Garthe et al., 2009; Burghardt et al., 2012; Swan et al., 2014; Berdugo-Vega et al., 2021). Increased post-training neurogenesis weakens memories acquired in the water maze, which ultimately enables later re-learning of the task (Epp et al., 2016). Therefore, abGCs might promote forgetting to subsequently support encoding of novel memories.

Discussion

Neural circuits require flexibility to adapt to changing environments, and stability to preserve information. The brain uses two main approaches to achieve transience: synaptic plasticity and cellular plasticity, or neurogenesis. Turnover of dendritic spines is undoubtedly the primary mechanism of structural plasticity behind learning, raising the question of why the DG needs neurogenesis beyond the synaptic modulation of mGCs.

Memory encoding by abGCs adds an anterograde form of transience to the hippocampus. Computational models support that abGCs optimize the balance between pattern separation and completion (Becker, 2005; Weisz and Argibay, 2009; O'Donnell and Sejnowski, 2014; Finnegan and Becker, 2015). abGCs might be used specifically to incorporate information about new experiences into engrams in familiar contexts (Aimone et al., 2009). Importantly, the inherent temporality of neurogenesis could hardly be replicated by synaptic plasticity. Most research into temporal sequence generation in the hippocampus has focused on CA1 and CA2 (MacDonald et al., 2013; Mankin et al., 2015), but the contribution of DG abGCs merits further investigations.

TABLE 1 Key studies on the effect of hippocampal neurogenesis on behavioral pattern separation and forgetting.

Experiment	Neurogenesis manipulation	Manipulation approach	abGC identification	Performance	Subjects (sex, age)	Supports involvement of abGCs?	References
Pattern separation							
CFC	↑	Genetic Bax ablation in NPCs	Dcx, BrdU	↑	MF 14–18 weeks	✓	Sahay et al., 2011; Besnard and Sahay, 2021
	↓	X-ray irradiation	Dcx	↓		✓	
	↓	Nestin-rtTA/Tet mice	CldU	↓	M 8 weeks	✓	Tronel et al., 2010
	Ablation	Nestin-HSV-TK mice	Ki67, NeuroD	↓ When contexts similar	M 10 weeks	✓	Niibori et al., 2012
Touchscreen location discrimination	↑	Voluntary exercise	BrdU	↑	M 3–22 months	✓	Creer et al., 2010
Radial arm maze Touchscreen location discrimination	↓	X-ray irradiation and viral Wnt knockdown	Dcx	↓ When contexts similar	F 8+ weeks	✓	Clelland et al., 2009
CFC with changed shock zone	Ablation	X-ray irradiation of GFAP-TK mice	Dcx	↓	M 10+ weeks	✓	Burghardt et al., 2012
Water maze	Ablation	Genetic Bax overexpression in NPCs	BrdU, Dcx, apoptotic marker	↓	M 14 weeks	✓	Dupret et al., 2008
Novel object recognition	↑	Voluntary exercise	Dcx	↑ When contexts similar	F 8+ weeks	✓	Bolz et al., 2015
Continuous novel object recognition	Silencing 4–7 weeks old abGCs	Optogenetic silencing in abGC-ArchT mice	Opto-tagging	↑	M 4–6 months	✓	McHugh et al., 2022
CFC	Postnatal ablation	DNMT1 knockout	BrdU	↑ In M	MF 3–5 months	X	Cushman et al., 2012
Touchscreen location discrimination	↓	GFAP-TK mice	Dcx	↑ In reversal phase	M 8+ weeks	X	Swan et al., 2014
Water maze	↓	GFAP-TK rats	Dcx	No effect ↓ Under cold-water stress	*M 12+ weeks	X	O'Leary et al., 2021
Neurogenesis-mediated forgetting							
CFC Water maze Incidental context learning	↑	Voluntary exercise or proneurogenic drugs	Retrovirus-driven GFP, Dcx, Ki67	Increased forgetting	? 8+ weeks	✓	Akers et al., 2014
	↓	Post-training temozolomide treatment or TK^+ mice		Improved retention		✓	
Water maze Odor-context paired-associates learning	↑	Voluntary exercise	Dcx	Increased forgetting but improved reversal learning	MF 8+ weeks	✓	Epp et al., 2016
	↓	Post-training vanganciclovir treatment or TK+ mice		Exercise failed to induce forgetting		✓	
CFC Water maze Paired associates learning	↑	Voluntary exercise	Dcx	Increased forgetting and improved reversal learning	*M ?	✓	Scott et al., 2021
CFC	↑	Voluntary exercise or p53 knockout	Dcx	Increased forgetting of recent memories	MF 8+ weeks	✓	Gao et al., 2018
CFC	↑	Memantine treatment	BrdU	Increased forgetting of remote memories after long re-exposures to training context	M 8+ weeks	✓	Ishikawa et al., 2016
Paired associates learning	↑	Voluntary exercise	Dcx	Increased forgetting	↑	✓	Epp et al., 2021
Water maze	↑	Voluntary exercise	BrdU, Dcx	No effect	*M 6+ weeks	X	Kodali et al., 2016
Water maze	↓	Post-training γ irradiation	BrdU, Dcx	No effect	*M 6+ weeks	X	Snyder et al., 2005

Information not reported in papers labeled with "?." Most studied use mouse models, while those labeled *use rats. M, males; F, females. Dcx, doubleortin (1–3 weeks old neurons); BrdU, CldU: thymidine analogs (proliferating cells); Ki67 (proliferating cells); NeuroD (immature neurons).

abGCs also confer retrograde transience on DG engrams through weakening and elimination of existing connections. Novel DG engrams may be "overfitted" and thus require generalization for optimal expression through neurogenesis, which acts as a regularizer in neuronal networks (Richards and Frankland, 2017; Tran et al., 2022). By eliminating unnecessary details while maintaining core features, neurogenesis may make memories easier to recall in changing or noisy environments. Neurogenesis also helps "clear up" remnants of remote hippocampal engrams already consolidated in the cortex, similar to sleep that serves the same function on a shorter timescale (Alam et al., 2018). Models support that neurogenesis makes room for new memories and prevents interferences (Wiskott et al., 2006).

As brains have become more complex throughout evolution, neurogenesis in the DG was maintained and repurposed. Some argue that it confers key functional benefits that underpin the evolutionary success of mammals (Kempermann, 2012), while others dismiss it as an evolutionary remnant, given its low rates, especially in highly cognitively developed species. As neurogenesis is associated with energy costs, oxidative stress, and oncogenesis (Walton et al., 2012; Batista et al., 2014), its maintenance may only be beneficial in animals that need to flexibly adapt to rapidly changing or enriched environments (Abrous et al., 2021). Indeed, most generalists (e.g., rodents) show neurogenesis, but mammals living in stable or homogenous environments do not (e.g., cetaceans).

The outstanding cognitive abilities of the human brain are thought to result from plasticity. Yet, the maintenance of DG neurogenesis throughout adulthood remains debated (Boldrini et al., 2018; Sorrells et al., 2018), mainly due to a lack of non-invasive research methods. Single-nucleus RNA sequencing recently verified the presence of scarce immature GCs in the adult human DG, with a marked reduction in Alzheimer's disease (Zhou et al., 2022). Whether these cells are actively generated during adulthood or retained in an immature state is unclear. Further research is required to establish if human neurogenesis has any cognitive benefits or functional implications in neuropsychiatric conditions (Mishra et al., 2022).

This review supports the idea that abGCs can participate in the formation of hippocampal memories and influence mGCs to help encoding, generalization, and forgetting. abGCs bring transience to the hippocampus both by adding and removing information about new events, experiences, or environments. Experimental standardization and technological advances can help resolve contradictions in the literature, for example, by combining abGC labeling, *in vivo* recording with engram cell- and synapse-tagging (Choi et al., 2018), and more advanced DG-specific behavioral paradigms. Standardized definitions of abGC versus mGC populations should also help draw clearer conclusions. Nevertheless if one accepts that, in addition to preserving information, a major goal of memory is to optimize behavior, a large body of evidence now supports adult neurogenesis as a meaningful contributor to hippocampal memory functions.

Author contributions

This work was originally written by OF as part of a 3rd year literature review assignment at Durham University. OF and VC: conceptualization. OF, ST, and VC: writing. VC: supervision. All authors contributed to the article and approved the submitted version.

Funding

Research in ST's laboratory is funded by the French National Research Agency (ANR-19-CE37-00036 and ANR-21-CE16-0015), the NARSAD BBRF (award 24925), and the Foundation NRJ-Institut de France. Research in VC's laboratory is funded by BBSRC (BB/W007347/1), the Royal Society (RGS\R1\221097), and Durham University Seedcorn Funds.

Conflict of interest

The authors declare that the research was conducted in the absence of any commercial or financial relationships that could be construed as a potential conflict of interest.

Publisher's note

All claims expressed in this article are solely those of the authors and do not necessarily represent those of their affiliated organizations, or those of the publisher, the editors and the reviewers. Any product that may be evaluated in this article, or claim that may be made by its manufacturer, is not guaranteed or endorsed by the publisher.

References

Abrous, D. N., Koehl, M., and Lemoine, M. (2021). A Baldwin interpretation of adult hippocampal neurogenesis: From functional relevance to physiopathology. *Mol. Psychiatry* 2021, 1–20. doi: 10.1038/s41380-021-01172-4

Aimone, J. B., Deng, W., and Gage, F. H. (2010). Adult neurogenesis: Integrating theories and separating functions. *Trends Cogn. Sci.* 14, 325–337. doi: 10.1016/J.TICS.2010.04.003

Aimone, J. B., Wiles, J., and Gage, F. H. (2006). Potential role for adult neurogenesis in the encoding of time in new memories. *Nat. Neurosci.* 9, 723–727. doi: 10.1038/NN1707

Aimone, J. B., Wiles, J., and Gage, F. H. (2009). Computational influence of adult neurogenesis on memory encoding. *Neuron* 61, 187–202. doi: 10.1016/J.NEURON.2008.11.026

Akers, K. G., Martinez-Canabal, A., Restivo, L., Yiu, A. P., de Cristofaro, A., Hsiang, H.-L., et al. (2014). Hippocampal neurogenesis regulates forgetting during adulthood and infancy. *Science* 344, 598–602. doi: 10.1126/SCIENCE.1248903

Alam, M. J., Kitamura, T., Saitoh, Y., Ohkawa, N., Kondo, T., and Inokuchi, K. (2018). Adult neurogenesis conserves hippocampal memory capacity. *J. Neurosci.* 38, 6854–6863. doi: 10.1523/JNEUROSCI.2976-17.2018

Alme, C. B., Buzzetti, R. A., Marrone, D. F., Leutgeb, J. K., Chawla, M. K., Schaner, M. J., et al. (2010). Hippocampal granule cells opt for early retirement. *Hippocampus* 20, 1109–1123. doi: 10.1002/HIPO.20810

Batista, C. M., Mariano, E. D., Barbosa, B. J. A. P., Morgalla, M., Marie, S. K. N., Teixeira, M. J., et al. (2014). Adult neurogenesis and glial oncogenesis: When the process fails. *Biomed. Res. Int.* 2014:438639. doi: 10.1155/2014/438639

Becker, S. (2005). A computational principle for hippocampal learning and neurogenesis. *Hippocampus* 15, 722–738. doi: 10.1002/HIPO.20095

Ben Abdallah, N., Slomianka, L., Vyssotski, A. L., and Lipp, H. P. (2010). Early age-related changes in adult hippocampal neurogenesis in C57 mice. *Neurobiol. Aging* 31, 151–161. doi: 10.1016/J.NEUROBIOLAGING.2008.03.002

Berdugo-Vega, G., Arias-Gil, G., López-Fernández, A., Artegiani, B., Wasielewska, J. M., Lee, C. C., et al. (2020). Increasing neurogenesis refines hippocampal activity rejuvenating navigational learning strategies and contextual memory throughout life. *Nat. Commun.* 11, 1–12. doi: 10.1038/s41467-019-14026-z

Berdugo-Vega, G., Lee, C. C., Garthe, A., Kempermann, G., and Calegari, F. (2021). Adult-born neurons promote cognitive flexibility by improving memory precision and indexing. *Hippocampus* 31, 1068–1079. doi: 10.1002/HIPO.23373

Bernier, B. E., Lacagnina, A. F., Ayoub, A., Shue, F., Zemelman, B. V., Krasne, F. B., et al. (2017). Dentate gyrus contributes to retrieval as well as encoding: Evidence from context fear conditioning, recall, and extinction. *J. Neurosci.* 37:6359. doi: 10.1523/JNEUROSCI.3029-16.2017

Besnard, A., and Sahay, A. (2021). Enhancing adult neurogenesis promotes contextual fear memory discrimination and activation of hippocampal-dorsolateral septal circuits. *Behav. Brain Res.* 399:112917. doi: 10.1016/J.BBR.2020.112917

Bliss, T. V. P., and Lømo, T. (1973). Long-lasting potentiation of synaptic transmission in the dentate area of the anaesthetized rabbit following stimulation of the perforant path. *J. Physiol.* 232, 331–356. doi: 10.1113/JPHYSIOL.1973.SP010273

Boldrini, M., Fulmore, C. A., Tartt, A. N., Simeon, L. R., Pavlova, I., Poposka, V., et al. (2018). Human hippocampal neurogenesis persists throughout aging. *Cell Stem Cell* 22, 589–599.e5. doi: 10.1016/J.STEM.2018.03.015

Bolz, L., Heigele, S., and Bischofberger, J. (2015). Running improves pattern separation during novel object recognition. *Brain Plast.* 1:129. doi: 10.3233/BPL-150010

Bruel-Jungerman, E., Davis, S., Rampon, C., and Laroche, S. (2006). Long-term potentiation enhances neurogenesis in the adult dentate gyrus. *J. Neurosci.* 26, 5888–5893. doi: 10.1523/JNEUROSCI.0782-06.2006

Burghardt, N. S., Park, E. H., Hen, R., and Fenton, A. A. (2012). Adult-born hippocampal neurons promote cognitive flexibility in mice. *Hippocampus* 22, 1795–1808. doi: 10.1002/HIPO.22013

Cai, D. J., Aharoni, D., Shuman, T., Shobe, J., Biane, J., Song, W., et al. (2016). A shared neural ensemble links distinct contextual memories encoded close in time. *Nature* 534, 115–118. doi: 10.1038/nature17955

Cameron, H. A., and Mckay, R. D. G. (2001). Adult neurogenesis produces a large pool of new granule cells in the dentate gyrus. *J. Comp. Neurol.* 435, 406–417. doi: 10.1002/CNE.1040

Chawla, M. K., Guzowski, J. F., Ramirez-Amaya, V., Lipa, P., Hoffman, K. L., Marriott, L. K., et al. (2005). Sparse, environmentally selective expression of Arc RNA in the upper blade of the rodent fascia dentata by brief spatial experience. *Hippocampus* 15, 579–586. doi: 10.1002/HIPO.20091

Choi, J., Sim, S., Kim, J., Choi, D., Oh, J., Ye, S., et al. (2018). Interregional synaptic maps among engram cells underlie memory formation. *Science* 360, 430–435. doi: 10.1126/SCIENCE.AAS9204

Ciric, T., Cahill, S. P., and Snyder, J. S. (2019). Dentate gyrus neurons that are born at the peak of development, but not before or after, die in adulthood. *Brain Behav.* 9:e01435. doi: 10.1002/BRB3.1435

Clelland, C. D., Choi, M., Romberg, C., Clemenson, G. D., Fragniere, A., Tyers, P., et al. (2009). A functional role for adult hippocampal neurogenesis in spatial pattern separation. *Science* 325, 210–213. doi: 10.1126/SCIENCE.1173215/SUPPL_FILE/CLELLAND.SOM-.PDF

Creer, D. J., Romberg, C., Saksida, L. M., van Praag, H., and Bussey, T. J. (2010). Running enhances spatial pattern separation in mice. *Proc. Natl. Acad. Sci. U.S.A.* 107, 2367–2372. doi: 10.1073/PNAS.0911725107

Cushman, J. D., Maldonado, J., Kwon, E. E., Denise Garcia, A., Fan, G., Imura, T., et al. (2012). Juvenile neurogenesis makes essential contributions to adult brain structure and plays a sex-dependent role in fear memories. *Front. Behav. Neurosci.* 6:3. doi: 10.3389/FNBEH.2012.00003

Danielson, N. B. B., Kaifosh, P., Zaremba, J. D. D., Lovett-Barron, M., Tsai, J., Denny, C. A. A., et al. (2016). Distinct contribution of adult-born hippocampal granule cells to context encoding. *Neuron* 90, 101–112. doi: 10.1016/J.NEURON.2016.02.019

Darcy, M. J., Trouche, S., Jin, S. X., and Feig, L. A. (2014). Ras-GRF2 mediates long-term potentiation, survival, and response to an enriched environment of newborn neurons in the hippocampus. *Hippocampus* 24, 1317–1329. doi: 10.1002/HIPO.22313

Dayer, A. G., Ford, A. A., Cleaver, K. M., Yassaee, M., and Cameron, H. A. (2003). Short-term and long-term survival of new neurons in the rat dentate gyrus. *J. Comp. Neurol.* 460, 563–572. doi: 10.1002/CNE.10675

de Vivo, L., Bellesi, M., Marshall, W., Bushong, E. A., Ellisman, M. H., Tononi, G., et al. (2017). Ultrastructural evidence for synaptic scaling across the wake/sleep cycle. *Science* 355, 507–510. doi: 10.1126/SCIENCE.AAH5982

Deisseroth, K., Singla, S., Toda, H., Monje, M., Palmer, T. D., and Malenka, R. C. (2004). Excitation-neurogenesis coupling in adult neural stem/progenitor cells. *Neuron* 42, 535–552. doi: 10.1016/S0896-6273(04)00266-1

Denny, C. A., Kheirbek, M. A., Alba, E. L., Tanaka, K. F., Brachman, R. A., Laughman, K. B., et al. (2014). Hippocampal memory traces are differentially modulated by experience, time, and adult neurogenesis. *Neuron* 83, 189–201. doi: 10.1016/J.NEURON.2014.05.018

Dupret, D., Revest, J. M., Koehl, M., Ichas, F., de Giorgi, F., Costet, P., et al. (2008). Spatial relational memory requires hippocampal adult neurogenesis. *PLoS One* 3:e1959. doi: 10.1371/JOURNAL.PONE.0001959

Engin, E., Zarnowska, E. D., Benke, D., Tsvetkov, E., Sigal, M., Keist, R., et al. (2015). Tonic inhibitory control of dentate gyrus granule cells by α5-containing GABAA receptors reduces memory interference. *J. Neurosci.* 35, 13698–13712. doi: 10.1523/JNEUROSCI.1370-15.2015

Epp, J. R., Botly, L. C. P., Josselyn, S. A., and Frankland, P. W. (2021). Voluntary exercise increases neurogenesis and mediates forgetting of complex paired associates memories. *Neuroscience* 475, 1–9. doi: 10.1016/J.NEUROSCIENCE.2021.08.022

Epp, J. R., Mera, R. S., Köhler, S., Josselyn, S. A., and Frankland, P. W. (2016). Neurogenesis-mediated forgetting minimizes proactive interference. *Nat. Commun.* 7, 1–8. doi: 10.1038/ncomms10838

Erwin, S. R., Sun, W., Copeland, M., Lindo, S., Spruston, N., and Cembrowski, M. S. (2020). A sparse, spatially biased subtype of mature granule cell dominates recruitment in hippocampal-associated behaviors. *Cell Rep.* 31:107551. doi: 10.1016/J.CELREP.2020.107551

Evans, A., Terstege, D. J., Scott, G. A., Tsutsui, M., and Epp, J. R. (2022). Neurogenesis mediated plasticity is associated with reduced neuronal activity in CA1 during context fear memory retrieval. *Sci. Rep.* 12, 1–16. doi: 10.1038/s41598-022-10947-w

Finnegan, R., and Becker, S. (2015). Neurogenesis paradoxically decreases both pattern separation and memory interference. *Front. Syst. Neurosci.* 9:136. doi: 10.3389/FNSYS.2015.00136

Frankland, P. W., and Bontempi, B. (2005). The organization of recent and remote memories. *Nat. Rev. Neurosci.* 6, 119–130. doi: 10.1038/nrn1607

Fyhn, M., Hafting, T., Treves, A., Moser, M. B., and Moser, E. I. (2007). Hippocampal remapping and grid realignment in entorhinal cortex. *Nature* 446, 190–194. doi: 10.1038/NATURE05601

Gao, A., Xia, F., Guskjolen, A. J., Ramsaran, A. I., Santoro, A., Josselyn, S. A., et al. (2018). Elevation of hippocampal neurogenesis induces a temporally graded pattern of forgetting of contextual fear memories. *J. Neurosci.* 38, 3190–3198. doi: 10.1523/JNEUROSCI.3126-17.2018

Garthe, A., Behr, J., and Kempermann, G. (2009). Adult-generated hippocampal neurons allow the flexible use of spatially precise learning strategies. *PLoS One* 4:e5464. doi: 10.1371/JOURNAL.PONE.0005464

Ge, S., Yang, C., Hsu, K., Ming, G., and Song, H. (2007). A critical period for enhanced synaptic plasticity in newly generated neurons of the adult brain. *Neuron* 54, 559–566. doi: 10.1016/J.NEURON.2007.05.002

Gould, E., Beylin, A., Tanapat, P., Reeves, A., and Shors, T. J. (1999). Learning enhances adult neurogenesis in the hippocampal formation. *Nat. Neurosci.* 2, 260–265. doi: 10.1038/6365

Gozel, O., and Gerstner, W. (2021). A functional model of adult dentate gyrus neurogenesis. *Elife* 10:e66463. doi: 10.1016/j.neulet.2021.136176

Gu, Y., Arruda-Carvalho, M., Wang, J., Janoschka, S. R., Josselyn, S. A., Frankland, P. W., et al. (2012). Optical controlling reveals time-dependent roles for adult-born dentate granule cells. *Nat. Neurosci.* 15, 1700–1706. doi: 10.1038/NN.3260

Guo, N., Soden, M. E., Herber, C., Kim, M. T. W., Besnard, A., Lin, P., et al. (2018). Dentate granule cell recruitment of feedforward inhibition governs engram maintenance and remote memory generalization. *Nat. Med.* 24, 438–449. doi: 10.1038/nm.4491

Guskjolen, A., Kenney, J., de la Parra, J., Yeung, B., Josselyn, S., and Frankland, P. (2018). Recovery of "Lost" infant memories in mice. *Curr. Biol.* 28, 2283–2290.e3. doi: 10.1016/J.CUB.2018.05.059

Hebb, D. O. (2005). *The organization of behavior: A neuropsychological theory*. New York, NY: Psychology Press. doi: 10.4324/9781410612403

Hendricks, W. D., Chen, Y., Bensen, A. L., Westbrook, G. L., and Schnell, E. (2017). Short-term depression of sprouted mossy fiber synapses from adult-born granule cells. *J. Neurosci.* 37, 5722–5735. doi: 10.1523/JNEUROSCI.0761-17.2017

Hochgerner, H., Zeisel, A., Lönnerberg, P., and Linnarsson, S. (2018). Conserved properties of dentate gyrus neurogenesis across postnatal development revealed by single-cell RNA sequencing. *Nat. Neurosci.* 21, 290–299. doi: 10.1038/s41593-017-0056-2

Ishikawa, R., Fukushima, H., Frankland, P. W., and Kida, S. (2016). Hippocampal neurogenesis enhancers promote forgetting of remote fear memory after hippocampal reactivation by retrieval. *Elife* 5:e17464. doi: 10.7554/ELIFE.17464

Jungenitz, T., Beining, M., Radic, T., Deller, T., Cuntz, H., Jedlicka, P., et al. (2018). Structural homo- and heterosynaptic plasticity in mature and adult newborn rat hippocampal granule cells. *Proc. Natl. Acad. Sci. U.S.A.* 115, E4670–E4679. doi: 10.1073/PNAS.1801889115

Kee, N., Teixeira, C. M., Wang, A. H., and Frankland, P. W. (2007). Preferential incorporation of adult-generated granule cells into spatial memory networks in the dentate gyrus. *Nat. Neurosci.* 10, 355–362. doi: 10.1038/NN1847

Kempermann, G. (2012). New neurons for "survival of the fittest.". *Nat. Rev. Neurosci.* 13, 727–736. doi: 10.1038/nrn3319

Kempermann, G., Gast, D., Kronenberg, G., Yamaguchi, M., and Gage, F. H. (2003). Early determination and long-term persistence of adult-generated new neurons in the hippocampus of mice. *Development* 130, 391–399. doi: 10.1242/DEV.00203

Kempermann, G., Kuhn, H. G., and Gage, F. H. (1997a). Genetic influence on neurogenesis in the dentate gyrus of adult mice. *Proc. Natl. Acad. Sci. U.S.A.* 94, 10409–10414.

Kempermann, G., Kuhn, H. G., and Gage, F. H. (1997b). More hippocampal neurons in adult mice living in an enriched environment. *Nature* 386, 493–495. doi: 10.1038/386493a0

Kesner, R. P., Hui, X., Sommer, T., Wright, C., Barrera, V. R., and Fanselow, M. S. (2014). The role of postnatal neurogenesis in supporting remote memory and spatial metric processing. *Hippocampus* 24, 1663–1671. doi: 10.1002/HIPO.22346

Kitamura, T., Ogawa, S. K., Roy, D. S., Okuyama, T., Morrissey, M. D., Smith, L. M., et al. (2017). Engrams and circuits crucial for systems consolidation of a memory. *Science* 356, 73–78. doi: 10.1126/SCIENCE.AAM6808

Kitamura, T., Saitoh, Y., Takashima, N., Murayama, A., Niibori, Y., Ageta, H., et al. (2009). Adult neurogenesis modulates the hippocampus-dependent period of associative fear memory. *Cell* 139, 814–827. doi: 10.1016/J.CELL.2009.10.020

Ko, S. Y., and Frankland, P. W. (2021). Neurogenesis-dependent transformation of hippocampal engrams. *Neurosci. Lett.* 762:136176. doi: 10.1016/J.NEULET.2021.136176

Kodali, M., Megahed, T., Mishra, V., Shuai, B., Hattiangady, B., and Shetty, A. K. (2016). Voluntary running exercise-mediated enhanced neurogenesis does not obliterate retrograde spatial memory. *J. Neurosci.* 36, 8112–8122. doi: 10.1523/JNEUROSCI.0766-16.2016

Kumar, D., Koyanagi, I., Carrier-Ruiz, A., Vergara, P., Srinivasan, S., Sugaya, Y., et al. (2020). Sparse activity of hippocampal adult-born neurons during REM sleep is necessary for memory consolidation. *Neuron* 107, 552–565.e10. doi: 10.1016/J.NEURON.2020.05.008

Lacefield, C. O., Itskov, V., Reardon, T., Hen, R., and Gordon, J. A. (2012). Effects of adult-generated granule cells on coordinated network activity in the dentate gyrus. *Hippocampus* 22, 106–116. doi: 10.1002/HIPO.20860

Leutgeb, J. K., Leutgeb, S., Moser, M. B., and Moser, E. I. (2007). Pattern separation in the dentate gyrus and CA3 of the hippocampus. *Science* 315, 961–966.

Li, L., He, Y., Zhao, M., and Jiang, J. (2013). Collective cell migration: Implications for wound healing and cancer invasion. *Burns Trauma* 1, 2321–3868.

Li, L., Sultan, S., Heigele, S., Schmidt-Salzmann, C., Toni, N., and Bischofberger, J. (2017). Silent synapses generate sparse and orthogonal action potential firing in adult-born hippocampal granule cells. *Elife* 6:e23612. doi: 10.7554/ELIFE.23612

Li, W., Ma, L., Yang, G., and Gan, W. B. (2017). REM sleep selectively prunes and maintains new synapses in development and learning. *Nat. Neurosci.* 20, 427–437. doi: 10.1038/nn.4479

Llorens-Martín, M., Jurado-Arjona, J., Avila, J., and Hernández, F. (2015). Novel connection between newborn granule neurons and the hippocampal CA2 field. *Exp. Neurol.* 263, 285–292. doi: 10.1016/J.EXPNEUROL.2014.10.021

Lods, M., Mortessagne, P., Pacary, E., Terral, G., Farrugia, F., Mazier, W., et al. (2022). Chemogenetic stimulation of adult neurogenesis, and not neonatal neurogenesis, is sufficient to improve long-term memory accuracy. *Prog. Neurobiol.* 219:102364. doi: 10.1016/J.PNEUROBIO.2022.102364

Lods, M., Pacary, E., Mazier, W., Farrugia, F., Mortessagne, P., Masachs, N., et al. (2021). Adult-born neurons immature during learning are necessary for remote memory reconsolidation in rats. *Nat. Commun.* 12, 1–14. doi: 10.1038/s41467-021-22069-4

Lois, C., and Alvarez-Buylla, A. (1993). Proliferating subventricular zone cells in the adult mammalian forebrain can differentiate into neurons and glia. *Proc. Natl. Acad. Sci. U.S.A.* 90, 2074–2077. doi: 10.1073/pnas.90.5.2074

Luna, V. M., Anacker, C., Burghardt, N. S., Khandaker, H., Andreu, V., Millette, A., et al. (2019). Adult-born hippocampal neurons bidirectionally modulate entorhinal inputs into the dentate gyrus. *Science* 364, 578–583. doi: 10.1126/SCIENCE.AAT8789

MacDonald, C. J., Carrow, S., Place, R., and Eichenbaum, H. (2013). Distinct hippocampal time cell sequences represent odor memories in immobilized rats. *J. Neurosci.* 33, 14607–14616. doi: 10.1523/JNEUROSCI.1537-13.2013

Mankin, E. A., Diehl, G. W., Sparks, F. T., Leutgeb, S., and Leutgeb, J. K. (2015). Hippocampal CA2 activity patterns change over time to a larger extent than between spatial contexts. *Neuron* 85, 190–201. doi: 10.1016/J.NEURON.2014.12.001

Martinez-Canabal, A., Akers, K. G., Josselyn, S. A., and Frankland, P. W. (2013). Age-dependent effects of hippocampal neurogenesis suppression on spatial learning. *Hippocampus* 23, 66–74. doi: 10.1002/HIPO.22054

McAvoy, K. M., Scobie, K. N., Berger, S., Russo, C., Guo, N., Decharatanachart, P., et al. (2016). Modulating neuronal competition dynamics in the dentate gyrus to rejuvenate aging memory circuits. *Neuron* 91, 1356. doi: 10.1016/J.NEURON.2016.08.009

McHugh, S. B., Lopes-dos-Santos, V., Gava, G. P., Hartwich, K., Tam, S. K. E., Bannerman, D. M., et al. (2022). Adult-born dentate granule cells promote hippocampal population sparsity. *Nat. Neurosci.* 25, 1481–1491. doi: 10.1038/s41593-022-01176-5

Mirescu, C., Peters, J. D., Noiman, L., and Gould, E. (2006). Sleep deprivation inhibits adult neurogenesis in the hippocampus by elevating glucocorticoids. *Proc. Natl. Acad. Sci. U.S.A.* 103, 19170–19175. doi: 10.1073/pnas.0608644103

Mishra, R., Phan, T., Kumar, P., Morrissey, Z., Gupta, M., Hollands, C., et al. (2022). Augmenting neurogenesis rescues memory impairments in Alzheimer's disease by restoring the memory-storing neurons. *J. Exp. Med.* 219:e20220391. doi: 10.1084/JEM.20220391

Mongiat, L. A., Espósito, M. S., Lombardi, G., and Schinder, A. F. (2009). Reliable activation of immature neurons in the adult hippocampus. *PLoS One* 4:e5320. doi: 10.1371/JOURNAL.PONE.0005320

Montaron, M. F., Charrier, V., Blin, N., Garcia, P., and Abrous, D. N. (2020). Responsiveness of dentate neurons generated throughout adult life is associated with resilience to cognitive aging. *Aging Cell* 19:e13161. doi: 10.1111/ACEL.13161

Murray, K. D., Liu, X. B., King, A. N., Luu, J. D., and Cheng, H. J. (2020). Age-related changes in synaptic plasticity associated with mossy fiber terminal integration during adult neurogenesis. *eNeuro* 7, 1–16. doi: 10.1523/ENEURO.0030-20.2020

Nakashiba, T., Buhl, D. L., McHugh, T. J., and Tonegawa, S. (2009). Hippocampal CA3 output is crucial for ripple-associated reactivation and consolidation of memory. *Neuron* 62, 781–787. doi: 10.1016/j.neuron.2009.05.013

Nakashiba, T., Cushman, J. D., Pelkey, K. A., Renaudineau, S., Buhl, D. L., McHugh, T. J., et al. (2012). Young dentate granule cells mediate pattern separation, whereas old granule cells facilitate pattern completion. *Cell* 149, 188–201. doi: 10.1016/J.CELL.2012.01.046

Ngwenya, L. B., Heyworth, N. C., Shwe, Y., Moore, T. L., and Rosene, D. L. (2015). Age-related changes in dentate gyrus cell numbers, neurogenesis, and associations with cognitive impairments in the rhesus monkey. *Front. Syst. Neurosci.* 9:102. doi: 10.3389/FNSYS.2015.00102

Niibori, Y., Yu, T. S., Epp, J. R., Akers, K. G., Josselyn, S. A., and Frankland, P. W. (2012). Suppression of adult neurogenesis impairs population coding of similar contexts in hippocampal CA3 region. *Nat. Commun.* 3, 1–7. doi: 10.1038/ncomms2261

O'Donnell, C., and Sejnowski, T. J. (2014). Selective memory generalization by spatial patterning of protein synthesis. *Neuron* 82, 398–412. doi: 10.1016/J.NEURON.2014.02.028

O'Leary, T. P., Askari, B., Lee, B., Darby, K., Knudson, C., Ash, A. M., et al. (2021). Inhibiting adult neurogenesis differentially affects spatial learning in females and males. *bioRxiv* [Preprint]. doi: 10.1101/2021.10.27.466135

Ohline, S. M., Wake, K. L., Hawkridge, M. V., Dinnunhan, M. F., Hegemann, R. U., Wilson, A., et al. (2018). Adult-born dentate granule cell excitability depends on the interaction of neuron age, ontogenetic age and experience. *Brain Struct. Funct.* 223, 3213–3228. doi: 10.1007/S00429-018-1685-2/FIGURES/6

Park, S., Kramer, E. E., Mercaldo, V., Rashid, A. J., Insel, N., Frankland, P. W., et al. (2016). Neuronal allocation to a hippocampal engram. *Neuropsychopharmacology* 41, 2987–2993. doi: 10.1038/npp.2016.73

Pilz, G. A., Bottes, S., Betizeau, M., Jörg, D. J., Carta, S., Simons, B. D., et al. (2018). Live imaging of neurogenesis in the adult mouse hippocampus. *Science* 359, 658–662.

Rapp, P. R., and Gallagher, M. (1996). Preserved neuron number in the hippocampus of aged rats with spatial learning deficits. *Proc. Natl. Acad. Sci. U.S.A.* 93, 9926–9930. doi: 10.1073/PNAS.93.18.9926

Restivo, L., Niibori, Y., Mercaldo, V., Josselyn, S. A., and Frankland, P. W. (2015). Development of adult-generated cell connectivity with excitatory and inhibitory cell populations in the hippocampus. *J. Neurosci.* 35, 10600–10612. doi: 10.1523/JNEUROSCI.3238-14.2015

Richards, B. A., and Frankland, P. W. (2017). The persistence and transience of memory. *Neuron* 94, 1071–1084. doi: 10.1016/J.NEURON.2017.04.037

Ruediger, S., Vittori, C., Bednarek, E., Genoud, C., Strata, P., Sacchetti, B., et al. (2011). Learning-related feedforward inhibitory connectivity growth required for memory precision. *Nature* 473, 514–518. doi: 10.1038/nature09946

Ryu, J. R., Hong, C. J., Kim, J. Y., Kim, E. K., Sun, W., and Yu, S. W. (2016). Control of adult neurogenesis by programmed cell death in the mammalian brain. *Mol. Brain* 9, 1–20. doi: 10.1186/S13041-016-0224-4

Sahay, A., Scobie, K. N., Hill, A. S., O'Carroll, C. M., Kheirbek, M. A., Burghardt, N. S., et al. (2011). Increasing adult hippocampal neurogenesis is sufficient to improve pattern separation. *Nature* 472, 466–470. doi: 10.1038/nature09817

Schmidt-Hieber, C., Jones, P., and Bischofberger, J. (2004). Enhanced synaptic plasticity in newly generated granule cells of the adult hippocampus. *Nature* 429, 184–187. doi: 10.1038/nature02553

Scott, G. A., Terstege, D. J., Roebuck, A. J., Gorzo, K. A., Vu, A. P., Howland, J. G., et al. (2021). Adult neurogenesis mediates forgetting of multiple types of memory in the rat. *Mol. Brain* 14, 1–13. doi: 10.1186/S13041-021-00808-4/FIGURES/4

Semon, R. (1921). *The mneme*. G. Allen & Unwin Limited. Available online at: https://books.google.com/books?hl=en&lr=&id=rFfuAgAAQBAJ&oi=fnd&pg=PA17&ots=4e3JbfekP2&sig=JteMg1F1IJQZNIsq8zU6xIhvXuc (accessed February 1, 2022).

Sippel, D., Schwabedal, J., Snyder, J. C., Oyanedel, C. N., Bernas, S. N., Garthe, A., et al. (2020). Disruption of NREM sleep and sleep-related spatial memory consolidation in mice lacking adult hippocampal neurogenesis. *Sci. Rep.* 10, 1–14. doi: 10.1038/s41598-020-72362-3

Snyder, J. S., Hong, N. S., McDonald, R. J., and Wojtowicz, J. M. (2005). A role for adult neurogenesis in spatial long-term memory. *Neuroscience* 130, 843–852. doi: 10.1016/J.NEUROSCIENCE.2004.10.009

Snyder, J. S., Soumier, A., Brewer, M., Pickel, J., and Cameron, H. A. (2011). Adult hippocampal neurogenesis buffers stress responses and depressive behaviour. *Nature* 476, 458–461. doi: 10.1038/nature10287

Sorrells, S. F., Paredes, M. F., Cebrian-Silla, A., Sandoval, K., Qi, D., Kelley, K. W., et al. (2018). Human hippocampal neurogenesis drops sharply in children to undetectable levels in adults. *Nature* 555, 377–381. doi: 10.1038/nature25975

Stone, S. S. D., Teixeira, C. M., Zaslavsky, K., Wheeler, A. L., Martinez-Canabal, A., Wang, A. H., et al. (2011). Functional convergence of developmentally and adult-generated granule cells in dentate gyrus circuits supporting hippocampus-dependent memory. *Hippocampus* 21, 1348–1362. doi: 10.1002/HIPO.20845

Suárez-Pereira, I., and Carrión, ÁM. (2015). Updating stored memory requires adult hippocampal neurogenesis. *Sci. Rep.* 5, 1–7. doi: 10.1038/srep13993

Suzuki, A., Josselyn, S. A., Frankland, P. W., Masushige, S., Silva, A. J., and Kida, S. (2004). Memory Reconsolidation and Extinction Have Distinct Temporal and Biochemical Signatures. *J. Neurosci.* 24, 4787–4795. doi: 10.1523/JNEUROSCI.5491-03.2004

Swan, A. A., Clutton, J. E., Chary, P. K., Cook, S. G., Liu, G. G., and Drew, M. R. (2014). Characterization of the role of adult neurogenesis in touch-screen discrimination learning. *Hippocampus* 24, 1581–1591. doi: 10.1002/HIPO.22337

Tashiro, A., Makino, H., and Gage, F. H. (2007). Experience-specific functional modification of the dentate gyrus through adult neurogenesis: A critical period during an immature stage. *J. Neurosci.* 27, 3252–3259. doi: 10.1523/JNEUROSCI.4941-06.2007

Tashiro, A., Sandler, V. M., Toni, N., Zhao, C., and Gage, F. H. (2006). NMDA-receptor-mediated, cell-specific integration of new neurons in adult dentate gyrus. *Nature* 442, 929–933. doi: 10.1038/nature05028

Temprana, S. G., Mongiat, L. A., Yang, S. M., Trinchero, M. F., Alvarez, D. D., Kropff, E., et al. (2015). Delayed coupling to feedback inhibition during a critical period for the integration of adult-born granule cells. *Neuron* 85, 116–130. doi: 10.1016/J.NEURON.2014.11.023

Toni, N., Laplagne, D. A., Zhao, C., Lombardi, G., Ribak, C. E., Gage, F. H., et al. (2008). Neurons born in the adult dentate gyrus form functional synapses with target cells. *Nat. Neurosci.* 11, 901–907. doi: 10.1038/nn.2156

Toni, N., Teng, E. M., Bushong, E. A., Aimone, J. B., Zhao, C., Consiglio, A., et al. (2007). Synapse formation on neurons born in the adult hippocampus. *Nat. Neurosci.* 10, 727–734. doi: 10.1038/NN1908

Tran, L. M., Santoro, A., Liu, L., Josselyn, S. A., Richards, B. A., and Frankland, P. W. (2022). Adult neurogenesis acts as a neural regularizer. *Proc. Natl. Acad. Sci. U.S.A.* 119, e2206704119.

Tronel, S., Fabre, A., Charrier, V., Oliet, S. H. R., Gage, F. H., and Abrous, D. N. (2010). Spatial learning sculpts the dendritic arbor of adult-born hippocampal neurons. *Proc. Natl. Acad. Sci. U.S.A.* 107, 7963–7968. doi: 10.1073/PNAS.0914613107

Trouche, S., Bontempi, B., Roullet, P., and Rampon, C. (2009). Recruitment of adult-generated neurons into functional hippocampal networks contributes to updating and strengthening of spatial memory. *Proc. Natl. Acad. Sci. U.S.A.* 106, 5919–5924. doi: 10.1073/PNAS.0811054106

van Praag, H., Christie, B. R., Sejnowski, T. J., and Gage, F. H. (1999). Running enhances neurogenesis, learning, and long-term potentiation in mice. *Proc. Natl. Acad. Sci. U.S.A.* 96, 13427–13431. doi: 10.1073/PNAS.96.23.13427

Walton, N. M., Shin, R., Tajinda, K., Heusner, C. L., Kogan, J. H., Miyake, S., et al. (2012). Adult neurogenesis transiently generates oxidative stress. *PLoS One* 7:e35264. doi: 10.1371/JOURNAL.PONE.0035264

Weisz, V. I., and Argibay, P. F. (2009). A putative role for neurogenesis in neuro-computational terms: Inferences from a hippocampal model. *Cognition* 112, 229–240. doi: 10.1016/J.COGNITION.2009.05.001

Wiskott, L., Rasch, M. J., and Kempermann, G. (2006). A functional hypothesis for adult hippocampal neurogenesis: Avoidance of catastrophic interference in the dentate gyrus. *Hippocampus* 16, 329–343. doi: 10.1002/HIPO.20167

Yasuda, M., Johnson-Venkatesh, E. M., Zhang, H., Parent, J. M., Sutton, M. A., and Umemori, H. (2011). Multiple forms of activity-dependent competition refine hippocampal circuits in vivo. *Neuron* 70, 1128–1142. doi: 10.1016/J.NEURON.2011.04.027

Zhao, C., Teng, E. M., Summers, R. G., Ming, G. L., and Gage, F. H. (2006). Distinct morphological stages of dentate granule neuron maturation in the adult mouse hippocampus. *J. Neurosci.* 26, 3–11. doi: 10.1523/JNEUROSCI.3648-05.2006

Zhou, Y., Su, Y., Li, S., Kennedy, B. C., Zhang, D. Y., Bond, A. M., et al. (2022). Molecular landscapes of human hippocampal immature neurons across lifespan. *Nature* 607, 527–533. doi: 10.1038/s41586-022-04912-w

frontiers | Frontiers in Neuroscience

TYPE Mini Review
PUBLISHED 02 March 2023
DOI 10.3389/fnins.2023.1150283

OPEN ACCESS

EDITED BY
Seiji Hitoshi,
Shiga University of Medical Science, Japan

REVIEWED BY
Tatsuhiro Hisatsune,
The University of Tokyo, Japan
Jenny Hsieh,
The University of Texas at San Antonio, United States

*CORRESPONDENCE
Kinichi Nakashima
✉ nakashima.kinichi.718@m.kyushu-u.ac.jp

SPECIALTY SECTION
This article was submitted to Neurodevelopment, a section of the journal Frontiers in Neuroscience

RECEIVED 24 January 2023
ACCEPTED 13 February 2023
PUBLISHED 02 March 2023

CITATION
Kasahara Y, Nakashima H and Nakashima K (2023) Seizure-induced hilar ectopic granule cells in the adult dentate gyrus. *Front. Neurosci.* 17:1150283. doi: 10.3389/fnins.2023.1150283

Seizure-induced hilar ectopic granule cells in the adult dentate gyrus

Yuka Kasahara, Hideyuki Nakashima and Kinichi Nakashima*

Department of Stem Cell Biology and Medicine, Graduate School of Medical Sciences, Kyushu University, Fukuoka, Japan

Epilepsy is a chronic neurological disorder characterized by hypersynchronous spontaneous recurrent seizures, and affects approximately 50 million people worldwide. Cumulative evidence has revealed that epileptogenic insult temporarily increases neurogenesis in the hippocampus; however, a fraction of the newly generated neurons are integrated abnormally into the existing neural circuits. The abnormal neurogenesis, including ectopic localization of newborn neurons in the hilus, formation of abnormal basal dendrites, and disorganization of the apical dendrites, rewires hippocampal neural networks and leads to the development of spontaneous seizures. The central roles of hilar ectopic granule cells in regulating hippocampal excitability have been suggested. In this review, we introduce recent findings about the migration of newborn granule cells to the dentate hilus after seizures and the roles of seizure-induced ectopic granule cells in the epileptic brain. In addition, we delineate possible intrinsic and extrinsic mechanisms underlying this abnormality. Finally, we suggest that the regulation of seizure-induced ectopic cells can be a promising target for epilepsy therapy and provide perspectives on future research directions.

KEYWORDS

epilepsy, neuroinflammation, adult neurogenesis, ectopic neurogenesis, E/I balance

Introduction

Epilepsy is a diverse group of neurological disorders characterized by excessive hypersynchronous discharge-induced seizures. The hippocampal dentate gyrus (DG) has been implicated in the development of epilepsy due to its unique circuitry (Jessberger and Parent, 2015; Danzer, 2019). The DG is the primary gating structure of the hippocampus, and its circuitry establishes an inhibitory feedback circuit comprised of interneuron microcircuits and regulates the flow of excitatory input from the cortex essential for spatial learning and memory (Sahay et al., 2011). Accumulated evidence has indicated that neural stem/progenitor cells (NS/PCs) are retained even in the adult subgranular zone of the DG (Eriksson et al., 1998; Boldrini et al., 2018; Terreros-Roncal et al., 2021; Zhou et al., 2022) and they proliferate and give rise to new neurons throughout life in a process referred to as adult neurogenesis (Gross, 2000; Gage, 2019). Adult-born granule cells (abGCs) are integrated into the existing mature brain networks and exhibit age-dependent effects on hippocampal network activity (Danielson et al., 2016; McHugh et al., 2022), contributing to brain plasticity and maintenance of proper brain functions. However, in the DG of temporal lobe epilepsy (TLE) animal models and patients, accelerated aberrant proliferation of NS/PCs, abnormal

abGC migration, formation of hilar basal dendrites and mossy fiber sprouting are observed, resulting in the aberrant integration of abGCs into the preexisting neural circuits (Jessberger and Parent, 2015; Danzer, 2019). This abnormal integration is thought to disrupt the dentate gate and increase the excitability of the hippocampus circuitry, leading to perpetuation of recurrent seizures (Parent et al., 1997; Overstreet Wadiche et al., 2005; Zhang et al., 2012; Zhou et al., 2019). Mapping analysis of large neuronal population dynamics has revealed that seizures are not simply recurrent bursts of hypersynchrony. Instead, it is becoming clear that seizures involve a complex interplay of different neural cell populations and circuits (Bui et al., 2015; Sparks et al., 2020). Based on computational modeling studies it is suggested that a network in which a small number of dentate GCs are hyperconnected to each other (hub network) is more effective at promoting seizure-like activity than a network wherein all dentate GCs are more interconnected than the control state (Morgan and Soltesz, 2008). Recent studies revealed that abGCs localized in the dentate hilus, hilar ectopic GCs, can play a role in the epileptic hub network (Scharfman and Pierce, 2012; Althaus et al., 2019; Lybrand et al., 2021). In this review, we discuss recent evidence demonstrating the characteristics and roles of hilar ectopic GCs in the epileptic brain and describe cell-intrinsic and extrinsic mechanisms underlying their mis-migration (**Figure 1**). Finally, we also offer some perspectives on future research directions.

Hilar ectopic granule cells

Prolonged seizure activity promotes NS/PC proliferation for several weeks after epileptogenic insult (Parent et al., 1997; Scott et al., 2000) and newborn GCs generated from these NS/PCs are integrated into neural networks heterogeneously (Murphy et al., 2011). Under healthy conditions, GCs exhibit a typical morphology: a round cell body located in the GC layer, fanlike dendritic trees extending to the molecular layer, and an absence of basal dendrites (Claiborne et al., 1990). By contrast, under epileptic conditions, a substantial fraction of newborn GCs migrate ectopically into the dentate hilus and the molecular layer and develop aberrant properties such as acquisition of hilar basal dendrites, mossy fiber sprouting, and increased dendritic arborization (Parent et al., 1997; Jessberger et al., 2007; **Figure 1**). A subpopulation of newborn GCs forms abnormal connections with neighboring GCs *via* sprouted mossy fibers or aberrant basal dendrites (Murphy et al., 2011; Du et al., 2017). Because abGCs exert a hippocampal network-level modulatory role throughout their maturation (McHugh et al., 2022), alterations in the network structure of abGCs may explain the effects on hippocampal excitability in the epileptic brain.

Hilar ectopic GCs are a pathological hallmark commonly observed in animal models and patients with TLE (Parent et al., 2006; Pierce et al., 2011). The abGCs are particularly vulnerable to epileptogenic insults. To determine the precise developmental stages at which GCs migrate ectopically, Kron et al. (2010) conducted cell birthdate studies in an experimental epilepsy model. They injected retroviral reporters to label dividing progenitor cells and suppressed neurogenesis by x-irradiation at specific times 2–4 weeks before or 4 days after pilocarpine-induced status epilepticus (SE) leading to the development of epilepsy. Only cells born post-SE were significantly more likely to migrate into the hilus (around 20% of labeled cells) and a fraction of the newborn GCs displayed hilar basal dendrites and mossy fiber sprouting (around 30% of labeled cells). Moreover, the study of Singh et al. (2015) clarified whether ectopic GCs arose ubiquitously throughout the NS/PC pool or were derived from a more restricted NS/PC subpopulation. They performed a clonal analysis study in mice expressing Brainbow fluorochromes in individual glioma-associated oncogene homolog1-expressing type 1 progenitor cells and identified a specific fraction of progenitors that produce the majority of ectopic GCs in response to an epileptogenic insult (Singh et al., 2015). Progenitor cells producing hilar ectopic GCs appear to generate only ectopic cells, whereas those producing the cells in the appropriate position in the dentate continued to do so. In epileptic conditions, the affected progenitors or their local microenvironments may become pathological, driving hilar ectopic cell migration. Alternatively, the affected progenitor cells may be functionally normal but misled to areas where migratory cues have been distorted, driving the generation of ectopic cells.

Open questions in the field include whether and how hilar ectopic cells contribute to network hyperexcitability leading to the development of epilepsy. To address this question, several groups have scrutinized features of the ectopic cells including the potential for burst firing and altered excitation/inhibition (E/I) ratios (Scharfman et al., 2000; Zhan and Nadler, 2009; Zhan et al., 2010; Althaus et al., 2015). Recently, Althaus et al. (2019) investigated the relationship between GCs' birthdate, morphology, and network integration in a pilocarpine TLE model. By recording spontaneous excitatory and inhibitory currents, they found that both early-born (P7) and adult-born (P60) populations of GCs received increased-excitatory input after the seizure, compared with age-matched sham controls. When abGCs were divided into normally integrated (normotopic) and aberrant (ectopic or hilar basal dendrites-containing) subpopulations, only the aberrant populations showed a relative increase in excitatory input. The ratio of excitatory-to-inhibitory input was most dramatically upregulated in hilar ectopic GCs, which implicates the ectopic GCs as drivers for network hyperexcitability in epileptic conditions. The authors hypothesized that these aberrantly integrated cells act as "hub cells" for initiating or propagating seizure activity. The diversity among the abGCs population highlights a key problem of experiments aiming to manipulate specific newborn GC subtypes in epilepsy. A study using an inducible transgenic alteration of mammalian target of rapamycin (mTOR) signaling to disrupt the normal development of a fraction of early-born GCs revealed that the generation of abnormal GCs including ectopic GCs is enough to induce spontaneous seizures (Pun et al., 2012). In support of this, pharmacogenetic suppression of the post-seizure aberrant neurogenesis including the generation of the ectopic GCs reduced the later development of spontaneous seizures (Cho et al., 2015; Hosford et al., 2016). Furthermore, chemogenetic silencing of abGCs reduced the number of ectopic GCs and seizure occurrence (Lybrand et al., 2021). However, it should be noted that reducing neurogenesis has not always been found to mitigate epilepsy development. Although Zhu et al. (2017) decreased abnormal integrations of abGCs into the neural circuit *via* the ablation of cells with methylazoxymethanol acetate, they found no effect on the development of spontaneous seizures in a pilocarpine model. Brulet et al. (2017) used a genetic approach to

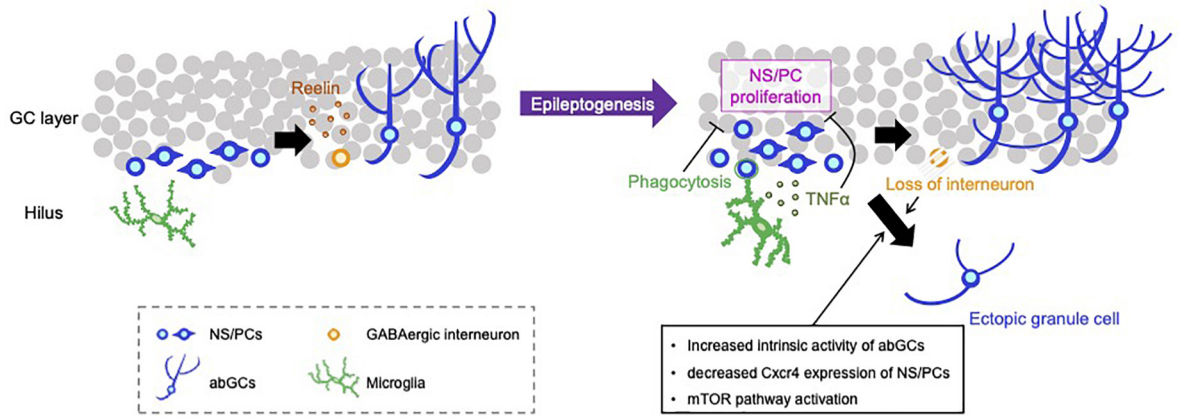

FIGURE 1
Representative negative and positive regulations for aberrant neurogenesis in the hippocampus. NS/PCs in the hippocampal subgranular zone proliferate and differentiate into GCs. Reelin released from GABAergic interneurons supports the integration processes of abGCs in the healthy brain **(left)**. SE induces an increase in the number of proliferating NS/PCs and subsequent depletion of NS/PCs, appearance of hilar ectopic GCs, mossy fiber sprouting, increased dendritic sprouting and loss of inhibitory interneurons **(right)**. Activated microglia phagocytose live newborn neurons and suppress the emergence of ectopic GCs. Microglia also attenuate the proliferation of NS/PCs by TLR9-mediated secretion of TNF-α, resulting in the reduction of aberrant neurogenesis. Loss of GABAergic neurons and intracellular alteration of abGCs properties, e.g., increased intrinsic neuronal activity, downregulation of Cxcr4 expression and activation of the mTOR pathway, can promote the mis-migration of abGCs to the hilus.

reduce neurogenesis by deleting the transcription factor *NeuroD1* gene in NS/PCs prior to SE. This conditional *NeuroD1* deletion indeed reduced abnormal integrations; however, seizure frequency did not change after pilocarpine administration (Brulet et al., 2017). These inconsistent results could be attributed to side effects of the drug, potential toxic effects of systemic antimitotic drugs, and/or insufficient reductions of ectopic GCs. The efficacy of manipulation of neurogenesis on seizure development may also depend on the time-point and targeted cell populations. It is conceivable that approaches targeting only abnormal cells would be more effective and broadly applicable, and would enable us to elucidate the role of hilar ectopic cells in the development of epilepsy. In the next section, we describe intrinsic and extrinsic mechanisms that help us to develop strategies to specifically manipulate hilar ectopic cells.

Cell-intrinsic mechanisms regulating the emergence of hilar ectopic granule cells

Accumulating evidence suggests that neuronal activity regulates adult neurogenesis (Kempermann et al., 2015; Denoth-Lippuner and Jessberger, 2021) and improper migration of abGCs has been linked to increased intrinsic neuronal activity (Sim et al., 2013). Recently, Lybrand et al. (2021) investigated whether activity during the maturation of immature abGCs plays a critical role to drive aberrant alterations of cellular behavior including ectopic migration. To manipulate the intrinsic activity of abGCs at different stages of maturation, proliferating NS/PCs were first infected with an excitatory designer receptor (hM3Dq)-expressing retrovirus and the synthetic ligand clozapine-N-oxide (CNO) was injected once daily to activate abGCs for the first (0–1 w) or second (1–2 w) week after retroviral infection. Activation during both the first and second periods of maturation promoted abnormal migration of abGCs into the hilus without dendrite developmental change. When the labeled 8 w-old mature GCs were activated with CNO, no effects on migration or cell morphology were observed. These results suggest that a critical time window during which neuronal activity is associated with aberrant maturation exists and activity during this period seems sufficient to promote the migration of abGCs to the hilus. Zero–1w and 1–2w activation provoked spontaneous recurrent seizures at 8 weeks post-infection in 60 and 80% of hM3Dq-virus injected mice, respectively. In the pilocarpine model, chemogenetically silencing immature aberrant abGCs through an inhibitory designer receptor (hM4Di) during this critical period reduced ectopic cells, abnormal dendritic morphology, and the occurrence of spontaneous seizures. They also found that 2w-old abGCs exhibited dynamic calcium fluctuations, and stimulation of both designer receptors (hM3Dq and hM4Di) could modulate the intracellular calcium of immature abGCs. These observations imply that cellular intrinsic activity *via* calcium response regulates the migration of newborn cells appropriately, but it is unclear how sustained elevation of intrinsic calcium levels affects abGCs' development and maturation. In mouse cerebellar granule cells, the amplitude and frequency of calcium transients, *via* voltage-gated calcium channels (VGCCs), are correlated positively with the rate of neuronal migration, suggesting that calcium acts as a speedometer to integrate various intrinsic/extrinsic cues that drive neuronal migration (Komuro and Rakic, 1996). Although the role of VGCCs in immature abGCs is poorly defined, it has been reported that VGCCs generate low-threshold somatic calcium spikes in immature abGCs before 3 weeks of age, which are trophic cues that promote neuronal development (Konur and Ghosh, 2005). In addition, enhanced VGCCs currents with altered properties occur in the dentate GCs of epileptic patients (Jeub et al., 1999; Djamshidian et al., 2002). These results suggest that increased VGCCs currents in immature abGCs promote improper cellular integration into existing dentate GCs circuits, causing the development of epilepsy

(**Figure 1**). Downstream regulators of calcium signaling in aberrant neurogenesis could also be potential targets for anti-epileptic drugs.

We have previously shown that prenatal exposure to valproic acid (VPA), which is known to function as an antiepileptic drug by inhibiting, e.g., gamma-aminobutyric acid (GABA) transaminase, leads to the reduction of adult neurogenesis and increase of the malpositioned GCs in the dentate hilus (Sakai et al., 2018). These effects were paired with an increase in the susceptibility to kainic acid (KA) -induced seizures in adulthood. To identify the mechanism underlying the accumulation of ectopic GCs, we performed RNA sequencing analysis and found that CXC motif chemokine receptor 4 (Cxcr4) expressed in the prenatally VPA-exposed NS/PCs was downregulated in the adult. Overexpression of *Cxcr4* selectively in NS/PCs using a retroviral strategy attenuated the ectopic migration of abGCs and seizure susceptibility. Although it has been reported that *Cxcr4* deletion consistently reduces adult neurogenesis and leads to the appearance of ectopic GCs (Schultheiß et al., 2013), how and why Cxcr4 expression has such an effect is not fully understood. One possible explanation is that *Cxcr4* overexpression restores the migratory cues needed for immature GCs to correctly integrate into the GC layer, reducing ectopic migration. VPA increases GABA levels in the brain and GABA can bind to and activate Cxcr4 (Guyon et al., 2013). Indeed, it was suggested that Cxcr4 ligand Cxcl12 is probably co-secreted with GABA from hippocampal interneurons, and thus they both may possibly affect NS/PC behavior (Bhattacharyya et al., 2008). By disrupting GABA and/or Cxcl12 signaling in the neurogenic niche, VPA may interfere with the Cxcr4-regulated migration of immature GCs. Another possibility is that VPA induces changes in the expression of many genes as an epigenetic drug because it has histone deacetylase inhibitor activity (Hsieh et al., 2004; Xu et al., 2007) that positively regulates gene expression by promoting histone acetylation. Understanding the contribution of epigenetic-mediated gene regulation may reveal new regulatory mechanisms of cell migration.

The mTOR pathway, which regulates neuronal migration, growth, and plasticity, is activated in several models of epilepsy (Zeng et al., 2009; Huang et al., 2010). Phosphatase and tensin homolog (PTEN) is a lipid phosphatase that targets the 3′ phosphate of phosphatidylinositol 3,4,5 triphosphate, acting in opposition to phosphatidylinositol 3-kinase (PI3K). mTOR is a major target in the PI3K pathway and deletion of PTEN leads to excess activation of mTOR (Kwon et al., 2003). Deletion of PTEN in postnatally produced GCs led to an increase in ectopically located cells, causing spontaneous seizures (Pun et al., 2012). PTEN-deficient GCs also recapitulate numerous other morphological pathologies associated with TLE, including mossy fiber sprouting, hypertrophy, the appearance of basal dendrites, and increased dendritic spine density (Kwon et al., 2001; Pun et al., 2012). After KA administration, treating animals with the mTOR antagonist rapamycin mitigates GC aberrant migration and mossy fiber sprouting, which directly links the mTOR pathway to these phenomena (Shima et al., 2015). mTOR signaling is involved in the regulation of GC dispersion and migration deeper into the GC layer closer to the molecular layer boundary (Getz et al., 2016). It is worthwhile noting that the mechanisms regulating the appearance of abnormal cells in two discrete locations, the hilus and the molecular layer, can be distinct.

Cell-extrinsic mechanisms regulating the emergence of hilar ectopic granule cells

Reelin, an extracellular matrix glycoprotein, plays an essential role in neuronal migration and the formation of laminated brain structures, such as the neocortex, hippocampus, and cerebellum (Chai and Frotscher, 2016). After cortical development and the demise of most Cajal-Retzius cells, Reelin is expressed primarily by interneurons in the adult brain (Lee and D'Arcangelo, 2016). Immunohistochemical studies revealed that the cell bodies of Reelin-expressing interneurons were located within the subgranular adult stem cell niche. These Reelin-expressing cells were identified as cholecystokinin-positive but not parvalbumin-positive cells (Pahle et al., 2020). Disorganized GC layer formation has been shown to be accompanied by a loss of Reelin-producing neurons in the epileptic hippocampus (Haas et al., 2002; Heinrich et al., 2006; Orcinha et al., 2016). In the DG of Reelin-deficient *reeler* mice, the GCs are scattered, suggesting a GC migration defect (Katsuyama and Terashima, 2009). Antibody-blockade of Reelin function in naive mice causes dispersion of GCs, and exogenous administration of Reelin after epileptogenic injury prevents the dispersion (Haas and Frotscher, 2010). Consistently, conditional knockout of the disabled-1 gene (*Dab1*), encoding an adaptor protein that is essential for Reelin signaling, in adult or postnatal NS/PCs results in abnormal migration, such that new granule neurons are scattered throughout the DG area (Teixeira et al., 2012; Korn et al., 2016). Both *reeler*- and *Dab1*-deficient mice lack spontaneous seizures but exhibit enhanced seizure susceptibility (Patrylo et al., 2006; Korn et al., 2016). In contrast, interneuron-specific Reelin knockout did not cause structural changes in the DG (Pahle et al., 2020). In this mouse, the number of Reelin-expressing Cajal-Retzius cells, which can function compensatorily for the loss of Reelin-expressing interneurons, increased, eventually resulting in the formation of an organized GC layer. However, it has become apparent that Reelin's functions are not simple. Using hippocampal slice culture and live imaging, Wang et al. (2018) revealed that Reelin acts as an attractant dictating the migration of GCs toward the molecular layer. In addition, Reelin has also been suggested to function as a local repulsing cue to ensconce mature GCs in the normotopic position, suppressing GC's aberrant migration under epileptic conditions (Orcinha et al., 2021).

Gamma-aminobutyric acid can directly control neurogenesis, and disruption of GABA homeostasis triggers abnormal neurogenesis (Tozuka et al., 2005; Nakamichi et al., 2009). In the DG, the primary sources of GABA are inhibitory interneurons, i.e., parvalbumin- and somatostatin-neurons. Immature dentate GCs express high levels of sodium, potassium, chloride cotransporter 1 (NKCC1), a cation-Cl^- importer, which changes the reversal potential for Cl^-, causing $GABA_A$ receptor activation to depolarize the cell (Ge et al., 2006). Immature abGCs initially receive the depolarizing GABA signal, which is necessary for their proper development (Overstreet Wadiche et al., 2005). A recent study showed that GABA-mediated amplification of intracellular calcium regulates the early critical period of activity associated with the aberrant maturation of abGCs (Lybrand et al., 2021). Treatment with the $GABA_A$ receptor agonist phenobarbital increases hilar ectopic GCs in normal rat pups and conversely, treatment with

the $GABA_A$ receptor antagonist picrotoxin decreased it in a postnatal febrile seizure (which is thought to be a triggering insult for TLE) model (Koyama et al., 2012; Kasahara et al., 2019). Following epileptogenic insults, GABAergic interneurons are overstimulated and presumably die *via* excitotoxicity, and surviving interneurons may compensate for this loss and become hyperexcitable abnormally (Kobayashi and Buckmaster, 2003; Wang et al., 2016). In hilar ectopic GCs, $GABA_A$ receptor signaling mediates tonic GABA currents that occur after SE (Zhan and Nadler, 2009). Increased depolarizing effect of GABA on immature abGCs would impose a hyperexcitable signal on mature dentate GCs and enhance hippocampal excitability. To enhance GABA's hyperpolarizing effect on mature neurons and attenuate hippocampal hyperexcitability, medial ganglionic eminence-derived GABAergic neuronal progenitor cells were grafted into the hippocampus and its antiepileptic effect was demonstrated (Hunt et al., 2013; Cunningham et al., 2014; Upadhya et al., 2019). Recently, Arshad et al. (2022) reported that following transplantation of GABAergic neuronal progenitors, ectopic immature abGCs decreased in epileptic model mice, while normotopic immature abGCs increased in not only the epileptic model but also in intact mice. These effects on migration/localization of abGCs could be due to Reelin released from the transplanted interneurons. Alternatively, modifying the E/I balance in the hippocampus may affect abGCs integration.

It has become clear from considerable evidence that glial cells modulate adult neurogenesis in the hippocampus (Cope and Gould, 2019). Microglia have been shown to regulate each step of adult neurogenesis, such as proliferation, survival, and maturation of newly generated cells both in the non-epileptic and epileptic brains (Luo et al., 2016a). We have previously shown that microglia suppress aberrant neurogenesis by inhibiting the hyper-proliferation of NS/PCs after KA-induced seizures through the activation of Toll-like receptor 9 (TLR9) in microglia (Matsuda et al., 2015). In the epileptic condition, microglia sense self-DNA, which is presumably released from degenerating neurons, *via* TLR9 and then secrete TNF-α, and TNF-α in turn attenuates hyper-proliferation of NS/PCs. After KA injection, GCs localized in the hilus increased in TLR9-deficient mice, and infusion of recombinant TNF-α into the ventricle reduced the hilar ectopic GCs. Furthermore, TLR9 deficiency exacerbated seizure-induced cognitive decline and recurrent seizure severity. These findings indicate that activated microglia reduce abnormally located newborn neurons through the secretion of TNF-α, resulting in antiepileptic effects. Microglia can also directly regulate the emergence of ectopic GCs by phagocytosis. In the healthy brain, microglia mainly engulf apoptotic abGCs, but after SE, activated microglia switch their target and prefer to engulf caspase-negative live abGCs (Luo et al., 2016b). Luo et al. (2016b) reported that the administration of minocycline, an inhibitor of microglial activation, reduced the number of engulfed newborn GCs, increasing the number of ectopic GCs. These results suggest that microglia suppress the appearance of excess newborn cells and eliminate abGCs after SE to inhibit the formation of abnormal neural circuits leading to the development of epilepsy. In contrast to these results, some studies reported that genetic ablation of microglia or suppression of microglial activation with minocycline reduced immature neurons, suggesting that microglia accelerate seizure-induced neurogenesis (Ali et al., 2015; Mo et al., 2019). Yang et al. (2010) demonstrated that after pilocarpine-induced SE, suppression of microglial activation with minocycline reduced the number of ectopic GCs. These discrepancies regarding the role of microglia in neurogenesis after SE may be attributable to differences in experimental settings to mimic epilepsy-like phenotypes. Indeed, microglia show different gene expressions depending on the types of chemoconvulsants, i.e., KA, and pilocarpine (Benson et al., 2015). In addition, "activated" microglia exhibit heterogeneity in their properties, which makes it difficult to corroborate the precise roles of microglia in adult neurogenesis.

Astrocytes also play roles in the proliferation and neuronal fate commitment of NS/PCs in the adult hippocampus (Song et al., 2002), and regulation of synapse integration into existing neural circuits through astrocytic vesicular release (Sultan et al., 2015). These findings suggest that astrocytes are important regulators of adult neurogenesis at all stages of the process. In the DG of the epileptic patient, astrocytes are activated and the length of astrocytic fibers around the GC layer significantly increases (Fahrner et al., 2007; Thom, 2014). However, whether and how astrocytes regulate aberrant adult neurogenesis in the epileptic brain remains largely unknown. Further studies are necessary to clarify the contribution of astrocytes to the aberrant neurogenesis characteristic of the epileptic brain.

Conclusion

Here, we review findings about seizure-induced ectopic GCs in animal models and humans with epilepsy. It is becoming clear that ectopic localization of abGCs in the dentate hilus radically alters the types of afferent inputs and efferent outputs, and that these ectopic cells exhibit hyperexcitable features. A key question that remained to be answered is whether ectopic GCs are the major player which rewires neural networks, accounting for hippocampal hyperexcitability, the characteristic of the epileptic brain. Several studies using distinct techniques have commonly demonstrated that targeted ablation of abGCs including hilar ectopic GCs can significantly reduce seizures, suggesting that abGC-specific manipulations could be beneficial for epilepsy treatment. However, there exist reports suggesting that abGCs ablation exacerbates epilepsy development, warranting further investigation to clearly elucidate the functional implications of hilar ectopic GCs acting as hub-like cells in the epileptic DG networks. Given the heterogeneous properties of abGCs after SE, populations of normotopically and ectopically integrated abGCs are likely to have opposing effects on neuronal excitability. Although current techniques for ablating or silencing abGCs affect all abGCs regardless of their subtypes, characterization and identification of the subtypes will enable us to target the specific hilar GC subtype for the therapeutic treatment of epilepsy. Elucidating the cellular and molecular mechanisms underlying seizure-induced ectopic abGCs would shed light on our understanding of brain plasticity attributable to adult neurogenesis. Taking all of these considerations together, we believe that seizure-induced hilar ectopic GCs represent a promising target for intervention in the treatment of human epilepsy and its comorbidities.

Author contributions

YK, HN, and KN: conceptualization and writing—review and editing. YK and HN: writing—original draft. All authors contributed to the article and approved the submitted version.

Funding

This research was supported by AMED under Grant Number: JP20gm1310008 to KN, Grants-in-Aid for Early-Career Scientists (no. 21K15272 to YK and no. 22K15201 to HN) from JSPS and by a Sasakawa Scientific Research Grant from the Japan Science Society to YK.

Conflict of interest

The authors declare that the research was conducted in the absence of any commercial or financial relationships that could be construed as a potential conflict of interest.

Publisher's note

All claims expressed in this article are solely those of the authors and do not necessarily represent those of their affiliated organizations, or those of the publisher, the editors and the reviewers. Any product that may be evaluated in this article, or claim that may be made by its manufacturer, is not guaranteed or endorsed by the publisher.

References

Ali, I., Chugh, D., and Ekdahl, C. T. (2015). Role of fractalkine-CX3CR1 pathway in seizure-induced microglial activation, neurodegeneration, and neuroblast production in the adult rat brain. *Neurobiol. Dis.* 74, 194–203. doi: 10.1016/j.nbd.2014.11.009

Althaus, A. L., Moore, S. J., Zhang, H., Du, X., Murphy, G. G., and Parent, J. M. (2019). Altered synaptic drive onto birthdated dentate granule cells in experimental temporal lobe epilepsy. *J. Neurosci.* 39, 7604–7614. doi: 10.1523/JNEUROSCI.0654-18.2019

Althaus, A. L., Sagher, O., Parent, J. M., and Murphy, G. G. (2015). Intrinsic neurophysiological properties of hilar ectopic and normotopic dentate granule cells in human temporal lobe epilepsy and a rat model. *J. Neurophysiol.* 113, 1184–1194. doi: 10.1152/jn.00835.2014

Arshad, M. N., Oppenheimer, S., Jeong, J., Buyukdemirtas, B., and Naegele, J. R. (2022). Hippocampal transplants of fetal GABAergic progenitors regulate adult neurogenesis in mice with temporal lobe epilepsy. *Neurobiol. Dis.* 174:105879. doi: 10.1016/j.nbd.2022.105879

Benson, M. J., Manzanero, S., and Borges, K. (2015). Complex alterations in microglial M1/M2 markers during the development of epilepsy in two mouse models. *Epilepsia* 56, 895–905. doi: 10.1111/epi.12960

Bhattacharyya, B. J., Banisadr, G., Jung, H., Ren, D., Cronshaw, D. G., Zou, Y., et al. (2008). The chemokine stromal cell-derived factor-1 regulates GABAergic inputs to neural progenitors in the postnatal dentate gyrus. *J. Neurosci.* 28, 6720–6730. doi: 10.1523/JNEUROSCI.1677-08.2008

Boldrini, M., Fulmore, C. A., Tartt, A. N., Simeon, L. R., Pavlova, I., Poposka, V., et al. (2018). Human hippocampal neurogenesis persists throughout aging. *Cell Stem Cell.* 22, 589–599.e5.

Brulet, R., Zhu, J., Aktar, M., Hsieh, J., and Cho, K. O. (2017). Mice with conditional NeuroD1 knockout display reduced aberrant hippocampal neurogenesis but no change in epileptic seizures. *Exp. Neurol.* 293, 190–198. doi: 10.1016/j.expneurol.2017.04.005

Bui, A., Kim, H. K., Maroso, M., and Soltesz, I. (2015). Microcircuits in epilepsy: heterogeneity and hub cells in network synchronization. *Cold Spring Harb. Perspect. Med.* 5:a022855. doi: 10.1101/cshperspect.a022855

Chai, X., and Frotscher, M. (2016). How does Reelin signaling regulate the neuronal cytoskeleton during migration? *Neurogenesis* 3:e1242455.

Cho, K. O., Lybrand, Z. R., Ito, N., Brulet, R., Tafacory, F., Zhang, L., et al. (2015). Aberrant hippocampal neurogenesis contributes to epilepsy and associated cognitive decline. *Nat. Commun.* 6:6606.

Claiborne, B. J., Amaral, D. G., and Cowan, W. M. (1990). Quantitative, three-dimensional analysis of granule cell dendrites in the rat dentate gyrus. *J. Comp. Neurol.* 302, 206–219.

Cope, E. C., and Gould, E. (2019). Adult neurogenesis, glia, and the extracellular matrix. *Cell. Stem Cell* 24, 690–705.

Cunningham, M., Cho, J. H., Leung, A., Savvidis, G., Ahn, S., Moon, M., et al. (2014). hPSC-derived maturing GABAergic interneurons ameliorate seizures and abnormal behavior in epileptic mice. *Cell. Stem Cell* 15, 559–573. doi: 10.1016/j.stem.2014.10.006

Danielson, N. B., Kaifosh, P., Zaremba, J. D., Lovett-Barron, M., Tsai, J., Denny, C. A., et al. (2016). Distinct contribution of adult-born hippocampal granule cells to context encoding. *Neuron* 90, 101–112.

Danzer, S. C. (2019). Adult neurogenesis in the development of epilepsy. *Epilepsy Curr.* 19, 316–320.

Denoth-Lippuner, A., and Jessberger, S. (2021). Formation and integration of new neurons in the adult hippocampus. *Nat. Rev. Neurosci.* 22, 223–236.

Djamshidian, A., Grassl, R., Seltenhammer, M., Czech, T., Baumgartner, C., Schmidbauer, M., et al. (2002). Altered expression of voltage-dependent calcium channel alpha(1) subunits in temporal lobe epilepsy with Ammon's horn sclerosis. *Neuroscience* 111, 57–69. doi: 10.1016/s0306-4522(01)00528-0

Du, X., Zhang, H., and Parent, J. M. (2017). Rabies tracing of birthdated dentate granule cells in rat temporal lobe epilepsy. *Ann. Neurol.* 81, 790–803. doi: 10.1002/ana.24946

Eriksson, P. S., Perfilieva, E., Björk-Eriksson, T., Alborn, A. M., Nordborg, C., Peterson, D. A., et al. (1998). Neurogenesis in the adult human hippocampus. *Nat. Med.* 4, 1313–1317.

Fahrner, A., Kann, G., Flubacher, A., Heinrich, C., Freiman, T. M., Zentner, J., et al. (2007). Granule cell dispersion is not accompanied by enhanced neurogenesis in temporal lobe epilepsy patients. *Exp. Neurol.* 203, 320–332.

Gage, F. H. (2019). Adult neurogenesis in mammals. *Science* 364, 827–828. doi: 10.1126/science.aav6885

Ge, S., Goh, E. L., Sailor, K. A., Kitabatake, Y., Ming, G. L., and Song, H. (2006). GABA regulates synaptic integration of newly generated neurons in the adult brain. *Nature* 439, 589–593. doi: 10.1038/nature04404

Getz, S. A., Despenza, T. Jr., Li, M., and Luikart, B. W. (2016). Rapamycin prevents, but does not reverse, aberrant migration in Pten knockout neurons. *Neurobiol. Dis.* 93, 12–20. doi: 10.1016/j.nbd.2016.03.010

Gross, C. G. (2000). Neurogenesis in the adult brain: death of a dogma. *Nat. Rev. Neurosci.* 1, 67–73. doi: 10.1038/35036235

Guyon, A., Kussrow, A., Olmsted, I. R., Sandoz, G., Bornhop, D. J., and Nahon, J. L. (2013). Baclofen and other GABAB receptor agents are allosteric modulators of the CXCL12 chemokine receptor CXCR4. *J. Neurosci.* 33, 11643–11654. doi: 10.1523/JNEUROSCI.6070-11.2013

Haas, C. A., and Frotscher, M. (2010). Reelin deficiency causes granule cell dispersion in epilepsy. *Exp. Brain Res.* 200, 141–149. doi: 10.1007/s00221-009-1948-5

Haas, C. A., Dudeck, O., Kirsch, M., Huszka, C., Kann, G., Pollak, S., et al. (2002). Role for reelin in the development of granule cell dispersion in temporal lobe epilepsy. *J. Neurosci.* 22, 5797–5802. doi: 10.1523/JNEUROSCI.22-14-05797.2002

Heinrich, C., Nitta, N., Flubacher, A., Müller, M., Fahrner, A., Kirsch, M., et al. (2006). Reelin deficiency and displacement of mature neurons, but not neurogenesis, underlie the formation of granule cell dispersion in the epileptic hippocampus. *J. Neurosci.* 26, 4701–4713. doi: 10.1523/JNEUROSCI.5516-05.2006

Hosford, B. E., Liska, J. P., and Danzer, S. C. (2016). Ablation of newly generated hippocampal granule cells has disease-modifying effects in epilepsy. *J. Neurosci.* 36, 11013–11023.

Hsieh, J., Nakashima, K., Kuwabara, T., Mejia, E., and Gage, F. H. (2004). Histone deacetylase inhibition-mediated neuronal differentiation of multipotent adult neural progenitor cells. *Proc. Natl. Acad. Sci. U.S.A.* 101, 16659–16664. doi: 10.1073/pnas.0407643101

Huang, X., Zhang, H., Yang, J., Wu, J., Mcmahon, J., Lin, Y., et al. (2010). Pharmacological inhibition of the mammalian target of rapamycin pathway suppresses acquired epilepsy. *Neurobiol. Dis.* 40, 193–199.

Hunt, R. F., Girskis, K. M., Rubenstein, J. L., Alvarez-Buylla, A., and Baraban, S. C. (2013). GABA progenitors grafted into the adult epileptic brain control seizures and abnormal behavior. *Nat. Neurosci.* 16, 692–697. doi: 10.1038/nn.3392

Jessberger, S., and Parent, J. M. (2015). Epilepsy and adult neurogenesis. *Cold Spring Harb. Perspect. Biol.* 7:a020677.

Jessberger, S., Zhao, C., Toni, N., Clemenson, G. D. Jr., Li, Y., and Gage, F. H. (2007). Seizure-associated, aberrant neurogenesis in adult rats characterized with retrovirus-mediated cell labeling. *J. Neurosci.* 27, 9400–9407. doi: 10.1523/JNEUROSCI.2002-07.2007

Jeub, M., Lie, A., Blümcke, I., Elger, C. E., and Beck, H. (1999). Loss of dynorphin-mediated inhibition of voltage-dependent Ca2+ currents in hippocampal granule cells isolated from epilepsy patients is associated with mossy fiber sprouting. *Neuroscience* 94, 465–471. doi: 10.1016/s0306-4522(99)00249-3

Kasahara, Y., Igata, H., Sasaki, T., Ikegaya, Y., and Koyama, R. (2019). The pharmacological assessment of GABA(A) receptor activation in experimental febrile seizures in mice. *eNeuro* 6:ENEURO.429–ENEURO.418. doi: 10.1523/ENEURO.0429-18.2019

Katsuyama, Y., and Terashima, T. (2009). Developmental anatomy of reeler mutant mouse. *Dev. Growth Differ.* 51, 271–286.

Kempermann, G., Song, H., and Gage, F. H. (2015). Neurogenesis in the adult hippocampus. *Cold Spring Harb. Perspect. Biol.* 7:a018812.

Kobayashi, M., and Buckmaster, P. S. (2003). Reduced inhibition of dentate granule cells in a model of temporal lobe epilepsy. *J. Neurosci.* 23, 2440–2452.

Komuro, H., and Rakic, P. (1996). Intracellular Ca2+ fluctuations modulate the rate of neuronal migration. *Neuron* 17, 275–285. doi: 10.1016/s0896-6273(00)80159-2

Konur, S., and Ghosh, A. (2005). Calcium signaling and the control of dendritic development. *Neuron* 46, 401–405.

Korn, M. J., Mandle, Q. J., and Parent, J. M. (2016). Conditional disabled-1 deletion in mice alters hippocampal neurogenesis and reduces seizure threshold. *Front. Neurosci.* 10:63. doi: 10.3389/fnins.2016.00063

Koyama, R., Tao, K., Sasaki, T., Ichikawa, J., Miyamoto, D., Muramatsu, R., et al. (2012). GABAergic excitation after febrile seizures induces ectopic granule cells and adult epilepsy. *Nat. Med.* 18, 1271–1278. doi: 10.1038/nm.2850

Kron, M. M., Zhang, H., and Parent, J. M. (2010). The developmental stage of dentate granule cells dictates their contribution to seizure-induced plasticity. *J. Neurosci.* 30, 2051–2059. doi: 10.1523/JNEUROSCI.5655-09.2010

Kwon, C. H., Zhu, X., Zhang, J., and Baker, S. J. (2003). mTor is required for hypertrophy of Pten-deficient neuronal soma in vivo. *Proc. Natl. Acad. Sci. U.S.A.* 100, 12923–12928.

Kwon, C. H., Zhu, X., Zhang, J., Knoop, L. L., Tharp, R., Smeyne, R. J., et al. (2001). Pten regulates neuronal soma size: a mouse model of Lhermitte-Duclos disease. *Nat. Genet.* 29, 404–411. doi: 10.1038/ng781

Lee, G. H., and D'Arcangelo, G. (2016). New insights into reelin-mediated signaling pathways. *Front. Cell Neurosci.* 10:122. doi: 10.3389/fncel.2016.00122

Luo, C., Ikegaya, Y., and Koyama, R. (2016a). Microglia and neurogenesis in the epileptic dentate gyrus. *Neurogenesis* 3:e1235525.

Luo, C., Koyama, R., and Ikegaya, Y. (2016b). Microglia engulf viable newborn cells in the epileptic dentate gyrus. *Glia* 64, 1508–1517. doi: 10.1002/glia.23018

Lybrand, Z. R., Goswami, S., Zhu, J., Jarzabek, V., Merlock, N., Aktar, M., et al. (2021). A critical period of neuronal activity results in aberrant neurogenesis rewiring hippocampal circuitry in a mouse model of epilepsy. *Nat. Commun.* 12:1423. doi: 10.1038/s41467-021-21649-8

Matsuda, T., Murao, N., Katano, Y., Juliandi, B., Kohyama, J., Akira, S., et al. (2015). TLR9 signalling in microglia attenuates seizure-induced aberrant neurogenesis in the adult hippocampus. *Nat. Commun.* 6:6514. doi: 10.1038/ncomms7514

McHugh, S. B., Lopes-Dos-Santos, V., Gava, G. P., Hartwich, K., Tam, S. K. E., Bannerman, D. M., et al. (2022). Adult-born dentate granule cells promote hippocampal population sparsity. *Nat. Neurosci.* 25, 1481–1491. doi: 10.1038/s41593-022-01176-5

Mo, M., Eyo, U. B., Xie, M., Peng, J., Bosco, D. B., Umpierre, A. D., et al. (2019). Microglial P2Y12 receptor regulates seizure-induced neurogenesis and immature neuronal projections. *J. Neurosci.* 39, 9453–9464. doi: 10.1523/JNEUROSCI.0487-19.2019

Morgan, R. J., and Soltesz, I. (2008). Nonrandom connectivity of the epileptic dentate gyrus predicts a major role for neuronal hubs in seizures. *Proc. Natl. Acad. Sci. U.S.A.* 105, 6179–6184. doi: 10.1073/pnas.0801372105

Murphy, B. L., Pun, R. Y., Yin, H., Faulkner, C. R., Loepke, A. W., and Danzer, S. C. (2011). Heterogeneous integration of adult-generated granule cells into the epileptic brain. *J. Neurosci.* 31, 105–117. doi: 10.1523/JNEUROSCI.2728-10.2011

Nakamichi, N., Takarada, T., and Yoneda, Y. (2009). Neurogenesis mediated by gamma-aminobutyric acid and glutamate signaling. *J. Pharmacol. Sci.* 110, 133–149.

Orcinha, C., Kilias, A., Paschen, E., Follo, M., and Haas, C. A. (2021). Reelin is required for maintenance of granule cell lamination in the healthy and epileptic hippocampus. *Front. Mol. Neurosci.* 14:730811. doi: 10.3389/fnmol.2021.730811

Orcinha, C., Münzner, G., Gerlach, J., Kilias, A., Follo, M., Egert, U., et al. (2016). Seizure-induced motility of differentiated dentate granule cells is prevented by the central reelin fragment. *Front. Cell Neurosci.* 10:183. doi: 10.3389/fncel.2016.00183

Overstreet Wadiche, L., Bromberg, D. A., Bensen, A. L., and Westbrook, G. L. (2005). GABAergic signaling to newborn neurons in dentate gyrus. *J. Neurophysiol.* 94, 4528–4532.

Pahle, J., Muhia, M., Wagener, R. J., Tippmann, A., Bock, H. H., Graw, J., et al. (2020). Selective inactivation of reelin in inhibitory interneurons leads to subtle changes in the dentate gyrus but leaves cortical layering and behavior unaffected. *Cereb Cortex* 30, 1688–1707. doi: 10.1093/cercor/bhz196

Parent, J. M., Elliott, R. C., Pleasure, S. J., Barbaro, N. M., and Lowenstein, D. H. (2006). Aberrant seizure-induced neurogenesis in experimental temporal lobe epilepsy. *Ann. Neurol.* 59, 81–91.

Parent, J. M., Yu, T. W., Leibowitz, R. T., Geschwind, D. H., Sloviter, R. S., and Lowenstein, D. H. (1997). Dentate granule cell neurogenesis is increased by seizures and contributes to aberrant network reorganization in the adult rat hippocampus. *J. Neurosci.* 17, 3727–3738.

Patrylo, P. R., Browning, R. A., and Cranick, S. (2006). Reeler homozygous mice exhibit enhanced susceptibility to epileptiform activity. *Epilepsia* 47, 257–266. doi: 10.1111/j.1528-1167.2006.00417.x

Pierce, J. P., Mccloskey, D. P., and Scharfman, H. E. (2011). Morphometry of hilar ectopic granule cells in the rat. *J. Comp. Neurol.* 519, 1196–1218. doi: 10.1002/cne.22568

Pun, R. Y., Rolle, I. J., Lasarge, C. L., Hosford, B. E., Rosen, J. M., Uhl, J. D., et al. (2012). Excessive activation of mTOR in postnatally generated granule cells is sufficient to cause epilepsy. *Neuron* 75, 1022–1034. doi: 10.1016/j.neuron.2012.08.002

Sahay, A., Scobie, K. N., Hill, A. S., O'carroll, C. M., Kheirbek, M. A., Burghardt, N. S., et al. (2011). Increasing adult hippocampal neurogenesis is sufficient to improve pattern separation. *Nature* 472, 466–470.

Sakai, A., Matsuda, T., Doi, H., Nagaishi, Y., Kato, K., and Nakashima, K. (2018). Ectopic neurogenesis induced by prenatal antiepileptic drug exposure augments seizure susceptibility in adult mice. *Proc. Natl. Acad. Sci. U.S.A.* 115, 4270–4275.

Scharfman, H. E., and Pierce, J. P. (2012). New insights into the role of hilar ectopic granule cells in the dentate gyrus based on quantitative anatomic analysis and three-dimensional reconstruction. *Epilepsia* 53(Suppl. 1), 109–115. doi: 10.1111/j.1528-1167.2012.03480.x

Scharfman, H. E., Goodman, J. H., and Sollas, A. L. (2000). Granule-like neurons at the hilar/CA3 border after status epilepticus and their synchrony with area CA3 pyramidal cells: functional implications of seizure-induced neurogenesis. *J. Neurosci.* 20, 6144–6158. doi: 10.1523/JNEUROSCI.20-16-06144.2000

Schultheiß, C., Abe, P., Hoffmann, F., Mueller, W., Kreuder, A. E., Schütz, D., et al. (2013). CXCR4 prevents dispersion of granule neuron precursors in the adult dentate gyrus. *Hippocampus* 23, 1345–1358. doi: 10.1002/hipo.22180

Scott, B. W., Wojtowicz, J. M., and Burnham, W. M. (2000). Neurogenesis in the dentate gyrus of the rat following electroconvulsive shock seizures. *Exp. Neurol.* 165, 231–236.

Shima, A., Nitta, N., Suzuki, F., Laharie, A. M., Nozaki, K., and Depaulis, A. (2015). Activation of mTOR signaling pathway is secondary to neuronal excitability in a mouse model of mesio-temporal lobe epilepsy. *Eur. J. Neurosci.* 41, 976–988. doi: 10.1111/ejn.12835

Sim, S., Antolin, S., Lin, C. W., Lin, Y., and Lois, C. (2013). Increased cell-intrinsic excitability induces synaptic changes in new neurons in the adult dentate gyrus that require Npas4. *J. Neurosci.* 33, 7928–7940. doi: 10.1523/JNEUROSCI.1571-12.2013

Singh, S. P., Lasarge, C. L., An, A., Mcauliffe, J. J., and Danzer, S. C. (2015). Clonal analysis of newborn hippocampal dentate granule cell proliferation and development in temporal lobe epilepsy. *eNeuro* 2:ENEURO.87–ENEURO.15. doi: 10.1523/ENEURO.0087-15.2015

Song, H., Stevens, C. F., and Gage, F. H. (2002). Astroglia induce neurogenesis from adult neural stem cells. *Nature* 417, 39–44.

Sparks, F. T., Liao, Z., Li, W., Grosmark, A., Soltesz, I., and Losonczy, A. (2020). Hippocampal adult-born granule cells drive network activity in a mouse model of chronic temporal lobe epilepsy. *Nat. Commun.* 11, 6138. doi: 10.1038/s41467-020-19969-2

Sultan, S., Li, L., Moss, J., Petrelli, F., Cassé, F., Gebara, E., et al. (2015). Synaptic integration of adult-born hippocampal neurons is locally controlled by astrocytes. *Neuron* 88, 957–972. doi: 10.1016/j.neuron.2015.10.037

Teixeira, C. M., Kron, M. M., Masachs, N., Zhang, H., Lagace, D. C., Martinez, A., et al. (2012). Cell-autonomous inactivation of the reelin pathway impairs adult neurogenesis in the hippocampus. *J. Neurosci.* 32, 12051–12065. doi: 10.1523/JNEUROSCI.1857-12.2012

Terreros-Roncal, J., Moreno-Jiménez, E. P., Flor-García, M., Rodríguez-Moreno, C. B., Trinchero, M. F., Cafini, F., et al. (2021). Impact of neurodegenerative diseases on human adult hippocampal neurogenesis. *Science* 374, 1106–1113.

Thom, M. (2014). Review: hippocampal sclerosis in epilepsy: a neuropathology review. *Neuropathol. Appl. Neurobiol.* 40, 520–543.

Tozuka, Y., Fukuda, S., Namba, T., Seki, T., and Hisatsune, T. (2005). GABAergic excitation promotes neuronal differentiation in adult hippocampal progenitor cells. *Neuron* 47, 803–815.

Upadhya, D., Hattiangady, B., Castro, O. W., Shuai, B., Kodali, M., Attaluri, S., et al. (2019). Human induced pluripotent stem cell-derived MGE cell grafting after status epilepticus attenuates chronic epilepsy and comorbidities via synaptic integration. *Proc. Natl. Acad. Sci. U.S.A.* 116, 287–296. doi: 10.1073/pnas.1814185115

Wang, S., Brunne, B., Zhao, S., Chai, X., Li, J., Lau, J., et al. (2018). Trajectory analysis unveils reelin's role in the directed migration of granule cells in the dentate gyrus. *J. Neurosci.* 38, 137–148. doi: 10.1523/JNEUROSCI.0988-17.2017

Wang, X., Song, X., Wu, L., Nadler, J. V., and Zhan, R. Z. (2016). Persistent hyperactivity of hippocampal dentate interneurons after a silent period in the rat pilocarpine model of epilepsy. *Front. Cell Neurosci.* 10:94. doi: 10.3389/fncel.2016.00094

Xu, W. S., Parmigiani, R. B., and Marks, P. A. (2007). Histone deacetylase inhibitors: molecular mechanisms of action. *Oncogene* 26, 5541–5552.

Yang, F., Liu, Z. R., Chen, J., Zhang, S. J., Quan, Q. Y., Huang, Y. G., et al. (2010). Roles of astrocytes and microglia in seizure-induced aberrant neurogenesis in the hippocampus of adult rats. *J. Neurosci. Res.* 88, 519–529. doi: 10.1002/jnr.22224

Zeng, L. H., Rensing, N. R., and Wong, M. (2009). The mammalian target of rapamycin signaling pathway mediates epileptogenesis in a model of temporal lobe epilepsy. *J. Neurosci.* 29, 6964–6972. doi: 10.1523/JNEUROSCI.0066-09.2009

Zhan, R. Z., and Nadler, J. V. (2009). Enhanced tonic GABA current in normotopic and hilar ectopic dentate granule cells after pilocarpine-induced status epilepticus. *J. Neurophysiol.* 102, 670–681. doi: 10.1152/jn.00147.2009

Zhan, R. Z., Timofeeva, O., and Nadler, J. V. (2010). High ratio of synaptic excitation to synaptic inhibition in hilar ectopic granule cells of pilocarpine-treated rats. *J. Neurophysiol.* 104, 3293–3304. doi: 10.1152/jn.00663.2010

Zhang, W., Huguenard, J. R., and Buckmaster, P. S. (2012). Increased excitatory synaptic input to granule cells from hilar and CA3 regions in a rat model of temporal lobe epilepsy. *J. Neurosci.* 32, 1183–1196. doi: 10.1523/JNEUROSCI.5342-11.2012

Zhou, Q. G., Nemes, A. D., Lee, D., Ro, E. J., Zhang, J., Nowacki, A. S., et al. (2019). Chemogenetic silencing of hippocampal neurons suppresses epileptic neural circuits. *J. Clin. Invest.* 129, 310–323. doi: 10.1172/JCI95731

Zhou, Y., Su, Y., Li, S., Kennedy, B. C., Zhang, D. Y., Bond, A. M., et al. (2022). Molecular landscapes of human hippocampal immature neurons across lifespan. *Nature* 607, 527–533. doi: 10.1038/s41586-022-04912-w

Zhu, K., Yuan, B., Hu, M., Feng, G. F., Liu, Y., and Liu, J. X. (2017). Reduced abnormal integration of adult-generated granule cells does not attenuate spontaneous recurrent seizures in mice. *Epilepsy Res.* 133, 58–66.

frontiers | Frontiers in Neuroscience

TYPE Review
PUBLISHED 07 March 2023
DOI 10.3389/fnins.2023.1141913

OPEN ACCESS

EDITED BY
Seiji Hitoshi,
Shiga University of Medical Science, Japan

REVIEWED BY
Kyoji Ohyama,
Tokyo Medical University, Japan
Katsuhiko Ono,
Kyoto Prefectural University of Medicine, Japan

*CORRESPONDENCE
Hitoshi Inada
✉ hinada@med.tohoku.ac.jp

SPECIALTY SECTION
This article was submitted to Neurodevelopment, a section of the journal Frontiers in Neuroscience

RECEIVED 11 January 2023
ACCEPTED 20 February 2023
PUBLISHED 07 March 2023

CITATION
Inada H, Corales LG and Osumi N (2023) A novel feature of the ancient organ: A possible involvement of the subcommissural organ in neurogenic/gliogenic potential in the adult brain.
Front. Neurosci. 17:1141913.
doi: 10.3389/fnins.2023.1141913

A novel feature of the ancient organ: A possible involvement of the subcommissural organ in neurogenic/gliogenic potential in the adult brain

Hitoshi Inada[1,2]*, Laarni Grace Corales[2] and Noriko Osumi[2]

[1]Laboratory of Health and Sports Sciences, Division of Biomedical Engineering for Health and Welfare, Graduate School of Biomedical Engineering, Tohoku University, Sendai, Japan, [2]Department of Developmental Neuroscience, Graduate School of Medicine, Tohoku University, Sendai, Japan

The subcommissural organ (SCO) is a circumventricular organ highly conserved in vertebrates from *Cyclostomata* such as lamprey to mammals including human. The SCO locates in the boundary between the third ventricle and the entrance of the aqueduct of Sylvius. The SCO functions as a secretory organ producing a variety of proteins such as SCO-spondin, transthyretin, and basic fibroblast growth factor (FGF) into the cerebrospinal fluid (CSF). A significant contribution of the SCO has been thought to maintain the homeostasis of CSF dynamics. However, evidence has shown a possible role of SCO on neurogenesis in the adult brain. This review highlights specific features of the SCO related to adult neurogenesis, suggested by the progress of understanding SCO functions. We begin with a brief history of the SCO discovery and continue to structural features, gene expression, and a possible role in adult neurogenesis suggested by the SCO transplant experiment.

KEYWORDS

subcommissural organ, neurogenesis, neural stem progenitor cell, Pax6, Sox2

Introduction

The subcommissural organ (SCO) is a circumventricular organ with a long history but is still enigmatic (Oksche et al., 1993; Meiniel et al., 1996; Rodriguez and Yulis, 2001; Kiecker, 2018). From *Cyclostomata* such as lamprey to mammals, the SCO is substantially conserved among vertebrates. The SCO is located at the boundary between the third ventricle and the entrance to the aqueduct of Sylvius (**Figures 1A, B**; Duvernoy and Risold, 2007; Kiecker, 2018; Corales et al., 2022). Its importance to maintaining the homeostasis of cerebrospinal fluid (CSF) dynamics has drawn attention to its functions (Perez-Figares et al., 2001; Guerra et al., 2015). The SCO has been hypothesized to play a role in neurogenesis (Guerra et al., 2015), although extensive research on dynamics of CSF and neuropathology of hydrocephalus has been conducted. Recent advancement in our understanding of the

function of the SCO have led us to hypothesize that the SCO possesses features relevant to adult neurogenesis. In this review, we overview how the SCO is discovered before discussing its structural characteristics, gene expression, and discuss a potential involvement in adult neurogenesis suggested by the SCO transplant experiment.

A brief history of the SCO

The first clear description of the SCO appears in the 1900's (Dendy, 1902). In an anatomical study on ammocoetes, a New Zealand Lamprey (*Geotria australis*), the SCO was described as "*a pair of ciliated grooves*" (**Figure 1C**), which in earlier study was referred as the epithelial layer (Edinger, 1892; Studnicka, 1900). The epithelium of the SCO is distinct from those in other brain regions due to its cylindrical structure. Dendy described it as follows; "They are most conspicuous beneath the commissure itself (figs. 1, 2), in which region they are lined by a sharply defined epithelium of very long columnar cells, totally different in appearance from the epithelium which lines the remainder of the brain-cavity." (Dendy, 1902). The SCO function was speculated, at that time, as making the circulation of the brain fluid due to its ciliated form and location. The term "Sub-Commissural Organ" was first proposed by Dendy and Nicholls in Dendy and Nicholls (1910). The same report also mentioned that the SCO exists in higher vertebrates such as mice, cats, and chimpanzees. At this time, "a pair of ciliated grooves" or "the epithelial layer beneath posterior commissure" was established as the "Sub-Commissural Organ."

Structural feature of the SCO

The SCO surface is sparsely ciliated and covered with microvilli, contrasting with the other ependymal areas, which are composed with multiciliated cells (Collins and Woollam, 1979; Rodriguez et al., 1998). The SCO consists of an inverted U-shape ependymal layer(s) lining the third ventricular side of the posterior commissure in the coronal section (Collins and Woollam, 1979; Rodriguez et al., 1998; **Figures 2A, B**). Later, it was proposed that the SCO is composed of two layers, ependyma and hypendyma, in vertebrates (Rodriguez et al., 1984). A small number of hypendymal cells are observed in amphibia and reptiles such as frogs, lizards, and snakes. In contrast, the hypendymal layer is more distinct in larger mammals such as bovines and primates, but its existence is species-dependent (Rodriguez et al., 1984). It appears that the presence of hypendymal cells is species-specific and be uncertain in animals with smaller brains. For example, a hypendymal layer is observed in rats but not in mice (**Figure 2C**; Corales et al., 2022).

As stated in the previous section, the SCO has been considered a secretory organ due to its cylindrical structure (**Figure 1D**). The SCO cells have an elongated shape, compared to typical ependymal cells, a large nucleus at the basal side adjacent to the posterior commissure (PC), the endoplasmic reticulum and the Golgi apparatus containing secretary molecules such as SCO-spondin and transthyretin (TTR). The apical pole of the SCO cells is exposed to the ventricular cavity. Apparent zonulae adherence is observed to connect adjacent cells. SCO-spondin secreted from the apical side forms the Reisner's fiber (RF) (Meiniel, 2001). This unique structure is also confirmed by a study using electron microscopy in detail (Meiniel, 2007).

Gene expression related to brain development in the SCO cells

Our knowledge on molecules expressed in the SCO is limited because of its restricted region, although a study reported a systematic DNA-chip analysis of circumventricular organs including SCO (Szathmari et al., 2013).

Secretory proteins

Due to their feature as secretory cells, two major secretory proteins, SCO-spondin and TTR, have been well studied in the SCO (Gobron et al., 1996; Montecinos et al., 2005).

Subcommissural organ-spondin is a giant glycoprotein with a large molecular weight (~540 kDa), which has been isolated as the SCO-specific transcript and identified as a component of Reissner's fiber (Meiniel et al., 1995; Gobron et al., 1996; Creveaux et al., 1998; Meiniel, 2001). SCO-spondin contains many functional domains (**Figure 3A**); elastin microfibril interface (EMI) domain, von Willebrand factor type-D (vWF-D) domains, FA5/8C domain, Low-density lipoprotein receptor class A (LDLrA) domains, trypsin inhibitor-like (TIL) domains, thrombospondin type I repeat (TSR) domains, von Willebrand factor type-C (vWF-C) domains, EGF-like domains, and CTCK domain (Gobron et al., 2000; Meiniel and Meiniel, 2007; Aboitiz and Montiel, 2021; Sepulveda et al., 2021). The SCO-spondin and its degradation products containing these domains have been proposed to function as neurogenesis regulators (Vera et al., 2013, 2015). SCO-spondin is also reported to have a neuroprotective effect (Deletage et al., 2021). Since the SCO-spondin contains many domains interacting with soluble factors, such as fibroblast growth factor 2 (FGF2), transforming growth factor-β (TGF-β), and vascular endothelial growth factor (VEGF), derivatives of the SCO-spondin could function as carriers or chelators of those soluble factors to regulate downstream signaling pathways (**Figure 3B**).

Transthyretin is a carrier for thyroid hormones in CSF (Alshehri et al., 2015; Richardson et al., 2015). It has previously been considered that only the choroid plexus produces TTR in the brain, although the SCO is shown to secrete TTR into the CSF (Montecinos et al., 2005). TTR might contribute to adult neurogenesis by regulating thyroid hormone homeostasis (Kapoor et al., 2015) since adult neural stem cell cycling *in vivo* requires thyroid hormone and its alpha receptor (Lemkine et al., 2005). Cell division and apoptosis are affected at the neural stem cell niche in the TTR null mice (Richardson et al., 2007).

The adult rat SCO shows strong expression of FGF2 (also known as a basic fibroblast growth factor, b-FGF) (Cuevas et al., 1996). FGF2 is critical in maintaining adult neurogenesis in the neurogenic niches (Mudo et al., 2009; Woodbury and Ikezu, 2014). The SCO also expresses Wnt1, a secretory glycoprotein critical for morphogenesis during brain development. Mutation in Wnt1 caused abnormal differentiation of the SCO in the mouse embryo

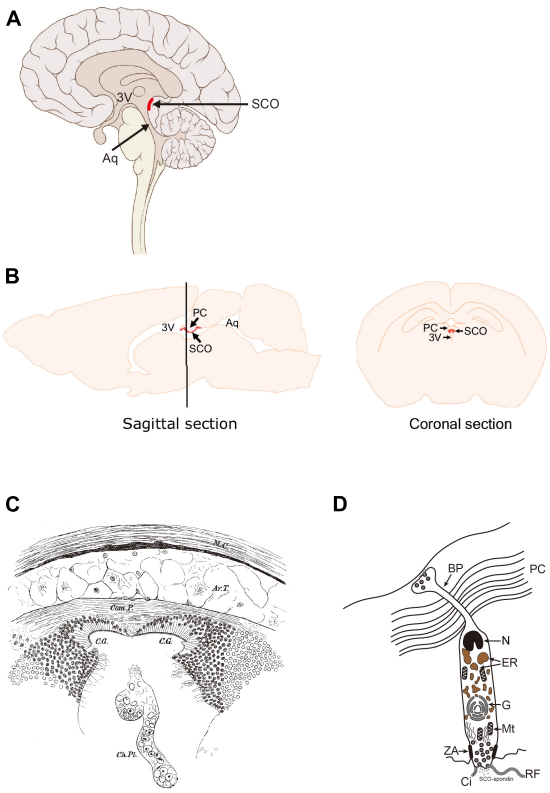

FIGURE 1
Location of the SCO in the adult human and rodent brains. **(A)** Sagittal section of human brain. **(B)** Sagittal and coronal sections of rodent brains. The SCO locates at the boundary between the third ventricle (3V) and the entrance of the aqueduct of Sylvius (Aq). The SCO is composed of an ependymal cell layer(s) lining the third ventricular side of the posterior commissure. In the coronal section, the SCO appears as an inverted U-shape underneath the posterior commissure (PC). 3V, third ventricle; Aq, aqueduct of Sylvius; PC, posterior commissure; SCO, subcommissural organ (Corales et al., 2022). **(C)** Illustration of "a pair of ciliated grooves". Ar.T., arachnoidal tissue; C.G., ciliated groove; Ch.PL, choroid plexus; Com.P., posterior commissure; M.C., connective tissue brain case. Used with permission of The Royal Society (U.K.), from Dendy (1902); permission conveyed through Copyright Clearance Center, Inc. **(D)** The secretory feature of the SCO ependymal cell. Scheme of an SCO secretory ependymal cell. The secretory proteins such as SCO-spondin and transthyretin are stored in the endoplasmic reticulum (ER), modified in the Golgi apparatus (G), and released both apically into the CSF and basally into the matrix of the posterior commissure. The SCO-spondin released into the CSF forms the RF. BP, basal process; Ci, cilia; ER, endoplasmic reticulum; G, Golgi apparatus; Mt, mitochondria; N, nucleus; PC, posterior commissure; RF, Reisner's fiber; ZA, zonula adherens.

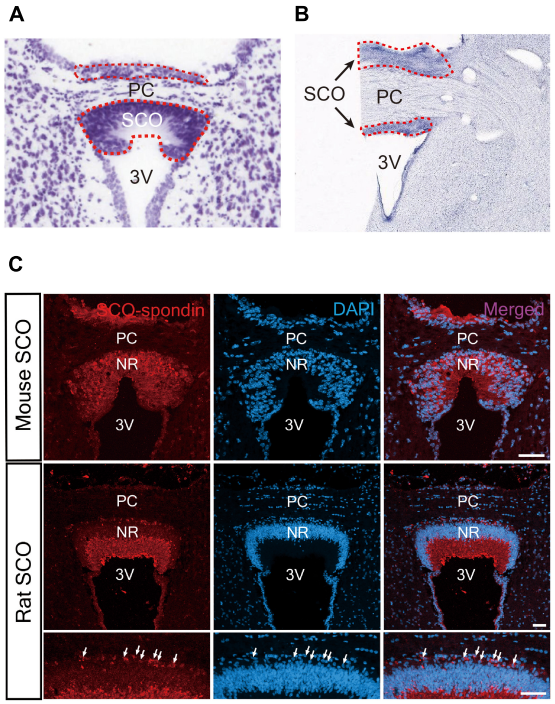

FIGURE 2
Histological structure of the SCO. **(A)** The SCO region of mouse brain. The SCO is composed of an ependymal cell layer(s) with an inverted U-shape lining the third ventricular side of the posterior commissure (Allen Brain Atlas: Mouse Brain, https://atlas.brain-map.org/). **(B)** The SCO region of human brain (BrainSpan Atlas of the Developing Human Brain, https://atlas.brain-map.org/). The SCO regions are surrounded by red dotted lines. **(C)** Immunostaining of SCO-spondin in the SCO region of the adult mouse and rat brain. The SCO-spondin staining pattern in the adult rat SCO shows a weak staining pattern in the nuclear region compared to the adult mouse SCO allowing better visualization of hypendymal cells between the ependymal layer and the posterior commissure. Arrows indicate hypendymal cells. Scale bars: 50 μm (Corales et al., 2022). 3V, third ventricle; Ep, ependymal cells; NR, nuclear region; PC, posterior commissure.

(Louvi and Wassef, 2000). Wnt1 expression is observed in the SCO at the RNA level based on Allen Mouse Brain Atlas.[1] Wnt signaling pathway has been reported to regulate neural differentiation from neural stem/progenitor cell (NSPCs) in early embryonic brain development (Hirabayashi et al., 2004; Machon et al., 2007; Munji et al., 2011; Inestrosa and Varela-Nallar, 2015).

These secretory proteins from the SCO could contribute to neurogenesis in the embryonic brain and adult neurogenesis (discussed later). In addition, these secretory proteins could also contribute to maintaining the SCO functions in an autocrine manner since the FGF2 receptor is expressed in the SCO (Szathmari et al., 2013).

The SCO development is consistent during embryonic stages among species, but its maintenance appears species dependent. For example, the SCO begins to differentiate at embryonic day 12.5 (E12.5) in mice, well developed by E16.5 (Estivill-Torrús et al., 2001), and appears to be maintained through postnatal stages (Corales et al., 2022). On the other hand, the SCO is well developed at embryonic stages (3- to 5-month-old fetuses) but gradually regresses the SCO structure after 5-month-old fetuses (Rodriguez et al., 2001). The SCO cells are significantly reduced in 1-year-old infants and lose their secretory features in the adult stages (Rodriguez et al., 2001).

Transcription factors

It has been reported that several transcription factors are critical for the formation of the SCO. Ectopic expression of Engrailed 1

1 https://mouse.brain-map.org/experiment/show/112644522

(En1), a homeobox transcription factor related to Wnt1 signaling, interferes with the differentiation of circumventricular organs, including the SCO (Louvi and Wassef, 2000). En1 expression is also confirmed in the SCO at the RNA level based on Allen Brain Atlas: Mouse Brain.[2] Deficiency in the function of Pax6, an essential transcription factor for neurogenesis in the embryonic and adult brain (Osumi et al., 2008), results in impairment of the SCO differentiation in early brain development (Estivill-Torrús et al., 2001). The SCO's structural and functional features as a secretory organ are completely lacking in the *Pax6*$^{Sey/Sey}$ mutant mouse, suggesting that Pax6 is critical for SCO formation. Msx1, a homeodomain transcription factor, is expressed in the SCO of the mouse embryonic brain, and a mutation in *Msx1* gene causes a defect in the SCO formation (Bach et al., 2003; Ramos et al., 2004). However, since these transcription factors are related to regionalization in early brain development, it remains unknown whether abnormality in the SCO might be directly caused by defects in these transcription factors or secondarily induced by compartmentation deficits.

Expressions of RFX3 and RFX4, members of the regulatory factor X gene family related to ciliogenesis, are also reported in the SCO. Their mutation or misexpression causes a severe hydrocephalus phenotype in mice, possibly by malformation of the SCO (Blackshear et al., 2003; Baas et al., 2006; Xu et al., 2018). Functional expression of CREB was also confirmed in the isolated SCO cells in an aspect to the cAMP-PKA pathway (Nurnberger and Schoniger, 2001; Schoniger et al., 2002).

As mentioned above, the secretory proteins from SCO could be associated with several signaling pathways, such as integrin, Wnt/β-catenin, and Notch signaling pathways (**Figure 3B**). Recent studies suggested that these signaling pathways are involved in multiciliated cell differentiation or hydrocephalus (Failler et al., 2021; Lewis and Stracker, 2021; Liu et al., 2023), emphasizing critical SCO roles on ciliogenesis and hydrocephalus caused by its malfunction.

Proliferation and differentiation potential of SCO cells: Neurogenic/gliogenic and embryonic/adult

A significant role of the SCO is maintaining CSF homeostasis by forming RF, which consists of SCO-spondin. However, several lines of evidence suggest its contribution to adult neurogenesis. Recently, we have reported that the SCO cells have a unique feature as immature neuroepithelial cells in the adult mouse brain (Corales et al., 2022). The SCO cells in the adult brain expressed known NSPC markers, i.e., Pax6, Sox2, and vimentin, and a proliferating marker, PCNA (**Figure 4**). Neither expression of another proliferation marker Ki67, indicating a G2/M phase, nor incorporation of BrdU, an indicator for DNA synthesis in the S phase, are undetectable, suggesting that the SCO cells have a potential for proliferation but are quiescent for cell division in the adult. The SCO cells also express other neuroepithelial cell markers, such as Nestin, as well as Notch 1, Hes1 and Hes3, Occludin, E-cadherin, MSI-1, Sox9, and BMI-1 at the RNA level based on Allen Brain Atlas.[3] These data demonstrate that the adult SCO cells maintain neuroepithelial cell characteristics, suggesting that the SCO is a possible adult neural stem cell niche.

The quiescent SCO might express its neurogenic activity by appropriate stimuli. For example, tanycytes in the adult hypothalamus are a subtype of ependymal cells with a long radial process (Rodriguez et al., 2005). It has been shown that sub-population of the tanycytes contain stimuli-responsive NSPCs (Lee et al., 2012; Cheng, 2013; Robins et al., 2013; Maggi et al., 2014). A recent study has reported that tanycyte-like ependymal cells in circumventricular organs (CVOs) and the central canal (CC) show a neural stem cell-like phenotype in the adult mouse brain (Furube et al., 2020). In the study, tamoxifen-induced EGFP labeling under the control of *Nestin-CreERT2* transgene has identified NSPCs and shown that the EGFP-labeled ependymal cells distribute in the organum vasculosum laminae terminalis (OVLT), subfornical organ (SFO), CC, and the arcuate nucleus (Arc) of the hypothalamus. Furthermore, EGFP-labeled ependymal cells increased by stimulation with FGF-2/EFG (Furube et al., 2020). The EGFP-labeled tanycyte-like ependymal cells of the OVLT and SFO express both GFAP and Sox2 but not Pax6, while the cells of the CC express those three marker proteins (Furube et al., 2020), which is similar to our results in the SCO (Corales et al., 2022). However, no EGFP-labeled ependymal cells in the SCO were mentioned in the study (Furube et al., 2020). Possibly, the SCO might be activated by the other factors than FGF-2/EFG. In addition, SCO cells are distinct from the tanycytes by structural features. The SCO cells have primary cilia while tanycytes or tanycyte-like cells are unciliated or unciliated/bi-ciliated, respectively (Langlet et al., 2013; Mirzadeh et al., 2017). The cytoplasm of the tanycyte often shows smooth endoplasmic reticulum (Wittkowski, 1998), while the cytoplasm of SCO cells are filled with rough endoplasmic reticulum (Rodriguez et al., 2001), consistent with their secretory function. Therefore, even though the SCO cells and tanycytes share a part of NSPC marker expression, they are different subtypes of ependymal cells.

Although the SCO cells share many properties with NSPCs in the gene expression, it is difficult to clarify whether they could express proliferation activity and whether they are neurogenic RG-like cells and/or gliogenic progenitors. At this point, what kind of cells could be produced from the SCO remains unknown. Considering its location near the posterior commissure and the existence of oligodendrocyte precursor cells (OPCs) at the periphery of the SCO (Corales et al., 2022), the SCO might be a niche for oligogenesis rather than neurogenesis.

Another possible involvement of the SCO in adult neurogenesis is obtained by transplantation of SCO cells into a lateral ventricle. In the study by Rodríguez et al., tissue blocks containing the SCO and the PC were transplanted into the left lateral ventricle in 2–3 months-old Sprague–Dawley rats (Rodriguez et al., 1999). It is observed that the grafted SCOs keep an ultrastructure similar to those of the SCO *in situ* and have the ability of production and secretion of SCO-spondin, resulting in the RF in the explanted lateral ventricle. The transplantation using bovine

2 https://mouse.brain-map.org/gene/show/13576

3 https://mouse.brain-map.org/

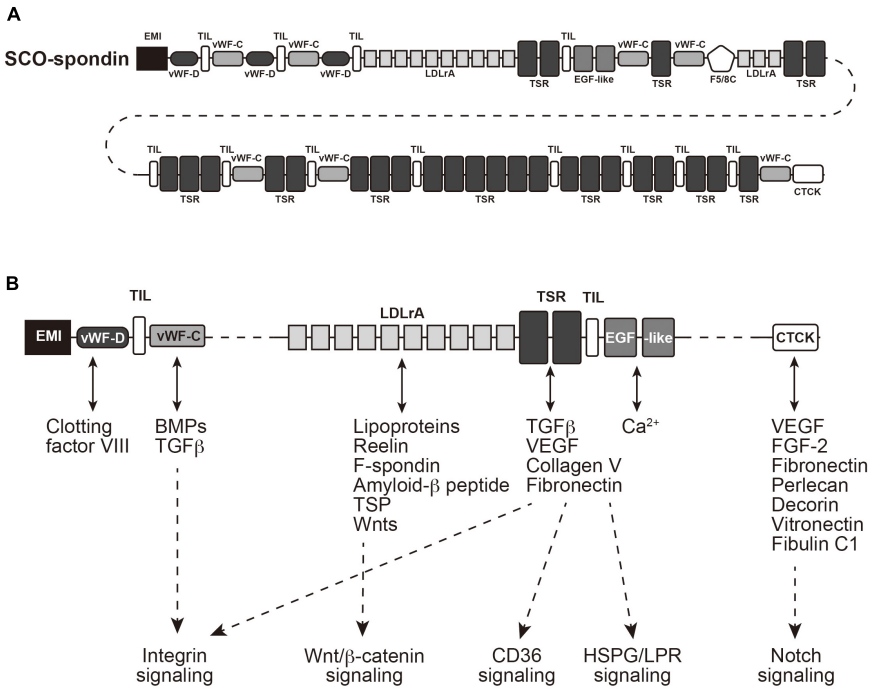

FIGURE 3
Structure of SCO-spondin and its downstream signaling pathways. **(A)** A cartoon of SCO-spondin structure. EMI, elastin microfibril interface; vWF-D, von Willebrand factor type-D; FA5/8C, Factor V/Factor VIII type C; LDLrA, low-density lipoprotein receptor class A; TIL, trypsin inhibitor-like; TSR thrombospondin type I repeat; vWF-C, von Willebrand factor type-C; EGF, epidermal growth factor; CTCK, C-terminal cystine knot-like. **(B)** Possible interactions of domains contained in SCO-spondin with soluble factors. FGF2, fibroblast growth factor 2; TGF-β, transforming growth factor-β; VEGF, vascular endothelial growth factor; HSPG, heparan sulfate proteoglycan; LPR, LDLr-related protein.

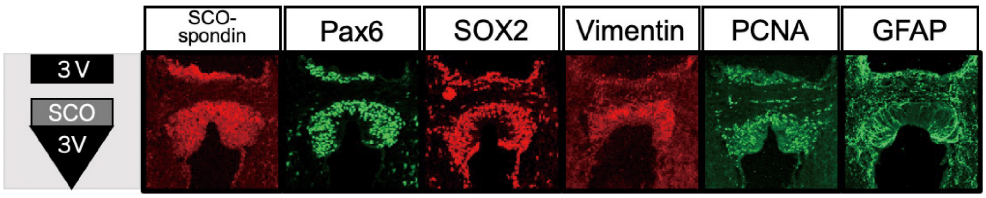

FIGURE 4
Expression of NSPC markers in the SCO. Immunostaining of NSPC markers in the mouse SCO (Corales et al., 2022).

SCO explants also support that the secretory active SCO can induce cell proliferation. The bovine SCO cultured *in vitro* for a few weeks express and secrete the SCO-spondin and TTR into the culture medium (Schobitz et al., 2001; Montecinos et al., 2005). Xenografts of bovine SCO explants into a lateral ventricle of rats indeed promote cell proliferation in the ipsilateral than contralateral SVZ niche (Guerra et al., 2015), suggesting that the SCO might contribute to the proliferation of NSPCs and possibly leading to neurogenesis through secreted factors CSF circulation in the adult brain.

One possible interpretation for the increased PCNA positive cells by the SCO transplant is that neuroprotective factors secreted by the grafted SCO might enhance or maintain cell proliferation, as suggested in the previous study where the SCO secretes SCO-spondin or TTR (Schobitz et al., 2001; Montecinos et al., 2005). This possibility can be supported by the contribution of the SCO to the early embryonic brain development. Especially, the SCO has been reported to show its contribution to neurogenesis during embryogenesis. In the embryonic stages, the SCO seems to regulate cell proliferation and neuronal differentiation through the secretion of the SCO-spondin (El-Bitar et al., 2001; Vera et al., 2013, 2015). SCO-spondin knockdown experiments using chick embryos have demonstrated that the protein released into embryonic CSF is required for neurogenesis and regulation of neuroepithelial cell proliferation/neuronal differentiation (Vera et al., 2013). A subsequent study showed that low-density lipoprotein (LDL) and SCO-spondin form a complex and that this interaction is essential in modulating the neuroepithelium differentiation generated by both molecules (Vera et al., 2015). However, *in ovo* inhibition of SCO-spondin using shRNA in the chick embryo has reduced neuronal cell number and increased PCNA-positive cells (Vera et al., 2013). A similar result was obtained by *in vitro* culture with the explanted optic tecta in the SCO explant conditioned medium and SCO-spondin-depleted embryonic CSF (Vera et al., 2015).

These results are inconsistent with those from SCO transplantation experiments. Cellular response to the SCO-spondin might be different between embryonic and adult brains, or among species.

Conclusion

In this review, we highlighted a possible role of the SCO in adult neurogenesis: as a neurogenesis/gliogenesis niche or a neurogenesis/gliogenesis regulatory region through secretory factors. Our knowledge about functions of the SCO in adult neurogenesis remains limited due to lacking SCO specific conditional knockout animals. Only a few studies related to functional disruption of the SCO, especially with SCO-spondin deficient animals, mainly focused on the relationship between the RF formation, CSF flow, and hydrocephalus (Perez-Figares et al., 2001; Sepulveda et al., 2021). For example, immunological blockage of the SCO function was able to induce a hydrocephalus phenotype in adult rats (Vio et al., 2000). Recently, a series of studies using zebrafish showed that a mutation in the SCO-spondin gene (*sspo*) causes a phenotype with an abnormal ventral curvature of the body axis and idiopathic scoliosis (Cantaut-Belarif et al., 2018; Lu et al., 2020; Rose et al., 2020). However, the effect of SCO disruption on adult neurogenesis has not been investigated. There are still enigmas on the SCO function on CSF homeostasis and neurogenesis. Comprehensive transcriptome analysis of genes expressed in the SCO and systematic analysis using SCO-specific conditional knockout animals of the related genes would be essential to elucidate the SCO contribution to adult neurogenesis.

Author contributions

HI was involved in writing the first manuscript. HI, LC, and NO contributed to the manuscript revision, reviewed, and approved the submitted version of the manuscript. All authors contributed to the article and approved the submitted version.

Funding

This work was supported by the Grants-in-Aid for Scientific Research (C) (17K08486) and (B) (19H03318) to HI and NO, respectively, from the Ministry of Education, Culture, Sports, Science and Technology of Japan (MEXT).

Acknowledgments

We thank Drs. Kotaro Hiraoka and Takako Kikkawa for the technical assistance, Shun Araki and Shinya Yamanaka for the data acquirement.

Conflict of interest

The authors declare that the research was conducted in the absence of any commercial or financial relationships that could be construed as a potential conflict of interest.

Publisher's note

All claims expressed in this article are solely those of the authors and do not necessarily represent those of their affiliated organizations, or those of the publisher, the editors and the reviewers. Any product that may be evaluated in this article, or claim that may be made by its manufacturer, is not guaranteed or endorsed by the publisher.

References

Aboitiz, F., and Montiel, J. F. (2021). The enigmatic Reissner's fiber and the origin of chordates. *Front. Neuroanat.* 15:703835. doi: 10.3389/fnana.2021.703835

Alshehri, B., D'Souza, D. G., Lee, J. Y., Petratos, S., and Richardson, S. J. (2015). The diversity of mechanisms influenced by transthyretin in neurobiology: development, disease and endocrine disruption. *J. Neuroendocrinol.* 27, 303–323. doi: 10.1111/jne.12271

Baas, D., Meiniel, A., Benadiba, C., Bonnafe, E., Meiniel, O., Reith, W., et al. (2006). A deficiency in RFX3 causes hydrocephalus associated with abnormal differentiation of ependymal cells. *Eur. J. Neurosci.* 24, 1020–1030. doi: 10.1111/j.1460-9568.2006.05002.x

Bach, A., Lallemand, Y., Nicola, M. A., Ramos, C., Mathis, L., Maufras, M., et al. (2003). Msx1 is required for dorsal diencephalon patterning. *Development* 130, 4025–4036. doi: 10.1242/dev.00609

Blackshear, P. J., Graves, J. P., Stumpo, D. J., Cobos, I., Rubenstein, J. L., and Zeldin, D. C. (2003). Graded phenotypic response to partial and complete deficiency of a brain-specific transcript variant of the winged helix transcription factor RFX4. *Development* 130, 4539–4552. doi: 10.1242/dev.00661

Cantaut-Belarif, Y., Sternberg, J. R., Thouvenin, O., Wyart, C., and Bardet, P. L. (2018). The reissner fiber in the cerebrospinal fluid controls morphogenesis of the body axis. *Curr. Biol.* 28, 2479–2486 e2474. doi: 10.1016/j.cub.2018.05.079

Cheng, M. F. (2013). Hypothalamic neurogenesis in the adult brain. *Front. Neuroendocrinol.* 34:167–178. doi: 10.1016/j.yfrne.2013.05.001

Collins, P., and Woollam, D. H. (1979). The ventricular surface of the subcommissural organ: a scanning and transmission electron microscopic study. *J. Anat.* 129, 623–631.

Corales, L. G., Inada, H., Hiraoka, K., Araki, S., Yamanaka, S., Kikkawa, T., et al. (2022). The subcommissural organ maintains features of neuroepithelial cells in the adult mouse. *J. Anat.* 241, 820–830. doi: 10.1111/joa.13709

Creveaux, I., Gobron, S., Meiniel, R., Dastugue, B., and Meiniel, A. (1998). Complex expression pattern of the SCO-spondin gene in the bovine subcommissural organ: toward an explanation for Reissner's fiber complexity? *Brain Res. Mol. Brain Res.* 55, 45–53. doi: 10.1016/S0169-328X(97)00357-4

Cuevas, P., Reimers, D., and Gimenez-Gallego, G. (1996). Loss of basic fibroblast growth factor in the subcommissural organ of old spontaneously hypertensive rats. *Neurosci. Lett.* 221, 25–28. doi: 10.1016/S0304-3940(96)13277-8

Deletage, N., Le Douce, J., Callizot, N., Godfrin, Y., and Lemarchant, S. (2021). SCO-spondin-derived peptide protects neurons from glutamate-induced excitotoxicity. *Neuroscience* 463, 317–336. doi: 10.1016/j.neuroscience.2021.02.005

Dendy, A. (1902). On a pair of cilliated grooves in the brain of the ammocoete. *Proc. R. Soc. Lond.* 69, 485–494. doi: 10.1098/rspl.1901.0136

Dendy, A., and Nicholls, G. E. (1910). On the occurrence of a mesocælic recess in the human brain, and its relation to the sub-commissural organ of lower vertebrates; with special reference to the distribution of Reissner's fibre in the vertebrate series and its possible function. *Proc. R. Soc. B Biol. Sci.* 82, 515–529. doi: 10.1098/rspb.1910.0046

Duvernoy, H. M., and Risold, P. Y. (2007). The circumventricular organs: an atlas of comparative anatomy and vascularization. *Brain Res. Rev.* 56, 119–147. doi: 10.1016/j.brainresrev.2007.06.002

Edinger, L. (1892). Untersuchungen über die vergleichende anatomie des gehirnes. *Abhandlungen der Senckenbergischen Naturforschenden Gesellschaft* 18, 1–55.

El-Bitar, F., Bamdad, M., Dastugue, B., and Meiniel, A. (2001). Effects of SCO-spondin thrombospondin type 1 repeats (TSR) in comparison to Reissner's fiber material on the differentiation of the B104 neuroblastoma cell line. *Cell Tissue Res.* 304, 361–369. doi: 10.1007/s004410100383

Estivill-Torrús, G., Vitalis, T., Fernández-Llebrez, P., and Price, D. J. (2001). The transcription factor Pax6 is required for development of the diencephalic dorsal midline secretory radial glia that form the subcommissural organ. *Mech. Dev.* 109, 215–224. doi: 10.1016/S0925-4773(01)00527-5

Failler, M., Giro-Perafita, A., Owa, M., Srivastava, S., Yun, C., Kahler, D. J., et al. (2021). Whole-genome screen identifies diverse pathways that negatively regulate ciliogenesis. *Mol. Biol. Cell* 32, 169–185. doi: 10.1091/mbc.E20-02-0111

Furube, E., Ishii, H., Nambu, Y., Kurganov, E., Nagaoka, S., Morita, M., et al. (2020). Neural stem cell phenotype of tanycyte-like ependymal cells in the circumventricular organs and central canal of adult mouse brain. *Sci. Rep.* 10:2826. doi: 10.1038/s41598-020-59629-5

Gobron, S., Creveaux, I., Meiniel, R., Didier, R., Herbet, A., Bamdad, M., et al. (2000). Subcommissural organ/Reissner's fiber complex: characterization of SCO-spondin, a glycoprotein with potent activity on neurite outgrowth. *Glia* 32, 177–191. doi: 10.1002/1098-1136(200011)32:2<177::AID-GLIA70>3.0.CO;2-V

Gobron, S., Monnerie, H., Meiniel, R., Creveaux, I., Lehmann, W., Lamalle, D., et al. (1996). SCO-spondin: a new member of the thrombospondin family secreted by the subcommissural organ is a candidate in the modulation of neuronal aggregation. *J. Cell Sci.* 109(Pt 5), 1053–1061. doi: 10.1242/jcs.109.5.1053

Guerra, M. M., Gonzalez, C., Caprile, T., Jara, M., Vio, K., Munoz, R. I., et al. (2015). Understanding how the subcommissural organ and other periventricular secretory structures contribute via the cerebrospinal fluid to neurogenesis. *Front. Cell Neurosci.* 9:480. doi: 10.3389/fncel.2015.00480

Hirabayashi, Y., Itoh, Y., Tabata, H., Nakajima, K., Akiyama, T., Masuyama, N., et al. (2004). The Wnt/beta-catenin pathway directs neuronal differentiation of cortical neural precursor cells. *Development* 131, 2791–2801. doi: 10.1242/dev.01165

Inestrosa, N. C., and Varela-Nallar, L. (2015). Wnt signalling in neuronal differentiation and development. *Cell Tissue Res.* 359, 215–223. doi: 10.1007/s00441-014-1996-4

Kapoor, R., Fanibunda, S. E., Desouza, L. A., Guha, S. K., and Vaidya, V. A. (2015). Perspectives on thyroid hormone action in adult neurogenesis. *J. Neurochem.* 133, 599–616. doi: 10.1111/jnc.13093

Kiecker, C. (2018). The origins of the circumventricular organs. *J. Anat.* 232, 540–553. doi: 10.1111/joa.12771

Langlet, F., Mullier, A., Bouret, S. G., Prevot, V., and Dehouck, B. (2013). Tanycyte-like cells form a blood-cerebrospinal fluid barrier in the circumventricular organs of the mouse brain. *J. Comp. Neurol.* 521, 3389–3405. doi: 10.1002/cne.23355

Lee, D. A., Bedont, J. L., Pak, T., Wang, H., Song, J., Miranda-Angulo, A., et al. (2012). Tanycytes of the hypothalamic median eminence form a diet-responsive neurogenic niche. *Nat. Neurosci.* 15, 700–702. doi: 10.1038/nn.3079

Lemkine, G. F., Raj, A., Alfama, G., Turque, N., Hassani, Z., Alegria-Prevot, O., et al. (2005). Adult neural stem cell cycling in vivo requires thyroid hormone and its alpha receptor. *Faseb J.* 19, 863–865. doi: 10.1096/fj.04-2916fje

Lewis, M., and Stracker, T. H. (2021). Transcriptional regulation of multiciliated cell differentiation. *Semin. Cell Dev. Biol.* 110, 51–60. doi: 10.1016/j.semcdb.2020.04.007

Liu, Q., Novak, M. K., Pepin, R. M., Maschhoff, K. R., and Hu, W. (2023). Different congenital hydrocephalus-associated mutations in Trim71 impair stem cell differentiation via distinct gain-of-function mechanisms. *PLoS Biol.* 21:e3001947. doi: 10.1371/journal.pbio.3001947

Louvi, A., and Wassef, M. (2000). Ectopic engrailed 1 expression in the dorsal midline causes cell death, abnormal differentiation of circumventricular organs and errors in axonal pathfinding. *Development* 127, 4061–4071. doi: 10.1242/dev.127.18.4061

Lu, H., Shagirova, A., Goggi, J. L., Yeo, H. L., and Roy, S. (2020). Reissner fibre-induced urotensin signalling from cerebrospinal fluid-contacting neurons prevents scoliosis of the vertebrate spine. *Biol. Open* 9:bio052027. doi: 10.1242/bio.052027

Machon, O., Backman, M., Machonova, O., Kozmik, Z., Vacik, T., Andersen, L., et al. (2007). A dynamic gradient of Wnt signaling controls initiation of neurogenesis in the mammalian cortex and cellular specification in the hippocampus. *Dev. Biol.* 311, 223–237. doi: 10.1016/j.ydbio.2007.08.038

Maggi, R., Zasso, J., and Conti, L. (2014). Neurodevelopmental origin and adult neurogenesis of the neuroendocrine hypothalamus. *Front. Cell Neurosci.* 8:440. doi: 10.3389/fncel.2014.00440

Meiniel, A. (2001). SCO-spondin, a glycoprotein of the subcommissural organ/Reissner's fiber complex: evidence of a potent activity on neuronal development in primary cell cultures. *Microsc. Res. Tech.* 52, 484–495. doi: 10.1002/1097-0029(20010301)52:5<484::AID-JEMT1034>3.0.CO;2-0

Meiniel, A. (2007). The secretory ependymal cells of the subcommissural organ: which role in hydrocephalus? *Int. J. Biochem. Cell Biol.* 39, 463–468. doi: 10.1016/j.biocel.2006.10.021

Meiniel, A., Meiniel, R., Didier, R., Creveaux, I., Gobron, S., Monnerie, H., et al. (1996). The subcommissural organ and Reissner's fiber complex. an enigma in the central nervous system? *Prog. Histochem. Cytochem.* 30, 1–66. doi: 10.1016/S0079-6336(96)80015-5

Meiniel, O., and Meiniel, A. (2007). The complex multidomain organization of SCO-spondin protein is highly conserved in mammals. *Brain Res. Rev.* 53, 321–327. doi: 10.1016/j.brainresrev.2006.09.007

Meiniel, R., Creveaux, I., Dastugue, B., and Meiniel, A. (1995). Specific transcripts analysed by in situ hybridization in the subcommissural organ of bovine embryos. *Cell Tissue Res.* 279, 101–107. doi: 10.1007/BF00300696

Mirzadeh, Z., Kusne, Y., Duran-Moreno, M., Cabrales, E., Gil-Perotin, S., Ortiz, C., et al. (2017). Bi- and uniciliated ependymal cells define continuous floor-plate-derived tanycytic territories. *Nat. Commun.* 8:13759. doi: 10.1038/ncomms13759

Montecinos, H. A., Richter, H., Caprile, T., and Rodriguez, E. M. (2005). Synthesis of transthyretin by the ependymal cells of the subcommissural organ. *Cell Tissue Res.* 320, 487–499. doi: 10.1007/s00441-004-0997-0

Mudo, G., Bonomo, A., Di Liberto, V., Frinchi, M., Fuxe, K., and Belluardo, N. (2009). The FGF-2/FGFRs neurotrophic system promotes neurogenesis in the adult brain. *J. Neural Transm.* 116, 995–1005. doi: 10.1007/s00702-009-0207-z

Munji, R. N., Choe, Y., Li, G., Siegenthaler, J. A., and Pleasure, S. J. (2011). Wnt signaling regulates neuronal differentiation of cortical intermediate progenitors. *J. Neurosci.* 31, 1676–1687. doi: 10.1523/JNEUROSCI.5404-10.2011

Nurnberger, F., and Schoniger, S. (2001). Presence and functional significance of neuropeptide and neurotransmitter receptors in subcommissural organ cells. *Microsc. Res. Tech.* 52, 534–540. doi: 10.1002/1097-0029(20010301)52:5<534::AID-JEMT1038>3.0.CO;2-R

Oksche, A., Rodriìguez, E. M., and Fernaìndez-Llebrez, P. (1993). "The subcommissural organ," in *Proceedings of the Ependymal Brain Gland: Symposium: Papers*, eds A. Oksche, E. M. Rodriguez and P. Fernandez-Llebrez (Berlin: Springer). doi: 10.1007/978-3-642-78013-4

Osumi, N., Shinohara, H., Numayama-Tsuruta, K., and Maekawa, M. (2008). Concise review: Pax6 transcription factor contributes to both embryonic and adult neurogenesis as a multifunctional regulator. *Stem Cells* 26, 1663–1672. doi: 10.1634/stemcells.2007-0884

Perez-Figares, J. M., Jimenez, A. J., and Rodriguez, E. M. (2001). Subcommissural organ, cerebrospinal fluid circulation, and hydrocephalus. *Microsc. Res. Tech.* 52, 591–607. doi: 10.1002/1097-0029(20010301)52:5<591::AID-JEMT1043>3.0.CO;2-7

Ramos, C., Fernandez-Llebrez, P., Bach, A., Robert, B., and Soriano, E. (2004). Msx1 disruption leads to diencephalon defects and hydrocephalus. *Dev. Dyn.* 230, 446–460. doi: 10.1002/dvdy.20070

Richardson, S. J., Lemkine, G. F., Alfama, G., Hassani, Z., and Demeneix, B. A. (2007). Cell division and apoptosis in the adult neural stem cell niche are differentially affected in transthyretin null mice. *Neurosci. Lett.* 421, 234–238. doi: 10.1016/j.neulet.2007.05.040

Richardson, S. J., Wijayagunaratne, R. C., D'Souza, D. G., Darras, V. M., and Van Herck, S. L. (2015). Transport of thyroid hormones via the choroid plexus into the brain: the roles of transthyretin and thyroid hormone transmembrane transporters. *Front. Neurosci.* 9:66. doi: 10.3389/fnins.2015.00066

Robins, S. C., Stewart, I., McNay, D. E., Taylor, V., Giachino, C., Goetz, M., et al. (2013). alpha-Tanycytes of the adult hypothalamic third ventricle include distinct populations of FGF-responsive neural progenitors. *Nat. Commun.* 4:2049. doi: 10.1038/ncomms3049

Rodriguez, E., and Yulis, C. R. (2001). Subcommissural organ. Cellular, molecular, physiological, and pathological aspects: one hundred years of subcommissural organ research. *Microsc. Res. Tech.* 52, 459–460. doi: 10.1002/1097-0029(20010301)52:5<459::AID-JEMT1031>3.0.CO;2-Y

Rodriguez, E. M., Blazquez, J. L., Pastor, F. E., Pelaez, B., Pena, P., Peruzzo, B., et al. (2005). Hypothalamic tanycytes: a key component of brain-endocrine interaction. *Int. Rev. Cytol.* 247, 89–164. doi: 10.1016/S0074-7696(05)47003-5

Rodriguez, E. M., Oksche, A., Hein, S., Rodriguez, S., and Yulis, R. (1984). Comparative immunocytochemical study of the subcommissural organ. *Cell Tissue Res.* 237, 427–441. doi: 10.1007/BF00228427

Rodriguez, E. M., Oksche, A., and Montecinos, H. (2001). Human subcommissural organ, with particular emphasis on its secretory activity during the fetal life. *Microsc. Res. Tech.* 52, 573–590. doi: 10.1002/1097-0029(20010301)52:5<573::AID-JEMT1042>3.0.CO;2-6

Rodriguez, E. M., Rodriguez, S., and Hein, S. (1998). The subcommissural organ. *Microsc. Res. Tech.* 41, 98–123. doi: 10.1002/(SICI)1097-0029(19980415)41:2<98::AID-JEMT2>3.0.CO;2-M

Rodriguez, S., Navarrete, E. H., Vio, K., Gonzalez, C., Schobitz, K., and Rodriguez, E. M. (1999). Isograft and xenograft of the subcommissural organ into the lateral ventricle of the rat and the formation of Reissner's fiber. *Cell Tissue Res.* 296, 457–469. doi: 10.1007/s004410051306

Rose, C. D., Pompili, D., Henke, K., Van Gennip, J. L. M., Meyer-Miner, A., Rana, R., et al. (2020). SCO-spondin defects and neuroinflammation are conserved mechanisms driving spinal deformity across genetic models of idiopathic scoliosis. *Curr. Biol.* 30, 2363–2373 e6. doi: 10.1016/j.cub.2020.04.020

Schobitz, K., Gonzalez, C., Peruzzo, B., Yulis, C. R., and Rodriguez, E. M. (2001). Organ culture of the bovine subcommissural organ: evidence for synthesis and release of the secretory material. *Microsc. Res. Tech.* 52, 496–509. doi: 10.1002/1097-0029(20010301)52:5<496::AID-JEMT1035>3.0.CO;2-R

Schoniger, S., Maronde, E., Kopp, M. D., Korf, H. W., and Nurnberger, F. (2002). Transcription factor CREB and its stimulus-dependent phosphorylation in cell and explant cultures of the bovine subcommissural organ. *Cell Tissue Res.* 308, 131–142. doi: 10.1007/s00441-002-0522-2

Sepulveda, V., Maurelia, F., Gonzalez, M., Aguayo, J., and Caprile, T. (2021). SCO-spondin, a giant matricellular protein that regulates cerebrospinal fluid activity. *Fluids Barriers CNS* 18:45. doi: 10.1186/s12987-021-00277-w

Studnicka, F. (1900). Untersuchungen über den bau des ependyms der nervösen central-organe. *Anat. Hefte* 15, 303–430. doi: 10.1007/BF02109682

Szathmari, A., Champier, J., Ghersi-Egea, J. F., Jouvet, A., Watrin, C., Wierinckx, A., et al. (2013). Molecular characterization of circumventricular organs and third ventricle ependyma in the rat: potential markers for periventricular tumors. *Neuropathology* 33, 17–29. doi: 10.1111/j.1440-1789.2012.01321.x

Vera, A., Recabal, A., Saldivia, N., Stanic, K., Torrejon, M., Montecinos, H., et al. (2015). Interaction between SCO-spondin and low density lipoproteins from embryonic cerebrospinal fluid modulates their roles in early neurogenesis. *Front. Neuroanat.* 9:72. doi: 10.3389/fnana.2015.00072

Vera, A., Stanic, K., Montecinos, H., Torrejon, M., Marcellini, S., and Caprile, T. (2013). SCO-spondin from embryonic cerebrospinal fluid is required for neurogenesis during early brain development. *Front. Cell Neurosci.* 7:80. doi: 10.3389/fncel.2013.00080

Vio, K., Rodriguez, S., Navarrete, E. H., Perez-Figares, J. M., Jimenez, A. J., and Rodriguez, E. M. (2000). Hydrocephalus induced by immunological blockage of the subcommissural organ-Reissner's fiber (RF) complex by maternal transfer of anti-RF antibodies. *Exp. Brain Res.* 135, 41–52. doi: 10.1007/s002210000474

Wittkowski, W. (1998). Tanycytes and pituicytes: morphological and functional aspects of neuroglial interaction. *Microsc. Res. Tech.* 41, 29–42. doi: 10.1002/(SICI)1097-0029(19980401)41:1<29::AID-JEMT4>3.0.CO;2-P

Woodbury, M. E., and Ikezu, T. (2014). Fibroblast growth factor-2 signaling in neurogenesis and neurodegeneration. *J. Neuroimmune Pharmacol.* 9, 92–101. doi: 10.1007/s11481-013-9501-5

Xu, P., Morrison, J. P., Foley, J. F., Stumpo, D. J., Ward, T., Zeldin, D. C., et al. (2018). Conditional ablation of the RFX4 isoform 1 transcription factor: allele dosage effects on brain phenotype. *PLoS One* 13:e0190561. doi: 10.1371/journal.pone.0190561

frontiers | Frontiers in Neuroscience

TYPE Original Research
PUBLISHED 28 June 2023
DOI 10.3389/fnins.2023.1149603

OPEN ACCESS

EDITED BY
Seiji Hitoshi,
Shiga University of Medical Science, Japan

REVIEWED BY
Akio Tsuboi,
Osaka University, Japan
Takeshi Kawauchi,
Kyoto University, Japan

*CORRESPONDENCE
Takaaki Kuniya
✉ taka1129@mol.f.u-tokyo.ac.jp
Yukiko Gotoh
✉ ygotoh@mol.f.u-tokyo.ac.jp

†PRESENT ADDRESS
Yujin Harada,
Laboratory of Neural Dynamics and Cognition,
The Rockefeller University,
New York, NY, United States

RECEIVED 22 January 2023
ACCEPTED 05 June 2023
PUBLISHED 28 June 2023

CITATION
Fang L, Kuniya T, Harada Y, Yasuda O, Maeda N, Suzuki Y, Kawaguchi D and Gotoh Y (2023) TIMP3 promotes the maintenance of neural stem-progenitor cells in the mouse subventricular zone.
Front. Neurosci. 17:1149603.
doi: 10.3389/fnins.2023.1149603

TIMP3 promotes the maintenance of neural stem-progenitor cells in the mouse subventricular zone

Lingyan Fang[1], Takaaki Kuniya[1*], Yujin Harada[1†], Osamu Yasuda[2], Nobuyo Maeda[2], Yutaka Suzuki[3], Daichi Kawaguchi[1] and Yukiko Gotoh[1,4*]

[1]Graduate School of Pharmaceutical Sciences, The University of Tokyo, Tokyo, Japan, [2]Department of Sports and Life Sciences, National Institute of Fitness and Sports in Kanoya, Kanoya, Japan, [3]Department of Computational Biology and Medical Sciences, Graduate School of Frontier Sciences, The University of Tokyo, Chiba, Japan, [4]International Research Center for Neurointelligence (WPI-IRCN), The University of Tokyo, Tokyo, Japan

Adult neural stem cells (NSCs) in the mouse subventricular zone (SVZ) serve as a lifelong reservoir for newborn olfactory bulb neurons. Recent studies have identified a slowly dividing subpopulation of embryonic neural stem-progenitor cells (NPCs) as the embryonic origin of adult NSCs. Yet, little is known about how these slowly dividing embryonic NPCs are maintained until adulthood while other NPCs are extinguished by the completion of brain development. The extracellular matrix (ECM) is an essential component of stem cell niches and thus a key determinant of stem cell fate. Here we investigated tissue inhibitors of metalloproteinases (TIMPs)—regulators of ECM remodeling—for their potential roles in the establishment of adult NSCs. We found that *Timp2*, *Timp3*, and *Timp4* were expressed at high levels in slowly dividing NPCs compared to rapidly dividing NPCs. Deletion of TIMP3 reduced the number of adult NSCs and neuroblasts in the lateral SVZ. In addition, overexpression of TIMP3 in the embryonic NPCs suppressed neuronal differentiation and upregulated the expression levels of Notch signaling relating genes. These results thus suggest that TIMP3 keeps the undifferentiated state of embryonic NPCs, leading to the establishment and maintenance of adult NSCs.

KEYWORDS

TIMP3, adult neural stem cell, embryonic neural stem-progenitor cell, stem cell maintenance, notch signaling

1. Introduction

In the subventricular zone (SVZ) of the adult mouse brain, neural stem cells (NSCs) remain in the quiescent state and produce neurons throughout life (Morshead et al., 1994; Doetsch and Alvarez-Buylla, 1996; Doetsch et al., 1999). Once activated, adult NSCs generate transit-amplifying progenitors (TAPs) and then differentiate into neuroblasts. Neuroblasts later migrate into the olfactory bulb and differentiate into interneurons, which integrate into existing circuitry and modify innate and cognitive functions (Bond et al., 2015; Lledo and Valley, 2016). The mechanism by which adult NSCs are established and maintained during development is under exploration. Recent studies have revealed that a slowly dividing subpopulation of neural stem-progenitor cells (NPCs) is set aside during development and later become adult NSCs in the SVZ, while other NPCs divide rapidly and contribute to brain development by generating neurons and

glial cells (Fuentealba et al., 2015; Furutachi et al., 2015). Compared with the rapidly dividing NPCs that are extinguished after development, slowly dividing NPCs must be maintained for a longer period to generate adult NSCs. However, the regulatory mechanisms that preferentially maintain slowly dividing NPCs are not fully understood.

Stem cells are maintained in specialized microenvironments, or niches. In adult SVZ, niche-specific extracellular matrix (ECM) has been characterized (Kerever et al., 2007; Kjell et al., 2020). Given the crucial roles of the ECM in regulating NSC fate (Kazanis and Ffrench-Constant, 2011; Faissner and Reinhard, 2015; Long and Huttner, 2019), we hypothesized that factors which modify the ECM may be important for the long-term maintenance of slowly dividing NPCs. ECM remodeling is controlled by the balance between matrix metalloproteinases (MMPs) and tissue inhibitors of metalloproteinases (TIMPs). MMPs degrade ECM proteins and promote ECM turnover (Nagase and Woessner, 1999; Page-McCaw et al., 2007), while TIMPs function as endogenous inhibitors of MMPs (Brew and Nagase, 2010; Murphy, 2011). Increasing evidence has indicated the roles of MMPs in the regulation of postnatal NSC proliferation in the SVZ. MMP12 regulates postnatal ECM organization and NSC proliferation (Shan et al., 2018). MT5-MMP (MMP24) controls NSC quiescence by cleaving N-cadherin (Porlan et al., 2014). However, the function of TIMPs in embryonic NPCs or adult NSCs remains largely unknown.

Here we found that TIMP3 is expressed at a higher level in slowly dividing NPCs than in rapidly dividing NPCs. Deletion of TIMP3 reduced the number of adult NSCs in the lateral SVZ. Meanwhile, overexpression of TIMP3 suppressed neuronal differentiation of embryonic NPCs. We also found that TIMP3 overexpression enhanced the expression of genes related to Notch signaling pathway. Our findings thus uncover a physiological role for TIMP3 in the maintenance of neural stem-progenitor cells.

2. Materials and methods

2.1. Mice

Slc:ICR (ICR) and C57BL/6JJcl (B6J) mice were obtained from SLC Japan and CLEA Japan. *Rosa26-rtTA* (#006965) and *TRE-mCMV-H2B-GFP* mice (#005104) were obtained from The Jackson Laboratory. *Timp3* KO mice were produced using the gene-targeting technique described previously (Kawamoto et al., 2006). Briefly, mice carrying the mutant allele were backcrossed with B6J mice to generate KO mice in a B6J background. All mice were maintained in a temperature- and relative humidity-controlled (23 ± 3°C and 50 ± 15%, respectively) environment with a normal 12-h light/dark cycle. They were housed two to six per sterile cage (Innocage, Innovive) with chips (PALSOFT, Oriental Yeast), and with irradiated food (CE-2, CLEA Japan) and filtered water available *ad libitum*. Mouse embryos were isolated at various ages, with E0.5 being considered the time of vaginal plug appearance. All animals were maintained and studied according to protocols approved by the Animal Care and Use Committee of The University of Tokyo.

2.2. Plasmid constructs

EGFP sequence was inserted into pCAGEN to generate pCAGEN-EGFP. pCAG2-IRES-EGFP (pCAG2IG) was used as previously described (Kawai et al., 2017). The coding sequence of mouse *Timp3* was inserted into pCAGEN and pCAG2IG to generate pCAGEN-TIMP3 and pCAG2IG-TIMP3, respectively.

2.3. Injection of 9TB-dox

9-*tert*-Butyl Doxycycline (9 TB-Dox) HCl (Echelon Biosciences) was dissolved in water to a final concentration of 2 μg/μL. 240–300 μg was injected intraperitoneally.

2.4. Flow cytometry

The lateral ganglionic eminences (LGEs) were dissected and subjected to enzymatic digestion with a papain-based solution (Wako). Dissociated cells were incubated first for 15 min on ice in 0.2% bovine serum albumin (BSA)/phosphate-buffered saline (PBS) with primary antibodies—PE/Cy7 anti-CD133 (1:100, BioLegend Cat# 141210, RRID:AB_2564069), APC anti-CD24 (1,100, BioLegend Cat# 101814, RRID:AB_439716), and anti-Isolectin B_4 (biotin conjugate) (1,1,000, Sigma-Aldrich Cat# L2140, RRID:AB_2313663)—and then for 5 min on ice in 0.2% BSA/PBS with Streptavidin PE (1,500, eBioscience Cat# 12-4317-87). Cells were sorted on FACSAria IIIu (BD Bioscience). Debris and aggregated cells were removed by gating based on forward and side scatter.

2.5. Quantitative RT-PCR analysis

Total RNA was isolated from sorted NPCs using RNAiso Plus (Takara). Reverse transcription (RT) was performed with a maximum of 0.5 μg of total RNA using ReverTra Ace qPCR Master Mix with gDNA remover (TOYOBO). The resulting cDNA was subjected to real-time PCR analysis in LightCycler 480 II (Roche) with KAPA SYBR Fast qPCR Kit (NIPPON Genetics). The amount of target mRNA was normalized by that of *Actb* mRNA. Primer sequences were as follows:

Actb
Forward: 5'-AATAGTCATTCCAAGTATCCATGAAA-3'
Reverse: 5'-GCGACCATCCTCCTCTTAG-3'.
Timp2
Forward: 5'-GTTGGAGGAAAGAAGGAGTATCTAA-3'
Reverse: 5'-ACAATGAAGTCACAGAGGGTA-3'.
Timp3
Forward: 5'-CCTGGCTATCAGTCCAAAC-3'
Reverse: 5'-GTTGCTGATGCTCTTGTCT-3'.
Timp4
Forward: 5'-ATCCATCTGTGCAACTACATT-3'
Reverse: 5'-GTTCTGGTGGTAGTGATGATTC-3'.
Sdc2
Forward: 5'-CTCATGGTGTCTGTCAATCA-3'
Reverse: 5'-CCAAATACATGCAGAATAACAATACTT-3'.

2.6. Immunohistofluorescence analysis

Mice were subjected to perfusion fixation with ice-cold 4% paraformaldehyde (Merck) in PBS. The brain was isolated and

exposed to the same fixative at 4°C for 120 min (postnatal) or 90 min (embryonic), equilibrated with 30% (w/v) sucrose in PBS, embedded in OCT compound (Tissue TEK), and frozen. Coronal sections (thickness of 12 μm) were exposed to Tris-buffered saline containing 0.1% Triton X-100 and 3% bovine serum albumin (blocking solution) for 2 h at room temperature, then incubated overnight at 4°C with primary antibodies in blocking solution and for 2 h at room temperature with Alexa Fluor-conjugated secondary antibodies (1:500, Thermo Fisher Scientific) and Hoechst 33342 (1:2000, Molecular Probes) in blocking solution, finally mounted in Mowiol (Calbiochem). Images were obtained with a laser confocal microscope (Leica TCS-SP5, Leica Mica, or Zeiss LSM 880) and were processed with LAS AF (Leica), ZEN (Zeiss), and Fiji (U.S. National Institutes of Health) software. Primary antibodies were as follows: anti-Ascl1 (1:500, BD Biosciences Cat# 556604, RRID:AB_396479), anti-Collagen IV (1:50, Abcam Cat# ab6586, RRID:AB_305584), anti-Dcx (1:1000, Abcam Cat# ab18723, RRID:AB_732011), anti-EGFR (1:500, Fitzgerald Industries International Cat# 20-ES04, RRID:AB_231428), anti-GFAP (1:1000, Abcam Cat# ab4674, RRID:AB_304558), anti-GFP (1:2000, Abcam Cat# ab13970, RRID:AB_300798; 1:1000, Nacalai Tesque Cat# GF090R, RRID:AB_2314545), anti-Ki67 (1:500, Agilent Cat# M7249, RRID:AB_2250503), anti-Sox2 (1:200, Cell Signaling Technology Cat# 3728, RRID:AB_2194037; 1:500, Santa Cruz Biotechnology Cat# sc-17320, RRID:AB_2286684), anti-S100β (1:200, Sigma-Aldrich Cat# S2657, RRID:AB_261477), anti-Tbr2 (1:1000, Millipore Cat# AB15894, RRID:AB_10615604; 1:500, Abcam Cat# ab23345, RRID:AB_778267), and anti-Tenascin C (1:50, Abcam Cat# ab108930, RRID:AB_10865908).

2.7. Administration of thymidine analogs

For identifying slowly dividing NPCs, 5-ethynyl-2'-deoxyuridine (EdU, Invitrogen, 5 mg/kg body weight) was injected intraperitoneally four times at 3-h intervals at embryonic day (E) 10.5. EdU was detected using Click-iT Plus EdU Cell Proliferation Kit for Imaging (Invitrogen).

2.8. *In utero* electroporation

The introduction of plasmid DNA into NPCs in the embryonic brain was performed as previously described (Tabata and Nakajima, 2001). In brief, plasmid DNA was injected into the lateral ventricle with an injector (FemtoJet, Eppendorf), electrodes were positioned at the flanking ventricular regions, and four–eight pulses of 35–45 V for 50 ms were applied at intervals of 950 ms using an electroporator (CUY21, NEPA GENE). The uterine horn was returned to the abdominal cavity so that the embryos continued to develop. The pCAGEN-EGFP plasmid was used to identify successfully electroporated cells.

2.9. RNA-sequencing (Quartz-Seq) analysis

RNA extraction, reverse transcription, and amplification of cDNA were performed on 1,000 cells aliquoted by FACS as described previously (Sasagawa et al., 2013). In brief, total RNA was purified using AMPure XP RNA cDNA (Beckman) and was subjected to reverse transcription with SuperScript III (Thermo Scientific). The cDNA was purified using AMPure XP (Beckman). Primers were digested by adding ExoI (Takara). Poly-A tail was added with terminal deoxynucleotidyl transferase (Roche). The cDNA was amplified using MightyAmp DNA polymerase (Takara) and was purified using PCR Extraction Kit (Nippon Genetics). Sequence data were obtained with a 36-base single-end on the Illumina HiSeq2500 platform. Approximately 2–4 million sequences were obtained from each sample. Sequences were mapped to the mouse genome (mm9) using ELAND v2 (Illumina). Only uniquely mapped reads with no base mismatches were used. Reads were normalized by TMM (weighted trimmed mean of M-values) normalization (Robinson and Oshlack, 2010) as implemented by the R package *edgeR* (RRID:SCR_012802) (Robinson et al., 2009). Differential gene expression analysis was performed using *edgeR*. Reads per kilobase of mRNA model per million total reads (RPKM) was calculated to analyze gene expression levels. Processed data of RNA sequence was shown in Supplementary Table 1. Gene ontology and pathway enrichment analysis were conducted with WebGestalt: WEB-based GEne SeT AnaLysis Toolkit (RRID:SCR_006786) (Liao et al., 2019).

2.10. Statistical analysis

Quantitative data are presented as means ± SEM and were compared with the two-tailed paired *t* test or the two-tailed Student's *t* test as indicated using GraphPad Prism (RRID:SCR_002798). A p value of <0.05 was considered statistically significant. The number of animals in each experiment is stated in the respective figure legends.

3. Results

3.1. *Timp2, Timp3*, and *Timp4* are highly expressed in slowly dividing embryonic NPCs and adult quiescent NSCs

We first compared the expression levels of TIMP family members between rapidly and slowly dividing NPCs in the lateral ganglionic eminences (LGEs). To monitor cell division frequency, we performed a histone 2B (H2B)-GFP retention analysis (Furutachi et al., 2015). Ubiquitous H2B-GFP expression was transiently induced at E9.5 by a single 9-tert-butyldoxycycline (9 TB-Dox) injection into pregnant *Rosa-rtTA;TRE-mCMV-H2B-GFP* mice. At E17.5, we collected two populations of $CD133^{+}CD24^{-}$Isolectin B_4^{-} NPCs from the LGE according to H2B-GFP fluorescence intensity: the bottom 10% as the rapidly dividing NPCs and the top 10% as the slowly dividing NPCs (Figures 1A,B). Quantitative RT-PCR analysis revealed that the abundance of *Timp2*, *Timp3*, and *Timp4* mRNAs was significantly higher in slowly dividing NPCs than in rapidly dividing NPCs (Figure 1C).

We also analyzed the expression levels of TIMPs in the adult SVZ. A previous study has performed single-cell RNA-sequencing from quiescent NSCs (qNSCs), activated NSCs (aNSCs), and TAPs from SVZs of young adult (3 months old) mice (Dulken et al., 2017). Reanalyzing the data, we found that *Timp2*, *Timp3*, and *Timp4* were expressed relatively at high levels in qNSCs compared to aNSCs and

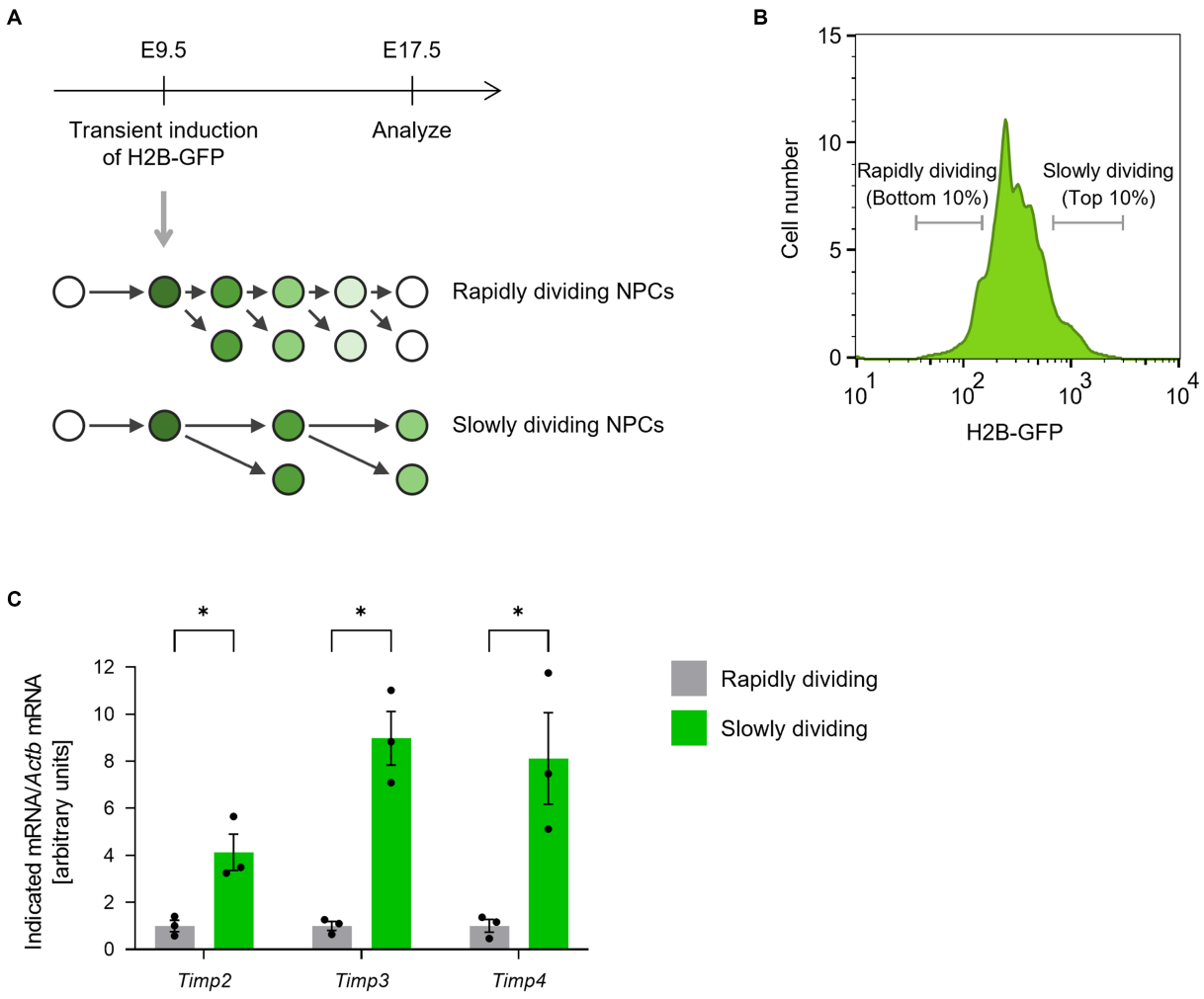

FIGURE 1
Timp2, *Timp3*, and *Timp4* are highly expressed in slowly dividing NPCs. **(A)** The scheme for isolating rapidly dividing and slowly dividing NPCs. H2B-GFP was transiently induced at E9.5 and the LGE was dissected at E17.5. NPCs were defined as cells positive for NPC marker CD133, negative for neuronal marker CD24, and negative for endothelial marker Isolectin B_4. **(B)** Representative flow cytometric histogram of H2B-GFP fluorescence intensity. Rapidly dividing NPCs (bottom 10% of NPCs for H2B-GFP intensity) and slowly dividing NPCs (top 10% of NPCs for H2B-GFP intensity) were collected. **(C)** Quantitative RT-PCR analysis of *Timp2*, *Timp3*, and *Timp4* mRNAs. Data are means ± SEM (n=3 independent experiments). *p<0.05 by two-tailed paired t test.

TAPs (Figure 2). Together, these results suggest that *Timp2*, *Timp3*, and *Timp4* are highly expressed in quiescent subpopulations of both embryonic NPCs and adult NSCs.

3.2. TIMP3 contributes to the establishment or maintenance of adult NSCs in the lateral SVZ

We next sought to examine the role of TIMPs in the genesis of adult NSCs. Here, we focused on TIMP3, given that TIMP2 has been shown to promote neuronal differentiation (Pérez-Martínez and Jaworski, 2005) and that TIMP4 is expressed relatively at a low level in NPCs in the embryonic mouse forebrain compared to TIMP2 and TIMP3 (La Manno et al., 2021). Since slowly dividing embryonic NPCs give rise to the majority of adult NSCs in the lateral wall of the SVZ (Furutachi et al., 2015), We examined whether TIMP3 is required for generating adult NSCs in the corresponding area (Figure 3A). We used *Timp3* knockout (KO) mice (postnatal day (P) 61–P111), which are viable and fertile and develop with no overt abnormalities (Kawamoto et al., 2006). Crucially, *Timp3* KO mice showed a reduced number of $GFAP^+Sox2^+S100\beta^-$ adult NSCs in the lateral SVZ compared with wild-type (WT) mice (Figures 3B,C). We further followed the effects of TIMP3 deletion on descendants of NSCs. Although the number of $GFAP^-EGFR^+S100\beta^-$ TAPs was not significantly changed (Supplementary Figures 1A,B), the number of Dcx^+ neuroblasts was decreased in *Timp3* KO mice (Figures 3D,E). Therefore, TIMP3 appears to play an important role in increasing adult NSCs and neurogenesis in the lateral SVZ.

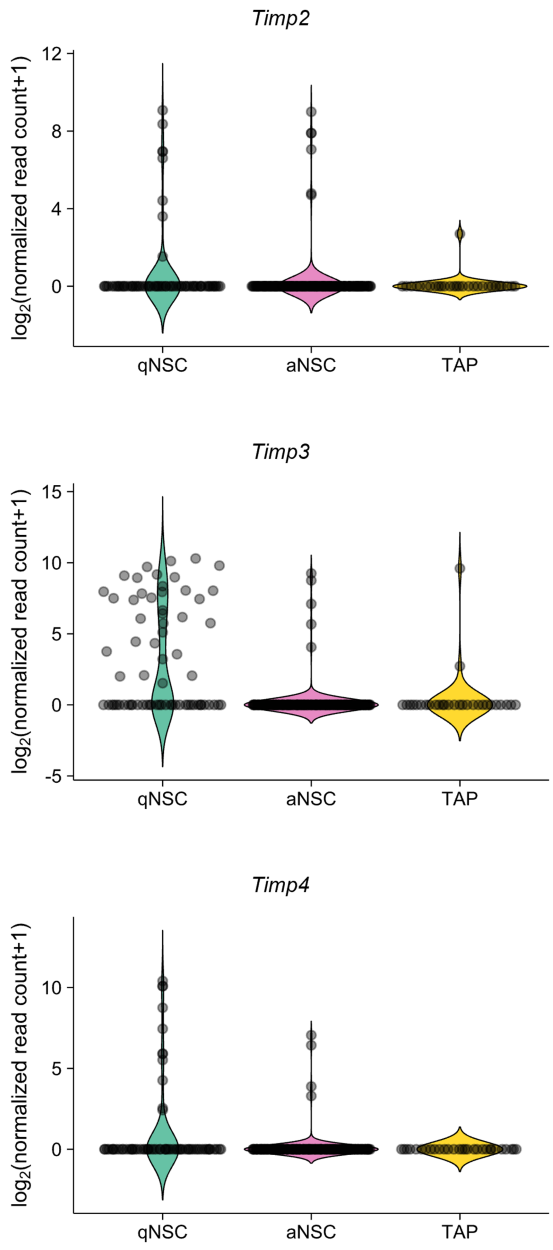

FIGURE 2
Timp2, *Timp3*, and *Timp4* are highly expressed in qNSCs in the adult SVZ. Expression of *Timp2*, *Timp3*, and *Timp4* in qNSCs, aNSCs, and TAPs (NPCs) from the SVZs of adult mice. Data were obtained from the previous study (Dulken et al., 2017).

3.3. TIMP3 is not essential for the emergence of slowly dividing embryonic NPCs

We then asked whether TIMP3 regulates the emergence of slowly dividing embryonic NPCs. Using *Timp3* KO mice, we tested whether TIMP3 deletion affects the abundance of slowly dividing NPCs. We detected slowly dividing NPCs based on 5-ethynyl-2′-deoxyuridine (EdU) retention at E17.5 after injecting it into pregnant mice at E10.5 (Figure 4A). No significant difference, however, was found in the number of EdU-retaining slowly dividing Sox2$^+$ NPCs in the dorsal LGE (dLGE) between WT mice and *Timp3* KO mice (Figures 4B,C). This result suggests that TIMP3 may not be required for the establishment of slowly dividing embryonic NPCs.

3.4. TIMP3 contributes to the maintenance of embryonic NPCs in the LGE

We then investigated the role for TIMP3 in the maintenance of slowly dividing NPCs. Slowly dividing embryonic NPCs are expected to be maintained in the undifferentiated state for a long period to become adult NSCs. We thus assumed that expression of TIMP3 at a high level might help maintain the undifferentiated state of slowly dividing NPCs. To test this possibility, we overexpressed TIMP3 in embryonic NPCs in the LGE at E14.5 by *in utero* electroporation (Figure 5A). Overexpression of TIMP3 significantly increased the percentage of Sox2$^+$Ascl1$^-$ undifferentiated cells at E17.5 (Figures 5B,C). This indicates the role of TIMP3 in maintaining the undifferentiated state of NPCs in the LGE.

3.5. TIMP3 promotes the maintenance of embryonic NPCs in the neocortex

To test whether the maintenance of undifferentiated state mediated by TIMP3 can also be seen in other brain regions, we ectopically overexpressed TIMP3 in neocortical NPCs, in which the level of endogenous *Timp3* appears to be lower than that in NPCs located in the LGE (Figure 6A; Supplementary Figure 2). Overexpression of TIMP3 at E14.5 increased the fraction of Sox2$^+$Tbr2$^-$ undifferentiated cells in the ventricular zone (VZ) (Figures 6B,C). Furthermore, we found that TIMP3 overexpression resulted in an increased proportion of GFP$^+$ cells residing in the VZ and a reduced proportion of GFP$^+$ cells in the cortical plate (CP) at E17.5 (Figures 6D,E). These results support the notion that TIMP3 promotes maintenance of the undifferentiated state of NPCs. Since cell cycle inhibition has been shown to promote NPC maintenance (Furutachi et al., 2015), we looked into the possible role of TIMP3 in regulating the cell cycle of NPCs. TIMP3 overexpression, however, did not change the fraction of cells positive for the proliferation marker Ki67 among Tbr2$^-$ cells in the VZ (Supplementary Figures 3A,B). Thus, the increased proportion of cells remaining in the VZ was not likely attributable to cell cycle arrest.

To investigate the mechanism by which TIMP3 promotes NPC maintenance, we collected CD133$^+$CD24$^-$ NPCs positive for GFP by FACS from the neocortex of E17.5 embryos and performed RNA-sequencing (Quartz-Seq). 2,725 differentially expressed genes (DEGs) were found using the R package *edgeR* (Robinson et al., 2009), with 2,106 genes upregulated and 619 genes downregulated by TIMP3 overexpression (Supplementary Table 1). Pathway enrichment analysis of DEGs showed that genes upregulated in TIMP3-overexpreesed NPCs are enriched with those related to Delta-Notch signaling (Figure 7A). TIMP3 overexpression increased the levels of Notch receptors (*Notch1* and *Notch3*), Notch downstream effector (*Hey1*), and Notch pathway co-factor (*Rbpj*) (Figure 7B). Furthermore, overexpression of TIMP3 reduced the level of *Neurog1*, a proneural transcription factor negatively regulated by Notch signaling (Figure 7B). These results suggest that Notch signaling may

10.3389/fnins.2023.1149603

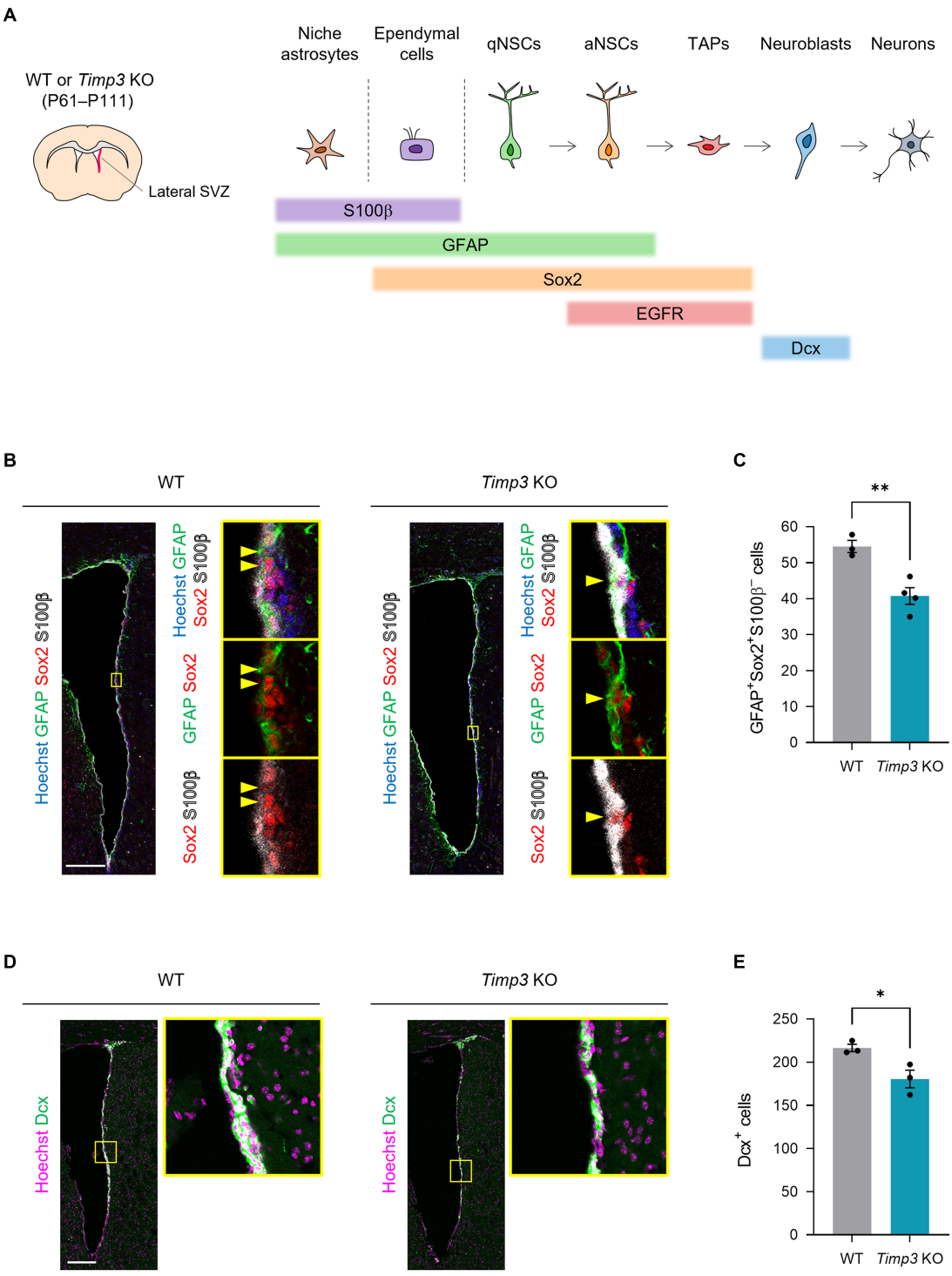

FIGURE 3
TIMP3 deletion reduces adult NSCs and neuroblasts. **(A)** Schematic showing the location of lateral SVZ and the makers for each cell type. WT mice and *Timp3* KO mice were sacrificed at P61–P111. The lateral wall of the SVZ was analyzed. **(B)** Immunohistofluorescence analysis of GFAP, Sox2, and S100β. Nuclei were stained with Hoechst 33342. Scale bar: 200μm. Arrowheads indicate $GFAP^+Sox2^+S100\beta^-$ adult NSCs. **(C)** Quantification of $GFAP^+Sox2^+S100\beta^-$ adult NSCs. Data are means ± SEM (n=3 and 4 animals for WT and *Timp3* KO, respectively). $^{**}p<0.01$ by two-tailed Student's t test. **(D)** Immunohistofluorescence analysis of Dcx. Nuclei were stained with Hoechst 33342. Scale bar: 200μm. **(E)** Quantification of Dcx^+ neuroblasts. Data are means ± SEM (n=3 and 3 animals for WT and *Timp3* KO, respectively). $^{*}p<0.05$ by two-tailed Student's t test.

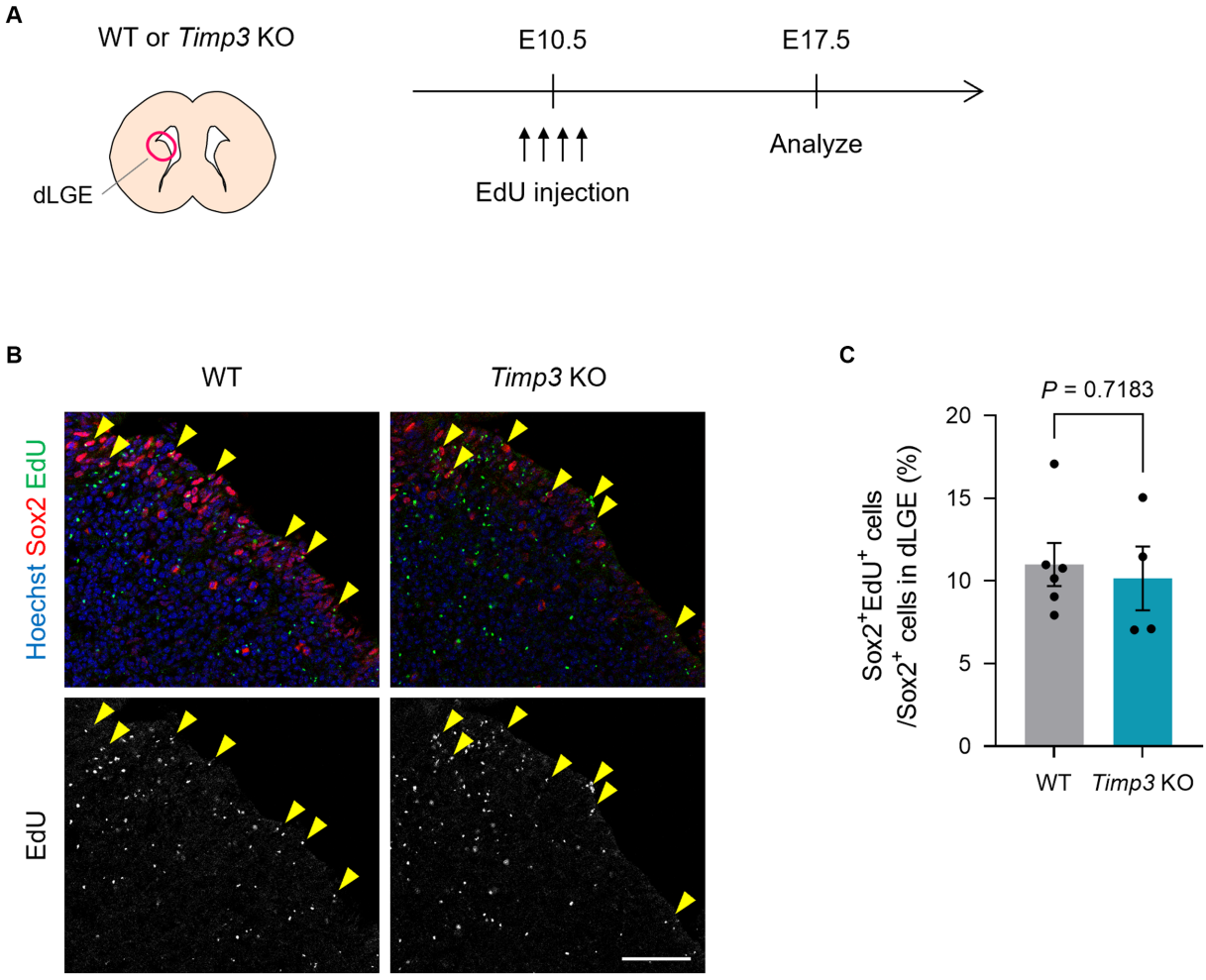

FIGURE 4
TIMP3 deletion does not change the number of slowly dividing embryonic NPCs. **(A)** Experimental design. EdU was injected intraperitoneally at E10.5 into pregnant WT and *Timp3* KO mice. Brain sections were obtained at E17.5 and dLGE was analyzed. **(B)** Immunohistofluorescence analysis of Sox2 and staining for EdU. Nuclei were stained with Hoechst 33342. Scale bar: 50μm. Arrowheads indicate $Sox2^+EdU^+$ slowly dividing NPCs. **(C)** Quantification of EdU^+ slowly dividing cells among $Sox2^+$ NPCs in the dLGE. Data are means ± SEM (n=6 and 4 embryos for WT and *Timp3* KO, respectively). Two-tailed Student's t test.

be activated in TIMP3-overexpressed NPCs and keep their undifferentiated state.

4. Discussion

The developmental process leading to the establishment of adult tissue stem cells is a fundamental question. A slowly dividing subpopulation of NPCs has been identified as the embryonic origin of adult NSCs. The regulatory mechanism of this population, however, is not well understood. In the present study, we show that TIMP3 is preferentially expressed in slowly dividing NPCs—an embryonic origin of adult NSCs—compared with rapidly dividing NPCs—a cellular source of brain development. Deletion of TIMP3 reduced the adult NSC pool in the lateral SVZ, without changing the initial population of slowly dividing embryonic NPCs. These results implicate TIMP3 in the long-term maintenance of slowly dividing NPCs, an essential basis for the genesis of adult NSCs.

How then does TIMP3 mediate the long-term maintenance of neural stem-progenitor cells at a molecular level? Overexpression of TIMP3 in the embryonic NPCs suppressed neural differentiation both in the GE and in the neocortex. Importantly, TIMP3-overexpressed NPCs showed increased levels of *Notch1*, *Notch3*, and *Hey1*, suggesting that Notch signaling is activated in TIMP3-overexpressed NPCs. Notch signaling plays a crucial role in the maintenance of the undifferentiated state of both embryonic NPCs and adult NSCs (Gaiano et al., 2000; Imayoshi et al., 2010; Kawaguchi et al., 2013; Engler et al., 2018; Sueda et al., 2019; Zhang et al., 2019). High levels of active Notch1 and its downstream effector Hey1 in slowly dividing NPCs have been implicated in robust maintenance of the undifferentiated state from the embryonic to postnatal stages (Harada et al., 2021). Notch3 has been shown to be responsible for the maintenance of quiescent adult NSCs (Kawai et al., 2017; Than-trong et al., 2018). Our results thus suggest that TIMP3 may maintain the undifferentiated state of neural stem-progenitor cells potentially through the activation of Notch signaling.

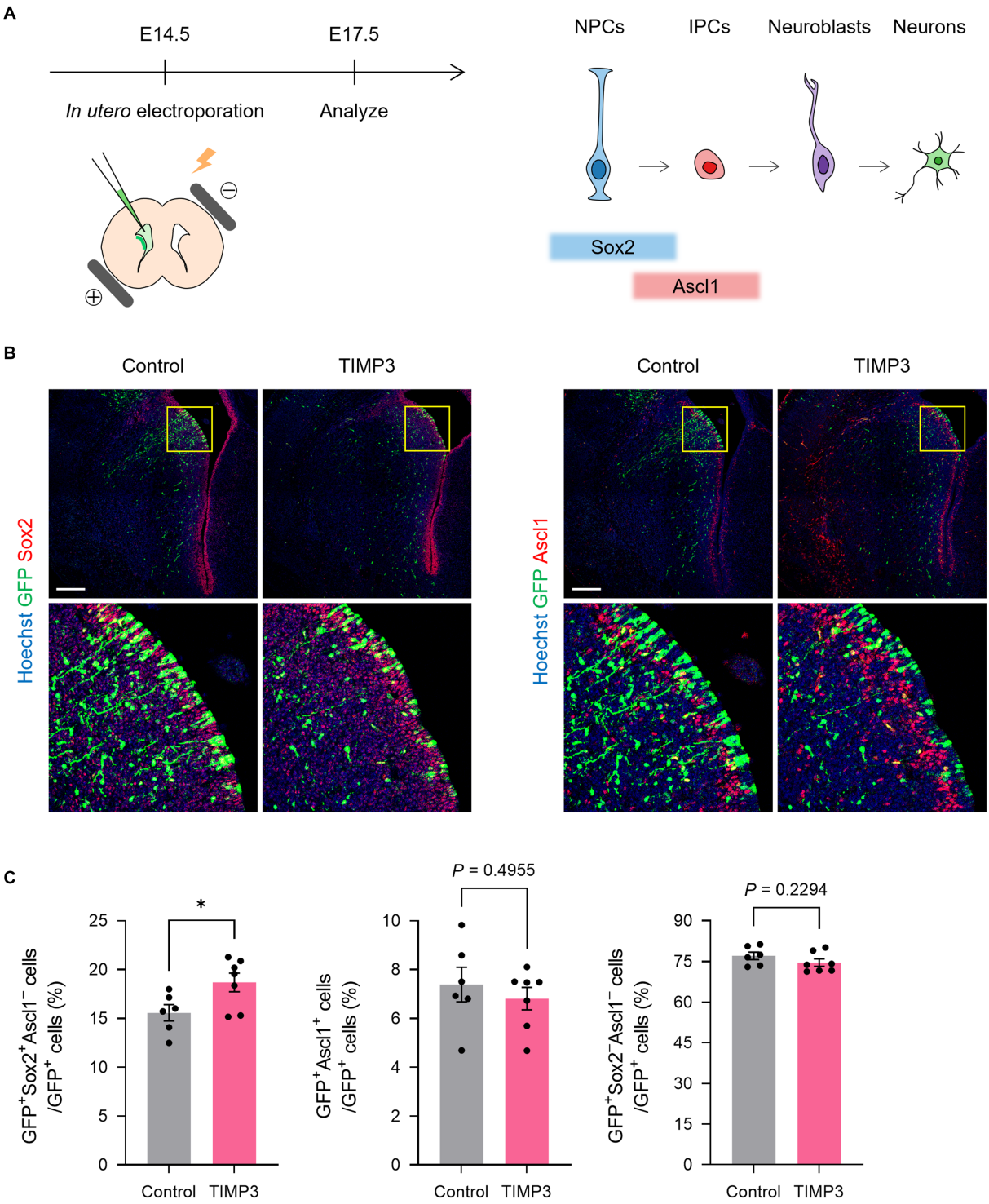

FIGURE 5
TIMP3 overexpression suppresses neuronal differentiation in the developing LGE. **(A)** Schematic showing the experimental design and the markers for each cell type. *In utero* electroporation was performed at E14.5 with plasmids expressing GFP, alone (control) or together with TIMP3. Embryos were analyzed at E17.5. NPC, neural progenitor cell; IPC, intermediate progenitor cell. **(B)** Immunohistofluorescence analysis of GFP, Sox2, and Ascl1. Nuclei were stained with Hoechst 33342. Scale bars: 200μm. **(C)** Quantification of the proportion of $Sox2^+Ascl1^-$ cells, $Ascl1^+$ cells, and $Sox2^-Ascl1^-$ cells among GFP^+ cells. Data are means ± SEM (n=6 and 7 embryos for control and *Timp3*, respectively). *p<0.05 by two-tailed Student's t test.

Considering the canonical functions of TIMP3 in ECM remodeling via MMP inhibition, it is of interest that gene ontology and pathway enrichment analysis showed that upregulated genes in neocortical NPCs by TIMP3 overexpression include those related to Hippo signaling, indicating the possibility that ECM dynamics were altered by TIMP3 overexpression (Supplementary Figure 4).

10.3389/fnins.2023.1149603

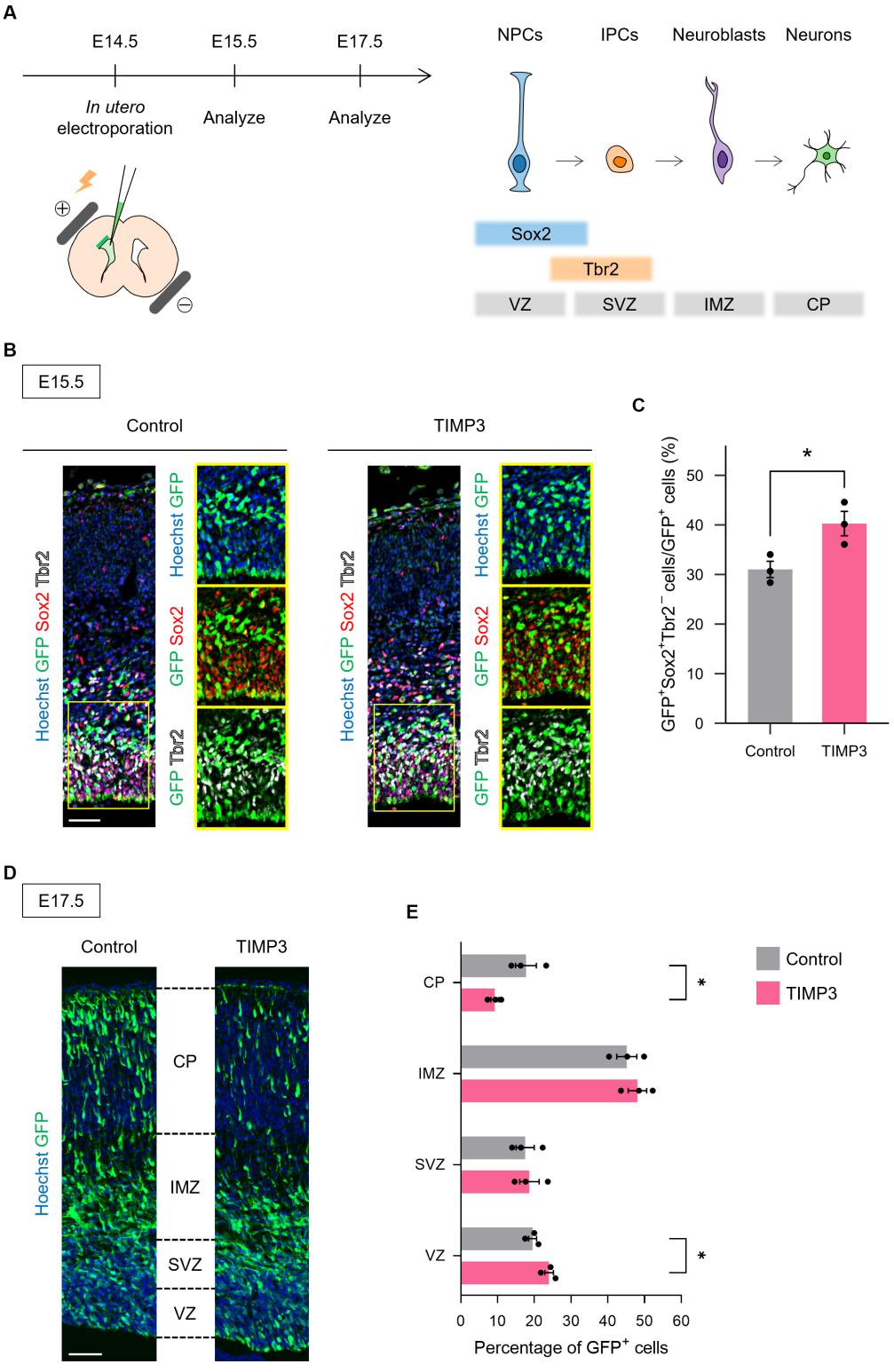

FIGURE 6
TIMP3 overexpression suppresses neuronal differentiation in the developing neocortex. **(A)** Schematic showing the experimental design and the markers for each cell type. *In utero* electroporation was performed at E14.5 with plasmids expressing GFP, alone (control) or together with TIMP3. NPC, neural progenitor cell; IPC, intermediate progenitor cell; VZ, ventricular zone; SVZ, subventricular zone; IMZ, intermediate zone; CP, cortical plate. **(B)** Embryos were subjected to immunohistofluorescence analysis of GFP, Sox2, and Tbr2 at E15.5. Nuclei were stained with Hoechst 33342. Scale bar: 50μm. **(C)** Quantification of the proportion of $Sox2^+Tbr2^-$ cells in the VZ among GFP^+ cells. Data are means ± SEM (n=3 and 3 embryos for control and TIMP3, respectively). *p<0.05 by two-tailed Student's t test. **(D)** Embryos were subjected to immunohistofluorescence analysis of GFP at E17.5. Nuclei were stained with Hoechst 33342. Scale bar: 50μm. **(E)** Distribution of GFP^+ cells. Data are means ± SEM (n=3 and 3 embryos for control and TIMP3, respectively). *p<0.05 by two-tailed Student's t test.

A

Pathway	FDR
PluriNetWork	8.7×10^{-7}
EGFR1 Signaling Pathway	2.1×10^{-4}
Signaling of Hepatocyte Growth Factor Receptor	1.3×10^{-3}
Insulin Signaling	4.6×10^{-3}
MAPK signaling pathway	7.0×10^{-3}
mRNA processing	7.0×10^{-3}
IL-2 Signaling Pathway	7.0×10^{-3}
Kit Receptor Signaling Pathway	1.1×10^{-2}
Regulation of Actin Cytoskeleton	1.1×10^{-2}
BMP Signaling Pathway in Eyelid Development	1.1×10^{-2}
MicroRNAs in Cardiomyocyte Hypertrophy	1.2×10^{-2}
IL-7 Signaling Pathway	2.3×10^{-2}
Toll Like Receptor signaling	2.3×10^{-2}
Delta-Notch Signaling Pathway	3.0×10^{-2}
TGF Beta Signaling Pathway	3.0×10^{-2}
G Protein Signaling Pathways	3.6×10^{-2}
EPO Receptor Signaling	4.6×10^{-2}
Endochondral Ossification	4.7×10^{-2}
ESC Pluripotency Pathways	5.2×10^{-2}
Hedgehog Signaling Pathway	5.2×10^{-2}

B

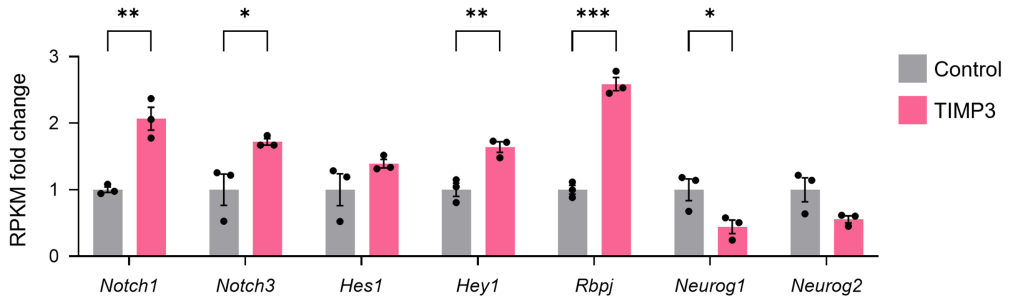

FIGURE 7
TIMP3 overexpression upregulates Notch signaling-related genes. **(A)** Pathway (WikiPathway) enrichment analysis of TIMP3-expressing NPCs enriched genes (*edgeR*; $p<0.05$). The top 20 are ranked by FDR. **(B)** RPKM fold change relative to the average of control samples. Data are means ± SEM ($n=3$ independent experiments). *$p<0.05$, **$p<0.01$, ***$p<0.001$ by two-tailed Student's *t* test.

We performed immunostaining for Collagen IV and Tenascin C, two major ECM proteins expressed in embryonic NPCs. However, we could not detect obvious changes in their expression levels and distribution by TIMP3 overexpression (Supplementary Figures 5A,B). Thus, there might be other extracellular matrix proteins that are regulated by TIMP3. For example, *Sdc2* (coding for the ECM protein Syndecan2) is highly expressed in slowly dividing NPCs than in rapidly dividing NPCs (Supplementary Figure 6). We also found that the level of *Sdc2* mRNA was increased by TIMP3 overexpression (Supplementary Figure 7). Of note, Syndecan2 and Syndecan3 have been found to promote Notch signaling through direct interactions with Notch3 and Notch1, respectively (Pisconti et al., 2010; Zhao et al., 2012). It is thus possible that TIMP3 promotes the direct interactions between syndecans and Notch receptors and thereby activates Notch signaling (Supplementary Figure 8). Beside ECM remodeling, other mechanisms might link TIMP3 to the activation of Notch signaling. MT1-MMP (MMP14), a candidate target of TIMP3, is expressed in the mouse developing forebrain (La Manno et al., 2021) and has been reported to negatively regulate Notch signaling by cleaving the Notch ligand Dll1 (Jin et al., 2011; Jiang et al., 2020). Therefore, TIMP3 may activate Notch signaling *via* suppression of MT1-MMP. Future investigation of MMPs and ECM remodeling would provide more insight into downstream mechanisms.

The mechanisms responsible for different expression levels of TIMP3 between slowly and rapidly dividing NPCs remain unclear. Of note, previous RNA sequencing data (Harada et al., 2021) revealed that cyclin-dependent kinase inhibitor p57 overexpression increased the mRNA level of *Timp3* in neocortical NPCs (Supplementary Figure 9). Given that p57 is highly expressed in slowly dividing NPCs compared to rapidly dividing ones, it is possible that p57 itself or cell cycle arrest upregulates *Timp3* expression level in slowly dividing NPCs.

In conclusion, we have here unveiled the role of TIMP3 in the maintenance of embryonic NPCs and adult NSCs in the mouse subventricular zone. In the hippocampus, the other known neurogenic region of the adult mammal brain, *Timp3* was also enriched in quiescent

NSCs and downregulated upon activation (Shin et al., 2015). Another study has reported that *Timp3* KO mice showed enhanced MMP activity in the hippocampus and delayed acquisition of spatial memory compared with WT mice (Baba et al., 2009). Since hippocampal neurogenesis is considered to be involved in memory formation, it will be of interest to examine the possible role of TIMP3 in hippocampal NSCs. Studies have shown the roles of TIMP3 in the regulation of other tissue stem cells as well. In mouse muscles, TIMP3 has been shown to suppress myogenic differentiation (Liu et al., 2010). The only *Drosophila timp* is required for normal oogenesis of the female germline stem cells (Pearson et al., 2016). Our findings thus provide novel evidence supporting the role of TIMP3 in long-term stem cell maintenance that may be shared by various adult tissue stem cells.

Data availability statement

The authors acknowledge that the data presented in this study must be deposited and made publicly available in an acceptable repository, prior to publication. Frontiers cannot accept a manuscript that does not adhere to our open data policies. The sequence data have been deposited in the DNA Data Bank of Japan (DDBJ) Sequence Read Archive under the following accession number: DRA016558.

Ethics Statement

The animal study was reviewed and approved by the Animal Care and Use Committee of the University of Tokyo.

Author contributions

LF: conception and design, collection and assembly of data, data analysis and interpretation, and manuscript writing. TK: conception and design, collection and assembly of data, data interpretation, and supervision. YH: data interpretation and supervision. OY and NM: generating *Timp3* KO mice. YS: performing RNA sequencing experiments and analysis of RNA sequencing data. DK: data interpretation, financial support, and supervision. YG: conception and design, data interpretation, financial support, administrative support, supervision, and manuscript writing. All authors contributed to the article and approved the submitted version.

Funding

This study was supported by the World-leading INnovative Graduate Study Program for Life Science and Technology of the University of Tokyo; by KAKENHI grants from the Ministry of Education, Culture, Sports, Science, and Technology of Japan and the Japan Society for the Promotion of Science (JP20J23093 to LF, JP16J03852 to TK, JP21K15180 to YH, JP21K06387 to DK, and JP15H05773, JP16H06279, JP16H06479, JP16H06481, JP22H00431, JP16H06279 to YG); by AMED-CREST of the Japan Agency for Medical Research and Development (JP19gm0610013, JP22gm1310004); by the Uehara Memorial Foundation; by the Japan Foundation for Applied Enzymology; and by the International Research Center for Neurointelligence (WPI-IRCN), the University of Tokyo Institutes for Advanced Study.

Acknowledgments

The authors thank M. Iwamoto for generating *Timp3* KO mice from frozen sperms; K. Imamura and T. Horiuchi (The University of Tokyo) for performing RNA-sequencing analysis. One-Stop Sharing Facility Center for Future Drug Discoveries (The University of Tokyo) for sharing instruments; and members of the Gotoh laboratory for technical assistance and discussion.

Conflict of interest

The authors declare that the research was conducted in the absence of any commercial or financial relationships that could be construed as a potential conflict of interest.

Publisher's note

Supplementary material

The Supplementary material for this article can be found online at: https://www.frontiersin.org/articles/10.3389/fnins.2023.1149603/full#supplementary-material

References

Baba, Y., Yasuda, O., Takemura, Y., Ishikawa, Y., Ohishi, M., Iwanami, J., et al. (2009). Timp-3 deficiency impairs cognitive function in mice. *Lab. Invest.* 89, 1340–1347. doi: 10.1038/labinvest.2009.101

Bond, A. M., Ming, G. L., and Song, H. (2015). Adult mammalian neural stem cells and neurogenesis: five decades later. *Cell Stem Cell* 17, 385–395. doi: 10.1016/j.stem.2015.09.003

Brew, K., and Nagase, H. (2010). The tissue inhibitors of metalloproteinases (TIMPs): an ancient family with structural and functional diversity. *Biochim. Biophys. Acta.* 1803, 55–71. doi: 10.1016/j.bbamcr.2010.01.003

Doetsch, F., and Alvarez-Buylla, A. (1996). Network of tangential pathways for neuronal migration in adult mammalian brain. *Proc. Natl. Acad. Sci.* 93, 14895–14900. doi: 10.1073/pnas.93.25.14895

Doetsch, F., Caille, I., Lim, D. A., García-Verdugo, J. M., Alvarez-Buylla, A., et al. (1999). Subventricular zone astrocytes are neural stem cells in the adult mammalian brain. *Cell* 97, 703–716. doi: 10.1016/S0092-8674(00)80783-7

Dulken, B. W., Leeman, D. S., Boutet, S. C., Hebestreit, K., and Brunet, A. (2017). Single-cell transcriptomic analysis defines heterogeneity and transcriptional dynamics in the adult neural stem cell lineage. *Cell Rep.* 18, 777–790. doi: 10.1016/j.celrep.2016.12.060

Engler, A., Rolando, C., Giachino, C., Saotome, I., Erni, A., Brien, C., et al. (2018). Notch2 signaling maintains NSC quiescence in the murine ventricular-subventricular zone. *Cell Rep.* 22, 992–1002. doi: 10.1016/j.celrep.2017.12.094

Faissner, A., and Reinhard, J. (2015). The extracellular matrix compartment of neural stem and glial progenitor cells. *Glia* 63, 1330–1349. doi: 10.1002/glia.22839

Fuentealba, L. C., Rompani, S. B., Parraguez, J. I., Obernier, K., Romero, R., Cepko, C. L., et al. (2015). Embryonic origin of postnatal neural stem cells. *Cell* 161, 1644–1655. doi: 10.1016/j.cell.2015.05.041

Furutachi, S., Miya, H., Watanabe, T., Kawai, H., Yamasaki, N., Harada, Y., et al. (2015). Slowly dividing neural progenitors are an embryonic origin of adult neural stem cells. *Nat. Neurosci.* 18, 657–665. doi: 10.1038/nn.3989

Gaiano, N., Nye, J. S., and Fishell, G. (2000). Radial glial identity is promoted by Notch1 signaling in the murine forebrain. *Neuron.* 26, 395–404. doi: 10.1016/S0896-6273(00)81172-1

Harada, Y., Yamada, M., Imayoshi, I., Kageyama, R., Suzuki, Y., Kuniya, T., et al. (2021). Cell cycle arrest determines adult neural stem cell ontogeny by an embryonic notch-nonoscillatory Hey1 module. *Nat. Commun.* 12, 1–16. doi: 10.1038/s41467-021-26605-0

Imayoshi, I., Sakamoto, M., Yamaguchi, M., Mori, K., and Kageyama, R. (2010). Essential roles of notch signaling in maintenance of neural stem cells in developing and adult brains. *J. Neurosci.* 30, 3489–3498. doi: 10.1523/JNEUROSCI.4987-09.2010

Jiang, Z., Zhou, J., Qin, X., Zheng, H., Gao, B., Liu, X., et al. (2020). MT1-MMP deficiency leads to defective ependymal cell maturation, impaired ciliogenesis, and hydrocephalus. *JCI Insight* 5:e132782. doi: 10.1172/jci.insight.132782

Jin, G., Zhang, F., Chan, K. M., Xavier Wong, H. L., Liu, B., Cheah, K. S. E., et al. (2011). MT1-MMP cleaves Dll1 to negatively regulate notch signalling to maintain normal B-cell development. *EMBO J.* 30, 2281–2293. doi: 10.1038/emboj.2011.136

Kawaguchi, D., Furutachi, S., Kawai, H., Hozumi, K., and Gotoh, Y. (2013). Dll1 maintains quiescence of adult neural stem cells and segregates asymmetrically during mitosis. *Nat. Commun.* 4, 1–12. doi: 10.1038/ncomms2895

Kawai, H., Kawaguchi, D., Kuebrich, B. D., Kitamoto, T., Yamaguchi, M., Gotoh, Y., et al. (2017). Area-specific regulation of quiescent neural stem cells by Notch3 in the adult mouse subependymal zone. *J. Neurosci.* 37, 11867–11880. doi: 10.1523/JNEUROSCI.0001-17.2017

Kawamoto, H., Yasuda, O., Suzuki, T., Ozaki, T., Yotsui, T., Higuchi, M., et al. (2006). Tissue inhibitor of Metalloproteinase-3 plays important roles in the kidney following unilateral ureteral obstruction. *Hyperten. Res.* 29, 285–294. doi: 10.1291/hypres.29.285

Kazanis, I., and Ffrench-Constant, C. (2011). Extracellular matrix and the neural stem cell niche. *Dev. Neurobiol.* 71, 1006–1017. doi: 10.1002/dneu.20970

Kerever, A., Schnack, J., Vellinga, D., Ichikawa, N., Moon, C., Arikawa-Hirasawa, E., et al. (2007). Novel extracellular matrix structures in the neural stem cell niche capture the neurogenic factor fibroblast growth factor 2 from the extracellular milieu. *Stem Cells* 25, 2146–2157. doi: 10.1634/stemcells.2007-0082

Kjell, J., Fischer-Sternjak, J., Thompson, A. J., Friess, C., Sticco, M. J., Salinas, F., et al. (2020). Defining the adult neural stem cell niche proteome identifies key regulators of adult neurogenesis. *Cell Stem Cell* 26, 277–293.e8. doi: 10.1016/j.stem.2020.01.002

la Manno, G., Siletti, K., Furlan, A., Gyllborg, D., Vinsland, E., Mossi Albiach, A., et al. (2021). Molecular architecture of the developing mouse brain. *Nature* 596, 92–96. doi: 10.1038/s41586-021-03775-x

Liao, Y., Wang, J., Jaehnig, E. J., Shi, Z., and Zhang, B. (2019). WebGestalt 2019: gene set analysis toolkit with revamped UIs and APIs. *Nucleic Acids Res.* 47, W199–W205. doi: 10.1093/nar/gkz401

Liu, H., Chen, S. E., Jin, B., Carson, J. A., Niu, A., Durham, W., et al. (2010). TIMP3: a physiological regulator of adult myogenesis. *J. Cell Sci.* 123, 2914–2921. doi: 10.1242/jcs.057620

Lledo, P. M., and Valley, M. (2016). Adult olfactory bulb neurogenesis. *Cold Spring Harb. Perspect. Biol.* 8:a018945. doi: 10.1101/cshperspect.a018945

Long, K. R., and Huttner, W. B. (2019). How the extracellular matrix shapes neural development. *Open Biol.* 9:180216. doi: 10.1098/rsob.180216

Morshead, C. M., Reynolds, B. A., Craig, C. G., McBurney, M. W., Staines, W. A., Morassutti, D., et al. (1994). Neural stem cells in the adult mammalian forebrain: a relatively quiescent subpopulation of subependymal cells. *Neuron* 13, 1071–1082. doi: 10.1016/0896-6273(94)90046-9

Murphy, G. (2011). Tissue inhibitors of metalloproteinases. *Genome Biol.* 12:233. doi: 10.1038/315768a0

Nagase, H., and Woessner, J. F. (1999). Matrix metalloproteinases. *J Biol Chem* 274, 21491–21494. doi: 10.1074/jbc.274.31.21491

Page-McCaw, A., Ewald, A. J., and Werb, Z. (2007). Matrix metalloproteinases and the regulation of tissue remodelling. *Nat. Rev. Mol. Cell Biol.* 8, 221–233. doi: 10.1038/nrm2125

Pearson, J. R., Zurita, F., Tomás-Gallardo, L., Díaz-Torres, A., Díaz de la Loza Mdel, C., Franze, K., et al. (2016). ECM-regulator timp is required for stem cell niche organization and cyst production in the Drosophila ovary. *PLoS Genet.* 12:e1005763. doi: 10.1371/journal.pgen.1005763

Pérez-Martínez, L., and Jaworski, D. M. (2005). Tissue inhibitor of metalloproteinase-2 promotes neuronal differentiation by acting as an anti-mitogenic signal. *J. Neurosci.* 25, 4917–4929. doi: 10.1523/JNEUROSCI.5066-04.2005

Pisconti, A., Cornelison, D. D. W., Olguín, H. C., Antwine, T. L., and Olwin, B. B. (2010). Syndecan-3 and notch cooperate in regulating adult myogenesis. *J. Cell Biol.* 190, 427–441. doi: 10.1083/jcb.201003081

Porlan, E., Martí-Prado, B., Morante-Redolat, J. M., Consiglio, A., Delgado, A. C., Kypta, R., et al. (2014). MT5-MMP regulates adult neural stem cell functional quiescence through the cleavage of N-cadherin. *Nat. Cell Biol.* 16, 629–638. doi: 10.1038/ncb2993

Robinson, M. D., McCarthy, D. J., and Smyth, G. K. (2009). edgeR: a bioconductor package for differential expression analysis of digital gene expression data. *Bioinformatics* 26, 139–140. doi: 10.1093/bioinformatics/btp616

Robinson, M. D., and Oshlack, A. (2010). A scaling normalization method for differential expression analysis of RNA-seq data. *Genome Biol.* 11, 1–9. doi: 10.1186/gb-2010-11-3-r25

Sasagawa, Y., Nikaido, I., Hayashi, T., Danno, H., Uno, K. D., Imai, T., et al. (2013). Quartz-Seq: a highly reproducible and sensitive single-cell RNA sequencing method, reveals nongenetic gene-expression heterogeneity. *Genome Biol.* 14:R31. doi: 10.1186/gb-2013-14-4-r31

Shan, X., Tomlinson, L., Yang, Q., and Colognato, H. (2018). Distinct requirements for extracellular and intracellular MMP12 in the development of the adult V-SVZ neural stem cell niche. *Stem Cell Reports* 10, 984–999. doi: 10.1016/j.stemcr.2018.01.038

Shin, J., Berg, D. A., Zhu, Y., Shin, J. Y., Song, J., Bonaguidi, M. A., et al. (2015). Single-cell RNA-Seq with waterfall reveals molecular cascades underlying adult neurogenesis. *Cell Stem Cell* 17, 360–372. doi: 10.1016/j.stem.2015.07.013

Sueda, R., Imayoshi, I., Harima, Y., and Kageyama, R. (2019). High Hes1 expression and resultant Ascl1 suppression regulate quiescent vs. active neural stem cells in the adult mouse brain. *Genes. Dev.* 33, 511–523. doi: 10.1101/gad.323196.118

Tabata, H., and Nakajima, K. (2001). Efficient in utero gene transfer system to the developing mouse brain using electroporation: visualization of neuronal migration in the developing cortex. *Neuroscience* 103, 865–872. doi: 10.1016/S0306-4522(01)00016-1

Than-Trong, E., Ortica-Gatti, S., Mella, S., Nepal, C., Alunni, A., and Bally-Cuif, L. (2018). Neural stem cell quiescence and stemness are molecularly distinct outputs of the Notch3 signalling cascade in the vertebrate adult brain. *Development* 145. doi: 10.1242/dev.161034

Zhang, R., Boareto, M., Engler, A., Louvi, A., Giachino, C., Iber, D., et al. (2019). Id4 downstream of Notch2 maintains neural stem cell quiescence in the adult Hippocampus article Id4 downstream of Notch2 maintains neural stem cell quiescence in the adult Hippocampus. *Cell Rep.* 28, 1485–1498.e6. doi: 10.1016/j.celrep.2019.07.014

Zhao, N., Liu, H., and Lilly, B. (2012). Reciprocal regulation of syndecan-2 and notch signaling in vascular smooth muscle cells. *J. Biol. Chem.* 287, 16111–16120. doi: 10.1074/jbc.M111.322107

frontiers | Frontiers in Neuroscience

TYPE Mini Review
PUBLISHED 29 June 2023
DOI 10.3389/fnins.2023.1179011

OPEN ACCESS

EDITED BY
Chitra D. Mandyam,
United States Department of Veterans Affairs, United States

REVIEWED BY
David Talmage,
National Institute of Neurological Disorders and Stroke (NIH), United States

*CORRESPONDENCE
Verdon Taylor
✉ verdon.taylor@unibas.ch

RECEIVED 03 March 2023
ACCEPTED 05 June 2023
PUBLISHED 29 June 2023

CITATION
Lampada A and Taylor V (2023) Notch signaling as a master regulator of adult neurogenesis. *Front. Neurosci.* 17:1179011. doi: 10.3389/fnins.2023.1179011

Notch signaling as a master regulator of adult neurogenesis

Aikaterini Lampada and Verdon Taylor *

Department of Biomedicine, University of Basel, Basel, Switzerland

Neurogenesis ceases in most regions of the mammalian brain before or shortly after birth, however, in a few restricted brain regions, the production of new neurons proceeds into adulthood. Neural stem cells (NSCs) in these neurogenic zones are integrated into niches that control their activity and fate. Most stem cells in the adult brain are mitotically inactive and these cells can remain quiescent for months or even years. One of the key questions is what are the molecular mechanisms that regulate NSC maintenance and differentiation. Notch signaling has been shown to be a critical regulator of stem cell activity and maintenance in many tissues including in the nervous system. In this mini-review we discuss the roles of Notch signaling and the functions of the different Notch receptors and ligands in regulating neurogenesis in the adult murine brain. We review the functions of Notch signaling components in controlling NSC quiescence and entry into cell cycle and neurogenesis.

KEYWORDS

Notch, neural stem cells, neurogenesis, subventricular zone, dentate gyrus

Introduction

The mammalian brain is formed during embryogenesis and early postnatal life, with most neurons being born before birth. However, in the 1960s, the field of neurogenesis was revolutionized by the discovery that neurons are continually generated in distinct regions of the adult mammalian brain including in the cerebral cortex and the hippocampus (Altman, 1962; Altman and Das, 1965; Obernier and Alvarez-Buylla, 2019). Hitherto, it is widely accepted that neurogenesis occurs throughout life in two specialized niches of the adult rodent brain, the ventricular-subventricular zone (V-SVZ) and the dentate gyrus (DG) of the hippocampus (Goncalves et al., 2016; Obernier and Alvarez-Buylla, 2019). Adult neurogenesis has been documented in the brains of many vertebrate species including fish, rodents, birds and primates and, although there is some controversy in the field, evidence suggests the production of neurons also in brains of adult humans (Boldrini et al., 2018; Kempermann et al., 2018; Sorrells et al., 2018).

Adult neural stem cells (NSCs) are the source of new neurons during adult neurogenesis. NSCs are specialized radial glia (RG) that reside in dedicated niches in the walls of the lateral ventricles (LV) forming the V-SVZ, and in the subgranular zone (SGZ) of the DG. V-SVZ NSCs give-rise to different interneuron populations that migrate to the olfactory bulb (OB) and the SGZ NSCs generate granule cells in the DG (Doetsch et al., 1999; Seri et al., 2001). NSCs in both adult neurogenic niches express glial markers and are maintained in a quiescent state. Once activated, quiescent NSCs (qNSCs) enter the cell cycle and become active NSCs (aNSCs). Several NSC intrinsic and extrinsic factors have been shown to regulate adult neurogenesis through altering the equilibrium between signals that maintain quiescence and those that induce NSC activation (Berg et al., 2013; Tong et al., 2014; Matsubara et al., 2021). This equilibrium between quiescence and activation defines the rate of neurogenesis as well as the long-term maintenance

of NSCs and neurogenesis in the brain niches (Bonaguidi et al., 2011; Encinas et al., 2011; Calzolari et al., 2015; Urban et al., 2016, 2019; Basak et al., 2018; Obernier et al., 2018; Pilz et al., 2018). Cell death of newborn neurons is also an important regulatory mechanism controlling the generation of mature neurons in the adult mouse brain (Sierra et al., 2010; Ryu et al., 2016; Pfisterer and Khodosevich, 2017).

In this review, we focus on the role of Notch signaling in the control of NSC activity and neurogenesis and address some of the unanswered questions about how this pathway plays different roles in the generation of neurons in the adult brain.

NSCs of the adult neurogenic niches

NSCs in the adult V-SVZ and the SGZ niches share many similarities, however, they also have important differences in the organization, location and architecture of their niches and in their fate potentials that will be discussed below [for reviews see (Goncalves et al., 2016; Obernier and Alvarez-Buylla, 2019; Urban et al., 2019)].

NSCs of the V-SVZ niche

NSCs in the adult V-SVZ (B1 cells) are generated by RGs during embryonic development. The majority of the V-SVZ NSC precursors are generated as early as embryonic day 13.5 and remain quiescent through the late stages of embryogenesis until postnatal and adult stages of life (Merkle et al., 2004; Fuentealba et al., 2015; Furutachi et al., 2015). V-SVZ NSCs are multipotent and are able to generate multiple neuron subtypes, astrocytes and oligodendrocytes (Menn et al., 2006; Mizrak et al., 2019; Obernier and Alvarez-Buylla, 2019). Most adult NSCs in the V-SVZ remain in an inactive and mitotically quiescent state, for long periods of time. A relatively small proportion of the NSCs in the V-SVZ enter the cell cycle at any one point in time and divide to generate more committed progeny. It has recently been described that most V-SVZ NSCs undergo symmetric, differentiating cell divisions but ~20% self-renew and remain in the V-SVZ for several months before they generate progeny (Obernier et al., 2018).

NSCs of the V-SVZ are polarized with an apical cilium that projects through the ependymal (E cells) lining of the ventricles into the cerebrospinal fluid (CSF) of the LV, and a long basal process that contacts blood vessels. The V-SVZ NSCs organize the E cells into pinwheel structures (Mirzadeh et al., 2008). During adult life, quiescent NSCs are activated to generate transient amplifying progenitors (C cells), which can divide further (three to four times) to give rise to neuroblasts (A cells) (Doetsch et al., 1999; Obernier et al., 2018). The newly formed neuroblasts in the V-SVZ migrate to the OB through the rostral migratory stream (RMS), where they differentiate into local interneurons that integrate into the local circuitry (Obernier and Alvarez-Buylla, 2019). V-SVZ NSCs are heterogeneous and, depending on their location, give-rise to different subtypes of interneurons of the OB (Merkle et al., 2007; Giachino et al., 2014; Giachino and Taylor, 2014; Merkle et al., 2014).

In addition to the NSCs in the lateral wall (LW) of the LV, recently gliogenic stem cells have been identified in the lateral septal wall (LSW) (Mizrak et al., 2019; Delgado et al., 2021), as well as a novel population of neurogenic NSCs in the dorsal septum (Lampada et al., 2022). LSW NSCs are predominantly in a quiescent state and induce pinwheel structures in the ependymal lining of the LV (Lampada et al., 2022). Stem cells in the LSW and V-SVZ have different lineage biases toward glia or neurons, indicating some mode of differential fate specification (Mizrak et al., 2019; Kjell et al., 2020; Delgado et al., 2021; Lampada et al., 2022). The roles of the stem cell populations in the forebrain outside the classic V-SVZ niche remain unclear.

NSCs of the SGZ niche

Like the NSCs of the V-SVZ, the NSCs of the adult SGZ of the DG are formed during embryonic development. Their precursors acquire a radial morphology reminiscent of adult NSCs, localize to the SGZ of the DG and become quiescent during the early postnatal period (Berg et al., 2019). In contrast to V-SVZ NSCs that mostly divide symmetrically, NSCs in the SGZ predominantly divide asymmetrically to generate a daughter stem cell and an intermediate progenitor cell or an astrocyte (Bonaguidi et al., 2011). However, a fraction of SGZ NSCs do divide symmetrically to expand the stem cell pool (Bonaguidi et al., 2011; Obernier et al., 2018; Pilz et al., 2018).

DG NSCs predominantly generate glutamatergic granule neurons and to a less extent astrocytes but not oligodendrocytes (van Praag et al., 2002; Bonaguidi et al., 2011; Lugert et al., 2012; Rolando et al., 2016; Bonzano et al., 2018; Pilz et al., 2018; Obernier and Alvarez-Buylla, 2019). The adult SGZ contains morphologically discrete populations of NSCs (Lugert et al., 2010, 2012). Radial and horizontal NSCs (type-1 cells) in the adult SGZ give-rise to mitotic intermediate progenitor cells (IPs; type-2 cells). IPs (type-2 cells) are subdivided into early IPs (type-2a cells) and late IPs (type-2b cells) (Lugert et al., 2012). SGZ NSCs generate early IPs (type-2a cells) through asymmetric divisions. Early IPs (type-2a cells) self-replicate through symmetric divisions and then generate late IPs (type-2b cells). Late IPs (type-2b) give-rise to neuroblasts (type-3 cells), which is a pool of committed progenitors that eventually differentiate into mature granule cells of the DG (Lugert et al., 2012; Goncalves et al., 2016; Engler et al., 2018b; Obernier and Alvarez-Buylla, 2019).

Notch signaling pathway overview

The mammalian genome contains four Notch receptor (*Notch1-4*) and five canonical ligand (*Dll1, Dll3 and Dll4* and *Jag1 and Jag2*) genes. Both the receptors and their ligands are type I transmembrane proteins, presented on the surface of cells and thus enabling direct cell-to-cell communication (Figure 1). The receptors and the ligands both contain EGF repeats in their ectodomains as well as specialized domains for ligand-receptor interaction and activation. The ligands have relatively short intracellular domains which are important for surface presentation and activation of the Notchs by promoting endocytosis and mechanical conformational changes in the receptor extracellular domains (Figure 1; Giaimo and Borggrefe, 2018; Zhang et al., 2018; Sprinzak and Blacklow, 2021).

Notch receptors are synthesized in the endoplasmic reticulum (ER) as proproteins and are then proteolytically processed by a Furin-like protease and post-translationally modified to generate the mature heterodimeric receptor. The mature Notch receptors are expressed on the plasma membrane with the Notch extracellular domain (NECD) linked to the transmembrane-intracellular domain through a calcium

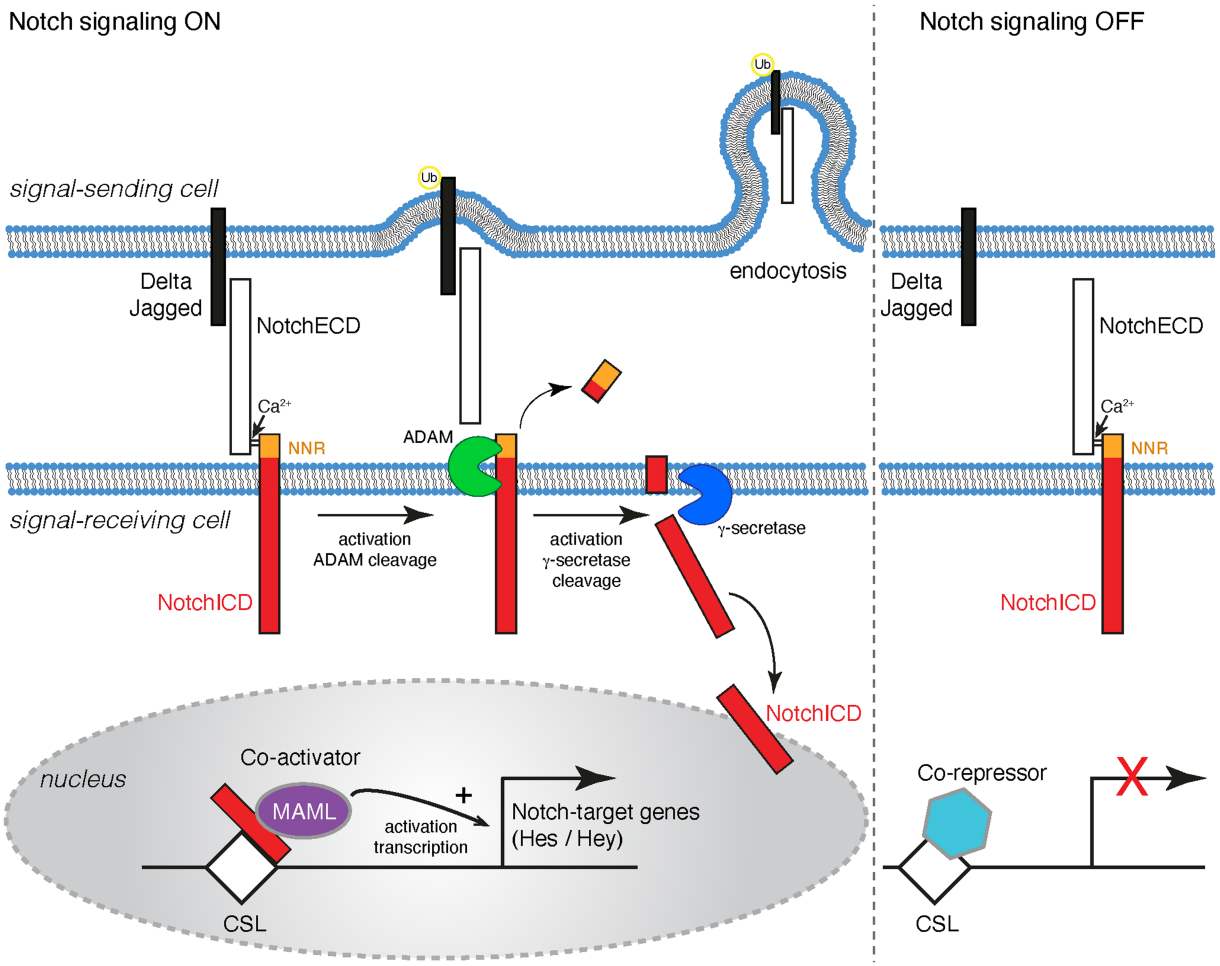

FIGURE 1
Schematic representation of the Notch signaling cascade. Notchs and their cognate ligands (Deltas and Jaggeds) are transmembrane proteins. Notch signaling occurs between cells that are in contact with one another. Notch signaling is activated when a ligand on a signal-sending cell binds to the Notch extracellular domain (NotchECD) on a signal-receiving cell. The Notch/ligand interaction triggers the ubiquitination (Ub) of the ligand intracellular domain, which results in endocytosis into the signal-sending cell. Endocytosis generates a pulling force that causes a conformational change on the NotchECD and reveals a proteolytic cleavage site for ADAM10/17 in the negative regulatory region (NRR) of the receptor. Two consecutive proteolytic cleavage events on the transmembrane portion of the Notch receptor are initiated. The first cleavage event by ADAM and the second by γ-secretase. These cleavage events release the Notch intracellular domain (NotchICD) into the cytoplasm of the signal-receiving cell. The The NotchICD translocates translocate to the nucleus where it interacts with the DNA-binding protein CSL and the co-activator Mastermind (MAML) to promote target gene transcription. Some Notch targets include genes of the *Hes* and *Hey* families. When Notch signaling is OFF, Notch receptors at the cell surface are heterodimers where the ADAM cleavage site is occluded. CSL is in the nucleus and interacts with co-repressors to inhibit the transcription of target genes.

bridge (Figure 1; Giaimo and Borggrefe, 2018; Zhang et al., 2018; Sprinzak and Blacklow, 2021).

Binding of a Notch to a ligand triggers the ubiquitination of the ligand, which results in endocytosis of the ligand and the bound NECD into the signal-sending cell. An endocytosis-mediated conformational change on the NECD reveals a proteolytic cleavage site for ADAM10/17 in the negative regulatory region (NRR) of the Notch receptor which facilitates the removal of the NECD. In the absence of a Notch/ligand interaction, the LNR (Lin-12/Notch Repeat) domains within the NRR prevent access and cleavage by ADAM proteases at the NECD, maintaining the Notch receptor in an inactive conformation (Sanchez-Irizarry et al., 2004; Gordon et al., 2007, 2009; Weinmaster and Fischer, 2011; Meloty-Kapella et al., 2012; Musse et al., 2012; Giaimo and Borggrefe, 2018; Handford et al., 2018; Lovendahl et al., 2018; Salazar and Yamamoto, 2018; Sprinzak and Blacklow, 2021). Cleavage by ADAM prevents reassociation of the ectodomain and results in intramembrane proteolysis of the remaining Notch transmembrane protein fragment by γ-secretase to release the intracellular domain (ICD) of the receptor. Apart from being present at the cell membrane, γ-secretase is also present in intracellular membrane compartments, including endosomes and lysosomes. It has been documented that γ-secretase can cleave Notch at the plasma membrane as well as in endocytic compartments, however it remains unclear whether γ-secretase primarily processes Notch receptors at the plasma membrane, within endocytic vesicles following Notch endocytosis, or in both compartments (Gupta-Rossi et al., 2004; Chyung et al., 2005; Hansson et al., 2005; Lange et al., 2011; Salazar and Yamamoto, 2018; Schnute et al., 2018; Steinbuck and Winandy, 2018). The intracellular domain of Notch proteins acts as a transcriptional regulator by binding to the CSL DNA-binding protein (RBPj, CBF1, Suppressor of Hairless, Lag-1), recruiting transcriptional coactivators and epigenetic regulators to target genes (Figure 1; Bray,

2016; Giaimo and Borggrefe, 2018; Lovendahl et al., 2018; Oswald and Kovall, 2018; Falo-Sanjuan and Bray, 2020; Sprinzak and Blacklow, 2021).

The NICD-CSL-MAML trimeric complex then recruits other co-activators and histone acetyltransferases to promote transcriptional activation of target genes. In the absence of Notch signal activation, CSL remains in the nucleus and interacts with several co-repressors to inhibit target gene transcription (Bray, 2016; Giaimo and Borggrefe, 2018; Lovendahl et al., 2018; Oswald and Kovall, 2018; Falo-Sanjuan and Bray, 2020; Sprinzak and Blacklow, 2021). The best characterized Notch targets genes include members of the hairy and enhancer of split (*Hes*) and hairy and enhancer of split-related with YRPW motif (*Hey*) families (Figure 1). HES and HEY proteins in the brain control the expression of several proneural genes (*Ascl1*, *Atoh1*, *Neurog1* and *Neurog2*) and are therefore important for NSC cell fate determination and neuronal differentiation (Bigas and Porcheri, 2018; Engler et al., 2018b; Urban et al., 2019).

Notch signaling is an important cell fate regulator in different organs, including in the brain, from embryogenesis through to adult homeostasis (Bray, 2016; Ho et al., 2018; Engler et al., 2018b; Ho et al., 2020). Control of NSC activity and fate is crucial for brain development and homeostasis. Misregulation of the Notch pathway in the central nervous system has been implicated in various pathological conditions, from progressive neurodegenerative diseases to cancer (Giachino et al., 2015; Zhang et al., 2018; Ho et al., 2020; Parmigiani et al., 2020, 2022). In this review, we will mainly discuss the regulation and function of the Notch signaling pathway in adult neurogenesis under homeostatic conditions with a focus on rodents and genetic experiments.

Notch signaling in adult neurogenesis

Expression of all four Notch receptor paralogs has been documented in various cell types of the adult mouse brain including by NSCs (Notch1, Notch2 and Notch3), astrocytes (Notch1 and Notch2), neurons (Notch1 and Notch2), endothelial cells (Notch1 and Notch4) and vascular smooth muscle cells and pericytes (Notch3) (Basak et al., 2012; Ehret et al., 2015; Llorens-Bobadilla et al., 2015; Shin et al., 2015; Kawai et al., 2017; Rieskamp et al., 2018; Engler et al., 2018a; Zhang et al., 2019; Ho et al., 2020). Furthermore, Notch receptors and many of their ligands are expressed by NSCs, progenitors and neuroblasts throughout the adult neurogenic lineage. However, downstream targets of the Notch pathway (Hes and Hey transcription factors) are only expressed by NSCs. This indicates that Notch signaling in the neurogenic niches is highly regulated and not only due to receptor or ligand expression by a cell (Figure 2A; Stump et al., 2002; Irvin et al., 2004; Nyfeler et al., 2005; Carlen et al., 2009; Aguirre et al., 2010; Lugert et al., 2010; Basak et al., 2012; Kawaguchi et al., 2013; Giachino et al., 2014; Lavado and Oliver, 2014; Ehret et al., 2015; Kawai et al., 2017; Semerci et al., 2017; Engler et al., 2018a,b; Zhang et al., 2018; Sueda et al., 2019; Zhang et al., 2019; Harada et al., 2021). Notch signaling can be regulated at multiple levels modulating the strength and dynamics of the signal outcome. The expression patterns of different Notch receptors and ligands, different modifications affecting ligand-receptor interactions and factors affecting the transcriptional activity of the Notch pathway contribute to differential regulation of NSC behavior and consequently adult neurogenesis.

Differential cell autonomous functions of Notch receptors on NSCs

Loss of function experimental approaches manipulating the expression of different components of the Notch pathway by NSCs combined with lineage tracing of the NSC population and their progeny have uncovered crucial roles for Notch signaling in adult mouse neurogenesis. Early studies investigated a cell autonomous role of Notch signaling in neurogenesis by ablating *Rbpj*, the common downstream effector of all Notch receptors. *Rbpj* deletion in NSCs of the V-SVZ and SGZ of the adult mouse brain caused an initial transient increase in neurogenesis that is followed by a total depletion of the NSC pool and loss of neurogenesis in the long-term (Ehm et al., 2010; Imayoshi et al., 2010; Lugert et al., 2010). These data indicated that Notch signaling plays a pivotal role in the regulation of NSC maintenance in both V-SVZ and SGZ neurogenic niches. However, any Rbpj-dependent but Notch-independent effects on adult neurogenesis could not be excluded by these experiments, and therefore further studies investigated the precise role of individual Notch receptors during adult neurogenesis.

The Notch1 receptor was found to be an important mediator of maintenance of a pool of proliferating undifferentiated cells in the adult SGZ and conditional deletion of *Notch1* from NESTIN positive progenitors led to a decrease in NSCs, IPs, NBs and mature neurons (Ables et al., 2010). Similarly, in the V-SVZ, ablation of *Notch1* from NESTIN positive progenitors resulted in a persistent defect in adult neurogenesis accompanied by a loss of mitotic progenitors and NBs. Interestingly, it was shown that Notch1 promotes the maintenance of aNSCs. Genetic ablation of *Notch1* from NSCs led to selective loss of the aNSC pool while qNSCs remain unchanged (Basak et al., 2012). qNSCs induced to enter cell cycle during regeneration and aging became Notch1-dependent and consequently failed to fully reinstate neurogenesis following *Notch1* deletion (Basak et al., 2012). This indicates that the qNSCs and aNSCs are in the same linage and that Notch1 is required at the activated stage (Basak et al., 2012). The observation that conditional deletion of *Rbpj* or *Notch1* from NSCs of the V-SVZ causes partially different phenotypes left open the possibility that other Notch receptors could functionally compensate the signals that repress activation of qNSCs through Rbpj.

Single cell transcriptomic analysis of NSCs in the adult V-SVZ reveals that *Notch2* expression is enriched in qNSCs (Llorens-Bobadilla et al., 2015). Engler et al. (2018a), performed conditional *Notch2* deletion in NSCs and revealed that Notch2 regulates adult NSC quiescence in the V-SVZ. Combinatorial conditional genetic deletion of *Notch1* and *Notch2* and *Rbpj* in NSCs uncovered distinct functions of Notch1 and Notch2 in regulating neurogenesis (Engler et al., 2018a).

Genome-wide gene expression analysis showed that *Notch2* deletion from V-SVZ NSCs affected genes associated with NSC proliferation and differentiation (Engler et al., 2018a). Indeed, qNSCs were rapidly activated and entered cell cycle shortly after deletion of *Notch2*, *Notch1Notch2* or *Rbpj*, but were not affected by *Notch1* deletion. The loss of *Notch2* led to an initial precocious differentiation and increased neurogenesis in the V-SVZ resulting in more neurons in the OB. However, 300 days after *Notch2* deletion the NSC pool had been exhausted leading to reduced V-SVZ neurogenic capacity, and a premature aging-like phenotype. Importantly, concomitant *Notch1Notch2* and *Rbpj* deletion gave similar phenotypes highlighting

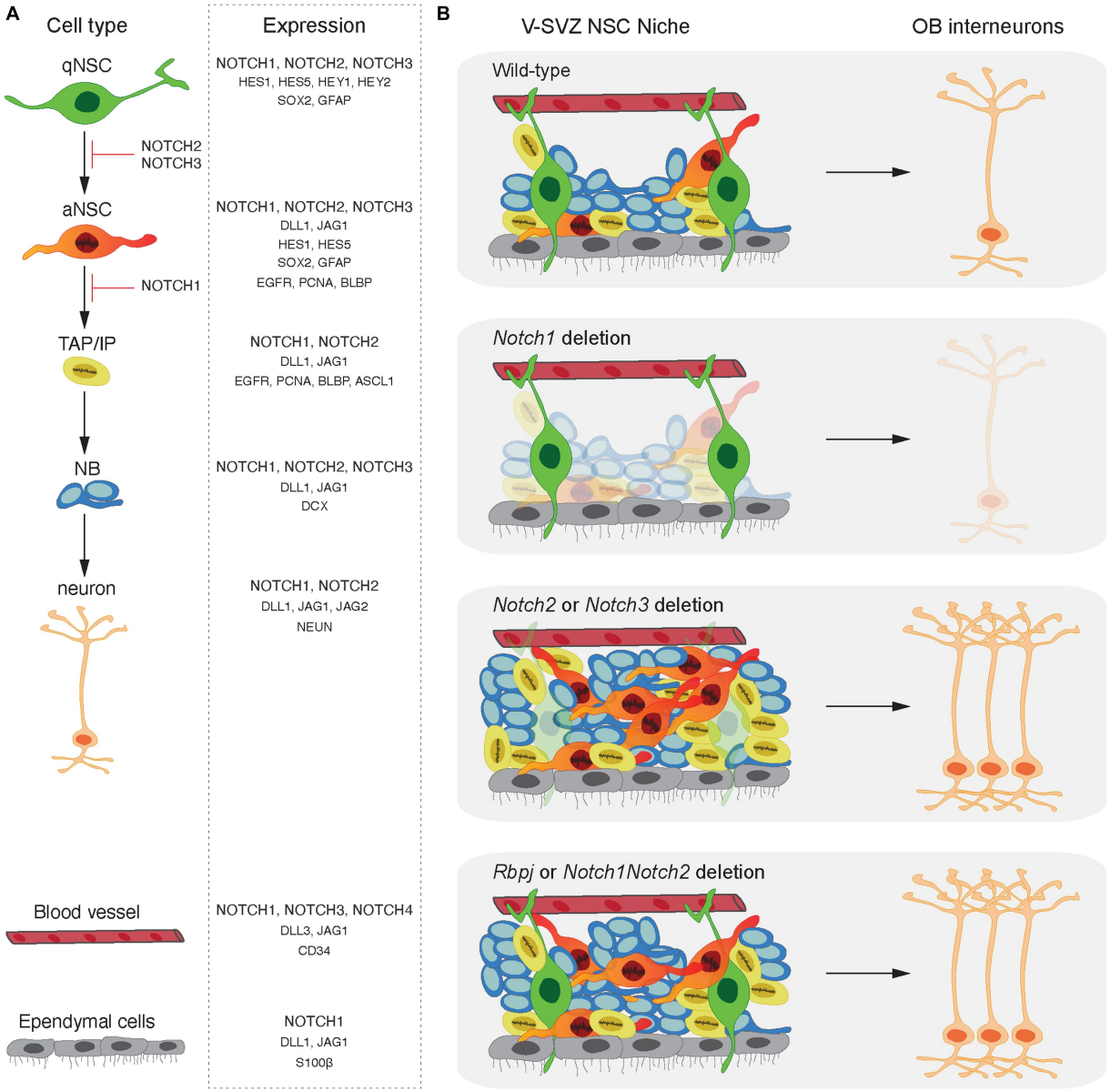

FIGURE 2
Notch signaling in adult neurogenesis. **(A)** Expression patterns of Notch ligands, receptors and downstream effectors in the neuronal lineage and cells of the adult NSC niche. Expression of Notch receptor paralogues and Rbpj has been documented in all cell types of the mouse adult-born neuronal lineage from NSCs to neurons. However, downstream effectors of the Notch signaling cascade (Hes and Hey factors) are present only in NSCs in both quiescent and activated states. Dll and Jagged ligands are expressed throughout the lineage apart from quiescent NSCs. **(B)** Functions of the Notch receptors and their common downstream effector, Rbpj, in the V-SVZ. Notch1 plays a role on the maintenance of the activated NSCs whereas Notch2 and Notch3 maintain NSC quiescence in the adult V-SVZ. Rbpj deletion and concomitant *Notch1Notch2* deletion result in similar phenotypes highlighting that Rbpj-mediated Notch signaling regulates NSC maintenance downstream of both Notch1 and Notch2 receptors.

that Rbpj-mediated Notch signaling regulates NSC maintenance downstream of both Notch1 and Notch2 (Engler et al., 2018a).

Similarly, *Notch2* deletion in Hes5 positive SGZ NSCs induced a rapid loss of qNSCs and an increase in proliferative progenitors, as well as NBs (Zhang et al., 2019). The effects culminated in a premature exhaustion of the SGZ NSC pool and neurogenic decline by 100 days after gene inactivation (Zhang et al., 2019). RNA-sequencing revealed that *Notch2* deletion downregulated quiescent NSC-associated genes while genes associated with NSC activation were upregulated (Zhang et al., 2019). *Notch2* activation by expression of the active form of *Notch2* (*Notch2ICD*) in SGZ NSCs maintained qNSCs, blocked NSC entry into cell cycle, and decreased mitotic progenitor, NB and neuron production (Zhang et al., 2019). Single cell RNA-sequencing of adult SGZ NSCs and their progeny indicate that quiescent adult NSCs express genes associated with different signaling pathways in the niche (Shin et al., 2015). Genes related by Notch signaling, including *Notch2*, are downregulated upon NSC exit from quiescence and entry into mitosis, further supporting the role of Notch2 in the regulation of

NSC quiescence (Shin et al., 2015). Recently, a population of quiescent NSCs with latent neurogenic potential was identified in the dorsal LSW of adult mice (Lampada et al., 2022). These dorsal LSW NSCs are dependent on Notch2 signaling which regulates quiescence and prevents their entry into the cell cycle and neurogenesis. These LSW NSCs respond to acute stress and elevated serotonin levels (Lampada et al., 2022). *Notch2* deletion increases proliferation and NB production in the dorsal LSW and generates new GABAergic interneurons that integrate into septal nuclei but which do not migrate to the OB (Lampada et al., 2022).

Similar to Notch2, Notch3 has also been described to play an important role in the maintenance of quiescent NSCs in the adult V-SVZ. Notch3 is expressed by qNSCs located at the lateral and ventral walls of the V-SVZ (Kawai et al., 2017). Germline deletion of *Notch3* led to a decrease in qNSCs, TAPs, NBs and Calbindin positive OB neurons without affecting the pool of aNSCs. It was suggested that qNSCs in *Notch3* knockout mice increase their activation but fail to complete lineage progression (Kawai et al., 2017). Nevertheless, acute knockdown of *Notch3* in NSCs in the lateral wall of the adult V-SVZ promotes qNSCs activation (Kawai et al., 2017; Rieskamp et al., 2018). Notch3 has also been associated with qNSCs in the adult SGZ. Using a transgenic mouse model overexpressing *Notch3*, Notch3 expression reduced precursor cell activation and proliferation without affecting levels of neurogenesis in the adult DG (Ehret et al., 2015).

Collectively, a differential mode of function of three Notch receptors expressed by NSCs has unveiled a pleiotropy in Notch signal function *in vivo*. Interestingly, the functions of the different Notch receptors are not compensated in NSCs. While Notch1 plays a role in the maintenance of aNSCs, Notch2 and Notch3 maintain NSC quiescence in both the adult V-SVZ and SGZ (Figure 2B; Ables et al., 2010; Ehm et al., 2010; Imayoshi et al., 2010; Basak et al., 2012; Ehret et al., 2015; Kawai et al., 2017; Engler et al., 2018a; Zhang et al., 2019). Even though the distinct functions of the Notch receptors can be attributed, at least in part, to their differential expression patterns on the different types of cells in the adult neurogenic lineages, an overlap in Notch1, Notch2 and Notch3 receptor expression by NSCs is clear (Ehret et al., 2015; Kawai et al., 2017; Engler et al., 2018a). The precise mechanism underlying the differential mode of function of Notch receptors and how they control different aspects of NSCs activity remains elusive.

Notch-mediated transcriptional responses in NSCs

Several transcriptional targets of the Notch pathway have been directly implicated in the maintenance and activation of quiescent NSCs and in their subsequent neuronal differentiation. *Hes5* expression distinguishes NSCs from intermediate progenitors in the neurogenic niches of the adult brain. However, both quiescent and activated NSCs in the V-SVZ and SGZ express Hes5 (Lugert et al., 2010, 2012; Giachino et al., 2014). The dynamics of Hes factor expression have been shown to control the balance between quiescent and activated states of NSCs during neurodevelopment. Specifically, Hes1/Hes5 levels oscillate out-of-phase with *Ascl1*, thereby promoting proliferation of mouse embryonic NSCs (Imayoshi et al., 2013). It remains unclear whether Hes factors are sustained or oscillatory in adult NSCs *in vivo*, however, *Hes1* expression does oscillate in some cells in cultured slices of the neurogenic regions of the adult brain (Sueda et al., 2019). Higher levels of *Hes1* expression were observed in qNSCs compared to aNSCs in both the V-SVZ and SGZ (Sueda et al., 2019; Sueda and Kageyama, 2020). Conditional deletion of *Hes1* in NSCs of *Hes3*/*Hes5*/*Hey1* knockout mice resulted in an activation of *Ascl1* expression and a transient increase in neurogenesis. This eventually resulted in depletion of the NSCs and termination of neurogenesis. Conversely, sustained *Hes1* expression repressed *Ascl1* expression and inhibited neurogenesis (Sueda et al., 2019; Sueda and Kageyama, 2020). Recently it has been suggested that the Notch-HEY1 axis also plays an important role in adult NSC ontogeny and long-term maintenance of quiescent embryonic NSCs through to adulthood. Interestingly, Hey1 has a non-oscillatory expression in NSCs (Harada et al., 2021).

The quiescence of adult NSCs has been linked to the expression of inhibitor of DNA-binding factors (IDs) in both the V-SVZ and SGZ (Llorens-Bobadilla et al., 2015; Shin et al., 2015; Blomfield et al., 2019; Zhang et al., 2019). In mammals, the *Id* family consists of four genes, *Id1-4*, that have been linked with stemness and proliferation (Niola et al., 2012). *Id2* and *Id3* expression are associated with quiescence in the adult V-SVZ (Llorens-Bobadilla et al., 2015). *Id3* and *Id4* were shown to be expressed by qNSCs in the DG and were both downregulated by mitotic cells (Shin et al., 2015). The ID1, ID3 and ID4 proteins are expressed in the SGZ of the DG of adult mice, and ID4 is expressed by the majority of the RG, and primarily by qNSCs (Blomfield et al., 2019). ID factors interact directly with Hes1 to form heterodimers. These heterodimers are responsible for releasing the negative feedback autorepression of Hes1 on its own promoter, in this way retaining *Hes1* expression and NSC maintenance (Bai et al., 2007). By combining mathematical modeling with analysis of published single-cell transcriptomic data, it was found that Notch signaling and ID factors control neurogenesis in a complementary manner. ID expression maintains NSCs in a quiescence state by blocking proneural gene expression and activity. Downregulation of IDs releases the complete repression of proneural activity mediated by sustained high levels of Hes expression. This promotes cell cycle entry by enabling proneural factor expression (Boareto et al., 2017). Recently, it was uncovered that quiescence in the adult SGZ is maintained by the expression of ID4 downstream of Notch2 signaling. Gene expression analysis and chromatin immunoprecipitation experiments identified *Id4* as a direct target of Notch2 signaling. *Id4* knockdown partially rescues the proliferation defect induced by *Notch2ICD* overexpression in SGZ NSCs, indicating that Notch2 and ID4 control proliferation in a complementary fashion *in vitro*. Genetic deletion and overexpression of *Id4* in adult SGZ NSCs confirmed that ID4 maintains NSC quiescence *in vivo* (Zhang et al., 2019).

Ligand-mediated regulation of Notch signaling in NSCs

The activation of Notch receptors on adult NSCs requires their interaction with cells expressing a ligand, underlying the

importance of the niche microenvironment in Notch signal regulation (Figure 1). Dll1 and Jagged1 were found to control Notch signaling in the V-SVZ and SGZ of adult mice (Nyfeler et al., 2005; Kawaguchi et al., 2013; Lavado and Oliver, 2014; Semerci et al., 2017). Apart from activating Notch on neighboring cells (*trans* interaction) Dll ligands are able to inactivate Notch signaling within the same cell (*cis* interaction/inhibition) (Sprinzak et al., 2010). In the adult V-SVZ, Dll1 was suggested to play an essential role in the maintenance of qNSCs (Kawaguchi et al., 2013). *Dll1* deletion from V-SVZ NSCs decreased the number of qNSCs while increasing the number of aNSCs, TAPs and NBs. Dll1 is expressed by cells negative for NICD expression that resided in close proximity to quiescent V-SVZ NSCs. Therefore, a model whereby Dll-expressing aNSCs control the dormancy of quiescent NSCs has been proposed (Kawaguchi et al., 2013). Jagged1 expression has been detected in both the neurogenic V-SVZ and DG regions of the adult brain (Stump et al., 2002; Irvin et al., 2004). Jagged1 was found to be expressed in the V-SVZ in a mutually exclusive manner to Notch1. Mice double hemizygous null for *Jagged1* and *Notch1* show reduced mitosis in the V-SVZ (Nyfeler et al., 2005). Ablation of *Jagged1* from adult V-SVZ neurospheres blocks NSC self-renewal potential, but do not affect their differentiation potential *in vitro* (Nyfeler et al., 2005). Conversely, treatment of V-SVZ neurospheres with a dimeric soluble Jagged1 induces NSC self-renewal and promotes neurogenic capacity *in vitro*. These findings suggest that Jagged1 plays a role in the maintenance of NSCs in the V-SVZ (Nyfeler et al., 2005). Similar to the V-SVZ, Jagged1 was found to play an essential role in neurogenesis in the adult SGZ by regulating NSC maintenance and proliferation. Conditional genetic deletion of *Jagged1* from SGZ NESTIN positive progenitors caused a transient increase in neurogenesis. However, *Jagged1* deletion eventually led to depletion of the SGZ NSC pool and obstructed neurogenesis (Lavado and Oliver, 2014).

It has been shown that Fringe-modified Notch receptors respond differently to ligand activating signals and modulate Notch activity. Fringe proteins (Lunatic, Manic and Radical in mammals) are β3-N-acetylglucosaminyltransferases that modify O-fucose on epidermal growth factor-like (EGF) repeats in the NECD. Specific fringe modifications therefore can enhance Notch binding to Dll1 resulting in activation of Notch signaling whereas others inhibit Notch activation by Jagged1 (Bray, 2016; Kakuda and Haltiwanger, 2017; Zhang et al., 2018). Recently, it has been described that Lunatic fringe (LFNG) is selectively expressed by NSCs in the adult SGZ together with Notch1. Additionally, Jagged1 was found to be expressed by amplifying neural progenitor cells and Dll1 by granule neurons of the DG, in close proximity to the NSCs. LFNG-mediated Notch signaling was therefore suggested to control SGZ NSC maintenance in the adult brain since genetic deletion of *Lfng* from NSCs leads to increased NSC proliferation, reduced numbers of amplifying neural progenitors and an increased tendency for astrocytic differentiation. Similar to *Lfng*, *Dll1* deletion leads to an increase in mitotic NSCs and less amplifying neural progenitors. On the other hand, genetic deletion of *Jagged1* causes NSCs to re-enter the cell cycle leading to an increase in amplifying neural progenitor production (Semerci et al., 2017). In summary, Notch signaling and its ligands play pivotal roles as niche molecules in the control of NSC activity and neurogenesis in the V-SVZ and SGZ of the DG. How the same pathway activated by different receptors can have such distinct functions in the different cells of the neurogenic lineages remains to be determined.

Discussion

In this review, we present an overview of our current knowledge about how the Notch signaling controls adult neurogenesis, with emphasis given to the roles of the pathway in NSC activity. It is now widely accepted that Notch signaling plays a pivotal role on NSC maintenance and neurogenesis. Different Notch receptor paralogues are able to control either the quiescent or activated state of NSCs through Rbpj and transcriptional regulation of target genes. In addition to Notch receptors, several Notch ligands and downstream transcriptional effectors play key roles in NSC maintenance and neurogenesis. However, the precise molecular mechanism that differentially controls Notch signaling in NSCs remains elusive and needs further investigation. The pleiotropic functions of Notch signaling in adult neurogenesis could be attributed to the complex nature and regulation of the pathway. Differential ligand-mediated activation of Notch receptors might control the quiescent or activated NSC state and maintenance. Additionally, differential transcriptional responses downstream of the Notch receptors might control the activation state of NSCs. It is intriguing to speculate that different Notch receptors modulate distinct gene networks and/or overlapping gene networks with distinctive strengths and dynamics. Additionally, the architecture of the NSC niches certainly adds another level of complexity to the regulation of Notch signaling in NSCs. Notch signaling mediates cell-to-cell communication between neighboring cells, and niche cells control NSC behavior, it could be that the expression of Notch ligands and/or other Notch interactors within the niche affects NSC fate and maintenance. The identification of new upstream or downstream effectors of the Notch signaling pathway will pave the way to a better understanding of NSC biology and fate switch.

There are still a number of important open questions about the role of Notch signaling in adult neurogenesis that need to be addressed in the future. Many of these unknowns are manifested in the fact that our current knowledge of Notch signaling cannot explain why cells in the same neurogenic niche express multiple Notch receptors which regulate either none compensated different processes or exert different functions.

Although it is clear that different Notch receptors play different roles in regulating the activity and fate of NSCs, how this is achieved for receptors that interact with the same set of ligands and use the same DNA binding molecule (CSL protein) is still not known. For example, it still remains unclear whether Notch receptors (Notch1-3) compete with each other for ligands, downstream effector proteins or target genes in order to modulate the response of the cell to different Notch receptor signals. Additionally, it is not known whether different ligands can activate Notch receptors to induce different downstream effectors of the pathway within the same cell. Although Notch1 has been shown to be target of its own signal in some cells, it remains to be shown whether Notch receptors can cross regulate the expression of other

Notch receptors at the transcriptional level in adult NSCs. Finally, the discrete or compensatory roles of the individual Notch ligands in the adult neurogenesis remain to be elucidated. In summary, there remains much to be learnt about the Notch signaling in the control of NSCs in the adult brain, and future findings may have important implications for other organs and even in diseases including cancer.

Author contributions

AL and VT wrote and edited the manuscript and designed and generated the figures. All authors contributed to the article and approved the submitted version.

Funding

This work was supported by the Swiss National Science Foundation (31003A_162609 and 31003A_182388 to VT).

Acknowledgments

We thank the members of the VT laboratory for helpful discussions. We apologize to colleagues who's work we were not able to cite due to space limitations.

Conflict of interest

The authors declare that the research was conducted in the absence of any commercial or financial relationships that could be construed as a potential conflict of interest.

Publisher's note

References

Ables, J. L., Decarolis, N. A., Johnson, M. A., Rivera, P. D., Gao, Z. L., Cooper, D. C., et al. (2010). Notch1 is required for maintenance of the reservoir of adult hippocampal stem cells. *J. Neurosci.* 30, 10484–10492. doi: 10.1523/JNEUROSCI.4721-09.2010

Aguirre, A., Rubio, M. E., and Gallo, V. (2010). Notch and EGFR pathway interaction regulates neural stem cell number and self-renewal. *Nature* 467, 323–327. doi: 10.1038/nature09347

Altman, J. (1962). Are new neurons formed in brains of adult mammals. *Science* 135, 1127–1128. doi: 10.1126/science.135.3509.1127

Altman, J., and Das, G. D. (1965). Autoradiographic and histological evidence of postnatal hippocampal neurogenesis in rats. *J. Comp. Neurol.* 124, 319–335. doi: 10.1002/cne.901240303

Bai, G., Sheng, N. Y., Xie, Z. H., Bian, W., Yokota, Y., Benezra, R., et al. (2007). Id sustains Hes1 expression to inhibit precocious neurogenesis by releasing negative autoregulation of Hes1. *Dev. Cell* 13, 283–297. doi: 10.1016/j.devcel.2007.05.014

Basak, O., Giachino, C., Fiorini, E., Macdonald, H. R., and Taylor, V. (2012). Neurogenic subventricular zone stem/progenitor cells are Notch1-dependent in their active but not quiescent state. *J. Neurosci.* 32, 5654–5666. doi: 10.1523/JNEUROSCI.0455-12.2012

Basak, O., Krieger, T. G., Muraro, M. J., Wiebrands, K., Stange, D. E., Frias-Aldeguer, J., et al. (2018). Troy+ brain stem cells cycle through quiescence and regulate their number by sensing niche occupancy. *Proc. Natl. Acad. Sci. U. S. A.* 115, E610–E619. doi: 10.1073/pnas.1715911114

Berg, D. A., Belnoue, L., Song, H. J., and Simon, A. (2013). Neurotransmitter-mediated control of neurogenesis in the adult vertebrate brain. *Development* 140, 2548–2561. doi: 10.1242/dev.088005

Berg, D. A., Su, Y. J., Jimenez-Cyrus, D., Patel, A., Huang, N., Morizet, D., et al. (2019). A common embryonic origin of stem cells drives developmental and adult neurogenesis. *Cells* 177, 654–668.e15. doi: 10.1016/j.cell.2019.02.010

Bigas, A., and Porcheri, C. (2018). Notch and stem cells. *Adv. Exp. Med. Biol.* 1066, 235–263. doi: 10.1007/978-3-319-89512-3_12

Blomfield, I. M., Rocamonde, B., Masdeu, M. D., Mulugeta, E., Vaga, S., Van Den Berg, D. L. C., et al. (2019). Id4 promotes the elimination of the pro-activation factor Ascl1 to maintain quiescence of adult hippocampal stem cells. *elife* 8:e48561. doi: 10.7554/eLife.48561

Boareto, M., Iber, D., and Taylor, V. (2017). Differential interactions between Notch and ID factors control neurogenesis by modulating Hes factor autoregulation. *Development* 144, 3465–3474. doi: 10.1242/dev.152520

Boldrini, M., Fulmore, C. A., Tartt, A. N., Simeon, L. R., Pavlova, I., Poposka, V., et al. (2018). Human hippocampal neurogenesis persists throughout aging. *Cell Stem Cell* 22:589. doi: 10.1016/j.stem.2018.03.015

Bonaguidi, M. A., Wheeler, M. A., Shapiro, J. S., Stadel, R. P., Sun, G. J., Ming, G. L., et al. (2011). In vivo clonal analysis reveals self-renewing and multipotent adult neural stem cell characteristics. *Cells* 145, 1142–1155. doi: 10.1016/j.cell.2011.05.024

Bonzano, S., Crisci, I., Podlesny-Drabiniok, A., Rolando, C., Krezel, W., Studer, M., et al. (2018). Neuron-astroglia cell fate decision in the adult mouse hippocampal neurogenic niche is cell-intrinsically controlled by COUP-TFI in vivo. *Cell Rep.* 24, 329–341. doi: 10.1016/j.celrep.2018.06.044

Bray, S. J. (2016). Notch signalling in context. *Nat. Rev. Mol. Cell Biol.* 17, 722–735. doi: 10.1038/nrm.2016.94

Calzolari, F., Michel, J., Baumgart, E. V., Theis, F., Gotz, M., and Ninkovic, J. (2015). Fast clonal expansion and limited neural stem cell self-renewal in the adult subependymal zone. *Nat. Neurosci.* 18, 490–492. doi: 10.1038/nn.3963

Carlen, M., Meletis, K., Goritz, C., Darsalia, V., Evergren, E., Tanigaki, K., et al. (2009). Forebrain ependymal cells are Notch-dependent and generate neuroblasts and astrocytes after stroke. *Nat. Neurosci.* 12, 259–267. doi: 10.1038/nn.2268

Chyung, J. H., Raper, D. M., and Selkoe, D. J. (2005). Gamma-secretase exists on the plasma membrane as an intact complex that accepts substrates and effects intramembrane cleavage. *J. Biol. Chem.* 280, 4383–4392. doi: 10.1074/jbc.M409272200

Delgado, A. C., Maldonado-Soto, A. R., Silva-Vargas, V., Mizrak, D., Von Kanel, T., Tan, K. R., et al. (2021). Release of stem cells from quiescence reveals gliogenic domains in the adult mouse brain. *Science* 372:1205. doi: 10.1126/science.abg8467

Doetsch, F., Caille, I., Lim, D. A., Garcia-Verdugo, J. M., and Alvarez-Buylla, A. (1999). Subventricular zone astrocytes are neural stem cells in the adult mammalian brain. *Cells* 97, 703–716. doi: 10.1016/S0092-8674(00)80783-7

Ehm, O., Goritz, C., Covic, M., Schaffner, I., Schwarz, T. J., Karaca, E., et al. (2010). RBPJ kappa-dependent signaling is essential for long-term maintenance of neural stem cells in the adult hippocampus. *J. Neurosci.* 30, 13794–13807. doi: 10.1523/JNEUROSCI.1567-10.2010

Ehret, F., Vogler, S., Pojar, S., Elliott, D. A., Bradke, F., Steiner, B., et al. (2015). Mouse model of CADASIL reveals novel insights into Notch3 function in adult hippocampal neurogenesis. *Neurobiol. Dis.* 75, 131–141. doi: 10.1016/j.nbd.2014.12.018

Encinas, J. M., Michurina, T. V., Peunova, N., Park, J. H., Tordo, J., Peterson, D. A., et al. (2011). Division-coupled astrocytic differentiation and age-related depletion of neural stem cells in the adult hippocampus. *Cell Stem Cell* 8, 566–579. doi: 10.1016/j.stem.2011.03.010

Engler, A., Rolando, C., Giachino, C., Saotome, I., Erni, A., Brien, C., et al. (2018a). Notch2 signaling maintains NSC quiescence in the murine ventricular-subventricular zone. *Cell Rep.* 22, 992–1002. doi: 10.1016/j.celrep.2017.12.094

Engler, A., Zhang, R. R., and Taylor, V. (2018b). Notch and neurogenesis. *Adv. Exp. Med. Biol.* 1066, 223–234. doi: 10.1007/978-3-319-89512-3_11

Falo-Sanjuan, J., and Bray, S. J. (2020). Decoding the Notch signal. *Develop. Growth Differ.* 62, 4–14. doi: 10.1111/dgd.12644

Fuentealba, L. C., Rompani, S. B., Parraguez, J. I., Obernier, K., Romero, R., Cepko, C. L., et al. (2015). Embryonic origin of postnatal neural stem cells. *Cells* 161, 1644–1655. doi: 10.1016/j.cell.2015.05.041

Furutachi, S., Miya, H., Watanabe, T., Kawai, H., Yamasaki, N., Harada, Y., et al. (2015). Slowly dividing neural progenitors are an embryonic origin of adult neural stem cells. *Nat. Neurosci.* 18:657. doi: 10.1038/nn.3989

Giachino, C., Basak, O., Lugert, S., Knuckles, P., Obernier, K., Fiorelli, R., et al. (2014). Molecular diversity subdivides the adult forebrain neural stem cell population. *Stem Cells* 32, 70–84. doi: 10.1002/stem.1520

Giachino, C., Boulay, J. L., Ivanek, R., Alvarado, A., Tostado, C., Lugert, S., et al. (2015). A tumor suppressor function for Notch signaling in forebrain tumor subtypes. *Cancer Cell* 28, 730–742. doi: 10.1016/j.ccell.2015.10.008

Giachino, C., and Taylor, V. (2014). Notching up neural stem cell homogeneity in homeostasis and disease. *Front. Neurosci.* 8:32. doi: 10.3389/fnins.2014.00032

Giaimo, B. D., and Borggrefe, T. (2018). Introduction to molecular mechanisms in Notch signal transduction and disease pathogenesis. *Adv. Exp. Med. Biol.* 1066, 3–30. doi: 10.1007/978-3-319-89512-3_1

Goncalves, J. T., Schafer, S. T., and Gage, F. H. (2016). Adult neurogenesis in the hippocampus: from stem cells to behavior. *Cells* 167, 897–914. doi: 10.1016/j.cell.2016.10.021

Gordon, W. R., Roy, M., Vardar-Ulu, D., Garfinkel, M., Mansour, M. R., Aster, J. C., et al. (2009). Structure of the Notch1-negative regulatory region: implications for normal activation and pathogenic signaling in T-ALL. *Blood* 113, 4381–4390. doi: 10.1182/blood-2008-08-174748

Gordon, W. R., Vardar-Ulu, D., Histen, G., Sanchez-Irizarry, C., Aster, J. C., and Blacklow, S. C. (2007). Structural basis for autoinhibition of Notch. *Nat. Struct. Mol. Biol.* 14, 295–300. doi: 10.1038/nsmb1227

Gupta-Rossi, N., Six, E., Lebail, O., Logeat, F., Chastagner, P., Olry, A., et al. (2004). Monoubiquitination and endocytosis direct gamma-secretase cleavage of activated Notch receptor. *J. Cell Biol.* 166, 73–83. doi: 10.1083/jcb.200310098

Handford, P. A., Korona, B., Suckling, R., Redfield, C., and Lea, S. M. (2018). Structural insights into Notch receptor-ligand interactions. *Adv. Exp. Med. Biol.* 1066, 33–46. doi: 10.1007/978-3-319-89512-3_2

Hansson, E. M., Stromberg, K., Bergstedt, S., Yu, G., Naslund, J., Lundkvist, J., et al. (2005). Aph-1 interacts at the cell surface with proteins in the active gamma-secretase complex and membrane-tethered Notch. *J. Neurochem.* 92, 1010–1020. doi: 10.1111/j.1471-4159.2004.02926.x

Harada, Y., Yamada, M., Imayoshi, I., Kageyama, R., Suzuki, Y., Kuniya, T., et al. (2021). Cell cycle arrest determines adult neural stem cell ontogeny by an embryonic Notch-nonoscillatory Hey1 module. *Nat. Commun.* 12:6562. doi: 10.1038/s41467-021-26605-0

Ho, D. M., Artavanis-Tsakonas, S., and Louvi, A. (2020). The Notch pathway in CNS homeostasis and neurodegeneration. *Wiley Interdiscipl. Rev. Develop. Biol.* 9:e358. doi: 10.1002/wdev.358

Ho, D. M., Guruharsha, K. G., and Artavanis-Tsakonas, S. (2018). The Notch interactome: complexity in signaling circuitry. *Adv. Exp. Med. Biol.* 1066, 125–140. doi: 10.1007/978-3-319-89512-3_7

Imayoshi, I., Isomura, A., Harima, Y., Kawaguchi, K., Kori, H., Miyachi, H., et al. (2013). Oscillatory control of factors determining multipotency and fate in mouse neural progenitors. *Science* 342, 1203–1208. doi: 10.1126/science.1242366

Imayoshi, I., Sakamoto, M., Yamaguchi, M., Mori, K., and Kageyama, R. (2010). Essential roles of Notch signaling in maintenance of neural stem cells in developing and adult brains. *J. Neurosci.* 30, 3489–3498. doi: 10.1523/JNEUROSCI.4987-09.2010

Irvin, D. K., Nakano, I., Paucar, A., and Kornblum, H. I. (2004). Patterns of Jagged1, Jagged2, delta-like 1 and delta-like 3 expression during late embryonic and postnatal brain development suggest multiple functional roles in progenitors and differentiated cells. *J. Neurosci. Res.* 75, 330–343. doi: 10.1002/jnr.10843

Kakuda, S., and Haltiwanger, R. S. (2017). Deciphering the fringe-mediated Notch code: identification of activating and inhibiting sites allowing discrimination between ligands. *Dev. Cell* 40, 193–201. doi: 10.1016/j.devcel.2016.12.013

Kawaguchi, D., Furutachi, S., Kawai, H., Hozumi, K., and Gotoh, Y. (2013). Dll1 maintains quiescence of adult neural stem cells and segregates asymmetrically during mitosis. *Nat. Commun.* 4:1880. doi: 10.1038/ncomms2895

Kawai, H., Kawaguchi, D., Kuebrich, B. D., Kitamoto, T., Yamaguchi, M., Gotoh, Y., et al. (2017). Area-specific regulation of quiescent neural stem cells by Notch3 in the adult mouse subependymal zone. *J. Neurosci.* 37, 11867–11880. doi: 10.1523/JNEUROSCI.0001-17.2017

Kempermann, G., Gage, F. H., Aigner, L., Song, H. J., Curtis, M. A., Thuret, S., et al. (2018). Human adult neurogenesis: evidence and remaining questions. *Cell Stem Cell* 23, 25–30. doi: 10.1016/j.stem.2018.04.004

Kjell, J., Fischer-Sternjak, J., Thompson, A. J., Friess, C., Sticco, M. J., Salinas, F., et al. (2020). Defining the adult neural stem cell niche proteome identifies key regulators of adult neurogenesis. *Cell Stem Cell* 26, 277–293.e8. doi: 10.1016/j.stem.2020.01.002

Lampada, A., Rolando, C., Freire, J., Giachino, C., Parmigiani, E., Engler, A., et al. (2022). Stress and elevation of serotonin from the raphe nuclei induce Septal neuron production in adult mice. *Cell Press Sneak Peek*. doi: 10.2139/ssrn.4084069

Lange, C., Prenninger, S., Knuckles, P., Taylor, V., Levin, M., and Calegari, F. (2011). The H(+) vacuolar ATPase maintains neural stem cells in the developing mouse cortex. *Stem Cells Dev.* 20, 843–850. doi: 10.1089/scd.2010.0484

Lavado, A., and Oliver, G. (2014). Jagged1 is necessary for postnatal and adult neurogenesis in the dentate gyrus. *Dev. Biol.* 388, 11–21. doi: 10.1016/j.ydbio.2014.02.004

Llorens-Bobadilla, E., Zhao, S., Baser, A., Saiz-Castro, G., Zwadlo, K., and Martin-Villalba, A. (2015). Single-cell transcriptomics reveals a population of dormant neural stem cells that become activated upon brain injury. *Cell Stem Cell* 17, 329–340. doi: 10.1016/j.stem.2015.07.002

Lovendahl, K. N., Blacklow, S. C., and Gordon, W. R. (2018). The molecular mechanism of Notch activation. *Adv. Exp. Med. Biol.* 1066, 47–58. doi: 10.1007/978-3-319-89512-3_3

Lugert, S., Basak, O., Knuckles, P., Haussler, U., Fabel, K., Gotz, M., et al. (2010). Quiescent and active hippocampal neural stem cells with distinct morphologies respond selectively to physiological and pathological stimuli and aging. *Cell Stem Cell* 6, 445–456. doi: 10.1016/j.stem.2010.03.017

Lugert, E., Vogt, M., Tchorz, J. S., Muller, M., Giachino, C., and Taylor, V. (2012). Homeostatic neurogenesis in the adult hippocampus does not involve amplification of Ascl1(high) intermediate progenitors. *Nat. Communicat.* 3:670. doi: 10.1038/ncomms1670

Matsubara, S., Matsuda, T., and Nakashima, K. (2021). Regulation of adult mammalian neural stem cells and neurogenesis by cell extrinsic and intrinsic factors. *Cells* 10:1145. doi: 10.3390/cells10051145

Meloty-Kapella, L., Shergill, B., Kuon, J., Botvinick, E., and Weinmaster, G. (2012). Notch ligand endocytosis generates mechanical pulling force dependent on dynamin, epsins, and actin. *Dev. Cell* 22, 1299–1312. doi: 10.1016/j.devcel.2012.04.005

Menn, B., Garcia-Verdugo, J. M., Yaschine, C., Gonzalez-Perez, O., Rowitch, D., and Alvarez-Buylla, A. (2006). Origin of oligodendrocytes in the subventricular zone of the adult brain. *J. Neurosci.* 26, 7907–7918. doi: 10.1523/JNEUROSCI.1299-06.2006

Merkle, F. T., Fuentealba, L. C., Sanders, T. A., Magno, L., Kessaris, N., and Alvarez-Buylla, A. (2014). Adult neural stem cells in distinct microdomains generate previously unknown interneuron types. *Nat. Neurosci.* 17, 207–214. doi: 10.1038/nn.3610

Merkle, F. T., Mirzadeh, Z., and Alvarez-Buylla, A. (2007). Mosaic organization of neural stem cells in the adult brain. *Science* 317, 381–384. doi: 10.1126/science.1144914

Merkle, F. T., Tramontin, A. D., Garcia-Verdugo, J. M., and Alvarez-Buylla, A. (2004). Radial glia give rise to adult neural stem cells in the subventricular zone. *Proc. Natl. Acad. Sci. U. S. A.* 101, 17528–17532. doi: 10.1073/pnas.0407893101

Mirzadeh, Z., Merkle, F. T., Soriano-Navarro, M., Garcia-Verdugo, J. M., and Alvarez-Buylla, A. (2008). Neural stem cells confer unique pinwheel architecture to the ventricular surface in neurogenic regions of the adult brain. *Cell Stem Cell* 3, 265–278. doi: 10.1016/j.stem.2008.07.004

Mizrak, D., Levitin, H. M., Delgado, A. C., Crotet, V., Yuan, J. Z., Chaker, Z., et al. (2019). Single-cell analysis of regional differences in adult V-SVZ neural stem cell lineages. *Cell Rep.* 26:394. doi: 10.1016/j.celrep.2018.12.044

Musse, A. A., Meloty-Kapella, L., and Weinmaster, G. (2012). Notch ligand endocytosis: mechanistic basis of signaling activity. *Semin. Cell Dev. Biol.* 23, 429–436. doi: 10.1016/j.semcdb.2012.01.011

Niola, F., Zhao, X., Singh, D., Castano, A., Sullivan, R., Lauria, M., et al. (2012). Id proteins synchronize stemness and anchorage to the niche of neural stem cells. *Nat. Cell Biol.* 14, 477–487. doi: 10.1038/ncb2490

Nyfeler, Y., Kirch, R. D., Mantei, N., Leone, D. P., Radtke, F., Suter, U., et al. (2005). Jagged1 signals in the postnatal subventricular zone are required for neural stem cell self-renewal. *EMBO J.* 24, 3504–3515. doi: 10.1038/sj.emboj.7600816

Obernier, K., and Alvarez-Buylla, A. (2019). Neural stem cells: origin, heterogeneity and regulation in the adult mammalian brain. *Development* 146:dev156059. doi: 10.1242/dev.156059

Obernier, K., Cebrian-Silla, A., Thomson, M., Parraguez, J. I., Anderson, R., Guinto, C., et al. (2018). Adult neurogenesis is sustained by symmetric self-renewal and differentiation. *Cell Stem Cell* 22, 221–234.e8. doi: 10.1016/j.stem.2018.01.003

Oswald, F., and Kovall, R. A. (2018). CSL-associated corepressor and coactivator complexes. *Adv. Exp. Med. Biol.* 1066, 279–295. doi: 10.1007/978-3-319-89512-3_14

Parmigiani, E., Ivanek, R., Rolando, C., Hafen, K., Turchinovich, G., Lehmann, F. M., et al. (2022). Interferon-gamma resistance and immune evasion in glioma develop via Notch-regulated co-evolution of malignant and immune cells. *Dev. Cell* 57, 1847–1865.e9. doi: 10.1016/j.devcel.2022.06.006

Parmigiani, E., Taylor, V., and Giachino, C. (2020). Oncogenic and tumor-suppressive functions of NOTCH signaling in Glioma. *Cells* 9:2304. doi: 10.3390/cells9102304

Pfisterer, U., and Khodosevich, K. (2017). Neuronal survival in the brain: neuron type-specific mechanisms. *Cell Death Dis.* 8:e2643. doi: 10.1038/cddis.2017.64

Pilz, G. A., Bottes, S., Betizeau, M., Jorg, D. J., Carta, S., Simons, B. D., et al. (2018). Live imaging of neurogenesis in the adult mouse hippocampus. *Science* 359:658. doi: 10.1126/science.aao5056

Rieskamp, J. D., Denninger, J. K., and Dause, T. J. (2018). Identifying the unique role of Notch3 in adult neural stem cell maintenance. *J. Neurosci.* 38, 3157–3159. doi: 10.1523/JNEUROSCI.3531-17.2018

Rolando, C., Erni, A., Grison, A., Beattie, R., Engler, A., Gokhale, P. J., et al. (2016). Multipotency of adult hippocampal NSCs in vivo is restricted by Drosha/NFIB. *Cell Stem Cell* 19, 653–662. doi: 10.1016/j.stem.2016.07.003

Ryu, J. R., Hong, C. J., Kim, J. Y., Kim, E. K., Sun, W., and Yu, S. W. (2016). Control of adult neurogenesis by programmed cell death in the mammalian brain. *Mol. Brain* 9:43. doi: 10.1186/s13041-016-0224-4

Salazar, J. L., and Yamamoto, S. (2018). Integration of Drosophila and human genetics to understand Notch signaling related diseases. *Adv. Exp. Med. Biol.* 1066, 141–185. doi: 10.1007/978-3-319-89512-3_8

Sanchez-Irizarry, C., Carpenter, A. C., Weng, A. P., Pear, W. S., Aster, J. C., and Blacklow, S. C. (2004). Notch subunit heterodimerization and prevention of ligand-independent proteolytic activation depend, respectively, on a novel domain and the LNR repeats. *Mol. Cell. Biol.* 24, 9265–9273. doi: 10.1128/MCB.24.21.9265-9273.2004

Schnute, B., Troost, T., and Klein, T. (2018). Endocytic trafficking of the Notch receptor. *Adv. Exp. Med. Biol.* 1066, 99–122. doi: 10.1007/978-3-319-89512-3_6

Semerci, F., Choi, W. T. S., Bajic, A., Thakkar, A., Encinas, J. M., Depreux, F., et al. (2017). Lunatic fringe-mediated Notch signaling regulates adult hippocampal neural stem cell maintenance. *elife* 6:e24660. doi: 10.7554/eLife.24660

Seri, B., Garcia-Verdugo, J. M., Mcewen, B. S., and Alvarez-Buylla, A. (2001). Astrocytes give rise to new neurons in the adult mammalian hippocampus. *J. Neurosci.* 21, 7153–7160. doi: 10.1523/JNEUROSCI.21-18-07153.2001

Shin, J., Berg, D. A., Zhu, Y. H., Shin, J. Y., Song, J., Bonaguidi, M. A., et al. (2015). Single-cell RNA-Seq with waterfall reveals molecular cascades underlying adult neurogenesis. *Cell Stem Cell* 17, 360–372. doi: 10.1016/j.stem.2015.07.013

Sierra, A., Encinas, J. M., Deudero, J. J., Chancey, J. H., Enikolopov, G., Overstreet-Wadiche, L. S., et al. (2010). Microglia shape adult hippocampal neurogenesis through apoptosis-coupled phagocytosis. *Cell Stem Cell* 7, 483–495. doi: 10.1016/j.stem.2010.08.014

Sorrells, S. F., Paredes, M. F., Cebrian-Silla, A., Sandoval, K., Qi, D. S., Kelley, K. W., et al. (2018). Human hippocampal neurogenesis drops sharply in children to undetectable levels in adults. *Nature* 555, 377–381. doi: 10.1038/nature25975

Sprinzak, D., and Blacklow, S. C. (2021). Biophysics of Notch signaling. *Annu. Rev. Biophys.* 50, 157–189. doi: 10.1146/annurev-biophys-101920-082204

Sprinzak, D., Lakhanpal, A., Lebon, L., Santat, L. A., Fontes, M. E., Anderson, G. A., et al. (2010). Cis-interactions between Notch and Delta generate mutually exclusive signalling states. *Nature* 465, 86–90. doi: 10.1038/nature08959

Steinbuck, M. P., and Winandy, S. (2018). A review of Notch processing with new insights into ligand-independent Notch signaling in T-cells. *Front. Immunol.* 9:1230. doi: 10.3389/fimmu.2018.01230

Stump, G., Durrer, A., Klein, A. L., Lutolf, S., Suter, U., and Taylor, V. (2002). Notch1 and its ligands Delta-like and jagged are expressed and active in distinct cell populations in the postnatal mouse brain. *Mech. Dev.* 114, 153–159. doi: 10.1016/S0925-4773(02)00043-6

Sueda, R., Imayoshi, I., Harima, Y., and Kageyama, R. (2019). High Hes1 expression and resultant Ascl1 suppression regulate quiescent vs. active neural stem cells in the adult mouse brain. *Genes Dev.* 33, 511–523. doi: 10.1101/gad.323196.118

Sueda, R., and Kageyama, R. (2020). Regulation of active and quiescent somatic stem cells by Notch signaling. *Develop. Growth Differ.* 62, 59–66. doi: 10.1111/dgd.12626

Tong, C. K., Chen, J. D., Cebrian-Silla, A., Mirzadeh, Z., Obernier, K., Guinto, C. D., et al. (2014). Axonal control of the adult neural stem cell niche. *Cell Stem Cell* 14, 500–511. doi: 10.1016/j.stem.2014.01.014

Urban, N., Blomfield, I. M., and Guillemot, F. (2019). Quiescence of adult mammalian neural stem cells: a highly regulated rest. *Neuron* 104, 834–848. doi: 10.1016/j.neuron.2019.09.026

Urban, N., Van Den Berg, D. L., Forget, A., Andersen, J., Demmers, J. A., Hunt, C., et al. (2016). Return to quiescence of mouse neural stem cells by degradation of a proactivation protein. *Science* 353, 292–295. doi: 10.1126/science.aaf4802

Van Praag, H., Schinder, A. F., Christie, B. R., Toni, N., Palmer, T. D., and Gage, F. H. (2002). Functional neurogenesis in the adult hippocampus. *Nature* 415, 1030–1034. doi: 10.1038/4151030a

Weinmaster, G., and Fischer, J. A. (2011). Notch ligand ubiquitylation: what is it good for? *Dev. Cell* 21, 134–144. doi: 10.1016/j.devcel.2011.06.006

Zhang, R. R., Boareto, M., Engler, A., Louvi, A., Giachino, C., Iber, D., et al. (2019). Id4 downstream of Notch2 maintains neural stem cell quiescence in the adult hippocampus. *Cell Rep.* 28:1485. doi: 10.1016/j.celrep.2019.07.014

Zhang, R. R., Engler, A., and Taylor, V. (2018). Notch: an interactive player in neurogenesis and disease. *Cell Tissue Res.* 371, 73–89. doi: 10.1007/s00441-017-2641-9

frontiers | Frontiers in Neuroscience

TYPE Brief Research Report
PUBLISHED 13 July 2023
DOI 10.3389/fnins.2023.1143130

OPEN ACCESS

EDITED BY
Seiji Hitoshi,
Shiga University of Medical Science, Japan

REVIEWED BY
Masahiro Yamaguchi,
Kōchi University, Japan
Jisoo Han,
University of California, Davis, United States

*CORRESPONDENCE
Kazunobu Sawamoto
✉ sawamoto@med.nagoya-cu.ac.jp

RECEIVED 12 January 2023
ACCEPTED 29 June 2023
PUBLISHED 13 July 2023

CITATION
Sawada M, Hamaguchi A, Mano N, Yoshida Y, Uemura A and Sawamoto K (2023) PlexinD1 signaling controls domain-specific dendritic development in newborn neurons in the postnatal olfactory bulb.
Front. Neurosci. 17:1143130.
doi: 10.3389/fnins.2023.1143130

PlexinD1 signaling controls domain-specific dendritic development in newborn neurons in the postnatal olfactory bulb

Masato Sawada[1,2], Ayato Hamaguchi[1], Naomichi Mano[1], Yutaka Yoshida[3,4,5], Akiyoshi Uemura[6] and Kazunobu Sawamoto[1,2]*

[1]Department of Developmental and Regenerative Neurobiology, Institute of Brain Science, Nagoya City University Graduate School of Medical Sciences, Nagoya, Japan, [2]Division of Neural Development and Regeneration, National Institute of Physiological Sciences, Okazaki, Japan, [3]Burke Neurological Institute, White Plains, NY, United States, [4]Brain and Mind Research Institute, Weill Cornell Medicine, New York, NY, United States, [5]Neural Circuit Unit, Okinawa Institute of Science and Technology Graduate University, Okinawa, Japan, [6]Department of Retinal Vascular Biology, Nagoya City University Graduate School of Medical Sciences, Nagoya, Japan

Newborn neurons show immature bipolar morphology and continue to migrate toward their destinations. After the termination of migration, newborn neurons undergo spatially controlled dendrite formation and change into a complex morphology. The mechanisms of dendritic development of newborn neurons have not been fully understood. Here, we show that in the postnatal olfactory bulb (OB), the Sema3E-PlexinD1 signaling, which maintains bipolar morphology of newborn neurons, also regulates their dendritic development after the termination of migration in a dendritic domain-specific manner. Genetic ablation of *Sema3E* or *PlexinD1* enhanced dendritic branching in the proximal domain of the apical dendrites of OB newborn granule cells, whereas PlexinD1 overexpression suppressed it in a Rho binding domain (RBD)-dependent manner. Furthermore, RhoJ, a small GTPase that directly binds to PlexinD1RBD in vascular endothelial cells, is expressed in migrating and differentiating newborn granule cells in the OB and is also involved in the suppression of proximal branching of their apical dendrites. These results suggest that the Sema3E-PlexinD1-RhoJ axis regulates domain-specific dendrite formation of newborn neurons in the postnatal OB.

KEYWORDS

postnatal neurogenesis, ventricular-subventricular zone, olfactory bulb, newborn neurons, dendrites, PlexinD1, RhoJ

Introduction

The brain of postnatal mammals contains neural stem cells (NSCs), which have the ability to generate new functional neurons. In the ventricular-subventricular-zone (V-SVZ) lining the lateral walls of the lateral ventricles, the largest neurogenic niche in the postnatal brain, newborn neurons generated from NSCs migrate toward the olfactory bulb (OB), a primary center for odor information processing (Bressan and Saghatelyan, 2020; Nakajima et al., 2021). After reaching the OB, most of the newborn neurons terminate their migration in the granule cell layer (GCL), develop their complex dendrites to precisely connect with preexisting OB circuits, and differentiate fully into granule cells, the major inhibitory interneurons in the OB (Luskin, 1993;

Lois and Alvarez-Buylla, 1994). Eliminating newborn neurons or blocking their synaptic transmission causes disruption of normal olfactory behaviors (Breton-Provencher et al., 2009; Sakamoto et al., 2014; Muthusamy et al., 2017). Thus, the integration of newborn neurons into mature OB circuits is critical for olfactory functions, and could be accomplished by appropriate dendritogenesis. However, its mechanism is still largely unknown.

In the OB, granule cells have short basal dendrites extending in the basal domain and a single long apical dendrite consisting of an unbranched proximal domain and a highly ramified distal domain (Price and Powell, 1970; Petreanu and Alvarez-Buylla, 2002; Kelsch et al., 2008). In the apical dendrite of granule cells, while the proximal domain receives centrifugal inputs from olfactory higher centers, the distal domain receives peripheral inputs from mitral/tufted cells, projection neurons in the OB (Shepherd et al., 2004). Therefore, the dendritic domains of granule cells are integrated into functionally distinct OB circuits, and their morphological regulation could be the basis of granule cell functions. Previous studies suggest that olfactory input (Saghatelyan et al., 2005) and 5T4 (Yoshihara et al., 2012) promote dendritic branching in the distal domain of the apical dendrites. However, the mechanism for suppression of dendritic branching in the proximal domain of apical dendrites remains unknown.

The secreted protein Sema3E and its receptor PlexinD1 are involved in morphogenesis of the nervous and vascular systems during development (Gay et al., 2011; Oh and Gu, 2013). In the central nervous system (CNS), PlexinD1 signaling is involved in the regulation of migration (Bribian et al., 2014; Sawada et al., 2018), survival (Cariboni et al., 2015), axonal elongation (Chauvet et al., 2007; Deck et al., 2013; Burk et al., 2017), and connections (Pecho-Vrieseling et al., 2009; Ding et al., 2011; Fukuhara et al., 2013; Mata et al., 2018) of neural cells. However, the role of PlexinD1 signaling in dendritogenesis in the CNS remains unclear. We have previously shown that PlexinD1 signaling suppresses the formation of filopodium-like lateral protrusions (FLPs), which branch laterally from the proximal domain of the leading process of migrating newborn neurons, thereby maintaining their immature bipolar morphology (Sawada et al., 2018). Therefore, we hypothesized that PlexinD1 signaling also suppresses dendritic branching in the proximal domain of apical dendrites in newborn granule cells after migration termination.

In this study, we show that PlexinD1 signaling is involved in the suppression of proximal branching of apical dendrites in newborn granule cells. We also show that this domain-specific regulation is controlled by the small GTPase RhoJ, a direct binding partner of PlexinD1.

Methods

Animals

Wild-type (WT) C57BL/6J mice were purchased from Japan SLC. *PlexinD1*-flox mice (Zhang et al., 2009) were described previously. *Sema3E*-KO mice (Gu et al., 2005) were provided by Dr. Fanny Mann (Institut de Biologie du Developpement de Marseille) and Dr. Christopher E. Henderson (Columbia University). *RhoJ*-KO mice were described previously (Kim et al., 2014). Both male and female animals were used in this study. All animals were maintained with their mother mouse during weaning and within 7 mice per cage after weaning on a 12 h light/dark cycle with *ad libitum* access to food and water. All of the animal experiments were performed in accordance with the guidelines and regulations of Nagoya City University (Approval No. 21-028).

Lentiviral vectors and plasmids

CSII-CMV-RfA-IRES2-Venus and CSII-EF-Venus lentiviral vectors were provided by Dr. Hiroyuki Miyoshi (RIKEN Tsukuba BioResource Center). CSII-CMV-PlexinD1-IRES2-Venus and CSII-CMV-PlexinD1ΔRBD-IRES2-Venus were described previously (Sawada et al., 2018). The pLV-CMV-tdTomato-IRES-Cre was provided by Dr. Magdalena Götz (Munich University). These viral vectors and the packaging vectors (pCAG-HIVgp and pCMV-VSV-G-RSV-Rev) were co-transfected into HEK293T cells using polyethylenimine to generate lentiviral particles, and then the culture supernatants were concentrated by centrifuging at 8,000 rpm for 16 h at 4°C using a refrigerated microcentrifuge (MX-307, Tomy) and resuspended with sterile phosphate buffered saline (PBS).

pEGFPC2 and pEGFPC2-RhoJ were described previously (Kusuhara et al., 2012; Fukushima et al., 2020). pCAGGS-DsRed was described previously (Sawada et al., 2018). These plasmids were amplified using *E. coli* and purified using a PureLink HiPure Plasmid Midiprep kit (Invitrogen).

In vitro V-SVZ cell culture

The V-SVZ cell culture was performed as described previously (Sawada et al., 2018). Briefly, the V-SVZ tissues were dissected from P0-1 WT, *PlexinD1*$^{+/fl}$, and *PlexinD1*$^{fl/fl}$ pups and dissociated with trypsin–EDTA (Invitrogen). The cells were washed two times in L-15 medium (Invitrogen) containing 40 μg/mL DNase I (Roche), seeded on coverglass (Matsunami) in 24-well cell culture plates, and cultured in Neurobasal medium (GIBCO) containing 10% fetal bovine serum, 2% NeuroBrew-21 (MACS Miltenyi Biotec), 2 mM L-glutamine (GIBCO), and 50 U/mL penicillin–streptomycin (GIBCO). At 4 days *in vitro* (div), 1 μL of lentiviral particles was added into the culture medium. At 10 div, cells were fixed with 4% paraformaldehyde (PFA) in 0.1 M phosphate buffer (PB) for 15 min at room temperature (RT) and subjected to immunocytochemistry.

In vivo lentiviral infection and electroporation

Injection of lentiviral suspension and plasmid solution was described previously (Ota et al., 2014; Sawada et al., 2018). For lentiviral infection, a 2 μL volume of lentiviral suspension was stereotaxically injected into the V-SVZ (1.8 mm anterior, 1.4 mm lateral to lambda and 1.5–2.0 mm deep) of male and female pups at postnatal day 1 (P1). For *in vivo* electroporation of P1 male and female pups, a 2 μL volume of plasmids (3.5 μg/μL) containing 0.05% Fast Green was stereotaxically injected into the lateral ventricle (1.8 mm anterior, 1.2 mm lateral to lambda and 2.0 mm deep), and electroporation was performed using an electroporator (CUY-21SC,

Nepagene) with a forceps-type electrode (CUY650P7, Nepagene). Lentivirus-injected or electroporated pups were allowed to recover on a heating pad and returned to their home cage.

Immunohistochemistry and immunocytochemistry

Immunohistochemistry was performed as described previously (Sawada et al., 2018). Briefly, the brain was fixed by transcardiac perfusion with 4% PFA in 0.1 M PB, and postfixed overnight in the same fixative at 4°C. Sixty-micrometer-thick coronal sections were prepared using a vibratome (VT-1200S, Leica) and incubated for 30 min at RT in blocking solution (10% normal donkey serum and 0.2% Triton X-100 in PBS). The sections were then incubated overnight at 4°C with the primary antibodies, and then for 2 h at RT with biotin- or Alexa Fluor-conjugated secondary antibodies (1:1,000, Invitrogen) in the blocking solution. For immunocytochemistry, fixed cells were incubated for 30 min at RT in blocking solution, overnight at 4°C with the primary antibodies, and then for 2 h at RT with Alexa Fluor-conjugated secondary antibodies (1:1,000, Invitrogen) in the blocking solution. The signal amplification and visualization were performed using the Vectastain Elite ABC kit (Vector Laboratories) and Tyramide Signal Amplification (Thermo Fisher Scientific), respectively. The following primary antibodies were used: mouse anti-βIII-tubulin (Tuj1) (1:1,000, Sigma); rat anti-CD31 (1:100, BD Pharmingen); rabbit anti-doublecortin (Dcx) (1:200, Cell Signaling Technology); guinea pig anti-Dcx (1:500, Chemicon); rabbit anti-DsRed (1:1,000, Clontech); rabbit anti-GFP (1:500, MBL); rat anti-GFP (1:500, Nakalai Tesque); rabbit anti-NeuN (1:1,000, abcam); goat anti-PlexinD1 (1:100, abcam); goat anti-PlexinD1 (1:100, R&D systems) antibodies. Nuclei were stained with Hoechst 33342 (1:5,000, Sigma).

Confocal image acquisition, quantification, and dendritic tracing of granule cells

Image acquisition and dendritic tracing of granule cells were performed as previously described (Sawada et al., 2018). Images of labeled granule cells of the postnatal OB were acquired by scanning at 2 µm intervals using an LSM 700 confocal laser-scanning microscope (Carl Zeiss) with a 20× objective lens (NA 0.8). For characterization of *RhoJ*$^{+/GFP}$-positive cells, three regions-of-interest (ROIs) were randomly selected from three consecutive sections (one ROI per section) from every sixth 60 µm-thick OB section and image acquisition was performed, and all of the positive cells in the ROIs were counted. The obtained proportions of *RhoJ*$^{+/GFP}$-positive cells were reported as mean ± SEM ($n = 3$ mice). Acquired z-stack images of virally labeled neurons were traced, reconstructed, and quantified using Neurolucida and Neurolucida Explorer software (MBF Bioscience) (Sawada et al., 2018). For analysis of apical and basal dendrites, all of the labeled granule cells showing complete neuronal morphologies observed in every sixth section were traced and analyzed. For analysis of dendritic branching in the proximal domain of the apical dendrite, all of the labeled granule cells showing >100 µm-length apical dendrites from soma were analyzed in this study. Dendritic branching in all domains of granule cells was expressed as branching in the dendritic domain per cell. For validation of PlexinD1 expression in neuronal culture, the signal intensity in the cell surface of labeled cells was measured using ZEN software (Carl Zeiss), and the average signal intensity (per µm), and normalized value (average value of control groups is 1.0) were calculated as reported previously (Sawada et al., 2018).

Statistical analysis

All of the data were two-tailed and analyzed using EZR (Kanda, 2013). The data distribution was analyzed by the Kolmogorov–Smirnov test. The equality of variance between groups was analyzed by the *F* test. Comparisons between two groups were analyzed by unpaired *t*-test or Mann–Whitney *U*-test. Comparisons among multiple groups were analyzed by one-way ANOVA test followed by a post-hoc Tukey–Kramer test, or Kruskal-Wallis test followed by a *post-hoc* Steel-Dwass test. All the numerical data are presented as the mean ± SEM and *p*-values less than 0.05 were considered statistically significant.

Results

PlexinD1 signaling specifically suppresses dendritic branching in the proximal domain of the apical dendrite of newborn granule cells in the postnatal OB

In the GCL of the postnatal OB, while Sema3E is expressed in mature granule cells, PlexinD1 is expressed in the leading process of migrating newborn neurons and is involved in suppressing FLP formation to maintain their immature morphology (Sawada et al., 2018). In this study, we investigated whether Sema3E-PlexinD1 signaling is also involved in the suppression of dendritic branching in the proximal domain of the apical dendrite of newborn granule cells that have terminated their migration.

First, we injected lentivirus encoding Venus into the V-SVZ of *Sema3E*$^{+/-}$ (control) and *Sema3E*$^{-/-}$ (*Sema3E*-KO) mice (Gu et al., 2005) at postnatal day 1 (P1) and analyzed the dendritic morphology of Venus+ granule cells in the GCL at 10 days post infection (dpi) (Figure 1A). The branch number in the proximal domain of the apical dendrite was significantly increased in *Sema3E*-KO mice compared with control mice (Figures 1B–D), suggesting that Sema3E suppresses dendritic branching in the proximal domain of the apical dendrite of newborn granule cells.

Next, to investigate the expression and role of PlexinD1 in this process, brain sections were stained with a PlexinD1 antibody. The PlexinD1 signal was observed in the proximal domain of the apical dendrite of differentiating granule cells (Supplementary Figure S1A). For functional analyses of PlexinD1, we used lentivirus encoding tdTomato and Cre recombinase. The decrease of PlexinD1 proteins by these vectors was confirmed in primary neuronal cultures (Figures 1E,F). To examine the function of PlexinD1 *in vivo*, we injected these lentiviral vectors into the V-SVZ of *PlexinD1*$^{+/flox}$ (control) and *PlexinD1*$^{flox/flox}$ (*PlexinD1*-cKO) mice (Zhang et al., 2009) at P1 and analyzed the dendritic morphology of tdTomato+ granule cells (Figure 1G). At 10 dpi, similar to the phenotype observed in *Sema3E*-KO mice, the branch number in the proximal domain of the apical dendrite was significantly increased by *PlexinD1* deficiency (Figures 1H–J). Moreover, at 28 dpi, when granule cells morphologically

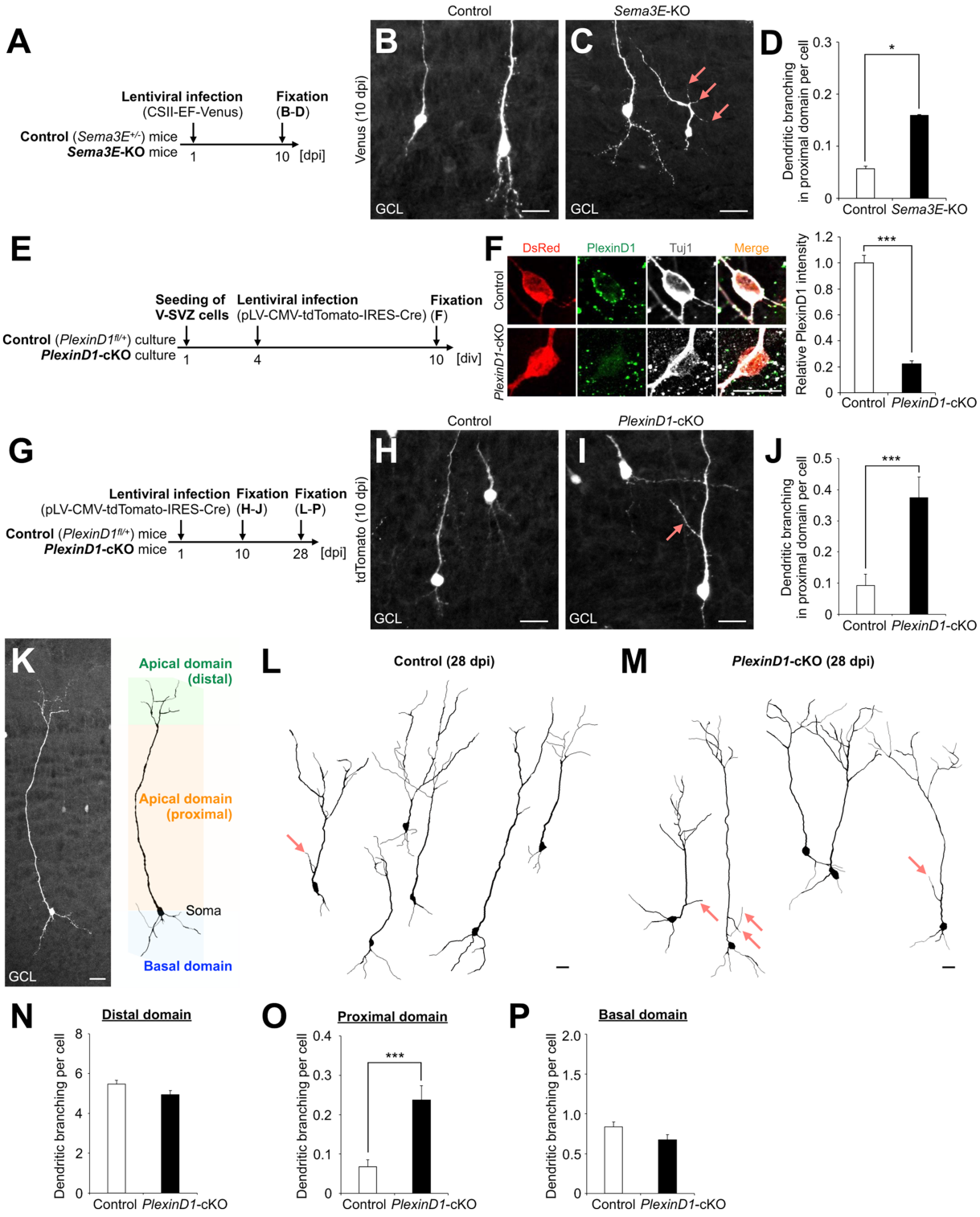

FIGURE 1
Sema3E-PlexinD1 signaling suppresses dendritic branching in the proximal domain of the apical dendrite of granule cells in the postnatal OB. **(A)** Experimental scheme in *Sema3E*-KO mice. **(B,C)** Representative projection images of Venus+ granule cells in control **(B)** and *Sema3E*-KO **(C)** mice at 10 dpi. **(D)** Dendritic branch number in the proximal domain of the apical dendrite in control (n=527 cells from 4 mice) and *Sema3E*-KO (n=962 cells from 5 mice) mice. **(E)** Experimental scheme of *PlexinD1*-cKO culture. **(F)** Representative images of DsRed+ (red) Tuj1+ (white) cultured control and *PlexinD1*-cKO neurons. Green indicates PlexinD1. Graph indicates relative PlexinD1 intensity in the infected neurons (control, n=35 cells; *PlexinD1*-cKO, n=30 cells; three independent experiments). **(G)** Experimental scheme in *PlexinD1*-cKO mice. **(H,I)** Representative projection images of Venus+ granule cells in Control **(H)** and *PlexinD1*-cKO **(I)** mice at 10 dpi. **(J)** Dendritic branch number in the proximal domain of the apical dendrite in control (n=206 cells from 6 mice) and *PlexinD1*-cKO (n=139 cells from 5 mice) mice at 10 dpi. **(K)** Classification of dendritic domains in granule cells. **(L,M)** Representative dendritic tracing of Venus+ granule cells in control [**(L)**; n=200 cells from 5 mice] and *PlexinD1*-cKO [**(M)**; n=138 cells from 5 mice]

(Continued)

FIGURE 1 (Continued)
mice. **(N–P)** Dendritic branch number in the distal [**(N)**; control, *n*=200 cells from 5 mice; KO, *n*=138 cells from 5 mice], proximal [**(O)**; control, *n*=200 cells from 5 mice; KO, *n*=138 cells from 5 mice], and basal [**(P)**; control, *n*=200 cells from 5 mice; KO, *n*=138 cells from 5 mice] domains in control and *PlexinD1*-cKO mice at 28 dpi. Pink arrows indicate dendritic branches in the proximal domain of apical dendrites. GCL, granule cell layer. *p<0.05, ***p<0.005. Scale bars: **(B)**, **(C)**, **(H)**, **(I)**, **(K)**, 20 μm; **(F)**, 10μm. Bars indicate mean±SEM.

mature (Petreanu and Alvarez-Buylla, 2002), the whole dendritic morphology of tdTomato+ granule cells was traced (Figure 1K). We found that the dendritic branch number in the proximal but not the distal or basal domain in tdTomato+ granule cells was significantly increased in *PlexinD1*-cKO mice compared to that in control mice (Figures 1L–P). The dendritic length of the apical and basal dendrites was not significantly different between control and *PlexinD1*-cKO mice (Supplementary Figures S1B–E). Taken together, these results suggest that Sema3E-PlexinD1 signaling is specifically involved in the suppression of dendritic branching in the proximal domain of the apical dendrite of newborn granule cells in the postnatal OB.

PlexinD1's RBD is involved in the PlexinD1-mediated suppression of dendritic branching at proximal domain of apical dendrites in newborn granule cells

The intracellular domain of Plexins has a Rho binding domain (RBD), which regulates cytoskeletal dynamics through binding to various Rho family small GTPases (Gay et al., 2011) (Figure 2A). To study the role of PlexinD1 and its RBD in dendritic development of newborn granule cells, we generated lentiviral vectors encoding PlexinD1 or its deletion mutant of RBD (PlexinD1ΔRBD), and confirmed their overexpression in primary neuronal cultures (Figures 2A–D). To examine the effects of PlexinD1 overexpression on the dendritic branching *in vivo*, we injected these lentiviruses into the V-SVZ and analyzed the dendritic morphology of infected granule cells in the OB at 10 dpi (Figure 2E). Overexpression of PlexinD1 decreased the number of dendritic branches in the proximal domain of the apical dendrite (Figures 2F,G,I). This effect was partially diminished when lentiviruses encoding PlexinD1ΔRBD were injected (Figures 2H,I). These results suggest that RBD is involved in the suppression of dendritic branching in the proximal domain of the apical dendrites of newborn granule cells by PlexinD1 overexpression.

Rhoj is expressed in migrating and differentiating granule cells, and suppresses dendritic branching of proximal domain of their apical dendrites

RhoJ, a member of Rho family small GTPases, is highly expressed in vascular endothelial cells and involved in Sema3E's repulsive effect by directly binding to the PlexinD1RBD to promote F-actin depolymerization (Fukushima et al., 2011, 2020). In the developing retina, RhoJ is expressed in not only vascular endothelial cells but also neurons (Fukushima et al., 2020). However, the function of RhoJ in the CNS remains unknown. Since RBD is involved in the PlexinD1-induced suppression of dendritic branching in the proximal domain of apical dendrites (Figure 2), we hypothesized that RhoJ contributes to this process.

First, to identify RhoJ-expressing cells in the V-SVZ-OB pathway, we analyzed GFP-expressing cell types in *RhoJ*$^{+/GFP}$ mice (Kim et al., 2014), in which EGFP replaces exon 1 of the *RhoJ* gene and is expressed under the control of the endogenous *RhoJ* promoter. EGFP was strongly expressed in the CD31+ vascular endothelial cells not only in the retina (Fukushima et al., 2020) but also in the brain (Figure 3A). We found that EGFP was not expressed in Dcx + cells in the V-SVZ, but was expressed in a subset of Dcx + and NeuN+ cells in the core and GCL of the OB (Figures 3B–E). These results suggest that newborn neurons express RhoJ during migration and maturation in the postnatal OB.

Next, to investigate the effect of forced expression of RhoJ on the dendritogenesis of newborn granule cells, plasmids encoding an EGFP-fused RhoJ were introduced into the V-SVZ by *in vivo* electroporation, and the dendritic morphology of labeled granule cells in the GCL was analyzed at 10 dpi (Figure 3F). The forced expression of RhoJ in granule cells significantly suppressed both their dendritic branching in the distal and proximal domains (Figures 3G–J) and dendritic length in the distal domain (Figure 3G; control, 340.0 ± 28.5 μm; RhoJ, 224.5 ± 29.0 μm; $p = 0.0063$, unpaired t-test). These results suggest that RhoJ overexpression has an inhibitory effect on dendritic branching and outgrowth *in vivo*.

Finally, to study the function of RhoJ on dendritogenesis of newborn granule cells, we introduced plasmids encoding DsRed into the V-SVZ of *RhoJ*$^{+/GFP}$ (control) and *RhoJ*$^{GFP/GFP}$ (*RhoJ*-KO) mice by *in vivo* electroporation and analyzed their dendritic morphology (Figure 3K). The dendritic branch number in the proximal but not distal or basal domain in DsRed+ granule cells was significantly increased in *RhoJ*-KO mice (Figures 3L–O). The dendritic length of the apical and basal dendrites was not significantly different between control and *RhoJ*-KO mice (Supplementary Figures S1B,F–H). Furthermore, the increase of dendritic branching in the proximal domain in *RhoJ*-KO neurons was partially diminished by PlexinD1 overexpression (Figures 3L–O). Together, these results suggest that RhoJ is specifically involved in the suppression of dendritic branching in the proximal domain of the apical dendrite of newborn granule cells in the postnatal OB.

Discussion

In this study, we demonstrated that Sema3E-PlexinD1 signaling is involved in the domain-specific dendritic branching of newborn granule cells in the postnatal OB. Furthermore, we showed that RhoJ, a small GTPase that directly binds to PlexinD1, is expressed in newborn granule cells during migration and maturation in the postnatal OB and involved in the proximal domain-specific inhibition of dendritic branching. These results provide new insights into the dendritogenesis of newborn neurons in the postnatal brain.

In the postnatal OB, granule cells receive centrifugal inputs in the proximal domain of the apical dendrite (Kaneko et al., 2006; Whitman and Greer, 2007; Yokoyama et al., 2011; Komano-Inoue et al., 2014). The distal domain of the apical dendrite undergoes many branchings, whereas the proximal domain maintains an unbranched state

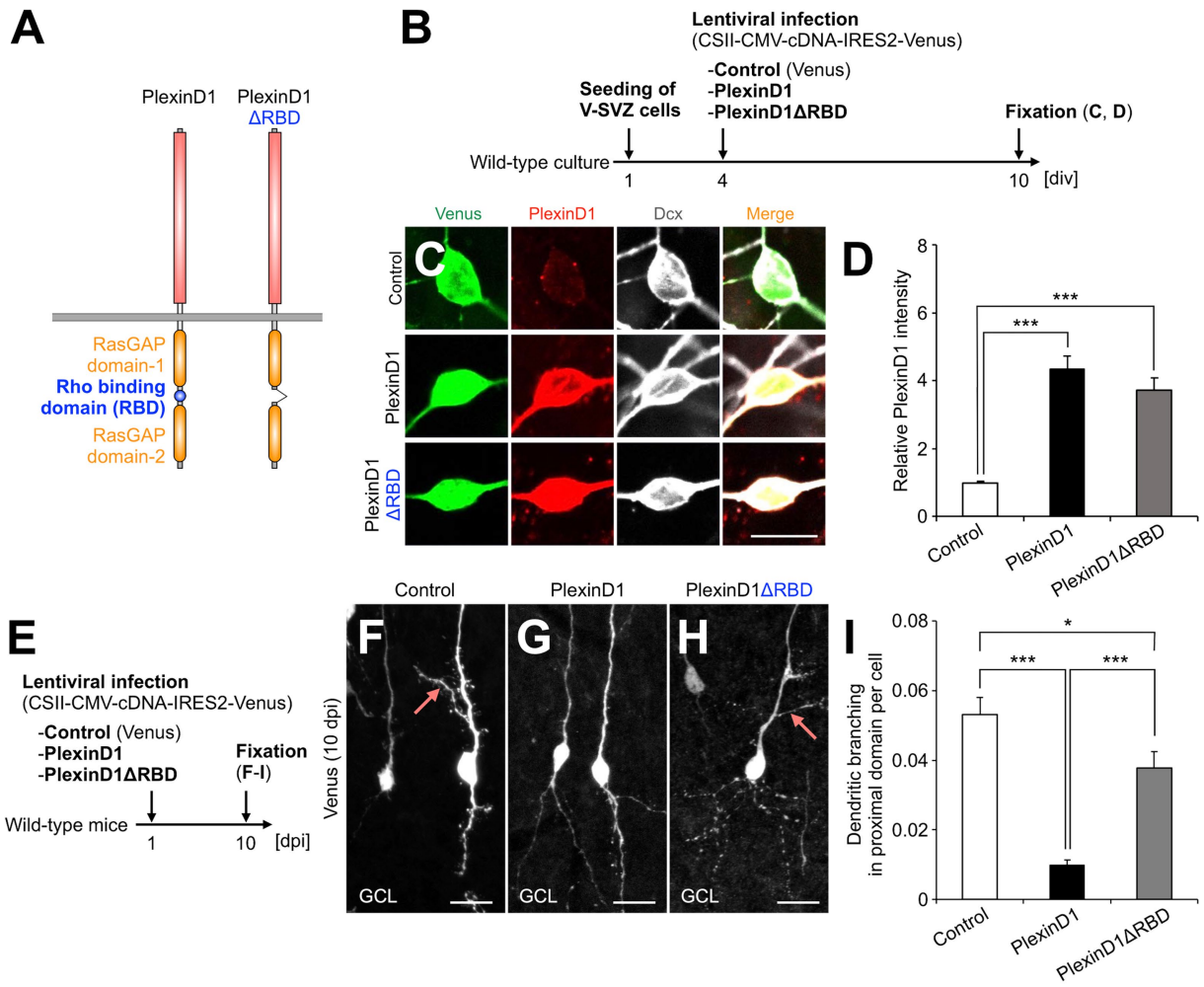

FIGURE 2
PlexinD1's RBD is involved in the PlexinD1-mediated suppression of lateral dendrite formation in granule cells in the postnatal OB. **(A)** Molecular structure of PlexinD1. **(B)** Experimental scheme of PlexinD1- and PlexinD1ΔRBD-overexpressing neuronal culture. **(C)** Representative images of Venus+ (green) Dcx+(white) cultured control, PlexinD1-overexpressing, and PlexinD1ΔRBD-overexpressing neurons. Red indicates PlexinD1. **(D)** Relative PlexinD1 intensity in the infected neurons (control, *n*=49 cells; PlexinD1, *n*=38 cells; PlexinD1ΔRBD, *n*=30 cells; three independent experiments). **(E)** Experimental scheme for PlexinD1 overexpression *in vivo*. **(F–H)** Representative projection images of Venus+ control **(F)**, PlexinD1-overexpressing **(G)**, and PlexinD1ΔRBD-overexpressing **(H)** granule cells at 10 dpi. **(I)** Proportions of lateral dendrite-bearing granule cells at 10 dpi (control, *n*=2,217 cells from 5 mice; PlexinD1, *n*=4,204 cells from 5 mice; PlexinD1ΔRBD, *n*=1,641 cells from 5 mice). Pink arrows indicate dendritic branches in the proximal domain of the apical dendrite. GCL, granule cell layer; RBD, Rho binding domain. *p<0.05, ***p<0.005. Scale bars: **(C)**, 10 μm; **(F–H)**, 20 μm. Bars indicate mean±SEM.

(Shepherd et al., 2004). Excessive centrifugal input to newborn granule cells may result in strong GABA-mediated feedback to mitral/tufted cells and excessively downregulated neuronal transmission from the OB toward the olfactory higher centers. Therefore, granule cells need a mechanism to inhibit dendritic branching in the proximal domain of the apical dendrite to prevent them from receiving too much centrifugal input. Our results indicate that PlexinD1 signaling not only determines the final positioning of newborn neurons by suppressing FLP formation during migration (Sawada et al., 2018), but also maintains the proximal domain of the apical dendrite unbranched after migration termination, thereby ensuring proper reception of centrifugal inputs.

Previous studies suggested that olfactory input (Saghatelyan et al., 2005) and 5T4 (Yoshihara et al., 2012) promote dendritic branching in the distal domain of granule cells. In contrast, the mechanism inhibiting their dendritic branching in the proximal domain has remained unknown. In this study, *PlexinD1*- or *RhoJ*-deficiency specifically enhanced dendritic branching in the proximal domain of the apical dendrite without affecting overall dendritic morphology or length in newborn granule cells. In newborn neurons migrating in the OB, PlexinD1 signaling suppresses FLP formation without affecting leading process formation (Sawada et al., 2018). Moreover, newborn neurons start to express RhoJ during their migration and maturation in the OB. Thus, our results suggest that Sema3E-PlexinD1-RhoJ signaling is involved in the proximal domain-specific suppression of branching both in the leading process during migration (Sawada et al., 2018) and in the apical dendrite after migration termination (this study).

FLPs are the cellular protrusions that link termination of migration and initiation of dendritogenesis in newborn neurons in the postnatal OB, and the timing of their formation is regulated by local PlexinD1 endocytosis during the process of migration termination (Sawada et al., 2018). Rac1 is locally activated in the proximal domain of the leading process to form FLPs (Sawada et al., 2018). On the other hand, this study showed that RhoJ suppresses dendritic branching in the proximal domain of apical dendrites. Since RhoJ, which is activated by

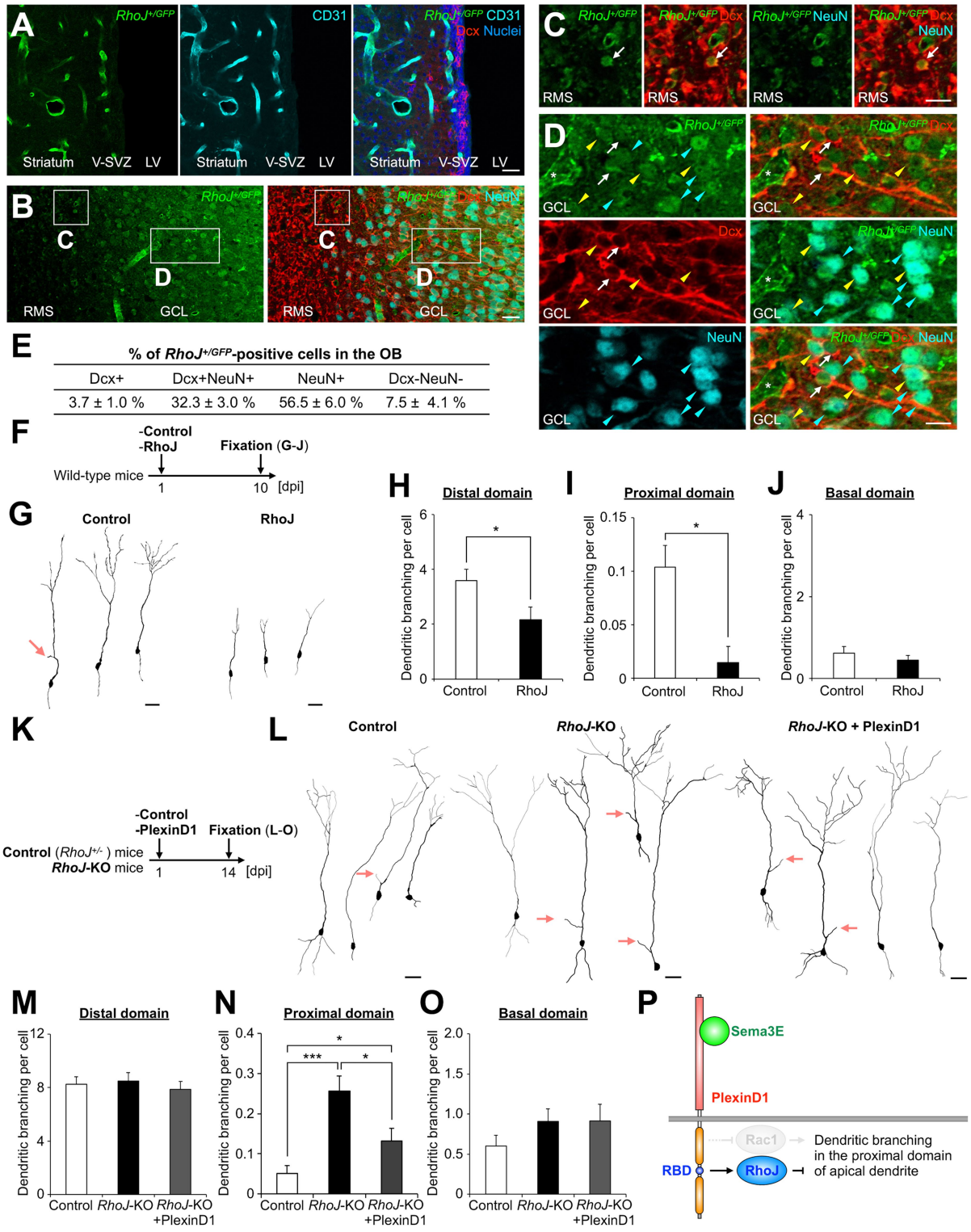

FIGURE 3
RhoJ is expressed in migrating and differentiating granule cells in the postnatal OB and involved in the suppression of their dendritic branching in the proximal domain of the apical dendrite. **(A)** Representative images of the coronal V-SVZ sections in *RhoJ*$^{+/GFP}$ mice stained for GFP (green), Dcx (red), and CD31 (cyan). Nuclei were stained with Hoechst 33342 (Blue). **(B–D)** Representative images of the coronal OB sections in *RhoJ*$^{+/GFP}$ mice stained for GFP (green), Dcx (red), and NeuN (cyan). Boxed area in **(B)** was enlarged in **(C)** and **(D)**. White arrows, yellow arrowheads, and cyan arrowheads **(C)** and **(D)** indicate GFP+Dcx+NeuN-, GFP+Dcx+NeuN+, and GFP+Dcx-NeuN+ granule cells, respectively. **(E)** Proportions of *RhoJ*$^{+/GFP}$-positive cells in the OB (n=3 mice; 144 cells analyzed). **(F)** Experimental scheme for RhoJ overexpression experiment. **(G)** Representative dendritic tracings of control (n=32 cells from 4 mice) and RhoJ-overexpressing (n=36 cells from 8 mice) granule cells at 10 day-post injection (dpi). **(H–J)** Dendritic branch numbers of distal [**(H)**; control, n=32 cells from 4 mice; RhoJ, n=36 cells from 8 mice], proximal [**(I)**; control, n=231 cells from 4 mice; RhoJ, n=67 cells from 8 mice], and basal [**(J)**; control, n=32 cells from 4 mice; RhoJ, n=36 cells from 8 mice] domains in control and RhoJ-overexpressing granule cells at 10 dpi.

(Continued)

FIGURE 3 (Continued)
(K) Experimental scheme for RhoJ loss-of-function experiment. **(L)** Representative dendritic tracings of control (n=43 cells from 3 mice), *RhoJ*-KO (n=47 cells from 3 mice), and PlexinD1-overexpressing *RhoJ*-KO (n=24 cells from 4 mice) granule cells at 14 dpi. **(M–O)** Dendritic branch numbers of distal [**(M)**; control, n=43 cells from 3 mice; *RhoJ*-KO, n=47 cells from 3 mice; *RhoJ*-KO+PlexinD1, n=24 cells from 4 mice], proximal [**(N)**; control, n=137 cells from 3 mice; *RhoJ*-KO, n=140 cells from 3 mice; *RhoJ*-KO+PlexinD1, n=128 cells from 4 mice], and basal [**(O)**; control, n=43 cells from 3 mice; *RhoJ*-KO, n=47 cells from 3 mice; *RhoJ*-KO+PlexinD1, n=24 cells from 4 mice] domains in control, *RhoJ*-KO, and PlexinD1-overexpressing *RhoJ*-KO granule cells at 14 dpi. **(P)** Mechanism of dendritic branching in the proximal domain of the apical dendrite in granule cells in the postnatal OB. Pink arrows indicate dendritic branches in the proximal domain of the apical dendrite. V-SVZ, ventricular-subventricular zone; LV, lateral ventricle; RMS, rostral migratory stream; GCL, granule cell layer. *p<0.05, ***p<0.005. Scale bars: **(A)**, **(B)**, **(G)**, **(L)**, 20μm; **(C)**, **(D)**, 10μm. Bars indicate mean±SEM.

Sema3E-PlexinD1 signaling, is localized in the perinuclear region and involved in F-actin depolymerization in vascular endothelial cells (Fukushima et al., 2020), it is possible that RhoJ is also localized in the proximal leading process and involved in the proximal domain-specific suppression of branching in migrating and maturing newborn neurons. Considering that PlexinD1 overexpression effects are partially diminished by RBD deletion (Figure 2I) or *RhoJ* deficiency (Figure 3N), our findings suggest that in newborn neurons, PlexinD1 activates RhoJ and inactivates Rac1 to suppress FLP formation during maintenance of migration, and its downregulation by local endocytosis relieves Rac1 inhibition and decreases RhoJ activation to promote FLP formation during termination of migration (Figure 3P). Thus, we propose that the PlexinD1-mediated regulation of the two opposing Rho GTPases has an advantage in the efficient transition from maintenance to termination of migration by controlling their timing of the branching of newborn neurons.

Conclusion

In this study, we showed a domain-specific mechanism for dendritic development in newborn granule cells in the postnatal OB. These results contribute to a better understanding of the development and function of newborn neurons in the postnatal OB circuits.

Data availability statement

The raw data supporting the conclusions of this article will be made available by the authors, without undue reservation.

Ethics statement

The animal study was reviewed and approved by Nagoya City University.

Author contributions

MS, AH, and NM performed experiments. MS, AH, NM, YY, AU, and KS analyzed the data. MS and KS wrote the manuscript. All authors contributed to the article and approved the submitted version.

Funding

This work was supported by research grants from Japan Agency for Medical Research and Development (AMED) (23gm1210007 to KS), Japan Society for the Promotion of Science (JSPS) KAKENHI (19H04757, 19H04785, 18KK0213, and 20H05700 to KS), (18 K14823 and 21 K06395 to MS), Bilateral Open Partnership Joint Research Projects (to KS), Core-to-core program "Neurogenesis Research & Innovation Center (NeuRIC)" (JPJSCCA20230007 to KS), Grant-in-Aid for Research at Nagoya City University (to MS and KS), and the Takeda Science Foundation (to MS and KS).

Acknowledgments

We thank F. Mann, C. E. Henderson, M. Götz, and H. Miyoshi for materials; Y. Fukushima for technical support; the Research Equipment Sharing Center and the Center for Experimental Animal Science at the Nagoya City University for technical and animal supports; and Sawamoto laboratory members for discussions.

Conflict of interest

The authors declare that the research was conducted in the absence of any commercial or financial relationships that could be construed as a potential conflict of interest.

Publisher's note

Supplementary material

The Supplementary material for this article can be found online at: https://www.frontiersin.org/articles/10.3389/fnins.2023.1143130/full#supplementary-material

SUPPLEMENTARY FIGURE S1
Dendritic length of newborn granule cells in PlexinD1-cKO and RhoJ-KO mice **(A)** Representative image of differentiating granule cells stained for Dcx (green) and PlexinD1 (red). Arrows indicate the signal of PlexinD1 protein in the proximal domain of the apical dendrite. **(B)** Classification of dendrites in newborn granule cells. **(C–H)** Length of apical dendrites **(C, F)**, dendritic branch in the proximal domain of the apical dendrite **(D, G)**, and basal dendrites **(E, H)** of granule cells in PlexinD1-cKO **(C–E)** and RhoJ-KO **(F–H)** mice. Scale bar, 10 μm. Bars indicate mean ± SEM.

References

Bressan, C., and Saghatelyan, A. (2020). Intrinsic mechanisms regulating neuronal migration in the postnatal brain. *Front. Cell. Neurosci.* 14:620379. doi: 10.3389/fncel.2020.620379

Breton-Provencher, V., Lemasson, M., Peralta, M. R. 3rd, and Saghatelyan, A. (2009). Interneurons produced in adulthood are required for the normal functioning of the olfactory bulb network and for the execution of selected olfactory behaviors. *J. Neurosci.* 29, 15245–15257. doi: 10.1523/JNEUROSCI.3606-09.2009

Bribian, A., Nocentini, S., Llorens, F., Gil, V., Mire, E., Reginensi, D., et al. (2014). Sema3E/PlexinD1 regulates the migration of hem-derived Cajal-Retzius cells in developing cerebral cortex. *Nat. Commun.* 5:4265. doi: 10.1038/ncomms5265

Burk, K., Mire, E., Bellon, A., Hocine, M., Guillot, J., Moraes, F., et al. (2017). Post-endocytic sorting of Plexin-D1 controls signal transduction and development of axonal and vascular circuits. *Nat. Commun.* 8:14508. doi: 10.1038/ncomms14508

Cariboni, A., Andre, V., Chauvet, S., Cassatella, D., Davidson, K., Caramello, A., et al. (2015). Dysfunctional SEMA3E signaling underlies gonadotropin-releasing hormone neuron deficiency in Kallmann syndrome. *J. Clin. Invest.* 125, 2413–2428. doi: 10.1172/JCI78448

Chauvet, S., Cohen, S., Yoshida, Y., Fekrane, L., Livet, J., Gayet, O., et al. (2007). Gating of Sema3E/PlexinD1 signaling by neuropilin-1 switches axonal repulsion to attraction during brain development. *Neuron* 56, 807–822. doi: 10.1016/j.neuron.2007.10.019

Deck, M., Lokmane, L., Chauvet, S., Mailhes, C., Keita, M., Niquille, M., et al. (2013). Pathfinding of corticothalamic axons relies on a rendezvous with thalamic projections. *Neuron* 77, 472–484. doi: 10.1016/j.neuron.2012.11.031

Ding, J. B., Oh, W. J., Sabatini, B. L., and Gu, C. (2011). Semaphorin 3E-Plexin-D1 signaling controls pathway-specific synapse formation in the striatum. *Nat. Neurosci.* 15, 215–223. doi: 10.1038/nn.3003

Fukuhara, K., Imai, F., Ladle, D. R., Katayama, K., Leslie, J. R., Arber, S., et al. (2013). Specificity of monosynaptic sensory-motor connections imposed by repellent Sema3E-PlexinD1 signaling. *Cell Rep.* 5, 748–758. doi: 10.1016/j.celrep.2013.10.005

Fukushima, Y., Nishiyama, K., Kataoka, H., Fruttiger, M., Fukuhara, S., Nishida, K., et al. (2020). RhoJ integrates attractive and repulsive cues in directional migration of endothelial cells. *EMBO J.* 39:e102930. doi: 10.15252/embj.2019102930

Fukushima, Y., Okada, M., Kataoka, H., Hirashima, M., Yoshida, Y., Mann, F., et al. (2011). Sema3E-PlexinD1 signaling selectively suppresses disoriented angiogenesis in ischemic retinopathy in mice. *J. Clin. Invest.* 121, 1974–1985. doi: 10.1172/JCI44900

Gay, C. M., Zygmunt, T., and Torres-Vázquez, J. (2011). Diverse functions for the semaphorin receptor PlexinD1 in development and disease. *Dev. Biol.* 349, 1–19. doi: 10.1016/j.ydbio.2010.09.008

Gu, C., Yoshida, Y., Livet, J., Reimert, D. V., Mann, F., Merte, J., et al. (2005). Semaphorin 3E and plexin-D1 control vascular pattern independently of neuropilins. *Science* 307, 265–268. doi: 10.1126/science.1105416

Kanda, Y. (2013). Investigation of the freely available easy-to-use software "EZR" for medical statistics. *Bone Marrow Transplant.* 48, 452–458. doi: 10.1038/bmt.2012.244

Kaneko, N., Okano, H., and Sawamoto, K. (2006). Role of the cholinergic system in regulating survival of newborn neurons in the adult mouse dentate gyrus and olfactory bulb. *Genes Cells* 11, 1145–1159. doi: 10.1111/j.1365-2443.2006.01010.x

Kelsch, W., Lin, C.-W., and Lois, C. (2008). Sequential development of synapses in dendritic domains during adult neurogenesis. *Proc. Natl. Acad. Sci. U. S. A.* 105, 16803–16808. doi: 10.1073/pnas.0807970105

Kim, C., Yang, H., Fukushima, Y., Saw, P. E., Lee, J., Park, J.-S., et al. (2014). Vascular RhoJ is an effective and selective target for tumor angiogenesis and vascular disruption. *Cancer Cell* 25, 102–117. doi: 10.1016/j.ccr.2013.12.010

Komano-Inoue, S., Manabe, H., Ota, M., Kusumoto-Yoshida, I., Yokoyama, T. K., Mori, K., et al. (2014). Top-down inputs from the olfactory cortex in the postprandial period promote elimination of granule cells in the olfactory bulb. *Eur. J. Neurosci.* 40, 2724–2733. doi: 10.1111/ejn.12679

Kusuhara, S., Fukushima, Y., Fukuhara, S., Jakt, L. M., Okada, M., Shimizu, Y., et al. (2012). Arhgef15 promotes retinal angiogenesis by mediating VEGF-induced Cdc42 activation and potentiating RhoJ inactivation in endothelial cells. *PLoS One* 7:e45858. doi: 10.1371/journal.pone.0045858

Lois, C., and Alvarez-Buylla, A. (1994). Long-distance neuronal migration in the adult mammalian brain. *Science* 264, 1145–1148. doi: 10.1126/science.8178174

Luskin, M. B. (1993). Restricted proliferation and migration of postnatally generated neurons derived from the forebrain subventricular zone. *Neuron* 11, 173–189. doi: 10.1016/0896-6273(93)90281-U

Mata, A., Gil, V., Pérez-Clausell, J., Dasilva, M., González-Calixto, M. C., Soriano, E., et al. (2018). New functions of Semaphorin 3E and its receptor PlexinD1 during developing and adult hippocampal formation. *Sci. Rep.* 8:1381. doi: 10.1038/s41598-018-19794-0

Muthusamy, N., Zhang, X., Johnson, C. A., Yadav, P. N., and Ghashghaei, H. T. (2017). Developmentally defined forebrain circuits regulate appetitive and aversive olfactory learning. *Nat. Neurosci.* 20, 20–23. doi: 10.1038/nn.4452

Nakajima, C., Sawada, M., and Sawamoto, K. (2021). Postnatal neuronal migration in health and disease. *Curr. Opin. Neurobiol.* 66, 1–9. doi: 10.1016/j.conb.2020.06.001

Oh, W.-J., and Gu, C. (2013). The role and mechanism-of-action of Sema3E and Plexin-D1 in vascular and neural development. *Semin. Cell Dev. Biol.* 24, 156–162. doi: 10.1016/j.semcdb.2012.12.001

Ota, H., Hikita, T., Sawada, M., Nishioka, T., Matsumoto, M., Komura, M., et al. (2014). Speed control for neuronal migration in the postnatal brain by Gmip-mediated local inactivation of RhoA. *Nat. Commun.* 5, 1–12. doi: 10.1038/ncomms5532

Pecho-Vrieseling, E., Sigrist, M., Yoshida, Y., Jessell, T. M., and Arber, S. (2009). Specificity of sensory-motor connections encoded by Sema3e-Plxnd1 recognition. *Nature* 459, 842–846. doi: 10.1038/nature08000

Petreanu, L., and Alvarez-Buylla, A. (2002). Maturation and death of adult-born olfactory bulb granule neurons: role of olfaction. *J. Neurosci.* 22, 6106–6113. doi: 10.1523/JNEUROSCI.22-14-06106.2002

Price, J. L., and Powell, T. P. (1970). The synaptology of the granule cells of the olfactory bulb. *J. Cell Sci.* 7, 125–155. doi: 10.1242/jcs.7.1.125

Saghatelyan, A., Roux, P., Migliore, M., Rochefort, C., Desmaisons, D., Charneau, P., et al. (2005). Activity-dependent adjustments of the inhibitory network in the olfactory bulb following early postnatal deprivation. *Neuron* 46, 103–116. doi: 10.1016/j.neuron.2005.02.016

Sakamoto, M., Ieki, N., Miyoshi, G., Mochimaru, D., Miyachi, H., Imura, T., et al. (2014). Continuous postnatal neurogenesis contributes to formation of the olfactory bulb neural circuits and flexible olfactory associative learning. *J. Neurosci.* 34, 5788–5799. doi: 10.1523/JNEUROSCI.0674-14.2014

Sawada, M., Ohno, N., Kawaguchi, M., Huang, S., Hikita, T., Sakurai, Y., et al. (2018). PlexinD1 signaling controls morphological changes and migration termination in newborn neurons. *EMBO J.* 37:e97404. doi: 10.15252/embj.201797404

Shepherd, G. M., Chen, W. R., and Greer, C. A. (2004). "Olfactory bulb" in *The synaptic organization of the BRAIN*. ed. G. M. Shepherd (New York: OXFORD), 165–216.

Whitman, M. C., and Greer, C. A. (2007). Synaptic integration of adult-generated olfactory bulb granule cells: basal axodendritic centrifugal input precedes apical dendrodendritic local circuits. *J. Neurosci.* 27, 9951–9961. doi: 10.1523/JNEUROSCI.1633-07.2007

Yokoyama, T. K., Mochimaru, D., Murata, K., Manabe, H., Kobayakawa, K., Kobayakawa, R., et al. (2011). Elimination of adult-born neurons in the olfactory bulb is promoted during the postprandial period. *Neuron* 71, 883–897. doi: 10.1016/j.neuron.2011.05.046

Yoshihara, S., Takahashi, H., Nishimura, N., Naritsuka, H., Shirao, T., Hirai, H., et al. (2012). 5T4 glycoprotein regulates the sensory input-dependent development of a specific subtype of newborn interneurons in the mouse olfactory bulb. *J. Neurosci.* 32, 2217–2226. doi: 10.1523/JNEUROSCI.5907-11.2012

Zhang, Y., Singh, M. K., Degenhardt, K. R., Lu, M. M., Bennett, J., Yoshida, Y., et al. (2009). Tie2Cre-mediated inactivation of PlexinD1 results in congenital heart, vascular and skeletal defects. *Dev. Biol.* 325, 82–93. doi: 10.1016/j.ydbio.2008.09.031

frontiers | Frontiers in Neuroscience

TYPE Original Research
PUBLISHED 27 July 2023
DOI 10.3389/fnins.2023.1178555

OPEN ACCESS

EDITED BY
Seiji Hitoshi,
Shiga University of Medical Science, Japan

REVIEWED BY
Naoko Kaneko,
Doshisha University Graduate School of Brain Science, Japan
Hidefumi Fukumitsu,
Gifu Pharmaceutical University, Japan

*CORRESPONDENCE
Eri Segi-Nishida
✉ eri.segi.nishida@rs.tus.ac.jp

RECEIVED 02 March 2023
ACCEPTED 13 July 2023
PUBLISHED 27 July 2023

CITATION
Kasakura N, Murata Y, Shindo A, Kitaoka S, Furuyashiki T, Suzuki K and Segi-Nishida E (2023) Overexpression of NT-3 in the hippocampus suppresses the early phase of the adult neurogenic process.
Front. Neurosci. 17:1178555.
doi: 10.3389/fnins.2023.1178555

Overexpression of NT-3 in the hippocampus suppresses the early phase of the adult neurogenic process

Nanami Kasakura[1], Yuka Murata[1], Asuka Shindo[1], Shiho Kitaoka[2], Tomoyuki Furuyashiki[3], Kanzo Suzuki[1] and Eri Segi-Nishida[1]*

[1]Department of Biological Science and Technology, Faculty of Advanced Engineering, Tokyo University of Science, Tokyo, Japan, [2]Department of Pharmacology, School of Medicine, Hyogo Medical University, Hyogo, Japan, [3]Division of Pharmacology, Kobe University Graduate School of Medicine, Kobe, Japan

The dentate gyrus (DG) of the hippocampus regulates stress-related emotional behaviors and ensures neurogenesis throughout life. Neurotrophin-3 (NT-3) is a neurotrophic factor that regulates neuronal differentiation, survival, and synaptic formation in both the peripheral and central nervous systems. NT-3 is expressed in the adult DG of the hippocampus; several chronic stress conditions enhance NT-3 expression in rodents. However, functional modulation of the adult DG by NT-3 signaling remains unclear. To directly investigate the impact of NT-3 on DG function, NT-3 was overexpressed in the hippocampal ventral DG by an adeno-associated virus carrying NT-3 (AAV-NT-3). Four weeks following the AAV-NT-3 injection, high NT-3 expression was observed in the ventral DG. We examined the influence of NT-3 overexpression on the neuronal responses and neurogenic processes in the ventral DG. NT-3 overexpression significantly increased the expression of the mature DG neuronal marker calbindin and immediate early genes, such as *Fos* and *Fosb*, thereby suggesting DG neuronal activation. During neurogenesis, the number of proliferating cells and immature neurons in the subgranular zone of the DG significantly decreased in the AAV-NT-3 group. Among the neurogenesis-related factors, *Vegfd, Lgr6, Bmp7,* and *Drd1* expression significantly decreased. These results demonstrated that high NT-3 levels in the hippocampus regulate the activation of mature DG neurons and suppress the early phase of neurogenic processes, suggesting a possible role of NT-3 in the regulation of adult hippocampal function under stress conditions.

KEYWORDS

NT-3, hippocampus, neurogenesis, dentate gyrus, maturation, AAV

Introduction

The hippocampus is a limbic structure implicated in the regulation of stress responses and pathophysiology of depression. The dentate gyrus (DG) is a part of the hippocampus that receives cortical inputs from the entorhinal cortex and projects them to the CA3 pyramidal cells. The DG is one of the few areas of the mammalian brain in which adult neurogenesis occurs (Ming and Song, 2005; Kempermann et al., 2015). The neurogenic processes include proliferation, differentiation, survival, and functional maturation. These processes are positively or negatively regulated by external stimuli, such as learning, exercise, antidepressant treatment,

and stress (Warner-Schmidt and Duman, 2006; Zhao et al., 2008; Leschik et al., 2021; Segi-Nishida and Suzuki, 2022).

Neurotrophin-3 (NT-3) is a neurotrophic factor that is known to regulate neuronal survival, differentiation, and synaptic function in both the peripheral and central nervous systems (Ernfors et al., 1994; Barbacid, 1995). In hippocampal neuronal cultures, NT-3 induced the expression of calbindin, a mature neuronal marker in the DG, and c-fos, a product of an immediate early gene (IEG) (Collazo et al., 1992), suggesting the effect of NT-3 on neuronal maturation and activation. In developmental neural stem cell culture, certain reports have demonstrated that NT-3 inhibits mitosis and lengthens the cell cycle (Ghosh and Greenberg, 1995; Lukaszewicz et al., 2002; Simpson et al., 2003), while others have reported that NT-3 promotes cell division and survival rate (Barnabe-Heider and Miller, 2003; Lu et al., 2011).

Although several studies have been reported, the role of NT-3 in adult neurogenesis *in vivo* remains unclear. One report revealed that the differentiation and survival, but not proliferation, of neuronal precursor cells were impaired in the DG of mice lacking NT-3 (Shimazu et al., 2006). However, another report demonstrated that the proliferation of neural stem cells in the subventricular zone, another neurogenic region in adults, was increased in NT-3 heterozygous mice, suggesting a suppressive role of NT-3 in neural stem cell proliferation (Delgado et al., 2014).

In rats, NT-3 is highly expressed in the central nervous system during development; however, its expression declines as these regions mature (Maisonpierre et al., 1990). Nevertheless, high expression of NT-3 is maintained in the hippocampus even in adult rats (Katoh-Semba et al., 1996). Although NT-3 is highly expressed in the DG compared to other hippocampal regions, such as CA1 and CA3 (Smith et al., 1995), its effects of NT-3 on the function of mature neurons in the DG remain unclear. We previously reported that chronic administration of antidepressants, such as fluoxetine, or electroconvulsive seizures, decreases NT-3 expression in the DG of adult mice (Imoto et al., 2017). Conversely, a previous study demonstrated that NT-3 expression was increased in the hippocampus following chronic unpredictable mild stress (Jiang et al., 2014). In addition, corticosterone administration increased NT-3 expression in the DG (Smith et al., 1995). However, whether increased NT-3 alters the neurogenic processes and neuronal maturation in the DG *in vivo* remains unclear.

The hippocampus reportedly plays functionally distinct roles in the dorsal and ventral regions (Fanselow and Dong, 2010), and both the regions respond to stress (Hawley et al., 2012; Maras et al., 2014). While the dorsal region is thought to be involved in stress-induced learning and memory changes, the ventral region contributes to stress response and emotions such as anxiety. Specifically, increased neurogenesis in the ventral DG reportedly contributes to stress resilience (Anacker et al., 2018), suggesting that identification of the key signaling pathway in the ventral DG would be important to understand the underlying mechanisms of stress response and emotion. While NT-3 is expressed in both the dorsal and ventral DG, we hypothesized that modulation of the NT-3 signals could alter the adult neurogenic processes and neuronal responses in the ventral DG.

In this study, we investigated the influence of high levels of NT-3 expression on the adult neurogenic processes and neuronal responses in the ventral DG using an adeno-associated virus (AAV) expression system. Elucidation of the function of NT-3 in the DG *in vivo* would result in a better understanding of the role of NT-3 in adult neurogenesis, as well as in the stress response.

Materials and methods

Experimental animals

Seven-to eight-week-old male C57BL/6 N mice (23–25 g) were purchased from Japan SLC (RRID5295404; Hamamatsu, Japan). The mice were housed in groups of six per cage. All the mice were housed under standard conditions (24 ± 2°C, 55% ± 5% humidity) with a 12 h light/dark cycle and *ad libitum* access to water and food. Weight gain of each mouse was recorded during the experiments to monitor the physical conditions of the animals. All the mice were habituated for longer than 1 week before the experimental procedures were performed. Animal use and procedures were performed according to the guidelines prescribed by the National Institute of Health and approved by the Animal Care and Use Committee of the Tokyo University of Science (approval number K20009, K21007, K22007).

AAV preparation and hippocampal administration

For the generation of AAV carrying NT-3 (AAV-NT-3) vector plasmids, an NT-3 coding sequence was amplified using polymerase chain reaction (PCR) from mouse hippocampal cDNA and inserted into the pcDNA3 plasmid (Thermo Fisher Scientific, Waltham, MA, USA). A CMV-NT-3 cassette was inserted into the MluI-EcoRV site of the pAAV-EF1α-DIO EYFP vector (Addgene #27056). For the generation of AAV carrying enhanced green fluorescent protein (AAV-EGFP), the NT-3 gene in the AAV-NT-3 was replaced with a gene encoding EGFP. To generate AAV-EF1α-Emerald-GFP (EmGFP), an EmGFP sequence was amplified using PCR from the pcDNA 6.2-GW/EmGFP-miR (Thermo Fisher Scientific) and inserted into the KpnI-EcoRV site of the pAAV-EF1α-DIO EYFP vector (Addgene #27056). AAV2/rh10 particles were produced as previously described with minor modifications (Shinohara et al., 2018). Briefly, the AAV-rep2/caprh10 expression plasmid (Addgene #112866), pHelper vector (#240071, Agilent Technologies, Santa Clara, CA), and the constructed AAV-vector plasmid were transfected into the AAV-293 cells (Agilent, #240073) using Lipofectamine 2000 (Thermo Fisher Scientific). The transfected AAV-293 cells were collected, resuspended in artificial cerebrospinal fluid, frozen, and thawed four times 3 days after transfection. Cell debris was eliminated by centrifugation at 10,000× *g* for 10 min, and the supernatant containing the virus was collected. The viral suspension was incubated with benzonase (Merck, Darmstadt, Germany) to degrade the residual DNA. The prepared AAV solution was aliquoted and stored at −80°C. The AAV titers were quantified using PCR. Under anesthesia with medetomidine (0.3 mg/kg, ZENOAQ, Fukushima, Japan), midazolam (4 mg/kg, Sandoz, Tokyo, Japan), and butorphanol (5 mg/kg, Meiji Seika Pharma, Tokyo, Japan) mixture, the mouse brain was fixed with stereotaxic instruments (Narishige, Tokyo, Japan). An AAV solution of 500 nL per injection site (2.5×10^8 copies) was stereotaxically injected at two sites in each hemisphere into the DG using a PV-820 Pneumatic PicoPump (World Precision Instruments,

Hessen, Germany) through a glass micropipette (World Precision Instruments) made with a PN-30 micropipette puller (Narishige). The stereotaxic coordinates were targeted to the ventral DG:3.2 mm posterior to the bregma, 2.7 mm lateral to the midline, and 3.0 mm ventral to the skull surface at the bregma according to a mouse brain atlas (Paxinos and Franklin, 2012). To visually detect viral infection, 5×10^7 copies of AAV-EF-1α-EmGFP were co-injected with AAV-NT-3 and AAV-EGFP in the DG of the hippocampus. The data were excluded from the analysis if fluorescence was not observed in the DG.

RNA extraction and real-time PCR

The mice were decapitated, and coronal brain slices (1 mm) were cut using a tissue slicer. To isolate the ventral DG, the hippocampal DG from the coronal brain slice of bregma −2.0 mm to −4.0 mm (Paxinos and Franklin, 2012) was dissected under a stereoscopic microscope. Total RNA was extracted using the Reliaprep RNA Cell Miniprep System (Promega, Madison, WI, USA) and reverse transcribed using ReverTra Ace (Toyobo, Osaka, Japan) followed by real-time PCR using the StepOne system (Applied Biosystems, Foster City, CA) and Thunderbird SYBR qPCR mix (Toyobo). The expression levels of each gene were quantified using standardized external dilutions. The relative expression levels of the target genes were normalized to those of 18S rRNA. The specificity of each primer set was confirmed by melt-curve analysis and the product size was examined using gel electrophoresis. Primer sequences for each gene are listed in Table 1.

Immunoblot

The mice were decapitated; coronal brain slices (1 mm) were cut using a tissue slicer and the ventral DG of the hippocampus was dissected under a stereoscopic microscope. The isolated DG was homogenized in a protein lysis buffer (50 mM Tris HCl pH 7.4, 150 mM NaCl, 0.5% sodium deoxycholate, 2 mM EDTA, 1 mM EGTA, 1% TritonX-100) containing protease inhibitor cocktail (Nacalai tesque, Kyoto, Japan) on ice and centrifuged at 16,000× *g* for 20 min at 4°C. Supernatants containing 10 μg proteins were separated on 12.5% sodium dodecyl sulfate (SDS)-polyacrylamide gel by electrophoresis and transferred onto the polyvinyl difluoride membrane. The membrane was first blocked with 5% skim milk in Tris-buffered saline for 1 h at room temperature and subsequently incubated with rabbit anti-NT-3 antibody (1:4500, kindly provided by Drs. Furuichi and Semba; Katoh-Semba et al., 1996), rabbit anti-GFP monoclonal antibody (1:500, #598, Medical and biological laboratories, Japan, RRID:AB_591819), or mouse anti-β-actin monoclonal antibody (1:4000, MA5-15739, Thermo Fisher Scientific, RRID:AB_10979409) at 4°C overnight. After washing, the membrane was incubated with horseradish peroxidase conjugated goat anti-rabbit IgG (1:5000, Jackson ImmunoResearch, Jackson ImmunoResearch, West Grove, PA, 111–035-144, RRID:AB_2307391) or horse anti-mouse IgG (1:2000, Vector Laboratories Inc., Burlingame, CA, PI-2000, RRID:AB_2336177) secondary antibody for 1 h at room temperature, and the bands were visualized with EzWestLumiOne (WSE-7110, ATTO, Tokyo, Japan) by LAS-4000 (GE Healthcare Life Science, Pittsburgh, PA).

TABLE 1 List of primers used for qPCR analysis.

Gene	Forward (5′ to 3′)	Reverse (5′ to 3′)
Ntf3	AGTTTGCCGGAAGACTCTCTC	GGGTGCTCTGGTAATTTTCCTTA
Trkc	CTGAGTGCTACAATCTAAGCCC	CACACCCCATAGAACTTGACAAT
Calb1	TCTGGCTTCATTTCGACGCTG	ACAAAGGATTTCATTTCCGGTGA
Fos	CAGAGCGGGAATGGTGAAGA	TCGGTGGGCTGCCAAAATAA
Fosb	TTTTCCCGGAGACTACGACTC	GTGATTGCGGTGACCGTTG
Arc	AGCGGGACCTGTACCAGAC	AGCTGCTCCAGGGTCTTG
Egr1	TATGAGCACCTGACCACAGAG	GCTGGGATAACTCGTCTCCA
Bdnf	GACAAGGCAACTTGGCCT AC	ACTGTCACACACGCTCAGCTC
Npas4	CAGATCAACGCCGAGATTCG	CACCCTTGCGAGTGTAGATGC
Vegfa	GCTGCACCCACGACAGAAG	CGCTGGTAGACATCCATGAAC
Figf/Vegfd	TTGAGCGATCATCCCGGTC	GCGTGAGTCCATACTGGCAAG
Wnt2	CTCGGTGGTGGAATCTGGCTCTG	CACATTGTCACACATCACCCT
Fzd6	TCTGCCCCTCGTAAGAGGAC	GGGAAGAACGTCATGTTGTAAGT
Lgr6	GAGGACGGCATCATGCTGTC	GCTCCGTGAGGTTGTTCATACT
Bmp2	GGGACCCGCTGTCTTCTAGT	TCAACTCAAATTCGCTGAGGAC
Bmp4	TTCCTGGTAACCGAATGCTGA	CCTGAATCTCGGCGACTTTTT
Bmp7	ACGGACAGGGCTTCTCCTAC	ATGGTGGTATCGAGGGTGGAA
Drd1	ACAGCAGCCCCTCCGATAG	GTTAGACCTGGGCAGATGAAG
Iba1/Aif1	ATCAACAAGCAATTCCTCGATGA	CAGCATTCGCTTCAAGGACATA

Sample isolation, immunohistochemistry and 5′-ethynyl-2′-deoxyuridine (EdU) detection

EdU and 5′-bromo-2′-deoxyuridine (BrdU) administration

To label dividing cells during the S-phase of mitosis, mice were administered BrdU (150 mg/kg, intraperitoneal [i.p.], Nacalai Tesque) twice a day, 2 to 4 days before the AAV injection, or EdU (100 mg/kg, i.p., Abcam, Cambridge, UK) 2 h before sacrifice.

Brain isolation and section preparation

For NT-3 immunostaining, mice were deeply anesthetized and transcardially perfused with cold saline followed by 0.25% glutaraldehyde and 2% paraformaldehyde in 0.1 M phosphate buffer (pH 7.4) and were post-fixed at 4°C for 24 h. For other immunostaining procedures, mice were perfused with cold saline followed by 4% paraformaldehyde in 0.1 M phosphate buffer (pH 7.4), and were post-fixed at 4°C for 48 h. The brains were cryoprotected in 20% sucrose for 48 h, then 30% sucrose for 24 h and stored at −80°C until further use. Serial sections (30 μm thick) were cut through the entire hippocampus using a cryostat (Leica 1510, Leica Microsystems, Wetzlar, German) and stored in 30% glycerol and 30% ethylene glycol in 0.02 M phosphate buffer (pH 7.4) at −20°C until staining.

Immunohistochemistry and EdU detection

The sections were washed with phosphate-buffered saline (PBS) and blocked using 10% equine serum (Cytiva, Tokyo, Japan, SH30074) in PBS containing 0.3% Triton X-100 (PBST) at room temperature for 60 min, followed by overnight incubation with rabbit anti-NT-3 (1:450), rabbit anti-doublecortin (DCX) (1:1000; Cell Signaling Technology, Danvers, MA, #4604, RRID:AB _561007), rabbit anti-calbindin (1:8000; Swant, Marly, Switzerland, CB38, AB_10000340), rabbit anti-FosB (1:1000; Abcam, ab184938, RRID: AB_2721123), mouse anti-NeuN (1:1000, Merck Millipore, Burlington, MA, MAB377, RRID: AB_2298772), rabbit anti-TrkC (1:1600, Cell Signaling Technology, #3376, RRID: AB_2155283), rabbit anti-pErk1/2 (1:200, Cell Signaling Technology, #4370, RRID:AB_2315112), rabbit anti-pPLC γ1 (1:100,Cell Signaling Technology #8713, RRID:AB_10890863), and rabbit anti-Iba1 (1:4000; Wako, Okasa, Japan, 019–19,741, RRID: AB_839504) at 4°C. For BrdU immunostaining, the sections were incubated in 50% formamide in 2 × saline sodium citrate buffer for 2 h at 60°C, followed by incubation in 2 M hydrogen chloride at 37°C for 30 min and neutralized with 0.1 M boric acid (pH 8.5) at room temperature for 10 min before blocking. After blocking, the sections were incubated overnight with monoclonal rat anti-BrdU (1:8000; Abcam, ab6326, RRID:AB_305426) at 4°C. After washing with PBST, the sections were incubated using donkey anti-rabbit IgG antibody conjugated with Alexa Fluor 555 (1:300 or 1:1000, Thermo Fisher Scientific, A-31572, RRID:AB_162543), rabbit anti-mouse IgG antibody conjugated with Alexa Fluor 555 (1:300, Thermo Fisher Scientific, A-21427, RRID:AB_2535848) and donkey anti-rat IgG antibody conjugated with Alexa Fluor 555 (1:1000, Abcam, ab150154, RRID:AB_2813834) for 60 min. After washing with PBST, the sections were incubated with 4′,6-diamidino-2-phenylindole (DAPI; 1:10000; Merck Millipore) and mounted on slides with Mowiol (Merck Millipore) after washing with PBS. For Iba1 and pERK staining, after washing with PBST, sections were incubated with biotinylated goat anti-rabbit IgG (1:200; Vector Laboratories Inc., Burlingame, CA, BA1000, RRID: AB_2313606) for 60 min. The sections were washed with PBST and incubated with the ABC Vectastain Kit (Vector), and antigen detection was performed with 0.02% 3,3′-diaminobenzidine (Wako, 049–22,831) staining. After washing, the sections were mounted on slides with Entellan New (Merck Millipore). EdU Detection was performed using Click-iT EdU imaging kit (Thermo Fisher Scientific), followed by mitotic staining with Alexa Fluor 555. *In situ* Apoptosis Detection kit was used for evaluating the levels of apoptosis according to the manufacturer's instructions (TaKaRa, MK500, Shiga, Japan).

Quantification of EdU-, BrdU-, doublecortin-, calbindin-, Iba1-, TrkC-, and FosB-positive cells

For EdU-labeled cell quantification in the dorsal and ventral DG, we used modified unbiased stereology protocol, which has been able to successfully quantify thymidine-analog labeling (West et al., 1991; Malberg et al., 2000). Briefly, every sixth section of the entire DG (30 μm) was selected to ensure that same cells will not be counted in two sections with the first half defined as the dorsal DG and the second half as the ventral DG. EdU-positive (+) cells were counted in the subgranular zone (SGZ) in either dorsal or ventral DG for cell proliferation using a fluorescent microscope (BZX-700, Keyence, Osaka, Japan). The SGZ was defined as a two cell-body width zone along the border of the granule cell layer and hilus. The sum of cell counts was multiplied by 6 to provide an estimate of the total number of EdU (+) cells in each DG region.

For BrdU-labeled cell quantification, 3–6 sections of the ventral DG were photographed using a microscope. The number of BrdU (+) cells is presented as the number of cells per 10,000 μm^2 area in the granule cell layer (GCL) in the DG using computer-assisted image analysis (ImageJ, NIH, Bethesda, MD, USA). For neuronal differentiation of BrdU-labeled cells, six slices were analyzed to determine if BrdU-labeled cells were colabeled with NeuN. For DCX (+) cell quantification, two or three sections of the ventral DG were photographed using a microscope. DCX (+) cells, in which dendrites did not reach the molecular layer, were subcategorized as DCX (+) cells with short dendrites, whereas DCX (+) cells, in which dendrites reached the molecular layer and had complex processes, were subcategorized as DCX (+) cells with long and branched dendrites. The number of DCX (+) cells was measured as the number of cells per 100 μm along the SGZ in the DG using ImageJ software. To quantify calbindin and TrkC immunoreactivity, three sections of the DG were photographed under a microscope. The molecular layer or GCL of the DG was set as the region of interest (ROI) and each ROI was measured. The average signal intensity of immunoreactivity in the molecular layer or GCL in the DG was quantified using ImageJ software. To measure the Iba1 immune-positive area, the grayscale image was converted into a binary image, and the Iba1 immune-positive area was measured within the ROI. To quantify FosB immunoreactivity, three sections of the ventral DG were photographed under a microscope. The number of FosB (+) cells is presented as the number of cells per 10,000 μm^2 area in the GCL in the DG using computer-assisted image analysis (QuPath, Bankhead et al., 2017).

Statistical analyses

All the data are presented as the mean ± standard error of mean. Statistical analysis was performed using the unpaired Student's *t*-test or Welch's *t*-test. Statistical significance was set at $p < 0.05$. Before performing *t*-test, normality of the data was examined using the Shapiro–Wilk test. If the data did not pass the normality test, a nonparametric test, the Mann–Whitney U test, was performed. Detailed statistical data are presented in Supplementary Table S1. All the analyses were performed using PRISM 9 software (GraphPad, San Diego, CA).

Results

Overexpression of NT-3 in the DG of the hippocampus

To examine the influence of NT-3 on adult neurogenesis in the DG, we used AAVrh10-CMV-NT-3 virus (AAV-NT-3) for NT-3 overexpression or AAVrh10-CMV-EGFP virus (AAV-EGFP) for control. To visually confirm viral infection, 10% AAVrh10-EF1α-EmGFP was mixed with these vectors and injected into the ventral DG of the hippocampus. Four to 5 weeks after viral injection, GFP expression was observed in the GCL and hilus region of the DG in both the groups (Figures 1A,B). In the GCL, most of the GFP-positive cells were neuronal marker NeuN-positive and immature neuronal marker DCX-negative (Supplementary Figure 1A), suggesting that the cells overexpressing NT-3 in the GCL were mostly mature neurons. However, strong immunostaining signals for the anti-NT-3 antibody were detected, especially in the hilus of the DG in the AAV-NT-3 group (Figure 1B). A robust increase in the NT-3 expression was confirmed by immunoblotting and real-time PCR analysis (Figures 1C,D, left), while no effect was observed in the NT-3 receptor *Trkc* expression by NT-3 overexpression (Figure 1D, right).

Since a high amount of NT-3 could exert a toxic effect, we evaluated the levels of microglial activation and apoptotic cell death in NT-3 overexpression. No difference was observed in the immune-positive area of Iba1 immunostaining in the molecular layer between the AAV-EGFP and AAV-NT-3 groups (Supplementary Figures 1B,C). We further quantified *Iba1(Aif1)* mRNA expression in the DG; however, these were similar in both groups (Supplementary Figure 1D). In addition, few apoptosis-positive signals were detected in the GCL and hilus regions in both groups (Supplementary Figure 1E).

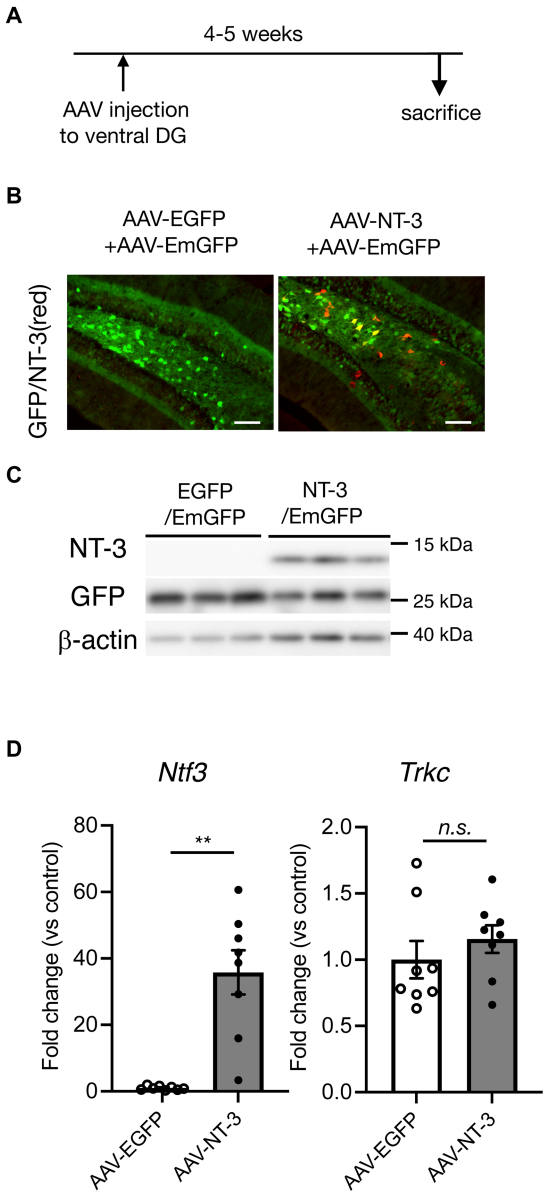

FIGURE 1
Overexpression of neurotrophin-3 (NT-3) in the DG of the hippocampus by AAV carrying NT-3 injection. **(A)** Time course of the experimental procedure. **(B)** The expression of GFP (green) and NT-3 (red) in the DG 4–5 weeks following AAV injection. Scale bars: 100 μm. **(C)** Confirmation of NT-3 protein overexpression in the DG. Typical immunoblots for anti-NT-3, anti-GFP, and anti-β-actin were shown. Each lane indicates different DG samples 4–5 weeks following AAV injection. **(D)** The confirmation of NT-3 mRNA overexpression (left, $p = 0.0012$) and the effect of NT-3 overexpression on the gene expression of *Trkc* (right, $p = 0.3282$) in the ventral DG. $n = 8$ each for the AAV-enhanced GFP group and AAV-NT-3 group. Data are expressed using dot plots and means ± standard error of mean. $^{**}p < 0.01$. n.s., not significant.

The responses of DG neurons to high NT-3 expression

In cultured hippocampal neurons, NT-3 increases the expression of calbindin and c-fos (Collazo et al., 1992; Boukhaddaoui et al., 2001). We examined the influence of high NT-3 levels on calbindin expression in mature neurons of the ventral DG. The calbindin immunoreactivity signals in the GCL and molecular layer of the ventral DG were significantly enhanced in the AAV-NT-3 group (Figures 2A,B). We also confirmed that the mRNA expression of *Calb1* in the ventral DG significantly increased in the AAV-NT-3 group (Figure 2C). We subsequently examined whether neuronal activation in the DG was modulated by NT-3 overexpression. FosB, including ΔFosB, is an indicator of prolonged cellular activity (Nestler et al., 1999). Therefore, we performed immunohistochemical analysis using FosB to evaluate the neuronal activity in the ventral DG. FosB-positive cells in the GCL were significantly increased in the AAV-NT-3 group (Figures 2D,E). We also examined the gene expression in

10.3389/fnins.2023.1178555

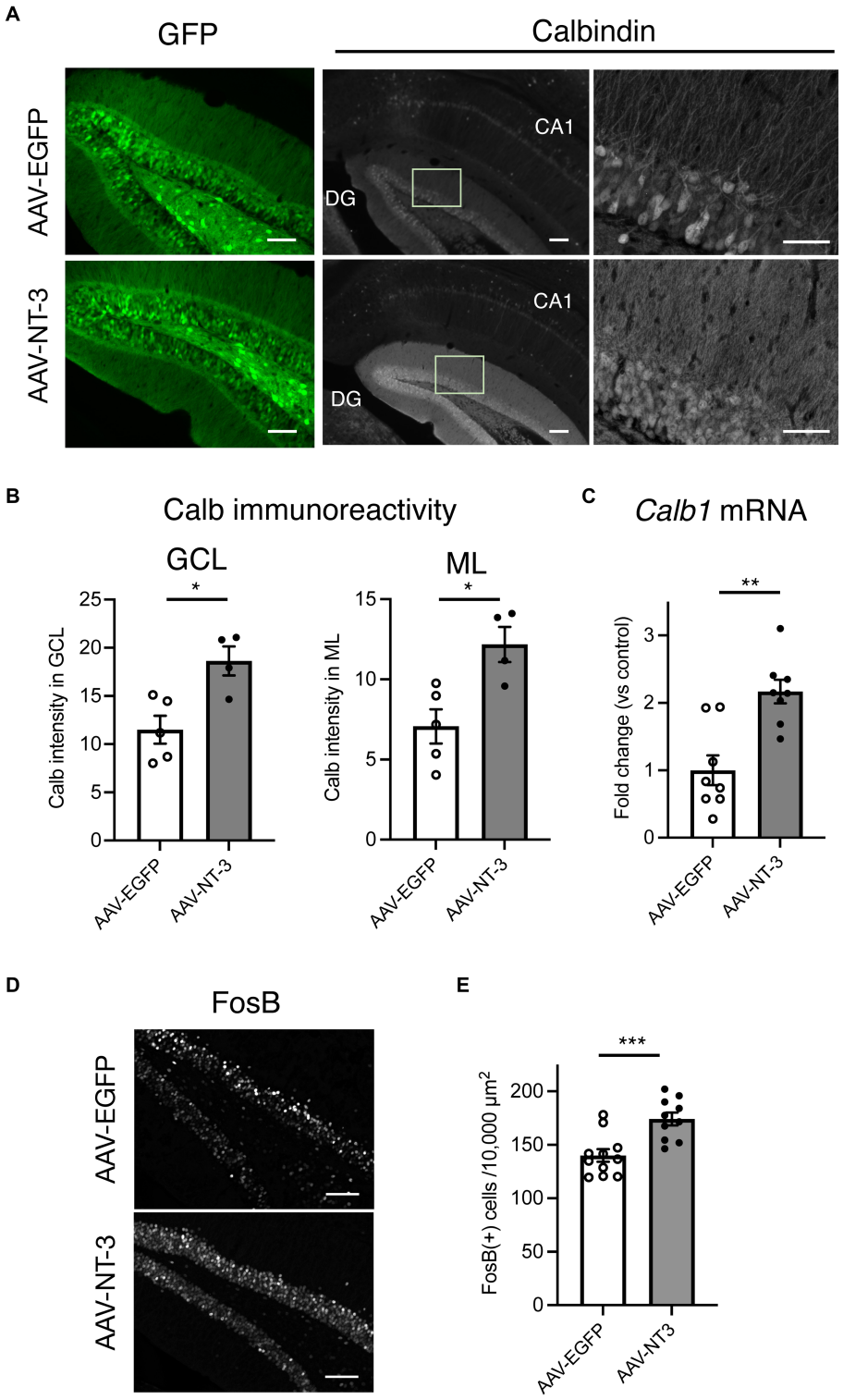

FIGURE 2
The response of hippocampal ventral DG neurons to high NT-3 expression. **(A)** The effect of NT-3 overexpression on the expression of mature neuronal marker, calbindin, in the ventral DG. Representative coronal images for GFP (left, scale bars: 100 μm) and anti-calbindin immunostaining (middle, scale bars: 100 μm) in the ventral DG are shown. The images on the right show the squares in the middle images (scale bars: 50 μm). **(B)** Quantification of the intensity of calbindin immunoreactivity in the granule cell layer (GCL, $p = 0.0117$) and molecular layer (ML, $p = 0.0131$). $n = 5$ for AAV-EGFP group and $n = 4$ AAV-NT-3 group. **(C)** The effect of NT-3 overexpression on the gene expression of *Calb1* ($p = 0.001$) in the ventral DG. $n = 8$ each for AAV-EGFP group and AAV-NT-3 group. **(D)** The expression of FosB in the ventral DG. Scale bars: 100 μm. **(E)** Quantification of FosB (+) cell numbers in the GCL. $p = 0.0007$, $n = 11$ for AAV-EGFP group and $n = 10$ AAV-NT-3 group. Data are expressed using dot plots and means ± standard error of mean. $^{*}p < 0.05$; $^{**}p < 0.01$; $^{***}p < 0.001$.

several types of IEGs in the ventral DG. NT-3 overexpression moderately, but significantly, increased the expression of *Fosb, Fos*, *Arc*, *Egr1*, and *Bdnf*, but not *Npas4* (Figure 3). These results suggest that NT-3 signaling directly or indirectly activates mature neurons in the GCL *in vivo*.

The influence of high NT-3 expression on the early phase of the neurogenic process in the DG of the hippocampus

Hippocampal adult neurogenesis is a multistep process, which includes proliferation, neuronal differentiation, and survival. We evaluated the effects of high NT-3 expression on the cell proliferation. EdU was administered 2 h before sacrifice to label the proliferating cells (Figure 4A). EdU-positive cells were detected in the SGZ of the DG (Figure 4B). The number of EdU-positive cells significantly decreased in the AAV-NT-3 group in the SGZ of both dorsal and ventral DG (Figure 4C), demonstrating a suppressive effect of NT-3 on cell proliferation in the entire DG. We subsequently examined the expression of an immature neuronal marker, DCX in the ventral DG. DCX-positive cells were subclassified into those with short dendrites and those with long and branched dendrites (Figures 4D,E, left). The number of DCX-positive cells with either short or long dendrites in the SGZ significantly decreased in the AAV-NT-3 group (Figure 4E). Most of the newborn cells in the DG reportedly die during 2–3 weeks following proliferation in mice (Ueno et al., 2019). To examine the effect of high NT-3 expression on the survival of newborn cells, BrdU was administered 2–4 days before AAV injection (Figure 4A). The number of BrdU-positive cells in the ventral DG was counted at 31–33 days of cell age (Figure 4F). While no difference was observed in the survival rate between the AAV-EGFP and AAV-NT-3 groups, the ratio of NeuN-positive cells in the

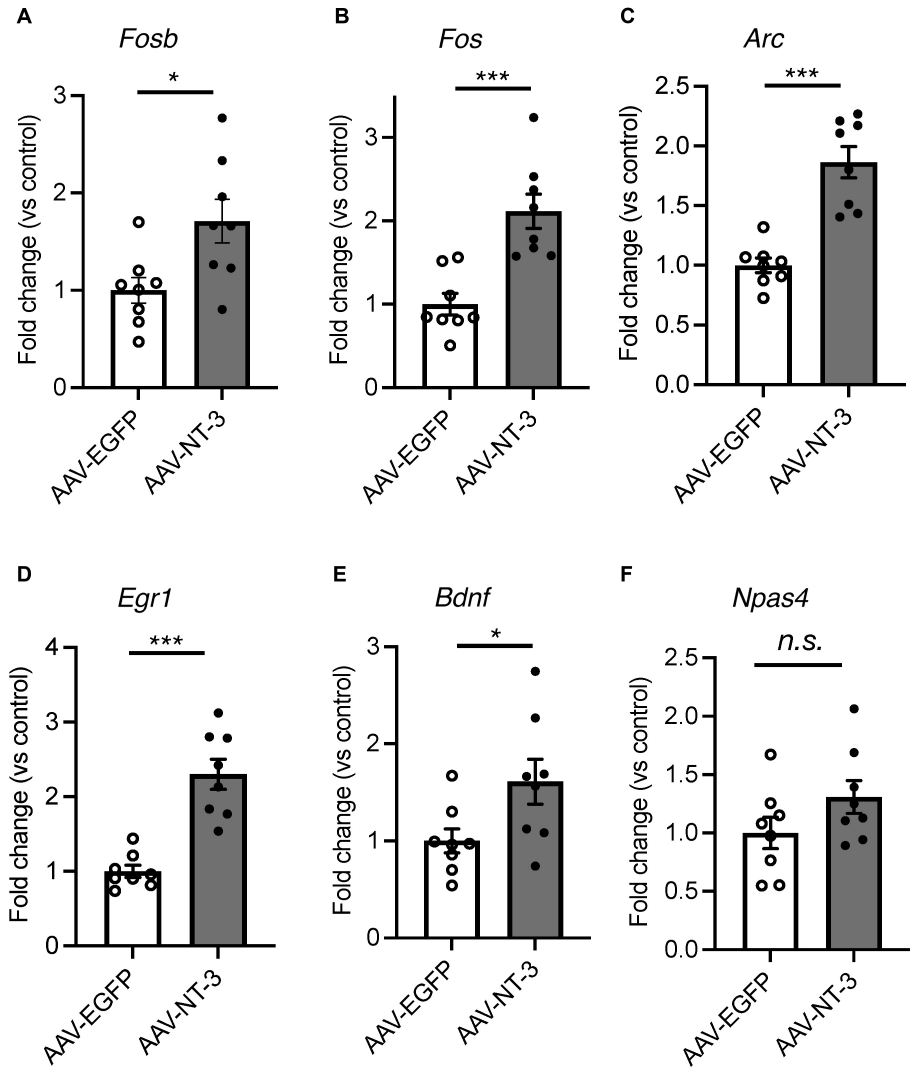

FIGURE 3
The effect of NT-3 overexpression on the gene expression of IEGs in the ventral DG. Expression of **(A)** *Fosb* ($p = 0.0163$), **(B)** *Fos* ($p = 0.0004$), **(C)** *Arc* ($p < 0.0001$), **(D)** *Egr1* ($p = 0.0002$), **(E)** *Bdnf* ($p = 0.0358$) and **(F)** *Napas4* ($p = 0.1349$) are shown. $n = 8$ each for AAV-EGFP group and AAV-NT-3 group. Data are expressed using dot plots and means ± standard error of mean. *$p < 0.05$; ***$p < 0.001$. n.s., not significant.

10.3389/fnins.2023.1178555

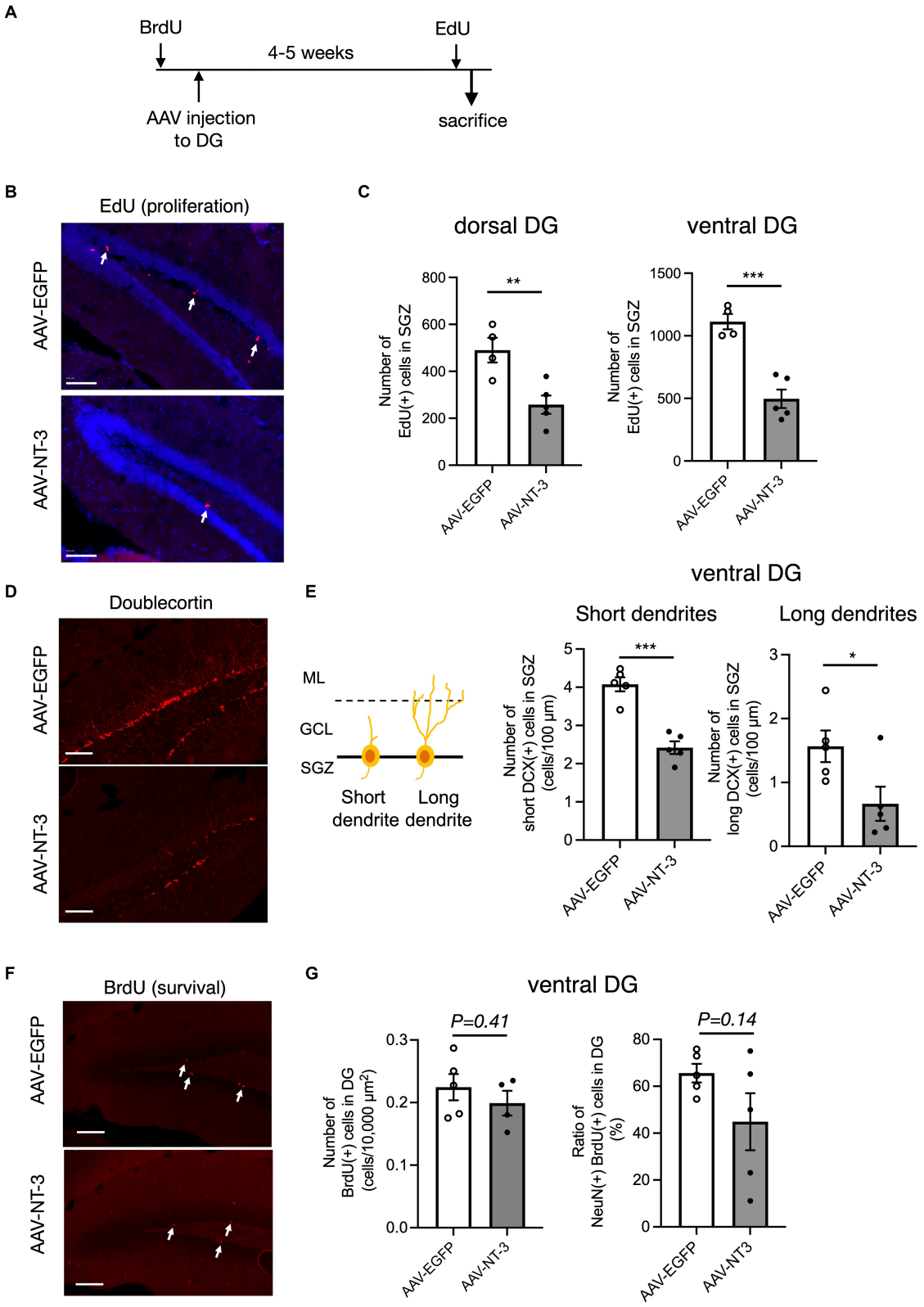

FIGURE 4
The effect of NT-3 overexpression on early phase of neurogenic process in the DG of the hippocampus. **(A)** Time course of the experimental procedure. **(B)** The effect of NT-3 overexpression on proliferation in the DG. Representative coronal images for EdU detection in the DG are shown. The arrows represent EdU(+) cells. **(C)** Quantification of EdU (+) cells in the subgranular zone (SGZ) of the dorsal (p = 0.008) and ventral (p = 0.0005) DG. n = 4 for AAV-EGFP group and n = 5 for AAV-NT-3 group. **(D)** The effect of NT-3 overexpression on cell number of doublecortin (DCX) (+) immature neurons in the ventral DG. Representative coronal images for anti-DCX immunostaining in the DG are shown. **(E)** DCX (+) cells with short or long dendrite in the SGZ (left). GCL, granule cell layer; ML, molecular layer. The numbers of DCX (+) cells with short dendrites (middle, p = 0.0002)

(Continued)

FIGURE 4 (Continued)
and DCX (+) cells with long dendrites (right, $p = 0.039$) are shown ($n = 5$ each for AAV-EGFP group and AAV-NT-3 group). **(F)** The effect of NT-3 overexpression on cell survival in the ventral DG. Representative coronal images for anti-BrdU immunostaining in the DG are shown. The arrows represent BrdU (+) cells. **(G)** The number of BrdU (+) cells (left, $p = 0.4138$) and the ratio of NeuN (+) cells among BrdU (+) cells (right, $p = 0.144$) in the ventral DG. $n = 5$ each for AAV-EGFP group and AAV-NT-3 group. Data are expressed using dot plots and means ± standard error of mean. $^{*}p < 0.05$; $^{**}p < 0.01$; $^{***}p < 0.001$. n.s., not significant. Scale bars: 100 μm.

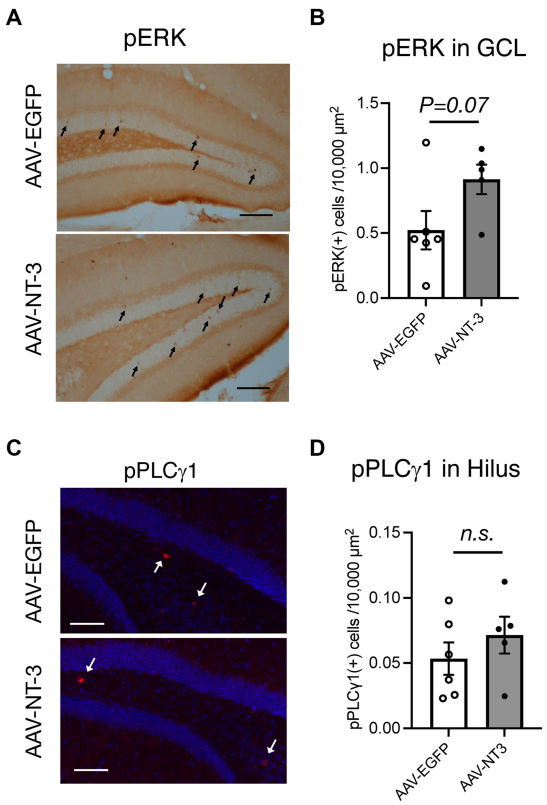

FIGURE 5
Downstream signaling of NT-3 overexpression in the ventral DG. Representative coronal images for pERK **(A)**, and pPLCγ1 **(C)** in the ventral DG are shown. Arrows in panels **(A,C)** show immune-positive cells. Scale bars: 100 μm. **(B,D)** Quantification of pERK (+) cells in the GCL (**B**, $p = 0.0733$), and pPLCγ1(+) cells in the hilus of the ventral DG (**D**, $p = 0.3609$). $n = 6$ for AAV-EGFP group and $n = 5$ for AAV-NT-3 group. Data are expressed using dot plots and means ± standard error of mean. n.s., not significant.

BrdU-positive population tended to decrease ($p = 0.1440$), although not significantly (Figure 4G). These results suggest that high NT-3 expression suppressed the early phase of the neurogenic process but had no effect on the late survival process.

The influence of high NT-3 expression on the intracellular signaling in the DG of the hippocampus

To explore the target cells for NT-3 signaling, we assessed the effect of NT-3 overexpression on its downstream signaling. We initially confirmed the localization of NT-3 receptor TrkC. In the Allen brain atlas database, *Trkc* mRNA expression is present in the GCL and hilus regions (Lein et al., 2007; Supplementary Figure 2A). Consistent with this, TrkC immunoreactivities were detected in the molecular layer, GCL, and hilus region in the AAV-EGFP and AAV-NT-3 group, while TrkC expression was decreased in the AAV-NT-3 group (Supplementary Figure 2B). These results indicate that NT-3 regulates downstream signaling *via* TrkC in these regions within DG, which may be subject to feedback regulation by long-term overexpression of NT-3. To determine whether NT-3 overexpression activates intracellular signaling in DG, phosphorylation of extracellular signal-regulated kinase (pERK) and phospholipase C γ1 (pPCL γ 1) were examined. pERK positive cells were scattered within the GCL. This activation tended to increase with NT-3 overexpression (Figures 5A,B). On the other hand, pPLC γ 1 positive cells were present in a small number of cells in the hilus region. This activation was not significantly altered by NT-3 overexpression (Figures 5C,D).

Neurogenic-related gene expression changes of hippocampal DG neurons by high NT-3 expression

Since our data suggested that NT-3 overexpression enhances neuronal activity and maturation in the DG, we would presume that it also regulates gene expression in an activity-dependent manner (Flavell and Greenberg, 2008). To investigate the mechanism of reduced neurogenesis by NT-3 overexpression, we examined the gene expression changes in factors related to neurogenic signals, such as vascular endothelial growth factor (VEGF) and Wnt (Lie et al., 2005; Han et al., 2015) in the DG. We found that the expression of *Vegfd (Figf)*, but not *Vegfa*, was significantly decreased by NT-3 overexpression (Figure 6A). The expression of *Wnt2* and *Fzd6*, which encode the Wnt receptor, was not altered by NT-3 overexpression, but *Lgr6*, which encodes the receptor involved in Wnt/β-catenin signaling (Liu et al., 2019), was significantly decreased in the AAV-NT-3 group (Figure 6B). We also investigated the expression of bone morphogenetic protein (BMP) families, which positively or negatively control the proliferation and neuronal differentiation in the DG during both development and adult neurogenesis (Mira et al., 2010; Mori et al., 2020). The expression of *Bmp7,* but not *Bmp2* and *Bmp4,* was significantly decreased in the AAV-NT-3 group (Figure 6C). We further found that the expression of dopamine receptor type 1 (*Drd1*), which mediates pro-neurogenic signals in the DG (Mishra et al., 2019), significantly decreased in the AAV-NT-3 group (Figure 6D). These findings may demonstrate that NT3 overexpression in the DG triggers activity-dependent gene expression that regulates the early phase of neurogenic processes.

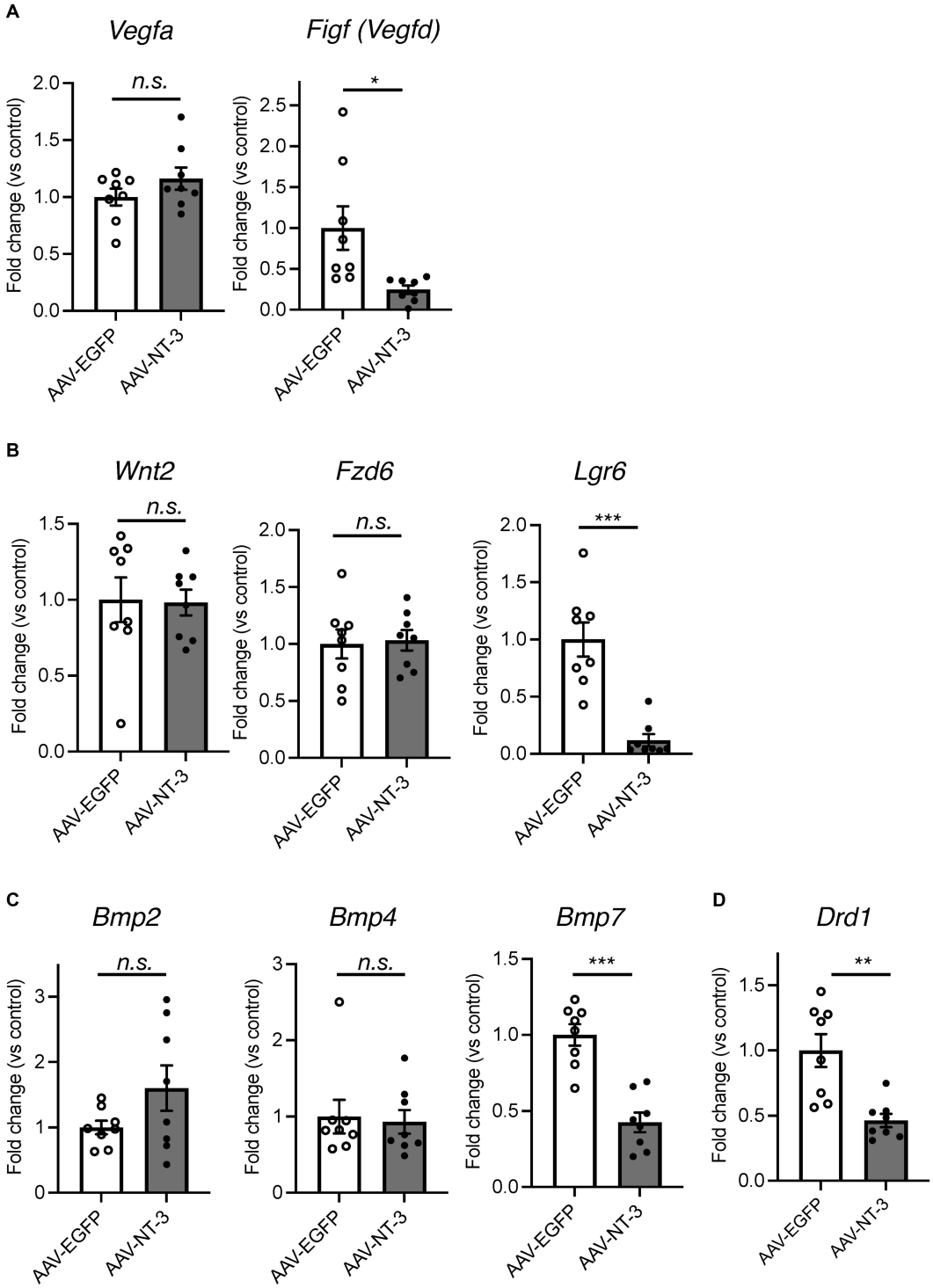

FIGURE 6
The gene expression changes of neurogenesis-related genes in the ventral DG by high NT-3 expression. **(A,B)** The effect of NT-3 overexpression on the expression of neurogenesis stimulant factors. Expression of *Vegfa* ($p = 0.2118$), *Figf* (*Vegfd*) ($p = 0.0248$), *Wnt2* ($p = 0.9160$), *Fz6* ($p = 0.8397$), *Lgr6* ($p = 0.0003$) are shown. **(C)** The expression of bone morphogenetic protein (BMP) families. Expression of *Bmp2* ($p = 0.1325$), *Bmp4* ($p = 0.7984$), and *Bmp7* ($p < 0.0001$) are shown. **(D)** The expression of D1 receptor (*Drd1*; $p = 0.0031$). $n = 8$ each for AAV-EGFP group and AAV-NT-3 group. Data are expressed using dot plots and means ± standard error of mean. *$p < 0.05$; **$p < 0.01$; ***$p < 0.001$. n.s., not significant.

Discussion

In this study, we investigated the influence of high levels of NT-3 expression on the neuronal responses and neurogenic processes in the mouse hippocampal DG using the AAV expression system. We found that the expression of the mature DG neuronal markers, calbindin and IEGs, such as *Fosb* and *Fos*, was moderately increased by NT-3 overexpression. We also demonstrated that NT-3 overexpression in the DG results in the suppression of the early processes of neurogenesis, including cell proliferation. Considering the

neurogenesis-related factors, the expression of *Vegfd, Lgr6, Bmp7,* and *Drd1* was significantly decreased. AAV mostly infected mature neurons in the GCL layer and cells in the hilus region of the DG. Since NT-3 is a release factor, neuronal/cell function would be affected not only in infected cells but also in surrounding ones.

During development, endogenous NT-3 is essential for the survival of peripheral sensory and sympathetic neurons (Ernfors et al., 1994; Farinas et al., 1994). In the adult central nervous system, NT-3 is highly expressed in the hippocampal DG (Smith et al., 1995). Importantly, several lines of evidence have demonstrated that NT-3 is a key regulator for the neurogenic processes, including proliferation, differentiation, and survival, in the DG of the hippocampus. A previous study demonstrated that the survival and neuronal differentiation, rather than proliferation, of the neuronal precursor cells were impaired in mice in which NT-3 expression was suppressed specifically in the brain using Nestin-Cre line (Shimazu et al., 2006). In the present study, we found that high expression of NT-3 in the DG with viral manipulation suppressed the proliferation but did not alter the survival. These findings suggest that the physiological levels of NT-3 do not affect the proliferation of neuronal precursor cells in the DG, but rather that excess amounts of NT-3 act to suppress cell proliferation. While we speculated that NT-3 overexpression can regulate cell survival, we did not observe a significant difference in the survival in NT-3 overexpression. These findings indicate that the physiological concentrations of NT-3 may be sufficient to maintain cell survival even though NT-3 is overexpressed. Interestingly, another study proposed that NT-3 can inhibit cell proliferation in the subventricular zone localized in the walls of the lateral ventricles, another neurogenic region in adults (Delgado et al., 2014). This study demonstrated that NT-3 heterozygous mice as well as endothelial NT-3 specific knockout Tie2-cre mice showed increased cell proliferation, suggesting an inhibitory effect of NT-3 on proliferation. This study may suggest that the inhibitory effect of NT-3 could occur in the SGZ of the DG in mice with NT-3 overexpression.

The role of NT-3 in neuronal differentiation remains unclear. We found a decrease in doublecortin-positive cells upon NT-3 overexpression but cannot distinguish whether this is due to inhibition of proliferation or neuronal differentiation. BrdU-labeled newborn cells at 31–33 days of cell age showed a decreasing trend in NeuN-positive neuronal differentiation, although survival remained unchanged. The effect of high expression of NT-3 on neuronal differentiation can be clarified by future analysis of surviving cells in combination with other differentiation markers for neuronal differentiation.

NT-3 overexpression resulted in an increase in Calb1 and FosB expression in the mature granule cells of the DG, suggesting that NT-3 directly or indirectly modulate their function. Hippocampal NT-3 expression is increased by chronic stress and corticosterone (Smith et al., 1995; Jiang et al., 2014). Expression of c-Fos was reportedly moderately increased in the ventral DG just after chronic social defeat stress (Anacker et al., 2018). Thus, we hypothesized that the stress-induced increase in NT-3 levels could contribute to the activation of mature neurons in the DG. A recent study reported that direct activation of the ventral DG promotes susceptibility to chronic stress (Anacker et al., 2018). Further research is warranted to clarify the influence of increased NT-3 levels in the ventral DG on emotional behaviors and stress responses.

We also found that gene expression of other types of IEGs and BDNF was enhanced by high levels of NT-3 in the DG. The cytoplasmic domains of TrkC receptors contain tyrosine phosphorylation sites that recruit various intracellular signaling molecules, including mitogen-activated protein (MAP) kinase, phosphoinositide 3-kinase (PI3K), and PLC-γ (Huang and Reichardt, 2003). Moreover, high NT-3 concentration can reportedly induce activation of adenosine 3′,5′-cyclic monophosphate (cAMP) response element binding (CREB) in cultured hippocampal neurons (Han et al., 2016), which regulate activity-dependent IEGs and BDNF expression (Esvald et al., 2022). Therefore, we investigated whether NT-3 overexpression could alter the downstream signaling pathways of NT-3-TrkC. In the present study, we detected pERK and pPLC-γ in different cells in the GCL or hilus of the DG. However, we did not observe a robust change in the downstream signals. Since our findings demonstrated that NT-3 overexpression supressed proliferation, other downstream signals or key signals could be altered by NT-3 overexpression in the SGZ of DG; however, this remains unclear. Future studies are warranted to identify the cell types in which TrkC is expressed and to identify NT-3 downstream signals according to the time course.

VEGF and Wnt signaling promote neural stem cell proliferation in the adult DG (Lie et al., 2005; Han et al., 2015). We found that the expression levels of *Vegfd* and *Lgr6* were significantly reduced by NT-3 overexpression. VEGF-D is a ligand for VEGF receptor 2 (Flk1) and VEGF receptor 3 (Flt4) (Achen et al., 1998), both of which promote neural stem cell proliferation (Segi-Nishida et al., 2008; Han et al., 2015). The expression of *Vegfd* in hippocampal neurons is regulated by nuclear calcium signaling, including Ca^{2+}/calmodulin-dependent protein kinase IV (CaMKIV) (Mauceri et al., 2011). The influence of persistent NT-3 on intracellular calcium signaling needs to be investigated. LGR6 binds to R-spondins and enhances Wnt/β-catenin signaling (Gong et al., 2012), which regulates adult hippocampal neurogenesis including stem cell proliferation (Lie et al., 2005). However, the contribution of LGR6 to hippocampal neurogenesis remains largely unknown. Investigating whether LGR6 is expressed in neural stem cells, and the influence of NT-3 on Wnt/β-catenin signaling is warranted.

BMP is a factor that inhibits neural stem cell proliferation (Bond et al., 2012). Unexpectedly, the expression level of *Bmp7* in the DG was reduced by NT-3 overexpression. The proliferation of neural stem cells has been investigated in mice in which the BMP receptor Bmpr1a was ablated in the hippocampal DG of adult mice (Mira et al., 2010). The proliferation of neural stem cells was increased shortly following Bmpr1a ablation. However, 4 weeks after Bmpr1a ablation, the proliferation of neural stem cells was reduced in mice. Therefore, chronic suppression of BMP signaling may reduce neural stem cell proliferation. Chronic NT-3 expression for 4 weeks in this study may have caused a chronic decrease in the signaling of BMP7, resulting in a decrease in the proliferating cells. We also found that the expression of the dopamine receptor gene *Drd1* was reduced by NT-3 overexpression. D1 receptor agonists reportedly enhance neural stem cell proliferation by positively regulating the Wnt/β-catenin signaling pathway in the hippocampus of Parkinson's disease rats (Mishra et al., 2019).

This study demonstrates that increased NT-3 expression in the DG possesses the potential to negatively regulate hippocampal neurogenesis *in vivo*. Since hippocampal neurogenic processes are

inhibited by chronic stress (Mitra et al., 2006; Van Bokhoven et al., 2011; Campos et al., 2013) and hippocampal NT-3 expression is increased by chronic stress (Smith et al., 1995; Jiang et al., 2014), we hypothesized that NT-3 is a key neurotrophic factor that suppresses adult hippocampal neurogenesis during chronic stress. However, it should be noted that *Ntf3* expression in the overexpression group increased by more than 30-fold. The increase in the *Ntf3* expression in the DG owing to chronic unpredictable stress and 7 days of corticosterone treatment was approximately 1.5- to 2-fold (Smith et al., 1995; Jiang et al., 2014). Thus, the results of this study may not merely mimic the influence of stress-induced increase in the NT-3 levels in the DG. Thus, comparing the levels of NT-3 protein production and/or downstream signaling between stress conditions and the overexpression system used in this study is warranted. In addition, we observed that NT-3 immunostaining signals localized to cells in the hilus region. The relationship between the stress-induced increase in *Ntf3* expression and cellular accumulation at the protein level needs to be investigated. Appropriate control of NT-3 expression may reveal the role of increased NT-3 expression in stressful environments.

Data availability statement

The original contributions presented in the study are included in the article/Supplementary material, further inquiries can be directed to the corresponding author.

Ethics statement

The animal study was reviewed and approved by the Animal Care and Use Committee of the Tokyo University of Science (approval numbers K20009, K21007, and K22007).

Author contributions

NK and YM designed the study, conducted the experiments, analyzed the data, and drafted the manuscript. AS conducted and analyzed the experiments. TF and SK contributed to the design and preparation of AAV. KS designed the study and drafted the manuscript. ES-N designed the study, analyzed the data, and drafted the manuscript. All authors have read and approved the final manuscript.

Funding

This work was supported in part by MEXT KAKENHI Grants 20K07090 (ES-N), 22K20697 (KS), 21K06576 (SK), 18H05429 (TF), and 21H04812 (TF); AMED grants (JP22gm0910012 and JP22wm0425001 to TF); Kato Memorial Bioscience Foundation (to KS); Brain Science Foundation (to KS).

Acknowledgments

We would like to thank Editage (www.editage.jp) for the English language editing. We are grateful to Sena Washizu for technical support; Teiichi Furuichi and Ritsuko Katoh-Semba for generously providing anti-NT-3 antibody.

Conflict of interest

The authors declare that the research was conducted in the absence of any commercial or financial relationships that could be construed as a potential conflict of interest.

Publisher's note

Supplementary material

The Supplementary material for this article can be found online at: https://www.frontiersin.org/articles/10.3389/fnins.2023.1178555/full#supplementary-material

References

Achen, M. G., Jeltsch, M., Kukk, E., Makinen, T., Vitali, A., Wilks, A. F., et al. (1998). Vascular endothelial growth factor D (VEGF-D) is a ligand for the tyrosine kinases VEGF receptor 2 (Flk1) and VEGF receptor 3 (Flt4). *Proc. Natl. Acad. Sci. U. S. A.* 95, 548–553. doi: 10.1073/pnas.95.2.548

Anacker, C., Luna, V. M., Stevens, G. S., Millette, A., Shores, R., Jimenez, J. C., et al. (2018). Hippocampal neurogenesis confers stress resilience by inhibiting the ventral dentate gyrus. *Nature* 559, 98–102. doi: 10.1038/s41586-018-0262-4

Bankhead, P., Loughrey, M. B., Fernandez, J. A., Dombrowski, Y., McArt, D. G., Dunne, P. D., et al. (2017). QuPath: open source software for digital pathology image analysis. *Sci. Rep.* 7:16878. doi: 10.1038/s41598-017-17204-5

Barbacid, M. (1995). Structural and functional properties of the TRK family of neurotrophin receptors. *Ann. N. Y. Acad. Sci.* 766, 442–458. doi: 10.1111/j.1749-6632.1995.tb26693.x

Barnabe-Heider, F., and Miller, F. D. (2003). Endogenously produced neurotrophins regulate survival and differentiation of cortical progenitors via distinct signaling pathways. *J. Neurosci.* 23, 5149–5160. doi: 10.1523/JNEUROSCI.23-12-05149.2003

Bond, A. M., Bhalala, O. G., and Kessler, J. A. (2012). The dynamic role of bone morphogenetic proteins in neural stem cell fate and maturation. *Dev. Neurobiol.* 72, 1068–1084. doi: 10.1002/dneu.22022

Boukhaddaoui, H., Sieso, V., Scamps, F., and Valmier, J. (2001). An activity-dependent neurotrophin-3 autocrine loop regulates the phenotype of developing hippocampal pyramidal neurons before target contact. *J. Neurosci.* 21, 8789–8797. doi: 10.1523/JNEUROSCI.21-22-08789.2001

Campos, A. C., Ortega, Z., Palazuelos, J., Fogaca, M. V., Aguiar, D. C., Diaz-Alonso, J., et al. (2013). The anxiolytic effect of cannabidiol on chronically stressed mice depends on hippocampal neurogenesis: involvement of the endocannabinoid system. *Int. J. Neuropsychopharmacol.* 16, 1407–1419. doi: 10.1017/S1461145712001502

Collazo, D., Takahashi, H., and McKay, R. D. (1992). Cellular targets and trophic functions of neurotrophin-3 in the developing rat hippocampus. *Neuron* 9, 643–656. doi: 10.1016/0896-6273(92)90028-c

Delgado, A. C., Ferron, S. R., Vicente, D., Porlan, E., Perez-Villalba, A., Trujillo, C. M., et al. (2014). Endothelial NT-3 delivered by vasculature and CSF promotes quiescence

of subependymal neural stem cells through nitric oxide induction. *Neuron* 83, 572–585. doi: 10.1016/j.neuron.2014.06.015

Ernfors, P., Lee, K. F., Kucera, J., and Jaenisch, R. (1994). Lack of neurotrophin-3 leads to deficiencies in the peripheral nervous system and loss of limb proprioceptive afferents. *Cells* 77, 503–512. doi: 10.1016/0092-8674(94)90213-5

Esvald, E. E., Tuvikene, J., Moistus, A., Rannaste, K., Koomagi, S., and Timmusk, T. (2022). Differential regulation of the BDNF gene in cortical and hippocampal neurons. *J. Neurosci.* 42, 9110–9128. doi: 10.1523/JNEUROSCI.2535-21.2022

Fanselow, M. S., and Dong, H. W. (2010). Are the dorsal and ventral hippocampus functionally distinct structures? *Neuron* 65, 7–19. doi: 10.1016/j.neuron.2009.11.031

Farinas, I., Jones, K. R., Backus, C., Wang, X. Y., and Reichardt, L. F. (1994). Severe sensory and sympathetic deficits in mice lacking neurotrophin-3. *Nature* 369, 658–661. doi: 10.1038/369658a0

Flavell, S. W., and Greenberg, M. E. (2008). Signaling mechanisms linking neuronal activity to gene expression and plasticity of the nervous system. *Annu. Rev. Neurosci.* 31, 563–590. doi: 10.1146/annurev.neuro.31.060407.125631

Ghosh, A., and Greenberg, M. E. (1995). Distinct roles for bFGF and NT-3 in the regulation of cortical neurogenesis. *Neuron* 15, 89–103. doi: 10.1016/0896-6273(95)90067-5

Gong, X., Carmon, K. S., Lin, Q., Thomas, A., Yi, J., and Liu, Q. (2012). LGR6 is a high affinity receptor of R-spondins and potentially functions as a tumor suppressor. *PLoS One* 7:e37137. doi: 10.1371/journal.pone.0037137

Han, J., Calvo, C. F., Kang, T. H., Baker, K. L., Park, J. H., Parras, C., et al. (2015). Vascular endothelial growth factor receptor 3 controls neural stem cell activation in mice and humans. *Cell Rep.* 10, 1158–1172. doi: 10.1016/j.celrep.2015.01.049

Han, K. A., Woo, D., Kim, S., Choii, G., Jeon, S., Won, S. Y., et al. (2016). Neurotrophin-3 regulates synapse development by modulating TrkC-PTPsigma synaptic adhesion and intracellular signaling pathways. *J. Neurosci.* 36, 4816–4831. doi: 10.1523/JNEUROSCI.4024-15.2016

Hawley, D. F., Morch, K., Christie, B. R., and Leasure, J. L. (2012). Differential response of hippocampal subregions to stress and learning. *PLoS One* 7:e53126. doi: 10.1371/journal.pone.0053126

Huang, E. J., and Reichardt, L. F. (2003). Trk receptors: roles in neuronal signal transduction. *Annu. Rev. Biochem.* 72, 609–642. doi: 10.1146/annurev.biochem.72.121801.161629

Imoto, Y., Segi-Nishida, E., Suzuki, H., and Kobayashi, K. (2017). Rapid and stable changes in maturation-related phenotypes of the adult hippocampal neurons by electroconvulsive treatment. *Mol. Brain* 10:8. doi: 10.1186/s13041-017-0288-9

Jiang, P., Dang, R. L., Li, H. D., Zhang, L. H., Zhu, W. Y., Xue, Y., et al. (2014). The impacts of swimming exercise on hippocampal expression of neurotrophic factors in rats exposed to chronic unpredictable mild stress. *Evid. Based Complement. Alternat. Med.* 2014:729827. doi: 10.1155/2014/729827

Katoh-Semba, R., Kaisho, Y., Shintani, A., Nagahama, M., and Kato, K. (1996). Tissue distribution and immunocytochemical localization of neurotrophin-3 in the brain and peripheral tissues of rats. *J. Neurochem.* 66, 330–337. doi: 10.1046/j.1471-4159.1996.66010330.x

Kempermann, G., Song, H., and Gage, F. H. (2015). Neurogenesis in the adult hippocampus. *Cold Spring Harb. Perspect. Biol.* 7:a018812. doi: 10.1101/cshperspect.a018812

Lein, E. S., Hawrylycz, M. J., Ao, N., Ayres, M., Bensinger, A., Bernard, A., et al. (2007). Genome-wide atlas of gene expression in the adult mouse brain. *Nature* 445, 168–176. doi: 10.1038/nature05453

Leschik, J., Lutz, B., and Gentile, A. (2021). Stress-related dysfunction of adult hippocampal neurogenesis-an attempt for understanding resilience? *Int. J. Mol. Sci.* 22: 7339. doi: 10.3390/ijms22147339

Lie, D. C., Colamarino, S. A., Song, H. J., Desire, L., Mira, H., Consiglio, A., et al. (2005). Wnt signalling regulates adult hippocampal neurogenesis. *Nature* 437, 1370–1375. doi: 10.1038/nature04108

Liu, S. L., Zhou, Y. M., Tang, D. B., Zhou, N., Zheng, W. W., Tang, Z. H., et al. (2019). LGR6 promotes osteogenesis by activating the Wnt/beta-catenin signaling pathway. *Biochem. Biophys. Res. Commun.* 519, 1–7. doi: 10.1016/j.bbrc.2019.08.122

Lu, H. X., Hao, Z. M., Jiao, Q., Xie, W. L., Zhang, J. F., Lu, Y. F., et al. (2011). Neurotrophin-3 gene transduction of mouse neural stem cells promotes proliferation and neuronal differentiation in organotypic hippocampal slice cultures. *Med. Sci. Monit.* 17:BR305-311. doi: 10.12659/msm.882039

Lukaszewicz, A., Savatier, P., Cortay, V., Kennedy, H., and Dehay, C. (2002). Contrasting effects of basic fibroblast growth factor and neurotrophin 3 on cell cycle kinetics of mouse cortical stem cells. *J. Neurosci.* 22, 6610–6622. doi: 10.1523/JNEUROSCI.22-15-06610.2002

Maisonpierre, P. C., Belluscio, L., Friedman, B., Alderson, R. F., Wiegand, S. J., Furth, M. E., et al. (1990). NT-3, BDNF, and NGF in the developing rat nervous system: parallel as well as reciprocal patterns of expression. *Neuron* 5, 501–509. doi: 10.1016/0896-6273(90)90089-x

Malberg, J. E., Eisch, A. J., Nestler, E. J., and Duman, R. S. (2000). Chronic antidepressant treatment increases neurogenesis in adult rat hippocampus. *J. Neurosci.* 20, 9104–9110. doi: 10.1523/JNEUROSCI.20-24-09104.2000

Maras, P. M., Molet, J., Chen, Y., Rice, C., Ji, S. G., Solodkin, A., et al. (2014). Preferential loss of dorsal-hippocampus synapses underlies memory impairments provoked by short, multimodal stress. *Mol. Psychiatry* 19, 811–822. doi: 10.1038/mp.2014.12

Mauceri, D., Freitag, H. E., Oliveira, A. M., Bengtson, C. P., and Bading, H. (2011). Nuclear calcium-VEGFD signaling controls maintenance of dendrite arborization necessary for memory formation. *Neuron* 71, 117–130. doi: 10.1016/j.neuron.2011.04.022

Ming, G. L., and Song, H. (2005). Adult neurogenesis in the mammalian central nervous system. *Annu. Rev. Neurosci.* 28, 223–250. doi: 10.1146/annurev.neuro.28.051804.101459

Mira, H., Andreu, Z., Suh, H., Lie, D. C., Jessberger, S., Consiglio, A., et al. (2010). Signaling through BMPR-IA regulates quiescence and long-term activity of neural stem cells in the adult hippocampus. *Cell Stem Cell* 7, 78–89. doi: 10.1016/j.stem.2010.04.016

Mishra, A., Singh, S., Tiwari, V., Parul, , and Shukla, S. (2019). Dopamine D1 receptor activation improves adult hippocampal neurogenesis and exerts anxiolytic and antidepressant-like effect via activation of Wnt/beta-catenin pathways in rat model of Parkinson's disease. *Neurochem. Int.* 122, 170–186. doi: 10.1016/j.neuint.2018.11.020

Mitra, R., Sundlass, K., Parker, K. J., Schatzberg, A. F., and Lyons, D. M. (2006). Social stress-related behavior affects hippocampal cell proliferation in mice. *Physiol. Behav.* 89, 123–127. doi: 10.1016/j.physbeh.2006.05.047

Mori, M., Murata, Y., Tsuchihashi, M., Hanakita, N., Terasaki, F., Harada, H., et al. (2020). Continuous psychosocial stress stimulates BMP signaling in dorsal hippocampus concomitant with anxiety-like behavior associated with differential modulation of cell proliferation and neurogenesis. *Behav. Brain Res.* 392:112711. doi: 10.1016/j.bbr.2020.112711

Nestler, E. J., Kelz, M. B., and Chen, J. (1999). DeltaFosB: a molecular mediator of long-term neural and behavioral plasticity. *Brain Res.* 835, 10–17. doi: 10.1016/s0006-8993(98)01191-3

Paxinos, G., and Franklin, K.B.J. (2012) *Paxinos and Franklin's the mouse brain in stereotaxic coordinates. 4th*. Cambridge, MA: Academic Press

Segi-Nishida, E., and Suzuki, K. (2022). Regulation of adult-born and mature neurons in stress response and antidepressant action in the dentate gyrus of the hippocampus. *Neurosci. Res.* doi: 10.1016/j.neures.2022.08.010

Segi-Nishida, E., Warner-Schmidt, J. L., and Duman, R. S. (2008). Electroconvulsive seizure and VEGF increase the proliferation of neural stem-like cells in rat hippocampus. *Proc. Natl. Acad. Sci. U. S. A.* 105, 11352–11357. doi: 10.1073/pnas.0710858105

Shimazu, K., Zhao, M., Sakata, K., Akbarian, S., Bates, B., Jaenisch, R., et al. (2006). NT-3 facilitates hippocampal plasticity and learning and memory by regulating neurogenesis. *Learn. Mem.* 13, 307–315. doi: 10.1101/lm.76006

Shinohara, R., Taniguchi, M., Ehrlich, A. T., Yokogawa, K., Deguchi, Y., Cherasse, Y., et al. (2018). Dopamine D1 receptor subtype mediates acute stress-induced dendritic growth in excitatory neurons of the medial prefrontal cortex and contributes to suppression of stress susceptibility in mice. *Mol. Psychiatry* 23, 1717–1730. doi: 10.1038/mp.2017.177

Simpson, P. J., Wang, E., Moon, C., Matarazzo, V., Cohen, D. R., Liebl, D. J., et al. (2003). Neurotrophin-3 signaling maintains maturational homeostasis between neuronal populations in the olfactory epithelium. *Mol. Cell. Neurosci.* 24, 858–874. doi: 10.1016/j.mcn.2003.08.001

Smith, M. A., Makino, S., Kvetnansky, R., and Post, R. M. (1995). Stress and glucocorticoids affect the expression of brain-derived neurotrophic factor and neurotrophin-3 mRNAs in the hippocampus. *J. Neurosci.* 15, 1768–1777. doi: 10.1523/JNEUROSCI.15-03-01768.1995

Ueno, M., Sugimoto, M., Ohtsubo, K., Sakai, N., Endo, A., Shikano, K., et al. (2019). The effect of electroconvulsive seizure on survival, neuronal differentiation, and expression of the maturation marker in the adult mouse hippocampus. *J. Neurochem.* 149, 488–498. doi: 10.1111/jnc.14691

Van Bokhoven, P., Oomen, C. A., Hoogendijk, W. J., Smit, A. B., Lucassen, P. J., and Spijker, S. (2011). Reduction in hippocampal neurogenesis after social defeat is long-lasting and responsive to late antidepressant treatment. *Eur. J. Neurosci.* 33, 1833–1840. doi: 10.1111/j.1460-9568.2011.07668.x

Warner-Schmidt, J. L., and Duman, R. S. (2006). Hippocampal neurogenesis: opposing effects of stress and antidepressant treatment. *Hippocampus* 16, 239–249. doi: 10.1002/hipo.20156

West, M. J., Slomianka, L., and Gundersen, H. J. (1991). Unbiased stereological estimation of the total number of neurons in the subdivisions of the rat hippocampus using the optical fractionator. *Anat. Rec.* 231, 482–497. doi: 10.1002/ar.1092310411

Zhao, C., Deng, W., and Gage, F. H. (2008). Mechanisms and functional implications of adult neurogenesis. *Cells* 132, 645–660. doi: 10.1016/j.cell.2008.01.033

frontiers | Frontiers in Neuroscience

TYPE Mini Review
PUBLISHED 28 July 2023
DOI 10.3389/fnins.2023.1217596

OPEN ACCESS

EDITED BY
Chitra D. Mandyam,
United States Department of Veterans Affairs, United States

REVIEWED BY
Igor Iskusnykh,
University of Tennessee Health Science Center (UTHSC), United States

*CORRESPONDENCE
Isabel Martinez-Garay
✉ martinezgarayi@cardiff.ac.uk

RECEIVED 05 May 2023
ACCEPTED 10 July 2023
PUBLISHED 28 July 2023

CITATION
Singh N, Siebzehnrubl FA and Martinez-Garay I (2023) Transcriptional control of embryonic and adult neural progenitor activity.
Front. Neurosci. 17:1217596.
doi: 10.3389/fnins.2023.1217596

Transcriptional control of embryonic and adult neural progenitor activity

Niharika Singh[1,2], Florian A. Siebzehnrubl[2] and Isabel Martinez-Garay[1]*

[1]Division of Neuroscience, School of Biosciences, Cardiff University, Cardiff, United Kingdom, [2]European Cancer Stem Cell Research Institute, Cardiff University School of Biosciences, Cardiff, United Kingdom

Neural precursors generate neurons in the embryonic brain and in restricted niches of the adult brain in a process called neurogenesis. The precise control of cell proliferation and differentiation in time and space required for neurogenesis depends on sophisticated orchestration of gene transcription in neural precursor cells. Much progress has been made in understanding the transcriptional regulation of neurogenesis, which relies on dose- and context-dependent expression of specific transcription factors that regulate the maintenance and proliferation of neural progenitors, followed by their differentiation into lineage-specified cells. Here, we review some of the most widely studied neurogenic transcription factors in the embryonic cortex and neurogenic niches in the adult brain. We compare functions of these transcription factors in embryonic and adult neurogenesis, highlighting biochemical, developmental, and cell biological properties. Our goal is to present an overview of transcriptional regulation underlying neurogenesis in the developing cerebral cortex and in the adult brain.

KEYWORDS

neurogenesis, transcription factor, embryonic, adult, bHLH, homeodomain, forkhead, Zeb1

Introduction

Neurogenesis happens primarily during embryonic stages, while the nervous system develops, although some regions in the adult brain retain the capacity to generate new neurons throughout life (Jurkowski et al., 2020). In both cases, neural progenitors need to balance their own proliferation with the production of differentiated cells to ensure that appropriate numbers of neurons and glia are made. During embryonic neurogenesis, progenitors first proliferate through symmetric divisions until about E11.5, when they change their division mode and start producing neurons through asymmetric divisions. Once all necessary neurons have been generated, they will begin generating glial cells in an irreversible switch that signifies the end of embryonic neurogenesis (Martynoga et al., 2012). Because transitions between phases cannot be reversed, accurate control of proliferation vs. differentiation is paramount to ensure the correct development of the nervous system. Postnatally, some radial glial cells become the specialized neural stem cells (NSCs) for postnatal and adult neurogenesis (Bond et al., 2020). In neurogenic regions [subventricular zone, hippocampus and hypothalamus, reviewed in Jurkowski et al., 2020], NSCs generate intermediate progenitor cells through asymmetric division. Intermediate progenitor cells expand rapidly and eventually differentiate into neuronal progenitor cells that migrate to their destination where they integrate into neuronal circuitry

TABLE 1 Role of different transcription factors in embryonic neurogenesis.

DNA-binding domain	Transcription factor	Role	References
Basic helix–loop–helix (bHLH)	HES1	Represses neuronal differentiation of NSC pool	Ishibashi et al. (1994), Nakamura et al. (2000), Shimojo et al. (2008), Dhanesh et al. (2016), and Gozlan and Sprinzak (2023)
		Heterogenous differentiation of NSCs	Kobayashi et al. (2009) and Kobayashi and Kageyama (2011)
	NGN2	Proneural differentiation of NSCs, regulation of progenitor maturation and of neuronal vs. glial fate decision	Nieto et al. (2001), Parras et al. (2002), Britz et al. (2006), Mattar et al. (2008), Miskinyte et al. (2018), and Han et al. (2021)
	ASCL1	Lineage commitment of NPCs to neuronal fate	Castro et al. (2011) and Vasconcelos and Castro (2014)
		Defines neurogenic patterning and cortical folding	Han et al. (2021)
Homeodomain	PAX6	Controls balance between neural stem cell (NSC) self-renewal and neurogenesis	Estivill-Torrus et al. (2002), Sansom et al. (2009), Mi et al. (2013), and Manuel et al. (2015)
		Dorsoventral patterning of the mammalian telencephalon	Toresson et al. (2000) and Yun et al. (2001)
	SOX2	Promotes progenitor proliferation and prevents differentiation	Miyagi et al., 2008
Zinc finger + leucine zipper + forkhead domain	FOXG1	Maintains balance between proliferation and differentiation in neural progenitors	Xuan et al. (1995), Dou et al. (1999), Hanashima et al. (2002), Shen et al. (2006), Eagleson et al. (2007), and Siegenthaler et al. (2008)
	FOXM1	Maintains stem cell pluripotency and self-renewal capacity of stem cells	Kalin et al. (2011) and Wu et al. (2014)
	FOXP1	Maintains progenitor pool by promoting progenitor self-renewal	Pearson et al. (2020)
		Promotes progenitor differentiation	Braccioli et al. (2017)
	FOXP2	Induces generation of intermediate progenitors	Tsui et al. (2013)
	FOXP4	Promotes progenitor differentiation	Rousso et al. (2012) and Li et al. (2023)
	FOXO 1/3/4	Mediate antiproliferative TGF-B signaling in early neural progenitors	Seoane et al. (2004)
Zinc finger homeodomain	ZEB1	Neuronal differentiation, and migration	Jiang et al. (2018) and Wang et al. (2019)
		Cleavage plane orientation in progenitors	Liu et al. (2019)

upon terminal differentiation. Contrastingly to embryonic neurogenesis, adult NSCs can simultaneously generate glial cells through a much less understood process.

The balance between proliferation and differentiation of neural stem and progenitor cells requires exquisite control at the transcriptional level. Transcriptional control of embryonic and adult neurogenesis relies on shared transcription factors (TFs) that become spatially confined over time, are expressed at specific timepoints, or both. The cell type-specific transcriptional activity of such neurogenic TFs is mediated by epigenetic signatures, chromatin changes, and other protein partners. In this mini-review, we provide a brief overview focusing on the role of some of the best-characterized TFs that control neurogenesis in the embryonic dorsal telencephalon (Table 1) and in the adult subgranular zone (SGZ) of the hippocampus and the subventricular zone (SVZ) of the lateral ventricles (Table 2). For more comprehensive analyses of the role of specific TFs, we refer the reader to appropriate reviews.

bHLH transcription factors in neurogenesis

Transcription factors of the bHLH (basic helix loop helix) superfamily work as dimers and bind DNA through a basic domain at their amino terminal end (Jones, 2004). Several bHLH TFs play important and sometimes opposing roles during embryonic and adult neurogenesis.

HES (Hairy and Enhancer of Split homologs) family members of the bHLH TF family are effectors of the Notch signaling pathway (Ohtsuka et al., 1999). During corticogenesis, they regulate cell

TABLE 2 Role of different transcription factors in postnatal/adult neurogenesis.

DNA-binding domain	Transcription factor	Role	References
Basic helix–loop–helix (bHLH)	HES1	Promotes/ regulates quiescence and proliferation of NSCs	Zhang et al. (2015), Sueda et al. (2019), and Kaise and Kageyama (2021)
	NGN2	Neuronal differentiation of progenitors	Ozen et al. (2007), Roybon et al. (2009), and Arai et al. (2017)
	ASCL1	Activation of quiescent NSCs, drives differentiation of NSPCs to neurogenic fate	Imayoshi et al. (2013), Andersen et al. (2014), Urbán et al. (2016), Pilz et al. (2018), and Harris et al. (2021)
		Defines SGZ and SVZ cells with long-term neurogenic potential	Kim et al. (2011)
Homeodomain	PAX6	Generation of neuronal progenitors and their specification into dopaminergic periglomerular phenotype	Hack et al. (2005), Kohwi et al. (2005), and Brill et al. (2008)
	SOX2	NSC maintenance	Ferri et al. (2004) and Favaro et al. (2009)
Zinc finger + leucine zipper + forkhead domain	FOXG1	Proliferation of neuronal progenitors in neurogenic niches	Shen et al. (2006), Tian et al. (2012), and Wang et al. (2022)
	FOXJ1	Maintains progenitor proliferation in SVZ through cell autonomous and non-autonomous mechanisms	Jacquet et al. (2009) and Jacquet et al. (2011)
	FOXO 1/3/4	Maintains the population of quiescent NSCs	Renault et al. (2009), Webb et al. (2013), Li et al. (2017), and Schäffner et al. (2018)
Zinc finger homeodomain	ZEB1	Self-renewal of active radial glia-like cells to favor an astroglial fate, shift in cell division polarity	Gupta et al. (2021)

proliferation, differentiation, and fate specification by maintaining stemness of progenitors and controlling the timing of differentiation (Kageyama et al., 2007; Gozlan and Sprinzak, 2023) in neuroepithelial and radial glial cells. Of the different *Hes* genes, *Hes1* is the most widely studied in the context of corticogenesis. HES1 levels in cortical neuronal progenitors experience cyclic oscillations, which are essential for the maintenance of neuronal progenitors (Shimojo et al., 2008). These oscillations result from the combination of *Hes1* expression induction by Notch signaling, an autoinhibitory effect of HES1 on its own transcription and the great instability of the *Hes1* mRNA and protein (Takebayashi et al., 1994; Hirata et al., 2002). In its capacity as an antineurogenic bHLH repressor (Nakamura et al., 2000), HES1 acts in two different ways. First, it represses expression of its target genes by directly binding to their promotors in a complex with co-repressors like Groucho/TLE-1 (Jiménez et al., 1997; Dhanesh et al., 2016). Second, HES1 interferes with the transcriptional activity of target TFs by binding to and sequestering E proteins such as E47, which are required by TFs like ASCL1 to function (Sasai et al., 1992; Dhanesh et al., 2016). Downstream targets of HES1 include cell-cycle regulators like the CDK inhibitor *Cdkn1B* (Murata et al., 2005), *Gadd45g*, cyclins D2 and E2, and the Notch ligand *Dll1* (Shimojo et al., 2008). In addition, HES1 also inhibits expression of several proneural bHLH TFs, including *Ascl1* and *Neurog2* (Shimojo et al., 2008). HES1 fluctuations drive oscillatory expression of these TFs and help maintain the progenitor population, especially during early stages of corticogenesis (Shimojo et al., 2011). In turn, expression, or lack thereof of the proneural bHLH TFs *Ascl1* and *Neurog2* define four different progenitor states, with expression of both TFs representing the least lineage restricted progenitors and those expressing only *Neurog2* committed to a neuronal lineage (Han et al., 2021). Furthermore, combined expression of *Ascl1* and *Neurog2* leads to cross-repression and to the production of Notch ligands that maintain proliferation in neighboring cells (Han et al., 2021).

During adult neurogenesis, sustained levels of HES1 are needed to keep aNSCs in the SVZ and SGZ in a quiescent state (Sueda et al., 2019), as constant, high HES1 indirectly leads to increased CDKN1A levels, inhibiting cell cycle progression (Maeda et al., 2023). This is accomplished through the interaction of HES1 with ID1, which represses HES1 autoinhibition (Bai et al., 2007). As NSCs activate, oscillating expression of HES1 drives a concomitant oscillatory expression of ASCL1, which is critical for NSC activation (Andersen et al., 2014). In fact, lower levels of ASCL1 are linked to higher numbers of resting NSCs (Urbán et al., 2016) and a proliferation vs. differentiation bias in progenitors (Imayoshi et al., 2013), while ASCL1 protein levels drop over time to ensure the maintenance of the aNSC pool (Harris et al., 2021).

Homeobox transcription factors in neurogenesis

There are 11 different classes of homeobox transcription factors, characterized by a helix-turn-helix homeodomain motif that mediates their binding to DNA (Holland et al., 2007). We discuss PAX6 and SOX2 here, but the roles of 21 homeobox TFs in vertebrate forebrain development have been comprehensively reviewed elsewhere (Leung et al., 2022).

PAX6 belongs to the paired-box homeodomain transcription factor family, harboring a second DNA binding domain, the paired

box, in addition to the homeodomain (Dahl et al., 1997). PAX6 is one of the main regulators of cortical neurogenesis, controlling cell cycle length and exit in a dose and context dependent manner [reviewed in Manuel et al. (2015)]. As such, loss of *Pax6* leads to shorter cell cycle length and a premature switch from proliferative to neurogenic divisions during early neurogenesis, with more pronounced effects in areas of higher *Pax6* expression (Estivill-Torrus et al., 2002; Mi et al., 2013). However, at later stages, *Pax6* loss leads to a longer cell cycle (Estivill-Torrus et al., 2002) and its overexpression decreases the number of proliferating progenitors in rostral and medial areas at E15.5 (Manuel et al., 2006). These results highlight the context dependent actions of this TF, which is needed both for progenitor proliferation and for neurogenesis. Interestingly, the effects of PAX6 during corticogenesis, except for its patterning role, are mediated by the paired-box, and not by the homeodomain (Haubst et al., 2004). PAX6 regulates progenitor cell proliferation in part by controlling expression of several genes involved in the G1/S transition, including cyclins and *Cdks* (Sansom et al., 2009; Mi et al., 2013). PAX6 has been shown to directly inhibit *Cdk6* expression, thereby reducing Rb phosphorylation and slowing down G1 progression (Mi et al., 2013). Regarding neurogenesis, PAX6 directly induces expression of *Tbr2*, which confers intermediate progenitor identity (Quinn et al., 2007; Sansom et al., 2009). In addition, PAX6 also stimulates expression of *Neurog2*, and participates in a transcriptional network with NEUROG2, ASCL1 and HES1 to control the outcome of neural progenitor cell division (Sansom et al., 2009).

During adult neurogenesis, PAX6 seems to play a similar role controlling proliferation and neuronal differentiation of aNSCs (Hack et al., 2005; Maekawa et al., 2005). In the SGZ, PAX6 induces expression of *Neurog2* and *NeuroD1* (Xu et al., 2021), which are needed to maintain NSC progenitors and induce neuronal fate, respectively (Roybon et al., 2009). It also acts through FABP7 to maintain NSC and progenitor cell proliferation and prevent exhaustion of the stem cell pool (Osumi et al., 2008). In the SVZ and the rostral migratory stream (RMS), PAX6 is needed to regulate neuronal precursor proliferation and for periglomerular neuron fate (Hack et al., 2005).

SOX2 (SRY-box binding transcription factor 2) is a member of the Sox family of transcription factors, which consists of 9 subfamilies (*SoxA, SoxB1, SoxB2, SoxC, SoxD, SoxE, SoxF, SoxG, SoxH*). *Sox2* is part of the *SoxB1* subgroup (together with *Sox1* and *Sox3*; Wegner, 2010) and is a master regulator of stemness in development and adult tissues (Sarkar and Hochedlinger, 2013). It is a pioneer factor that can initiate transcription in epigenetically silenced chromatin regions (Dodonova et al., 2020). SOX transcription factors bind the consensus sequence TTGT through their high-mobility-group (HMG) box (Wegner, 2010), with specificity of individual SOX factors conveyed by DNA regions flanking the consensus motif (Sarkar and Hochedlinger, 2013). SOX2 is expressed throughout embryonic and adult neurogenesis, as well as in pluripotent embryonic stem cells and *Sox2* knockout (KO) is lethal during early embryogenesis (Avilion et al., 2003). In the developing brain SOX2 promotes progenitor proliferation and prevents cell differentiation, functions that overlap with SOX1 and SOX3 (Wegner and Stolt, 2005; Miyagi et al., 2008). Interestingly, Sox2 hypomorphism also affects differentiation into GABAergic interneurons in the cortex and olfactory bulb at E17.5 (Cavallaro et al., 2008).

In the adult CNS, SOX2 is expressed in all neurogenic niches, and conditional deletion of *Sox2* results in impaired NSC proliferation, increased apoptosis, and reduced neurogenesis in the SVZ and SGZ (Ferri et al., 2004; Favaro et al., 2009). The wide-ranging functions of SOX2 in the brain are reviewed in more detail in Pevny and Nicolis (2010) and Mercurio et al. (2019).

Forkhead transcription factors in neurogenesis

Forkhead transcription factors are characterized by the presence of the so-called forkhead domain, which mediates their interaction with DNA. This domain consists of three α-helices and three β-sheets surrounded by two loops that form the "winged" region (Hannenhalli and Kaestner, 2009). Forkhead family members are classified into 19 subfamilies from *FoxA* to *FoxS* (Jackson et al., 2010). Members of the *FoxG, FoxJ, FoxM, FoxO*, and *FoxP* subfamilies have been implicated in embryonic and/or adult neurogenesis and play sometimes opposing roles in the regulation of neural stem cell behavior.

Foxg1 KO animals die at birth with severe brain hypoplasia (Xuan et al., 1995; Dou et al., 1999) and heterozygous animals display decreased cortical, hippocampal and striatal size, along with reduced numbers of TBR2+ intermediate progenitors (Shen et al., 2006; Eagleson et al., 2007; Siegenthaler et al., 2008). Those changes reflect the role of FOXG1 in maintaining the correct balance between proliferation and differentiation in neural progenitors, with lack of *Foxg1* leading to lengthening of the cell cycle and premature cell cycle exit (Xuan et al., 1995; Hanashima et al., 2002). At the molecular level, FOXG1 antagonizes TGF-B signaling by repressing the expression of TGF-B family members BMP2, 4, 6, and 7, which are all ectopically upregulated in *Foxg1* KOs. This repression requires the DNA binding domain of FOXG1 (Dou et al., 1999; Hanashima et al., 2002). FOXG1 also interferes with the ability of the TGF-B signaling effectors SMADs to promote expression of CDK inhibitors. The SMAD partner FAST-2 is needed for the transcriptional activation of *Cdkn2b*, but binding of FOXG1 to FAST-2 interferes with TGF-B signaling and antagonizes its growth inhibition effects (Dou et al., 2000). To activate *Cdkn1a* expression, SMAD proteins need to form a complex with members of the FOXO subfamily (Seoane et al., 2004). FOXG1 can reduce *Cdkn1a* expression levels by repressing expression of *Foxo1* (Vezzali et al., 2016). Furthermore, FOXG1 interacts with FOXO at the protein level, forming a ternary complex with SMADs that can no longer activate *Cdkn1a* expression (Seoane et al., 2004). In addition, FOXG1 inhibition of *Cdkn1a* expression can also be mediated by its interaction with the polycomb protein BMI-1 (Fasano et al., 2009). FOXG1 could also potentially interfere with the expression of *Cdkn1b*, as its expression is stimulated by BMP treatment (Nakamura et al., 2003; Sharov et al., 2006) and by expression of *Foxo1*, 3 and 4 (Medema et al., 2000).

FOXG1 has also been indirectly linked to Notch signaling, as it interacts with TLE1, which enhances the repressive ability of FOXG1 (Yao et al., 2001). This interaction has been shown *in vitro* and in the E15.5 developing telencephalon. Moreover, TLE1 enables the interaction between FOXG1 and HES1, which increases HES1-mediated transcriptional repression (Yao et al., 2001), suggesting that FOXG1 might act to amplify the effect of Notch signaling in early neural progenitors, as all three proteins are expressed in cultures derived from E12.5 telencephalic progenitors.

Other forkhead family members are also involved in neurogenesis. FOXM1 stimulates expression of genes needed for G1/S transition and DNA replication, while simultaneously diminishing protein stability of CDK inhibitors (Kalin et al., 2011). These roles could explain why cortical progenitors derived from E14 ER^{T2}Cre *FoxM1*$^{fl/fl}$ animals display a reduction in the number of neurospheres formed after tamoxifen addition (Wang et al., 2011). FOXM1 also regulates expression of *Sox2* and Bmi1, which are necessary for neural progenitor self-renewal (Wang et al., 2011). However, conditional deletion of *Foxm1* does not lead to major abnormalities in the brain (Schüller et al., 2007), suggesting the presence of compensatory mechanisms. From the FOXP family members, FOXP1 works to maintain the progenitor pool by promoting progenitor self-renewal, at least in part through the induction of vertical division angles and symmetric divisions (Pearson et al., 2020). However, FOXP1 has also been shown to inhibit Notch signaling in the developing cortex, thereby promoting progenitor differentiation (Braccioli et al., 2017). FOXP2 might regulate the generation of TBR2+ intermediate progenitors (Tsui et al., 2013) and FOXP4 promotes neuronal differentiation of neural progenitors by repressing N-Cadherin expression, therefore favoring detachment from the ventricular zone (Rousso et al., 2012; Li et al., 2023).

FOXG1 is strongly expressed in the SGZ of the dentate gyrus and the lateral ventricle SVZ (Shen et al., 2006; Schäffner et al., 2023). In aNSCs of the DG, FOXG1 plays a similar role of balancing proliferation and differentiation as it does in embryonic progenitors (Wang et al., 2022), with partial or total loss leading to defects in size and morphology of this anatomical structure. Progressive loss of progenitors, altered neuronal differentiation and reduced neuronal survival have been described in these mutant animals, as well as a failure to form the secondary radial glia scaffold (Shen et al., 2006; Tian et al., 2012). Remarkably, generation of olfactory interneurons in the SVZ does not seem to be affected by heterozygous lack of *Foxg1* (Shen et al., 2006), suggesting a region-specific function of FOXG1 in adult neurogenesis.

FOXO1 and FOXO3 are also expressed in aNSCs of the SVZ and the SGZ (Paik et al., 2009; Renault et al., 2009). In a *Foxo1/3/4* triple mutant, aNSCs get depleted over time due to decreased self-renewal and increased activation of progenitors early on (Paik et al., 2009; Schäffner et al., 2018). These effects are due to increased expression of cyclins and CDKs and decreased expression of CDK inhibitors, as well as derepression of the centrosomal gene *Aspm*, a known regulator of NSCs divisions (Paik et al., 2009). Very similar results are obtained in *Foxo3* single KO animals (Renault et al., 2009). Transcriptional analysis has revealed that FOXO3 targets are enriched in cell quiescence-related genes, oxidative stress response and cell metabolism, further supporting the notion that FOXO proteins are necessary to maintain the population of quiescent NSCs over the lifespan of the animals by preventing excessive cell cycle reentry (Renault et al., 2009; Ro et al., 2013). This transcriptional control is mediated in part by the interaction of FOXO3 with the methylcytosine dioxygenase TET2 (Li et al., 2017). Moreover, FOX3 restricts the neurogenic effects of ASCL1 in adult NPCs by preventing ASCL1-dependent transcription (Webb et al., 2013) Additionally, lack of *Foxo3* also impacts the outcome of aNSC progeny, with a bias toward astrocytes and reduced production of neurons and oligodendrocytes (Renault et al., 2009).

Finally, FOXJ1 has also been linked to adult neurogenesis in the SVZ of the lateral ventricle. This TF is required for ependymal cell specification during the transition to postnatal stages (Jacquet et al., 2009), but it also defines a subpopulation of progenitors that rely on FOXJ1 expression for its proliferative ability (Jacquet et al., 2011). FOXJ1 deficient progenitors produce fewer neurospheres and are biased toward a glial fate, with defective neurogenic potential. Interestingly, beyond the cell autonomous effect of FOXJ1 in the FOXJ1+ lineage, an additional non-autonomous effect on the remaining aNSCs in the SEZ has been described (Jacquet et al., 2011).

ZEB1 in neurogenesis

The transcription factor ZEB1 (zinc finger E-box binding homeobox 1) is emerging as a new regulator of self-renewal and fate choice in the CNS. The ZEB family of TFs consists of two members, *Zeb1* and *Zeb2*, which are both core regulators of epithelial-mesenchymal transition (Vandewalle et al., 2009). Epithelial-mesenchymal transition is developmental program that has more recently garnered attention for its role in stemness and lineage regulation (Goossens et al., 2017). *Zeb1*-mutant mice show aberrant T cell development, underlining its involvement in lineage regulation (Higashi et al., 1997). Structurally, ZEB proteins comprise of two C_2H_2-type zinc finger domains that flank a central homeodomain. The zinc finger domains are necessary for DNA binding, with each zinc finger independently binding to separate E-box motifs in gene promoters with the consensus sequence 5′-CACCT(G)-3; Sekido et al., 1996, 1997; Remacle et al., 1999). The homeodomain mediates interaction with other proteins (e.g., CTBP, YAP) that are necessary for transcriptional regulation (Furusawa et al., 1999; Feldker et al., 2020). Depending on their interaction partners, ZEB TFs can activate or repress transcription, with E-cadherin repression and Vimentin activation being the best-known examples (Vandewalle et al., 2009). Phosphorylation of Thr-867 is necessary for nuclear import of ZEB1 (Llorens et al., 2016), otherwise the effects of post-transcriptional ZEB1 modifications are poorly understood.

In embryonal neurogenesis, ZEB1 is expressed in the subventricular zone and overlaps with proliferating progenitor cells between E14 and E18 (Yen et al., 2001). Constitutive deletion of *Zeb1* causes defects in proliferation of embryonic neural progenitors in the ventricular zone of the lateral ventricles and the hypothalamus at E15.5 (Liu et al., 2008). ZEB1 blocks neuronal lineage progression as well as migration of cortical neuroblasts (Wang et al., 2019). Conditional loss of *Zeb1* at E14.5 does not affect cell proliferation or radial glia cell maintenance but causes premature neuronal differentiation (Wang et al., 2019). *Zeb1* overexpression at E14.5 results in reduced neurogenesis, migration defects and subcortical band heterotopia (Wang et al., 2019).

In the adult brain, ZEB1 is important for the self-renewal of adult hippocampal radial glia-like (RGL) cells. *Zeb1* loss in RGL cells results in their precocious differentiation into the neuronal lineage (Gupta et al., 2021). This is accompanied by reduced differentiation into the astroglial lineage, but it remains to be resolved whether this is due to an as-yet unspecified role of ZEB1 in glial fate determination or a natural consequence of the increased neurogenesis. Hence, ZEB1 blocks neuronal lineage progression during embryonal and adult neurogenesis. In adult neural stem/progenitor cells, ZEB1 is associated

with activation and proliferation, and loss of *Zeb1* results in depletion of the stem cell pool. Contrastingly, ZEB1 functions in neural progenitors during embryonic neurogenesis appear to be separated in time, with *Zeb1* loss affecting proliferation of progenitors in a constitutive knockout model, but not of later radial glia cells when deleted at E14.5 (Liu et al., 2008; Wang et al., 2019). In both adult and embryonic neurogenesis, *Zeb1* loss is associated with a change in cell division type (symmetric vs. asymmetric) which promotes differentiation of the stem/progenitor cell pool. Interestingly, *Zeb1* loss during embryogenesis promoted asymmetric divisions that prevented expansion of neural progenitors (and therefore caused premature differentiation), whereas in the adult hippocampus *Zeb1* KO causes increased symmetric divisions of neural stem/progenitor cells which are necessary for self-renewal, thus promoting their differentiation (Liu et al., 2019; Gupta et al., 2021).

Conclusion

Although neurogenic transcription factors are expressed during embryonic and adult neurogenesis their functions often show differences during both processes. These differences include increased spatial confinement and spatial heterogeneity in adult neurogenic niches, different activities in neural progenitor cells at various developmental stages, and/or different effects on downstream progenitor cells. It is important to consider epigenetic modifications, post-translational modifications, and differential expression of interacting partners at different developmental stages to unravel the functions of each neurogenic transcription factor at specific points in time and space. For example, changes in ASCL1 post-translational degradation result in different behavior of adult neural stem cells in juvenile and adult hippocampal neurogenesis (Harris et al., 2021). Integrated analysis of neurogenic transcription factors across development and aging is needed to reveal the specific co-factors contributing to the differential functions in embryonic and adult neurogenesis.

Data availability statement

No new data was created during this study.

Author contributions

All authors listed have made a substantial, direct, and intellectual contribution to the work and approved it for publication.

Funding

NS was the recipient of a Biotechnology and Biological Sciences Research Council (BBSRC) PhD studentship (BB/T008741/1). FS was supported by MRC grant MR/S007709/1. IM-G was supported by funding from the BBSRC (BB/S002359/1). Open access publication fees were covered by the Cardiff University's Open Access Institutional Fund.

Conflict of interest

The authors declare that the research was conducted in the absence of any commercial or financial relationships that could be construed as a potential conflict of interest.

Publisher's note

All claims expressed in this article are solely those of the authors and do not necessarily represent those of their affiliated organizations, or those of the publisher, the editors and the reviewers. Any product that may be evaluated in this article, or claim that may be made by its manufacturer, is not guaranteed or endorsed by the publisher.

References

Andersen, J., Urbán, N., Achimastou, A., Ito, A., Simic, M., Ullom, K., et al. (2014). A Transcriptional Mechanism Integrating Inputs from Extracellular Signals to Activate Hippocampal Stem Cells. *Neuron* 83, 1085–1097. doi: 10.1016/j.neuron.2014.08.004

Arai, M. D., Zhan, B., Maruyama, A., Matsui-Harada, A., Horinouchi, K., and Komai, S. (2017). Enriched environment and Mash1 transfection affect neural stem cell differentiation after transplantation into the adult somatosensory cortex. *J. Neurol. Sci.* 373, 73–80. doi: 10.1016/j.jns.2016.12.013

Avilion, A. A., Nicolis, S. K., Pevny, L. H., Perez, L., Vivian, N., and Lovell-Badge, R. (2003). Multipotent cell lineages in early mouse development depend on SOX2 function. *Genes Dev.* 17, 126–140. doi: 10.1101/gad.224503

Bai, G., Sheng, N., Xie, Z., Bian, W., Yokota, Y., Benezra, R., et al. (2007). Id Sustains Hes1 Expression to Inhibit Precocious Neurogenesis by Releasing Negative Autoregulation of Hes1. *Dev. Cell* 13, 283–297. doi: 10.1016/j.devcel.2007.05.014

Bond, A. M., Ming, G., and Song, H. (2020). Ontogeny of adult neural stem cells in the mammalian brain. *Curr. Top. Dev. Biol.* 142, 67–98. doi: 10.1016/bs.ctdb.2020.11.002

Braccioli, L., Vervoort, S. J., Adolfs, Y., Heijnen, C. J., Basak, O., Pasterkamp, R. J., et al. (2017). FOXP1 Promotes Embryonic Neural Stem Cell Differentiation by Repressing Jagged1 Expression. *Stem Cell Rep* 9, 1530–1545. doi: 10.1016/j.stemcr.2017.10.012

Brill, M. S., Snapyan, M., Wohlfrom, H., Ninkovic, J., Jawerka, M., Mastick, G. S., et al. (2008). A Dlx2- and Pax6-Dependent Transcriptional Code for Periglomerular Neuron Specification in the Adult Olfactory Bulb. *J. Neurosci.* 28, 6439–6452. doi: 10.1523/JNEUROSCI.0700-08.2008

Britz, O., Mattar, P., Nguyen, L., Langevin, L.-M., Zimmer, C., Alam, S., et al. (2006). A Role for Proneural Genes in the Maturation of Cortical Progenitor Cells. *Cereb. Cortex* 16, i138–i151. doi: 10.1093/cercor/bhj168

Castro, D. S., Martynoga, B., Parras, C., Ramesh, V., Pacary, E., Johnston, C., et al. (2011). A novel function of the proneural factor Ascl1 in progenitor proliferation identified by genome-wide characterization of its targets. *Genes Dev.* 25, 930–945. doi: 10.1101/gad.627811

Cavallaro, M., Mariani, J., Lancini, C., Latorre, E., Caccia, R., Gullo, F., et al. (2008). Impaired generation of mature neurons by neural stem cells from hypomorphic Sox2 mutants. *Development* 135, 541–557. doi: 10.1242/dev.010801

Dahl, E., Koseki, H., and Balling, R. (1997). Pax genes and organogenesis. *Bioessays* 19, 755–765. doi: 10.1002/bies.950190905

Dhanesh, S. B., Subashini, C., and James, J. (2016). Hes1: the maestro in neurogenesis. *Cell. Mol. Life Sci.* 73, 4019–4042. doi: 10.1007/s00018-016-2277-z

Dodonova, S. O., Zhu, F., Dienemann, C., Taipale, J., and Cramer, P. (2020). Nucleosome-bound SOX2 and SOX11 structures elucidate pioneer factor function. *Nature* 580, 669–672. doi: 10.1038/s41586-020-2195-y

Dou, C., Lee, J., Liu, B., Liu, F., Massague, J., Xuan, S., et al. (2000). BF-1 Interferes with Transforming Growth Factor β Signaling by Associating with Smad Partners. *Mol. Cell. Biol.* 20, 6201–6211. doi: 10.1128/MCB.20.17.6201-6211.2000

Dou, C.-L., Li, S., and Lai, E. (1999). Dual Role of Brain Factor-1 in Regulating Growth and Patterning of the Cerebral Hemispheres. *Cereb. Cortex* 9, 543–550. doi: 10.1093/cercor/9.6.543

Eagleson, K. L., McFadyen-Ketchum, L. J. S., Ahrens, E. T., Mills, P. H., Does, M. D., Nickols, J., et al. (2007). Disruption of Foxg1 expression by knock-in of Cre recombinase: Effects on the development of the mouse telencephalon. *Neuroscience* 148, 385–399. doi: 10.1016/j.neuroscience.2007.06.012

Estivill-Torrus, G., Pearson, H., Heyningen, V., Price, D. J., and Rashbass, P. (2002). Pax6 is required to regulate the cell cycle and the rate of progression from symmetrical to asymmetrical division in mammalian cortical progenitors. *Development* 129, 455–466. doi: 10.1242/dev.129.2.455

Fasano, C. A., Phoenix, T. N., Kokovay, E., Lowry, N., Elkabetz, Y., Dimos, J. T., et al. (2009). Bmi-1 cooperates with Foxg1 to maintain neural stem cell self-renewal in the forebrain. *Genes Dev.* 23, 561–574. doi: 10.1101/gad.1743709

Favaro, R., Valotta, M., Ferri, A. L. M., Latorre, E., Mariani, J., Giachino, C., et al. (2009). Hippocampal development and neural stem cell maintenance require Sox2-dependent regulation of Shh. *Nat. Neurosci.* 12, 1248–1256. doi: 10.1038/nn.2397

Feldker, N., Ferrazzi, F., Schuhwerk, H., Widholz, S. A., Guenther, K., Frisch, I., et al. (2020). Genome-wide cooperation of EMT transcription factor ZEB1 with YAP and AP-1 in breast cancer. *EMBO J.* 39:e103209. doi: 10.15252/embj.2019103209

Ferri, A. L. M., Cavallaro, M., Braida, D., Cristofano, A. D., Canta, A., Vezzani, A., et al. (2004). Sox2 deficiency causes neurodegeneration and impaired neurogenesis in the adult mouse brain. *Development* 131, 3805–3819. doi: 10.1242/dev.01204

Furusawa, T., Moribe, H., Kondoh, H., and Higashi, Y. (1999). Identification of CtBP1 and CtBP2 as Corepressors of Zinc Finger-Homeodomain Factor δEF1. *Mol. Cell. Biol.* 19, 8581–8590. doi: 10.1128/MCB.19.12.8581

Goossens, S., Vandamme, N., Vlierberghe, P. V., and Berx, G. (2017). EMT transcription factors in cancer development re-evaluated: Beyond EMT and MET. *Biochimica Et Biophys Acta Bba Rev Cancer* 1868, 584–591. doi: 10.1016/j.bbcan.2017.06.006

Gozlan, O., and Sprinzak, D. (2023). Notch signaling in development and homeostasis. *Development* 150:1138. doi: 10.1242/dev.201138

Gupta, B., Errington, A. C., Jimenez-Pascual, A., Eftychidis, V., Brabletz, S., Stemmler, M. P., et al. (2021). The transcription factor ZEB1 regulates stem cell self-renewal and cell fate in the adult hippocampus. *Cell Rep.* 36:109588. doi: 10.1016/j.celrep.2021.109588

Hack, M. A., Saghatelyan, A., Chevigny, A., Pfeifer, A., Ashery-Padan, R., Lledo, P.-M., et al. (2005). Neuronal fate determinants of adult olfactory bulb neurogenesis. *Nat. Neurosci.* 8, 865–872. doi: 10.1038/nn1479

Han, S., Okawa, S., Wilkinson, G. A., Ghazale, H., Adnani, L., Dixit, R., et al. (2021). Proneural genes define ground-state rules to regulate neurogenic patterning and cortical folding. *Neuron* 109, 2847–2863.e11. doi: 10.1016/j.neuron.2021.07.007

Hanashima, C., Shen, L., Li, S. C., and Lai, E. (2002). Brain Factor-1 Controls the Proliferation and Differentiation of Neocortical Progenitor Cells through Independent Mechanisms. *J. Neurosci.* 22, 6526–6536. doi: 10.1523/JNEUROSCI.22-15-06526.2002

Hannenhalli, S., and Kaestner, K. H. (2009). The evolution of Fox genes and their role in development and disease. *Nat. Rev. Genet.* 10, 233–240. doi: 10.1038/nrg2523

Harris, L., Rigo, P., Stiehl, T., Gaber, Z. B., Austin, S. H. L., Masdeu, M. D. M., et al. (2021). Coordinated changes in cellular behavior ensure the lifelong maintenance of the hippocampal stem cell population. *Cell Stem Cell* 28, 863–876.e6. doi: 10.1016/j.stem.2021.01.003

Haubst, N., Berger, J., Radjendirane, V., Graw, J., Favor, J., Saunders, G. F., et al. (2004). Molecular dissection of Pax6 function: the specific roles of the paired domain and homeodomain in brain development. *Development* 131, 6131–6140. doi: 10.1242/dev.01524

Higashi, Y., Moribe, H., Takagi, T., Sekido, R., Kawakami, K., Kikutani, H., et al. (1997). Impairment of T Cell Development in δEF1 Mutant Mice. *J. Exp. Med.* 185, 1467–1480. doi: 10.1084/jem.185.8.1467

Hirata, H., Yoshiura, S., Ohtsuka, T., Bessho, Y., Harada, T., Yoshikawa, K., et al. (2002). Oscillatory Expression of the bHLH Factor Hes1 Regulated by a Negative Feedback Loop. *Science* 298, 840–843. doi: 10.1126/science.1074560

Holland, P. W., Booth, H. A. F., and Bruford, E. A. (2007). Classification and nomenclature of all human homeobox genes. *BMC Biol.* 5:47. doi: 10.1186/1741-7007-5-47

Imayoshi, I., Isomura, A., Harima, Y., Kawaguchi, K., Kori, H., Miyachi, H., et al. (2013). Oscillatory Control of Factors Determining Multipotency and Fate in Mouse Neural Progenitors. *Science* 342, 1203–1208. doi: 10.1126/science.1242366

Ishibashi, M., Moriyoshi, K., Sasai, Y., Shiota, K., Nakanishi, S., and Kageyama, R. (1994). Persistent expression of helix-loop-helix factor HES-1 prevents mammalian neural differentiation in the central nervous system. *EMBO J.* 13, 1799–1805. doi: 10.1002/j.1460-2075.1994.tb06448.x

Jackson, B. C., Carpenter, C., Nebert, D. W., and Vasiliou, V. (2010). Update of human and mouse forkhead box (FOX) gene families. *Hum. Genomics* 4:345. doi: 10.1186/1479-7364-4-5-345

Jacquet, B. V., Muthusamy, N., Sommerville, L. J., Xiao, G., Liang, H., Zhang, Y., et al. (2011). Specification of a Foxj1-dependent lineage in the forebrain is required for embryonic-to-postnatal transition of neurogenesis in the olfactory bulb. *J Neurosci Official J Soc Neurosci* 31, 9368–9382. doi: 10.1523/jneurosci.0171-11.2011

Jacquet, B. V., Salinas-Mondragon, R., Liang, H., Therit, B., Buie, J. D., Dykstra, M., et al. (2009). FoxJ1-dependent gene expression is required for differentiation of radial glia into ependymal cells and a subset of astrocytes in the postnatal brain. *Development* 136, 4021–4031. doi: 10.1242/dev.041129

Jiang, Y., Yan, L., Xia, L., Lu, X., Zhu, W., Ding, D., et al. (2018). Zinc finger E-box–binding homeobox 1 (ZEB1) is required for neural differentiation of human embryonic stem cells. *J. Biol. Chem.* 293, 19317–19329. doi: 10.1074/jbc.RA118.005498

Jiménez, G., Paroush, Z., and Ish-Horowicz, D. (1997). Groucho acts as a corepressor for a subset of negative regulators, including Hairy and Engrailed. *Genes Dev.* 11, 3072–3082. doi: 10.1101/gad.11.22.3072

Jones, S. (2004). An overview of the basic helix-loop-helix proteins. *Genome Biol.* 5:226. doi: 10.1186/gb-2004-5-6-226

Jurkowski, M. P., Bettio, L., Woo, E. K., Patten, A., Yau, S.-Y., and Gil-Mohapel, J. (2020). Beyond the Hippocampus and the SVZ: Adult Neurogenesis Throughout the Brain. *Front. Cell. Neurosci.* 14:576444. doi: 10.3389/fncel.2020.576444

Kageyama, R., Ohtsuka, T., and Kobayashi, T. (2007). The Hes gene family: repressors and oscillators that orchestrate embryogenesis. *Development* 134, 1243–1251. doi: 10.1242/dev.000786

Kaise, T., and Kageyama, R. (2021). Hes1 oscillation frequency correlates with activation of neural stem cells. *Gene Expr. Patterns* 40:119170. doi: 10.1016/j.gep.2021.119170

Kalin, T. V., Ustiyan, V., and Kalinichenko, V. V. (2011). Multiple faces of FoxM1 transcription factor. *Cell Cycle* 10, 396–405. doi: 10.4161/cc.10.3.14709

Kim, E. J., Ables, J. L., Dickel, L. K., Eisch, A. J., and Johnson, J. E. (2011). Ascl1 (Mash1) Defines Cells with Long-Term Neurogenic Potential in Subgranular and Subventricular Zones in Adult Mouse Brain. *PLoS One* 6:e18472. doi: 10.1371/journal.pone.0018472

Kobayashi, T., and Kageyama, R. (2011). Hes1 Oscillations Contribute to Heterogeneous Differentiation Responses in Embryonic Stem Cells. *Genes* 2, 219–228. doi: 10.3390/genes2010219

Kobayashi, T., Mizuno, H., Imayoshi, I., Furusawa, C., Shirahige, K., and Kageyama, R. (2009). The cyclic gene Hes1 contributes to diverse differentiation responses of embryonic stem cells. *Genes Dev.* 23, 1870–1875. doi: 10.1101/gad.1823109

Kohwi, M., Osumi, N., Rubenstein, J. L. R., and Alvarez-Buylla, A. (2005). Pax6 Is Required for Making Specific Subpopulations of Granule and Periglomerular Neurons in the Olfactory Bulb. *J. Neurosci.* 25, 6997–7003. doi: 10.1523/JNEUROSCI.1435-05.2005

Leung, R. F., George, A. M., Roussel, E. M., Faux, M. C., Wigle, J. T., and Eisenstat, D. D. (2022). Genetic Regulation of Vertebrate Forebrain Development by Homeobox Genes. *Front. Neurosci.* 16:843794. doi: 10.3389/fnins.2022.843794

Li, X., Yao, B., Chen, L., Kang, Y., Li, Y., Cheng, Y., et al. (2017). Ten-eleven translocation 2 interacts with forkhead box O3 and regulates adult neurogenesis. *Nat. Commun.* 8:15903. doi: 10.1038/ncomms15903

Li, X., Zou, S., Tu, X., Hao, S., Jiang, T., and Chen, J.-G. (2023). Inhibition of Foxp4 Disrupts Cadherin-based Adhesion of Radial Glial Cells, Leading to Abnormal Differentiation and Migration of Cortical Neurons in Mice. *Neurosci. Bull.* 1–15:7. doi: 10.1007/s12264-022-01004-7

Liu, Y., El-Naggar, S., Darling, D. S., Higashi, Y., and Dean, D. C. (2008). Zeb1 links epithelial-mesenchymal transition and cellular senescence. *Development* 135, 579–588. doi: 10.1242/dev.007047

Liu, J., Liu, Y., Shao, J., Li, Y., Qin, L., Shen, H., et al. (2019). Zeb1 is important for proper cleavage plane orientation of dividing progenitors and neuronal migration in the mouse neocortex. *Cell Death Differ.* 26, 2479–2492. doi: 10.1038/s41418-019-0314-9

Llorens, M. C., Lorenzatti, G., Cavallo, N. L., Vaglienti, M. V., Perrone, A. P., Carenbauer, A. L., et al. (2016). Phosphorylation Regulates Functions of ZEB1 Transcription Factor. *J. Cell. Physiol.* 231, 2205–2217. doi: 10.1002/jcp.25338

Maeda, Y., Isomura, A., Masaki, T., and Kageyama, R. (2023). Differential cell-cycle control by oscillatory versus sustained Hes1 expression via p21. *Cell Rep.* 42:112520. doi: 10.1016/j.celrep.2023.112520

Maekawa, M., Takashima, N., Arai, Y., Nomura, T., Inokuchi, K., Yuasa, S., et al. (2005). Pax6 is required for production and maintenance of progenitor cells in postnatal hippocampal neurogenesis. *Genes Cells* 10, 1001–1014. doi: 10.1111/j.1365-2443.2005.00893.x

Manuel, M., Georgala, P. A., Carr, C. B., Chanas, S., Kleinjan, D. A., Martynoga, B., et al. (2006). Controlled overexpression of Pax6 in vivo negatively autoregulates the Pax6 locus, causing cell-autonomous defects of late cortical progenitor proliferation with little effect on cortical arealization. *Development* 134, 545–555. doi: 10.1242/dev.02764

Manuel, M. N., Mi, D., Mason, J. O., and Price, D. J. (2015). Regulation of cerebral cortical neurogenesis by the Pax6 transcription factor. *Front. Cell. Neurosci.* 9:70. doi: 10.3389/fncel.2015.00070

Martynoga, B., Drechsel, D., and Guillemot, F. (2012). Molecular Control of Neurogenesis: A View from the Mammalian Cerebral Cortex. *Cold Spring Harb. Perspect. Biol.* 4:a008359. doi: 10.1101/cshperspect.a008359

Mattar, P., Langevin, L. M., Markham, K., Klenin, N., Shivji, S., Zinyk, D., et al. (2008). Basic Helix-Loop-Helix Transcription Factors Cooperate To Specify a Cortical Projection Neuron Identity. *Mol. Cell. Biol.* 28, 1456–1469. doi: 10.1128/MCB.01510-07

Medema, R. H., Kops, G. J., Bos, J. L., and Burgering, B. M. (2000). AFX-like Forkhead transcription factors mediate cell-cycle regulation by Ras and PKB through p27kip1. *Nature* 404, 782–787. doi: 10.1038/35008115

Mercurio, S., Serra, L., and Nicolis, S. K. (2019). More than just Stem Cells: Functional Roles of the Transcription Factor Sox2 in Differentiated Glia and Neurons. *Int. J. Mol. Sci.* 20:4540. doi: 10.3390/ijms20184540

Mi, D., Carr, C. B., Georgala, P. A., Huang, Y.-T., Manuel, M. N., Jeanes, E., et al. (2013). Pax6 exerts regional control of cortical progenitor proliferation via direct

repression of Cdk6 and hypophosphorylation of pRb. *Neuron* 78, 269–284. doi: 10.1016/j.neuron.2013.02.012

Miskinyte, G., Hansen, M. G., Monni, E., Lam, M., Bengzon, J., Lindvall, O., et al. (2018). Transcription factor programming of human ES cells generates functional neurons expressing both upper and deep layer cortical markers. *PLoS One* 13:e0204688. doi: 10.1371/journal.pone.0204688

Miyagi, S., Masui, S., Niwa, H., Saito, T., Shimazaki, T., Okano, H., et al. (2008). Consequence of the loss of Sox2 in the developing brain of the mouse. *FEBS Lett.* 582, 2811–2815. doi: 10.1016/j.febslet.2008.07.011

Murata, K., Hattori, M., Hirai, N., Shinozuka, Y., Hirata, H., Kageyama, R., et al. (2005). Hes1 Directly Controls Cell Proliferation through the Transcriptional Repression of p27Kip1. *Mol. Cell. Biol.* 25, 4262–4271. doi: 10.1128/MCB.25.10.4262-4271.2005

Nakamura, Y., Ozaki, T., Koseki, H., Nakagawara, A., and Sakiyama, S. (2003). Accumulation of p27KIP1 is associated with BMP2-induced growth arrest and neuronal differentiation of human neuroblastoma-derived cell lines. *Biochem Bioph Res* 307, 206–213. doi: 10.1016/S0006-291X(03)01138-0

Nakamura, Y., Sakakibara, S., Miyata, T., Ogawa, M., Shimazaki, T., Weiss, S., et al. (2000). The bHLH Gene Hes1 as a Repressor of the Neuronal Commitment of CNS Stem Cells. *J. Neurosci.* 20, 283–293. doi: 10.1523/JNEUROSCI.20-01-00283.2000

Nieto, M., Schuurmans, C., Britz, O., and Guillemot, F. (2001). Neural bHLH Genes Control the Neuronal versus Glial Fate Decision in Cortical Progenitors. *Neuron* 29, 401–413. doi: 10.1016/S0896-6273(01)00214-8

Ohtsuka, T., Ishibashi, M., Gradwohl, G., Nakanishi, S., Guillemot, F., and Kageyama, R. (1999). Hes1 and Hes5 as Notch effectors in mammalian neuronal differentiation. *EMBO J.* 18, 2196–2207. doi: 10.1093/emboj/18.8.2196

Osumi, N., Shinohara, H., Numayama-Tsuruta, K., and Maekawa, M. (2008). Concise Review: Pax6 Transcription Factor Contributes to both Embryonic and Adult Neurogenesis as a Multifunctional Regulator. *Stem Cells* 26, 1663–1672. doi: 10.1634/stemcells.2007-0884

Ozen, I., Galichet, C., Watts, C., Parras, C., Guillemot, F., and Raineteau, O. (2007). Proliferating neuronal progenitors in the postnatal hippocampus transiently express the proneural gene Ngn2. *Eur. J. Neurosci.* 25, 2591–2603. doi: 10.1111/j.1460-9568.2007.05541.x

Paik, J., Ding, Z., Narurkar, R., Ramkissoon, S., Muller, F., Kamoun, W. S., et al. (2009). FoxOs Cooperatively Regulate Diverse Pathways Governing Neural Stem Cell Homeostasis. *Cell Stem Cell* 5, 540–553. doi: 10.1016/j.stem.2009.09.013

Parras, C. M., Schuurmans, C., Scardigli, R., Kim, J., Anderson, D. J., and Guillemot, F. (2002). Divergent functions of the proneural genes Mash1 and Ngn2 in the specification of neuronal subtype identity. *Genes Dev.* 16, 324–338. doi: 10.1101/gad.940902

Pearson, C. A., Moore, D. M., Tucker, H. O., Dekker, J. D., Hu, H., Miquelajáuregui, A., et al. (2020). Foxp1 Regulates Neural Stem Cell Self-Renewal and Bias Toward Deep Layer Cortical Fates. *Cell Rep.* 30, 1964–1981.e3. doi: 10.1016/j.celrep.2020.01.034

Pevny, L. H., and Nicolis, S. K. (2010). Sox2 roles in neural stem cells. *Int. J. Biochem. Cell Biol.* 42, 421–424. doi: 10.1016/j.biocel.2009.08.018

Pilz, G. A., Bottes, S., Betizeau, M., Jörg, D. J., Carta, S., Simons, B. D., et al. (2018). Live imaging of neurogenesis in the adult mouse hippocampus. *Science* 359, 658–662. doi: 10.1126/science.aao5056

Quinn, J. C., Molinek, M., Martynoga, B. S., Zaki, P. A., Faedo, A., Bulfone, A., et al. (2007). Pax6 controls cerebral cortical cell number by regulating exit from the cell cycle and specifies cortical cell identity by a cell autonomous mechanism. *Dev. Biol.* 302, 50–65. doi: 10.1016/j.ydbio.2006.08.035

Remacle, J. E., Kraft, H., Lerchner, W., Wuytens, G., Collart, C., Verschueren, K., et al. (1999). New mode of DNA binding of multi-zinc finger transcription factors: δEF1 family members bind with two hands to two target sites. *EMBO J.* 18, 5073–5084. doi: 10.1093/emboj/18.18.5073

Renault, V. M., Rafalski, V. A., Morgan, A. A., Salih, D. A. M., Brett, J. O., Webb, A. E., et al. (2009). FoxO3 Regulates Neural Stem Cell Homeostasis. *Cell Stem Cell* 5, 527–539. doi: 10.1016/j.stem.2009.09.014

Ro, S.-H., Liu, D., Yeo, H., and Paik, J. (2013). FoxOs in neural stem cell fate decision. *Arch. Biochem. Biophys.* 534, 55–63. doi: 10.1016/j.abb.2012.07.017

Rousso, D. L., Pearson, C. A., Gaber, Z. B., Miquelajauregui, A., Li, S., Portera-Cailliau, C., et al. (2012). Foxp-mediated suppression of N-cadherin regulates neuroepithelial character and progenitor maintenance in the CNS. *Neuron* 74, 314–330. doi: 10.1016/j.neuron.2012.02.024

Roybon, L., Hjalt, T., Stott, S., Guillemot, F., Li, J.-Y., and Brundin, P. (2009). Neurogenin2 Directs Granule Neuroblast Production and Amplification while NeuroD1 Specifies Neuronal Fate during Hippocampal Neurogenesis. *PLoS One* 4:e4779. doi: 10.1371/journal.pone.0004779

Sansom, S. N., Griffiths, D. S., Faedo, A., Kleinjan, D.-J., Ruan, Y., Smith, J., et al. (2009). The Level of the Transcription Factor Pax6 Is Essential for Controlling the Balance between Neural Stem Cell Self-Renewal and Neurogenesis. *PLoS Genet.* 5:e1000511. doi: 10.1371/journal.pgen.1000511

Sarkar, A., and Hochedlinger, K. (2013). The Sox Family of Transcription Factors: Versatile Regulators of Stem and Progenitor Cell Fate. *Cell Stem Cell* 12, 15–30. doi: 10.1016/j.stem.2012.12.007

Sasai, Y., Kageyama, R., Tagawa, Y., Shigemoto, R., and Nakanishi, S. (1992). Two mammalian helix-loop-helix factors structurally related to Drosophila hairy and Enhancer of split. *Genes Dev.* 6, 2620–2634. doi: 10.1101/gad.6.12b.2620

Schäffner, I., Minakaki, G., Khan, M. A., Balta, E.-A., Schlötzer-Schrehardt, U., Schwarz, T. J., et al. (2018). FoxO Function Is Essential for Maintenance of Autophagic Flux and Neuronal Morphogenesis in Adult Neurogenesis. *Neuron* 99, 1188–1203.e6. doi: 10.1016/j.neuron.2018.08.017

Schäffner, I., Wittmann, M.-T., Vogel, T., and Lie, D. C. (2023). Differential vulnerability of adult neurogenic niches to dosage of the neurodevelopmental-disorder linked gene Foxg1. *Mol. Psychiatry* 28, 497–514. doi: 10.1038/s41380-022-01497-8

Schüller, U., Zhao, Q., Godinho, S. A., Heine, V. M., Medema, R. H., Pellman, D., et al. (2007). Forkhead Transcription Factor FoxM1 Regulates Mitotic Entry and Prevents Spindle Defects in Cerebellar Granule Neuron Precursors. *Mol. Cell. Biol.* 27, 8259–8270. doi: 10.1128/MCB.00707-07

Sekido, R., Murai, K., Kamachi, Y., and Kondoh, H. (1997). Two mechanisms in the action of repressor δEF1: binding site competition with an activator and active repression. *Genes Cells* 2, 771–783. doi: 10.1046/j.1365-2443.1997.1570355.x

Sekido, R., Takagi, T., Okanami, M., Moribe, H., Yamamura, M., Higashi, Y., et al. (1996). Organization of the gene encoding transcriptional repressor δEF1 and cross-species conservation of its domains. *Gene* 173, 227–232. doi: 10.1016/0378-1119(96)00185-0

Seoane, J., Le, H.-V., Shen, L., Anderson, S. A., and Massagué, J. (2004). Integration of Smad and Forkhead Pathways in the Control of Neuroepithelial and Glioblastoma Cell Proliferation. *Cells* 117, 211–223. doi: 10.1016/S0092-8674(04)00298-3

Sharov, A. A., Sharova, T. Y., Mardaryev, A. N., Vignano, A. T., Atoyan, R., Weiner, L., et al. (2006). Bone morphogenetic protein signaling regulates the size of hair follicles and modulates the expression of cell cycle-associated genes. *Proc Natl Acad Sci* 103, 18166–18171. doi: 10.1073/pnas.0608899103

Shen, L., Nam, H., Song, P., Moore, H., and Anderson, S. A. (2006). FoxG1 haploinsufficiency results in impaired neurogenesis in the postnatal hippocampus and contextual memory deficits. *Hippocampus* 16, 875–890. doi: 10.1002/hipo.20218

Shimojo, H., Ohtsuka, T., and Kageyama, R. (2008). Oscillations in notch signaling regulate maintenance of neural progenitors. *Neuron* 58, 52–64. doi: 10.1016/j.neuron.2008.02.014

Shimojo, H., Ohtsuka, T., and Kageyama, R. (2011). Dynamic Expression of Notch Signaling Genes in Neural Stem/Progenitor Cells. *Front. Neurosci.* 5:78. doi: 10.3389/fnins.2011.00078

Siegenthaler, J. A., Tremper-Wells, B. A., and Miller, M. W. (2008). Foxg1 Haploinsufficiency Reduces the Population of Cortical Intermediate Progenitor Cells: Effect of Increased p21 Expression. *Cereb. Cortex* 18, 1865–1875. doi: 10.1093/cercor/bhm209

Sueda, R., Imayoshi, I., Harima, Y., and Kageyama, R. (2019). High Hes1 expression and resultant Ascl1 suppression regulate quiescent vs. active neural stem cells in the adult mouse brain. *Genes Dev.* 33, 511–523. doi: 10.1101/gad.323196.118

Takebayashi, K., Sasai, Y., Sakai, Y., Watanabe, T., Nakanishi, S., and Kageyama, R. (1994). Structure, chromosomal locus, and promoter analysis of the gene encoding the mouse helix-loop-helix factor HES-1. Negative autoregulation through the multiple N box elements. *J. Biol. Chem.* 269, 5150–5156. doi: 10.1016/S0021-9258(17)37668-8

Tian, C., Gong, Y., Yang, Y., Shen, W., Wang, K., Liu, J., et al. (2012). Foxg1 has an essential role in postnatal development of the dentate gyrus. *J Neurosci Official J Soc Neurosci* 32, 2931–2949. doi: 10.1523/JNEUROSCI.5240-11.2012

Toresson, H., Potter, S. S., and Campbell, K. (2000). Genetic control of dorsal-ventral identity in the telencephalon: opposing roles for Pax6 and Gsh2. *Development* 127, 4361–4371. doi: 10.1242/dev.127.20.4361

Tsui, D., Vessey, J. P., Tomita, H., Kaplan, D. R., and Miller, F. D. (2013). FoxP2 Regulates Neurogenesis during Embryonic Cortical Development. *J. Neurosci.* 33, 244–258. doi: 10.1523/JNEUROSCI.1665-12.2013

Urbán, N., Berg, D. L. C., Forget, A., Andersen, J., Demmers, J. A. A., Hunt, C., et al. (2016). Return to quiescence of mouse neural stem cells by degradation of a proactivation protein. *Science* 353, 292–295. doi: 10.1126/science.aaf4802

Vandewalle, C., Roy, F. V., and Berx, G. (2009). The role of the ZEB family of transcription factors in development and disease. *Cell. Mol. Life Sci.* 66, 773–787. doi: 10.1007/s00018-008-8465-8

Vasconcelos, F. F., and Castro, D. S. (2014). Transcriptional control of vertebrate neurogenesis by the proneural factor Ascl1. *Front. Cell. Neurosci.* 8:412. doi: 10.3389/fncel.2014.00412

Vezzali, R., Weise, S. C., Hellbach, N., Machado, V., Heidrich, S., and Vogel, T. (2016). The FOXG1/FOXO/SMAD network balances proliferation and differentiation of cortical progenitors and activates Kcnh3 expression in mature neurons. *Oncotarget* 7, 37436–37455. doi: 10.18632/oncotarget.9545

Wang, Z., Park, H. J., Carr, J. R., Chen, Y., Zheng, Y., Li, J., et al. (2011). FoxM1 in Tumorigenicity of the Neuroblastoma Cells and Renewal of the Neural Progenitors. *Cancer Res.* 71, 4292–4302. doi: 10.1158/0008-5472.CAN-10-4087

Wang, H., Xiao, Z., Zheng, J., Wu, J., Hu, X.-L., Yang, X., et al. (2019). ZEB1 Represses Neural Differentiation and Cooperates with CTBP2 to Dynamically Regulate Cell Migration during Neocortex Development. *Cell Rep.* 27, 2335–2353.e6. doi: 10.1016/j.celrep.2019.04.081

Wang, J., Zhai, H.-R., Ma, S.-F., Shi, H.-Z., Zhang, W.-J., Yun, Q., et al. (2022). FOXG1 Contributes Adult Hippocampal Neurogenesis in Mice. *Int. J. Mol. Sci.* 23:14979. doi: 10.3390/ijms232314979

Webb, A. E., Pollina, E. A., Vierbuchen, T., Urbán, N., Ucar, D., Leeman, D. S., et al. (2013). FOXO3 Shares Common Targets with ASCL1 Genome-wide and Inhibits ASCL1-Dependent Neurogenesis. *Cell Rep.* 4, 477–491. doi: 10.1016/j.celrep.2013.06.035

Wegner, M. (2010). All purpose Sox: The many roles of Sox proteins in gene expression. *Int. J. Biochem. Cell Biol.* 42, 381–390. doi: 10.1016/j.biocel.2009.07.006

Wegner, M., and Stolt, C. C. (2005). From stem cells to neurons and glia: a Soxist's view of neural development. *Trends Neurosci.* 28, 583–588. doi: 10.1016/j.tins.2005.08.008

Wu, X., Gu, X., Han, X., Du, A., Jiang, Y., Zhang, X., et al. (2014). A Novel Function for Foxm1 in Interkinetic Nuclear Migration in the Developing Telencephalon and Anxiety-Related Behavior. *J. Neurosci.* 34, 1510–1522. doi: 10.1523/JNEUROSCI.2549-13.2014

Xu, C., Fan, W., Zhang, Y., Loh, H. H., and Law, P. (2021). Kappa opioid receptor controls neural stem cell differentiation via a miR-7a/Pax6 dependent pathway. *Stem Cells* 39, 600–616. doi: 10.1002/stem.3334

Xuan, S., Baptista, C. A., Balas, G., Tao, W., Soares, V. C., and Lai, E. (1995). Winged helix transcription factor BF-1 is essential for the development of the cerebral hemispheres. *Neuron* 14, 1141–1152. doi: 10.1016/0896-6273(95)90262-7

Yao, J., Lai, E., and Stifani, S. (2001). The Winged-Helix Protein Brain Factor 1 Interacts with Groucho and Hes Proteins To Repress Transcription. *Mol. Cell. Biol.* 21, 1962–1972. doi: 10.1128/MCB.21.6.1962-1972.2001

Yen, G., Croci, A., Dowling, A., Zhang, S., Zoeller, R. T., and Darling, D. S. (2001). Developmental and functional evidence of a role for Zfhep in neural cell development. *Mol. Brain Res.* 96, 59–67. doi: 10.1016/S0169-328X(01)00267-4

Yun, K., Potter, S., and Rubenstein, J. L. (2001). Gsh2 and Pax6 play complementary roles in dorsoventral patterning of the mammalian telencephalon. *Development* 128, 193–205. doi: 10.1242/dev.128.2.193

Zhang, Z., Gao, F., Kang, X., Li, J., Zhang, L., Dong, W., et al. (2015). Exploring the potential relationship between Notch pathway genes expression and their promoter methylation in mice hippocampal neurogenesis. *Brain Res. Bull.* 113, 8–16. doi: 10.1016/j.brainresbull.2015.02.003

frontiers | Frontiers in Neuroscience

TYPE Original Research
PUBLISHED 03 August 2023
DOI 10.3389/fnins.2023.1224941

OPEN ACCESS

EDITED BY
Ashok K. Shetty,
Texas A&M University School of Medicine, United States

REVIEWED BY
Gamze Yalcinkaya Colak,
Bozok University, Türkiye
Michael John Hylin,
Southern Illinois University Carbondale, United States
Pablo Chamero,
INRA Centre Val de Loire, France

*CORRESPONDENCE
Nathalie Mandairon
✉ nathalie.mandairon@cnrs.fr

†These authors have contributed equally to this work

RECEIVED 18 May 2023
ACCEPTED 17 July 2023
PUBLISHED 03 August 2023

CITATION
Athanassi A, Breton M, Chalençon L, Brunelin J, Didier A, Bath K and Mandairon N (2023) Chronic unpredictable mild stress alters odor hedonics and adult olfactory neurogenesis in mice.
Front. Neurosci. 17:1224941.
doi: 10.3389/fnins.2023.1224941

Chronic unpredictable mild stress alters odor hedonics and adult olfactory neurogenesis in mice

Anna Athanassi[1†], Marine Breton[1†], Laura Chalençon[1], Jérome Brunelin[2,3], Anne Didier[1], Kevin Bath[4,5†] and Nathalie Mandairon[1*†]

[1]INSERM, U1028, CNRS UMR5292, Neuropop Team, Lyon Neuroscience Research Center, Université Claude Bernard Lyon 1, Université Jean Monnet, Bron, France, [2]Centre Hospitalier Le Vinatier, Bron, France, [3]INSERM, U1028, CNRS UMR5292, PSYR2 Team, Lyon Neuroscience Research Center, Université Claude Bernard Lyon 1, Université Jean Monnet, Bron, France, [4]Division of Developmental Neuroscience, New York State Psychiatric Institute, Research Foundation for Mental Hygiene, New York, NY, United States, [5]Department of Psychiatry, Columbia University Medical College, New York, NY, United States

Experiencing chronic stress significantly increases the risk for depression. Depression is a complex disorder with varied symptoms across patients. However, feeling of sadness and decreased motivation, and diminished feeling of pleasure (anhedonia) appear to be core to most depressive pathology. Odorants are potent signals that serve a critical role in social interactions, avoiding danger, and consummatory behaviors. Diminished quality of olfactory function is associated with negative effects on quality of life leading to and aggravating the symptoms of depression. Odor hedonic value (I like or I dislike this smell) is a dominant feature of olfaction and guides approach or avoidance behavior of the odor source. The neural representation of the hedonic value of odorants is carried by the granule cells in the olfactory bulb, which functions to modulate the cortical relay of olfactory information. The granule cells of the olfactory bulb and those of the dentate gyrus are the two major populations of cells in the adult brain with continued neurogenesis into adulthood. In hippocampus, decreased neurogenesis has been linked to development or maintenance of depression symptoms. Here, we hypothesize that chronic mild stress can alter olfactory hedonics through effects on the olfactory bulb neurogenesis, contributing to the broader anhedonia phenotype in stress-associated depression. To test this, mice were subjected to chronic unpredictable mild stress and then tested on measures of depressive-like behaviors, odor hedonics, and measures of olfactory neurogenesis. Chronic unpredictable mild stress led to a selective effect on odor hedonics, diminishing attraction to pleasant but not unpleasant odorants, an effect that was accompanied by a specific decrease in adult neurogenesis and of the percentage of adult-born cells responding to pleasant odorants in the olfactory bulb.

KEYWORDS

olfactory bulb, odor hedonics, adult neurogenesis, chronic mild stress, emotional alteration

Introduction

Depressive symptoms can be complex and vary widely between individuals as well as within individuals with recurrent episodes. In major depressive disorder (MDD), core symptoms include anhedonia and diminished motivation. In humans, depression is often also associated with disturbance in olfactory sensory function (Negoias et al., 2016; Croy and Hummel, 2017; Pabel et al., 2018; Athanassi et al., 2021). Like depression, olfactory sensory function is complex (including features such as familiarity, intensity, and identity) with the hedonic perception of odor dominating. Hedonic value is generally the first criterion used by humans to describe and categorized odorants (Schiffman, 1974; Richardson and Zucco, 1989; Yeshurun and Sobel, 2010) and represents a valuable source of information for decision-making and guiding goal-oriented motivated behaviors. Across species (including humans), the hedonic value of odorants is a critical driving force for food intake or social interactions supporting survival and regulation of the emotional state. Interestingly, odor hedonic value (pleasantness) is the dimension of olfactory perception most strongly affected in depression (Naudin et al., 2012). Consequently, altered odor hedonics can cause disturbances in food intake or mood which worsen depressive symptoms and contribute significantly to negative outcomes across a range of diseases with comorbid depression. The critical neural substrate influencing odor hedonics appears to be the granule cell layer of the olfactory bulb (OB), a modulator of the first cortical relay of olfactory information (Kermen et al., 2016). Optogenetic inhibition of granule cell activity modulates approach behavior to odorants in rodents, which is used to evaluate whether an odorant is pleasant or unpleasant in an animal model (Kermen et al., 2016; Midroit et al., 2021). The granule cells, significantly influence processing of hedonic information and interestingly are the largest population of cells with ongoing adult neurogenesis (Lledo and Valley, 2016). Stem cells located in the subventricular zone of the lateral ventricles give rise to neuroblasts that migrate along the rostral migratory stream to reach the OB and functionally integrate the pre-existing network (Alvarez-Buylla and Garíca-Verdugo, 2002; Carlén et al., 2002; Belluzzi et al., 2003; Carleton et al., 2003; Magavi et al., 2005). These new neurons are key elements of odor processing by shaping the activity of the relay cells (Schoppa and Urban, 2003; Lledo et al., 2005; Lledo and Saghatelyan, 2005). The other major brain structure with high rates of adult neurogenesis, is the hippocampus (Lledo et al., 2006; Kempermann, 2015). Prior work has implicated alterations in hippocampal neurogenesis on both the development and response to treatment for depression (Santarelli et al., 2003; Planchez et al., 2019). Like the hippocampus, the OB serves a significant role in cognitive processes, memory formation and retrieval, and emotional regulation (Bagur et al., 2021; Mofleh and Kocsis, 2021; Salimi et al., 2022).

Despite prior work implicating disturbance in neurogenesis in hippocampus with depression few studies have investigated the relationship between depressive-like behaviors and OB neurogenesis and olfactory processing (Lledo and Valley, 2016; Siopi et al., 2016). Chronic stress is known to increase the risk for depression, alter morphology and functioning of the hippocampus including alteration of adult neurogenesis (McEwen and Magarinos, 1997). Prior work has established that chronic unpredictable mild stress (CUMS) can reliably induce behavioral profiles in mice that resemble depressive symptoms in humans (Pothion et al., 2004; Nollet et al., 2012; van Boxelaere et al., 2017).

Here, the aim of this work was to test the impact of CUMS on olfactory hedonics in mice, its effects on adult OB neurogenesis, and the activity of adult-born neurons during hedonic valuation. In CUMS exposed and control mice, behavioral measures of both depressive-like and anxiety-like behaviors (Willner et al., 1987; Papp and Moryl, 1994; Willner, 2017) were assessed. In conjunction, the hedonic processing of olfactory signals was tested in an olfactory preference test (Kermen et al., 2016; Midroit et al., 2021). Finally, measures of adult-born neuron number and activity were measured in the OB of mice following hedonic preference testing. The CUMS protocol led to higher levels of anhedonia and increased anxiety-like behaviors compared with control mice. Importantly, the CUMS paradigm induced olfactory hedonic alteration, significantly diminishing interest in pleasant but not unpleasant odorants. At the cellular level, CUMS decreased the density of adult-born neurons in the OB as well as the percentage of adult-born neurons responding to pleasant but not unpleasant odorants.

Materials and methods

Animals

Twenty adult male C57Bl6/J mice (8 weeks, Charles River Laboratories, L'Arbresle, France) were used in this study. Mice were randomly assigned to one of two groups, one control group ($n = 10$; housed in groups of five in standard laboratory cages) and one stressed group ($n = 10$; placed in individual standard laboratory cages). All experiments were done in accordance with the European Community Council Directive of 22nd September 2010 (2010/63/UE) and the National Ethics Committee (Agreement APAFIS#20702_2019072614086203_v2). Mice were kept on a 12 h light/dark cycle at a constant temperature of 22°C with food and water *ad libitum* except during the stress protocol (Table 1). All efforts were made to minimize animal suffering.

TABLE 1 CUMS protocol stressors (see Supplementary Table 1 for examples of daily sequences of events).

Stimuli	Duration
Sawdust bedding removed	About 6 h
Mouse cage change	Permanent
Cage titling at 45°	About 1 h
Wet sawdust (200 mL of water for 100 g sawdust)	3 to 12 h
Nycthemeral rhythm perturbation	About 3 h through the night
Food and water deprivation	About 12 h
Mice pair housed (with or without dry or wet sawdust)	About 3 h or through the night
Mice hung by their tail	About 1 min
Change sawdust	Twice (each hour)

Chronic unpredictable mild stress

The CUMS protocol was performed every day over 7 weeks in which mice were subjected to mild stressors several times per day (Table 1). Some stressors were combined such as: cage tilting and wet sawdust, mice were housed 2 per cage for food and water deprivation, mice were placed 2 per cage for cage tilting, etc. Details of the procedure are described in Supplementary Table 1. All stress manipulations were performed in a room different from the housing room. When no overnight stress was planned, mice were returned to and remained in the housing room.

Behavioral testing

Sucrose Preference Test. Animals were placed in a cage with free access to two pipettes connected to two bottles of water: one contained only water and the other one contained 1% sucrose dissolved in water. The test was conducted during 3 days (d1 to d3). The sucrose solution was freshly prepared each day. To avoid neophobia, sucrose at 1% was presented to all animals for a period of 24 h, a week before the test. During the test, the pipettes and bottles containing sucrose were reversed every 12 h to avoid potential side biases. Sucrose preference was calculated as follow: Sucrose Consumption (mg)/Total Consumption (mg). Preference of CUMS mice was expressed as a percentage of that of control mice.

Light/Dark Box test. This apparatus is composed of two compartments: one (2/3 of the box) is directly highly illuminated (820 lm) and the other on (1/3 of the box) is dark. The animal can move freely from one compartment to another. For testing, a single mouse was placed in the left corner of the highly illuminated compartment of the box and the trajectory of the mouse was video recorded and analyzed using A2V Volcano®. The time spent in the illuminated side was used as a measure of anxiety-like behavior with avoidance of the brightly lit area being considered a measure of heightened anxiety-like behavior. The test lasted 5 min and the box was cleaned after each trial.

OpenField test. Animals were placed in an OpenField maze composed of a wall-enclosed area to prevent the mouse from escaping. For testing, a single mouse was placed at the top left corner, several motor and behavioral activities were video recorded for 5 min, including: time spent in the inner zone, number of entries into the inner zone, duration of grooming, number of fecal boli deposited, latency and number of rearing events (mouse standing on their hind limbs). An increased number of fecal boli, increased rearing, decreased latency of rearing and decreased grooming as well as decreased time spent in the inner zone were used as metrics of increased anxiety-like behavior.

Odor hedonic value assessment. Based on work done in mice (Kermen et al., 2016; Midroit et al., 2021), we selected six odorants for this test: three well documented to have positive hedonic values (Limonene + Lim; 5,989-27-5; 0.2% dilution for 1 Pa vapor), Citronellol (Citro; 106-22-9; 17.8% dilution for 1 Pa vapor) and Camphor (Cam; 76-22-2; 0.46% dilution for 1 Pa vapor) and three with well-documented negative hedonic values (Guaiacol (Gua; 90-05-1; 2.08% dilution for 1 Pa vapor), P-cresol (Cre; 6,032-29-7; 1.8% dilution for 1 Pa vapor), and Pyridine (Pyr; 110-86-1; 2% dilution for 1 Pa vapor)). Hedonic preference was defined as approach and avoidance behavior and was validated in reference to investigation times for biologically relevant odors with known aversive or appetitive properties (Kermen et al., 2016). All odorants were diluted on the day of the test in order to have similar vapor pressures (1 Pa; similar perceived intensity) (Mandairon et al., 2006; Moreno et al., 2009).

The test was performed on the one hole-board apparatus as follows: 60 µL of pure odorant was put on cotton batting and placed at the bottom of a pot covered with bedding. The pot was put in the central hole of the board. Mice were placed at the bottom right corner of the board and allowed to freely explore for 2 min. After the 2 min test, the mouse and the pot were removed, and the board was cleaned. The order of odor presentation was randomized. The total time spent exploring the hole (as measured by a photobeam break at the hole entrance) was recorded for each mouse.

Neurogenesis assessment

Sacrifice. To identify populations of cells that were activated in response to a given odorant, mice were odor stimulated for 1 hour with either an unpleasant odorant (Guaiacol; 100 µL of odorant at 1 Pa) or a pleasant odorant (+Limonene; 100 µL of odorant at 1 Pa). Odorants were presented in a tea ball. One hour after the end of odor stimulation, mice were sacrificed by Urethane injection (2 g/kg) followed by intracardiac perfusion of 50 mL of cold fixative (paraformaldehyde 4% in PBS, pH 7.4). Brains were dissected, sunk in sucrose and sectioned (14 µm thick).

BrdU injections. Adult-born cells of the OB require several days to migrate from the subventricular zone to the OB, where they differentiate into mature granule and periglomerular cells. To determine the impact of CUMS on integration and differentiation of adult-born cells in the OB, mice were injected with bromodeoxyuridine (BrdU; Sigma; 50 mg/kg in saline three times daily at 2 h intervals, i.p.) 20 d after the beginning of stress procedure. The CUMS procedure continued for several weeks following BrdU injection, with animals being sacrificed at the completion of behavioral testing (38 d after the BrdU injections). This time course of BrdU administration allowed for assessment of CUMS effects on the birth, differentiation, and survival of adult-born cells in the OB during the CUMS procedure.

BrdU immunocytochemistry. The protocol has been described in detail previously (Forest et al., 2019). Sections were incubated overnight in a mouse anti-BrdU antibody (1:100, Millipore Bioscience Research Reagents) at 4°C followed by a biotinylated anti-mouse secondary antibody (1:200, Vector Laboratories) for 2 h. The sections were then processed through an avidin-biotin-peroxidase complex (ABC Elite Kit, Vector Laboratories). Following dehydration in graded ethanols, the sections were defatted in xylene and coverslipped in DPX (Fluka, Sigma).

Double labelling BrdU/cFos immunocytochemistry. To investigate the density of BrdU-positive cells responding to pleasant and unpleasant odorants, double labelling was performed using mouse anti BrdU (1/100, Merck) and monoclonal rat anti c-Fos (1/2000, Synaptic System) respectively. Appropriate secondary antibodies were used (goat anti-mouse Alexa 546 (1/200, Molecular probes); goat anti-rat Alexa 488 (1/200, Molecular probes) to label cBrdU+/-Fos + cells.

Data analysis (BrdU and c-Fos levels)

Every fifth coronal section of the olfactory bulb was processed for immunostaining (sampling interval = 70 µm; 3–5 sections per animal

were analyzed). Within each analyzed section, every BrdU-positive cell was counted in the granule layer of the right OB using mapping software (Mercator, Explora Nova, La Rochelle, France) coupled to a Zeiss microscope. The mean positive cell density was calculated and averaged within each experimental group.

Fluorescent counting was done using AxioVision (Zeiss) software coupled to a pseudo-confocal Zeiss microscope. We calculated the percentage of BrdU+ cells expressing c-Fos per mouse and averaged the values per group (23 ± 5 cells per animal were assessed). As an additional control, we also counted the density of c-Fos+/BrdU$^-$ in the OB (3 sections were analyzed and averaged per animal). All counting was done blind with regards to the identity and treatment group of the animal.

Statistics

All analyses were performed using Rstudio. For behavioral experiments were used, preliminary tests including Kolmogorov–Smirnov and Levene tests for normality for all data. This resulted in the use of parametric tests: repeated measures analysis of variance (ANOVA) (day as factor) followed by Bonferroni-corrected *post-hoc* *t*-tests for the sucrose consumption test and two-ways ANOVA (group and hedonic as factors) followed by Bonferroni-corrected *post hoc* *t*-tests for the olfactory preference test and cellular analysis. For other behavioral tests and analysis of cellular densities, the 2 experimental groups were compared using two sample *t*-tests. Unilateral *t*-tests were used when prior evidence of effects of the CUMS model on depressive-like behavior and anxiety in rodents were reported (Antoniuk et al., 2019; Markov, 2022). The validity of the *t*-test positive results was confirmed using permutation tests. No statistical methods were used to predetermine sample sizes, but our sample sizes were similar to those reported in previous publications (Forest et al., 2019). Data collection and animal assignation to the various experimental groups were randomized and data collected blind to condition.

Results

Chronic unpredictable mild stress induced emotional changes in adult mice

To confirm the effectiveness of the CUMS protocol to alter expression of anxiety and depressive-like behaviors, sucrose preference was assessed in mice over 3 days (Goodwill et al., 2019). The repeated measures ANOVA revealed a day effect on sucrose consumption in CUMS compared to control group ($F(2,18) = 3.82$, $p = 0.04$). More precisely, CUMS mice showed a significant reduction of sucrose consumption at D2 and D3 compared to controls (unilateral one sample *t*-test D1 $p = 0.6$; D2 $p = 0.006$; D3 $p = 0.03$; Figure 1A).

To assess the impact of CUMS on the level of anxiety-like behaviors, mice were tested on two standard behavioral assays, the Light/Dark Box and the OpenField. The Light/Dark Box test relies on the relative time spent exploring each of the two compartments (one illuminated and the other dark). A decrease in time spent in the illuminated compartment is used as a measure of increased of anxiety-like behavior. Results showed that the CUMS group spent less time in the illuminated compartment compared to the control group (unpaired unilateral *t*-test, $p = 0.02$; permutation test, $p = 0.03$, 100,000 permutations; Figure 1B), suggesting a higher level of anxiety in CUMS mice. Similarly, the middle of the OpenField, is generally considered more anxiogenic. Thus, the amount of time that the animal spent in the inner zone (center) of the setup, and the number of entries into center was used as an index of anxiety-like behavior. Here, no significant differences were found between CUMS and control mice (unpaired *t*-test, $p = 0.96$ and $p = 0.93$ respectively; Figures 1Ci,ii). As additional measures, CUMS mice spent a similar amount of time to control animals grooming (unpaired *t*-test, $p = 0.25$; Figure 1Ciii). We observed an increase in time spent rearing (unpaired *t*-test, $p = 0.005$; permutation test, $p < 0.0001$, 100,000 permutations; Figure 1Civ) and a decrease of latency to rear (unpaired *t*-test, $p = 0.0003$; permutation test, $p = 0.001$, 100,000 permutations; Figure 1Cv) in CUMS compared to control mice. To ensure that these effects were not due to changes in locomotor activity, we assessed the total distance travelled by animals in the OpenField for the two groups and found no difference between control and CUMS groups (unpaired *t*-test, $p = 0.44$; Figure 1Cvi). Taken together, these results suggest that CUMS influences multiple aspects of anxiety and depressive-like behavior.

Chronic unpredictable mild stress induced alterations in odor hedonics

Odor hedonics were automatically assessed using an odor preference test (Mandairon and Linster, 2009), and the time the mouse investigated the odorants was used as an index of odor hedonics (Kermen et al., 2016; Midroit et al., 2021; Figure 2 and Supplementary Figure 1) As expected, investigation time of pleasant odorants was higher compared to unpleasant ones in control mice (2-ways-ANOVA, odor effect: $F(1.36) = 5.039$, $p = 0.03$; Bonferroni *post-hoc* test, $p = 0.02$; Figure 2). Interestingly, we observed a significant effect of experimental group (CUMS versus control: 2-ways-ANOVA; $F(1.36) = 8.035$, $p = 0.007$) and an interaction ($F(1.36) = 4.2$, $p = 0.04$) indicating that the effect of the experimental group depends on the odor hedonic value. In particular, the investigation time of the pleasant odorants was lower in the CUMS group compared to the control one (Bonferroni *post hoc* test, $p = 0.007$; Figure 2) while the investigation time of the unpleasant odorants remained unchanged (Bonferroni *post hoc* test $p = 0.9$; Figure 2).

Chronic unpredictable mild stress altered adult neurogenesis and reduced the density of adult-born cells responding to pleasant odorants in the OB

We then tested whether the altered odor hedonic perception after CUMS protocol was associated with changes in olfactory neurogenesis. To do this, we labelled a cohort of adult-born cells integrating in the OB during CUMS protocol by injecting BrdU 20 days after the beginning of the CUMS procedure. This delay allows neuroblasts to migrate from the subventricular zone to the OB and integrate into the pre-existing neural network. We assessed adult-born cell density in the granule cell layer. We found a lower density of BrdU-positive cell in the OB in CUMS compared to control group (unpaired bilateral *t*-test, $p = 0.006$; permutation test, $p = 0.0043$, 924 permutations; Figure 3A).

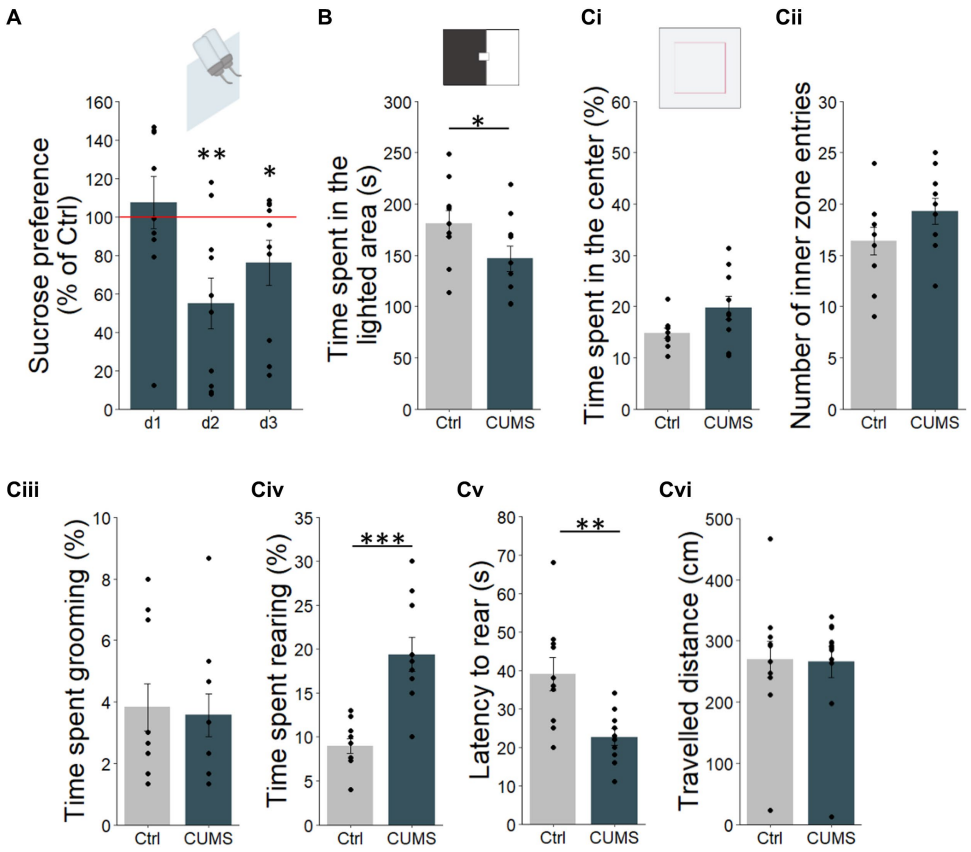

FIGURE 1
CUMS protocol impacted the mouse emotional behavior. **(A)** The percentage of sucrose consumption was lower at d2 and d3 in CUMS compared to control (Ctrl) mice. **(B)** The CUMS mice showed a significant decrease of time spent in the illuminated compartment compared to the control group in the Light/Dark Box test. **(Ci)** No difference was found between groups in terms of time spent. **(Cii)** nor number of entries in the center of the OpenField apparatus. **(Ciii)** The CUMS mice showed similar levels of grooming to controls, **(Civ)** however they displayed more rearing, **(Cv)** and reared sooner than control mice. **(Cvi)** Locomotion of mice was not altered by CUMS. Points represent individual data means ± s.e.m. Statistical significance depicted as ***$p < 0.001$, **$p < 0.01$, and *$p < 0.05$. $n = 10$/group.

We then assessed the effect of CUMS on the activity of adult-born neurons responding to pleasant versus unpleasant odorants by analyzing c-Fos expression in BrdU labeled cells 1 h following stimulation with either a hedonically pleasant or unpleasant odorant. Using 2-way-ANOVA, we found an effect of experimental group ($F(1.36) = 19.837$, $p = 0.0007$), of odor hedonics ($F(1.36) = 5.039$, $p = 0.03$) and an interaction ($F(1.36) = 6.634$, $p = 0.02$) indicating that the effect of the experimental group depended on the odor hedonics. Specifically, we found that while the percentage of double labelled BrdU/c-Fos cells is not different between the two experimental groups in response to unpleasant odorant (Bonferoni post-hoc test, $p = 0.3$; Figure 3B), a lower percentage of double labelled cells was found in response to pleasant odorant in CUMS compared to control group (Bonferoni post-hoc test, $p = 0.0002$; Figure 3B). This was not due to an overall decrease in neuronal activity in the OB of CUMS animals. Indeed, when assessing the density of c-Fos+/BrdU-labeled cells), a 2-way-ANOVA revealed no effect of experimental group ($F(1.13) = 0.45$, $p = 0.51$), nor of the hedonic value of odorants ($F(1.13) = 0.972$, $p = 0.7$) (Figure 3C). Thus, the decrease in BrdU/c-Fos double labelling reflects less involvement of adult-born neurons in processing pleasant odorants in CUMS group, and not an overall decrease in sensitivity of CUMS animals to pleasant odorants.

Discussion

In the current experiments, the CUMS paradigm evoked patterns of behavior consistent with increased anxiety and depressive-like behavior and also altered olfactory hedonics. Specifically, our findings confirmed that CUMS induced depressive-like state, with evidence of anhedonia in the sucrose preference test. We also observed an increased anxiety-like behavior in the Light/Dark Box test and the assessment of rearing behavior in the open field. Importantly, we made the novel observation that that CUMS altered odorant hedonics by specifically lowering interest for pleasant odorants. To date, the focus of studies assessing the effect of stress and depression on olfactory perception focus on threshold or intensity (Schablitzky and Pause, 2014). Here, in order to focus on odor hedonics, we chose the strategy of using largely supraliminal concentration of odorants so that the mice, even if they had an altered threshold for odor detection, could still detect the odorant. This is confirmed by the fact that the level of investigation of unpleasant odorants is the same for control and CUMS mice. In addition, simple discrimination is known to be unaffected by chronic stress (Athanassi et al., 2021). While olfactory hedonics is almost never studied in rodent models of stress, several studies in humans have found that pleasant odorants were perceived

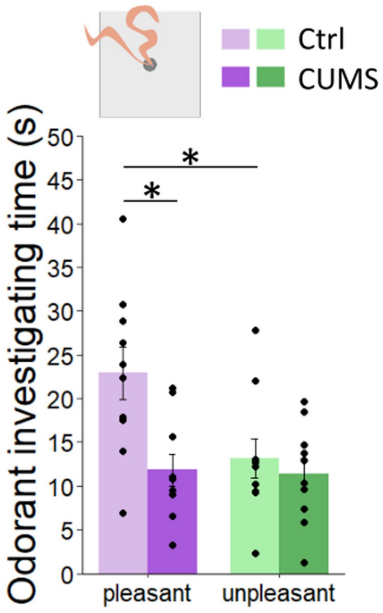

FIGURE 2
CUMS protocol altered the perception of pleasant odorants. (Top) Experimental set up. (Bottom) (Ctrl) mice spent more time investigating pleasant odorants compared to unpleasant ones. Odor investigation time of the unpleasant odorants was similar between control and CUMS mice while it was reduced for the pleasant odorants in CUMS compared to control group. Points represent individual data means ± s.e.m. Statistical significance depicted as *$p < 0.05$. $n = 10$/group.

as less pleasant in patients with depression (anhedonia) and unpleasant ones perceived as more unpleasant (negative alliesthesia) (Atanasova et al., 2010; Naudin et al., 2012; Kazour et al., 2020). In the present study, no difference between control and CUMS groups were found in response to unpleasant odorants suggesting a specific effect of CUMS on the perception of pleasant odorant but a preserved avoidance behavior for unpleasant odorants.

A neural signature of odor hedonics is believed to reside in the granule cell layer of the OB (Kermen et al., 2016). As OB granule cells are born throughout life, we investigated the impact of CUMS on adult neurogenesis. More specifically, we studied the impact of CUMS on the density of adult-born in the OB and their response to odorants to test a possible neural bases for observed effects on olfactory hedonics. First, our results showed that CUMS decreased the density of adult-born neurons in the OB. The lower cell density in the OB could be the result of a reduction of adult-born cell survival in the OB and/or of cell proliferation in the subventricular zone. Here, the time course of labeling was designed to assess aggregate effects on proliferation, integration, and survival of newly born cells, but did not test for selective effects on proliferation. Thus, the contribution of CUMS effects on proliferation versus survival remains open since other studies using various stressors showed different effects on olfactory proliferation (Yang et al., 2011; Belnoue et al., 2013; Siopi et al., 2016; Czarnabay et al., 2019; Wang et al., 2022). The diversity of findings may indicate that the impact of stress on neurogenesis may rely on either discrete (proliferation vs. survival) or synergistic (proliferation and survival) mechanisms in the OB as well as the hippocampus since in the hippocampus, neurogenesis levels and more specifically cell proliferation is altered after stress (corticosterone injections), or CUMS (Guo et al., 2009; Roni and Rahman, 2015; Huang et al., 2019; Li et al., 2021, 2022; Parul et al., 2021). Here, we did not test for changes in hippocampal neurogenesis in our model. While some olfactory associative tasks may involve the hippocampus (Kesner et al., 2011), many of them do not and do not modulate hippocampal neurogenesis (Kaut and Bunsey, 2001; Kaut et al., 2003; Sultan et al., 2010, 2011; Mandairon et al., 2011). Moreover, the olfactory preference task that we use here is a spontaneous olfactory task that do not rely on learning or recall. Thus, even though many studies have found alterations in hippocampal neurogenesis by CUMS, there is no evidence that hippocampal recruitment is involved in olfactory preference testing. Thus it is unlikely that CUMS effects on hippocampal neurogenesis explain olfactory anhedonia.

Interestingly, hippocampal (Huang et al., 2019) and bulbar (Lledo et al., 2006; Hitoshi et al., 2007; Siopi et al., 2016) neurogenesis are restored after anti-depressive treatment. It would be interesting in this context to assess the effect of anti-depressive treatment on olfactory hedonics.

Here, we provided evidence of impaired activity of adult-born granule cells in response to pleasant but not unpleasant odorants after CUMS. Indeed, stressed animals not only displayed lower neurogenesis but also a weaker integration of these cells to the mature network of adult-born granule cells processing pleasant odorants specifically. This suggests that adult born neurons involved in processing pleasant but not unpleasant odorants are not correctly integrated. This suggests a specific sensitivity of OB sub circuits that underlie response to pleasant odorants and could be due to a vulnerability of olfactory sensory neurons recognizing specific molecular features of pleasant odorants and/or a vulnerability of feedback projections to the OB that may modulate survival of newly born cells. This alteration of odor hedonics and bulbar neurogenesis is consistent with recent studies revealing a link between adult-born neuron activity in the hippocampus and hedonic behavior with alleviated depression-like behaviors and an increased resilience against chronic stress when the activity of adult-born neurons is increased (Anacker et al., 2018; Rawat et al., 2022). Finally, granule cells coding for olfactory hedonics regulate mitral cell activity projecting directly to the olfactory tubercle, another key structure of odor hedonics (Midroit et al., 2021). Therefore, any functional alterations of adult-born granule cells in the OB would modulate olfactory processing in the OB and possibly also one of its direct targets, the olfactory tubercle, contributing to odor hedonic impairment.

Olfactory perception and emotional behavior have a bidirectional relationship with olfactory disturbances leading to behavioral profiles indicative of depression-like state in rodents and humans and *vice-versa* (Atanasova et al., 2008; Croy and Hummel, 2017; Taalman et al., 2017; Rochet et al., 2018). Since the OB is tightly linked to the limbic system whose structures are involved in emotional regulation, changes in OB outputs can also modify emotional circuit functioning and behavior (Eiland et al., 2012; Ma et al., 2021). Conversely, alteration of structures of the emotional circuit after stress, like the amygdala, which projects to the OB granule cells (Wen et al., 2019), can lead to change in olfactory processing and perception. Altogether, this may explain why the olfactory perception can be a marker of depression (Croy and Hummel, 2017). Finally, strategies increasing adult hippocampal neurogenesis can alleviate anhedonia (Eliwa et al., 2021), leading to questions about whether a similar mechanism could be employed in the olfactory bulb.

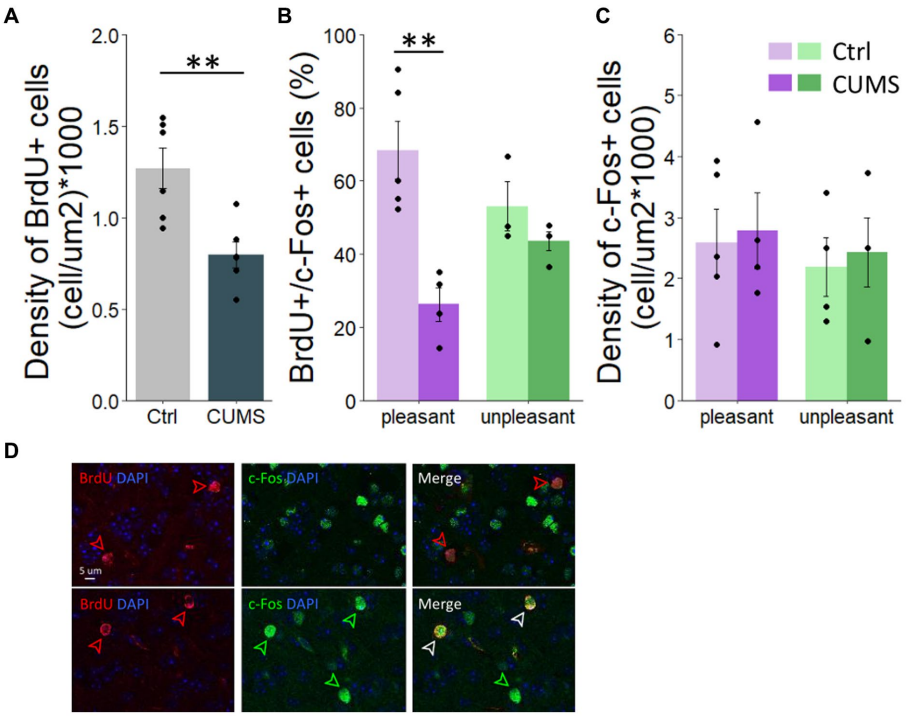

FIGURE 3
CUMS protocol altered adult-born survival and the activity of adult-neurons involved in pleasant odorant processing. **(A)** The density of BrdU-positive cells was lower in CUMS compared to controls. **(B)** The percentage of BrdU-positive cells responding to pleasant odorants was lower in CUMS mice compared to controls while no difference was found in response to unpleasant odorants. **(C)** The density of c-Fos + cell is similar between groups and hedonic value of odorants. **(D)** Photo of BrdU$^+$ cells (red arrows), c-Fos + cell (green arrows) and BrdU+/c-Fos + double-labelled cells (white arrows). Points represent individual data means ± s.e.m. Statistical significance depicted as $^{**}p < 0.001$. $n = 5$ control and 4 CUMS mice stimulated with pleasant odorants and $n = 3$ control and 4 stressed mice stimulated with unpleasant odorants.

In summary, these represent the first study linking CUMS with altered hedonic processing of odorants, a phenotype that is associated with increased anxiety and depressive-like behavior. We provide novel data indicating that CUMS effects on either integration and activity of adult- born cells may underlie alterations in olfactory hedonics. However, more specific characterization of the activity and interaction of adult-born and pre-existing neurons would be an asset to better understand the mechanistic underpinnings of the altered odor hedonics observed here. Such change in OB activity could contribute significantly to our understanding of the mechanisms of hedonic disturbance of olfactory signals in human population and their contribution to either symptom presentation or worsening quality of life in depressed populations. In addition to enhancing our understanding of the mechanisms underlying impairments in pleasant odor perception in depression, our findings could provide useful information to set up more naturalistic, non-pharmacological approaches to improve olfactory perception, and thereby overall well-being of individuals who have suffered from chronic stress. Indeed, by demonstrating a specific effect of CUMS on positive odor hedonics, future studies could focus on the effects of olfactory training on the hedonic response to odors in order to assess if its effects are mediated by an increase in olfactory hedonic perception. Furthermore, fostering training with consensual pleasant odorants could be more efficient in improving mood disorders in humans, than previous studies using odorants without considering their hedonic value (Umezu, 1999; Ceccarelli et al., 2004; de Almeida et al., 2004; Tokumo et al., 2006; Faturi et al., 2010; Linck et al., 2010; Cryan and Sweeney, 2011; Birte-Antina et al., 2018; Pieniak et al., 2022).

Data availability statement

The raw data supporting the conclusions of this article will be made available by the authors, without undue reservation.

Ethics statement

The animal study was reviewed and approved by European Community Council Directive of 22nd September 2010 (2010/63/UE) and the National Ethics Committee (Agreement APAFIS#20702_2019072614086203_v2).

Author contributions

MB, AD, and NM contributed to conception and design of the study. MB performed the behavioral tests. AA performed the cellular analysis. AA and LC performed the statistical analysis. LC, AA, JB, KB, and NM wrote sections of the manuscript. All authors contributed to the article and approved the submitted version.

Funding

This work was supported by the CNRS, Inserm, Lyon 1 University (LC), FRM doctoral fellowship (AA) and ENS doctoral fellowship (MB).

Acknowledgments

We thank Samuel Kumar for his technical support.

Conflict of interest

The authors declare that the research was conducted in the absence of any commercial or financial relationships that could be construed as a potential conflict of interest.

Publisher's note

Supplementary material

The Supplementary material for this article can be found online at: https://www.frontiersin.org/articles/10.3389/fnins.2023.1224941/full#supplementary-material

References

Alvarez-Buylla, A., and Garíca-Verdugo, J. M. (2002). Neurogenesis in adult subventricular zone. *J. Neurosci.* 22, 629–634. doi: 10.1523/JNEUROSCI.22-03-00629.2002

Anacker, C., Luna, V. M., Stevens, G. S., Millette, A., Shores, R., Jimenez, J. C., et al. (2018). Hippocampal neurogenesis confers stress resilience by inhibiting the ventral dentate gyrus. *Nature* 559, 98–102. doi: 10.1038/s41586-018-0262-4

Antoniuk, S., Bijata, M., Ponimaskin, E., and Wlodarczyk, J. (2019). Chronic unpredictable mild stress for modeling depression in rodents: meta-analysis of model reliability. *Neurosci. Biobehav. Rev.* 99, 101–116. doi: 10.1016/j.neubiorev.2018.12.002

Atanasova, B., El-Hage, W., Chabanet, C., Gaillard, P., Belzung, C., and Camus, V. (2010). Olfactory anhedonia and negative olfactory alliesthesia in depressed patients. *Psychiatry Res.* 176, 190–196. doi: 10.1016/j.psychres.2008.11.016

Atanasova, B., Graux, J., El Hage, W., Hommet, C., Camus, V., and Belzung, C. (2008). Olfaction: a potential cognitive marker of psychiatric disorders. *Neurosci. Biobehav. Rev.* 32, 1315–1325. doi: 10.1016/j.neubiorev.2008.05.003

Athanassi, A., Dorado Doncel, R., Bath, K. G., and Mandairon, N. (2021). Relationship between depression and olfactory sensory function: a review. *Chem. Senses* 46:bjab044. doi: 10.1093/chemse/bjab044

Bagur, S., Lefort, J. M., Lacroix, M. M., de Lavilléon, G., Herry, C., Chouvaeff, M., et al. (2021). Breathing-driven prefrontal oscillations regulate maintenance of conditioned-fear evoked freezing independently of initiation. *Nat. Commun.* 12:2605. doi: 10.1038/s41467-021-22798-6

Belluzzi, O., Benedusi, M., Ackman, J., and LoTurco, J. J. (2003). Electrophysiological differentiation of new neurons in the olfactory bulb. *J. Neurosci.* 23, 10411–10418. doi: 10.1523/JNEUROSCI.23-32-10411.2003

Belnoue, L., Grosjean, N., Ladevèze, E., Abrous, D. N., and Koehl, M. (2013). Prenatal stress inhibits hippocampal neurogenesis but spares olfactory bulb neurogenesis. *PLoS One* 8:e72972. doi: 10.1371/journal.pone.0072972

Birte-Antina, W., Ilona, C., Antje, H., and Thomas, H. (2018). Olfactory training with older people. *Int. J. Geriatr. Psychiatry* 33, 212–220. doi: 10.1002/gps.4725

Carlén, M., Cassidy, R. M., Brismar, H., Smith, G. A., Enquist, L. W., and Frisén, J. (2002). Functional integration of adult-born neurons. *Curr. Biol.* 12, 606–608. doi: 10.1016/S0960-9822(02)00771-6

Carleton, A., Petreanu, L. T., Lansford, R., Alvarez-Buylla, A., and Lledo, P.-M. (2003). Becoming a new neuron in the adult olfactory bulb. *Nat. Neurosci.* 6, 507–518. doi: 10.1038/nn1048

Ceccarelli, I., Lariviere, W. R., Fiorenzani, P., Sacerdote, P., and Aloisi, A. M. (2004). Effects of long-term exposure of lemon essential oil odor on behavioral, hormonal and neuronal parameters in male and female rats. *Brain Res.* 1001, 78–86. doi: 10.1016/j.brainres.2003.10.063

Croy, I., and Hummel, T. (2017). Olfaction as a marker for depression. *J. Neurol.* 264, 631–638. doi: 10.1007/s00415-016-8227-8

Cryan, J. F., and Sweeney, F. F. (2011). The age of anxiety: role of animal models of anxiolytic action in drug discovery. *Br. J. Pharmacol.* 164, 1129–1161. doi: 10.1111/j.1476-5381.2011.01362.x

Czarnabay, D., Dalmago, J., Martins, A. S., Queiroz, A., Sperling, L.-E., Reis, K. P., et al. (2019). Repeated 3-hour maternal deprivation as a model of early-life stress alters maternal behavior, olfactory learning and neural development. *Neurobiol. Learn. Mem.* 163:107040. doi: 10.1016/j.nlm.2019.107040

de Almeida, R. N., Motta, S. C., de Brito Faturi, C., Catallani, B., and Leite, J. R. (2004). Anxiolytic-like effects of rose oil inhalation on the elevated plus-maze test in rats. *Pharmacol. Biochem. Behav.* 77, 361–364. doi: 10.1016/j.pbb.2003.11.004

Eiland, L., Ramroop, J., Hill, M. N., Manley, J., and McEwen, B. S. (2012). Chronic juvenile stress produces corticolimbic dendritic architectural remodeling and modulates emotional behavior in male and female rats. *Psychoneuroendocrinology* 37, 39–47. doi: 10.1016/j.psyneuen.2011.04.015

Eliwa, H., Brizard, B., Le Guisquet, A.-M., Hen, R., Belzung, C., and Surget, A. (2021). Adult neurogenesis augmentation attenuates anhedonia and HPA axis dysregulation in a mouse model of chronic stress and depression. *Psychoneuroendocrinology* 124:105097. doi: 10.1016/j.psyneuen.2020.105097

Faturi, C. B., Leite, J. R., Alves, P. B., Canton, A. C., and Teixeira-Silva, F. (2010). Anxiolytic-like effect of sweet orange aroma in Wistar rats. *Prog. Neuro-Psychopharmacol. Biol. Psychiatry* 34, 605–609. doi: 10.1016/j.pnpbp.2010.02.020

Forest, J., Chalençon, L., Midroit, M., Terrier, C., Caillé, I., Sacquet, J., et al, (2020). *Role of adult-born versus preexisting neurons born at P0 in olfactory perception in a complex olfactory environment in mice. Cerebral cortex.* 30(2), 534–549. doi: 10.1093/cercor/bhz105

Goodwill, H. L., Manzano-Nieves, G., Gallo, M., Lee, H.-I., Oyerinde, E., Serre, T., et al. (2019). Early life stress leads to sex differences in development of depressive-like outcomes in a mouse model. *Neuropsychopharmacology* 44, 711–720. doi: 10.1038/s41386-018-0195-5

Guo, Y., Zhang, Z., Wang, S., Sui, Y., and Sun, Y. (2009). Notch1 signaling, hippocampal neurogenesis and behavioral responses to chronic unpredicted mild stress in adult ischemic rats. *Prog. Neuro-Psychopharmacol. Biol. Psychiatry* 33, 688–694. doi: 10.1016/j.pnpbp.2009.03.022

Hitoshi, S., Maruta, N., Higashi, M., Kumar, A., Kato, N., and Ikenaka, K. (2007). Antidepressant drugs reverse the loss of adult neural stem cells following chronic stress. *J. Neurosci. Res.* 85, 3574–3585. doi: 10.1002/jnr.21455

Huang, H.-J., Chen, X.-R., Han, Q.-Q., Wang, J., Pilot, A., Yu, R., et al. (2019). The protective effects of ghrelin/GHSR on hippocampal neurogenesis in CUMS mice. *Neuropharmacology* 155, 31–43. doi: 10.1016/j.neuropharm.2019.05.013

Kaut, K. P., and Bunsey, M. D. (2001). The effects of lesions to the rat hippocampus or rhinal cortex on olfactory and spatial memory: retrograde and anterograde findings. *Cogn. Affect. Behav. Neurosci.* 1, 270–286. doi: 10.3758/cabn.1.3.270

Kaut, K. P., Bunsey, M. D., and Riccio, D. C. (2003). Olfactory learning and memory impairments following lesions to the hippocampus and perirhinal-entorhinal cortex. *Behav. Neurosci.* 117, 304–319. doi: 10.1037/0735-7044.117.2.304

Kazour, F., Richa, S., Abi Char, C., Surget, A., Elhage, W., and Atanasova, B. (2020). Olfactory markers for depression: differences between bipolar and unipolar patients. *PLoS One* 15:e0237565. doi: 10.1371/journal.pone.0237565

Kempermann, G. (2015). Astrocytes, makers of new neurons. *Neuron* 88, 850–851. doi: 10.1016/j.neuron.2015.11.017

Kermen, F., Midroit, M., Kuczewski, N., Forest, J., Thévenet, M., Sacquet, J., et al. (2016). Topographical representation of odor hedonics in the olfactory bulb. *Nat. Neurosci.* 19, 876–878. doi: 10.1038/nn.4317

Kesner, R. P., Hunsaker, M. R., and Ziegler, W. (2011). The role of the dorsal and ventral hippocampus in olfactory working memory. *Neurobiol. Learn. Mem.* 96, 361–366. doi: 10.1016/j.nlm.2011.06.011

Li, Y., Fan, C., Gao, R., Lan, T., Wang, W., and Yu, S. Y. (2021). Hippocampal miR-211-5p regulates neurogenesis and depression-like behaviors in the rat. *Neuropharmacology* 194:108618. doi: 10.1016/j.neuropharm.2021.108618

Li, F., Wang, Y., Wang, X., Zhao, Y., Xie, F., and Qian, L.-J. (2022). Dynamic effects of chronic unpredictable mild stress on the hippocampal transcriptome in rats. *Mol. Med. Rep.* 25:110. doi: 10.3892/mmr.2022.12626

Linck, V. M., da Silva, A. L., Figueiró, M., Caramão, E. B., Moreno, P. R. H., and Elisabetsky, E. (2010). Effects of inhaled linalool in anxiety, social interaction and aggressive behavior in mice. *Phytomedicine* 17, 679–683. doi: 10.1016/j.phymed.2009.10.002

Lledo, P.-M., Alonso, M., and Grubb, M. S. (2006). Adult neurogenesis and functional plasticity in neuronal circuits. *Nat. Rev. Neurosci.* 7, 179–193. doi: 10.1038/nrn1867

Lledo, P.-M., Gheusi, G., and Vincent, J.-D. (2005). Information processing in the mammalian olfactory system. *Physiol. Rev.* 85, 281–317. doi: 10.1152/physrev.00008.2004

Lledo, P.-M., and Saghatelyan, A. (2005). Integrating new neurons into the adult olfactory bulb: joining the network, life-death decisions, and the effects of sensory experience. *Trends Neurosci.* 28, 248–254. doi: 10.1016/j.tins.2005.03.005

Lledo, P.-M., and Valley, M. (2016). Adult olfactory bulb neurogenesis. *Cold Spring Harb. Perspect. Biol.* 8:a018945. doi: 10.1101/cshperspect.a018945

Ma, H., Li, C., Wang, J., Zhang, X., Li, M., Zhang, R., et al. (2021). Amygdala-hippocampal innervation modulates stress-induced depressive-like behaviors through AMPA receptors. *Proc. Natl. Acad. Sci. U. S. A.* 118:e2019409118. doi: 10.1073/pnas.2019409118

Magavi, S. S. P., Mitchell, B. D., Szentirmai, O., Carter, B. S., and Macklis, J. D. (2005). Adult-born and preexisting olfactory granule neurons undergo distinct experience-dependent modifications of their olfactory responses in vivo. *J. Neurosci.* 25, 10729–10739. doi: 10.1523/JNEUROSCI.2250-05.2005

Mandairon, N., and Linster, C. (2009). Odor perception and olfactory bulb plasticity in adult mammals. *J. Neurophysiol.* 101, 2204–2209. doi: 10.1152/jn.00076.2009

Mandairon, N., Stack, C., Kiselycznyk, C., and Linster, C. (2006). Enrichment to odors improves olfactory discrimination in adult rats. *Behav. Neurosci.* 120, 173–179. doi: 10.1037/0735-7044.120.1.173

Mandairon, N., Sultan, S., Nouvian, M., Sacquet, J., and Didier, A. (2011). Involvement of newborn neurons in olfactory associative learning? The operant or non-operant component of the task makes all the difference. *J. Neurosci.* 31, 12455–12460. doi: 10.1523/JNEUROSCI.2919-11.2011

Markov, D. D. (2022). Sucrose preference test as a measure of anhedonic behavior in a chronic unpredictable mild stress model of depression: outstanding issues. *Brain Sci.* 12:1287. doi: 10.3390/brainsci12101287

McEwen, B. S., and Magarinos, A. M. (1997). Stress effects on morphology and function of the hippocampus. *Ann. N. Y. Acad. Sci.* 821, 271–284. doi: 10.1111/j.1749-6632.1997.tb48286.x

Midroit, M., Chalençon, L., Renier, N., Milton, A., Thevenet, M., Sacquet, J., et al. (2021). Neural processing of the reward value of pleasant odorants. *Curr. Biol.* 31, 1592–1605.e9. doi: 10.1016/j.cub.2021.01.066

Mofleh, R., and Kocsis, B. (2021). Delta-range coupling between prefrontal cortex and hippocampus supported by respiratory rhythmic input from the olfactory bulb in freely behaving rats. *Sci. Rep.* 11:8100. doi: 10.1038/s41598-021-87562-8

Moreno, M. M., Linster, C., Escanilla, O., Sacquet, J., Didier, A., and Mandairon, N. (2009). Olfactory perceptual learning requires adult neurogenesis. *Proc. Natl. Acad. Sci.* 106, 17980–17985. doi: 10.1073/pnas.0907063106

Naudin, M., El-Hage, W., Gomes, M., Gaillard, P., Belzung, C., and Atanasova, B. (2012). State and trait olfactory markers of major depression. *PLoS One* 7:e46938. doi: 10.1371/journal.pone.0046938

Negoias, S., Hummel, T., Symmank, A., Schellong, J., Joraschky, P., and Croy, I. (2016). Olfactory bulb volume predicts therapeutic outcome in major depression disorder. *Brain Imaging Behav.* 10, 367–372. doi: 10.1007/s11682-015-9400-x

Nollet, M., Gaillard, P., Tanti, A., Girault, V., Belzung, C., and Leman, S. (2012). Neurogenesis-independent antidepressant-like effects on behavior and stress axis response of a dual orexin receptor antagonist in a rodent model of depression. *Neuropsychopharmacology* 37, 2210–2221. doi: 10.1038/npp.2012.70

Pabel, L. D., Hummel, T., Weidner, K., and Croy, I. (2018). The impact of severity, course and duration of depression on olfactory function. *J. Affect. Disord.* 238, 194–203. doi: 10.1016/j.jad.2018.05.033

Papp, M., and Moryl, E. (1994). Antidepressant activity of non-competitive and competitive NMDA receptor antagonists in a chronic mild stress model of depression. *Eur. J. Pharmacol.* 263, 1–7. doi: 10.1016/0014-2999(94)90516-9

Parul, M. A., Singh, S., Singh, S., Tiwari, V., Chaturvedi, S., Wahajuddin, M., et al. (2021). Chronic unpredictable stress negatively regulates hippocampal neurogenesis and promote anxious depression-like behavior via upregulating apoptosis and inflammatory signals in adult rats. *Brain Res. Bull.* 172, 164–179. doi: 10.1016/j.brainresbull.2021.04.017

Pieniak, M., Oleszkiewicz, A., Avaro, V., Calegari, F., and Hummel, T. (2022). Olfactory training – thirteen years of research reviewed. *Neurosci. Biobehav. Rev.* 141:104853. doi: 10.1016/j.neubiorev.2022.104853

Planchez, B., Surget, A., and Belzung, C. (2019). Animal models of major depression: drawbacks and challenges. *J. Neural Transm.* 126, 1383–1408. doi: 10.1007/s00702-019-02084-y

Pothion, S., Bizot, J.-C., Trovero, F., and Belzung, C. (2004). Strain differences in sucrose preference and in the consequences of unpredictable chronic mild stress. *Behav. Brain Res.* 155, 135–146. doi: 10.1016/j.bbr.2004.04.008

Rawat, R., Tunc-Ozcan, E., McGuire, T. L., Peng, C.-Y., and Kessler, J. A. (2022). Ketamine activates adult-born immature granule neurons to rapidly alleviate depression-like behaviors in mice. *Nat. Commun.* 13:2650. doi: 10.1038/s41467-022-30386-5

Richardson, J. T. E., and Zucco, G. M. (1989). Cognition and olfaction: a review. *Psychol. Bull.* 105, 352–360. doi: 10.1037/0033-2909.105.3.352

Rochet, M., El-Hage, W., Richa, S., Kazour, F., and Atanasova, B. (2018). Depression, olfaction, and quality of life: a mutual relationship. *Brain Sci.* 8:80. doi: 10.3390/brainsci8050080

Roni, M. A., and Rahman, S. (2015). The effects of lobeline on depression-like behavior and hippocampal cell proliferation following chronic stress in mice. *Neurosci. Lett.* 584, 7–11. doi: 10.1016/j.neulet.2014.10.009

Salimi, M., Tabasi, F., Abdolsamadi, M., Dehghan, S., Dehdar, K., Nazari, M., et al. (2022). Disrupted connectivity in the olfactory bulb-entorhinal cortex-dorsal hippocampus circuit is associated with recognition memory deficit in Alzheimer's disease model. *Sci. Rep.* 12:4394. doi: 10.1038/s41598-022-08528-y

Santarelli, L., Saxe, M., Gross, C., Surget, A., Battaglia, F., Dulawa, S., et al. (2003). Requirement of hippocampal neurogenesis for the behavioral effects of antidepressants. *Science* 301, 805–809. doi: 10.1126/science.1083328

Schablitzky, S., and Pause, B. (2014). Sadness might isolate you in a non-smelling world: olfactory perception and depression. *Front. Psychol.* 5:45. doi: 10.3389/fpsyg.2014.00045

Schiffman, S. S. (1974). Physicochemical correlates of olfactory quality: a series of physicochemical variables are weighted mathematically to predict olfactory quality. *Science* 185, 112–117. doi: 10.1126/science.185.4146.112

Schoppa, N. E., and Urban, N. N. (2003). Dendritic processing within olfactory bulb circuits. *Trends Neurosci.* 26, 501–506. doi: 10.1016/S0166-2236(03)00228-5

Siopi, E., Denizet, M., Gabellec, M.-M., de Chaumont, F., Olivo-Marin, J.-C., Guilloux, J.-P., et al. (2016). Anxiety- and depression-like states lead to pronounced olfactory deficits and impaired adult neurogenesis in mice. *J. Neurosci.* 36, 518–531. doi: 10.1523/JNEUROSCI.2817-15.2016

Sultan, S., Mandairon, N., Kermen, F., Garcia, S., Sacquet, J., and Didier, A. (2010). Learning-dependent neurogenesis in the olfactory bulb determines long-term olfactory memory. *FASEB J.* 24, 2355–2363. doi: 10.1096/fj.09-151456

Sultan, S., Rey, N., Sacquet, J., Mandairon, N., and Didier, A. (2011). Newborn neurons in the olfactory bulb selected for long-term survival through olfactory learning are prematurely suppressed when the olfactory memory is erased. *J. Neurosci.* 31, 14893–14898. doi: 10.1523/JNEUROSCI.3677-11.2011

Taalman, H., Wallace, C., and Milev, R. (2017). Olfactory functioning and depression: a systematic review. *Front. Psych.* 8:190. doi: 10.3389/fpsyt.2017.00190

Tokumo, K., Tamura, N., Hirai, T., and Nishio, H. (2006). Effects of (Z)-3-hexenol, a major component of green odor, on anxiety-related behavior of the mouse in an elevated plus-maze test and biogenic amines and their metabolites in the brain. *Behav. Brain Res.* 166, 247–252. doi: 10.1016/j.bbr.2005.08.008

Umezu, T. (1999). Anticonflict effects of plant-derived essential oils. *Pharmacol. Biochem. Behav.* 64, 35–40. doi: 10.1016/S0091-3057(99)00115-X

van Boxelaere, M., Clements, J., Callaerts, P., D'Hooge, R., and Callaerts-Vegh, Z. (2017). Unpredictable chronic mild stress differentially impairs social and contextual discrimination learning in two inbred mouse strains. *PLoS One* 12:e0188537. doi: 10.1371/journal.pone.0188537

Wang, Z., Zhou, L. Q., Lee, C. M., Shi, J. Y., Liu, L., Yang, X. J., et al. (2022). Prenatal maternal stress promotes neural stem cell proliferation in the ependymal-subventricular zone of adult male offspring. *PLos One* 15:e520572. doi: 10.1101/2022.12.15.520572

Wen, P., Rao, X., Xu, L., Zhang, Z., Jia, F., He, X., et al. (2019). Cortical Organization of Centrifugal Afferents to the olfactory bulb: mono- and trans-synaptic tracing with recombinant neurotropic viral tracers. *Neurosci. Bull.* 35, 709–723. doi: 10.1007/s12264-019-00385-6

Willner, P. (2017). The chronic mild stress (CMS) model of depression: history, evaluation and usage. *Neurobiol. Stress* 6, 78–93. doi: 10.1016/j.ynstr.2016.08.002

Willner, P., Towell, A., Sampson, D., Sophokleous, S., and Muscat, R. (1987). Reduction of sucrose preference by chronic unpredictable mild stress, and its restoration by a tricyclic antidepressant. *Psychopharmacology* 93, 358–364. doi: 10.1007/BF00187257

Yang, D., Li, Q., Fang, L., Cheng, K., Zhang, R., Zheng, P., et al. (2011). Reduced neurogenesis and pre-synaptic dysfunction in the olfactory bulb of a rat model of depression. *Neuroscience* 192, 609–618. doi: 10.1016/j.neuroscience.2011.06.043

Yeshurun, Y., and Sobel, N. (2010). An odor is not worth a thousand words: from multidimensional odors to unidimensional odor objects. *Annu. Rev. Psychol.* 61, 219–241. doi: 10.1146/annurev.psych.60.110707.163639

frontiers | Frontiers in Neuroscience

TYPE Original Research
PUBLISHED 14 August 2023
DOI 10.3389/fnins.2023.1232670

OPEN ACCESS

EDITED BY
Ashok K. Shetty,
Texas A&M University School of Medicine, United States

REVIEWED BY
Adriana Berenice Silva Gómez,
Benemérita Universidad Autónoma de Puebla, Mexico
J. Martin Wojtowicz,
University of Toronto, Canada

*CORRESPONDENCE
Alexander A. Lazutkin
✉ lazutkin.a.a@gmail.com
Grigori Enikolopov
✉ grigori.enikolopov@stonybrookmedicine.edu

†These authors have contributed equally to this work and share first authorship

RECEIVED 31 May 2023
ACCEPTED 28 July 2023
PUBLISHED 14 August 2023

CITATION
Amelchenko EM, Bezriadnov DV, Chekhov OA, Anokhin KV, Lazutkin AA and Enikolopov G (2023) Age-related decline in cognitive flexibility is associated with the levels of hippocampal neurogenesis. *Front. Neurosci.* 17:1232670. doi: 10.3389/fnins.2023.1232670

Age-related decline in cognitive flexibility is associated with the levels of hippocampal neurogenesis

Evgeny M. Amelchenko[1,2†], Dmitri V. Bezriadnov[3†], Olga A. Chekhov[1,2], Konstantin V. Anokhin[3,4], Alexander A. Lazutkin[1,2,5*] and Grigori Enikolopov[1,2*]

[1]Center for Developmental Genetics, Stony Brook, NY, United States, [2]Department of Anesthesiology, Stony Brook University, Stony Brook, NY, United States, [3]P.K. Anokhin Research Institute of Normal Physiology RAS, Moscow, Russia, [4]Institute for Advanced Brain Studies, Lomonosov Moscow State University, Moscow, Russia, [5]Institute of Higher Nervous Activity and Neurophysiology RAS, Moscow, Russia

Aging is associated with impairments in learning, memory, and cognitive flexibility, as well as a gradual decline in hippocampal neurogenesis. We investigated the performance of 6-and 14-month-old mice (considered mature adult and late middle age, respectively) in learning and memory tasks based on the Morris water maze (MWM) and determined their levels of preceding and current neurogenesis. While both age groups successfully performed in the spatial version of MWM (sMWM), the older mice were less efficient compared to the younger mice when presented with modified versions of the MWM that required a reassessment of the previously acquired experience. This was detected in the reversal version of MWM (rMWM) and was particularly evident in the context discrimination MWM (cdMWM), a novel task that required integrating various distal cues, local cues, and altered contexts and adjusting previously used search strategies. Older mice were impaired in several metrics that characterize rMWM and cdMWM, however, they showed improvement and narrowed the performance gap with the younger mice after additional training. Furthermore, we analyzed the adult-born mature and immature neurons in the hippocampal dentate gyrus and found a significant correlation between neurogenesis levels in individual mice and their performance in the tasks demanding cognitive flexibility. These results provide a detailed description of the age-related changes in learning and memory and underscore the importance of hippocampal neurogenesis in supporting cognitive flexibility.

KEYWORDS

adult-born neurons, aging, cognitive flexibility, hippocampal neurogenesis, neuronal maturation, search strategies, spatial learning

Introduction

In humans and animals, aging is associated with a gradual impairment of learning, memory, and executive function (Salthouse, 2009; Samson and Barnes, 2013; Nyberg and Pudas, 2019; McQuail et al., 2020). Aging is also associated with a decrease in cognitive (behavioral) flexibility – the ability to switch between mental tasks, adapt to new environments, and adjust strategies in response to changing circumstances. Cognitive flexibility is a critical component of the executive function and deficits in cognitive flexibility may contribute to age-related cognitive decline.

Not all cognitive functions show deterioration with age, as certain aspects such as procedural, automatic, and verbal memory tend to be preserved during normal aging (Nyberg and Pudas, 2019; McQuail et al., 2020). Furthermore, the decline in certain cognitive functions can be partially mitigated by increased learning and cognitive training. While a wide range of specialized tests can detect subtle age-related changes in cognitive performance in humans, there is a limited repertoire of such tests available for animal models, such as rodents. As a result, certain nuanced features affected by aging may go unnoticed due to the lower resolution of behavioral tasks designed for animals.

Another hallmark of aging is the decrease in production of new neurons in the dentate gyrus (DG) of the hippocampus, a brain region that supports neurogenesis in humans and animals long after birth (Kuhn et al., 1996; Encinas et al., 2011; Boldrini et al., 2018; Kempermann et al., 2018; Pilz et al., 2018; Shetty et al., 2018; Sorrells et al., 2018; Lazutkin et al., 2019; Tobin et al., 2019; Toda et al., 2019; Urban et al., 2019; Bottes et al., 2021; Ibrayeva et al., 2021; Wu et al., 2023). Adult-born hippocampal neurons are believed to play diverse roles, including their involvement in distinguishing subtle differences in familiar contexts (pattern separation), supporting behavioral flexibility, and promoting active forgetting (Saxe et al., 2006; Clelland et al., 2009; Arruda-Carvalho et al., 2011; Sahay et al., 2011b; Burghardt et al., 2012; Niibori et al., 2012; Tronel et al., 2012; Aimone et al., 2014; Akers et al., 2014; Epp et al., 2016; McAvoy et al., 2016; Anacker and Hen, 2017; Toda et al., 2019; Yu et al., 2019; Lods et al., 2021; Koehl et al., 2022). A growing body of evidence indicates that decreased hippocampal neurogenesis is associated with impaired performance in a variety of learning and memory tasks [e.g., MWM and contextual fear conditioning (Hernandez-Mercado and Zepeda, 2021)]; moreover, experimental enhancement of neurogenesis has been shown to improve performance in relevant cognitive tests (Sahay et al., 2011a; McAvoy and Sahay, 2017; Berdugo-Vega et al., 2020; Montaron et al., 2020).

In this study we aimed to investigate whether the effects of aging can be detected using a novel set of tasks that we developed to assess changes in cognitive flexibility in mice (Amelchenko et al., 2023). We show that aging leads to the adoption of inefficient and spatially imprecise search strategies, resulting in impaired learning; however, this deficiency can be overcome through an extended training period. Furthermore, we sought to characterize the decline in production of neural stem and progenitor cells that accompanies aging. We found a pronounced correlation between the levels of immature and mature neurons in the dentate gyri of individual mice and their performance in tasks that require cognitive flexibility. Thus, our study reveals age-dependent impairment of several features that characterize learning, memory, and cognitive flexibility in mice and provides evidence for a correlation between adult hippocampal neurogenesis and cognitive flexibility.

Materials and methods

Mice

Adult male Nestin-CFPnuc mice (Mignone et al., 2004; Encinas et al., 2006; Enikolopov et al., 2015) maintained on C57BL/6J background, were used for all experiments. Prior and during the experiment, mice were housed in groups of 2–4 animals per cage under standard conditions with 12/12 h light–dark cycle, in cages 36x21x13.5 cm, with food and water available *ad libitum*. All experiments were conducted in compliance with the requirements, regulations, and guidelines issued by the National Institutes of Health and Stony Brook University.

We examined mice of different ages, dividing them into two groups. The first group consisted of mice that were 6 months old at the start of the behavioral training sessions (referred to as the 6MO group, $n = 13$). The second group consisted of mice that were 14 months old at the start of the behavioral training sessions (referred to as the 14MO group, $n = 15$). The same animals from the 6MO and 14MO groups were used for all experiments.

Cell labeling

To label dividing cells in the brain, experimental animals were injected with 5-ethynyl-2′-deoxyuridine (EdU, 123 mg/kg, Invitrogen, USA) intraperitoneally (Podgorny et al., 2018; Ivanova et al., 2022) 6 weeks before behavioral training. After the injection, all mice were returned to their home cages and housed under conventional conditions before the beginning of behavioral experiments.

Morris water maze training

Mice were transferred from the animal facility to the experimental room 1 h prior to the beginning of the experimental procedures. The mice were subjected to three consecutive Morris water maze-(MWM)-based tasks: spatial MWM (sMWM), followed by reversal MWM (rMWM), which was followed by context discrimination MWM (cdMWM). For the training in the sMWM (Figure 1), animals were presented with a circular pool (120 cm in diameter) made of blue plastic (Noldus, the Netherlands). The water was made opaque with non-toxic white paint and maintained at 23–24°C. Several distal cues were affixed to the walls surrounding the pool. Each mouse performed five 60 s trials per day, with 30 min inter-trial intervals, for five consecutive days, with the objective to locate a submerged platform positioned 0.5 cm below the water surface in one of the virtual quadrants (the target quadrant, T). At the beginning of each trial, a mouse was released into the pool from one of three virtual quadrants that did not contain the platform. If a mouse failed to find the platform, the experimenter gently guided it to the platform. The mouse was allowed to remain on the platform for 30 s. The platform position remained constant throughout the five training days. On day 6, the mice underwent a spatial memory test involving swimming for 60 s in the pool without the platform.

Training in rMWM (Figure 1) started 2 h after the sMWM memory test. The hidden platform was reintroduced to the pool but was placed in the quadrant opposite to that used during sMWM training. The distal cues on the walls remained the same and were located at the same positions relative to the pool. The mice were given three additional days to learn the new platform location. The overall procedure was identical to that described for sMWM. On day 9, the mice were subjected to a 60 s memory test without the platform.

cdMWM training (Figure 1) began 2 h after the rMWM memory test (day 9). The same blue plastic pool and the same distal cues on the

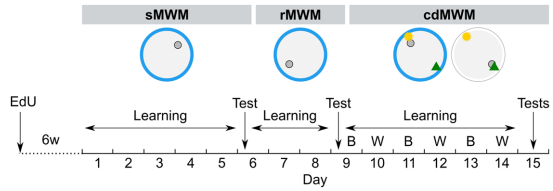

FIGURE 1
Experimental timeline. Mice were trained in succession of three tasks: spatial MWM (sMWM) learning – days 1–5, sMWM memory test – day 6; reversal MWM (rMWM) learning – days 6–8, rMWM memory test – day 9; context discrimination (cdMWM) learning in daily alternating blue (B) and white (W) pools with a pair of local cues, that context-dependently signaled platform location – days 9–14, cdMWM memory tests in the blue and white pools – day 15. Blue ring represents the blue swimming pool, white ring represents the white swimming pool, small grey circle represents platform location, note different platform location in different tasks; yellow star and green triangle represents local cues introduced for training in the cdMWM task.

walls were used. The platform was relocated to a new quadrant and two local cues (beacons) – a yellow rubber ball and a multicolor pyramid – were suspended 20 cm above the water surface. One beacon was placed above the platform (the goal cue), while the other was positioned above the opposite quadrant (the false cue). On the following day (day 10), each mouse was placed in a pool identical to the blue pool except it was constructed from white plastic. This pool was located in the adjacent room with different distal cues on the walls. Two beacons identical to those used in the blue pool (a ball and a pyramid) were suspended above the pool, but the goal cue and the false cue were switched, i.e., if the ball indicated the platform location in the blue pool, it served as the false cue in the white pool, while the pyramid became the new goal cue. The assignment of beacons indicating the platform location was counterbalanced between the pools: for half of the animals in each group in a particular pool the goal cue was the ball, whereas for the other half in the same pool the goal cue was the pyramid. Therefore, to choose the correct local cue indicating the platform location, each mouse needed to discriminate among the contextual factors of the room, pool color, and distal cues. Each mouse underwent five daily sessions lasting 60 s each, and after reaching the platform was allowed an additional 30 s on the platform. The pools were alternated daily for six days (day 9 through day 14). On day 15, the mice underwent 60 s memory tests in the blue and white pools, separated by a 2 h interval. The timeline of the tasks is depicted in Figure 1.

Behavioral parameters and analysis

Animals' behavior was recorded with the video camera mounted above the pool. For behavioral tracking, EthoVision XT, versions 8 and 17 (Noldus, the Netherlands) was used, and the following behavioral parameters were extracted from the video: *escape latency* – time to reach the platform in training trial; *fraction of time spent in each quadrant* (in %) in the memory test. For the classification analysis of the search strategies, we used the Pathfinder software (Cooke et al., 2019). Raw tracking files with *xy coordinates over time* were extracted from the EthoVision XT and uploaded to the Pathfinder. The following parameters, empirically determined for our combination of the pool and platform size and location were used: Goal Position (x,y): varied between sMWM, rMWM, cdMWM; Goal Diameter (cm): 10; Maze Diameter (cm): 120; Maze Centre (x,y): 0,0; Angular Corridor Width (degrees): 20; Chaining Angular Width (cm): 15; Thigmotaxis Zone Size (cm): 15. A trial was truncated when the animal reached goal location. As a result, each track was assigned to one of the seven search strategies: direct path, directed search, focal search, indirect search, scanning, random search, thigmotaxis (from the most spatially precise and efficient to the least one). In wild-type healthy rodents, learning leads to a decrease of the fraction of inefficient, spatially imprecise search strategies (presumably, hippocampal-independent) and is accompanied by an increase of the fraction of more efficient, spatially specific, and, presumably, hippocampal-dependent, strategies (indirect search, focal search, directed search, direct path) (Garthe et al., 2009, 2014, 2016; Cooke et al., 2019). The repertoire of strategies used in every trial was presented as a percentage of each strategy used by animals for each group. *The ideal path error* (IPE) extracted from the Pathfinder output file was calculated as follows: *the summed error of the search path (cm) = the cumulative actual path distance (cm) – the cumulative ideal path (cm)*. This parameter served as another metric to characterize effectiveness of search strategies: the IPE is expected to be lower if mostly spatially precise strategies were used, and higher if mostly spatially imprecise strategies were used. *The preference score* was calculated as the time spent in the target (T) quadrant divided by the cumulative time spent in both the T quadrant and the opposite (O) quadrant: *(time in T) × 100/(time in T + time in O)* was used to directly compare the quadrant discrimination between the experimental groups. *The correct first choice (CFC)* score was calculated by subtracting the latency to reach the goal cue from the latency to reach the false cue.

Immunohistochemistry

After the completion of behavioral testing, mice were deeply anesthetized with a mixture of Zoletil 100 (40 mg/kg) and xylazine (5 mg/kg) and transcardially perfused with 30 mL of ice-cold PBS followed by 30 mL of 4% paraformaldehyde (PFA) in phosphate buffer (PBS), pH 7.4. Brains were removed from the skull and postfixed in 4% PFA overnight at 4°C. The following day, the brains were transferred into PBS and stored until sectioning. Free-floating 50 µm-thick sagittal sections were obtained using a Leica VT1000S vibratome (Leica, Germany). The sections were collected in PBS and kept in PBS at 4°C or in cryoprotectant (1 volume of ethylene glycol, 1 volume of glycerin, and 2 volumes of PBS) at −20°C until staining. For permeabilization and blocking, sections were incubated in a solution containing 2% Triton-X100 in PBS (2% TBS) and 5% normal goat serum (Abcam, USA, ab7481) for 1 h at room temperature on a rocking platform. Next, the sections were incubated with primary antibodies in 0.2% TBS and 3% normal goat serum overnight at room temperature on a rocking platform. After washing three times in 0.2% TBS, sections were incubated with secondary antibodies in 0.2% TBS and 3% normal goat serum for 2 h at room temperature in darkness on a rocking platform. The following antibodies were used: guinea pig anti-DCX (1:2000, Millipore, USA, AB2253) and goat anti-guinea pig AlexaFluor 647 (1:500, Molecular Probes, USA, A21450); mouse anti-NeuN (1:1000, Millipore AB377) and goat anti-mouse AlexaFluor 488

(1:400, Molecular Probes, A32723). After three washings in 0.2% TBS, the click reaction was performed with AlexaFluor 555 Azide, triethylammonium salt (Invitrogen, USA, A20012) according to Salic and Mitchison (2008) and Ivanova et al. (2022). After three washes in 0.2% TBS and three washes in PBS, the sections were glass-mounted using Fluorescent Mounting Medium (DAKO, USA, S3023). The glass slides were dried horizontally overnight at room temperature in darkness, then stored at 4°C until imaging.

Imaging and cell counting

Cell counting was performed by means of design-based stereology (Encinas and Enikolopov, 2008). One brain hemisphere was randomly selected for each animal. The hemisphere was sagittally sectioned in the lateral-to-medial direction, from the beginning of the lateral ventricle to the midline, thus covering the entire DG region. The sections were 50 µm thick and were collected in six parallel sets; thus, each set was comprised of sections that were 300 µm apart from each other in the brain. One set of 8–9 sections on average, covering the DG, was used for cell counting. The sections were imaged using a spinning-disc confocal microscope (Andor Revolution WD, Oxford Instruments, UK) with the iQ 3.1 software (Oxford Instruments, UK) and a 20x NA 0.75 objective (Nikon, Japan). All images were imported into Imaris software (v.7.6.4, Bitplane, UK) and cells were counted manually by an experimenter who was blinded to the group assignment. The cell counts for the section set were averaged, normalized to the average number of sections from all animals, and then multiplied by 6 and by 2 (the number of wells and hemispheres, respectively) to represent the total number of cells per two hippocampi.

To control the validity of cell counts, we compared the impact of between-sample variability of cell counts (i.e., the variance of cell counts within a set of brain sections from the same animal) with the impact of between-animals variability. We calculated the mean coefficient of error (CE) for the mice and compared it to the group variance (CV) (Slomianka and West, 2005; Basler et al., 2017; Slomianka, 2021). A $\frac{\text{mean } CE^2_{sampling}}{CV^2_{group}}$ ratio less than 0.5 would indicate that between-sample variability in cell counts contributed less than 50% to the overall variability between the animals, a value considered to be acceptable as a measure of the results' validity in most cases (Slomianka, 2021).

Statistical analysis

Statistical analysis was performed using Prism (version 6.04, GraphPad Software, USA) and SPSS (version 28.0.0, IBM, USA). We used unpaired (independent samples, repeated measures) design for the experiments. For the analysis of escape latencies we used two-way repeated measures ANOVA followed by multiple comparisons with Sidak's correction, with a family-wise significance level set to 0.05 ($\alpha = 0.05$). For the analysis of the effect of age on the search strategies, we used Generalized Linear Mixed Model (GLMM). The response variable was the strategy used by an animal to reach platform in each trial. If a spatially precise strategy (direct path, directed search, focal search, indirect search) was used, it was scored "1"; if a spatially imprecise strategy (scanning, random search, thigmotaxis) was used, it was scored "0." Age and the day of training were the predictor variables; subjects (individual animals) were added to model a random effect. A separate GLMM analysis was conducted for each of the MWM tasks. The results were presented as odds ratio (OR) of using precise search strategies over imprecise search strategies in the aged (14MO) group compared to the mature adult (6MO) group; a significant difference for the between-group pairwise comparison was determined with Bonferroni correction. The ideal path error (IPE) data were analyzed with two-way repeated measures ANOVA followed by multiple comparisons with Sidak's correction.

To assess the distribution of time spent in quadrants in the test trials for uniformity we applied the Dirichlet distribution, using the "Dirichlet package" (Maugard et al., 2019). If the distribution was found to diverge from a uniform distribution, we performed *post-hoc* single sample *t*-tests with Bonferroni correction to compare the percentage of time spent in a particular quadrant with a theoretical value of 25%. The average distributions of the track points (mouse locations) in the test trials were represented as heatmaps generated in Ethovision XT. For the preference score (transformed with probit function from non-normally distributed data to normally distributed) and the CFC score analysis, we used Mann–Whitney *t*-test.

For the cell counts, we used Mann–Whitney *t*-test, with a significance level set to 0.05 ($\alpha = 0.05$). A total of 10 mice from the 6MO group and 14 mice from the 14MO group were examined. In the 6MO group, one animal had pronounced hydrocephaly and was excluded from the analysis. The brain sections from two other animals showed unexpectedly high number of DCX^+ cells [three-fold higher than in the other 24 animals; values identified as outliers using the ROUT method (Motulsky and Brown, 2006)] and were excluded from the further cell count analysis. In the 14MO group, sections from one animal were damaged during staining and processing and could not be included in the cell number analysis. Of note, these four mice did not differ significantly from the remaining mice in each of the behavioral tests.

To assess potential joint variation of individual behavioral parameters and neurogenesis, we performed correlation analysis. We used (a) escape latencies (averaged across five training trials) or cumulative number of precise search strategies used by individual mice on specific days of training (ranging from 0 – if a mouse did not use any of precise search strategies in each of five training trials, to 5 – if a mouse used only precise search strategies in each of five training trials), and (b) cell counts (DCX^+ and $EdU^+NeuN^+DCX^-$ cells per DG) for the same animals. We used Spearman rank correlation (following D'Agostino & Pearson omnibus normality test), with a significance level set to 0.05 ($\alpha = 0.05$).

Graphs were plotted in Prism, the "Dirichlet package," and Ethovision XT. Images were obtained in Imaris. Final figures were prepared in Inkscape 1.1.

Results

Experimental design

To investigate the effects of aging on learning, memory, behavioral flexibility, and neurogenesis, we focused on two age groups: mice that are considered mature adult (6 months old, the 6MO group) and those considered to be of late middle age (14

months old, the 14MO group), i.e., on the ages before the overt manifestation of impairments characteristic of old age (Flurkey et al., 2007). We assessed the animals' performance in a series of consecutive MWM tasks designed to evaluate various behavioral domains and analyzed several parameters to quantify the age-related changes (scheme in Figure 1). Additionally, we tagged dividing cells using the thymidine analog EdU, administered 6 weeks prior to the start of the MWM series.

Both the 6MO and 14MO groups were first trained for 5 days to locate a hidden escape platform in the standard spatial MWM (sMWM) task (Figure 1). On day 6, the platform was removed, and a memory test was conducted. Next, the same animals underwent 3 days of training (days 6–8) in the reversal MWM (rMWM) task where the platform was moved to the quadrant opposite to that used in the sMWM task. Following another memory test without the platform on day 9, the mice underwent training for 6 days (days 9–14) in the context discrimination MWM (cdMWM), with the color of the pool (blue and white) and the position of the beacons (a ball and a pyramid) alternating daily. The training in cdMWM was followed by memory tests in both pool configurations, with the platform removed. To evaluate the overall fitness of the animals for the task series, we measured an average swimming speed on days 1, 6, and 10 of training and found no significant differences between the 6MO and 14MO groups, indicating comparable locomotor activity of the mice of both ages (Figure 2).

Learning, search strategies, and memory in the sMWM, rMWM, and cdMWM tasks in 6- and 14-month-old mice

sMWM

Both groups of mice successfully learned the platform location, as evidenced by a significant reduction in escape latencies throughout the training period (Figure 3A). Two-way repeated measures ANOVA indicated a significant effect of the training day ($p < 0.0001$), but not of the animals' age or the training day × age interaction ($p > 0.05$ for both). *Post-hoc* comparison using Sidak's correction revealed a decrease in escape latencies from day 1 to day 5 of training in both the 6MO group ($p < 0.0001$) and the 14MO group ($p < 0.0001$), indicating improved performance in the sMWM task for both age groups.

We further analyzed the navigation strategies used by the mice during the search for the escape platform. For each trial, the overall search path was assigned to one of seven distinct search strategies (Cooke et al., 2019), ranging from inefficient spatially imprecise (e.g., thigmotaxis and random search), to highly efficient spatially precise (e.g., directed path, directed search and focal search). Over the 5 days of sMWM training, both groups showed an increase in the proportion of spatially precise search strategies and a decrease in spatially imprecise strategies (Figure 3B).

As another approach to characterize the use of different search strategies by the 6MO and 14MO groups, we applied Generalized Linear Mixed Model (GLMM) analysis to determine the relationship between the outcome variable (search strategy) and predictor variables (age and day of training). The GLMM did not reveal a significant effect of the training day × age interaction ($p = 0.990$) or of age alone ($p = 0.895$), but it did indicate a significant effect of training day ($p < 0.001$) (Figure 3C). Thus, in the sMWM task, the age of the animals did not affect the odds of using spatially precise search strategies compared to spatially imprecise strategies.

As yet another measure of the efficiency of the platform search, we determined the ideal path error (IPE), which represents the difference between the ideal path (a straight line from the release site to the platform) and the actual path taken by the mouse during the search. Both groups showed a significant decrease in the IPE from day 1 to day 5 of the sMWM task (effect of training day: $p < 0.0001$), with no effect of age ($p = 0.1269$), or the training day × age interaction ($p = 0.8977$) (Figure 3D). This indicated improved performance during learning, without significant difference in IPE between the 6MO and 14MO groups.

We next assessed the performance of the mice in the memory test by examining whether the time spent searching the platform was uniformly distributed between the quadrants. Using the Dirichlet distribution to account for the constant-sum constraints of the MWM test (Maugard et al., 2019), we found that in both age groups the distribution of time spent in the four quadrants significantly deviated from a uniform distribution (6MO: $p < 0.0001$; 14MO: $p < 0.0001$, Bonferroni correction applied here and later) (Figure 3E). *Post-hoc* single sample *t*-tests revealed that the mice spent more time in the target (T) quadrant than would be expected by chance (25%) (6MO: $p < 0.0001$; 14MO: $p < 0.0001$). Heatmaps depicting the average spatial distributions of the track points (i.e., mouse locations in the pool during the sessions) further confirmed that mice from both age groups localized their search to the general area of the platform (Figure 3E). Lastly, to compare the ability of the two groups to discriminate the quadrants, we calculated quadrant preference scores

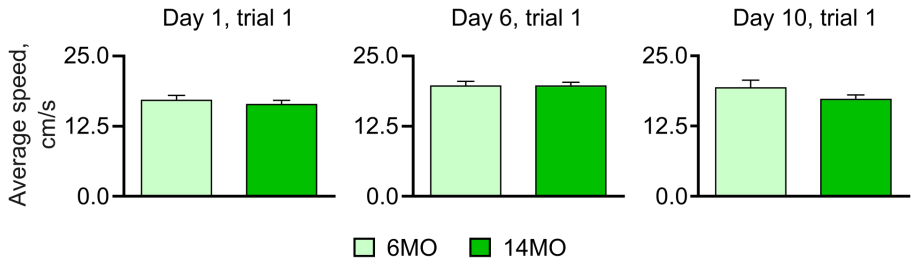

FIGURE 2
Average swim speed measured in course of training; no significant difference between the groups was found (Mann–Whitney *t*-test), data presented as Mean ± SEM.

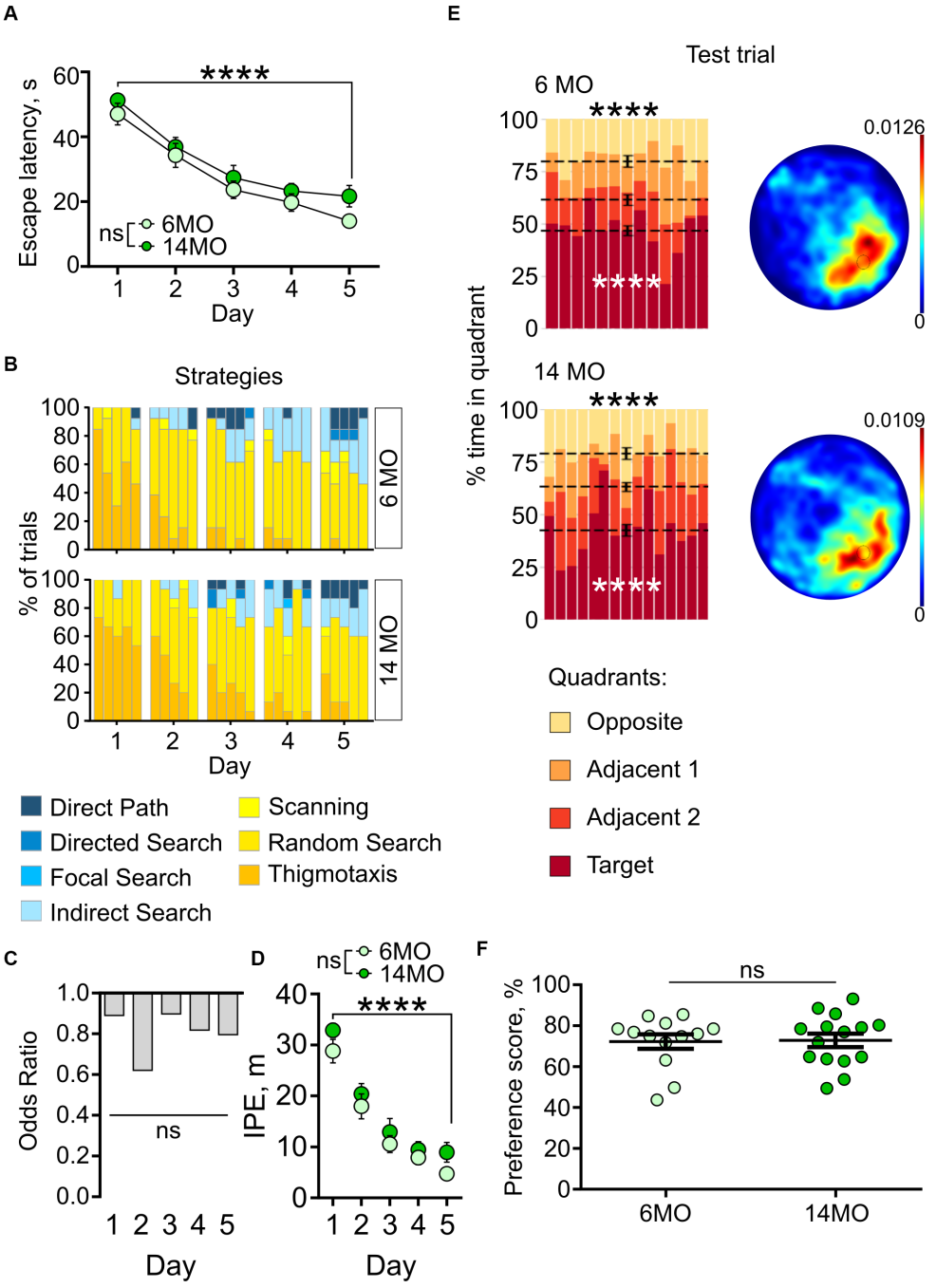

FIGURE 3
Behavior in spatial MWM (sMWM) of 6-month-old (6MO, $n = 13$) and 14-month-old (14MO, $n = 15$) mice. **(A)** Escape latencies (time to reach a hidden platform) during training; ****$p < 0.0001$ for each of two groups, ns – $p > 0.05$ (two-way ANOVA, multiple comparisons with Sidak's correction), data presented as Mean ± SEM; **(B)** Search strategies in sMWM; each block of stacked bars indicates strategies used for the 5 trials for each day; **(C)** Odds ratio of spatially precise strategies use in 14MO compared with the 6MO in sMWM; ns – $p > 0.05$ (p values determined by fitting a generalized linear mixed effect model with binomial distribution); **(D)** Ideal path error (IPE) in sMWM; ****$p < 0.0001$ for each of two groups, ns – $p > 0.05$ for effect of age (two-way ANOVA, multiple comparisons with Sidak's correction), data presented as Mean ± SEM; **(E)** Time spent in quadrants (in %) during test following sMWM training; each column represents an animal and each color represents the percent of time spent in each quadrant. Mean value for the fraction of time spent in each quadrant is represented by a black dash line and the error bar on the mean is approximated with the inverse Fisher information, ****$p < 0.0001$, in black symbols the results of Dirichlet distribution analysis are shown, in white symbols the results of *post-hoc* single sample *t*-test comparison (with Bonferroni correction) with the theoretical value 25% are shown; heatmaps represent average distribution of the track points (mouse locations) in the pool during test trial; **(F)** Preference score, relative time spent in T quadrant in test, dots represent individual values, ns – $p > 0.05$, data presented as Mean ± SEM.

and found no overall difference between the 6MO and 14MO groups (Mann–Whitney *t*-test) (Figure 3F). Thus, each of the applied tests and metrics indicates that spatial learning and memory in the sMWM task were not impaired in the older mice compared to the younger mice.

rMWM

We next assessed the re-learning ability of the mice by presenting them with the rMWM task. A two-way repeated measures ANOVA of the escape latencies revealed significant effects of the training day ($p < 0.0001$) and of the animals' age ($p = 0.0033$); it did not indicate a significant interaction between the training days and age ($p > 0.05$). *Post-hoc* comparison with Sidak's correction showed a decrease in escape latencies from day 6 to day 8 of training in both the 6MO and 14MO groups (day 8 vs day 6: $p = 0.0104$ for 6MO and $p = 0.0016$ for 14MO) (Figure 4A), indicating improved performance in the rMWM task for both age groups. Furthermore, the between-groups comparisons showed that the 14MO group had longer escape latency than the 6MO group on day 6 ($p = 0.0263$), with a trend toward longer latencies on days 7 and 8 ($p = 0.056$ and $p = 0.059$, respectively) (Figure 4A). These findings suggest that while both the 6MO and 14MO mice were capable of learning the new platform location, the 14MO mice exhibited significant impairment compared to the 6MO mice.

The impaired learning of the 14MO group was further corroborated by the analysis of search strategies. Initially, both groups predominantly utilized spatially imprecise strategies (Figure 4B, day 6 trial 1). However, starting from trial 2 on day 6 and continuing on days 7 and 8, the 6MO mice demonstrated a higher reliance on spatially precise strategies compared to the 14MO mice (Figure 4B).

The GLMM analysis revealed a significant effect of age ($p = 0.003$), but no effect of the training day or the training day × age interaction ($p = 0.100$ and $p = 0.388$, respectively) (Figure 4C). The odds ratio (OR) of using spatially precise over spatially imprecise strategies in the 14MO group compared to the 6MO group were 0.166 ($p = 0.005$) on day 6, 0.381 ($p = 0.076$) on day 7, and 0.366 ($p = 0.056$) on day 8.

For the IPE, a two-way repeated measures ANOVA revealed a significant effect of the training day ($p = 0.0001$) and age ($p = 0039$), but not of the day × age interaction ($p = 0.0685$) (Figure 4D). Further *post-hoc* analysis revealed a significantly higher IPE in the 14MO group than in the 6MO group on days 6 and 7 ($p = 0.0098$ and 0.0427, respectively). Together, these metrics indicate a pronounced learning deficit in the 14MO mice compared to the 6MO mice.

In the memory test, the distribution of time spent in the four quadrants significantly deviated from a uniform distribution for both groups (6MO: $p < 0.0001$; 14MO: $p < 0.0001$) (Figure 4E). *Post-hoc* single sample *t*-tests demonstrated that in each group mice spent more time in the T quadrant and less time in the opposite (O) quadrant than would be expected by chance: $p = 0.0003$ for 6MO and $p = 0.0005$ for 14MO for the T quadrant and $p = 0.0004$ for 6MO and $p = 0.0012$ for 14MO for the O quadrant. The heatmaps illustrated that the spatial distributions of the track points for mice from both groups were localized to the area of the platform location (Figure 4E). The preference scores for the 6MO and 14MO groups did not differ significantly ($p > 0.05$, Mann–Whitney *t*-test) (Figure 4F). Finally, as an additional approach to evaluate the animals' memory for the platform location, we determined the correct first choice score (CFC score) by subtracting the latency to reach the (former) platform location in the rMWM task from the latency in the sMWM task. There was no difference in the CFC scores between the groups ($p > 0.05$, Mann–Whitney *t*-test) (Figure 4G). Thus, while the spatial learning of the older mice was impaired in the rMWM task compared to the younger mice, their memory remained unaffected.

cdMWM

Next, we compared the performance of both age groups in cdMWM, a complex paradigm which included varying contexts and local cues, in addition to the varying platform position relative to the distal cues characteristic of the sMWM and rMWM tasks. Mice were exposed to daily alternating contexts (pool color) and different positions of the local cues [beacons (Figure 5)]. Two-way ANOVA of escape latencies revealed significant effects of the training day ($p < 0.0001$) and age ($p = 0.0266$), but no significant interaction between training day and age ($p > 0.05$). When analyzing the daily performance, *post-hoc* comparisons indicated a longer escape latency in the 14MO group than in the 6MO group on day 11 in the blue pool ($p = 0.039$) (Figure 5A). These results suggest that learning in the cdMWM task was affected in the 14MO group.

The analysis of search strategies supported the observation of impaired learning in the 14MO group. In both groups the contribution of spatially precise strategies, such as direct path, increased compared to the sMWM and rMWM tasks, starting from the first trial on day 9 (likely due to the introduction of the local cues) (Figure 5B). The reliance on spatially precise search strategies gradually increased over the training days in both groups; however, during the initial days of training, 14MO mice exhibited a noticeable delay in their adoption of these efficient strategies compared to the younger mice. Nevertheless, by the end of training, the disparity in the use of spatially precise strategies between the older and younger mice diminished.

The GLMM analysis indicated significant effects of the training day and age ($p < 0.001$ and $p < 0.001$, respectively), but not of the day × age interaction ($p = 0.979$) (Figure 5C). The ORs for using efficient strategies were significantly lower for the 14MO group compared to the 6MO group: 0.278 ($p = 0.003$) on day 9, 0.393 ($p = 0.034$) on day 10, 0.276 ($p = 0.005$) on day 11, 0.351 ($p = 0.018$) on day 12, 0.365 ($p = 0.045$) on day 13, and 0.361 ($p = 0.078$) on day 14.

Significant effects of the training day and age were also observed for the IPE ($p < 0.0001$, $p = 0.0289$, respectively), but the day × age interaction was non-significant ($p = 0.213$). *Post-hoc* analysis revealed significantly higher IPE in the 14MO group compared to the 6MO group on day 9 ($p = 0.0228$) (Figure 5D). Taken together, the results with cdMWM indicate a significant learning deficit in the 14MO mice compared to the 6MO mice.

In the memory test, similar to the sMWM and rMWM tasks, the distribution of time spent by both groups in the four quadrants of both pools significantly deviated from a uniform distribution ($p < 0.0001$ both for the 6MO and 14MO groups in the blue and in the white pool) (Figure 5E). *Post-hoc* single sample *t-tests* revealed that while the 6MO group spent significantly more time in the T quadrant than in the O quadrant of the blue pool, the fraction of time spent by the 14MO group in each quadrant did not significantly differ from the expected chance value of 25% (6MO: T quadrant: $p < 0.0001$, O quadrant: $p = 0.7291$; 14MO: T quadrant: $p > 0.05$ for both the T and O quadrants). In the white pool, both the 6MO and 14MO groups spent more time in the T quadrant than the chance value of 25% ($p < 0.0001$), while there was no significant difference in time spent by either group in the O quadrant ($p > 0.05$).

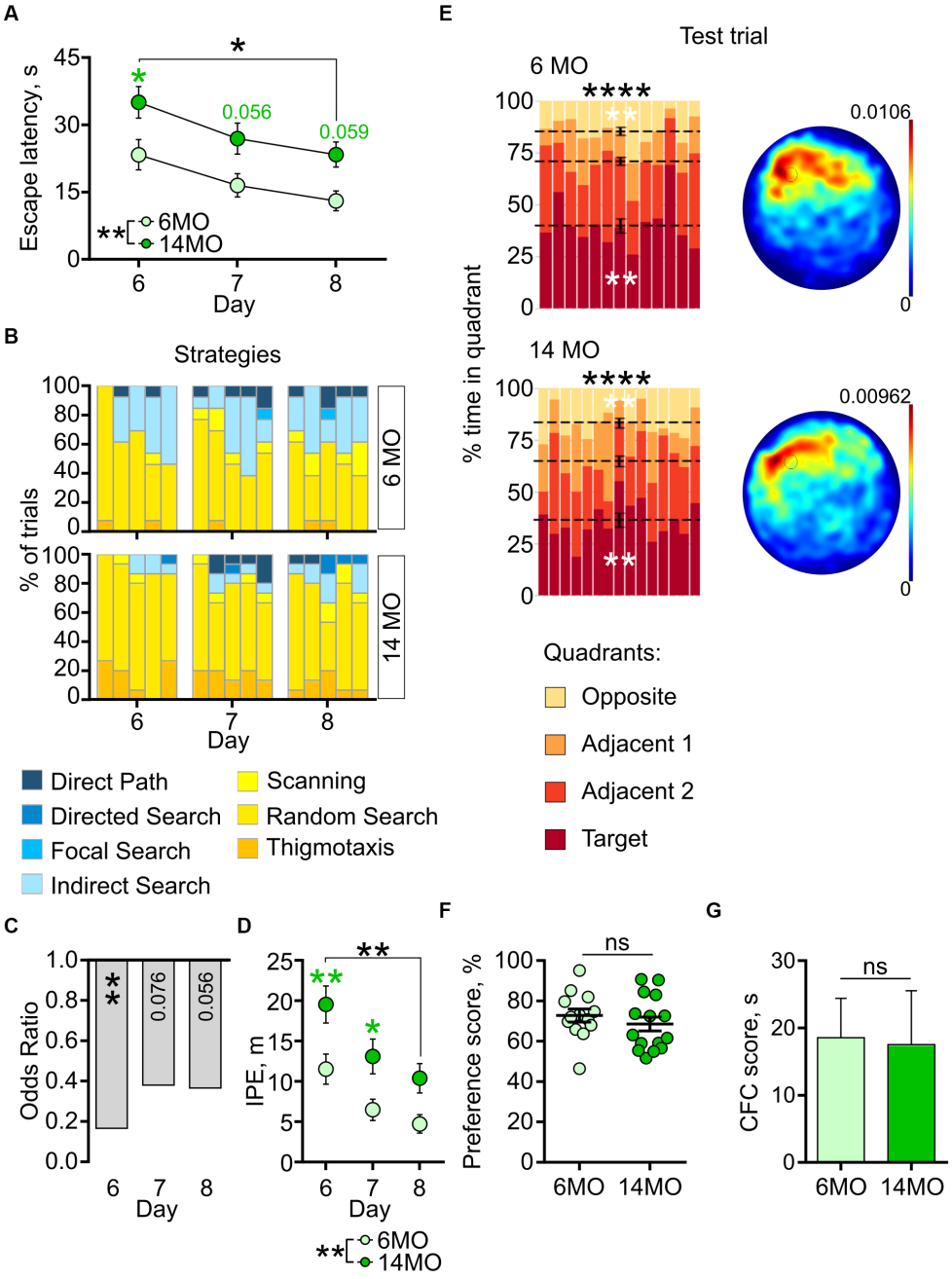

FIGURE 4
Behavior in reversal MWM (rMWM) of 6-month-old (6MO, $n = 13$) and 14-month-old (14MO, $n = 15$) mice. **(A)** Escape latencies (time to reach a hidden platform) during training; black asterisks: *$p < 0.05$ for day 6 vs day 8 for each of two groups, **$p < 0.01$ effect of age; green symbols: 14MO vs 6MO, *$p < 0.05$ (two-way ANOVA, multiple comparisons with Sidak's correction), data presented as Mean ± SEM; **(B)** Search strategies in rMWM; each block of stacked bars indicates strategies used for the 5 trials for each training day; **(C)** Odds ratio of spatially precise strategies use in 14MO compared with the 6MO in rMWM; **$p < 0.01$ (p values determined by fitting a generalized linear mixed effect model with binomial distribution); **(D)** Ideal path error (IPE) in rMWM; black asterisks: both groups or between-group comparison **$p < 0.01$ for day 6 vs day 8 for each of two groups, **$p < 0.01$ effect of age; green asterisks: 14MO vs 6MO, *$p < 0.05$, **$p < 0.01$ (two-way ANOVA, multiple comparisons with Sidak's correction), data presented as Mean ± SEM; **(E)** Time spent in quadrants (in %) during test following sMWM training; each column represents an animal and each color represents the percent of time spent in each quadrant. Mean value for the fraction of time spent in each quadrant is represented by a black dash line and the error bar on the mean is approximated with the inverse Fisher information, **$p < 0.01$, ****$p < 0.0001$, in black symbols the results of Dirichlet distribution analysis are shown, in white symbols the results of *post-hoc* single sample t-test comparison (with Bonferroni correction) with the theoretical value 25% are shown; heatmaps represent average distribution of the track points (mouse locations) in the pool during test trial; **(F)** Preference score, relative time spent in T quadrant in test, dots represent individual values, ns – $p > 0.05$, data presented as Mean ± SEM; **(G)** Correct first choice (CFC) score (latency to reach the false cue – latency to reach goal cue); ns – $p > 0.05$, data presented as Mean ± SEM.

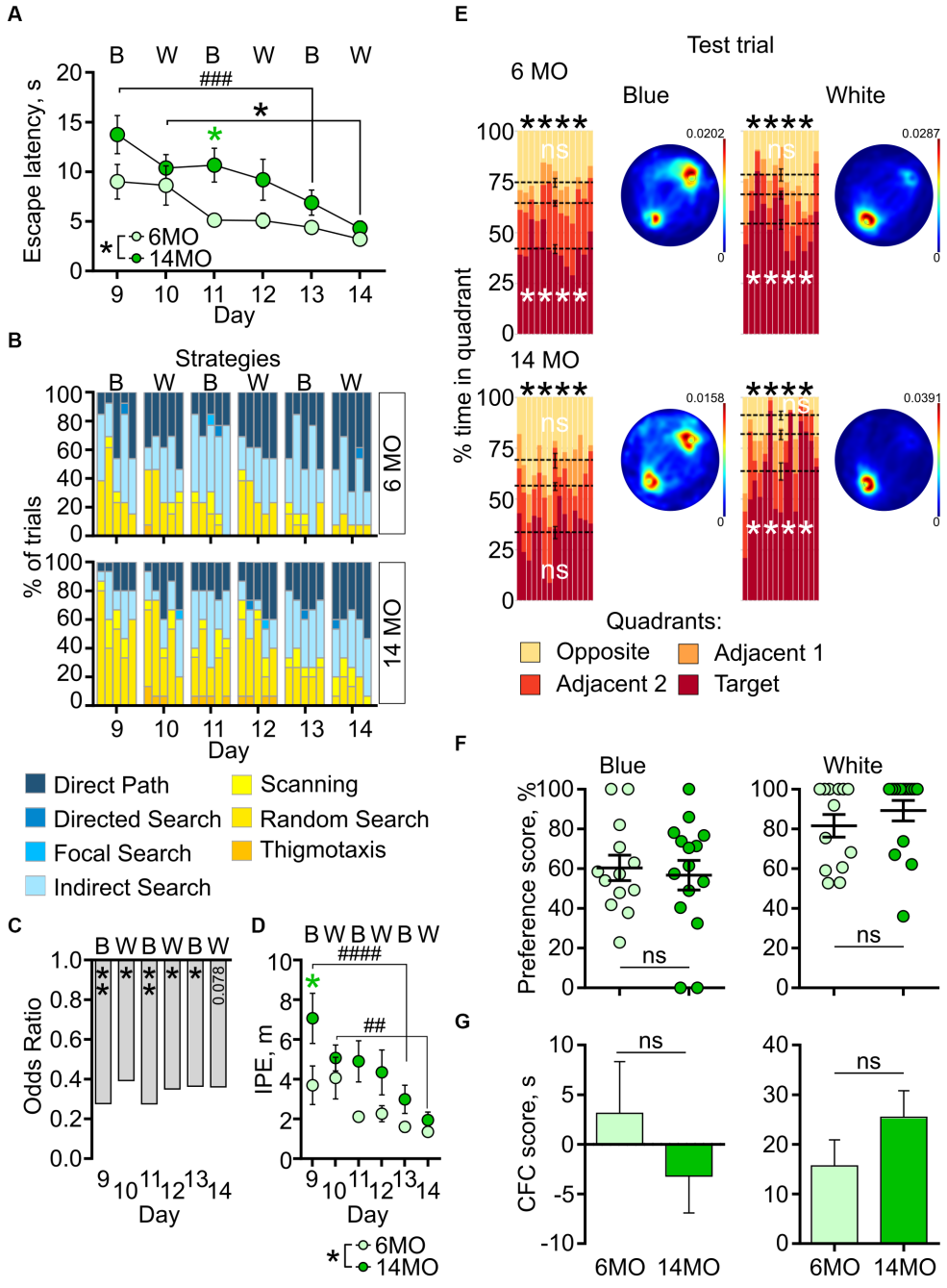

FIGURE 5
Behavior in context discrimination MWM (cdMWM) of 6-month-old (6MO, $n = 13$) and 14-month-old (14MO, n = 15) mice. **(A)** Escape latencies (time to reach a hidden platform) during training; black asterisks: both groups or effect of age, $^{*}p < 0.05$, $^{\#\#\#}p < 0.001$ day 9 vs day 13 for the 14MO group; green asterisk: comparison of 14MO vs 6MO on specific day, $^{*}p < 0.05$ (two-way ANOVA, multiple comparisons with Sidak's correction), data presented as Mean ± SEM; **(B)** Search strategies in cdMWM; each block of stacked bars indicates strategies used for the 5 trials for each training day; **(C)** Odds ratio of spatially precise strategies use by the 14MO group compared to the 6MO groups in cdMWM; $^{*}p < 0.05$, $^{**}p < 0.01$ (p values determined by fitting a generalized linear mixed effect model with binomial distribution); **(D)** Ideal path error (IPE) in cdMWM; black symbols: $^{*}p < 0.05$ for effect of age, $^{\#\#}p < 0.01$, $^{\#\#\#}p < 0.001$ day 9 vs day 13 or day 10 vs day 14 for the 14MO group; green asterisk: 14MO vs 6MO, $^{*}p < 0.05$ (two-way ANOVA, multiple comparisons with Sidak's correction), data presented as Mean ± SEM; **(E)** Time spent in quadrants (in %) during test following sMWM training; each column represents an animal and each color represents the percent of time spent in each quadrant. Mean value for the fraction of time spent in each quadrant is represented by a black dash line and the error bar on the mean is approximated with the inverse Fisher information, $^{****}p < 0.0001$, ns – $p > 0.05$, in black symbols the results of Dirichlet distribution analysis are shown, in white symbols the results of *post-hoc* single sample *t*-test comparison (with Bonferroni correction) with the theoretical value 25% are shown; heatmaps represent average distribution of the track points (mouse locations) in the pool during test trial; **(F)** Preference score, relative time spent in T quadrant in test; dots represent individual values, ns – $p > 0.05$, data presented as Mean ± SEM; **(G)** Correct first choice (CFC) score (latency to reach the false cue – latency to reach goal cue); ns – $p > 0.05$, data presented as Mean ± SEM.

These findings were further illustrated by the heatmaps: in the blue pool, there was a higher density of track points in the area of platform, but a second focus of higher track point density was observed in the opposite quadrant; in the white pool, the density of track points was higher in the area of the platform in both groups (Figure 5E).

The preference scores and CFC scores did not significantly differ between the 6MO and 14MO groups in either pool ($p > 0.05$, Mann–Whitney *t*-test) (Figures 5F,G). To address the possibility that in the test session with the local cues present, mice might have initially visited the goal cue but, in the absence of the platform, explored other locations in the pool, and this may have blurred the difference in the preference scores, we compared the preference scores obtained during the first 10 s of the 60-s test trial in the cdMWM task; no between-group differences in preference scores were observed in either pool ($p > 0.05$). Thus, while the cumulative time spent in the T quadrant was altered in 14MO mice in the blue pool (but not in the white pool), analysis of their behavior toward the cues did not show any difference compared to the 6MO mice, suggesting that memory in 14MO mice was similar to that of 6MO mice.

In summary, compared to the younger 6MO mice, 14MO mice exhibited intact learning in the sMWM task but showed deficits in the rMWM and cdMWM tasks. Furthermore, we did not find evidence of memory impairment in 14MO mice after multiple days of training in the sMWM, rMWM, and cdMWM tasks.

Hippocampal neurogenesis and the MWM task performance of individual mice

Certain aspects of learning and memory, particularly in complex settings, have been shown to rely on ongoing hippocampal neurogenesis. As the division of neural stem cells and production of new neurons in the DG continuously decline with age (Kuhn et al., 1996; Ben Abdallah et al., 2010; Encinas et al., 2011; Kirschen and Ge, 2019), it is plausible that age-related changes in animals' performance in the learning and memory tests are associated with the changes in hippocampal neurogenesis. Therefore, we investigated neurogenesis in 6MO and 14MO mice and explored its potential connection to their test performance.

Six weeks prior to the start of learning and memory training (i.e., 8 weeks at the time of the final cdMWM test, Figure 1), mice from both age groups were administered a synthetic thymidine analog EdU. Following completion of the test, the mice hippocampi were examined for the EdU labeling and expression of NeuN and DCX markers. The EdU signal identifies cells that were undergoing DNA duplication at the time of EdU administration, NeuN expression marks differentiated neurons in the DG, and DCX expression marks advanced neuronal precursors and immature neurons (Kronenberg et al., 2003; Encinas and Enikolopov, 2008; Podgorny et al., 2018). Thus, $EdU^+NeuN^+DCX^-$ cells correspond to newly generated fully differentiated mature neurons derived from progenitors that were dividing at the time of the EdU administration; DCX^+ cells encompass a broad range of neuronal precursors; and EdU^+DCX^+ cells correspond to neuronal precursors that were in the cell cycle at the time when the label was injected (representative images are shown in Figures 6A,B).

We found a significantly lower number of EdU^+, $EdU^+NeuN^+DCX^-$, and DCX^+ cells in the DG of 14MO mice compared to 6MO mice ($p < 0.0001$, $p = 0.0018$, and $p < 0.0001$, respectively) (Figures 6C–E), in line with previous reports (Bondolfi et al., 2004; van Praag et al., 2005; Gil-Mohapel et al., 2013). As expected, we did not detect any EdU^+DCX^+ cells in either group.

Notably, when we assessed the impact of between-sample variability on the total variability, we found that the $\frac{\text{mean } CE^2_{sampling}}{CV^2_{group}}$ ratio was lower than 0.5 for each cell count in either group: 0.282 and 0.25 for the EdU^+ cells in the 6MO and 14MO groups, respectively; 0.20 and 0.0133 for the $EdU^+NeuN^+DCX^-$ cells in the 6MO and 14MO, respectively; and 0.130 and 0.0803 for the DCX^+ cells in the 6MO and 14MO groups, respectively. This indicates that the variability introduced by the sampling procedure was less than half of the total variability, thus, supporting the validity of our cell counts (particularly relevant for the older animals).

Given the involvement of newly generated hippocampal neurons in a range of behavioral responses, we further investigated whether the number of newly produced cells in individual animals correlated with their performance in the learning and memory tasks. Specifically, we correlated the numbers of DCX^+ and $EdU^+NeuN^+DCX^-$ cells (representing immature and mature neurons, respectively) in each mouse with their escape latency and with their use of spatially precise strategies during the initial days of training in the sMWM, rMWM, and cdMWM tasks (day 1, day 6, and days 9–10 of the training sequence, respectively).

On the first day of training in sMWM we did not find a significant correlation (Spearman's *r* here and later) between the number of DCX^+ immature neurons in individual animals and their task performance (Figure 7A). Of note, the evident bimodal distribution of the cell counts reflects the difference in the number of these cells between the 6MO and 14MO groups.

During the initial training in rMWM, the correlation between the number of DCX^+ cells and the animal's escape latency or use of spatially precise search strategies did not reach statistical significance (Figure 7B, $r = -0.3643$, $p = 0.0801$, $r = 0.3867$, $p = 0.0619$, respectively). However, on the first and second days of training in cdMWM (in the blue and white pools, respectively), there were significant correlations between the number of DCX^+ cells and the escape latencies (Figure 7C (left graph), day 9: $r = -0.4292$; $p = 0.0364$; day 10: $r = -0.5576$; $p = 0.0046$). Additionally, there was a trend for a correlation between the number of DCX^+ cells and the use of spatially precise search strategies on the first day of cdMWM (Figure 7C (right graph), day 9: $r = 0.4023$, $p = 0.0513$), and a significant correlation on the second day of cdMWM (Figure 7C (right graph), day 10: $r = 0.4512$, $p = 0.0269$).

On the first day of training in the sMWM, the number of adult-born differentiated neurons ($EdU^+NeuN^+DCX^-$) was correlated with the escape latency, but not with the use of spatially precise search strategies ($r = -0.4774$, $p = 0.0183$ and $r = -0.1152$, $p = 0.5920$, respectively) (Figure 7D). The number of adult-born differentiated neurons ($EdU^+NeuN^+DCX^-$) showed correlations with the escape latency (Figure 7E, $r = -0.6649$, $p = 0.0004$) and the use of spatially precise search strategies ($r = 0.4567$, $p = 0.0249$) on the first day of training in the rMWM task. Furthermore, the number of mature neurons correlated with the average escape latency (day 9: $r = -0.6224$, $p = 0.0012$; day 10: $r = -0.4749$, $p = 0.0190$) and the use of spatially precise search strategies (day 9: $r = 0.6699$, $p = 0.0003$; day 10: $r = 0.4554$, $p = 0.0253$) during the initial days of training in cdMWM (Figure 7F). Moreover, when comparing the data for the mice in the two age groups, we found a significant correlation ($p = 0.0205$) and a highly significant correlation ($p < 0.0001$) between the number of

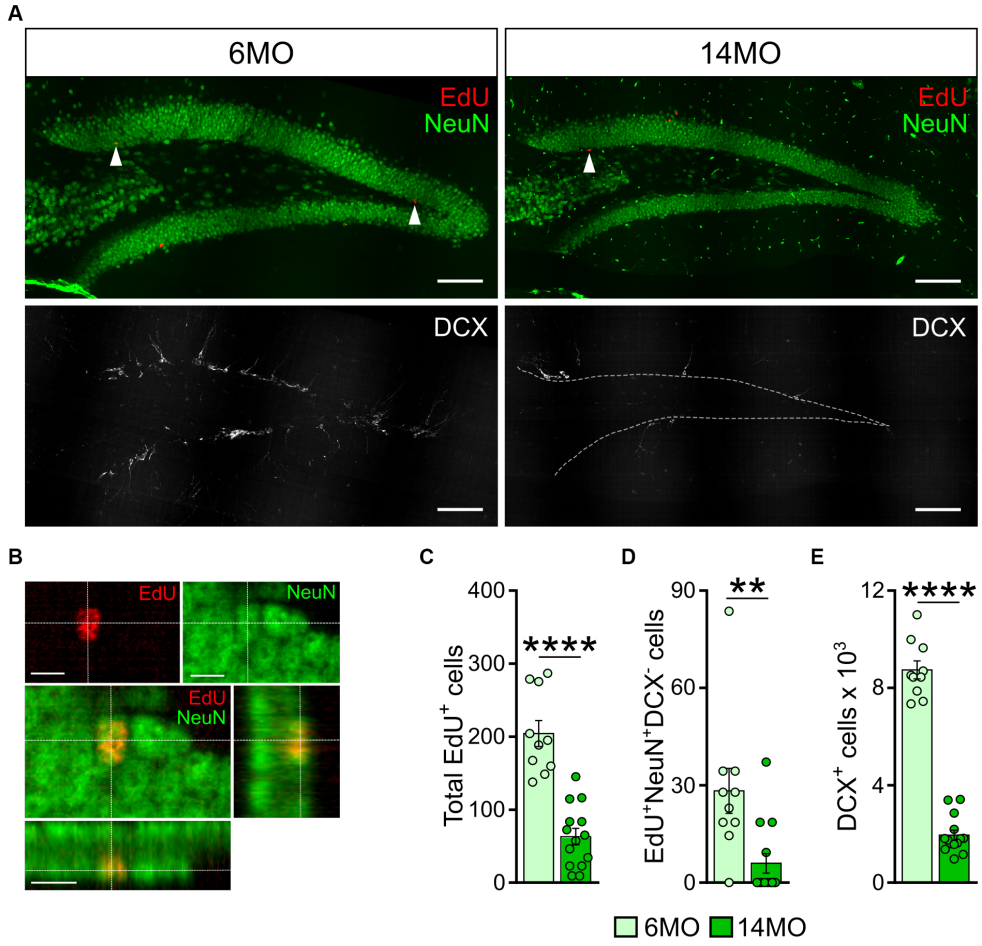

FIGURE 6
Neurogenesis in 6-and 14-month-old mice: **(A)** Images of sections from 6MO (left column) and 14MO (right column) mice stained for EdU, NeuN (top row), and DCX (bottom row); arrows on two top images indicate EdU$^+$ cells; white dash line in lower right image outlines the borders of the granule cell layer of the DG; scale bar – 100 μm; **(B)** Example confocal images and cross sections representing EdU labeling co-localized with NeuN expression in the same cell of the granule cell layer of the DG of a 14MO mouse; scale bar – 10 μm; **(C)** number of EdU$^+$-cells per DG; ****$p < 0.0001$; **(D)** Number of EdU$^+$NeuN$^+$DCX$^-$-cells (mature adult-born neurons) per DG, **$p < 0.01$; **(E)** Number of DCX$^+$ cells (immature adult-born neurons) per DG. ****$p < 0.0001$; **(C–E)** Data presented as Mean ± SEM, all comparisons – Mann–Whitney *t*-tests.

mature neurons and their escape latencies on day 6 of rMWM, and on days 9 and 10 of cdMWM, respectively, in individual 14MO mice but not in 6MO mice. Importantly, this correlation in 14MO mice disappeared by the end of training in each of these tasks (day 8 of rMWM, days 13 and 14 for cdMWM, all $p > 0.05$; not shown). Taken together, these findings suggest that individual animals with higher levels of adult-born immature and mature neurons perform better at the beginning of training in tasks that require flexible adaptation to the changed demands of the task.

Discussion

Our results highlight a decline in cognitive flexibility during the adult period of mice lifespan. This decline is manifested as a reduced ability to adjust previous experiences in order to solve tasks that involve new combinations of familiar cues and contexts. Notably, the impairment of cognitive flexibility in older animals can be partially mitigated through additional training. Furthermore, our results suggest a correlation between the decline in cognitive flexibility within individual animals and a decrease in the numbers of recently generated mature neurons or immature neuronal precursors in their hippocampi. Together, our results suggest that while adult hippocampal neurogenesis may not be essential for learning a new task, it plays a critical role in circumstances that require the modification of previously acquired experience.

We focused our investigation on mature adult-middle age period of the mice lifespan (6 and 14 month at the start of the training series) to mitigate the effect of some of the confounding factors of the young and old age (e.g., sexual maturation, continuous growth, and metabolic changes in younger mice and increase in the markers of senescence and inflammation and decrease in locomotor activity and grip strength in older mice) (Flurkey et al., 2007; Yanai and Endo, 2021). Furthermore, this period is also characterized by the least relative changes in various behavioral tests related to learning and memory, anxiety, and pain sensitivity (e.g., MWM, Barnes maze, fear conditioning, open field, marble burying, shock sensitivity) (Yanai and Endo, 2021). Indeed, consistent with previous studies (Frick et al., 2000; de Fiebre et al., 2006; Driscoll et al., 2006; Gil-Mohapel et al., 2013; Shoji and Miyakawa, 2019;

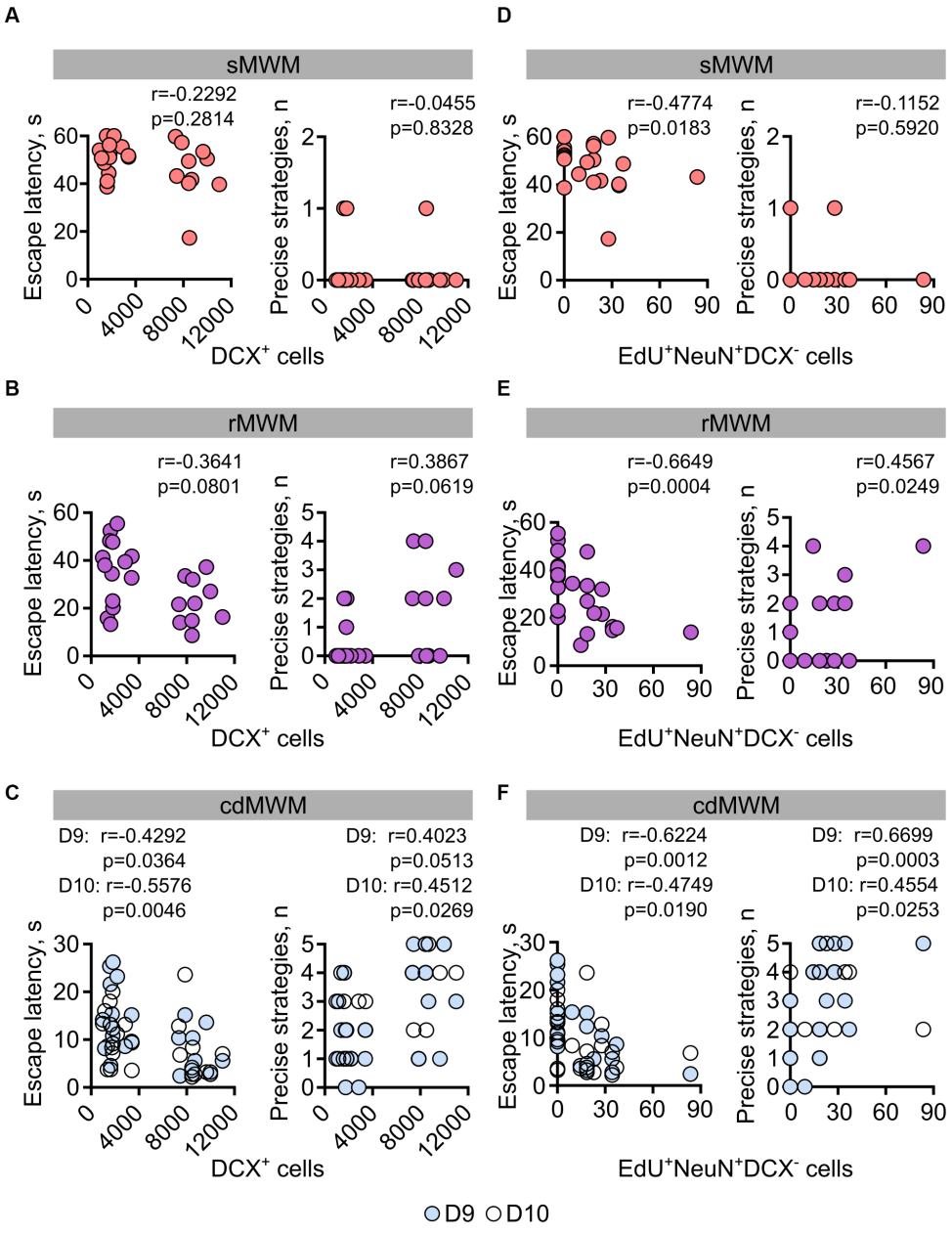

FIGURE 7
Correlation analysis (Spearman's *r*) for mice individual performance parameters on the first days of training in: **(A,D)** – sMWM; **(B,E)** –rMWM, **(C,F)** – in cdMWM with the numbers of adult-born immature (DCX⁺) and mature (EdU⁺NeuN⁺DCX⁻) neurons.

Yanai and Endo, 2021), we did not observe learning or memory deficits in the older group compared to the younger group in the conventional spatial version of the MWM (sMWM). We also did not detect aging effects on the repertoire of search strategies in the sMWM, furthermore, in both groups we observed a gradual increase of spatially precise search strategies during the learning trials, in line with published findings (Garthe et al., 2009; Garthe and Kempermann, 2013; Gil-Mohapel et al., 2013; Bowers et al., 2020). Moreover, the responses of both age groups were similar across all metrics that we used to assess mice behavior.

However, differences between the age groups were detected when mice were tested in the reversal version of the MWM (rMWM), which requires a degree of cognitive flexibility. Older mice exhibited longer escape latencies, a reliance on spatially imprecise search strategies, and increased IPE compared to younger mice. Interestingly, the difference between the groups was evident only at the beginning of the rMWM training, with the difference in corresponding metrics becoming non-significant by the end of training. Of note, the differences in reversal learning in the MWM have been reported for mice of contrasting ages (2 and 18 months) (Hamieh et al., 2021), but not when comparing mature adult and aged mice (Frick et al., 2000; de Fiebre et al., 2006; Shoji and Miyakawa, 2019).

The differences between older and younger mice were particularly evident in the cdMWM task (Amelchenko et al., 2023), which introduced additional variables such as alternating local cues and contexts and required further reevaluation and adjustment of the previously successful strategies. The older mice exhibited impaired

performance during learning, as compared to the younger mice; this was evident across multiple metrics, including escape latency, the use of spatially imprecise search strategies during training, odds ratio of using efficient strategies, IPE, and time spent in the correct quadrant during the memory test (Figure 5). Similar to the rMWM task, the performance gap between the age groups diminished with additional training (which may explain comparable memory scores in both groups). Note that if the cdMWM had been presented as the first task, without prior exposure to the sMWM or rMWM, it would have primarily assessed the mice's capacity for learning and memory, rather than cognitive flexibility which involves exposure to preceding rounds of learning and the ability to readjust the learned strategy in a novel setting.

Our findings demonstrate a remarkable degree of correlation between the level of hippocampal neurogenesis in individual animals and their performance in tasks that rely on cognitive flexibility (Figure 7), in line with previous reports (Drapeau et al., 2003; Leuner et al., 2004; Gil-Mohapel et al., 2013). Notably, this correlation was only partially revealed in allegedly simpler tasks that focus on efficient learning and memory, but, unlike cdMWM, do not require (sMWM) or have a lesser requirement for (rMWM) the reevaluation of previously acquired knowledge and adaption to new environment. Moreover, our results suggest that cells at different stages of neuronal differentiation play distinct roles in tasks requiring cognitive flexibility: specifically, the number of immature DCX^+ hippocampal neurons correlated with individual animals' performance in the cdMWM task, but not in the sMWM or rMWM tasks; in contrast, the number of mature EdU^+ neurons correlated with performance in all three tasks.

Potentially, the increased physical activity and enriched environment during the training period and process of learning itself may affect the cascade of neuronal differentiation at various stages: stem and progenitor cell division, selective cell elimination, differentiation, and maturation of the young neurons of different ontogenic age and their integration into the preexisting circuitry (Kempermann et al., 1997; van Praag et al., 1999; Bergami et al., 2015; Denoth-Lippuner and Jessberger, 2021). In our experimental setting this might be particularly relevant to the DCX^+ population, the bulk of which was born and has been maturing during the training period and therefore may be affected by the tasks themselves. However, the $EdU^+NeuN^+DCX^-$ cells correspond to the cohort that was born at the time of the EdU administration, i.e., 6 weeks before the start of the training sequence, and have already differentiated and matured by the start of the training sequence; thus, their number is unlikely to be affected by the training process.

Interestingly, the correlation between neurogenesis and performance was specifically observed in the older animals. Notably, in older mice the correlation between the number of differentiated neurons and escape latency was present during the first days of training (day 6 for rMWM and days 9 and 10 for cdMWM) but disappeared by the end of training (days 8 for rMWM and days 13 and 14 for cdMWM). This may indicate that mature adult-born neurons are crucial when the animal is adjusting its relevant experience but become less critical at the later stages, when the performance of older animals approaches that of younger ones. Together, our results provide further evidence for the association between hippocampal neurogenesis and cognitive flexibility, particularly in older animals.

Our study underscores the importance of employing multiple metrics to characterize animal behavior in complex tasks, such as those assessing cognitive flexibility. Studies in which the escape latency, determined at a single time point, serves as a sole measure of the animals' performance, may miss important differences. Dissecting the animals' patterns of spatial navigation into defined spatially precise and spatially imprecise (and thus efficient and inefficient, respectively) strategies and following them across each trial reveals fine differences and provides critical insights into the learning process (Garthe et al., 2009; Garthe and Kempermann, 2013; Gil-Mohapel et al., 2013; Cooke et al., 2019; Berdugo-Vega et al., 2020; Bowers et al., 2020; Hernandez-Mercado and Zepeda, 2021; Yanai and Endo, 2021; Villarreal-Silva et al., 2022). Supplementing these parameters with additional metrics, such as OR, IPE, comparison of quadrant time distribution, path heatmaps, preference score, CFC score, and the correlation analysis between individual animals' performance and their level of hippocampal neurogenesis, offers a more comprehensive and precise representation of learning, memory, and cognitive flexibility.

Data availability statement

The raw data supporting the conclusions of this article will be made available by the authors, without undue reservation.

Ethics statement

The animal study was approved by Institutional Animal Care and Use Committee of the Stony Brook University. The study was conducted in accordance with the local legislation and institutional requirements.

Author contributions

EA, DB, KA, GE, and AL designed the experiments. EA, DB, OC, and AL performed experiments. GE and KA provided funding. All authors interpreted the results, made direct, and intellectual contribution to the project, and approved the final version of the manuscript.

Funding

This study was supported by grants R01 AG057705-01 and R01 AG076937-01 to GE from the National Institute on Aging and by grant 20-15-00283 to DB and KA (learning and memory tasks in aged mice) from the Russian Science Foundation.

Acknowledgments

The authors thank Yulia Orlova and Lidiya Zamyatina for technical assistance. The authors thank Jie Yang (Renaissance School of Medicine at Stony Brook University Biostatistical Consulting Core) for her consultation on statistical analysis.

Conflict of interest

The authors declare that the research was conducted in the absence of any commercial or financial relationships that could be construed as a potential conflict of interest.

Publisher's note

References

Aimone, J. B., Li, Y., Lee, S. W., Clemenson, G. D., Deng, W., and Gage, F. H. (2014). Regulation and function of adult neurogenesis: from genes to cognition. *Physiol. Rev.* 94, 991–1026. doi: 10.1152/physrev.00004.2014

Akers, K. G., Martinez-Canabal, A., Restivo, L., Yiu, A. P., De Cristofaro, A., Hsiang, H. L., et al. (2014). Hippocampal neurogenesis regulates forgetting during adulthood and infancy. *Science* 344, 598–602. doi: 10.1126/science.1248903

Amelchenko, E., Bezrriadnov, D. V., Chekhov, O. A., Ivanova, A., Kedrov, A. V., Anokhin, K. V., et al. (2023). Cognitive flexibility is selectively impaired by radiation and is associated with differential recruitment of adult-born neurons. *J. Neurosci. Press.* doi: 10.1523/JNEUROSCI.0161-22.2023

Anacker, C., and Hen, R. (2017). Adult hippocampal neurogenesis and cognitive flexibility – linking memory and mood. *Nat. Rev. Neurosci.* 18, 335–346. doi: 10.1038/nrn.2017.45

Arruda-Carvalho, M., Sakaguchi, M., Akers, K. G., Josselyn, S. A., and Frankland, P. W. (2011). Posttraining ablation of adult-generated neurons degrades previously acquired memories. *J. Neurosci.* 31, 15113–15127. doi: 10.1523/JNEUROSCI.3432-11.2011

Basler, L., Gerdes, S., Wolfer, D. P., and Slomianka, L. (2017). Sampling the mouse hippocampal dentate gyrus. *Front. Neuroanat.* 11:123. doi: 10.3389/fnana.2017.00123

Ben Abdallah, N. M., Slomianka, L., Vyssotski, A. L., and Lipp, H. P. (2010). Early age-related changes in adult hippocampal neurogenesis in C57 mice. *Neurobiol. Aging* 31, 151–161. doi: 10.1016/j.neurobiolaging.2008.03.002

Berdugo-Vega, G., Arias-Gil, G., Lopez-Fernandez, A., Artegiani, B., Wasielewska, J. M., Lee, C. C., et al. (2020). Increasing neurogenesis refines hippocampal activity rejuvenating navigational learning strategies and contextual memory throughout life. *Nat. Commun.* 11:135. doi: 10.1038/s41467-019-14026-z

Bergami, M., Masserdotti, G., Temprana, S. G., Motori, E., Eriksson, T. M., Gobel, J., et al. (2015). A critical period for experience-dependent remodeling of adult-born neuron connectivity. *Neuron* 85, 710–717. doi: 10.1016/j.neuron.2015.01.001

Boldrini, M., Fulmore, C. A., Tartt, A. N., Simeon, L. R., Pavlova, I., Poposka, V., et al. (2018). Human hippocampal neurogenesis persists throughout aging. *Cell Stem Cell* 22:e585, 589–599.e5. doi: 10.1016/j.stem.2018.03.015

Bondolfi, L., Ermini, F., Long, J. M., Ingram, D. K., and Jucker, M. (2004). Impact of age and caloric restriction on neurogenesis in the dentate gyrus of C57BL/6 mice. *Neurobiol. Aging* 25, 333–340. doi: 10.1016/S0197-4580(03)00083-6

Bottes, S., Jaeger, B. N., Pilz, G. A., Jorg, D. J., Cole, J. D., Kruse, M., et al. (2021). Long-term self-renewing stem cells in the adult mouse hippocampus identified by intravital imaging. *Nat. Neurosci.* 24, 225–233. doi: 10.1038/s41593-020-00759-4

Bowers, M., Liang, T., Gonzalez-Bohorquez, D., Zocher, S., Jaeger, B. N., Kovacs, W. J., et al. (2020). FASN-dependent lipid metabolism links neurogenic stem/progenitor cell activity to learning and memory deficits. *Cell Stem Cell* 27:e111, 98–109.e11. doi: 10.1016/j.stem.2020.04.002

Burghardt, N. S., Park, E. H., Hen, R., and Fenton, A. A. (2012). Adult-born hippocampal neurons promote cognitive flexibility in mice. *Hippocampus* 22, 1795–1808. doi: 10.1002/hipo.22013

Clelland, C. D., Choi, M., Romberg, C., Clemenson, G. D. Jr., Fragniere, A., Tyers, P., et al. (2009). A functional role for adult hippocampal neurogenesis in spatial pattern separation. *Science* 325, 210–213. doi: 10.1126/science.1173215

Cooke, M. B., Oleary, T. P., Harris, P., Ma, R., Brown, R. E., and Snyder, J. S. (2019). Pathfinder: open source software for analyzing spatial navigation search strategies. *F1000Res* 8:1521. doi: 10.12688/f1000research.20352.1

De Fiebre, N. C., Sumien, N., Forster, M. J., and De Fiebre, C. M. (2006). Spatial learning and psychomotor performance of C57BL/6 mice: age sensitivity and reliability of individual differences. *Age (Dordr.)* 28, 235–253. doi: 10.1007/s11357-006-9027-3

Denoth-Lippuner, A., and Jessberger, S. (2021). Formation and integration of new neurons in the adult hippocampus. *Nat. Rev. Neurosci.* 22, 223–236. doi: 10.1038/s41583-021-00433-z

Drapeau, E., Mayo, W., Aurousseau, C., Le Moal, M., Piazza, P. V., and Abrous, D. N. (2003). Spatial memory performances of aged rats in the water maze predict levels of hippocampal neurogenesis. *Proc. Natl. Acad. Sci. U. S. A.* 100, 14385–14390. doi: 10.1073/pnas.2334169100

Driscoll, I., Howard, S. R., Stone, J. C., Monfils, M. H., Tomanek, B., Brooks, W. M., et al. (2006). The aging hippocampus: a multi-level analysis in the rat. *Neuroscience* 139, 1173–1185. doi: 10.1016/j.neuroscience.2006.01.040

Encinas, J. M., and Enikolopov, G. (2008). Identifying and quantitating neural stem and progenitor cells in the adult brain. *Methods Cell Biol.* 85, 243–272. doi: 10.1016/S0091-679X(08)85011-X

Encinas, J. M., Michurina, T. V., Peunova, N., Park, J. H., Tordo, J., Peterson, D. A., et al. (2011). Division-coupled astrocytic differentiation and age-related depletion of neural stem cells in the adult hippocampus. *Cell Stem Cell* 8, 566–579. doi: 10.1016/j.stem.2011.03.010

Encinas, J. M., Vaahtokari, A., and Enikolopov, G. (2006). Fluoxetine targets early progenitor cells in the adult brain. *Proc. Natl. Acad. Sci. U. S. A.* 103, 8233–8238. doi: 10.1073/pnas.0601992103

Enikolopov, G., Overstreet-Wadiche, L., and Ge, S. (2015). Viral and transgenic reporters and genetic analysis of adult neurogenesis. *Cold Spring Harb. Perspect. Biol.* 7:a018804. doi: 10.1101/cshperspect.a018804

Epp, J. R., Silva Mera, R., Kohler, S., Josselyn, S. A., and Frankland, P. W. (2016). Neurogenesis-mediated forgetting minimizes proactive interference. *Nat. Commun.* 7:10838. doi: 10.1038/ncomms10838

Flurkey, K., Currer, J. M., and Harrison, D. E. (2007). Mouse models in aging research. *Mouse Biomed. Res.* III, 637–672. doi: 10.1016/B978-012369454-6/50074-1

Frick, K. M., Burlingame, L. A., Arters, J. A., and Berger-Sweeney, J. (2000). Reference memory, anxiety and estrous cyclicity in C57BL/6NIA mice are affected by age and sex. *Neuroscience* 95, 293–307. doi: 10.1016/S0306-4522(99)00418-2

Garthe, A., Behr, J., and Kempermann, G. (2009). Adult-generated hippocampal neurons allow the flexible use of spatially precise learning strategies. *PLoS One* 4:e5464. doi: 10.1371/journal.pone.0005464

Garthe, A., Huang, Z., Kaczmarek, L., Filipkowski, R. K., and Kempermann, G. (2014). Not all water mazes are created equal: cyclin D2 knockout mice with constitutively suppressed adult hippocampal neurogenesis do show specific spatial learning deficits. *Genes Brain Behav.* 13, 357–364. doi: 10.1111/gbb.12130

Garthe, A., and Kempermann, G. (2013). An old test for new neurons: refining the Morris water maze to study the functional relevance of adult hippocampal neurogenesis. *Front. Neurosci.* 7:63. doi: 10.3389/fnins.2013.00063

Garthe, A., Roeder, I., and Kempermann, G. (2016). Mice in an enriched environment learn more flexibly because of adult hippocampal neurogenesis. *Hippocampus* 26, 261–271. doi: 10.1002/hipo.22520

Gil-Mohapel, J., Brocardo, P. S., Choquette, W., Gothard, R., Simpson, J. M., and Christie, B. R. (2013). Hippocampal neurogenesis levels predict WATERMAZE search strategies in the aging brain. *PLoS One* 8:e75125. doi: 10.1371/journal.pone.0075125

Hamieh, A. M., Camperos, E., Hernier, A. M., and Castagne, V. (2021). C57BL/6 mice as a preclinical model to study age-related cognitive deficits: executive functions impairment and inter-individual differences. *Brain Res.* 1751:147173. doi: 10.1016/j.brainres.2020.147173

Hernandez-Mercado, K., and Zepeda, A. (2021). Morris water maze and contextual fear conditioning tasks to evaluate cognitive functions associated with adult hippocampal neurogenesis. *Front. Neurosci.* 15:782947. doi: 10.3389/fnins.2021.782947

Ibrayeva, A., Bay, M., Pu, E., Jorg, D. J., Peng, L., Jun, H., et al. (2021). Early stem cell aging in the mature brain. *Cell Stem Cell* 28:e957, 955–966.e7. doi: 10.1016/j.stem.2021.03.018

Ivanova, A., Gruzova, O., Ermolaeva, E., Astakhova, O., Itaman, S., Enikolopov, G., et al. (2022). Synthetic thymidine analog labeling without misconceptions. *Cells* 11:1888. doi: 10.3390/cells11121888

Kempermann, G., Gage, F. H., Aigner, L., Song, H., Curtis, M. A., Thuret, S., et al. (2018). Human adult neurogenesis: evidence and remaining questions. *Cell Stem Cell* 23, 25–30. doi: 10.1016/j.stem.2018.04.004

Kempermann, G., Kuhn, H. G., and Gage, F. H. (1997). More hippocampal neurons in adult mice living in an enriched environment. *Nature* 386, 493–495. doi: 10.1038/386493a0

Kirschen, G. W., and Ge, S. (2019). Young at heart: insights into hippocampal neurogenesis in the aged brain. *Behav. Brain Res.* 369:111934. doi: 10.1016/j.bbr.2019.111934

Koehl, M., Ladeveze, E., Montcouquiol, M., and Abrous, D. N. (2022). Vangl2, a Core component of the WNT/PCP pathway, regulates adult hippocampal neurogenesis and age-related decline in cognitive flexibility. *Front. Aging Neurosci.* 14:844255. doi: 10.3389/fnagi.2022.844255

Kronenberg, G., Reuter, K., Steiner, B., Brandt, M. D., Jessberger, S., Yamaguchi, M., et al. (2003). Subpopulations of proliferating cells of the adult hippocampus respond differently to physiologic neurogenic stimuli. *J. Comp. Neurol.* 467, 455–463. doi: 10.1002/cne.10945

Kuhn, H. G., Dickinson-Anson, H., and Gage, F. H. (1996). Neurogenesis in the dentate gyrus of the adult rat: age-related decrease of neuronal progenitor proliferation. *J. Neurosci.* 16, 2027–2033. doi: 10.1523/JNEUROSCI.16-06-02027.1996

Lazutkin, A., Podgorny, O., and Enikolopov, G. (2019). Modes of division and differentiation of neural stem cells. *Behav. Brain Res.* 374:112118. doi: 10.1016/j.bbr.2019.112118

Leuner, B., Mendolia-Loffredo, S., Kozorovitskiy, Y., Samburg, D., Gould, E., and Shors, T. J. (2004). Learning enhances the survival of new neurons beyond the time when the hippocampus is required for memory. *J. Neurosci.* 24, 7477–7481. doi: 10.1523/JNEUROSCI.0204-04.2004

Lods, M., Pacary, E., Mazier, W., Farrugia, F., Mortessagne, P., Masachs, N., et al. (2021). Adult-born neurons immature during learning are necessary for remote memory reconsolidation in rats. *Nat. Commun.* 12:1778. doi: 10.1038/s41467-021-22069-4

Maugard, M., Doux, C., and Bonvento, G. (2019). A new statistical method to analyze Morris water maze data using Dirichlet distribution. *F1000Res* 8:1601. doi: 10.12688/f1000research.20072.2

Mcavoy, K. M., and Sahay, A. (2017). Targeting adult neurogenesis to optimize hippocampal circuits in aging. *Neurotherapeutics* 14, 630–645. doi: 10.1007/s13311-017-0539-6

Mcavoy, K. M., Scobie, K. N., Berger, S., Russo, C., Guo, N., Decharatanachart, P., et al. (2016). Modulating neuronal competition dynamics in the dentate gyrus to rejuvenate aging memory circuits. *Neuron* 91, 1356–1373. doi: 10.1016/j.neuron.2016.08.009

Mcquail, J. A., Dunn, A. R., Stern, Y., Barnes, C. A., Kempermann, G., Rapp, P. R., et al. (2020). Cognitive Reserve in Model Systems for mechanistic discovery: the importance of longitudinal studies. *Front. Aging Neurosci.* 12:607685. doi: 10.3389/fnagi.2020.607685

Mignone, J. L., Kukekov, V., Chiang, A. S., Steindler, D., and Enikolopov, G. (2004). Neural stem and progenitor cells in nestin-GFP transgenic mice. *J. Comp. Neurol.* 469, 311–324. doi: 10.1002/cne.10964

Montaron, M. F., Charrier, V., Blin, N., Garcia, P., and Abrous, D. N. (2020). Responsiveness of dentate neurons generated throughout adult life is associated with resilience to cognitive aging. *Aging Cell* 19:e13161. doi: 10.1111/acel.13161

Motulsky, H. J., and Brown, R. E. (2006). Detecting outliers when fitting data with nonlinear regression – a new method based on robust nonlinear regression and the false discovery rate. *BMC Bioinformatics* 7:123. doi: 10.1186/1471-2105-7-123

Niibori, Y., Yu, T. S., Epp, J. R., Akers, K. G., Josselyn, S. A., and Frankland, P. W. (2012). Suppression of adult neurogenesis impairs population coding of similar contexts in hippocampal CA3 region. *Nat. Commun.* 3:1253. doi: 10.1038/ncomms2261

Nyberg, L., and Pudas, S. (2019). Successful memory aging. *Annu. Rev. Psychol.* 70, 219–243. doi: 10.1146/annurev-psych-010418-103052

Pilz, G. A., Bottes, S., Betizeau, M., Jorg, D. J., Carta, S., Simons, B. D., et al. (2018). Live imaging of neurogenesis in the adult mouse hippocampus. *Science* 359, 658–662. doi: 10.1126/science.aao5056

Podgorny, O., Peunova, N., Park, J. H., and Enikolopov, G. (2018). Triple S-phase labeling of dividing stem cells. *Stem Cell Rep.* 10, 615–626. doi: 10.1016/j.stemcr.2017.12.020

Sahay, A., Scobie, K. N., Hill, A. S., O'carroll, C. M., Kheirbek, M. A., Burghardt, N. S., et al. (2011a). Increasing adult hippocampal neurogenesis is sufficient to improve pattern separation. *Nature* 472, 466–470. doi: 10.1038/nature09817

Sahay, A., Wilson, D. A., and Hen, R. (2011b). Pattern separation: a common function for new neurons in hippocampus and olfactory bulb. *Neuron* 70, 582–588. doi: 10.1016/j.neuron.2011.05.012

Salic, A., and Mitchison, T. J. (2008). A chemical method for fast and sensitive detection of DNA synthesis *in vivo*. *Proc. Natl. Acad. Sci. U. S. A.* 105, 2415–2420. doi: 10.1073/pnas.0712168105

Salthouse, T. A. (2009). When does age-related cognitive decline begin? *Neurobiol. Aging* 30, 507–514. doi: 10.1016/j.neurobiolaging.2008.09.023

Samson, R. D., and Barnes, C. A. (2013). Impact of aging brain circuits on cognition. *Eur. J. Neurosci.* 37, 1903–1915. doi: 10.1111/ejn.12183

Saxe, M. D., Battaglia, F., Wang, J. W., Malleret, G., David, D. J., Monckton, J. E., et al. (2006). Ablation of hippocampal neurogenesis impairs contextual fear conditioning and synaptic plasticity in the dentate gyrus. *Proc. Natl. Acad. Sci. U. S. A.* 103, 17501–17506. doi: 10.1073/pnas.0607207103

Shetty, A. K., Kodali, M., Upadhya, R., and Madhu, L. N. (2018). Emerging anti-aging strategies-scientific basis and efficacy. *Aging Dis.* 9, 1165–1184. doi: 10.14336/AD.2018.1026

Shoji, H., and Miyakawa, T. (2019). Age-related behavioral changes from young to old age in male mice of a C57BL/6J strain maintained under a genetic stability program. *Neuropsychopharmacol. Rep.* 39, 100–118. doi: 10.1002/npr2.12052

Slomianka, L. (2021). Basic quantitative morphological methods applied to the central nervous system. *J. Comp. Neurol.* 529, 694–756. doi: 10.1002/cne.24976

Slomianka, L., and West, M. J. (2005). Estimators of the precision of stereological estimates: an example based on the CA1 pyramidal cell layer of rats. *Neuroscience* 136, 757–767. doi: 10.1016/j.neuroscience.2005.06.086

Sorrells, S. F., Paredes, M. F., Cebrian-Silla, A., Sandoval, K., Qi, D., Kelley, K. W., et al. (2018). Human hippocampal neurogenesis drops sharply in children to undetectable levels in adults. *Nature* 555, 377–381. doi: 10.1038/nature25975

Tobin, M. K., Musaraca, K., Disouky, A., Shetti, A., Bheri, A., Honer, W. G., et al. (2019). Human hippocampal neurogenesis persists in aged adults and Alzheimer's disease patients. *Cell Stem Cell* 24:e973, 974–982.e3. doi: 10.1016/j.stem.2019.05.003

Toda, T., Parylak, S. L., Linker, S. B., and Gage, F. H. (2019). The role of adult hippocampal neurogenesis in brain health and disease. *Mol. Psychiatry* 24, 67–87. doi: 10.1038/s41380-018-0036-2

Tronel, S., Belnoue, L., Grosjean, N., Revest, J. M., Piazza, P. V., Koehl, M., et al. (2012). Adult-born neurons are necessary for extended contextual discrimination. *Hippocampus* 22, 292–298. doi: 10.1002/hipo.20895

Urban, N., Blomfield, I. M., and Guillemot, F. (2019). Quiescence of adult mammalian neural stem cells: a highly regulated rest. *Neuron* 104, 834–848. doi: 10.1016/j.neuron.2019.09.026

Van Praag, H., Kempermann, G., and Gage, F. H. (1999). Running increases cell proliferation and neurogenesis in the adult mouse dentate gyrus. *Nat. Neurosci.* 2, 266–270. doi: 10.1038/6368

Van Praag, H., Shubert, T., Zhao, C., and Gage, F. H. (2005). Exercise enhances learning and hippocampal neurogenesis in aged mice. *J. Neurosci.* 25, 8680–8685. doi: 10.1523/JNEUROSCI.1731-05.2005

Villarreal-Silva, E. E., Gonzalez-Navarro, A. R., Salazar-Ybarra, R. A., Quiroga-Garcia, O., Cruz-Elizondo, M. A. J., Garcia-Garcia, A., et al. (2022). Aged rats learn Morris water maze using non-spatial search strategies evidenced by a parameter-based algorithm. *Transl. Neurosci.* 13, 134–144. doi: 10.1515/tnsci-2022-0221

Wu, Y., Bottes, S., Fisch, R., Zehnder, C., Cole, J. D., Pilz, G. A., et al. (2023). Chronic *in vivo* imaging defines age-dependent alterations of neurogenesis in the mouse hippocampus. *Nat. Aging* 3, 380–390. doi: 10.1038/s43587-023-00370-9

Yanai, S., and Endo, S. (2021). Functional aging in male C57BL/6J mice across the life-span: a systematic behavioral analysis of motor, emotional, and memory function to define an aging phenotype. *Front. Aging Neurosci.* 13:697621. doi: 10.3389/fnagi.2021.697621

Yu, R. Q., Cooke, M., Seib, D. R., Zhao, J., and Snyder, J. S. (2019). Adult neurogenesis promotes efficient, nonspecific search strategies in a spatial alternation water maze task. *Behav. Brain Res.* 376:112151. doi: 10.1016/j.bbr.2019.112151

frontiers | Frontiers in Neuroscience

TYPE Original Research
PUBLISHED 17 August 2023
DOI 10.3389/fnins.2023.1237176

OPEN ACCESS

EDITED BY
Ashok K. Shetty,
Texas A&M University School of Medicine, United States

REVIEWED BY
Jianqin Niu,
Army Medical University, China
Walter Low,
University of Minnesota Twin Cities, United States
Henrik Ahlenius,
Lund University, Sweden

*CORRESPONDENCE
Daniel A. Peterson
✉ daniel.peterson@rosalindfranklin.edu

†PRESENT ADDRESS
Stanley F. Bazarek,
Department of Neurosurgery, Brigham and Women's Hospital, Harvard Medical School, Boston, MA, United States

RECEIVED 09 June 2023
ACCEPTED 31 July 2023
PUBLISHED 17 August 2023

CITATION
Bazarek SF, Thaqi M, King P, Mehta AR, Patel R, Briggs CA, Reisenbigler E, Yousey JE, Miller EA, Stutzmann GE, Marr RA and Peterson DA (2023) Engineered neurogenesis in naïve adult rat cortex by Ngn2-mediated neuronal reprogramming of resident oligodendrocyte progenitor cells.
Front. Neurosci. 17:1237176.
doi: 10.3389/fnins.2023.1237176

Engineered neurogenesis in naïve adult rat cortex by Ngn2-mediated neuronal reprogramming of resident oligodendrocyte progenitor cells

Stanley F. Bazarek[1†], Mentor Thaqi[1,2], Patrick King[1,2], Amol R. Mehta[1], Ronil Patel[1], Clark A. Briggs[2], Emily Reisenbigler[1,2], Jonathon E. Yousey[1,2], Elis A. Miller[1], Grace E. Stutzmann[1,2], Robert A. Marr[1,2] and Daniel A. Peterson[1,2*]

[1]Center for Stem Cell and Regenerative Medicine, The Chicago Medical School, Rosalind Franklin University of Medicine and Science, North Chicago, IL, United States, [2]Center for Neurodegenerative Disease and Therapeutics, The Chicago Medical School, Rosalind Franklin University of Medicine and Science, North Chicago, IL, United States

Adult tissue stem cells contribute to tissue homeostasis and repair but the long-lived neurons in the human adult cerebral cortex are not replaced, despite evidence for a limited regenerative response. However, the adult cortex contains a population of proliferating oligodendrocyte progenitor cells (OPCs). We examined the capacity of rat cortical OPCs to be re-specified to a neuronal lineage both *in vitro* and *in vivo*. Expressing the developmental transcription factor Neurogenin2 (Ngn2) in OPCs isolated from adult rat cortex resulted in their expression of early neuronal lineage markers and genes while downregulating expression of OPC markers and genes. Ngn2 induced progression through a neuronal lineage to express mature neuronal markers and functional activity as glutamatergic neurons. *In vivo* retroviral gene delivery of Ngn2 to naive adult rat cortex ensured restricted targeting to proliferating OPCs. Ngn2 expression in OPCs resulted in their lineage re-specification and transition through an immature neuronal morphology into mature pyramidal cortical neurons with spiny dendrites, axons, synaptic contacts, and subtype specification matching local cytoarchitecture. Lineage re-specification of rat cortical OPCs occurred without prior injury, demonstrating these glial progenitor cells need not be put into a reactive state to achieve lineage reprogramming. These results show it may be feasible to precisely engineer additional neurons directly in adult cerebral cortex for experimental study or potentially for therapeutic use to modify dysfunctional or damaged circuitry.

KEYWORDS

oligodendrocyte precursor cell, NeuroD1 transcription factor, Neurogenin 2, NG2 cell, reprogramming and differentiation, neuronal replacement, neural stem/progenitor cells

Introduction

Direct *in vivo* reprogramming of resident tissue cells to re-specify cell lineage has been achieved in the pancreas (Zhou et al., 2008) and heart (Qian et al., 2012; Song et al., 2012), providing a potential approach to therapeutic cell replacement that could avoid the immunogenicity, time, and expense of grafting exogenous cells (Bazarek and Peterson, 2014; Torper and Gotz, 2017). However, neurons are specified into highly distinct subtypes (Molyneaux et al., 2007) and effective neuronal replacement will require engineering authentic, subtype-specific neurons (Bazarek and Peterson, 2014). Whereas neuronal turnover has been demonstrated in adult human hippocampus (Eriksson et al., 1998) and striatum (Ernst et al., 2014), the human cerebral cortex is normally devoid of adult neurogenesis (Kornack and Rakic, 2001; Bhardwaj et al., 2006) with a limited regenerative response reported following ischemic cortical injury (Jin et al., 2006; Lindvall and Kokaia, 2015).

The demonstration that expressing select developmental transcription factors in cultured mouse astrocytes resulted in their conversion to functional, subtype-specific neurons (Heins et al., 2002; Heinrich et al., 2010; Kempf et al., 2021) suggested that direct *in vivo* conversion of resident glia to neurons could be a potential approach for brain repair Indeed, a growing number of studies show *in vivo* conversion of astrocytes to various neuronal subtypes in mouse spinal cord (Tai et al., 2021; Zhou et al., 2021) and mouse striatum (Giehrl-Schwab et al., 2022; Zhang et al., 2022). Reprogramming in the cerebral cortex and hippocampus reportedly requires the targeted glia to be in a reactive state to achieve neuronal induction (Buffo et al., 2005; Grande et al., 2013; Guo et al., 2013; Heinrich et al., 2014; Lentini et al., 2021). However, injury responses are highly variable and poorly defined and may not feature in dysregulated circuitry, such as epilepsy, addictive disorders, and psychiatric disorders, where newly engineered neurons could play a modulatory role (Southwell et al., 2014).

Despite reports of success with neuronal reprogramming in a number of brain regions, approaches to direct *in vivo* reprogramming have recently come under criticism. The controversy largely stems from a lack of certitude that pre-existing neurons were not inadvertently targeted, as this would make interpretation of the outcomes problematic (Calzolari and Berninger, 2021; Wang et al., 2021; Chen et al., 2022; Cooper and Berninger, 2022). Suggested considerations to allay concerns in further studies included demonstrating cell-specific targeting of reprogramming factors and demonstrating progression from early to late neuronal lineage states as confirmation of an induced neuron.

With this perspective in mind, we undertook a study to reprogram oligodendrocyte progenitor cells (OPCs). OPCs, also known as NG2 Glia, represent an attractive alternative to astrocytes as a target cell for neuronal reprogramming. OPCs have a diverse developmental origin that may contribute to their apparent regional heterogeneity in the adult CNS, with cortical OPCs arising postnatally from the dorsal ventricular zone (Newville et al., 2017). OPCs are characterized by their expression of Olig2, Sox10, NG2, and Pdgfa. Definitive OPCs gradually reduce expression of NG2 and Pdgfa upon progressing to terminal differentiation as oligodendrocytes (Nishiyama et al., 2016). OPCs are the largest dividing cell population in the healthy, naive adult cortex (Dawson et al., 2003), respond to injury (Simon et al., 2011; von Streitberg et al., 2021), and homeostatically maintain a latticed distribution (Hughes et al., 2013) throughout the entire cortical region. As their primary role is understood to be a reserve population to proceed to terminal differentiation as oligodendrocytes when needed, OPCs offer an abundant and renewable cell population for neuronal reprogramming.

Here we show that retroviral gene delivery of the transcription factor neurogenin2 (Ngn2) can reprogram isolated adult rat OPCs into functional neurons and produce phenotypically mature neurons from naïve OPCs in the adult rat cortex. We isolated gray matter OPCs from adult rat cortex and screened developmental transcription factors for functional neuronal induction capacity (Heinrich et al., 2011). Ngn2 reprogrammed OPCs into functional neurons *in vitro* and subsequent *in vivo* expression of Ngn2 in normally proliferating naive OPCs reprogrammed these cells through a transitional immature neuronal phenotype into mature glutamatergic pyramidal neurons with authentic dendritic arbor, axonal extension, and synaptic contacts from pre-existing neurons. Our results demonstrate direct *in vivo* engineering of mature neurons in multiple areas of the naive adult rat cortex. Engineering precise neuronal subtypes by reprogramming resident glia in this fashion may prove useful for experimental and potentially therapeutic manipulation of neuronal circuitry in the intact brain and for endogenous cell replacement following disease or neurological injury.

Materials and methods

OPC isolation and culture

Adult Hooded Long Evans Rats ($n = 4$) were deeply anesthetized, guillotined, and brains removed. Brains were cut into 2 mm slabs with a coronal brain matrix and the neocortex carefully dissected to avoid inclusion of white matter under a dissecting microscope in chilled HBSS buffer. Tissue was dissociated using a papain-based neural dissociation kit (Miltenyi) and cells were selected for the O4 antigen via Magnetic Activated Cell Sorting (MACS) and cultured as described previously (Dincman et al., 2012). OPCs were grown and passaged on PDL/laminin coated plastic dishes or glass coverslips in OPC growth medium (DMEM/F12, BSA (0.1%), N2 (1%), PDGFaa (10 ng/mL), FGF2 (20 ng/mL), and Insulin (5 μg/mL)) at 5% CO_2. Cells were passaged, cryopreserved, and maintained as a primary cell line with no later than passage 7 used in experiments.

Differentiation assays

Differentiation potential was assessed by replacing OPC growth media with Oligodendrocyte Differentiation Media (DMEM/F12, N2 (1%), B-27 Supplement (B27 1%), Penicillin/Streptomycin/Fungizone (PSF 1%), Insulin (50 ng/mL), Triiodothyronine (T3 40 ng/mL)) or Astrocyte Differentiation Media (DMEM/F12, Fetal Bovine Serum (10%), PSF (1%)). Experiments were performed in triplicate.

Neuronal reprogramming

OPCs were transduced with OPC growth media containing retroviral constructs carrying the transgene for candidate neurogenic

transcription factors (Supplementary Table S1). *In vitro* screening studies initially used a mixture of the constitutive CAG promoter or the OPC-specific NG2 promoter in different constructs. No advantage was conferred by NG2-promoter expression and to avoid potential silencing with neuronal differentiation, we chose to standardize on the CAG promoter for our studies. After 24 h, transduction media was replaced with Neuronal Reprogramming Media (Neuralbasal Media, B27 (2%), Glutamax (1%), PSF (1%)) at 10% CO2 with BDNF (20 ng/mL) added on Day 5 and every 4 days thereafter with no media changes (Heinrich et al., 2011). For co-culture experiments, PN1 rat neurons (derivation described in Sun et al., 2008) were plated onto reprogrammed neurons within 48 h of their transduction. Experiments were performed in triplicate. Time-lapse imaging studies were conducted using a Leica SP8 resonance confocal microscope equipped with an environmental stage (Okolab) and cultures were maintained at 37°C and 5% CO_2 for the duration of the imaging session.

Immunofluorescence staining for cell culture

Coverslips were transferred and rinsed in a well of PBS and fixed in 4% paraformaldehyde (0.1 M phosphate buffer). Three rinses in Tris-buffered saline (TBS) preceded a 1 h block in 5% donkey serum/0.25% TritonX-100/TBS solution (TBS++). For multiple immunostaining, sections were incubated overnight (at 4°C on a shaker table) with primary antibodies diluted in TBS with 0.25% TritonX-100 (TBS+). Primary antibodies used are listed in Supplementary Table S2. Following two 30 min block/rinses with TBS++, sections were incubated for 2 h with Alexa Fluor 488 (Molecular Probes), Cy3, or Cy5 (Jackson Immunoresearch) diluted in TBS+ (1:500) for 2 h at room temperature. Following two 15-min rinses with TBS, cells were counterstained with DAPI, rinsed with TBS, and coverslips were mounted onto slides, with a glycerol-polyvinyl alcohol plus DABCO (1,4 diazabicyclo [2.2.2] octane; Sigma D2522, Sigma-Aldrich, Inc., St. Louis, MO, United States) PVA-DABCO solution to self-seal and prevent fading, and stored at 4°C in the dark. Negative controls lacking primary antibodies were run along samples.

In vitro quantitation

To assess the efficiency of both viral transduction and neuronal conversion, the number of total cells (DAPI), virally transduced cells (GFP), and converted neurons (beta-III-tubulin) was estimated at each time in the screening assay by systematic sampling of coverslips in triplicate. Coverslips were imaged on an Olympus Spinning Disk (DSU) confocal microscope under the control of stereological software (StereoInvestigator, MBF Bioscience, Inc.) to achieve systematic, fractionated sampling. The entire coverslip was defined as a contour and the sampling density adjusted to acquire images at 10 sites with a randomized start site. This approach assured that all regions of the coverslip had an equal probability of being sampled. Confocal stacks (20 focal planes at 1 µm intervals) were automatically collected by the software at each site for each channel of fluorescence. Cells of each phenotype (DAPI, GFP, and beta-III-tubulin) were counted using the software to obtain an estimate of total cells (DAPI), transduction efficiency (GFP cells over DAPI cells), and conversion efficiency (beta-III-tubulin cells over GFP cells) per coverslip. The extent of colocalization of beta-III-tubulin was also calculated. As the physical parameters of the coverslip did not change, the results are expressed as the sum of the 10 fields sampled. Efficiency calculations were defined as the mathematical ratio of the mean values.

Molecular analysis

Cells were rinsed with PBS and harvested with no more than 5×10^5 cells resuspended in 1 mL CCM, then lysed and extracted with the RNeasy Plus Micro kit (Qiagen) using larger volumes for the purification of RNA from cells protocol. RNA concentrations were obtained using a Nanodrop 1000 (Thermo Scientific) using 1.5 µL RNA. Each sample was then assessed for quality using the Experion Capillary Electrophoresis System (Bio-Rad). Samples were diluted, denatured and prepared according to the manufacturer's directions for the Experion RNA HighSens analysis kit (Bio-Rad). They were run on the same chip as an extraction negative control and a positive control and compared using the Bio-Rad Experion software (v3.2.243.0) to a supplied denatured, diluted RNA ladder. Only samples with an RQI (RNA Quality Indicator) number greater than 7.0 were used for arrays. 400 ng of RNA from each sample was reverse transcribed using the ImpromII Reverse Transcription system (Promega, manufacturer's directions). 91 µL of RNase-free water was added to the cDNA for each sample. The PCR component mix was made up using iTaq Universal SYBR Green supermix (Bio-Rad) for 96-well format A for use in a Bio-Rad iCycler as instructed by the manufacturer (Qiagen). Each sample was pipetted into a Rat Neurogenesis array (Qiagen PARN-404Z) and performed on a Bio-Rad iCycler. The same threshold was set for all arrays and controls checked. The rat genomic DNA contamination control indicated the absence of genomic DNA. The positive PCR control wells were within 2 cycles of a Ct of 20, indicating a lack of inhibitors. Data was analyzed using the RT2 Profiler PCR Array Data Analysis software (v3.5) from Qiagen. Three reference genes that had a difference in Ct values of <2 across all samples were chosen to analyze the data. Delta-delta Ct was calculated for each well to find genes that were under and over expressed by more than 4 fold in the 7dpt and 15dpt day groups when compared to the OPC control cells.

Electrophysiological recordings

Electrophysiological recordings were conducted at room temperature (22°C) using standard whole-cell patch-clamp techniques, extracellular artificial cerebrospinal fluid gassed with 95% O_2/5% CO_2 and containing (in mM) 130 NaCl, 2.5 KCl, 2.0 $CaCl_2$, 1.2 $MgSO_4$, 1.25 KH_2PO_4, 25 $NaHCO_3$ and 10 dextrose, and intracellular solution containing 135 K-gluconate, 2.0 $MgCl_2$, 4.0 Na_2-ATP, 0.4 Na-GTP, 10 Na-phosphocreatine and 10 HEPES adjusted to pH 7.3 with KOH. Cells were selected based upon neuron-like morphology and GFP marker expression ($n = 15$ from triplicate preparations). Recordings were conducted in both current-clamp and voltage-clamp modes with cell potential adjusted to −70 mV using Axon Instruments Multiclamp 700B amplifier, Digidata 1,440 analog-digital converter and pClamp 10.2 software. Input resistance was measured with −20

pA, 500 msec current steps and neuron-like excitability (action potential firing) was tested using 500 msec current steps ranging from −50 to +100 pA in current-clamp. Sodium currents and spontaneous excitatory postsynaptic currents (sEPSCs) were measured in voltage-clamp. sEPSCs were detected and measured offline using Minianalysis software with threshold amplitude set to 7.5 pA to avoid false positives from noise. Datasets of three 1-min recording epochs before, during and after CNQX per cell ($n = 4$) were analyzed by 1-way ANOVA followed by Tukey's multiple comparisons test.

Viral-vector preparation

3rd generation (self-inactivating) VSV-G pseudotyped Murine Moloney Leukemia Virus vector were produced by transfection of packaging (Gag/Pol, VSV-G) and vector plasmids into 293 T cells with the retroviral vectors collected into the cell culture supernatant or into Opti-MEM medium (serum free) for concentration by ultracentrifugation (Tiscornia et al., 2006). All vector transgenes were driven by the CAG promoter and co-expressed eGFP or dsRed under an internal ribosomal entry site (IRES) sequence. See Supplementary Table S1 for the origins of each retroviral vector plasmid.

In vivo delivery and histology

Seven to eight week-old young adult male Long Evans Hooded rats were purchased from Harlan Sprague Dawley (Indiana, United States) for sole use in this study. Rats were housed two to three per cage under standard laboratory conditions with a light/dark cycle of 12 h with food and water *ad libitum*. All experiments were performed according to and approved by national and institutional guidelines (NIH, IACUC). Intracranial injection procedures adopted to minimize mechanical trauma to the cortex included careful drilling of a skull opening so that no mechanical compression of the dura or parenchyma occurs, use of a small gage needle to superficially create an opening in the dura for insertion of the delivery needle without contact with the cortical surface, and use of a specially designed 33G needle (Hamilton Neuros Syringe) to minimize needle track volume combined with slow delivery of viral volume. With these procedures, neuronal loss is confined to the volume of the 33G needle and hypertrophy of astrocytes is confined to the lining of the needle track and the cortical surface at the site of insertion. Rats were randomly assigned to viral delivery groups for the different transgenes. Viral injections were done for each transgene in groups of three to minimize wastage of the virus. Rats within each group were randomly assigned for collection of brains at the different analysis times. Rats were anesthetized with Isoflurane inhalant and injected with 3ul of concentrated retroviral CAG-eGFP (3×10^8) or CAG-Neurogenin2-IRES-eGFP (3×10^8) using a motorized stereotaxic injector (Stoelting) with delivery at 0.2 µL/min into either the right motor cortex or the right entorhinal cortex. The following coordinates were used: for motor cortex [from Bregma (mm): nosepiece −0.3; A/P: +0.5; M/L: −2.5; D/V(from dura): −2.0 raised 0.1 every minute] and for entorhinal cortex [from Bregma (mm): nosepiece: −7.0; A/P: ±9.2; M/L: −5.0; D/V(from dura): −4.5 raised 0.1 every 1 m 30 s].

Brains were collected at 1 and 2–3 weeks post injection following transcardial perfusion with 0.9% saline wash, followed by 4% paraformaldehyde (PFA) in phosphate buffer, then post-fixed in 4% PFA overnight at 4°C, equilibrated in 30% sucrose, and sectioned at 40 µm on a freezing stage microtome (Leica). Using unstained wet-mounted sections, all brains were screened for the detection of native GFP expression; brains that did not contain fluorescent cells or brains where the injection reached the corpus callosum or otherwise were not entirely within the cortex were not included in the study. Final group sizes were GFP (27) and Ngn2 (27). For immunofluorescence staining, net inserts (Corning Costar) were used to transfer free-floating sections between solutions and minimize handling. To remove cryoprotectant, all sections were rinsed multiple times in TBS followed by 3 h block in TBS++. For multiple immunostaining, sections were incubated for 72 h (at 4°C on a shaker table) with primary antibody diluted in TBS+. Primary antibodies and dilutions used are listed in Supplementary Table S2. Following two 1 h blocks with TBS++, sections were incubated for 48 h with Alexa Fluor 488 (Molecular Probes), Cy3, or Cy5 (Jackson Immunoresearch) diluted in TBS+ (1:500) for 2 h at room temperature. Following two 15-min rinses with TBS, all sections were mounted onto slides, cover slipped with PVA-DABCO mounting media, and stored at 4°C in the dark. Negative controls lacking primary antibodies were run along samples. The use of different reporter genes in some cases prevented the blinding of investigators to group identity.

Microscopy and imaging

Confocal images were acquired using an Olympus DSU, Olympus Fluoview XV, Fluoview 500, or Leica SP8 resonance confocal microscope. Appropriate apertures and Nyquist sampling were used to acquire optimal resolution confocal stacks. Signal intensity was set objectively against a signal distribution histogram and with reference to positive and negative imaging controls to ensure an appropriate acquisition without oversaturation. Three-dimensional colocalization of signal was performed by generation of orthogonal views or through rendered three-dimensional visualization with rotation and orthogonal sectioning of the image volume using NeuroLucida software (MBF Bioscience, Inc.). Figures were composed in Adobe Photoshop with minimal adjustment to normalize signal distribution between panels and images were not otherwise manipulated.

Quantitative stereology

The Navigator feature of the Leica LASX software was used to acquire a three-dimensional virtual tissue section of all sections containing GFP-positive cells. Imaging was performed on a Leica SP8 resonance confocal microscope using the 25 × 0.95 NA water immersion lens with a z-axis sampling interval of 1 µm to generate a focal series throughout the entire section thickness. All image stacks were stitched together to generate a virtual section. The series of virtual sections for each site of gene delivery were sampled using the StereoInvestigator software (MBF Bioscience, Inc.) to implement Optical Fractionator sampling to produce an estimate of total cell number (Peterson, 2004; Peterson, 2014). The sampling parameters

used were: section series- every third section; area fraction 65 × 65 µm counting frame and a 125 × 125 µm sampling grid; optical disector height of 12 µm with a mean section thickness of 24.6 (±1.04) µm. This sampling density generated a mean coefficient of error (CE) value of 0.16 (±0.02). Cells were counted as they first came into focus using the optical disector counting rules and scored for single or multiple expression of fluorescent labeling. Data was summarized and analyzed using Prism 9.4 software (GraphPad, Inc.) with an initial ANOVA followed by a Bonferroni *post-hoc* test for significance with significance accepted at $p \leq 0.05$.

Results

Characterization of adult-derived rat cortical OPCs

To prepare for future studies of neurogenic engineering in rat models of injury and dysfunction, we isolated and cultured adult rat cortical OPCs for use as an *in vitro* assay to identify successful transcription factors for subsequent *in vivo* cortical delivery to induce neurons from resident non-reactive OPCs (Figures 1A–C). To screen developmentally relevant pro-neuronal transcription factors (Imayoshi and Kageyama, 2014) (Supplementary Table S1), adult OPCs were isolated from cortical gray matter to replicate the target cell population for *in vivo* reprogramming. OPCs were selected for expression of the O4 antigen (Dincman et al., 2012) from dissociated adult rat neocortical gray matter, and could be cultured with the ability to expand, passage, and cryopreserve cells (Figures 1B,D). All adult cortical-OPCs expressed pan-oligodendroglial markers, Olig2 and Sox10 (Nishiyama et al., 2009) (Figure 1E) and NG2 (Figure 1F), but displayed maturational heterogeneity within the OPC lineage with a concomitant loss of nestin and increased O4 expression as cells progressed from early bipolar to later multipolar morphologies (Figure 1F). Under OPC growth conditions, most cells retained an OPC phenotype and the premyelinating oligodendrocyte marker RIP was rarely observed (Figure 1G). However, under oligodendrocyte differentiation conditions, RIP became strongly expressed (Figure 1H) confirming that the isolated OPCs were indeed within the oligodendroglial lineage and could proceed to terminal differentiation as oligodendrocytes with appropriate instruction.

In vitro neuronal reprogramming

Delivery of neurogenic transcription factors (Supplementary Table S1) cloned into retroviral vectors resulted in robust expression of the neuronal lineage marker ß-III-tubulin by 7 days (Figures 2A–E) following delivery of the single factors Neurogenin2 (Ngn2; 50% efficiency) or NeuroD1 (50% efficiency), and to a lesser extent with the combined delivery of Ascl1 and Dlx2 (15% efficiency), but not in any of the other combinations, including GFP-reporter control (0%) and Pax6 (0%). Ngn2-induced neurons (Ngn2-iNs) expressed ß-III-tubulin as early as 3 days post transduction (dpt) and expressed Map2 (Figure 2E′). Non-infected cells continued to express Olig2 and O4, while these were downregulated in Ngn2-infected cells (Figure 2F). Initial transduction efficiency was approximately 60% and of those GFP-expressing cells, neuronal conversion efficiency was approximately 25% (i.e., 15% of total cells; Figures 2G,H).

To confirm lineage progression from OPCs to induced neurons, we performed time-lapse imaging over 70 h from four to 6 days post-infection and conducted a trajectory analysis on the lineage progression of individual cells (Figure 3). Single frame images from

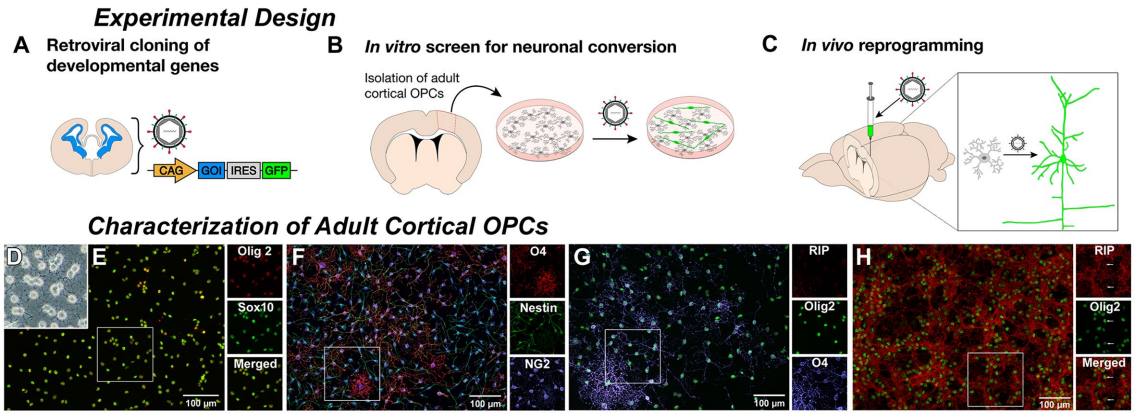

FIGURE 1
Derivation of adult rat cortical oligodendrocyte progenitor cells (OPCs). Experimental Design: **(A)** Genes encoding relevant developmental transcription factors were cloned into a retroviral vector with a fluorescent reporter gene. **(B)** Adult rat cortical gray matter was dissociated and O4-positive oligodendrocyte progenitor cells (OPCs) were selected, cultured, and transduced by retroviral delivery. β-III-tubulin expression of reporter-labeled cells served as a readout of neuronal induction. **(C)** Retrovirus containing successful constructs is then delivered to the cortex of a naïve animal to infect resident proliferating OPCs and induce neuronal reprogramming. Characterization of Adult Cortical OPCs: **(D)** Cultured O4-selected phase-bright multipolar cells with morphology consistent with an OPC identity. **(E)** Cells stain positive for pan-oligodendroglial lineage markers Olig2 and Sox10. **(F)** Isolated OPCs are NG2-positive and demonstrate a concomitant loss of nestin and increased O4 expression as cells progressed from early bipolar to later multipolar morphologies. **(G)** Under growth conditions, only the most elaborate O4-positive cells contained detectable staining for the premyelinating oligodendrocyte marker RIP. However, under oligodendrocyte differentiation media, **(H)** nearly all OPCs matured into RIP-positive oligodendrocytes, while maintaining expression of Olig2.

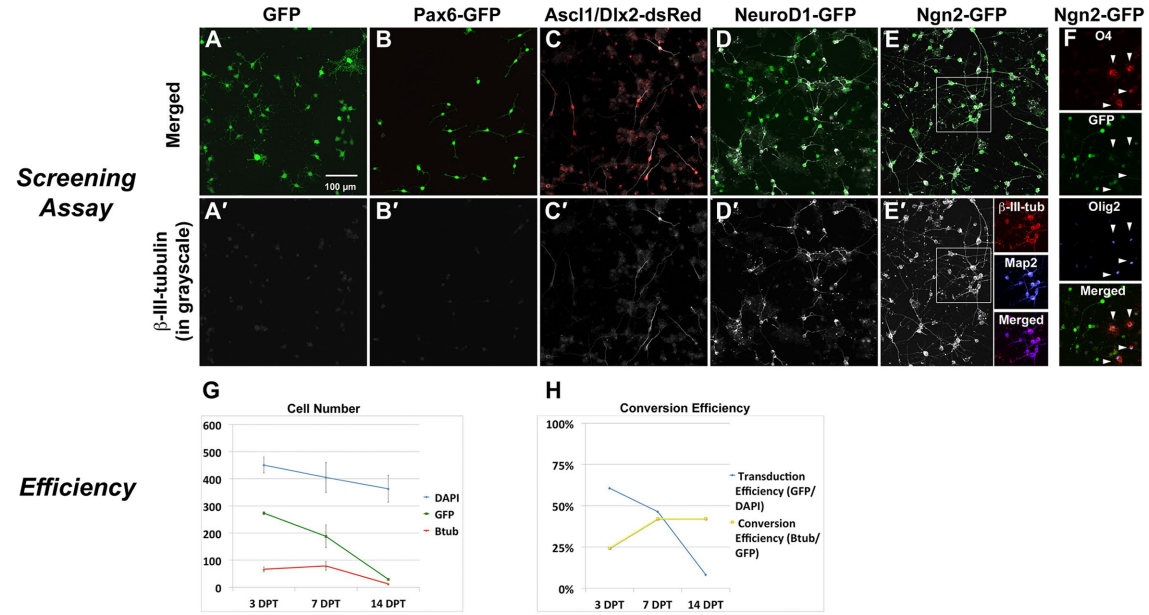

FIGURE 2
In vitro screen for reprogramming to phenotypic neurons. Screening Assay: OPC cultures received retroviral vectors for neurogenic transcription factors and were evaluated for neuronal induction based upon expression of the early neuronal marker β-III-tubulin. **(A)** GFP alone or **(B)** Pax6-GFP transduced OPCs but did not induce β-III-tubulin. Co-delivery of **(C)** Ascl1-dsRed and Dlx2-dsRed or **(D)** NeuroD1-GFP did induce β-III-tubulin. **(E)** Ngn2-GFP strongly induced β-III-tubulin, and induced neurons also expressed Map2. **(F)** Only non-transduced OPCs (non-GFP cells) continue to express Olig2 or O4 (arrowheads), indicating successful lineage respecification by Ngn2. Efficiency of Ngn2-induction: **(G)** The total number of cells in culture (DAPI) was reduced by about 20% over the course of the screening assay (14 days). Not all cells were transduced and the number of GFP-positive cells declined by about 90% over the course of the assay. Ngn2 successfully induced neurons, but the number of β-III-tubulin cells decreased by 80% by day 14. At all times, nearly 100% of β-III-tubulin cells were GFP-positive. Thus, loss of GFP positive cells occurred mainly in the portion that did not successfully convert into neurons. Values are mean ± standard deviation. **(H)** When stated in terms of efficiency, retroviral-Ngn2 transduced 60% of the cells and induced β-III-tubulin in 25% of those cells (i.e., 15% of total cells). Thus, over time, as the number of GFP cells declined, the apparent conversion efficiency increased.

each day during the imaging period (Figures 3A–C) illustrate morphological progression from multipolar short processes of OPCs to the eventual long processes typical of neuronal morphology that contact neighboring cells. The dynamic nature of this interaction can be seen in the Supplementary Video S1 (https://doi.org/10.5281/zenodo.8189544). Immunostaining immediately following confirmed the expression in these cultures of the mature neuronal marker, NeuN (Figures 3D–F).

As an assessment of neuronal function following Ngn2 delivery, a neurogenesis-themed PCR array found that GFP-control vector largely matched the expression profile of OPCs while Ngn2-iNs upregulated neuronal genes (ie. DCX, Grin1) and the pro-neuronal transcription factor NeuroD1, but downregulated Olig2 by 7 dpt (Figures 4A,B). When co-cultured with P1 rat cortical neurons, Ngn2-iNs developed elaborate dendritic processes with punctate synaptophysin-positive contacts (Figures 4C–E), showed strong neuron-like voltage gated sodium current (Figure 4F), generated action potentials upon depolarization (Figure 4F), and displayed spontaneous excitatory post-synaptic currents that were inhibited by the glutamatergic AMPA receptor blocker, CNQX (Figures 4I,J). Thus, in addition to showing morphological and phenotypic features consistent with a neuronal identity, Ngn2-iNs evidence a similarity in transcriptional profile. Furthermore, Ngn2-iNs exhibited functional contacts and neuronal membrane properties consistent with a glutamatergic phenotype.

Specificity of *in vivo* retroviral delivery for cortical OPCs

We next asked if *in vivo* retroviral delivery of Ngn2 could also reprogram non-reactive OPCs within the naive rat cerebral cortex into neurons. As predicted from the fact that OPCs are the primary proliferative cells in the naive adult cortex, we found that GFP-reporter labeled cells expressed the pan-oligodendroglial marker, Olig2, with characteristic OPC morphology (Figures 5A,B). Based upon viral delivery parameters, each injection infected a fraction of Olig2-positive cells in this cortical volume in the rat, reflecting the proportion of OPCs undergoing cell cycle at the time of retroviral availability. With GFP-reporter only delivery, infected cells rarely express markers for immature (DCX) neurons and then only weakly. However, GFP-positive cells did not co-express markers for mature (NeuN) neurons, mature astrocytes (S100ß), or microglia (Iba1) at 7 days post injection (dpi; Figures 5A–D). By using detection of soma-localized S100ß for astrocytes, we were able to unambiguously exclude co-localization of astrocytes with retroviral GFP-reporter (Figure 5D).

Olig2 is a transcription factor expressed throughout the oligodendrocyte lineage apart from mature oligodendrocytes, while Sox10 is a transcription factor expressed from early OPCs to terminal oligodendrocytes. OPCs begin to downregulate expression of NG2 as they progress to becoming mature oligodendrocytes. To further characterize the proliferating cell population targeted by retroviral

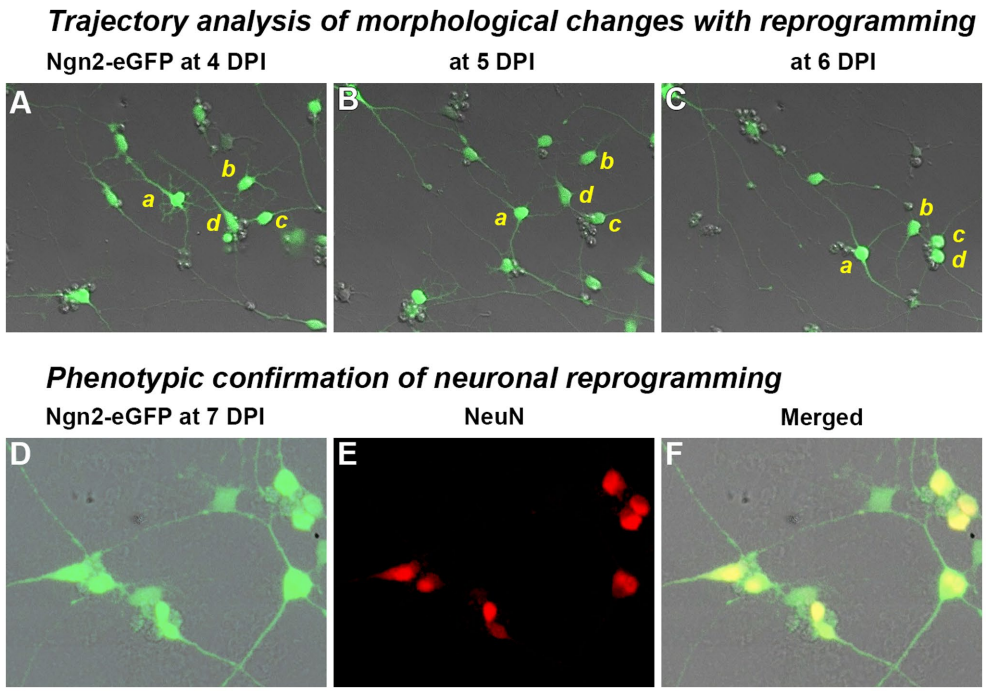

FIGURE 3
Trajectory analysis of Ngn2-expressing OPCs during the process of neuronal reprogramming. Trajectory analysis: Following retroviral delivery of Ngn2-eGFP (0 days post-infection or DPI), OPC cultures were observed by time-lapse imaging. A video summarizing the changes with neuronal reprogramming is included as Supplementary Material and can also be found at https://doi.org/10.5281/zenodo.8189544. **(A–C)** Four cells (*a–d*) are shown at 24 h intervals as they move, change morphology, and remodel their neurite extensions (see video for a dynamic view). Cells *a* and *b* exhibit a multipolar morphology at 4 DPI, while cells *c* and *d* are already showing more bipolar processes at this time. By 6 DPI, all four cells exhibit rounded cell bodies and distinct neurite processes that connect with neighboring induced neurons. Neuronal phenotype confirmation: **(D–F)** Cultures were fixed and immunostained at 7 DPI, revealing that nearly all GFP-positive cells expressed the neuronal marker, NeuN. Morphological progression and NeuN-positive cells were not observed in control cultures receiving retroviral eGFP-only delivery.

gene delivery, which infects only dividing cells, we analyzed control eGFP-only *in vivo* retroviral delivery at the 7 day post-injection interval and found that 85.9% (±2.6%) were Sox10+/NG2+ OPCs and the remaining 13.8% (±2.7%) were Sox10+/NG2− oligodendrocytes. Thus, 99.7% (±0.03%) of GFP-expressing cells are OPCs or OPCs progressing toward terminal differentiation. As only proliferating OPCs were targeted by retroviral delivery, only 23.4% (±5.8%) of OPCs present at the point of retroviral delivery expressed GFP.

In vivo cortical neuronal reprogramming by Ngn2

Retroviral delivery of Ngn2 induced DCX expression in nearly all Ngn2-GFP-positive cells by 7 days (Figures 6A–D). Ngn2-iNs began to express NeuN, although at weaker levels than pre-existing neurons by 7 dpi. Given the robust process extension and morphological remodeling observed of Ngn2-iNs *in vitro* at a similar time (Figure 3 and Supplementary Video S1), it is perhaps not surprising that *in vivo* Ngn2-iNs exhibited substantial process extension and complexity with cell polarity suggesting a transitional immature neuronal morphology (Figure 6E). These Ngn2-iNs also expressed the early neuronal lineage marker DCX, confirming their progression through a neuronal lineage (Figure 6E).

As Ngn2 reprogramming *in vitro* also drove very high expression of NeuroD1 (Figures 4A,B), we next asked if *in vivo* Ngn2 reprogramming alone was sufficient to generate pyramidal neuronal morphology with glutamatergic subtype specification. By 3 weeks, Ngn2-iNs were observed in superficial layers of the cortex (Figures 7A–C) showing a continuum of progression toward a mature neuronal morphology with distinct dendritic and axonal processes and, in all cases, distinctly co-expressing the mature neuronal marker NeuN. In all cases, signal co-expression was assessed in three-dimensions to verify that signals overlap in the same cellular compartments. All neurons, including the Ngn2-iNs, were closely associated with Iba-1-positive microglia (Figures 7A–C), but no microglia were observed to co-express GFP, indicating the absence of non-specific GFP uptake.

Ngn2-iNs were also observed by 3 weeks in deep cortical layers (Figures 7D–F) that distinctly co-expressed NeuN and exhibited cytoarchitecturally appropriate pyramidal cortical neuron morphology, including primary and basal dendrites, dendritic arbor elaboration, and dendritic spines. Evaluation of GFAP-positive cells confirmed the absence of GFP expression in astrocytes. Separate Ngn2-GFP gene delivery to the phylogenetically older entorhinal cortex (allocortex) also resulted in the generation of induced neurons by 3 weeks (Figures 7G–I) demonstrating that OPCs in regions other than neocortex may be amenable to neuronal reprogramming.

In vitro data had demonstrated that Ngn2-iNs established functional glutamatergic contacts (Figure 4). To determine if Ngn2-iNs generated following *in vivo* gene delivery adopt a glutamatergic neuronal subtype specification, GFP-positive Ngn2-iNs were examined for co-expression

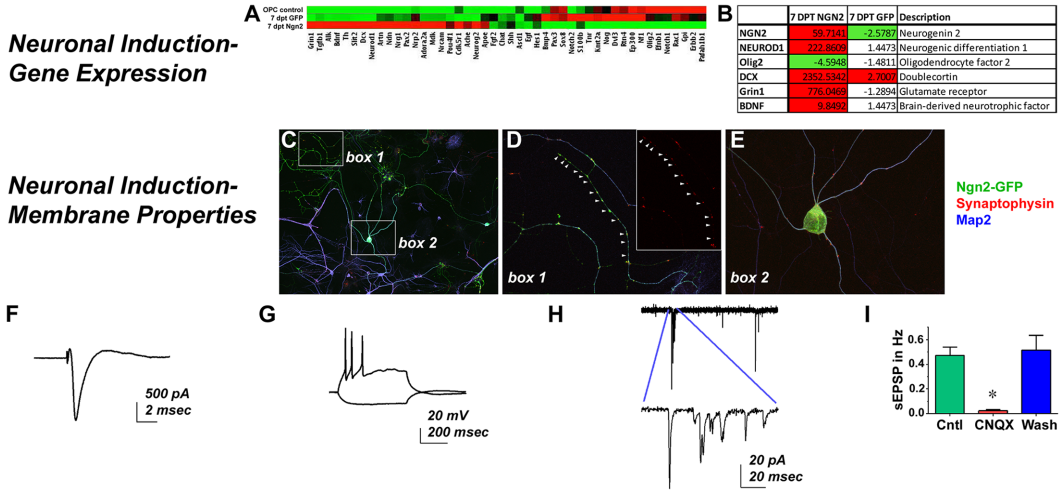

FIGURE 4
Ngn2 Expression Reprograms OPCs into Functional Neurons. Neuronal Induction-Gene Expression: **(A)** Control GFP-only transduced cells exhibited a largely similar gene expression profile to OPCs in a neurogenesis pathway PCR array, while Ngn2-induced neurons demonstrate distinct gene expression changes. **(B)** There was greater than a 4-fold expression increase in Ngn2-induced neurons for selected genes relevant to neuronal lineage, including NeuroD1 and DCX. Olig2, a pan-oligodendroglial lineage marker was actually reduced by more than 4-fold. Neuronal Induction-Membrane Properties: **(C)** Ngn2-GFP induced neurons (green) co-cultured with neonatal primary rat cortical neurons elaborate Map2-positive processes (blue). Primary neurons stain only with Map2. **(D)** There were extensive synaptophysin-positive contacts (red) on Ngn2-GFP dendrites. Inset shows synaptophysin staining alone. **(E)** Synaptic contacts were also found on dendrites near the soma and frequently on the soma itself. *In vitro* patch clamp recordings demonstrate **(F)** strong sodium currents **(G)** repetitive firing of action potentials upon depolarizing injection, and **(H)** spontaneous excitatory post-synaptic current activity that is **(I)** largely blocked by the glutamatergic AMPA receptor antagonist CNQX, indicative of synaptic input. Values are mean ± SEM, F (2, 6) = 23.28, p = 0.0015.

of the cortical glutamatergic neuronal markers Tbr1 and Cam-II-kinase-α. Evaluation of three-dimensional imaging (Figures 7J–L) revealed that both markers were detected, indicating that rat cortical OPCs had been reprogrammed by Ngn2 expression alone in the absence of prior injury into a glutamatergic neuronal subtype. We next evaluated dendrites and dendritic spines on Ngn2-iNs (Figures 7M–O) and identified synaptophysin-positive contacts on both GFP-positive dendrites and dendritic spines indicating the presence of morphological contacts with the pre-existing cortical circuitry.

Stereological quantification of neuronal reprogramming

We performed stereological quantitation (Figure 8) to assess the number of GFP-positive cells in total for neocortical retroviral gene delivery of both control GFP-only and Ngn2-GFP at three time points (7, 14, and 21 days post-delivery). Cells were counted based upon their expression of GFP alone, or coexpression with the early neuronal lineage marker DCX (7 and 14 day groups) or the mature neuronal marker NeuN (21 day group). The volume of cortex occupied by GFP-positive cells did not differ between control and Ngn2 induction at any time point but did reveal a decline over time (Figure 8A). The basis for this volumetric decline can be seen by the estimation of total GFP-positive cell number (Figure 8B). Although there was no difference at any time between control GFP-only and Ngn2-GFP conditions, overall the populations of cells declined. The extent of initial gene delivery distribution within the cortex varies from subject to subject. This variable, and likely other nuances of intracerebral delivery, contributed to substantial variance with the result that statistical evaluation by ANOVA did not produce adequate significance to proceed with subsequent between group tests.

Estimation of the number of GFP-positive cells that showed neuronal lineage commitment (Figure 8C) demonstrated that the Ngn2-induced groups significantly generated induced neurons compared to the control GFP-only group. In fact, the control GFP-only group had few GFP-positive cells that were weakly DCX-positive. Despite the weakness of staining, these cells were included in the counts for 7 and 14 day groups. In the 21 day group for the GFP-only control condition, no GFP-positive cells were detected that co-expressed NeuN apart from a single GFP-positive cell that showed weak positivity for NeuN. This cell was included in the count, which also enabled statistical testing to be performed for the 21 day group. When evaluated for neuronal lineage commitment as a percentage of GFP-positive cells (Figure 8D), the weakly DCX-positive cells in the control GFP-only condition represent less than 4% of GFP-positive cells in the 14 day group. The single weakly NeuN positive cell represents less than 1% of GFP-positive cells in the 21 day group. In contrast, neuronal lineage commitment is significantly higher in the Ngn2-induced condition, with more than 85% of GFP-positive cells identified as neurons by 21 days.

Discussion

In this report, we demonstrate that delivery of a single transcription factor, Ngn2, can reprogram resident cortical OPCs into morphologically mature, subtype-specific pyramidal neurons in multiple rat cortical regions (including neocortex and allocortex) that are otherwise entirely devoid of neurogenesis. The relatively rapid expression of mature neuronal features we observed *in vitro* and *in vivo* may be explained by the reports that forced Ngn2 expression produces rapid expression of many mature neuronal transcriptional programs (Masserdotti et al., 2015; Kempf et al., 2021). Although possibly still in the process of maturing, these Ngn2-iNs receive multiple contacts on

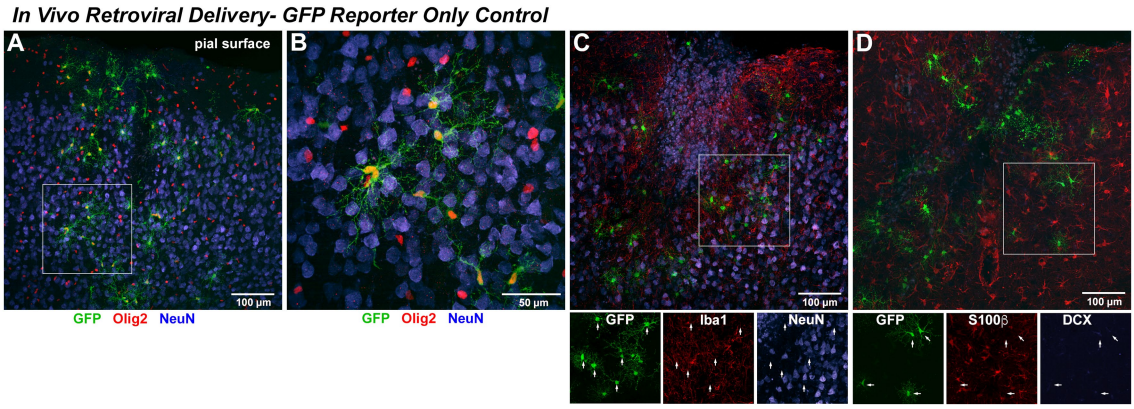

FIGURE 5
In vivo retroviral delivery of GFP reporter-only control infects proliferating OPCs but does not induce any detectable neuronal phenotype. *In Vivo* Retroviral Delivery-GFP Reporter Only Control: As retrovirus infects only dividing cells and the vast majority of proliferating cells in the naïve brain are OPCs, it was expected that this population would be targeted by retroviral delivery. By 7 days following *in vivo* cortical delivery of retroviral-GFP control vector, a distinct population of transduced cells was observed. **(A)** GFP-positive cells with a complex branching morphology consistent with NG2 Glia were uniformly distributed. A systematic, quantitative examination of coexpression with GFP revealed that 99.7% of GFP-positive cells observed in the control condition were positive for the OPC marker Olig2 (red) or Sox10 (not shown) by 7 DPI. **(B)** GFP-positive cells were distributed amongst mature neurons (NeuN, blue) and were often closely associated with, but distinct from, neurons. NeuN-positive cells were never observed to coexpress GFP. To verify that no GFP-positive cells were other neural cell types, adjacent sections were stained for **(C)** Iba1 (red) to detect microglia or **(D)** S100β (red) to detect astrocytes. In no case were GFP-positive microglia or astrocytes observed, as would be predicted for a naïve brain without previous injury where these cells are not actively proliferating. Staining for the early neuronal marker DCX revealed an absence of DCX expression in GFP-only positive cells (DCX detection in the hippocampal dentate gyrus within the same section was used as a positive control for validation of imaging parameters).

their dendrites and dendritic spines from pre-existing neurons. Neuronal electrophysiological properties were evident in Ngn2-iNs by 1 week *in vitro*. By using retroviral delivery of the reprogramming factor, we avoided targeting preexisting neurons, as has been a possibility with AAV delivery (Calzolari and Berninger, 2021; Wang et al., 2021; Chen et al., 2022; Cooper and Berninger, 2022). However, this experimental design also precluded employing the strategy of prior injury, reportedly important to achieve reprogramming (Grande et al., 2013; Guo et al., 2013; Heinrich et al., 2014; Torper and Gotz, 2017; Lentini et al., 2021), as this would have induced proliferation in a broader population of cells and prevented our goal of targeting the OPC population. Nevertheless, retroviral delivery of Ngn2 to proliferating OPCs resulted in their reprogramming into neurons, suggesting that the cortical environment of the adult rat can continue to foster neuronal maturation.

Specificity of reprogramming factor delivery

Retroviral transgene expression is restricted to cells undergoing cell division and thus also serves as a marker of cell cycle (Morshead and van der Kooy, 1992; Torper and Gotz, 2017). We therefore anticipated that retroviral delivery of reprograming factors to the naïve cortex would primarily target OPCs (Dawson et al., 2003), while also serving as a control for the inability to infect pre-existing post mitotic neurons. This straightforward delivery strategy also avoids potential false positive detection due to leaky expression of Cre under OPC-specific promoters that has been responsible for mistaken *in vivo* differentiation of OPCs to neurons (Richardson et al., 2011). Although a previous report (Guo et al., 2013) identified retroviral infection of astrocytes in mouse cortex, these cells only proliferate several days following an injury, and astrocyte proliferation may be misidentified and overstated due to the extent of GFAP upregulation (Burda and Sofroniew, 2014; Dimou and Gotz, 2014). This study design avoided any prior injury or activation of glial cells into a reactive state that would also stimulate proliferation in other cell types (Hampton et al., 2004), resulting in the absence of any retrovirally-delivered GFP detected in cells other than the constitutively proliferating OPC population. Thus although it is possible that occasional proliferating pericytes, endothelial cells, microglia, or astrocytes could potentially be included among infected cells, on a population basis, these other cell types were not detected to express GFP and the infected cell population was primarily OPCs, consistent with the non-reactive milieu at the time of viral infection. In control GFP-only conditions, we observed a portion of the GFP-expressing cells were Sox10-positive without NG2 expression. It is possible that some of these cells may have been oligodendrocytes proliferating at the time of retroviral delivery (Simon et al., 2011). The remaining population may have been OPCs at the time of retroviral delivery that subsequently downregulated NG2 as they progressed over the 7 days toward terminal differentiation as oligodendrocytes, a number and timeframe that is consistent with another report (Shimizu et al., 2020). Furthermore, we were able to exclude the participation of SVZ-derived neuroblasts as the source of our identified Ngn2-iNs based upon their absence in control GFP-only conditions and the identification of Ngn2-iNs in the entorhinal cortex, the most remote cortical region from the anterior SVZ.

Ngn2 reprogramming induced progression through neuronal lineage

Neurons have distinct phenotypic subtypes and the generation of new generic neurons without these properties and without appropriate

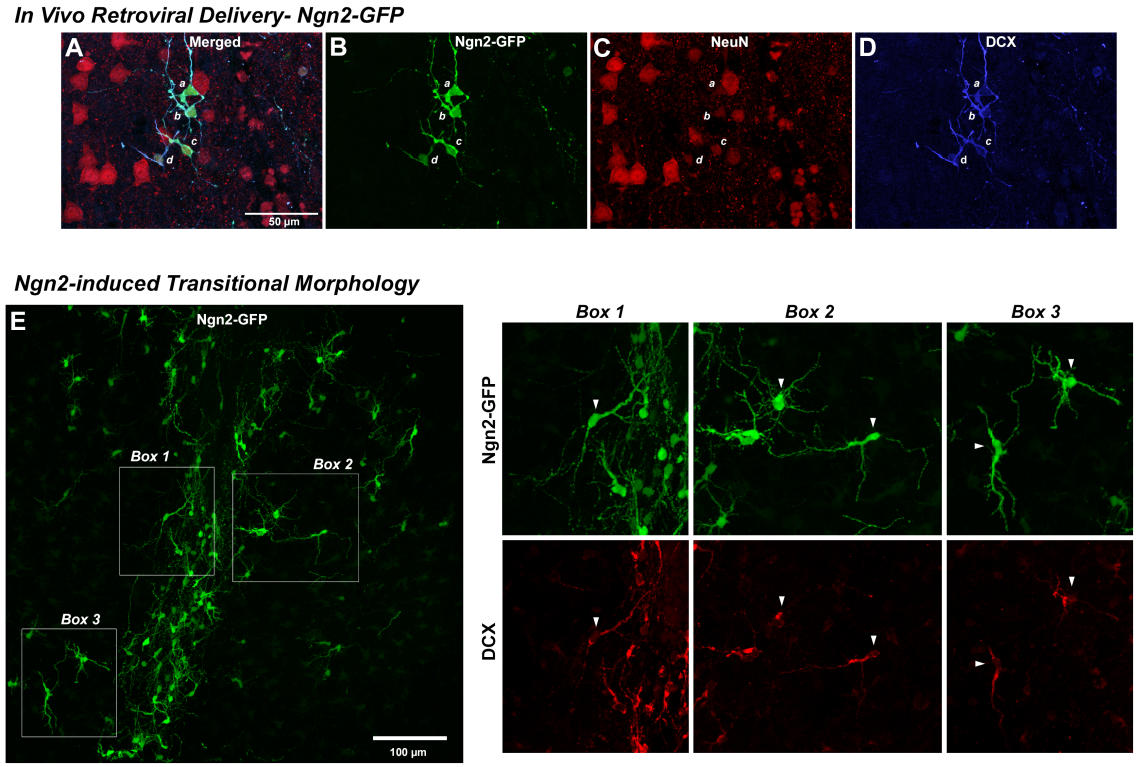

FIGURE 6
Reprogramming *in vivo* OPCs by Ngn2 induces neuronal lineage commitment. *In Vivo* Retroviral Delivery-Ngn2-GFP: Within 7 days, delivery of Ngn2-GFP resulted in a population of cells (four of which are identified by *a*, *b*, *c*, and *d*) expressing the GFP reporter **(A,B)**. Ngn2-induction also initiated neuronal lineage commitment evidenced by their co-labeling with DCX **(D)** and in some cells there may be some weak expression of NeuN **(C)**, indicating a further progression toward neuronal maturation. Ngn2-induced Transitional Morphology: **(E)** Ngn2-GFP-positive cells exhibited elaborate process extension with the adoption of defined cell polarity, similar to the dynamic morphological transition observed *in vitro* in Figure 4. Cells indicated in the boxed regions are shown at right with their co-expression of DCX. The elaboration of polarized cell morphology, extensive varicose process extension, weak NeuN expression, and discontinuous DCX staining suggests adoption of early neuronal lineage with eventual transition from DCX-positive neuroblasts to NeuN-positive neurons with a mature morphology. While some very weak DCX staining was observed at 7 days following retroviral GFP control delivery, this distinct DCX-positive phenotype and polarized cell morphology was only observed following retroviral Ngn2-delivery.

morphology may be of limited value for repair. Thus, our goal was to achieve reprogramming of naive OPCs to distinct neuronal subtypes with cytoarchitecturally appropriate neuronal morphology. An important validation to the authenticity of neuronal reprogramming is the progression from earlier to more mature neuronal phenotypes (Calzolari and Berninger, 2021). Both our *in vitro* and *in vivo* data demonstrated that expression of Ngn2 in OPCs resulted initially in a transition in morphology and the expression of early neuronal lineage commitment markers. By following the morphological trajectory of cultured rat OPCs expressing GFP, the transition to a neuronal morphology could be confirmed in individual cells and the expression of mature neuronal markers subsequently confirmed.

Following *in vivo* delivery, Ngn2-iNs begin to adopt more mature neuronal morphologies and express more mature phenotypic markers and evidence of synaptic contact with the pre-existing neuronal circuitry. Newly Ngn2-engineered neurons were detected in both more superficial and deep layers of the motor cortex (neocortex) and also the phylogenetically distinct entorhinal cortex (allocortex). The appropriate pyramidal neuron phenotype of Ngn2-iNs was confirmed by their expression of the cortical glutamatergic neuronal markers that matched adjacent pre-existing mature neurons and indicates phenotypic subtype specification, consistent with the *in vitro* functional data indicating glutamatergic specification. The adoption of cytoarchitecturally appropriate, location specific morphology also suggests competence to respond to remaining local environmental factors in establishing final maturation. For example, inverted pyramidal neurons comprise a small projection neuron subset confined to the deep cortical layers (Mendizabal-Zubiaga et al., 2007), and this morphology is appropriately induced in a subset of Ngn2-iNs in the deep layers. Similarly, entorhinal Ngn2-iNs adopt a location appropriate morphology. Thus, our ability to target OPCs almost exclusively by using retroviral gene delivery and the demonstrated progression from earlier to mature neuronal lineage validate that these are newly generated neurons and argue against the concerns that have been identified with some previous studies (Calzolari and Berninger, 2021; Wang et al., 2021; Chen et al., 2022; Cooper and Berninger, 2022).

Authenticity of neuronal reprogramming

Apart from a single weakly NeuN-positive cell observed in one GFP-control subject at 21 days, no GFP-neurons were detected in control GFP-only injected animals. Nevertheless, the observation of morphologically appropriate neurons emerging by 21 days following

10.3389/fnins.2023.1237176

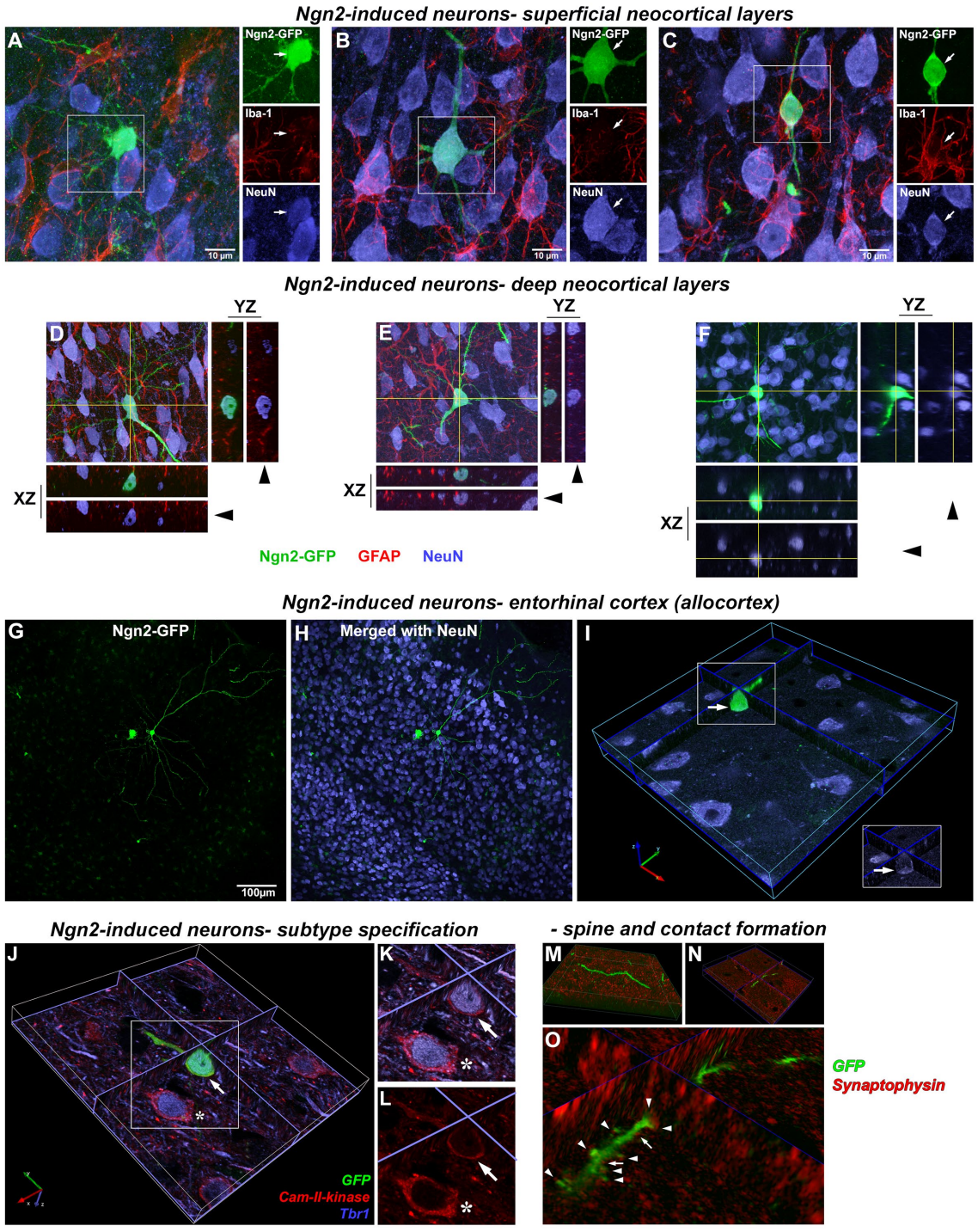

FIGURE 7
Morphologically mature neurons induced by *in vivo* Ngn2-reprogramming. Superficial cortical layers: by 3 weeks, Ngn2-GFP induced neurons showed an advancement in neuronal lineage commitment as evidenced by a more mature and cytoarchitecturally appropriate neuronal morphology. Superficial cortical layers contained induced neurons exhibiting a continuum of morphological maturation, but also showing coexpression of the mature neuronal marker NeuN (blue). **(A)** Some Ngn2-GFP-positive cells evidenced less maturation by 3 weeks, exhibiting incomplete process polarity, varicosities in processes and a lack of dendritic spines, but still expressing NeuN as evidence of neuronal lineage commitment. However, Ngn2-induced neurons did not co-express Iba1 (red), indicating the absence of non-specific uptake of GFP by microglia. **(B)** Other Ngn2-induced neurons exhibited a distinctly mature neuronal morphology with dendritic branching and a descending axon that left the plane of section within 50 µm from the soma along with strong NeuN co-expression. **(C)** Yet other Ngn2-induced neurons exhibited a less complex morphology, but still strongly expresses NeuN. GFP signal outside of the boxed region belongs to other induced neurons and their processes that lay beyond the focal planes included in this image. Images are presented as a maximum projection of a number of focal planes to provide a three-dimensional representation. Deep cortical layers: Deeper cortical layers also contained Ngn2-induced newly-generated neurons with layer-appropriate cytoarchitecture including an Ngn2-induced neuron **(D)** with an inverted pyramidal morphology only seen in cortical layer V neurons. Orthogonal projections in the XZ and YZ planes at

(Continued)

FIGURE 7 (Continued)
the level indicated by the yellow lines are included for each maximum projection image to validate coexpression of staining in three-dimensions. Confocal image stacks showing three examples of Ngn2-induced neurons **(D–F)** confirm these cells are NeuN positive (blue); arrowheads indicate removal of GFP-signal. Panels **(D,E)** also illustrate the absence of GFP coexpression in GFAP-positive astrocytes (red). In fact, no GFAP-positive astrocytes were observed to express GFP. Entorhinal cortex (Allocortex): In addition to the motor cortex, OPCs can be induced by retroviral Ngn2 delivery to convert to a neuronal lineage in other cortical regions. Retroviral delivery of Ngn2-GFP to the entorhinal cortex (allocortex) also induced new neurons by 3 weeks, including this example in entorhinal cortical layer III **(G,H)**. However not all infected cells survived the reprogramming instruction as shown by the dying cell to the left of a cytoarchitecturally appropriate new neuron. The successfully reprogrammed new neuron on the right also expresses NeuN **(I)** as evidenced by the three-dimensional image shown digitally sectioned at the planes indicated at the blue lines. The boxed region in inset validates the colocalization with NeuN following the removal of the GFP-signal overlay (arrow). Neuronal subtype specification: The subtype specification of GFP-positive Ngn2-induced new neurons (**J**; arrow) to a glutamatergic phenotype is shown by their co-expression of Tbr1 (blue) and Cam-II-kinase (red). This expression is identical to adjacent pre-existing neurons (asterisk). **(K)** Inset shows digital resectioning of a confocal image stack at the planes indicated at the blue lines with digital removal of the GFP signal (arrow) leaving the combined Tbr1 (blue) and Cam-II-kinase (red) signal. **(L)** Digital removal of the Tbr1 signal leaves only the Cam-II-kinase expression, cumulatively demonstrating the coexpression of these glutamatergic phenotype markers in the induced neuron. Dendritic spine and synaptic contact formation: Apical and basal dendrites of all newly-generated neurons contain abundant small spines **(M,N)** shown in different orientations from a confocal image stack. Three-dimensional rendering of dendrites and spines **(O)** reveals that both spines (arrowheads) and dendritic shafts (arrows) receive synaptophysin-positive contacts (red) indicating that preexisting axons are making synaptic contact with the newly-generated neurons.

retroviral delivery of Ngn2 led us to examine the possibility of a fusion event or other artifact, whereby GFP was simply transferred to a pre-existing neuron. Fusion events have been reported in neonatal brain, where it was mediated by infected microglia, but not in adult cortex (Ackman et al., 2006). We carefully examined Ngn2-iNs using high-resolution imaging and 3-dimensional rendering and found no cases of process fusion or double nuclei. Ngn2-iNs were contacted by Iba1-positive microglia, as were pre-existing neurons but in no cases were the Iba1 cells also GFP-positive. Furthermore, Ngn2-iNs passed through an immature, DCX-expressing neuronal state with advanced morphological complexity prior to the appropriate neuronal morphology seen later. In addition, Ngn2-iNs are not synchronous in their lineage progression and display a range of maturation, further arguing against transfer of GFP to pre-existing neurons.

Efficiency of neuronal reprogramming

The reduction in number of infected cells prior to maturation suggests that only fully reprogrammed Ngn2-iNs survive the reprogramming experience (Gascon et al., 2016). This low survival rate is not entirely surprising as 50–80% of adult newborn dentate granule cells die in an environment that is normally supportive of adult neurogenesis (Dayer et al., 2003; Sandoval et al., 2011). Similar outcomes in efficiency of neuronal reprogramming have been linked to regional heterogeneity of astrocytes (Hu et al., 2019) and this may also be true of OPCs. The efficiency of neuronal reprogramming is consistent with that seen in our *in vitro* data and in other reports (Guo et al., 2013), suggesting the possible death of cells that fail to achieve full re-specification. Furthermore, we estimate that only some 25% of available OPCs were targeted using retroviral delivery of the reprogramming factor. Increasing the number of cells targeted and the reprogramming efficiency to generate more induced neurons will be a goal for future studies.

Reprogramming capacity of the naïve rat cortex

There are two additional aspects that distinguish this report from most previous studies investigating cortical neuronal reprogramming. Previous studies in mouse cortex made the point that activation of astrocytes or glial progenitor cells by injury prior to delivery of reprograming factors was needed to achieve neuronal induction (Guo et al., 2013; Heinrich et al., 2014; Lentini et al., 2021). Using transcription factors alone for neuronal re-specification had not achieved this goal, suggesting that the prior injury or pathology was needed to generate a reactive or environmental state where the cells could be amenable to reprogramming (Grande et al., 2013; Guo et al., 2013; Heinrich et al., 2014; Torper and Gotz, 2017). In the present study, our retroviral targeting design avoided the establishment of an injury response state and provided insight as to the autonomous capacity of transcription factors to re-specify lineage (Guo et al., 2013; Heinrich et al., 2014). We reasoned these data could then also provide insight in regard to experimental or potential therapeutic modulation of local circuitry in disorders without a proximal injury response, such as psychiatric or addictive disorders (Southwell et al., 2014). This is not to say that an injury response after delivery of the reprogramming factor may not play a role in the process of lineage respecification. For example, some astrocytic hypertrophy was observed at the injection sites at 7 days post-injection and more severe cortical injury models note substantial proliferation of microglia and NG2-positive cells within 2–4 days (Hampton et al., 2004; Simon et al., 2011; von Streitberg et al., 2021). However, the data reported here demonstrate that neuronal reprogramming is possible without previously generating a reactive state in the target cell.

Another distinguishing feature of the present study is that the capacity for neuronal reprogramming is demonstrated in the naïve rat cortex, not the mouse cortex, which most studies to date have used. While mouse models are undeniably powerful research tools, many other important disease and behavior models have been developed using rats. Here, we demonstrate that cortical neuronal reprogramming is possible in naïve rat CNS, supporting the feasibility of extending studies of cell lineage specification into this important research tool.

Conclusion

This study is primarily a proof of concept for developing OPC reprogramming for neural regeneration. While, there is some possibility that retroviral vectors could be developed for safe use in the clinic in the

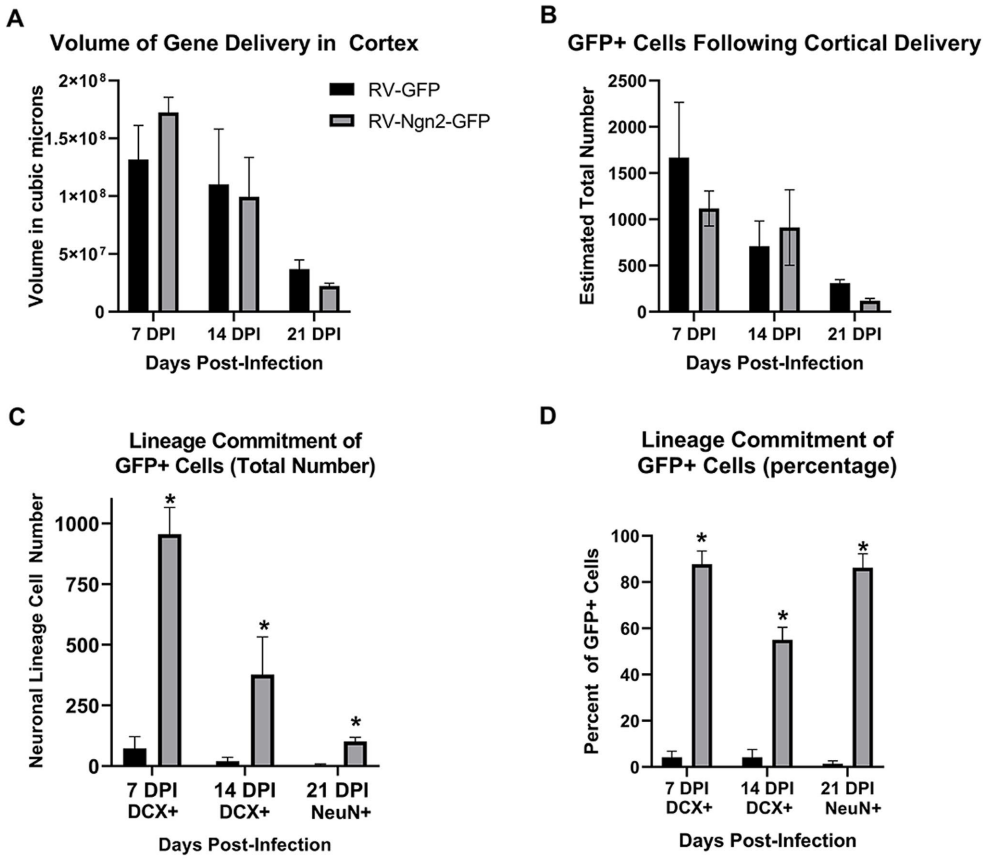

FIGURE 8
Stereological quantitation of OPC infection by retroviral delivery and subsequent neuronal reprogramming outcomes. **(A)** The volume of cortex containing GFP-positive cells following retroviral delivery did not differ between the control, GFP-only vector, and the experimental, Ngn2-GFP vector, at any time point. However, the reduction in cell survival over time is reflected in the declining volume occupied by GFP-positive cells over time. **(B)** The determination of total number of GFP-positive cells likewise showed no difference between GFP-only and Ngn2-GFP infection at any time point, although a decline in total number is evident over time. **(C)** GFP-positive cells were quantified for coexpression of the early neuronal lineage marker DCX at 7 days or 14 days, or coexpression with the mature neuronal lineage marker NeuN at 21 days. The GFP-only control group contained only few cells expressing some weak DCX labeling at early time points and only a single cell was observed to weakly express NeuN at 21 days. The number of GFP-positive cells expressing neuronal markers in the Ngn2-GFP group is significantly higher at all time points. **(D)** When expressed as a percentage of GFP-positive cells for each condition at each time point, retroviral delivery of Ngn2 resulted in a high percentage of all remaining GFP-positive cells being induced neurons at all time points.

future, it is far more likely that therapeutic delivery would ultimately utilize a host of other vector systems with better safety profiles. However, complex retrovirus vectors are being used clinically (Jogalekar et al., 2022) and past incidence of simple retroviral vector oncogenesis (Hacein-Bey-Abina et al., 2008) has been linked to the oncogenic nature of the transgene itself and not to the vector alone (Woods et al., 2006). It should also be noted that the expression of differentiation factors should inhibit oncogenesis (Lacomme et al., 2012).

While further studies are needed to elucidate the mechanisms of neuronal lineage re-specification, increase the efficiency of reprogramming OPCs into neurons, and to evaluate the functional integration of newly induced neurons into existing neuronal circuitry, the present study demonstrates the feasibility of neuronal reprogramming in the naïve rat cortex. These data suggest that direct *in vivo* fate reprogramming of resident non-reactive OPCs may provide a potential avenue for repair in the adult brain, both for neuronal replacement to restore circuitry and conceivably for neuronal addition to modulate circuitry in neurological disorders.

Data availability statement

The raw data supporting the conclusions of this article will be made available by the authors, without undue reservation.

Ethics statement

The animal study was approved by Rosalind Franklin University Institutional Animal Care and Use Committee. The study was conducted in accordance with the local legislation and institutional requirements.

Author contributions

SB, AM, RP, and MT isolated cortical progenitor cells and performed and analyzed *in vitro* studies. MT conducted the time-lapse

in vitro imaging. SB, CB, and GS conducted and analyzed electrophysiological studies. ER and RM designed vectors and produced virus. ER conducted and analyzed gene expression studies. SB, MT, RM, and DP performed *in vivo* gene delivery studies. SB, MT, JY, EM, and DP performed histological processing and imaging. PK and DP performed quantitative stereological analysis. SB, GS, RM, and DP conceived and designed the study and contributed to the writing of the manuscript. All authors contributed to the article and approved the submitted version.

Funding

This work was supported by NIH awards AG20047 and NS100514 to DP.

Acknowledgments

We thank Benedikt Berninger, Gong Chen, and Magdalena Götz for providing vector plasmids that were used to subclone transgenes into new retroviral vector plasmids or used unaltered for the production of virus (see Supplementary Table 1). We thank M. Rose Rogers for her assistance with figure composition and Scott Whittemore and his laboratory for their guidance with OPC isolation and culture. We thank Sarah Schuck and John Nino for technical assistance.

Conflict of interest

The authors declare that the research was conducted in the absence of any commercial or financial relationships that could be construed as a potential conflict of interest.

Publisher's note

All claims expressed in this article are solely those of the authors and do not necessarily represent those of their affiliated organizations, or those of the publisher, the editors and the reviewers. Any product that may be evaluated in this article, or claim that may be made by its manufacturer, is not guaranteed or endorsed by the publisher.

Supplementary material

The Supplementary material for this article can be found online at: https://www.frontiersin.org/articles/10.3389/fnins.2023.1237176/full#supplementary-material

References

Ackman, J. B., Siddiqi, F., Walikonis, R. S., and LoTurco, J. J. (2006). Fusion of microglia with pyramidal neurons after retroviral infection. *J. Neurosci.* 26, 11413–11422. doi: 10.1523/JNEUROSCI.3340-06.2006

Bazarek, S., and Peterson, D. A. (2014). Prospects for engineering neurons from local neocortical cell populations as cell-mediated therapy for neurological disorders. *J. Comp. Neurol.* 522, 2857–2876. doi: 10.1002/cne.23618

Bhardwaj, R. D., Curtis, M. A., Spalding, K. L., Buchholz, B. A., Fink, D., Björk-Eriksson, T., et al. (2006). Neocortical neurogenesis in humans is restricted to development. *Proc. Natl. Acad. Sci. U. S. A.* 103, 12564–12568. doi: 10.1073/pnas.0605177103

Buffo, A., Vosko, M. R., Erturk, D., Hamann, G. F., Jucker, M., Rowitch, D., et al. (2005). Expression pattern of the transcription factor Olig2 in response to brain injuries: implications for neuronal repair. *Proc. Natl. Acad. Sci. U. S. A.* 102, 18183–18188. doi: 10.1073/pnas.0506535102

Burda, J. E., and Sofroniew, M. V. (2014). Reactive gliosis and the multicellular response to CNS damage and disease. *Neuron* 81, 229–248. doi: 10.1016/j.neuron.2013.12.034

Calzolari, F., and Berninger, B. (2021). cAAVe phaenomena: beware of appearances! *Cells* 184, 5303–5305. doi: 10.1016/j.cell.2021.09.027

Chen, W., Zheng, Q., Huang, Q., Ma, S., and Li, M. (2022). Repressing PTBP1 fails to convert reactive astrocytes to dopaminergic neurons in a 6-hydroxydopamine mouse model of Parkinson's disease. *elife* 11:e75636. doi: 10.7554/eLife.75636

Cooper, A., and Berninger, B. (2022). Gatekeeping astrocyte identity. *elife* 11:e80232. doi: 10.7554/eLife.80232

Dawson, M. R., Polito, A., Levine, J. M., and Reynolds, R. (2003). NG2-expressing glial progenitor cells: an abundant and widespread population of cycling cells in the adult rat CNS. *Mol. Cell. Neurosci.* 24, 476–488. doi: 10.1016/S1044-7431(03)00210-0

Dayer, A. G., Ford, A. A., Cleaver, K. M., Yassaee, M., and Cameron, H. A. (2003). Short-term and long-term survival of new neurons in the rat dentate gyrus. *J. Comp. Neurol.* 460, 563–572. doi: 10.1002/cne.10675

Dimou, L., and Gotz, M. (2014). Glial cells as progenitors and stem cells: new roles in the healthy and diseased brain. *Physiol. Rev.* 94, 709–737. doi: 10.1152/physrev.00036.2013

Dincman, T. A., Beare, J. E., Ohri, S. S., and Whittemore, S. R. (2012). Isolation of cortical mouse oligodendrocyte precursor cells. *J. Neurosci. Methods* 209, 219–226. doi: 10.1016/j.jneumeth.2012.06.017

Eriksson, P. S., Perfilieva, E., Bjork-Eriksson, T., Alborn, A.-M., Nordborg, C., Peterson, D. A., et al. (1998). Neurogenesis in the adult human hippocampus. *Nat. Med.* 4, 1313–1317. doi: 10.1038/3305

Ernst, A., Alkass, K., Bernard, S., Salehpour, M., Perl, S., Tisdale, J., et al. (2014). Neurogenesis in the striatum of the adult human brain. *Cells* 156, 1072–1083. doi: 10.1016/j.cell.2014.01.044

Gascon, S., Murenu, E., Masserdotti, G., Ortega, F., Russo, G. L., Petrik, D., et al. (2016). Identification and successful negotiation of a metabolic checkpoint in direct neuronal reprogramming. *Cell Stem Cell* 18, 396–409. doi: 10.1016/j.stem.2015.12.003

Giehrl-Schwab, J., Giesert, F., Rauser, B., Lao, C. L., Hembach, S., Lefort, S., et al. (2022). Parkinson's disease motor symptoms rescue by CRISPRa-reprogramming astrocytes into GABAergic neurons. *EMBO Mol. Med.* 14:e14797. doi: 10.15252/emmm.202114797

Grande, A., Sumiyoshi, K., Lopez-Juarez, A., Howard, J., Sakthivel, B., Aronow, B., et al. (2013). Environmental impact on direct neuronal reprogramming *in vivo* in the adult brain. *Nat. Commun.* 4:2373. doi: 10.1038/ncomms3373

Guo, Z., Zhang, L., Wu, Z., Chen, Y., Wang, F., and Chen, G. (2013). *In vivo* direct reprogramming of reactive glial cells into functional neurons after brain injury and in an Alzheimer's disease model. *Cell Stem Cell* 14, 188–202. doi: 10.1016/j.stem.2013.12.001

Hacein-Bey-Abina, S., Garrigue, A., Wang, G. P., Soulier, J., Lim, A., Morillon, E., et al. (2008). Insertional oncogenesis in 4 patients after retrovirus-mediated gene therapy of SCID-X1. *J. Clin. Invest.* 118, 3132–3142. doi: 10.1172/JCI35700

Hampton, D. W., Rhodes, K. E., Zhao, C., Franklin, R. J., and Fawcett, J. W. (2004). The responses of oligodendrocyte precursor cells, astrocytes and microglia to a cortical stab injury, in the brain. *Neuroscience* 127, 813–820. doi: 10.1016/j.neuroscience.2004.05.028

Heinrich, C., Bergami, M., Gascon, S., Lepier, A., Vigano, F., Dimou, L., et al. (2014). Sox2-mediated conversion of NG2 glia into induced neurons in the injured adult cerebral cortex. *Stem Cell Rep.* 3, 1000–1014. doi: 10.1016/j.stemcr.2014.10.007

Heinrich, C., Blum, R., Gascon, S., Masserdotti, G., Tripathi, P., Sánchez, R., et al. (2010). Directing astroglia from the cerebral cortex into subtype specific functional neurons. *PLoS Biol.* 8:e1000373. doi: 10.1371/journal.pbio.1000373

Heinrich, C., Gascon, S., Masserdotti, G., Lepier, A., Sanchez, R., et al. (2011). Generation of subtype-specific neurons from postnatal astroglia of the mouse cerebral cortex. *Nat. Protoc.* 6, 214–228. doi: 10.1038/nprot.2010.188

Heins, N., Malatesta, P., Cecconi, F., Nakafuku, M., Tucker, K. L., Hack, M. A., et al. (2002). Glial cells generate neurons: the role of the transcription factor Pax6. *Nat. Neurosci.* 5, 308–315. doi: 10.1038/nn828

Hu, X., Qin, S., Huang, X., Yuan, Y., Tan, Z., Gu, Y., et al. (2019). Region-restrict astrocytes exhibit heterogeneous susceptibility to neuronal reprogramming. *Stem Cell Rep.* 12, 290–304. doi: 10.1016/j.stemcr.2018.12.017

Hughes, E. G., Kang, S. H., Fukaya, M., and Bergles, D. E. (2013). Oligodendrocyte progenitors balance growth with self-repulsion to achieve homeostasis in the adult brain. *Nat. Neurosci.* 16, 668–676. doi: 10.1038/nn.3390

Imayoshi, I., and Kageyama, R. (2014). bHLH factors in self-renewal, multipotency, and fate choice of neural progenitor cells. *Neuron* 82, 9–23. doi: 10.1016/j.neuron.2014.03.018

Jin, K., Wang, X., Xie, L., Mao, X. O., Zhu, W., Wang, Y., et al. (2006). Evidence for stroke-induced neurogenesis in the human brain. *Proc. Natl. Acad. Sci. U. S. A.* 103, 13198–13202. doi: 10.1073/pnas.0603512103

Jogalekar, M. P., Rajendran, R. L., Khan, F., Dmello, C., Gangadaran, P., and Ahn, B. C. (2022). CAR T-cell-based gene therapy for cancers: new perspectives, challenges, and clinical developments. *Front. Immunol.* 13:925985. doi: 10.3389/fimmu.2022.925985

Kempf, J., Knelles, K., Hersbach, B. A., Petrik, D., Riedemann, T., Bednarova, V., et al. (2021). Heterogeneity of neurons reprogrammed from spinal cord astrocytes by the proneural factors Ascl1 and Neurogenin2. *Cell Rep.* 36:109409. doi: 10.1016/j.celrep.2021.109409

Kornack, D. R., and Rakic, P. (2001). Cell proliferation without neurogenesis in adult primate neocortex. *Science* 294, 2127–2130. doi: 10.1126/science.1065467

Lacomme, M., Liaubet, L., Pituello, F., and Bel-Vialar, S. (2012). NEUROG2 drives cell cycle exit of neuronal precursors by specifically repressing a subset of cyclins acting at the G1 and S phases of the cell cycle. *Mol. Cell. Biol.* 32, 2596–2607. doi: 10.1128/MCB.06745-11

Lentini, C., d'Orange, M., Marichal, N., Trottmann, M. M., Vignoles, R., Foucault, L., et al. (2021). Reprogramming reactive glia into interneurons reduces chronic seizure activity in a mouse model of mesial temporal lobe epilepsy. *Cell Stem Cell* 28:e10, 2104–2121.e10. doi: 10.1016/j.stem.2021.09.002

Lindvall, O., and Kokaia, Z. (2015). Neurogenesis following stroke affecting the adult brain. *Cold Spring Harb. Perspect. Biol.* 7:a019034. doi: 10.1101/cshperspect.a019034

Masserdotti, G., Gillotin, S., Sutor, B., Drechsel, D., Irmler, M., Jørgensen, H. F., et al. (2015). Transcriptional mechanisms of proneural factors and REST in regulating neuronal reprogramming of astrocytes. *Cell Stem Cell* 17, 74–88. doi: 10.1016/j.stem.2015.05.014

Mendizabal-Zubiaga, J. L., Reblet, C., and Bueno-Lopez, J. L. (2007). The underside of the cerebral cortex: layer V/VI spiny inverted neurons. *J. Anat.* 211, 223–236. doi: 10.1111/j.1469-7580.2007.00779.x

Molyneaux, B. J., Arlotta, P., Menezes, J. R., and Macklis, J. D. (2007). Neuronal subtype specification in the cerebral cortex. *Nat. Rev. Neurosci.* 8, 427–437. doi: 10.1038/nrn2151

Morshead, C. M., and van der Kooy, D. (1992). Postmitotic death is the fate of constitutively proliferating cells in the subependymal layer of the adult mouse brain. *J. Neurosci.* 12, 249–256. doi: 10.1523/JNEUROSCI.12-01-00249.1992

Newville, J., Jantzie, L. L., and Cunningham, L. A. (2017). Embracing oligodendrocyte diversity in the context of perinatal injury. *Neural Regen. Res.* 12, 1575–1585. doi: 10.4103/1673-5374.217320

Nishiyama, A., Boshans, L., Goncalves, C. M., Wegrzyn, J., and Patel, K. D. (2016). Lineage, fate, and fate potential of NG2-glia. *Brain Res.* 1638, 116–128. doi: 10.1016/j.brainres.2015.08.013

Nishiyama, A., Komitova, M., Suzuki, R., and Zhu, X. (2009). Polydendrocytes (NG2 cells): multifunctional cells with lineage plasticity. *Nat. Rev. Neurosci.* 10, 9–22. doi: 10.1038/nrn2495

Peterson, D. A. (2004). "The use of fluorescent probes in cell counting procedures" in *Quantitative methods in neuroscience- a neuroanatomical approach*. eds. S. M. Evans, A. M. Janson and J. R. Nyengaard (Oxford: Oxford University Press), 85–114.

Peterson, D. A. (2014) in *High-resolution estimation of multiple cell populations in tissue using confocal microscopy in fluorescence microscopy: Super-resolution and other novel techniques*. eds. M. Conn and A. Cornea (Oxford: Academic Press), 171–184.

Qian, L., Huang, Y., Spencer, C. I., Foley, A., Vedantham, V., Liu, L., et al. (2012). *In vivo* reprogramming of murine cardiac fibroblasts into induced cardiomyocytes. *Nature* 485, 593–598. doi: 10.1038/nature11044

Richardson, W. D., Young, K. M., Tripathi, R. B., and McKenzie, I. (2011). NG2-glia as multipotent neural stem cells: fact or fantasy? *Neuron* 70, 661–673. doi: 10.1016/j.neuron.2011.05.013

Sandoval, C. J., Martinez-Claros, M., Bello-Medina, P. C., Perez, O., and Ramirez-Amaya, V. (2011). When are new hippocampal neurons, born in the adult brain, integrated into the network that processes spatial information? *PLoS One* 6:e17689. doi: 10.1371/journal.pone.0017689

Shimizu, T., Ishida, A., Hagiwara, M., Ueda, Y., Hattori, A., Tajiri, N., et al. (2020). Social defeat stress in adolescent mice induces depressive-like behaviors with reduced Oligodendrogenesis. *Neuroscience* 443, 218–232. doi: 10.1016/j.neuroscience.2020.07.002

Simon, C., Gotz, M., and Dimou, L. (2011). Progenitors in the adult cerebral cortex: cell cycle properties and regulation by physiological stimuli and injury. *Glia* 59, 869–881. doi: 10.1002/glia.21156

Song, K., Nam, Y. J., Luo, X., Qi, X., Tan, W., Huang, G. N., et al. (2012). Heart repair by reprogramming non-myocytes with cardiac transcription factors. *Nature* 485, 599–604. doi: 10.1038/nature11139

Southwell, D. G., Nicholas, C. R., Basbaum, A. I., Stryker, M. P., Kriegstein, A. R., Rubenstein, J. L., et al. (2014). Interneurons from embryonic development to cell-based therapy. *Science* 344:1240622. doi: 10.1126/science.1240622

Sun, X., Milovanovic, M., Zhao, Y., and Wolf, M. E. (2008). Acute and chronic dopamine receptor stimulation modulates AMPA receptor trafficking in nucleus accumbens neurons cocultured with prefrontal cortex neurons. *J. Neurosci.* 28, 4216–4230. doi: 10.1523/JNEUROSCI.0258-08.2008

Tai, W., Wu, W., Wang, L. L., Ni, H., Chen, C., Yang, J., et al. (2021). *In vivo* reprogramming of NG2 glia enables adult neurogenesis and functional recovery following spinal cord injury. *Cell Stem Cell* 28:e4, 923–937.e4. doi: 10.1016/j.stem.2021.02.009

Tiscornia, G., Singer, O., and Verma, I. M. (2006). Production and purification of lentiviral vectors. *Nat. Protoc.* 1, 241–245. doi: 10.1038/nprot.2006.37

Torper, O., and Gotz, M. (2017). Brain repair from intrinsic cell sources: turning reactive glia into neurons. *Prog. Brain Res.* 230, 69–97. doi: 10.1016/bs.pbr.2016.12.010

von Streitberg, A., Jakel, S., Eugenin von Bernhardi, J., Straube, C., Buggenthin, F., Marr, C., et al. (2021). NG2-glia transiently overcome their homeostatic network and contribute to wound closure after brain injury. *Front. Cell Dev. Biol.* 9:662056. doi: 10.3389/fcell.2021.662056

Wang, L. L., Serrano, C., Zhong, X., Ma, S., Zou, Y., and Zhang, C. L. (2021). Revisiting astrocyte to neuron conversion with lineage tracing *in vivo*. *Cells* 184:e16, 5465–5481.e16. doi: 10.1016/j.cell.2021.09.005

Woods, N. B., Bottero, V., Schmidt, M., von Kalle, C., and Verma, I. M. (2006). Therapeutic gene causing lymphoma. *Nature* 440:1123. doi: 10.1038/4401123a

Zhang, Y., Li, B., Cananzi, S., Han, C., Wang, L. L., Zou, Y., et al. (2022). A single factor elicits multilineage reprogramming of astrocytes in the adult mouse striatum. *Proc. Natl. Acad. Sci. U. S. A.* 119:e2107339119. doi: 10.1073/pnas.2107339119

Zhou, Q., Brown, J., Kanarek, A., Rajagopal, J., and Melton, D. A. (2008). *In vivo* reprogramming of adult pancreatic exocrine cells to beta-cells. *Nature* 455, 627–632. doi: 10.1038/nature07314

Zhou, M., Tao, X., Sui, M., Cui, M., Liu, D., Wang, B., et al. (2021). Reprogramming astrocytes to motor neurons by activation of endogenous Ngn2 and Isl1. *Stem Cell Rep.* 16, 1777–1791. doi: 10.1016/j.stemcr.2021.05.020

frontiers | Frontiers in Neuroscience

TYPE Original Research
PUBLISHED 18 September 2023
DOI 10.3389/fnins.2023.1204012

OPEN ACCESS

EDITED BY
Seiji Hitoshi,
Shiga University of Medical Science, Japan

REVIEWED BY
Ataulfo Martinez-Torres,
National Autonomous University of Mexico, Mexico
Hirotaka James Okano,
Jikei University School of Medicine, Japan

*CORRESPONDENCE
Kyoji Ohyama
✉ kyohyama@tokyo-med.ac.jp

RECEIVED 11 April 2023
ACCEPTED 29 August 2023
PUBLISHED 18 September 2023

CITATION
Ohyama K, Shinohara HM, Omura S, Kawachi T, Sato T and Toda K (2023) PSmad3+/Olig2– expression defines a subpopulation of *gfap*-GFP+/Sox9+ neural progenitors and radial glia-like cells in mouse dentate gyrus through embryonic and postnatal development. *Front. Neurosci.* 17:1204012. doi: 10.3389/fnins.2023.1204012

PSmad3+/Olig2– expression defines a subpopulation of *gfap*-GFP+/Sox9+ neural progenitors and radial glia-like cells in mouse dentate gyrus through embryonic and postnatal development

Kyoji Ohyama*, Hiroshi M. Shinohara, Shoichiro Omura, Tomomi Kawachi, Toru Sato and Keiko Toda

Department of Histology and Neuroanatomy, Tokyo Medical University, Tokyo, Japan

In mouse dentate gyrus, radial glia-like cells (RGLs) persist throughout life and play a critical role in the generation of granule neurons. A large body of evidence has shown that the combinatorial expression of transcription factors (TFs) defines cell types in the developing central nervous system (CNS). As yet, the identification of specific TFs that exclusively define RGLs in the developing mouse dentate gyrus (DG) remains elusive. Here we show that phospho-Smad3 (PSmad3) is expressed in a subpopulation of neural progenitors in the DG. During embryonic stage (E14-15), PSmad3 was predominantly expressed in *gfap*-GFP-positive (GFP+)/Sox2+ progenitors located at the lower dentate notch (LDN). As the development proceeds (E16-17), the vast majority of PSmad3+ cells were GFP+/Sox2+/Prox1$_{low}$+/Ki67+ proliferative progenitors that eventually differentiated into granule neurons. During postnatal stage (P1–P6) PSmad3 expression was observed in GFP+ progenitors and astrocytes. Subsequently, at P14–P60, PSmad3 expression was found both in GFP$^+$ RGLs in the subgranular zone (SGZ) and astrocytes in the molecular layer (ML) and hilus. Notably, PSmad3+ SGZ cells did not express proliferation markers such as PCNA and phospho-vimentin, suggesting that they are predominantly quiescent from P14 onwards. Significantly PSmad3+/GFP+ astrocytes, but not SGZ cells, co-expressed Olig2 and S100β. Together, PSmad3+/Olig2– expression serves as an exclusive marker for a specific subpopulation of GFP+ neural progenitors and RGLs in the mouse DG during both embryonic and postnatal period.

KEYWORDS

Smad3, GFAP, Olig2, SGZ, radial glia-like cells, astrocytes, dentate gyrus

Introduction

Using *gfap*-GFP transgenic mice expressing GFP under the control of mouse *gfap* promoter, it has previously been shown that *gfap*-GFP+ (GFP+) progenitors around the dentate notch (DN) contribute to granule neurons in the dentate gyrus (DG) during development (Altman and Bayer, 1990; Seki et al., 2014). The GFP+ progenitors have also been suggested to contribute

to other cell types: radial glia-like cells (RGLs) and protoplasmic astrocytes (Brunne et al., 2013). After birth, neurogenesis takes place mainly in the hilus and its border from the granule cell layer (GCL), becoming confined to the subgranular zone (SGZ) by postnatal day 14 (P14; Namba et al., 2005; Seki et al., 2014). Some GFP+ progenitors are converted to adult type RGLs immediately after birth (Matsue et al., 2017). However, the mechanism by which RGLs are specified during DG development is largely unknown.

There is considerable evidence that combinatorial expressions of TFs under the influence of signaling molecules define progenitor cell types in the developing CNS. However, it is currently unknown what TF code distinguishes RGLs from astrocytes, both of which appear mostly during the early postnatal period. Molecular markers for RGLs such as Sox9 are important to maintain RGLs in adulthood. However, they are also expressed in astrocytes, making it difficult to understand the mechanism by which RGLs and astrocytes develop in different ways.

Previous studies have shown that varieties of signals control the development of the dentate gyrus (DG) both in the embryo and the adult. Both BMP7 and Wnt signals regulate the expression of transcription factor Prox1, thereby governing the fate of granule neurons in the DG (Galceran et al., 2000; Choe et al., 2013). Sox2-dependent Shh signaling plays a key role both in the development of RGLs and sustained neurogenesis at the SGZ in adult mice (Li et al., 2013). ALK5-dependent TGFβ signaling through pSmad2 maintains late events during adult hippocampal neurogenesis (He et al., 2014). Smad3 is crucial for neuronal survival and adult neurogenesis in the hippocampus (Tapia-González et al., 2013). However, lack of TGFβ-Smad signaling does not affect the development of dentate granule neurons (Choe et al., 2013). These studies suggest that TGFβ-Smad2/3 signaling is essential for the development of adult but not embryonic granule neurons in the hippocampus. However, it remains unclear whether TGFβ-Smad signaling plays a role for other cell types that derived from GFP+ progenitors, namely astrocytes in the developing DG.

Phospho-Smad3 (PSmad3) has been shown to regulate not only progenitor specification and neuronal differentiation in the embryonic spinal cord (García-Campmany and Martí, 2007). As yet its expression pattern in the developing mouse DG has not been well studied. A recent study pointed out that TGFβ-PSmad3 pathway controls the glioblastoma stemness (Ikushima et al., 2009). Given the migratory and proliferative properties of the GFP+ DG progenitors (Seki et al., 2014), they may share some properties. In this study, we therefore examined the expression patterns of PSmad3 in the developing mouse DG. We show that PSmad3 is expressed in both a subpopulation of GFP+/Sox9+ progenitors, RGLs, and astrocytes throughout the embryonic and postnatal period. It is worthy of note that Olig2 expression distinguishes astrocytes from the RGLs. Together, PSmad3+/Olig2− expression defines a subpopulation of GFP+/Sox9+ neural progenitors and RGLs at the SGZ in both embryonic and postnatal mouse DG.

Materials and methods

Animals

Gfap-GFP transgenic mice that express GFP under the control of mouse *gfap* promoter (Suzuki et al., 2003) were housed under a standard condition (12-h light/dark cycle) in the animal care facility of Tokyo Medical University. All experiments were carried out in accordance with the guideline of the Institutional Animal Care and Use Committees and conform to the National Institutes of Health Guide for the Care and Use of Laboratory Animals (NIH Publication No. 80-23) revised in 1996. All efforts were made to minimize the number of animals used and their suffering. Embryos and pups of the *gfap*-GFP transgenic mice above were used. The day on which a vaginal plug was found was designated as embryonic day 0.5 (E0.5), and the day of birth was designated as postnatal day 0.5 (P0.5).

Tissue preparation

Embryos were harvested at E14.5—E18.5, and postnatal mice were anesthetized and perfused with 4% paraformaldehyde (PFA) in 0.1 M phosphate buffer (PB), pH7.4, at room temperature. The brains were removed and washed with PBS and immersed in 30% sucrose/0.1 M PB. The forebrains were embedded into OCT compound and stored at −70°C. Cryosections were cut at 25 μm thickness.

Antibodies

Antibodies used in this study are in the followings: mouse anti-E-cad (BD Transduction Laboratories 61081, 1:250); chick anti-GFAP (Millipore, 1:5,000); chick anti-GFP IgY (Abcam ab13970, 1:5,000); rabbit anti-GLAST polyclonal antibody (Covalab (France) PA-INS, 1:1,000); rabbit anti-Ki67 polyclonal antibody (Novocastra, NCL-Ki67p, 1:1,000); goat anti-NeuroD antibody (N-19; Santa Cruz, sc-1,084, 1:1,000); rabbit anti-Olig2 IgG (Millipore, AB9610, 1:1,000); goat anti-Olig2 (R&D systems, 1:1,000); mouse anti-PCNA (Novocastra, PC-10, 1:100); rabbit anti-PSmad3(S423/S425) polyclonal antibody (Millipore 07-1389, 1:1,000); mouse anti-phospho-vimentin IgG (MBL, D076-3S, 1:1,000); goat anti-Prox1 IgG (R&D systems, 1:1,000); mouse anti-S100β (Sigma, 1:1,000); rabbit Sox2 antibody (Millipore, 1:1,000); goat anti-Sox2 IgG (R&D systems, 1:1,000); goat anti-Sox9 polyclonal antibody (R&D systems, 1:1,000).

Immunohistochemistry

Cryosections were processed for immunohistochemistry as described previously (Ohyama et al., 2005; Seki et al., 2014). Briefly, cryosection of the hippocampus were incubated with primary antibodies overnight at 4°C. For some antibody labeling experiments (Ki67, phospho-vimentin), antigen retrieval with Histo VT One (Nacalai, Japan) was carried out following manufacturer's instructions. After wash with PBS three times, the sections were incubated with secondary antibodies for 45 min at room temperature. After wash with PBS three times, the sections were mounted with Vectashield (Vector lab). Images were taken with a Zeiss confocal microscope LSM700. In some cases, fluorescence images were digitally zoomed at 0.5x to 2x. Stacks of optical sections (1.8 μm in thickness/optical section) were obtained at 0.9 μm increments on the z-axis using x20 objective. The images were corrected for brightness and contrast and composed using Zeiss Image Browser, ZEN software (Zeiss,

Thomwood, NY) and Adobe Photoshop CS6 (San Jose, CA). Mice ($n = 3–6$) were examined for individual experiments, and, for quantification of some experiments, 9 sections at least were analyzed for each using Fiji of image J. Mean ± SE was indicated in the results.

Results

Gfap-GFP+ cells contribute to RGLs at the SGZ and astrocytes in the molecular layer and hilus

Using *gfap*-GFP mice (Seki et al., 2014; Matsue et al., 2017), we first monitored the contributions of *gfap*-GFP-positive (GFP+) progenitors in the developing mouse dentate gyrus (DG). GFP+ progenitors were found in the ventricular zone (VZ) around the dentate notch (DN) and in the primordium of the DG at E14–E16 (Figures 1A,B). At postnatal day1 (P1), many GFP+ progenitors accumulate in the developing DG (Figure 1C). By P6 hilus, granule cell layer (GCL), and molecular layer (ML) become apparent (Figure 1D). GFP+ cells were observed not only in the hilus of the DG, but also in the ML. At P14-21, in addition to the GFP+ astrocytes in the hilus and ML, GFP+ cells were also found at the SGZ where RGLs reside postnatally (Figures 1E,F). Taken together, our data indicate that GFP+ progenitors contribute to both RGLs at the SGZ and astrocytes in the hilus and ML over time (Supplementary Figure 1).

PSmad3 expression in GFP+ RGLs in early developing mouse DG

PSmad3 has been shown to control the proliferative and migratory behavior of glioblastoma (Ikushima et al., 2009). GFP+/Sox2+ neural progenitors also possess both proliferative and migratory properties (Seki et al., 2014). This led us to examine whether PSmad3 is expressed in the GFP+/Sox2+ neural progenitors in developing mouse DG. At E14, PSmad3 expression was found in the ventricular zone (VZ) of the lower part of the DN and in a migrating stream of GFP+/Sox2+ progenitors toward the DG primordium ($n = 3$; Figures 2A1–B8).

At E16-P3, 64.4% ± 6.4% of Sox2+ cells co-expressed PSmad3 in the DG ($n = 4$), and 44.3% ± 3.4% of Sox2+ cells were Ki67+ proliferative cells (Figures 3A1–A4,C1–C3; $n = 4$). PSmad3 and GFP were co-expressed in dentate progenitors. 32.5% ± 3.6% of PSmad3+ cells were $Prox1_{low}$ +before birth (33% ± 3%, $n = 5$; Figures 3B1,B2,D1–D4,E1–E8). Given that GFP+ progenitors give rise to Prox1+ granule neurons (Seki et al., 2014), these data suggest that PSmad3 is expressed in a subpopulation of GFP+ progenitors that give rise to granule neurons.

PSmad3 expression in GFP+ RGLs and astrocytes in the postnatal DG

PSmad3 was also expressed in GFP+ RGLs at P1–P6 (45.4% ± 2.7%, $n = 5$; Figures 4A1–D3). At P1 GFP+ cells co-expressed GLAST, another marker for RGLs in the DG (Supplementary Figures 2A1–A6). Given that PSmad3 is a regulator of epithelial mesenchymal transition (EMT),

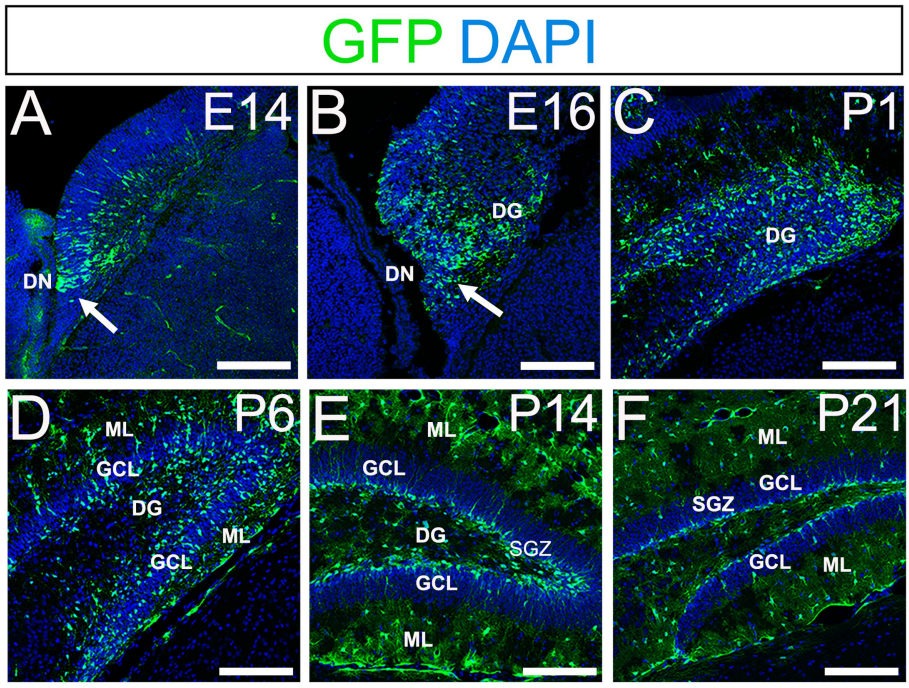

FIGURE 1
Gfap-GFP+ (GFP+) progenitors contribute to RGLs and astrocytes in developing mouse DG **(A,B)** GFP+ cells are found at the DN and forming DG at E14 and E16. **(C,D)** Many GFP+ cells are observed in the developing DG at P1 and P6. **(E,F)** GFP+ cells are located at SGZ and ML of the DG at P14-21. DN, dentate notch; DG, dentate gyrus; GCL, granule cell layer; ML, molecular layer; SGZ, subgranular zone. Scale bars: all 200 μm.

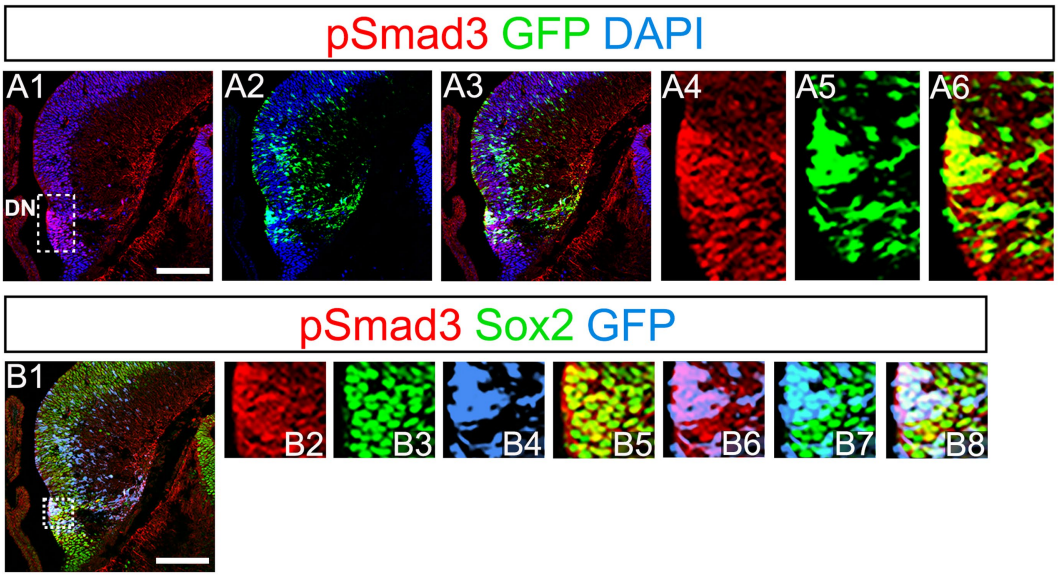

FIGURE 2
PSmad3 expression in GFP+/Sox2+ cells at the lower DN and their migratory stream toward developing DG **(A1–A6)** PSmad3 expression was found in GFP+ cells at the lower DN and their migratory stream toward the DG primordium at E14. **(B1–B8)** Co-expression of pSmad3, Sox2, and GFP+ at E14. Box in panels **(A1,B1)** indicates region shown in panels (**A4-A6**,**B2–B8**, respectively). Scale bars: all 200 μm. PSmad3 is expressed in GFP+/Sox2+ cells at E14 **(A1–A6)** PSmad3 is expressed in GFP+ cells. **(B1–B8)** Many PSmad3+/GFP+ cells co-express Sox2. Box in panels **(A1,B1)** indicates region shown in panels (**A4–A6**,**B2–B8**, respectively).

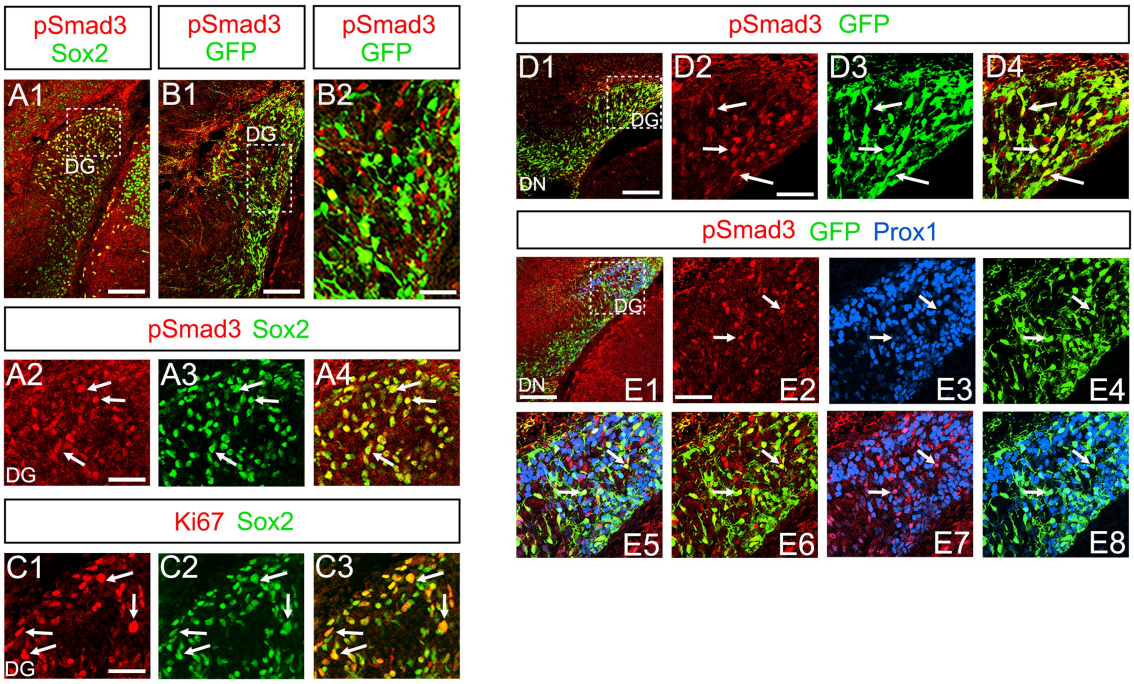

FIGURE 3
PSmad3+/GFP+ cells are Ki67+ proliferative RGLs and co-express $Prox1_{Low}$ in embryonic DG **(A1–A4)** PSmad3 co-express Sox2 at E16. **(B1,B2)** PSmad3+ cells co-express GFP at E17. **(C1–C3)** 44% of Sox2+ cells were Ki67+ proliferating cells. **(D1–D4)** PSmad3+/ GFP+ cells observed at E17. **(E1–E8)** PSmad3 is expressed in GFP+/$Prox1_{low}$ + cells at E18 (arrows). Scale bars: 200 μm in **A1,B1,D1,E1**; 50 μm in **A2–A4,B2,C1–C3,D2–D4,E2–E8**.

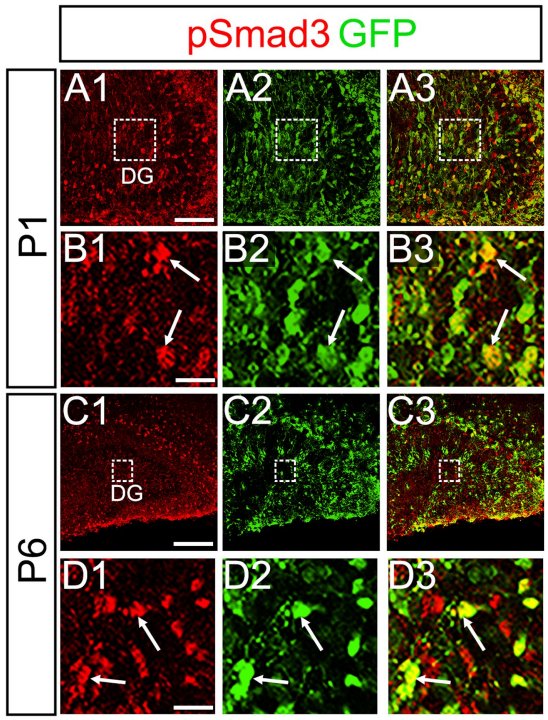

FIGURE 4
PSmad3 is expressed in GFP+ RGLs in early postnatal DG **(A1–D3)** PSmad3 expression in GFP+ RGLs at P1 and P6 (arrows in **B1–B3,D1–D3**). Box in panels (**A1–A3,C1–C3**) indicates region shown in panels (**B1–B3,D1–D3**). Scale bars: 200 μm in **A1–A3,C1–C3**; 50 μm in **B1–B3,D1–D3**.

and that an EMT-like mechanism operates in the developing CNS (Itoh et al., 2013; Singh and Solecki, 2015; Singh et al., 2016), we compared an expression pattern of PSmad3 with that of E cadherin (E-cad), a marker for epithelial cells. PSmad3+ cells were enriched alongside the pial surface of the DG where E-cad was less abundant (Figures 5A1–A3). Instead, vimentin expression was prominent in the DG (data not shown). Moreover, at P1–P6 the PSmad3+/GFP+ cells were found to co-express phospho-vimentin (pVim), a marker for proliferative RGLs both in the DN and DG ($n = 3$; Figures 5B1–I5). pVim expression was also found in Sox2+ cells at P6, and some pVim+ nuclei highlighted a mitotic feature of PSmad3+ RGLs (data not shown). PSmad3+/GFP+ cells were PCNA+ at P3–P6 ($n = 3$, Supplementary Figures 3A1–B6). Consistent with this, Ki67 expression was also found in the GFP+ RGLs ($28 \pm 5\%$, $n = 6$; Supplementary Figures 4A1–A6).

Previous studies have suggested that Sox9 contributes to the maintenance stemness in a variety of tissue-specific stem cells (Furuyama et al., 2011; Guo et al., 2012), including RGLs/neural stem cells (Scott et al., 2010). Our data showed that PSmad3 was expressed in $74\% \pm 3\%$ of Sox9+ cells ($n = 4$), and that Sox9 was expressed in GFP+ RGLs at P1–P6 ($69.5 \pm 3.2\%$, $n = 9$; Figures 6A1–A6,B1–B6,C1–C4). These data suggest that PSmad3 is expressed in a subpopulation of RGLs. In contrast, a vast majority of PSmad3+ RGLs did not express NeuroD, a marker for neuronal progenitors and early differentiating neurons at P3 ($n = 6$; Figures 6D1–D4). In summary, our data suggest that many PSmad3+ cells are proliferative RGLs during the first postnatal week.

At P14 the formation of the GCL and SGZ was almost complete (Figure 7A1). PSmad3 expression was found in the GFP+ cells at SGZ and astrocytes in the ML at P14–P30 ($n = 3$; Figures 7A1–C4). Intriguingly, many of the Ki67+ cells at the SGZ were Tbr2+ neuronal progenitors ($n = 3$; Figures 8A1–A8), and only a small proportion of the GFP+ cells were Ki67+ and PCNA+ ($n = 3$; Figures 8B1–C8). Consistent with this, PSmad3+ cells at P14-P21 were predominantly pVim−/PCNA− (Figures 8D1–E8). These data suggest that the PSmad3+ RGLs are mostly quiescent after the second postnatal week.

Olig2 expression in PSmad3+/GFP+ astrocytes but not in RGLs at SGZ

Our data have shown that PSmad3 is expressed in GFP+ RGLs and astrocytes (Figures 2–7). However, the TFs expression that could discern the two distinct cell types remains unclear. Given that Olig2 is expressed not only in oligodendrocyte progenitors but also in astrocyte progenitors (Marshall et al., 2005; Zhu et al., 2012; Ohayon et al., 2018; Tatsumi et al., 2018; Wang et al., 2021), we next examined whether Olig2 is expressed in astrocytes of the developing DG. Very few Olig2+ cells were found in DG at E16 (Figures 9A1–A6). A small population of Olig2+/GFP+ cells was found in the DN and DG at E18 (Figures 9B1–B6,C1–C6). Many more Olig2+/GFP+ cells were observed in both DN and DG at P3 (Figures 9D1–D6,E1–E6). $32 \pm 6\%$ of the GFP+ cells were Olig2+ ($n = 4$). The Olig2+ cells were mainly located in the ML, with some in the hilus and GCL at P3–P6 (Figures 9D1–F6). Olig2 is expressed in $42.1\% \pm 2.9\%$ of Sox9+ cells ($n = 5$). GFAP is expressed in RGLs and astrocytes but not in oligodendrocyte progenitors (OLPs). Hence our data suggest that Olig2+/GFP+ cells are astrocytes. Meanwhile, Olig2+/GFP− oligodendrocyte progenitors (OLPs; $68.7\% \pm 4.3\%$ of Olig2+ cells, $n = 4$) were found in the hilus, GCL, and ML (Figures 9D1–F6). At P14, Olig2+/GFP+ astrocytes were also found in the ML but not in the SGZ (Figures 9G1–G9), and they co-expressed an astrocytic marker Sox9 (Figures 9H1–H8). To confirm that Olig2 expression is associated with glial progenitors in the DG, no Olig2+ cells co-expressed a neuronal progenitor marker NeuroD (Figures 10A1–D8).

Our data further showed that PSmad3 is expressed in Olig2+ cells at the ML at P3 ($n = 3$, Figures 11A1–A4). At P14, PSmad3+ cells in the ML co-expressed Olig2, whereas those at the SGZ did not ($n = 3$, Figures 11B1–B4, also see Figures 9G4–G9). Collectively, our data show that PSmad3+ cells in the ML but not the SGZ of early postnatal DG are Olig2+/GFP+ astrocytes. Consistent with this, PSmad3 was expressed in S100β + and GFAP+ astrocytes in the ML at P14 ($n = 3$, Figures 12A1–A3,B1–B3, respectively). Moreover, at P60, whereas PSmad3+ cells in the ML co-expressed either S100β or GFP, PSmad3+ cells in the SGZ did not ($n = 3$, Figures 12C1–C8).

Taken together, GFP+ and Sox9+ cells are either RGLs or astrocytes in the postnatal DG. Approximately 60%–70% of them correspond to RGLs (Sox9 + Olig2− or GFP+ Olig2−). The remaining 30%–40% are astrocytes (Olig2 + GFP+ or Olig2 + Sox9+). Approximately 70% of the Sox9+ cells (RGLs or astrocytes) co-express PSmad3. Approximately 30% of the GFP^+ cells (RGLs or astrocytes) are proliferating (Ki67+) at during the first postnatal week. In conclusion, the present study has revealed that there are distinct types

10.3389/fnins.2023.1204012

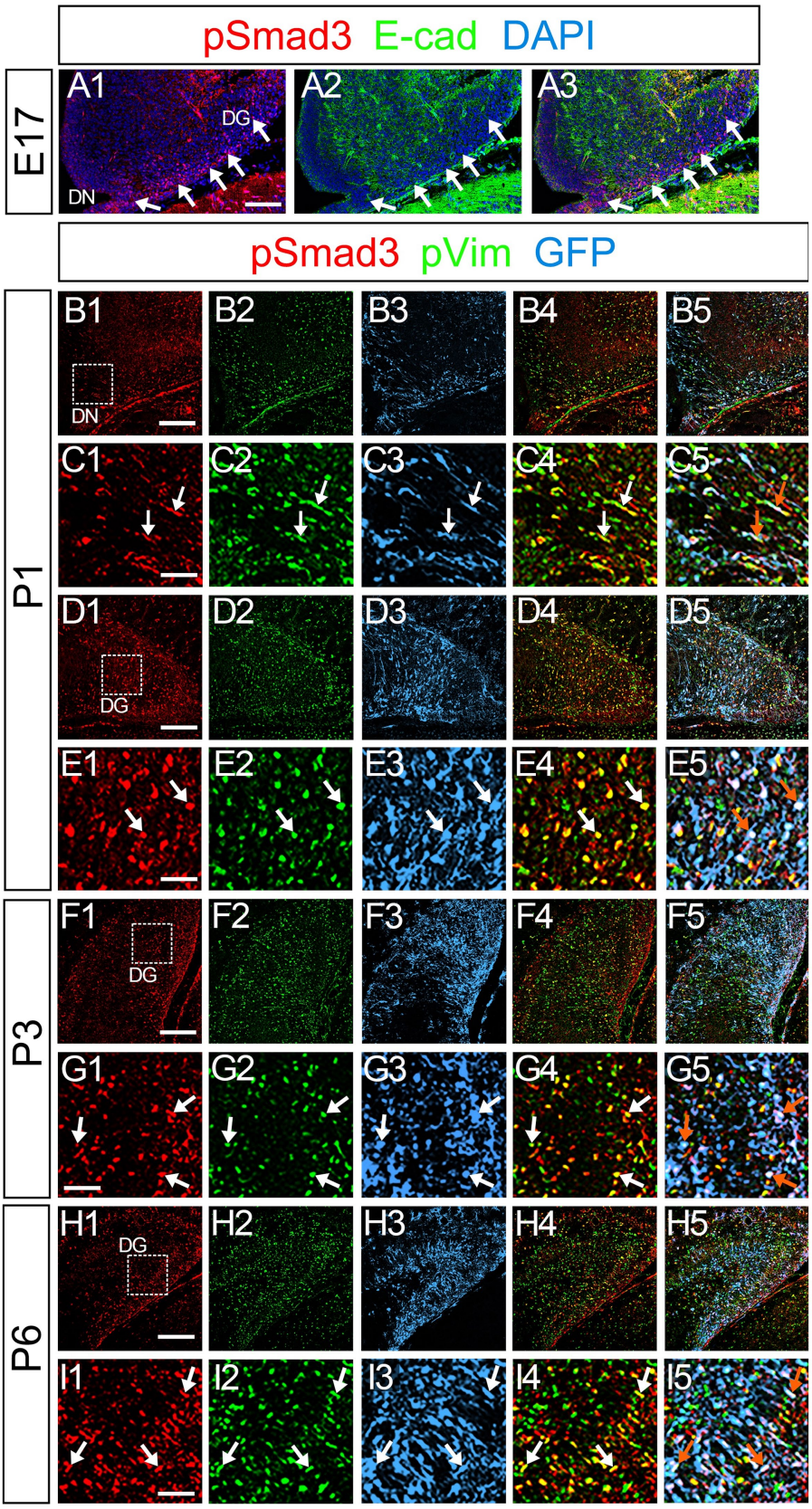

FIGURE 5
PSmad3+/GFP+ cells are pVim+ proliferating basal RGLs in postnatal DG **(A1–A3)** PSmad3 expression is abundant in E-Cad-negative area of the DG at E17. **(B1–I5)** PSmad3+/GFP+ cells co-express a proliferative basal RGLs marker pVim at DN and DG at P1–P6 (arrows in **C1–C5,E1–E5,G1–G5,I1–I5**). Box in panels (**B1,D1,F1,H1**) indicates region shown in panels (**C1–C5,E1–E5,G1–G5,I1–I5**, respectively). Scale bars: 200 μm in **A1–A3,B1–B5,D1–D5,F1–F5,H1–H5**; 100 μm in **C1–C5,E1–E5,G1–G5,I1–I5**.

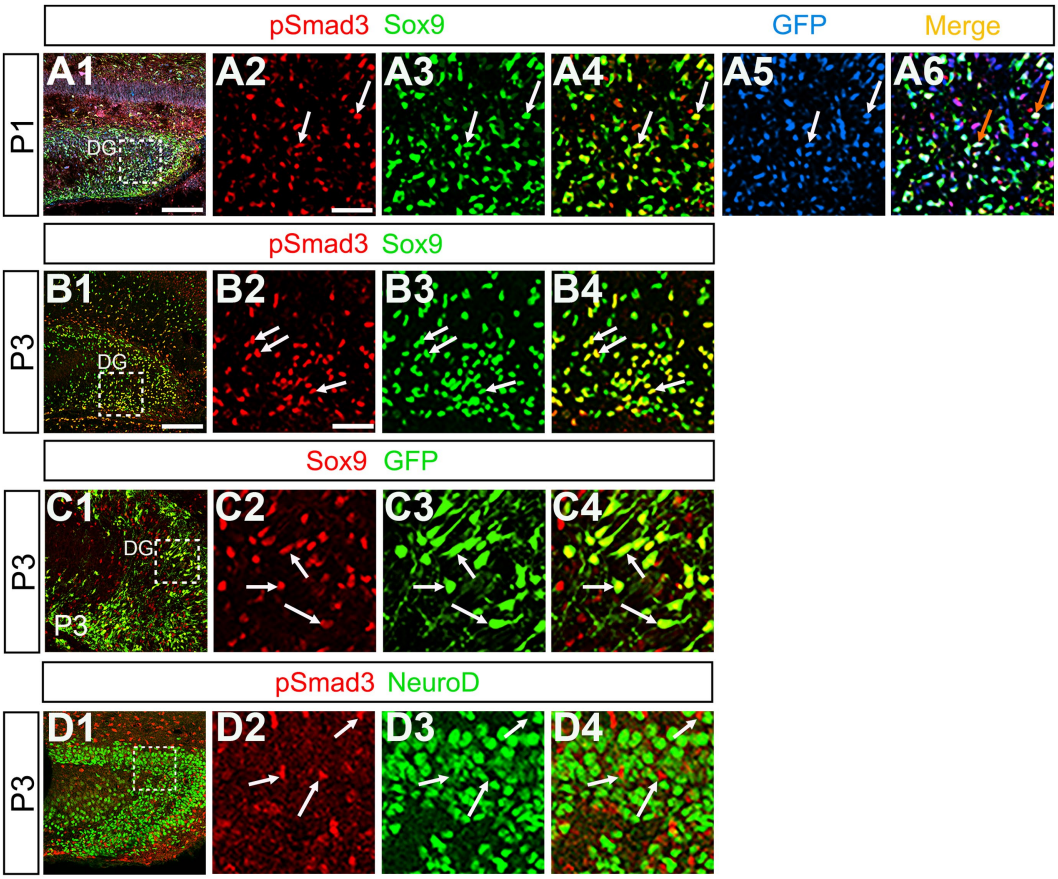

FIGURE 6
PSmad3+/GFP+ RGLs express Sox9 but not NeuroD **(A1–A6)** PSmad3 + cells co-express Sox9 in DG at P1 (arrows in **A2–A4**). The PSmad3+/Sox9+ cells also co-express GFP (arrows in **A5,A6**). **(B1–B4)** Co-expression of PSmad3 and Sox9 in DG at P3 (arrows in **B2–B4**). **(C1–C4)** Sox9 expression in GFP+ RGLs in DG at P3 (arrows in **C2–C4**). **(D1–D4)** PSmad3+ RGLs do not co-express NeuroD (arrows in **D2–D4**). Box in panels (**A1,B1,C1,D1**) indicates region shown in panels (**A2–A6,B2–B4,C2–C4,D2–D4**). Scale bars = 200 μm in **A1,B1,C1,D1**; 50 μm in **A2–A6,B2–B4,C2–C4,D2–D4**.

of PSmad3+/GFP+ cells in both embryonic and postnatal mouse DG: neural progenitors, RGLs, and Olig2+ astrocytes (Figure 13).

Discussion

Development of PSmad3+ RGLs

Gfap-GFP+ (GFP+) DG progenitors express Sox2 and migrate away from the VZ of the DN, and they are found in the SGZ, ML, and hilus in the postnatal DG (Figure 1). These data suggest that both the GFP+ RGLs in the SGZ and the astrocytes in the ML and hilus are derived from the DN. Consistent with this, PSmad3 expression was found in both GFP+/Prox1 + $_{low}$ progenitors, GFP+ RGLs, and GFP+/Olig2+ astrocytes. Given the Prox1$_{low}$ + expression, the PSmad3+/ GFP+ progenitors seem to possess a property of neurogenic cells that give rise to Prox1$_{high}$ + dentate granule neurons. Interestingly, PSmad3+/ GFP+/Prox1$_{low}$ + progenitors were also observed in early postnatal DG (data not shown). However, the developmental origin of PSmad3+ RGLs and astrocytes remains elusive. Given that PSmad3+ cells are observed mostly in the lower DN and fimbria-dentate junction at E14–17, the PSmad3+ RGLs are likely to originate from the lower DN. Consistent with this, PSmad3 is expressed in a subpopulation of GFP+/Sox9+ cells that are likely to originate from a broader region around the DN (Figure 6). While our data imply that PSmad3+/ GFP+/Prox1 $_{low}$ + neurogenic progenitors may originate from the lower DN, a genetic lineage tracing analysis will be necessary to further clarify this issue.

It has previously been shown that expansion of RGLs is prominent during the first week after birth (Matsue et al., 2017). In support of this notion, the expansion of PSmad3+/GFP+ RGLs becomes evident during the perinatal period (Figure 5; Supplementary Figure 3). The majority of the PSmad3+ RGLs co-express Sox2, Sox9, pVim, and PCNA (Figures 3, 5, 6; Supplementary Figure 3), supporting their proliferative capacity in the first postnatal week.

The TGFβ-pSmad2/3-Sox2 pathway has been implicated in regulating the stemness of glioma-initiating cells (Ikushima et al., 2009). Recent studies have also shown that PSmad3 can bind to Sox9 and activate Sox9-dependent transcription (Furumatsu et al., 2009), and that Sox9 and Slug co-operate to maintain cancer stem cells (Guo et al., 2012). While Slug is not expressed in the developing brain

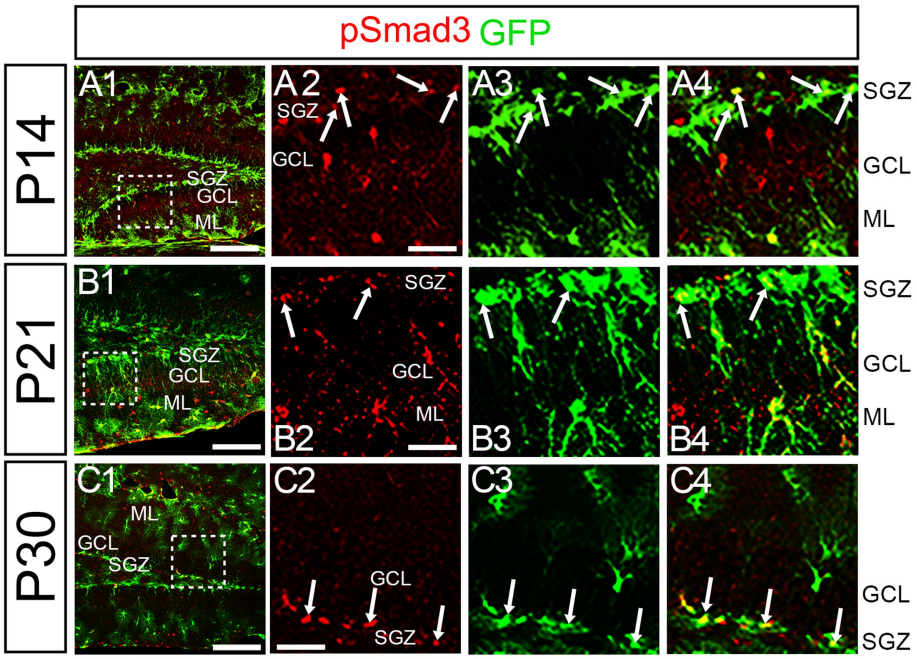

FIGURE 7
PSmad3 is expressed in GFP+ RGLs at P14 and onward **(A1–C4)** PSmad3 is expressed in GFP+ RGLs at SGZ and astrocytes in ML at P14, P21, and P30 (arrows in **A2–A4,B2–B4,C2–C4**). Box in panels (**A1,B1,C1**) indicates region shown in panels (**A2–A4,B2–B4,C2–C4**). Scale bars = 200 μm in **A1,B1,C1**; 50 μm in **A2–A4,B2–B4,C2–C4**.

(Marin and Nieto, 2004), Snail1, a cousin of Slug controls the number of neural progenitors at the SGZ of the hippocampus (Zander et al., 2014). Similarly, Zeb1 at the downstream of PSmad3 maintains RGLs in the DG (Gupta et al., 2021). PSmad3 may contribute to control the proliferative property of RGLs in the DG through the regulation of the EMT-TFs Sox9, Snail1, and Zeb1.

Sufu acts as a positive regulator of Shh signal, thereby RGLs expansion in the DG (Noguchi et al., 2019). TGFβ2 induces Gli1 expression in a PSmad3-dependent manner after ischemia/reperfusion injury (Peng et al., 2019). Future analysis of the crosstalk between the TGFb-PSmad3 pathway and Shh signaling will also shed light on the mechanism controlling the expansion of postnatal RGLs in the DG.

Accumulating evidence suggests that EMT prevents oncogene-induced senescence (OIS) early in tumor progression (Weinberg, 2008). EMT TFs such as Twist and Zeb1 promote EMT and simultaneously inhibit OIS (Ansieau et al., 2008; Chaffer et al., 2013). Deficiency of the senescence regulator $p21^{CIP1}$ induces EMT vice versa (Lin et al., 2012). B-catenin associates with PSmad3 to promote TGFβ-induced EMT (Tian et al., 2012). In contrast, downregulation of Wnt-β-catenin signaling triggers the onset of cellular senescence (Ye et al., 2007). Thus, it is possible that TGFβ and Wnt signaling may cooperate at the level of PSmad3 and β-catenin to escape senescence in RGLs, thereby maintaining their stemness.

Tapia-Gonzalez et al. showed that Smad3 is expressed in early intermediate progenitors but not in Sox2+ RGLs in adult mouse DG. Smad3 mRNA was observed in the granule cell layer (GCL) in addition to the SGZ. Our data show that PSmad3 is expressed in GFP+/Sox2+/Sox9+ progenitors and RGLs. These data appear to be somewhat contradictory each other. Tapia-Gonzalez et al. analyzed the DG of 3–4 month old female mice. In our data, PSmad3 expression was observed in the SGZ, hilus, and ML in male mice at P60 (Figure 12). It is also worth noting that PSmad3 was very weakly expressed in the GCL of the mouse DG at P60 but not at P30 (Figures 7, 12). Intriguingly, at 6 months old of age, PSmad3 was strongly expressed in the GCL in addition to the SGZ, hilus, and ML (data not shown). It seems that the expression pattern of PSmad3 is somehow slightly different between adolescent and adult mouse DG.

Our data clearly show that PSmad3 is expressed in subpopulation of GFP+ cells. This also explain why in Tapia-Gonzalez et al., PSmad3 expression was not observed in Sox2+ and GFAP+ RGLs at the SGZ of 3–4 month old mouse DG (Tapia-González et al., 2013). GFP+ expression can label many more GFAP-expressing cells, compared to immunolabeling with GFAP antibody. Given our data that some GFP+ cells at the SGZ express Tbr2 (unpublished data), and that Tbr2+ intermediate progenitors at the SGZ express Ascl1 (Tapia-González et al., 2013), this may explain why we were able to detect PSmad3+/GFP+ RGLs at the SGZ, whereas PSmad3 expression was detected in Ascl1+ progenitors (Tapia-González et al., 2013).

Taken together, PSmad3 is expressed in a subpopulation of GFP+/Sox2+/Sox9+ dentate progenitors in the embryo, and the RGLs and astrocytes in the postnatally developing mouse DG. Although this also seems to be the case in the adult, further careful analysis of PSmad3 expression in combination with various markers of distinct cell types

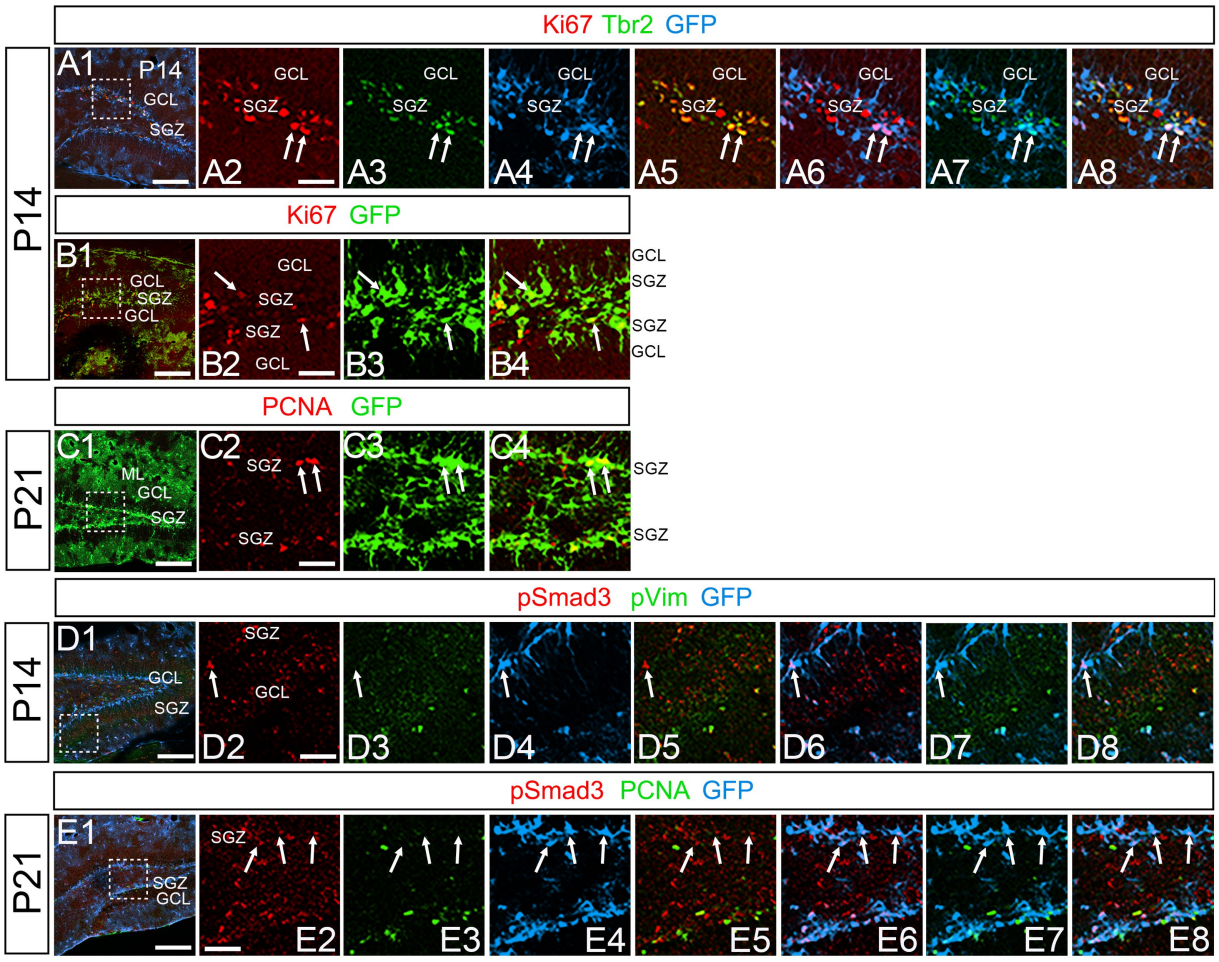

FIGURE 8
PSmad3+/GFP+ RGLs at SGZ are mostly in quiescence **(A1–A8)** Ki67 expression in Tbr2+/GFP+ progenitors at P14 (arrows in **A2–A8**). A majority of GFP+ RGLs at SGZ do not co-express Ki67. **(B1–B4)** Ki67 expression is found in some GFP+ RGLs at P14 (arrows in **B2–B4**). **(C1–C4)** PCNA expression in some GFP+ RGLs at SGZ at P21. **(D1–D8)** PSmad3+/GFP+ RGLs do not express pVim at P14 (arrows in **D2–D8**). **(E1–E8)** PSmad3+/GFP+ RGLs do not express PCNA at P21 (arrows in E2-E8). Box in panels **(A1,B1,C1,D1,E1)** indicates region shown in panels (**A2–A8,B2–B4,C2–C4,D2–D8,E2–E8**). Scale bars, 200 μm in **A1,B1,C1,D1,E1**; 50 μm in **A2–A8,B2–B4,C2–C4,D2–D8,E2–E8**.

is necessary to accurately describe the expression pattern of PSmad3 throughout life.

Development of PSmad3+/Olig2+ astrocytes

While PSmad3+ progenitors were found in the DN at E14–E16, very few Olig2+ cells were found in both the DN and DG at E16 (Figures 1, 2, 9). Olig2+ progenitors appear at the upper DN at E18 (Figures 9B1–B6). At P1-6 PSmad3+/GFP+ progenitors were found around both upper and lower DN, and many of them co-expressed Olig2 (data not shown). These data suggest that the Olig2+ astrocytes seem to originate from the VZ around the DN from E18 onwards.

Recent studies have shown that Olig2+ astrocytes are present in both embryonic and adult CNS (Ohayon et al., 2018; Tatsumi et al., 2018; Wang et al., 2021). While it has previously been shown that the majority of Olig2+ astrocytes are GFAP− in the adult CNS (Tatsumi et al., 2018; Wang et al., 2021), we were able to detect Olig2+/GFP+ astrocytes by using *gfap*-GFP mice (Figure 9). Nonetheless, there may be Olig2+/GFP− astrocytes in the DG. More careful analysis of Olig2+ astrocytes will be necessary to clarify the heterogeneity of Olig2+ astrocytes. In terms of the function of Olig2+ astrocytes, while Olig2+ OLPs respond to brain injury such as hypoxia and increase in number, the role of Olig2+ astrocytes remains unclear (Allan et al., 2021). It will be interesting to see whether Olig2+ astrocytes act as reactive astrocytes after brain injury.

In conclusion, we have provided evidence that PSmad3 is expressed in a subpopulation of GFP+/Sox9+ neural progenitors, RGLs, and astrocytes in the mouse DG during embryonic and postnatal development, and that Olig2 expression is allocated with astrocytes but not RGLs. While the roles of PSmad3 and Olig2 in the development of RGLs and astrocytes remain elusive, combinatorial expression of these TFs will be useful to identify RGLs and Olig2+ astrocytes to investigate their development and function in the mouse DG.

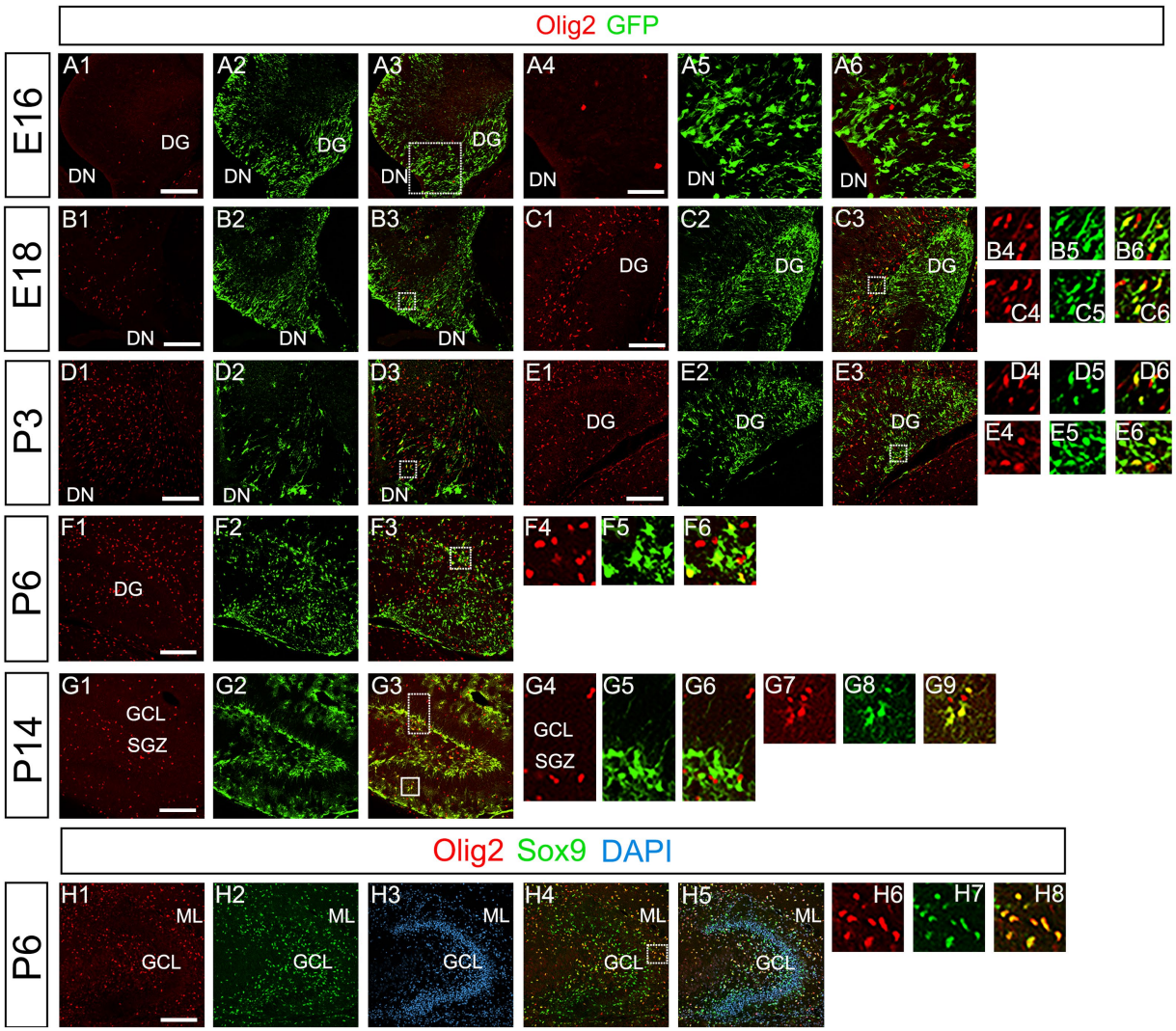

FIGURE 9
Olig2 expression in GFP+/Sox9+ astrocytes of the ML but not in the SGZ RGLs of developing mouse DG **(A1–A6)** Only a few Olig2+ cells were found in DN at E16. They are immuno-negative for GFP **(A4–A6)**. **(B1–B3,C1–C6,D1–D3,E1–E6)** Some Olig2+/GFP+ astrocytes were found both in DN and DG at E18 and P3. **(F1–F6)** Olig2+/GFP+ astrocytes are found in the ML of DG at P6. **(G1–G9)** While GFP+ cells at the SGZ do not express Olig2 **(G4–G6)**, those at the ML co-express Olig2 **(G7–G9)**, indicating that the latter are astrocytes. **(H1–H8)** Olig2+/Sox9+ cells were found in the DG at P6, suggesting that the Olig2+/GFP+/Sox9+ cells are astrocytes. Box in panels **(A3,B3,C3,D3,E3,F3,G3,H4)** indicates region shown in panels **(A4-A6, B4-B6,C4-C6,D4-D6,E4-E6,F4-F6,G4-G6,G7-G9,H6-H8)**. Scale bars, 200μm in **A1–A3,B1–B3,C1–C3,D1–D3,E1–E3,F1–F3,G1–G3,H1–H5**; 50μm in **A4–A6**.

Data availability statement

The original contributions presented in the study are included in the article/Supplementary material, further inquiries can be directed to the corresponding author.

Ethics statement

The animal study was approved by Ethics committee of Animal Experiments in Tokyo Medical University. The study was conducted in accordance with the local legislation and institutional requirements.

Author contributions

KO: experimental design. KO, SO, TK, TS, and KT: acquisition of data. KO and HS: analysis and interpretation of data and writing and editing the manuscript. All authors contributed to the article and approved the submitted version.

Funding

This study was supported by Mitsui Sumitomo Insurance Welfare Foundation (to KO), Japan Society for the Promotion of Science (JSPS) KAKENHI [Grant numbers 19K11726 (to KO), 22H03367 (to KO), 23K05995 (to KO), 16K18983 (to HS), and 20K07233 (to HS)], the Center

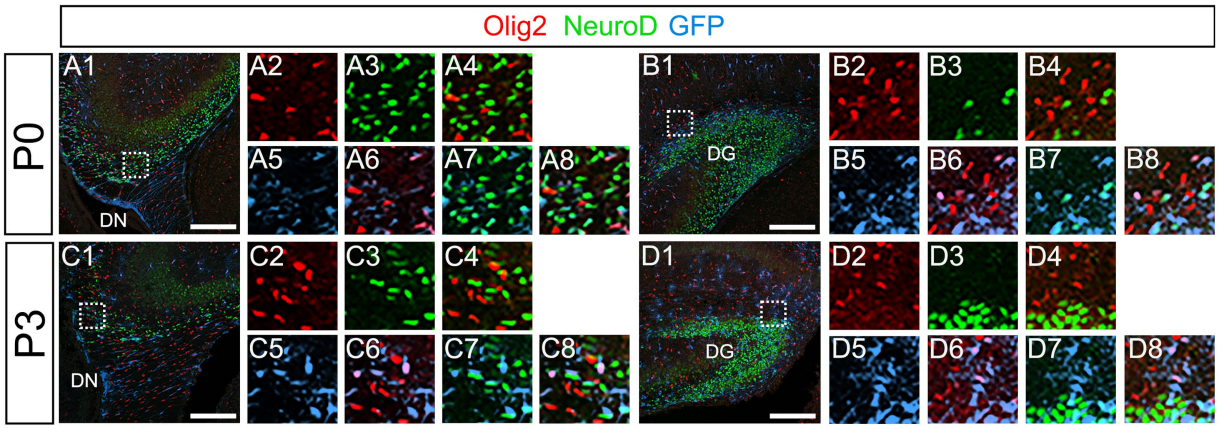

FIGURE 10
Olig2+ cells do not co-express NeuroD. **(A1–A8,B1–B8)** Olig2+/GFP+ cells do not co-express NeuroD at DN **(A1–A8)** and DG **(B1–B8)** at P0. **(C1–C8,D1–D8)** Olig2+/GFP+ cells do not co-express NeuroD at DN **(C1–C8)** and DG **(D1–D8)** at P3. Box in panels **(A1,B1,C1,D1)** indicates region shown in panels **(A2-A8,B2-B8,C2-C8,D2-D8)**. Scale bars, 200 μm in **A1,B1,C1,D1**.

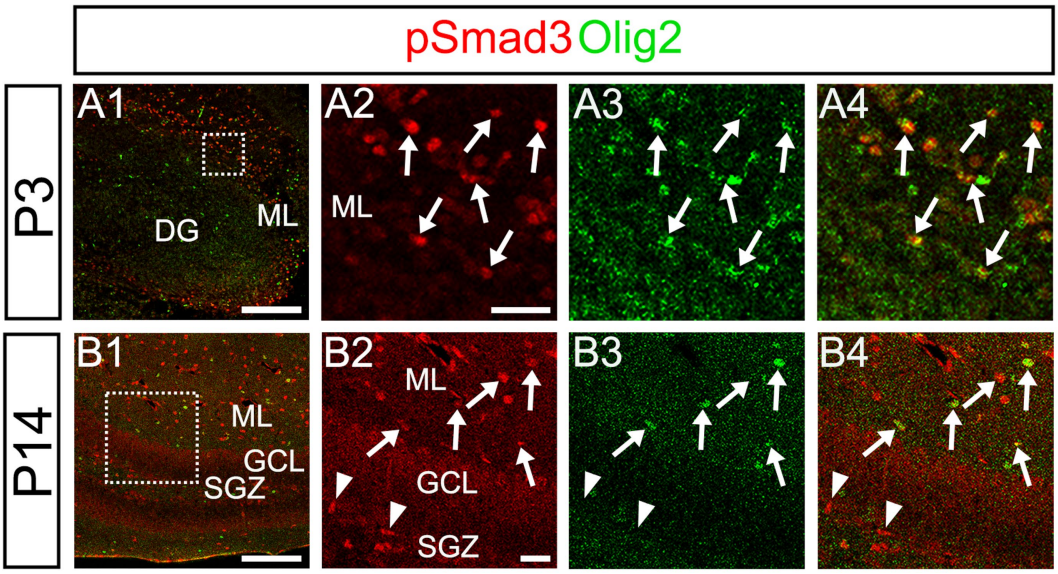

FIGURE 11
While pSmad3+ cells in the ML co-express Olig2, PSmad3+ SGZ cells do not. **(A1–A4)** PSmad3+ cells in the ML co-express Olig2 at P3 (arrows in **A2–A4**). **(B1–B4)** While PSmad3+ cells in the ML co-express Olig2 (arrows in **B2–B4**), PSmad3+ cells (red) at SGZ do not co-express Olig2 (arrowheads in **B2–B4**). Box in panels **(A1,B1)** indicates region shown in panels **(A2–A4,B2–B4)**. Scale bars, 200 μm in **A1,B1**; 50 μm in **A2–A4,B2–B4**.

10.3389/fnins.2023.1204012

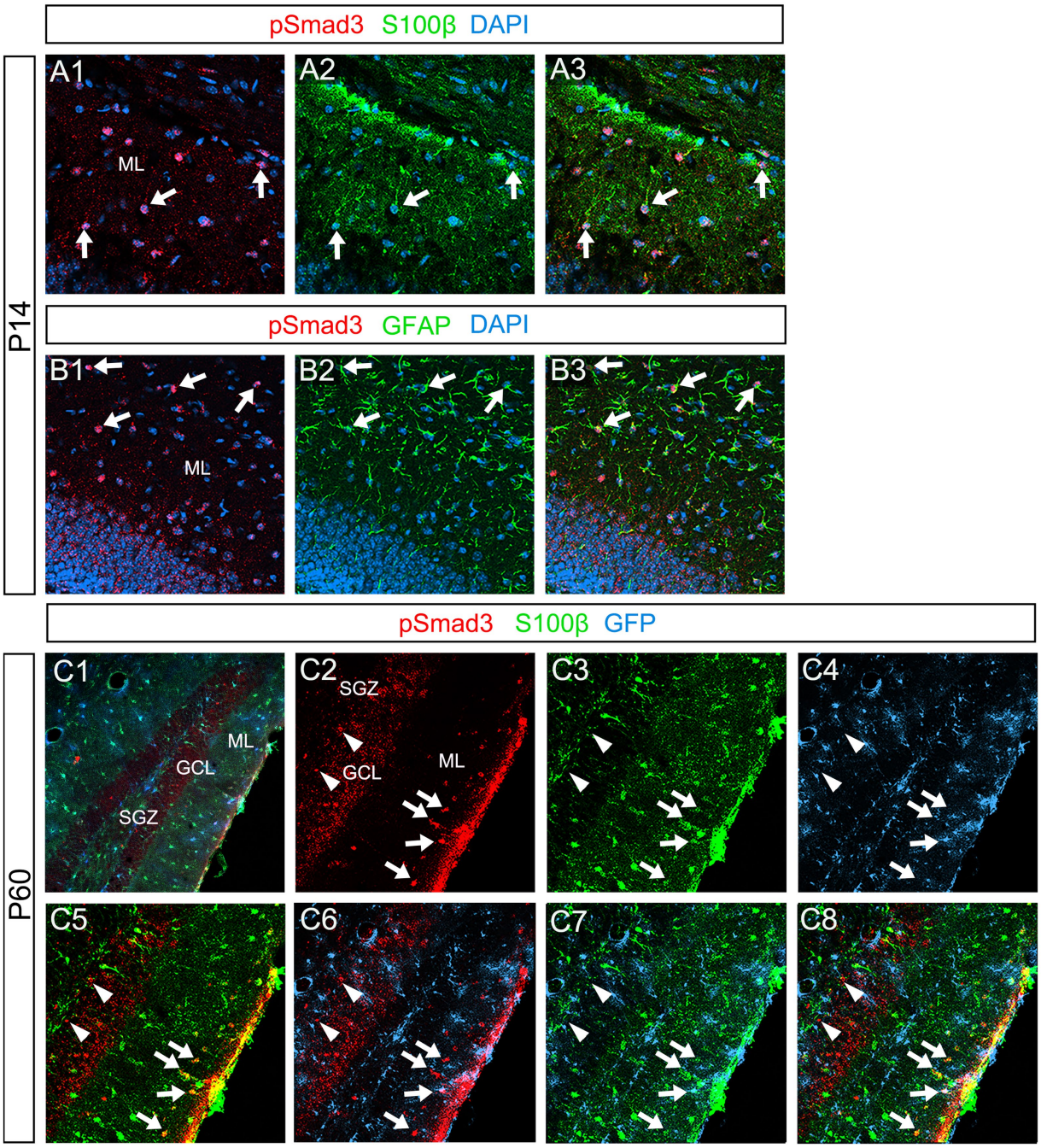

FIGURE 12
PSmad3+ cells in the ML, but not at the SGZ, co-express S100β in postnatal and adult mouse DG **(A1–A3)** PSmad3+ cells co-express S100β at ML at P14 (arrows). **(B1–B3)** PSmad3+ cells co-express GFAP at P14 (arrows). **(C1–C8)** At P60 pSmad3 is co-expressed with both S100β and GFP in the ML but not at the SGZ (arrows in **C2–C8**, arrowheads in **C2–C8**, respectively).

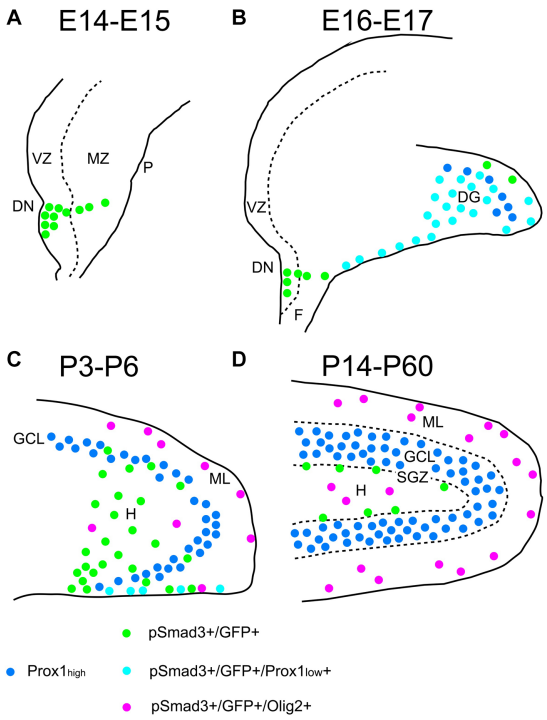

FIGURE 13
Schematic drawing of the PSmad3+/GFP+ RGLs and PSmad3+/GFP+/Olig2+ astrocytes in developing mouse DG **(A)** At E14-E15 PSmad3+/GFP+ cells (green) are located mainly at the VZ of lower DN, forming a migratory stream to the MZ. **(B)** At E16-E18 PSmad3+/GFP+/Prox1 + $_{low}$ cells (light blue) are found in the subpial region and the DG, suggesting that they are the RGLs that give rise to granule neuronal progenitors. Very few GFP+ cells co-express Olig2. **(C)** At P3-P6 PSmad3+/GFP+ cells accumulate in the hilus (H) and ML (green, light blue, or purple). Some PSmad3+/GFP+ cells co-express either Prox1 + $_{low}$ (blue; data not shown) or Olig2 (purple). **(D)** At P14-60 PSmad3+/GFP+ cells located at the ML and H, but not at the SGZ, co-express Olig2 (purple). Together, expressions of PSmad3 and Olig2 in combination defines RGLs (PSmad3+/Olig2– in either green or light blue) and astrocytes (PSmad3+/Olig2+ in purple) both in embryonic and postnatal DG. DG, dentate gyrus; DN, dentate notch; F, fimbria; GCL, granule cell layer (Prox1$_{high}$ + in blue); H, hilus; MZ, mantle zone; P, pia; VZ, ventricular zone.

for Diversity at Tokyo Medical University TMUCD-202202 (to HS), and Research promotion grant from Tokyo Medical University (to KO).

Acknowledgments

The authors thank T. Seki for encouragement and helpful discussions, T. Takahashi for feedback on the manuscript, and S. Shioda for providing *gfap*-GFP mice.

Conflict of interest

The authors declare that the research was conducted in the absence of any commercial or financial relationships that could be construed as a potential conflict of interest.

Publisher's note

Supplementary material

The Supplementary material for this article can be found online at: https://www.frontiersin.org/articles/10.3389/fnins.2023.1204012/full#supplementary-material

References

Allan, K. C., Hu, L. R., Scavuzzo, M. A., Morton, A. R., Gevorgyan, A. S., Cohn, E. F., et al. (2021). Non-canonical targets of HIF1a impair oligodendrocyte progenitor cell function. *Cell Stem Cell* 28, 257–272. doi: 10.1016/j.stem.2020.09.019

Altman, J., and Bayer, S. A. (1990). Mosaic organization of the hippocampal neuroepithelium and the multiple germinal sources of dentate granule cells. *J. Comp. Neurol.* 301, 325–342. doi: 10.1002/cne.903010302

Ansieau, S., Bastid, J., Doreau, A., Morel, A.-P., Bouchet, B. P., Thomas, C., et al. (2008). Induction of EMT by twist proteins as a collateral effect of tumor-promoting inactivation of premature senescence. *Cancer Cell* 14, 79–89. doi: 10.1016/j.ccr.2008.06.005

Brunne, B., Franco, S., Bouché, E., Herz, J., Howell, B. W., Pahle, J., et al. (2013). Role of the postnatal radial glial scaffold for the development of the dentate gyrus as revealed by Reelin signaling mutant mice. *Glia* 61, 1347–1363. doi: 10.1002/glia.22519

Chaffer, C. L., Marjanovic, N. D., Lee, T., Bell, G., Kleer, C. G., Reinhardt, F., et al. (2013). Poised chromatin at the ZEB1 promoter enables breast cancer cell plasticity and enhances tumorigenicity. *Cells* 154, 61–74. doi: 10.1016/j.cell.2013.06.005

Choe, Y., Kozlova, A., Graf, D., and Pleasure, S. J. (2013). Bone morphogenic protein signaling is a major determinant of dentate development. *J. Neurosci.* 33, 6766–6775. doi: 10.1523/JNEUROSCI.0128-13.2013

Furumatsu, T., Ozaki, T., and Asahara, H. (2009). Smad3 activates the Sox9-dependent transcription on chromatin. *Int. J. Biochem. Cell Biol.* 41, 1198–1204. doi: 10.1016/j.biocel.2008.10.032

Furuyama, K., Kawaguchi, Y., Akiyama, H., Horiguchi, M., Kodama, S., Kuhara, T., et al. (2011). Continuous cell supply from a Sox9-expressing progenitor zone in adult liver, exocrine pancreas and intestine. *Nat. Genet.* 43, 34–41. doi: 10.1038/ng.722

Galceran, J., Miyashita-Lin, E. M., Devaney, E., Rubenstein, J. L. R., and Grosschedl, R. (2000). Hippocampus development and generation of dentate gyrus granule cells is regulated by LEF1. *Development* 127, 469–482. doi: 10.1242/dev.127.3.469

García-Campmany, L., and Martí, E. (2007). The TGFβ intracellular effector Smad3 regulates neuronal differentiation and cell fate specification in the developing spinal cord. *Development* 134, 65–75. doi: 10.1242/dev.02702

Guo, W., Keckesova, Z., Donaher, J. L., Shibue, T., Tischler, V., Reinhardt, F., et al. (2012). Slug and Sox9 cooperatively determine the mammary stem cell state. *Cells* 148, 1015–1028. doi: 10.1016/j.cell.2012.02.008

Gupta, B., Errington, A. C., Jimenez-Pascual, A., Eftychidis, V., Brabletz, S., Stemmler, M. P., et al. (2021). The transcription factor ZEB1 regulates stem cell self-renewal and cell fate in the adult hippocampus. *Cell Rep.* 36:109588. doi: 10.1016/j.celrep.2021.109588

He, Y., Zhang, H., Yung, A., Villeda, S. A., Jaeger, P. A., Olayiwola, O., et al. (2014). ALK5-dependent TGF-b signaling is a major determinant of late-stage adult neurogenesis. *Nat. Neurosci.* 17, 943–952. doi: 10.1038/nn.3732

Ikushima, H., Todo, T., Ino, Y., Takahashi, M., Miyazawa, K., and Miyazono, K. (2009). Autocrine TGF-b signaling maintains tumorigenicity of glioma-initiating cells through Sry-related HMG-box factors. *Cell Stem Cell* 5, 504–514. doi: 10.1016/j.stem.2009.08.018

Itoh, Y., Moriyama, Y., Hasegawa, T., Endo, T. A., Toyoda, T., and Gotoh, Y. (2013). Scratch regulates neuronal migration onset via an epithelial-mesenchymal transition–like mechanism. *Nat. Neurosci.* 16, 416–425. doi: 10.1038/nn.3336

Li, G., Fang, L., Fernandez, G., and Pleasure, S. J. (2013). The ventral hippocampus is the embryonic origin for adult neural stem cells in the dentate gyrus. *Neuron* 78, 658–672. doi: 10.1016/j.neuron.2013.03.019

Lin, S., Yang, J., Elkahloun, A. G., Bandyopadhyay, A., Wang, L., Cornell, J. E., et al. (2012). Attenuation of TGF-β signaling suppresses premature senescence in a p21-dependent manner and promotes oncogenic Ras-mediated metastatic transformation in human mammary epithelial cells. *Mol. Biol. Cell* 23, 1569–1581. doi: 10.1091/mbc.E11-10-0849

Marin, F., and Nieto, M. A. (2004). Expression of chicken *slug* and *snail* in mesenchymal components of the developing central nervous system. *Dev. Dyn.* 230, 144–148. doi: 10.1002/dvdy.20027

Marshall, C. A. G., Novitch, B. G., and Goldman, J. E. (2005). Olig2 directs astrocyte and oligodendrocyte formation in postnatal subventricular zone cells. *J. Neurosci.* 25, 7289–7298. doi: 10.1523/JNEUROSCI.1924-05.2005

Matsue, K., Minakawa, S., Kashiwagi, T., Toda, K., Sato, T., Shioda, S., et al. (2017). Dentate granule progenitor cell properties are rapidly altered soon after birth. *Brain Struct. Funct.* 223, 357–369. doi: 10.1007/s00429-017-1499-7

Namba, T., Mochizuki, H., Onodera, M., Mizuno, Y., Namiki, H., and Seki, T. (2005). The fate of neural progenitor cells expressing astrocytic and radial glial markers in the postnatal rat dentate gyrus. *Eur. J. Neurosci.* 22, 1928–1941. doi: 10.1111/j.1460-9568.2005.04396.x

Noguchi, H., Castillo, J. G., Nakashima, K., and Pleasure, S. J. (2019). Suppressor of fused controls perinatal expansion and quiescence of future dentate adult neural stem cells. *Elife* 8:e42918. doi: 10.7554/eLife.42918

Ohayon, D., Escalas, N., Cochard, P., Glise, B., Danesin, C., and Soula, C. (2018). Sulfatase 2 promotes generation of a spinal cord astrocyte subtype that stands out through the expression of Olig2. *Glia* 67, 478–1495. doi: 10.1002/glia.23621

Ohyama, K., Ellis, P., Kimura, S., and Placzek, M. (2005). Directed differentiation of neural cells to hypothalamic dopaminergic neurons. *Development* 132, 5185–5197. doi: 10.1242/dev.02094

Peng, L., Yang, C., Yin, J., Ge, M., Wang, S., Zhang, G., et al. (2019). TGF-β2 induces Gli1 in a Smad3-dependent manner against cerebral ischemia/reperfusion injury after isoflurane post-conditioning in rats. *Front. Neurosci.* 13:636. doi: 10.3389/fnins.2019.00636

Scott, C. E., Wynn, S. L., Sesay, A., Cruz, C., Cheung, M., Gomez Gaviro, M.-V., et al. (2010). SOX9 induces and maintains neural stem cells. *Nat. Neurosci.* 13, 1181–1189. doi: 10.1038/nn.2646

Seki, T., Sato, T., Toda, K., Osumin, N., Imura, T., and Shioda, S. (2014). Distinctive population of gfap-expressing neural progenitors arising around the dentate notch migrate and form the granule cell layer in the developing hippocampus. *J. Comp. Neurol.* 522, 261–283. doi: 10.1002/cne.23460

Singh, S., Howell, D., Trivedi, N., Kessler, K., Ong, T., Rosmaninho, P., et al. (2016). Zeb1 controls neuron differentiation and germinal zone exit by a mesenchymal-epithelial-like transition. *Elife* 5:717. doi: 10.7554/eLife.12717

Singh, S., and Solecki, D. J. (2015). Polarity transitions during neurogenesis and germinal zone exit in the developing central nervous system. *Front. Cell. Neurosci.* 9:62. doi: 10.3389/fncel.2015.00062

Suzuki, R., Watanabe, J., Arata, S., Funahashi, H., Kikuyama, S., and Shioda, S. (2003). A transgenic mouse model for the detailed morphological study of astrocytes. *Neurosci. Res.* 47, 451–454. doi: 10.1016/j.neures.2003.08.008

Tapia-González, S., Muñoz, M. D., Cuartero, M. I., and Sánchez-Capelo, A. (2013). Smad3 is required for the survival of proliferative intermediate progenitor cells in the dentate gyrus of adult mice. *Cell Commun. Signal* 11:93. doi: 10.1186/1478-811X-11-93

Tatsumi, K., Isonishi, A., Yamasaki, M., Kawabe, Y., Morita-Takemura, S., Nakahara, K., et al. (2018). Olig2-lineage astrocytes: a distinct subtype of astrocytes that differs from GFAP astrocytes. *Front. Neuroanat.* 12:8. doi: 10.3389/fnana.2018.00008

Tian, X., Zhang, J., Tan, T. K., Lyons, J. G., Zhao, H., Niu, B., et al. (2012). Association of β-catenin with P-Smad3 but not LEF-1 dissociates in vitro profibrotic from anti-inflammatory effects of TGF-β1. *J. Cell Sci.* 126, 67–76. doi: 10.1242/jcs.103036

Wang, H., Xu, L., Lai, C., Hou, K., Chen, J., Guo, Y., et al. (2021). Region-specific distribution of Olig2-expressing astrocytes in adult mouse brain and spinal cord. *Mol. Brain* 14:36. doi: 10.1186/s13041-021-00747-0

Weinberg, R. A. (2008). Twisted epithelial–mesenchymal transition blocks senescence. *Nat. Cell Biol.* 10, 1021–1023. doi: 10.1038/ncb0908-1021

Ye, X., Zerlanko, B., Kennedy, A., Banumathy, G., Zhang, R., and Adams, P. D. (2007). Downregulation of Wnt signaling is a trigger for formation of facultative heterochromatin and onset of cell senescence in primary human cells. *Mol. Cell* 27, 183–196. doi: 10.1016/j.molcel.2007.05.034

Zander, M. A., Cancino, G. I., Gridley, T., Kaplan, D. R., and Miller, F. D. (2014). The snail transcription factor regulates the numbers of neural precursor cells and newborn neurons throughout mammalian life. *PloS One* 9:e104767. doi: 10.1371/journal.pone.0104767

Zhu, X., Zuo, H., Maher, B. J., Serwanski, D. R., LoTurco, J. J., Lu, Q. R., et al. (2012). Olig2-dependent developmental fate switch of NG2 cells. *Development* 139, 2299–2309. doi: 10.1242/dev.094524

Frontiers in Neuroscience

Provides a holistic understanding of brain function from genes to behavior

Part of the most cited neuroscience journal series which explores the brain - from the new eras of causation and anatomical neurosciences to neuroeconomics and neuroenergetics.

Discover the latest Research Topics

See more →

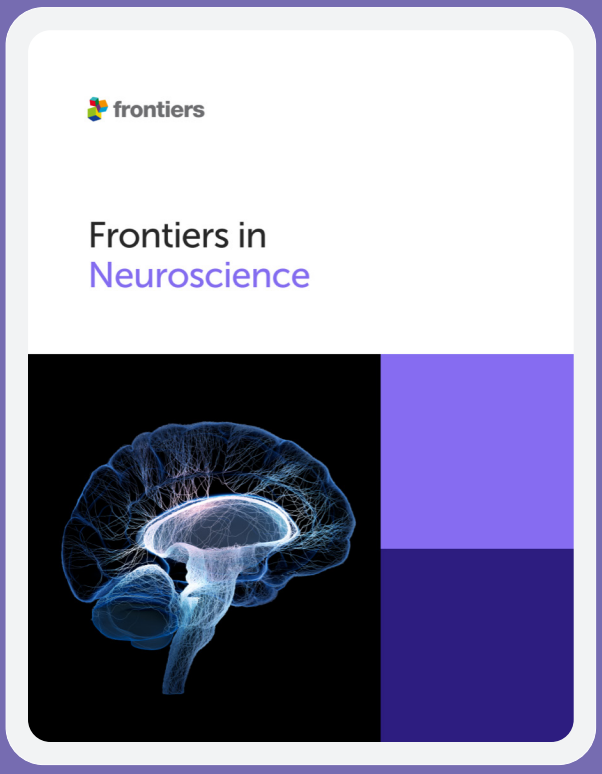

Frontiers

Avenue du Tribunal-Fédéral 34
1005 Lausanne, Switzerland
frontiersin.org

Contact us

+41 (0)21 510 17 00
frontiersin.org/about/contact